USGS
science for a changing world

Prepared in cooperation with the city of Santa Barbara

Santa Barbara and Foothill Groundwater Basins Geohydrology and Optimal Water Resources Management—Developed using Density Dependent Solute Transport and Optimization Models

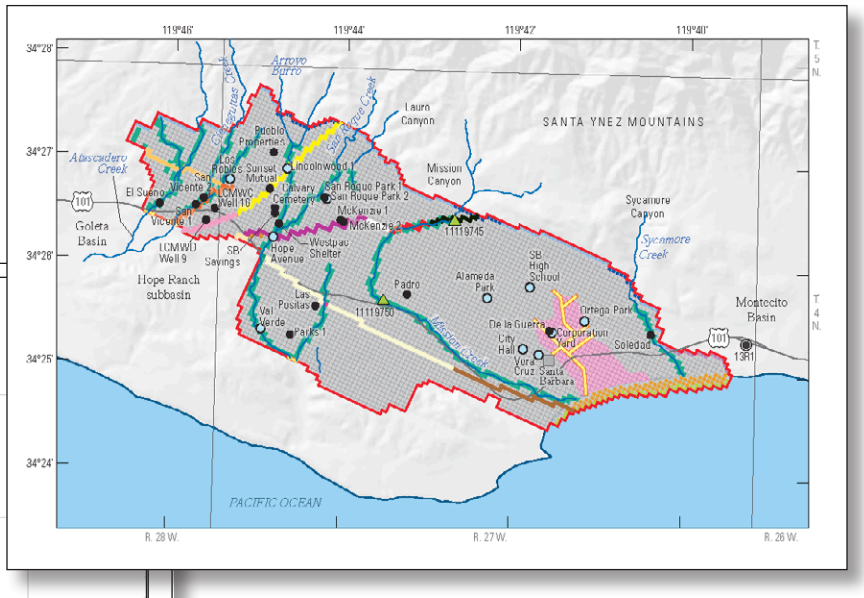

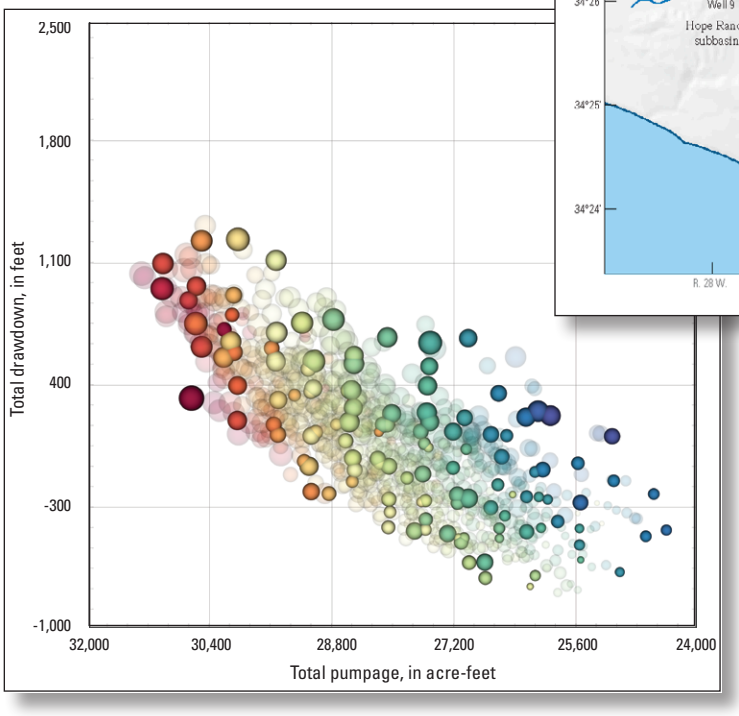

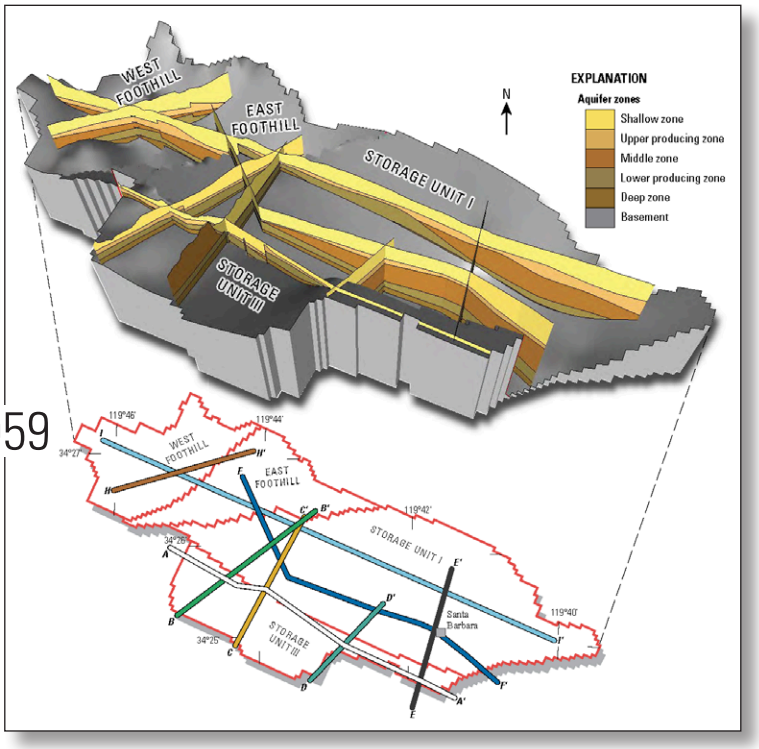

Scientific Investigation Report 2018–5059

U.S. Department of the Interior
U.S. Geological Survey

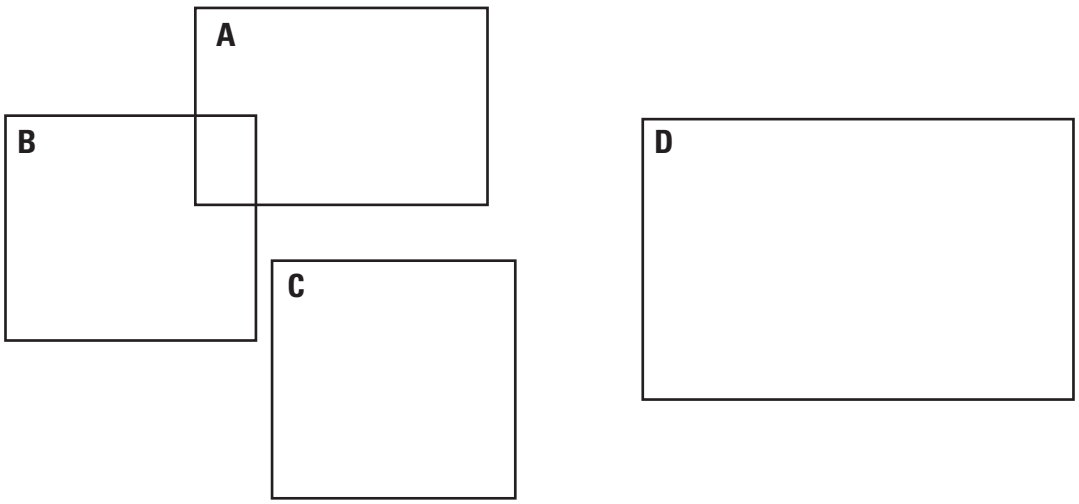

Cover photographs:

Front cover: *A*, Distribution of flow barriers, general-head boundaries, drains, small-catchment recharge, and creek recharge in the Santa Barbara flow and transport model, Santa Barbara, California.

B, Santa Barbara multi-object management model, Santa Barbara, California.

C, Hydrogeologic framework model results by fence diagram, Santa Barbara and Foothill groundwater basins, Santa Barbara, California: *A*, geometric framework model showing subsurface extent of the five aquifer zones, and *B*, texture model showing the distribution of coarse- and fine-grained material in each aquifer zone, with percent-coarse intervals for drillers' well logs and geophysical e-logs (locations of all logs are also shown on the inset diagram). Fence diagrams shown with five times vertical exaggeration.

Back cover: *D*, Photograph showing mission reflection in pond (Photograph taken by Claudia C. Faunt, U.S. Geological Survey).

Santa Barbara and Foothill Groundwater Basins Geohydrology and Optimal Water Resources Management—Developed using Density Dependent Solute Transport and Optimization Models

Edited by Tracy Nishikawa

Chapter A
Introduction and Overview of Geology and Hydrogeology
By Scott R. Paulinski and Tracy Nishikawa

Chapter B
Overview of Hydrogeologic Framework Model
By Geoffrey Cromwell and Scott E. Boyce

Chapter C
Numerical Model of Groundwater Flow and Solute Transport
By Scott R. Paulinski

Chapter D
Multi-Objective Simulation-Optimization Model
By Zachary P. Stanko and Tracy Nishikawa

Prepared in cooperation with the city of Santa Barbara

Scientific Investigations Report 2018–5059

U.S. Department of the Interior
U.S. Geological Survey

U.S. Department of the Interior
RYAN K. ZINKE, Secretary

U.S. Geological Survey
James F. Reilly II, Director

U.S. Geological Survey, Reston, Virginia: 2018

For more information on the USGS—the Federal source for science about the Earth, its natural and living resources, natural hazards, and the environment—visit https://www.usgs.gov or call 1–888–ASK–USGS.

For an overview of USGS information products, including maps, imagery, and publications, visit https://store.usgs.gov.

Suggested citation:
Nishikawa, T., ed., 2018, Santa Barbara and Foothill groundwater basins Geohydrology and optimal water resources management—Developed using density dependent solute transport and optimization models, U.S. Geological Survey, Scientific Investigations Report 2018-5059, 4 chap. (A–D), variously paged, https://doi.org/10.3133/sir20185059.

ISSN 2328-0328(online)

Contents

Contents—Continued

Contents—Continued

Figures

Chapter A

Figures—Continued

Figures—Continued

Figures—Continued

Chapter D

Figures—Continued

Figures—Continued

Figures—Continued

Tables

Chapter A

Chapter B

Tables—Continued

Conversion Factors

U.S. customary units to International System of Units

Multiply	By	To obtain
	Length	
inch (in.)	25.4	millimeter (mm)
inch (in.)	0.0254	meter (m)
foot (ft)	0.3048	meter (m)
mile (mi)	1.609	kilometer (km)
	Area	
acre	4,047	meter^2 (m^2)
square mile (mi^2)	2.590	square kilometer (km^2)
	Volume	
acre-foot (acre-ft)	1,233	cubic meter (m^3)
gallon per day (gal/d)	3.78541	liter per day (L/d)
	Flow rate	
acre-foot per day (acre-ft/d)	0.01427	cubic meter per second (m^3/s)
acre-foot per year (acre-ft/yr)	1,233	cubic meter per year (m^3/yr)
foot per day (ft/d)	0.3048	meter per day (m/d)
foot per year (ft/yr)	0.3048	meter per year (m/yr)
gallon per day (gal/d)	0.003785	cubic meter per day (m^3/d)

Temperature in degrees Celsius (°C) may be converted to degrees Fahrenheit (°F) as follows:

$$°F = (1.8 \times °C) + 32.$$

Temperature in degrees Fahrenheit (°F) may be converted to degrees Celsius (°C) as follows:

$$°C = (°F - 32) / 1.8.$$

Datum

Vertical coordinate information is referenced to the North American Vertical Datum of 1988 (NAVD 88).

Horizontal coordinate information is referenced to the North American Datum of 1983 (NAD 83).

Elevation, as used in this report, refers to distance above the vertical datum.

Supplemental Information

Concentrations of chemical constituents in water are given in either milligrams per liter (mg/L) or micrograms per liter (µg/L).

Abbreviations

bls	below land surface
bsl	below sea level
CSS	composite scaled sensitivity
GHB	general-head boundary package
HFB	horizontal-flow barrier package
HFM	hydrogeologic-framework model
HK	horizontal hydraulic conductivity
LCM	La Cumbre Mutual Water Company
MUD	multi-unit dwellings
P	porosity
PRISM	Parameter-elevation Regressions on Independent Slopes Model
RCH	recharge package
RIV	river package
SBFTM	Santa Barbara Flow and Transport Model
SFR	single-family residences
SGMA	Sustainable Groundwater Management Act
SS	specific storage
SY	specific yield
USGS	U.S. Geological Survey
VK	vertical hydraulic conductivity
WEL	well package

Santa Barbara and Foothill Groundwater Basins Geohydrology and Optimal Water Resources Management—Developed using Density Dependent Solute Transport and Optimization Models

Abstract

Groundwater has been a part of the city of Santa Barbara's water-supply portfolio since the 1800s; however, since the 1960s, the majority of the city's water has come from local surface water, and the remainder has come from groundwater, State Water Project, recycled water, increased water conservation, and as needed, seawater desalination. Although groundwater from the Santa Barbara and Foothill groundwater basins only accounts for a small percentage of the long-term supply, it is an important source of supplemental water during times of surface-water shortages. During the late 1980s and early 1990s, production wells extracted additional groundwater to compensate for drought related water-delivery shortfalls from other sources; in response, water levels declined substantially in the Santa Barbara and Foothill groundwater basins (below sea level in the Santa Barbara groundwater basin).

In coastal basins that have groundwater extraction near shore, seawater intrusion is often a problem. Seawater intrusion in the Santa Barbara groundwater basin is thought to be more limited than in other coastal basins because of an offshore fault that acts as a partial barrier to groundwater flow. During the late 1980s and early 1990s, seawater intrusion was observed in the Santa Barbara groundwater basin, as indicated by increased chloride concentrations at several monitoring wells that ranged from 200 ft to 1,300 ft from the ocean and as close as 2,900 ft to the nearest pumping well. This demonstrated that seawater can intrude into the Santa Barbara groundwater basin when groundwater levels fall below sea level near the coast.

The city of Santa Barbara is interested in developing a better understanding of the sustainability of its groundwater supplies. In 2014, California adopted historic legislation to manage its groundwater: the Sustainable Groundwater Management Act (SGMA). The SGMA requires the development and implementation of "Groundwater Sustainability Plans" in 127 priority groundwater basins; although Santa Barbara was not a designated priority basin, the city is taking steps to achieve sustainability. Sustainability was defined in the SGMA in terms of avoiding undesirable results: significant and unreasonable groundwater-level declines, reduction in groundwater storage, seawater intrusion, water-quality degradation, land subsidence, and surface-water depletion.

In this project, a cooperative study between the U.S. Geological Survey (USGS) and the city of Santa Barbara, sustainable yield is defined as the volume of groundwater that can be pumped from storage without causing water-level drawdowns and the associated increases in seawater intrusion (as indicated by increases in measured chloride concentrations) at selected wells. In order to estimate the sustainability of Santa Barbara's groundwater basins, a three-dimensional density-dependent groundwater-flow and solute-transport model (the Santa Barbara Flow and Transport Model, or SBFTM) was developed on the basis of an existing groundwater-flow model. To simulate seawater intrusion to the Santa Barbara Basin under various management strategies, the SBFTM uses the USGS code SEAWAT to simulate salinity transport and variable-density flow. The completed SBFTM was coupled with a management optimization tool, in this case a multi-objective evolutionary algorithm, to determine optimal pumping strategies that maximize the sustainable yield and at the same time satisfy user-defined drawdown and chloride-concentration constraints.

As part of this study, a three-dimensional hydrogeologic framework model was developed to quantify the extent and hydrogeologic characteristics of the Santa Barbara and Foothill groundwater basins and to help define the discretization and hydraulic properties used in the SBFTM. The development of the hydrogeologic framework model required the collection and reconciliation of geologic and geophysical data from existing maps, reports, and databases, along with geologic and hydrologic data from recently drilled wells. These data were integrated into a three-dimensional hydrogeologic framework model that defines the stratigraphy and geometry of the aquifer zones and the major geologic structures in the basin. The hydrogeologic framework model also quantifies the variation in sediment grain size within each aquifer zone as the percentage of coarse-grained sediment. Previous studies indicated that there are two principal water-producing zones in the Santa Barbara groundwater basin, the upper and lower producing zones; an additional thin, productive zone was identified as part of this study. This "middle producing zone" is not as areally extensive as the upper and lower producing zones and only exists in the coastal part of Storage Unit I. These producing zones are bounded at depth by less productive shallow, middle, and deep zones.

Two versions of the SBFTM were constructed: an initial-condition model and a modern transient model. The initial-condition model is a long-term transient model that simulates flow and solute-transport conditions during a period with limited anthropogenic influences preceeding the modern transient model. The simulation-transient model simulates flow and transport conditions from 1929 through 2013; however, because of data availability, the focus of the model calibration was 1972–2013. The SBFTM was calibrated to measured groundwater levels and drawdown, as well as measured chloride concentrations and change in concentrations, using a combination of automated and trial-and-error parameter-estimation techniques.

A sensitivity analysis indicated that, in general, the SBFTM was most sensitive to recharge- and pumping-distribution parameters, specifically those controlling the amount of small-catchment recharge and the distribution of water extraction by hydrogeologic layer for production wells. The model was also sensitive to parameters controlling stream-recharge rates, horizontal and vertical hydraulic conductivity, and porosity.

From 1929 to 1971, most of the water entering the area represented by the SBFTM was from creek and small-catchment recharge, and the majority of water leaving the SBFTM area was from pumping, discharge to creeks, and drains. In addition, about 37 percent of the total pumpage came from a net reduction in groundwater storage. From 1972 to 2013, the amount of water entering and leaving the SBFTM was fairly similar as that from 1929 to 1971, except the reduction in pumpage added about 17,000 acre-ft of water to storage. During this later period, there were also times of storage loss. For example, during July 1990, a month when approximately 705 acre-ft of groundwater was pumped in the study area, the pumpage was much greater than all sources of recharge combined, and about 382 acre-ft of water was removed from groundwater storage.

Simulated hydraulic heads replicated the observed data to an acceptable matching of the measured water-level, flow direction, and vertical gradients. Simulated hydrographs for selected wells were in good agreement with the measured data, with an average residual of -2.7 ft and a standard deviation of 14.5 ft, indicating that the simulated heads, on average, underestimated the observed water levels. An examination of the model fit indicated that most of the discrepancies were lower simulated heads at wells proximal to production well sites.

The simulated chloride concentrations reasonably matched the rising limbs of the measured breakthrough curves in terms of timing and magnitude; however, the simulation overestimated the chloride concentrations on the falling limbs. The overestimation of low chloride concentrations was attributed to the model overestimating the advance of the chloride front during periods of heavy pumping and underestimating the retreat of the chloride front during periods of low pumping. These simulation errors would result in a conservative response by local water managers to seawater intrusion.

The SBFTM was used to develop a collection of predictive simulations optimized to produce pumping schedules that maximize yield, subject to a set of constraints and competing objectives. The simulations were grouped as scenarios that differed in their time horizon, initial conditions for groundwater levels and chloride concentrations, as well as precipitation, which was incorporated into the model through simulated recharge. Overall, five scenarios were developed in a multi-objective framework to obtain optimal pumping rates for all of the wells managed by the city, while minimizing excessive drawdown and seawater intrusion.

For the current study, complexities in the simulation model and the optimization formulation required additional considerations. Incorporating the solute-transport equations to simulate chloride transport added a highly nonlinear process that is solved iteratively in each time step of the groundwater-flow model. These nonlinearities, coupled with the highly refined grid in the current model, creates challenges for many traditional optimization methods. Therefore, an optimization method was needed that could address nonlinear relationships as well as a very large problem size. Lastly, the optimization problem was reformulated to include multiple objectives without requiring convergence to a single solution. This approach, guided by the city's objectives, allowed the maximum extraction of information from the complex simulation.

Borg, a multi-objective evolutionary algorithm, was chosen as the optimization algorithm for this study for several reasons: (1) it is very computationally efficient; (2) it can run in parallel; (3) it requires little user input; and (4) it can solve for multiple competing objectives. The first three points allow the algorithm to proceed toward the optimal solutions at the fastest possible rate. The fourth point is advantageous for large, complex optimization problems because it is difficult to formulate the optimization problem in a way that produces only one optimal solution.

The problem formulation consisted of four competing objectives and a constraint set in accordance with the main concerns of the city. The objectives were maximizing total pumpage, minimizing seawater intrusion, minimizing total drawdown in production wells, and minimizing the maximum drawdown. The constraints were pump capacity, meeting drinking-water standards for chloride, maintaining a specified minimum flowrate to a groundwater treatment plant, and maintaining minimum water levels in pumping wells. The decision variables either were quarterly pumpage by well or total pumpage by basin.

Five optimization scenarios were developed that allow the decision makers to evaluate a range of optimal solutions for a variety of water levels and chloride concentrations as well as potential future climatic conditions. Three scenarios (1, 2, and 5) were multi-objective optimization formulations that allowed for variations in management preferences and climatic conditions. The other two scenarios (3 and 4) were designed to examine the optimization results to answer specific questions. Scenario 1 described the best-case sustainable yield assuming a "full" basin (that is, high initial water levels) and typical climate conditions for 10 years. Scenario 2 also started with a "full" basin; however, this was followed by a 10-year drought. Scenario 3 determined if an "empty" basin (that is, low initial water levels) would recover to full conditions (1998 conditions) given climate assumptions and optimal pumping schedules from scenarios 1 and 2. Scenario 4 was designed to produce decision rules that can be used by water managers to help choose an optimal pumping schedule based on measured water-level or chloride data. Scenario 5 identified future pumping schedules based on short-term climate variations during a 2-year management horizon.

The results from scenarios 1 and 2 described the differences in maximum pumpage in the basin under typical and dry long-term climate projections, respectively. The scenario 1 results indicated the maximum 10-year pumpage of the basin was about 31,300 acre-ft under typical conditions and controlling simulated seawater intrusion and drawdowns. For scenario 2, less recharge over the 10-year dry climate produced a maximum pumpage estimate of 30,000 acre-ft to control seawater intrusion and drawdowns. The larger pumpage for scenario 1 resulted in more seawater intrusion, but less total drawdown, compared to that of scenario 2.

Results for scenarios 3 and 4 showed the basin's response to management actions combined with climate projections. Both scenarios used the optimal pumping schedules and the 10-year climates from scenarios 1 and 2. The scenario 3 results showed that under minimal pumping, the basin did not fully recover to 1998 water levels within 10 years under either climate scenario. The relatively larger recharge from the typical climate resulted in less drawdown at coastal monitoring wells after the 10-year recovery period than that from the dry climate. The location of the seawater intrusion front was not appreciably different between the scenarios, however. Scenario 4 used the optimal results from scenarios 1 and 2 to produce decision-rule curves that illustrated the pumpage for each basin, given measured levels of chloride concentration or drawdown. This allowed the use of additional measurements at monitoring wells to assess future management decisions on the basis of the sensitivity of observations of drawdown and seawater intrusion to various pumping rates.

Scenario 5 allowed managers to investigate the effects of short-term climate variations on optimal pumping schedules. Three specific 2-year simulations were optimized: typical-to-dry (scenario 5A), dry-to-typical (scenario 5B), and dry-to-dry (scenario 5C). The most noteable result from scenario 5 was the overall reduction in optimal pumpage for most schedules in scenario 5C, when the climate is simulated as dry-to-dry. There are also many optimal pumping schedules that produced an overall increase in waterlevels over the two-year simulation period, regardless of climatic condition. Similar to scenario 2, the scenario 5C results represents conservative yield estimates under a minimal-precipitation climatic condition.

Chapter A: Introduction and Overview of Geology and Hydrogeology

By Scott R. Paulinski and Tracy Nishikawa

Introduction

Groundwater has been a part of the city of Santa Barbara's water supply since the 1800s, when it was the city's primary source of water. Surface water became the primary water source after the early 1910s. In 1991, the city completed construction of wastewater-treatment facilities that supply recycled water for irrigation purposes. The recycled-water project has the capacity to treat and deliver up to 1,400 acre-feet per year (acre-ft/yr) of recycled water. The city also completed construction of a desalination plant in 1992 (City of Santa Barbara, 2015), which was in long-term standby mode until the recent drought. The city reactivated the desalination plant and it became operational in spring 2017. In July 1997, the city gained access to California State Water Project water and is entitled to 3,300 acre-ft/yr, subject to availability (City of Santa Barbara, 2015). In a typical non-drought year, about 82 percent of the city's water supply comes from surface water; the remainder comes from groundwater, the State Water Project, and recycled water (City of Santa Barbara, 2015).

Despite the increased use of surface water, pumping in the Santa Barbara groundwater basin increased from less than 1,000 acre-ft/yr in the late 1950s to about 3,000 acre-ft/yr in the 1960s. Although groundwater only accounts for a small percentage of the long-term demand, it is an important source of supplemental water during water shortages. For example, groundwater was an important addition to the water supply during the severe drought in the late 1980s to early 1990s (Freckleton and others, 1998). Production wells extracted more groundwater to compensate for water-delivery shortfalls from other sources, and water levels declined noticeably in the Santa Barbara and Foothill groundwater basins (fig. 1).

In coastal basins with groundwater extraction near shore, seawater can intrude into freshwater resources. Many of the city of Santa Barbara's production wells are in the Santa Barbara groundwater basin between 3,500 and 5,000 feet (ft) from the ocean; these wells can be susceptible to seawater intrusion during times of intensive pumping, causing below-sea-level groundwater levels. Seawater intrusion into the Santa Barbara groundwater basin is thought to be limited by the presence of an assumed offshore fault, which acts as a partial barrier to groundwater flow. During the 1980s and early 1990s, however, seawater intrusion was observed at several monitoring wells in the Santa Barbara groundwater basin between about 200 and 1,300 ft from the ocean and as close as 2,900 ft to the nearest pumping well (Martin, 1984). These observations demonstrated that seawater can intrude into the basin when water levels fall below sea level at the coastal boundary of the basin.

The city of Santa Barbara is interested in developing a better understanding of the sustainability of its groundwater supplies. In 2014, California adopted historic legislation to manage its groundwater: the Sustainable Groundwater Management Act (SGMA). The SGMA requires the development and implementation of "Groundwater Sustainability Plans" in 127 priority groundwater basins; although Santa Barbara was not a priority basin as of 2017, the city is taking steps to achieve sustainability. Sustainability is defined in the SGMA in terms of avoiding undesirable results: large and unreasonable groundwater-level declines, reduction in groundwater storage, seawater intrusion, water-quality degradation, land subsidence, and surface-water depletion (U.S. Geological Survey, 2018).

In order to estimate the sustainability of the Santa Barbara and Foothill groundwater basins, a three-dimensional, density-dependent solute-transport model was developed by the U.S. Geological Survey (USGS) in cooperation with city of Santa Barbara. For this work, sustainable yield is defined, with respect to seawater intrusion, as the volume of groundwater that can be pumped from storage without causing water-level drawdowns and associated increases in seawater intrusion (as indicated by increases in measured chloride concentrations) at selected wells. The groundwater-flow model developed by Freckleton and others (1998) provided the basis for solute-transport modeling.

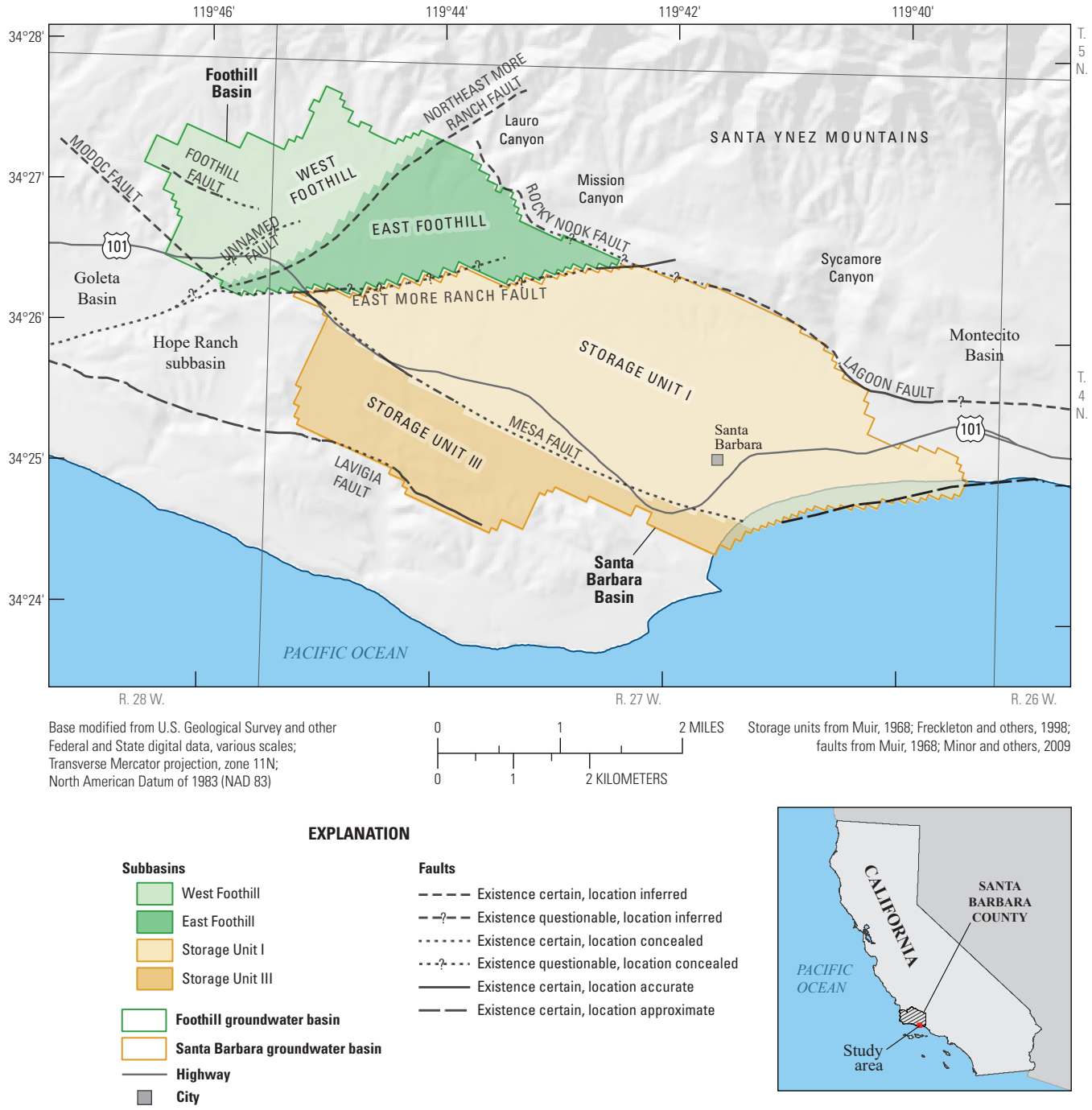

Figure 1. Location and general features of the Santa Barbara and Foothill groundwater basins, Santa Barbara, California.

Purpose and Scope

This report describes the solute-transport model that was used in conjunction with a management optimization model, in this case a multi-objective evolutionary algorithm, to determine the optimal pumping strategies that maximize the sustainable yield yet satisfy user-defined drawdown and chloride-concentration constraints. In addition to developing the solute-transport and optimization models, new hydrogeologic framework and textural models of the Santa Barbara and Foothill groundwater basins were developed. These models were used in the construction of the solute-transport model.

The study is summarized in this four-chapter report describing the hydrogeology and the hydrogeologic framework, groundwater-flow, and solute-transport models of the Santa Barbara and Foothill groundwater basins. This chapter (chapter A) introduces the study, presenting a description of the study area, an overview of previous work, and an overview of the geology and hydrogeology of the study area. Chapter B presents a hydrogeologic framework model of the study area. This hydrogeologic framework model includes a three-dimensional interpretation of the geologic features associated with producing zones that supply most of the city of Santa Barbara's groundwater. The textural component of the hydrogeologic framework model provides a three-dimensional gradational distribution of the coarse and fine sediments in the Santa Barbara and Foothill groundwater basins. Chapter C presents the numerical groundwater-flow and solute-transport model of the Santa Barbara and Foothill groundwater basins (Santa Barbara Flow and Transport Model or SBFTM), which simulates groundwater flow and transport of chloride in the study area from 1929 through 2013. Chapter D presents a simulation-optimization model of the study area that enables use of the solute-transport model within a management optimization approach for water-management decision support.

Previous Studies

The Santa Barbara groundwater basin has been the subject of a number of USGS studies in the last 50 years. As groundwater levels declined throughout the 1960s, a study by the USGS, in cooperation with the Santa Barbara County Water Agency, developed the information needed to ensure sufficient water for the future needs of the county. A study of the geology, hydrogeology, water quality, and inflow/outflow of the Santa Barbara and Montecito area (Muir, 1968) concluded that groundwater pumping had removed 6,000 acre-feet (acre-ft) of water from groundwater storage in the Santa Barbara area between 1959 and 1964. The study also concluded that seawater intrusion during this time was limited to near-shore shallow alluvial deposits and that there was no direct connection between the deeper water-bearing zones and the ocean. This lack of connection was attributed to an offshore fault.

In 1977, the USGS, in cooperation with the city of Santa Barbara, began to develop and implement a three-phase groundwater-monitoring program focused on "Storage Unit I" of the Santa Barbara groundwater basin (fig. 1 *in* Hutchinson, 1979). The monitoring program's main focus was to study the effects of pumping in Storage Unit I on groundwater levels and seawater intrusion. During phase 1 of the study, coastal monitoring wells were constructed and sampled to detect sea intrusion into the freshwater aquifer. The study concluded that observed elevated levels of chloride in coastal monitoring wells could either be due to connate water or to underflow across the offshore fault (Hutchinson, 1979). Phase 2 of the groundwater monitoring program focused on characterizing the geohydrology of the Santa Barbara groundwater basin (Martin, 1984). The number of monitoring wells in the Santa Barbara groundwater basin was increased from 17 to 30, and data from the monitoring wells were used to assess the effects of pumping on water levels and water quality. The study concluded that several methods, including decreased pumpage, artificial recharge, and relocation of the city well field, could be used to displace intruded ocean water in the basin and force it seaward (Martin, 1984). A three-dimensional groundwater-flow model for Storage Unit I was developed for phase 3 of the study (Martin and Berenbrock, 1986). Results from the groundwater-flow model indicated that increased municipal pumpage resulted in increased inflow across the offshore fault at a rate of about 580 acre-ft/yr.

The USGS, in cooperation with the city of Santa Barbara, extended the three-phase groundwater study to include the Foothill groundwater basin, where additional groundwater monitoring wells were installed, a geohydrologic assessment was performed, and a three-dimensional, finite-difference, two-layer model was developed to confirm estimates of basin recharge and natural discharge and to evaluate water-level response to groundwater pumping (Freckleton, 1989).

In July and September of 1987, streamflow gains and losses were measured along Mission Creek (McFadden and others, 1991). As part of the study, water was released from a reservoir to Mission Creek; streamflow was measured at 10 sites downstream; and seepage was calculated along 10 segments of Mission Creek. The rate of streamflow gain or loss between stations varied greatly. Results along some segments were substantially different from a 1979 study by the USGS, when the water table was lower (Martin, 1984).

In the 1990s, the USGS, in cooperation with the city of Santa Barbara, developed an area-wide groundwater-flow model of the Santa Barbara and Foothill groundwater basins, including the previously unmodeled Storage Unit III (Freckleton and others, 1998). During the simulation period, from 1978 to 1992, the model simulated water moving landward, across the offshore fault, to the Santa Barbara groundwater basin. Based on this groundwater-flow model, a two-dimensional simulation-optimization density-dependent groundwater-flow and transport model was developed to aid in making management decisions regarding the city of Santa Barbara's water resources (Nishikawa and Martin, 1998). Selected optimal pumping strategies were simulated to determine the effect on seawater intrusion during a 5-year management period.

Study Area

The study area is situated on a south-facing section of coastline in southeastern Santa Barbara County, in southern California about 85 miles (mi) west-northwest of Los Angeles. The study area includes the Santa Barbara and Foothill groundwater basins on the Santa Barbara coastal plain, a narrow strip of land about 2 mi wide between the Santa Ynez Mountains to the north and the Pacific Ocean to the south (fig. 1). The coastal plain extends beyond the study area to the Goleta groundwater basin to the west and the Montecito groundwater basin to the east.

The study area includes much of the city of Santa Barbara, which had an estimated population of 91,842 in 2015 (United States Census Bureau, 2017). The city of Santa Barbara covers approximately 19 square miles and has a population density of approximately 4,800 people per square mile.

Climate

The study area has a Mediterranean-like climate, with warm summers and mild winters. Average temperatures range from highs around 65 degrees Fahrenheit (°F) and lows around 45 °F in the winter to highs around 75 °F and lows around 60 °F in the summer (National Weather Service, 2016). The study area has distinct wet and dry seasons; between 1972 and 2013, about 83 percent of the rain fell between November and May. The average annual rainfall from 1899 to 2013 measured at a rain gage at the Santa Barbara County building in downtown Santa Barbara was 18.55 inches (in.; County of Santa Barbara, 2014). The least and most recorded precipitation in the city of Santa Barbara fell in water year 2007 (6.41 in.) and water year 1998 (46.97 in.), respectively (County of Santa Barbara, 2014; fig. 2*A*). From 1900 to 2013, the study area has experienced several sequences of wet and dry periods, as indicated by a cumulative-departure from the mean curve (fig. 2*B*).

Land Use

Land use during the study period (1929–2013) was relatively stable, and it was assumed that the 1992 land-use map was representative of the land-use conditions during the study period. In 1992, 70 percent of the land use was residential and commercial-industrial; 21 percent was shrub-forest or grassland; 5 percent was planted or cultivated land or planted grasses; 2 percent was barren; and less than 1 percent was wetlands (fig. 3). Commercial-industrial land use was most prevalent in downtown Santa Barbara near the coast. Small parks and golf courses were scattered throughout the study area. Forests, shrubs, and grasslands characterized the parks, and planted grasses were used in the golf courses. Small ranches in the foothills of the northern region of the western study area accounted for much of the planted and cultivated land use. Wetlands were confined to areas along the coast in the eastern-most area of the study area.

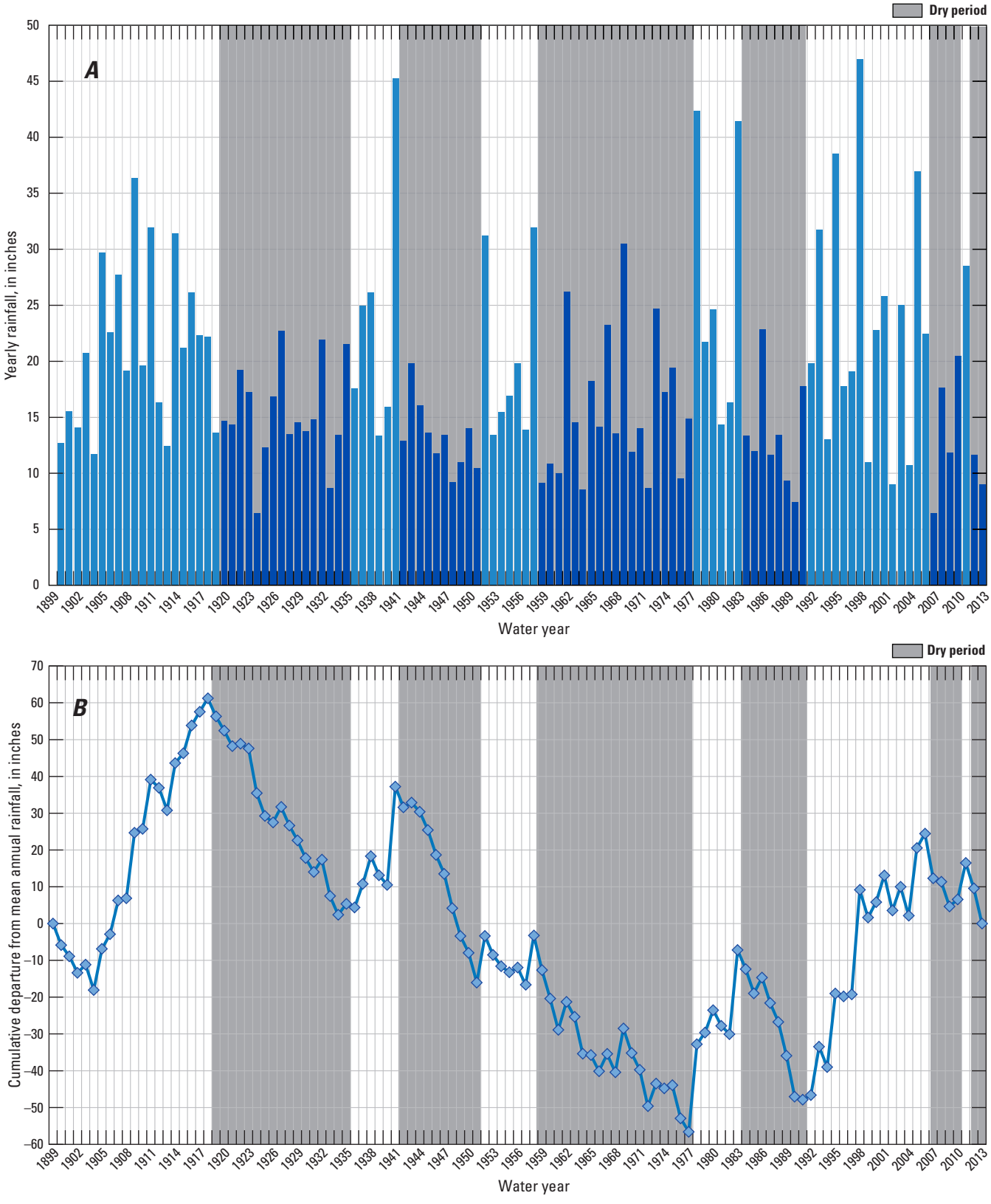

Figure 2. Precipitation measured at the Santa Barbara County building (1899–2013), by water year, Santa Barbara, California: *A*, total annual precipitation, and *B*, cumulative departure from mean.

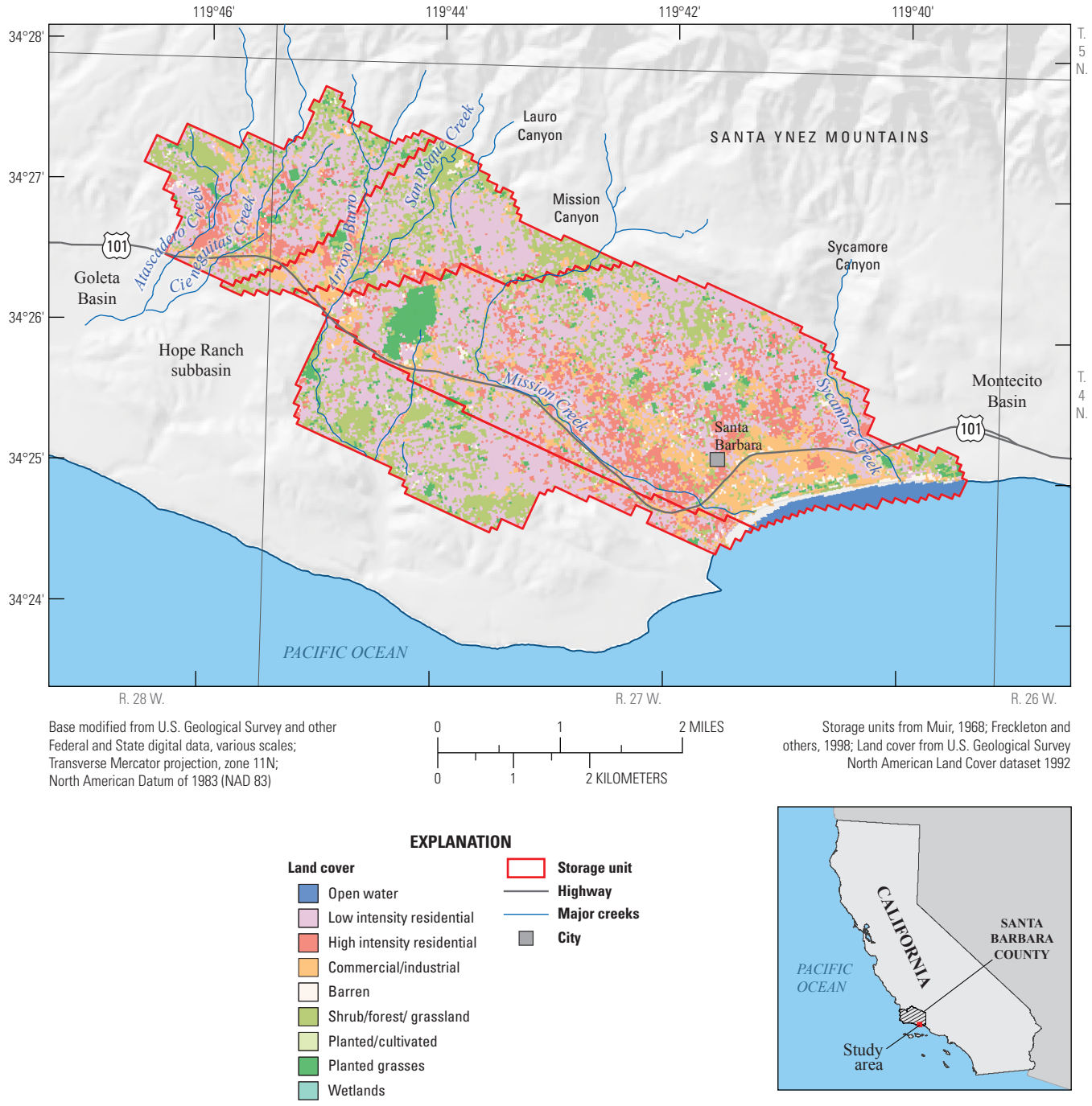

Figure 3. Distribution of land-use patterns, North American Land Cover Dataset 1992, Santa Barbara, California.

Geology and Structure

Previous studies have described the geology and structure of the Santa Barbara groundwater basin in great detail (summarized by Minor and others, 2009). A general overview of the geology is presented in this report; the reader is referred to Minor and others (2009) for additional information.

The Santa Barbara groundwater basin is part of the coastal plain and is in the western Transverse Ranges physiographic province (Minor and others, 2009). The western Transverse Ranges consist mainly of variably deformed marine and nonmarine sedimentary rocks and deposits that range in age from Jurassic to the present. The coastal plain includes several mesas and hills that represent potentially active structures of the Santa Barbara fold and fault belt that transects the coastal plain. The study area is dominated by oblique-slip reverse and thrust faulting. Bounding the study area are the Rocky Nook and Lagoon faults to the north and the Lavigia and Modoc faults to the south (fig. 4). An unnamed fault, about 0.25 mi offshore extending from the Mesa fault eastward, truncates deeper deposits so they lie against consolidated deposits on the seaward side of the fault. Outcrops of sedimentary rock can be observed in the local Santa Ynez Mountains where oblique-slip reverse and thrust faulting has uplifted and overturned many of the formations (Minor and others, 2009).

The Santa Barbara groundwater basin consists of tertiary sedimentary rock overlain by unconsolidated to partially consolidated deposits. The sedimentary rock, mostly marine in origin, consists primarily of shale, mudstone, sandstone, and conglomerate.

Overlying the consolidated units are marine and non-marine unconsolidated and partially consolidated deposits of the Santa Barbara Formation of late Pliocene and Pleistocene age and alluvium of Holocene age. A medium- to coarse-grained sand with fine gravel near the base of the Santa Barbara Formation extends inland several miles from the coast. Most of the surficial deposits in the study area are either Pleistocene moderately consolidated poorly sorted sands, gravels, and conglomerates deposited as alluvial fans from the Santa Ynez Mountains or Holocene and upper Pleistocene poorly consolidated silts, sands, and gravels deposited from modern drainages, alluvial fans, and floodplains (Minor and others, 2009). The study area also contains small areas of Holocene estuarine deposits of organically rich clay, silt, and sand along low-lying coastal areas (fig. 4).

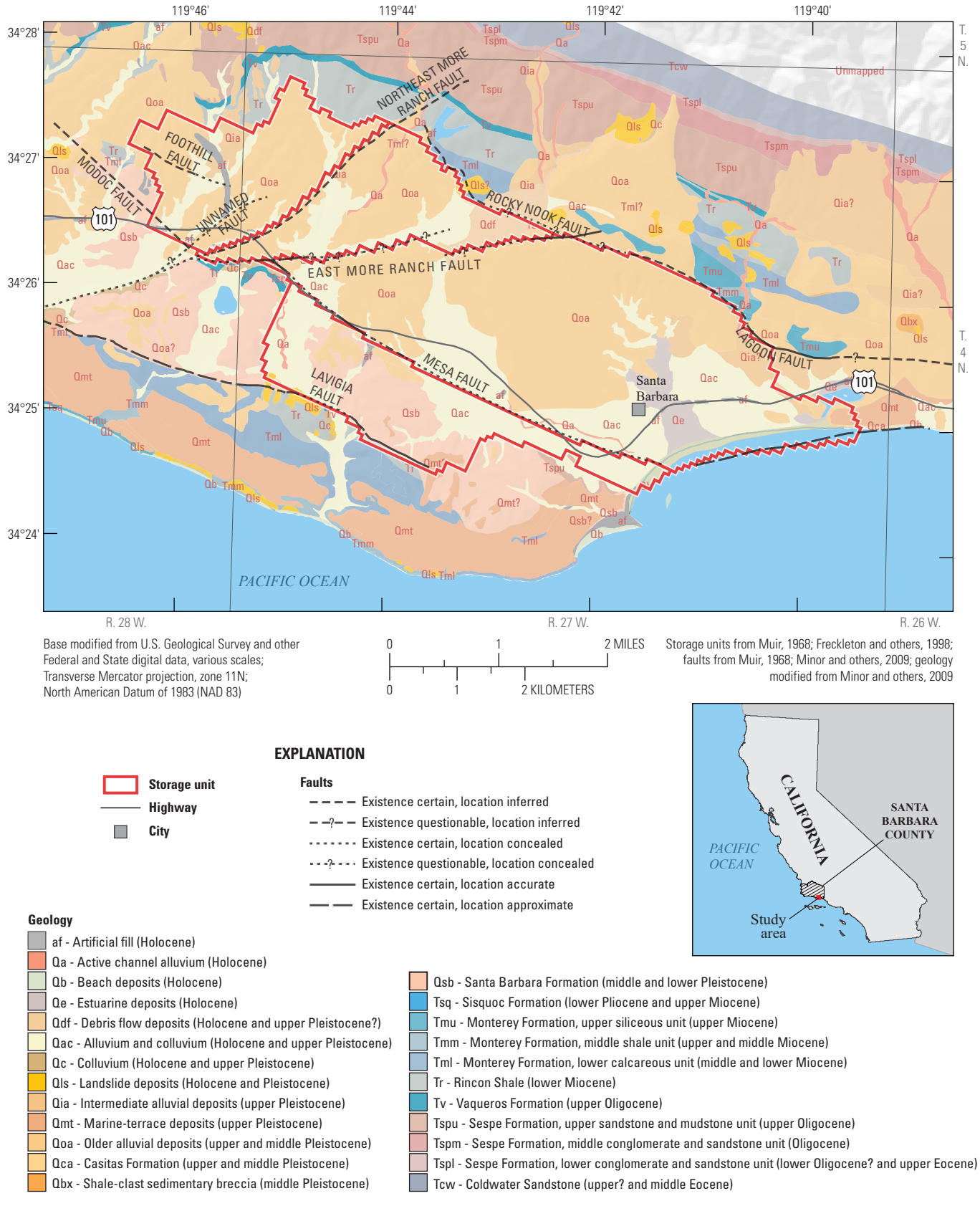

Figure 4. Surface geology and faults of the Santa Barbara area, California.

Hydrogeology

The hydrogeology of the Santa Barbara and Foothill groundwater basins was defined by summarizing previously published research (for example, Muir, 1968; Martin and Berenbrock, 1986; Freckleton and others, 1998). In addition, a new hydrogeologic zone is described.

Description of the Aquifer System

There are two main groundwater basins in the study area that are separated by faults: the Santa Barbara groundwater basin and the Foothill groundwater basin (fig. 5). The Santa Barbara groundwater basin contains two subbasins, "Storage Unit I" and "Storage Unit III" (Muir, 1968). The Foothill basin is divided by a fault into two subbasins; for the purposes of this report, these subbasins are named the East and West Foothill subbasins (fig. 5). Storage Unit I underlies the main part of the city of Santa Barbara and is the main focus of this report; less emphasis is placed on Storage Unit III and the two Foothill subbasins. Storage Unit I and the Foothill subbasins are the main sources of potable groundwater for the city of Santa Barbara.

Faults and Groundwater Flow

In the study area, many of the faults separate the subbasins and act as partial barriers to groundwater flow (Freckleton and others, 1998). The Rocky Nook and Lagoon faults to the north and the Lavigia and Modoc faults to the south (fig. 4) are assumed to restrict groundwater flow into the basin and, therefore, define parts of the basin boundary. The East More Ranch fault acts as a groundwater barrier separating the Foothill groundwater basin from the Santa Barbara groundwater basin. The Mesa fault divides Storage Unit I from Storage Unit III in the Santa Barbara groundwater basin. Additionally, the Northeast More Ranch fault divides the Foothill groundwater basin into two subbasins, East Foothill and West Foothill (Minor and others, 2009, fig. 4). The Foothill fault and an unnamed fault could act as groundwater barriers in the West Foothill subbasin. The unnamed fault about 0.25 mi offshore that extends from the Mesa fault eastward is thought to impede groundwater flow (Freckleton and others, 1998).

Hydrogeologic Zones

The Santa Barbara and Foothill groundwater basins consist primarily of unconsolidated silts, sands, and gravels deposited from drainages, alluvial fans, and floodplains. Based on electric and geologic logs, Martin and Berenbrock (1986) divided the unconsolidated deposits into five zones representing the hydraulic characteristics of the layers: the shallow, upper producing, middle, lower producing, and deep zones. Based on additional analyses, the middle zone contains a thin, not very extensive, but productive zone, referred to as the "middle producing zone." The three main productive zones in the basins and their extents are shown on figure 6. A description of each of the zones and how the middle producing zone was defined is given below. Chapter B describes a hydrogeologic framework model defining the extent and characteristics of all the zones.

Shallow Zone

The shallow zone includes alluvium from land surface to the top of the upper producing zone. In general, it is composed of fine-grained deposits that confine or partly confine the upper producing zone.

Upper Producing Zone

The upper producing zone, one of the main water-bearing units in the study area, consists predominately of medium- to coarse-grained sand and fine gravel. It averages about 50 ft thick (fig. 7). The upper producing zone extends through much of the Santa Barbara and Foothill groundwater basins and pinches out to the north near the Santa Ynez foothills in Storage Unit I and East Foothill subbasin and to the east of Las Positas Creek in Storage Unit III (fig. 6*A*).

Middle Zone

As defined by Martin and Berenbrock (1986), the middle zone consists of fine-grained deposits interspersed with sporadic coarse-grained water-bearing deposits, which confine or partially confine the lower producing zone. The middle zone separates the upper and lower producing zones in most of the study area. The middle zone pinches out in the northwestern part of Storage Unit I, where the upper and lower producing zones are in contact with each other. A downhole-velocity survey of the Corporation Yard well (4N/27W-15Q10, fig. 5) and resistivity logs from several wells perforated in the middle zone indicated a thin, not very extensive, but productive zone of coarse-grained deposits at a depth of about 360–380 ft below NAVD 88 near the coast (Pueblo Water Resources, written commun., 2013). The results from the velocity survey indicated that 17 percent of total production from the Corporation Yard well was extracted from 410 to 430 ft bls, 21 percent was from the upper producing zone, and 36 percent was from the lower producing zone (table 1); the balance of production was extracted from other formations. The middle producing zone was not identified in previous studies, but was identified in this study.

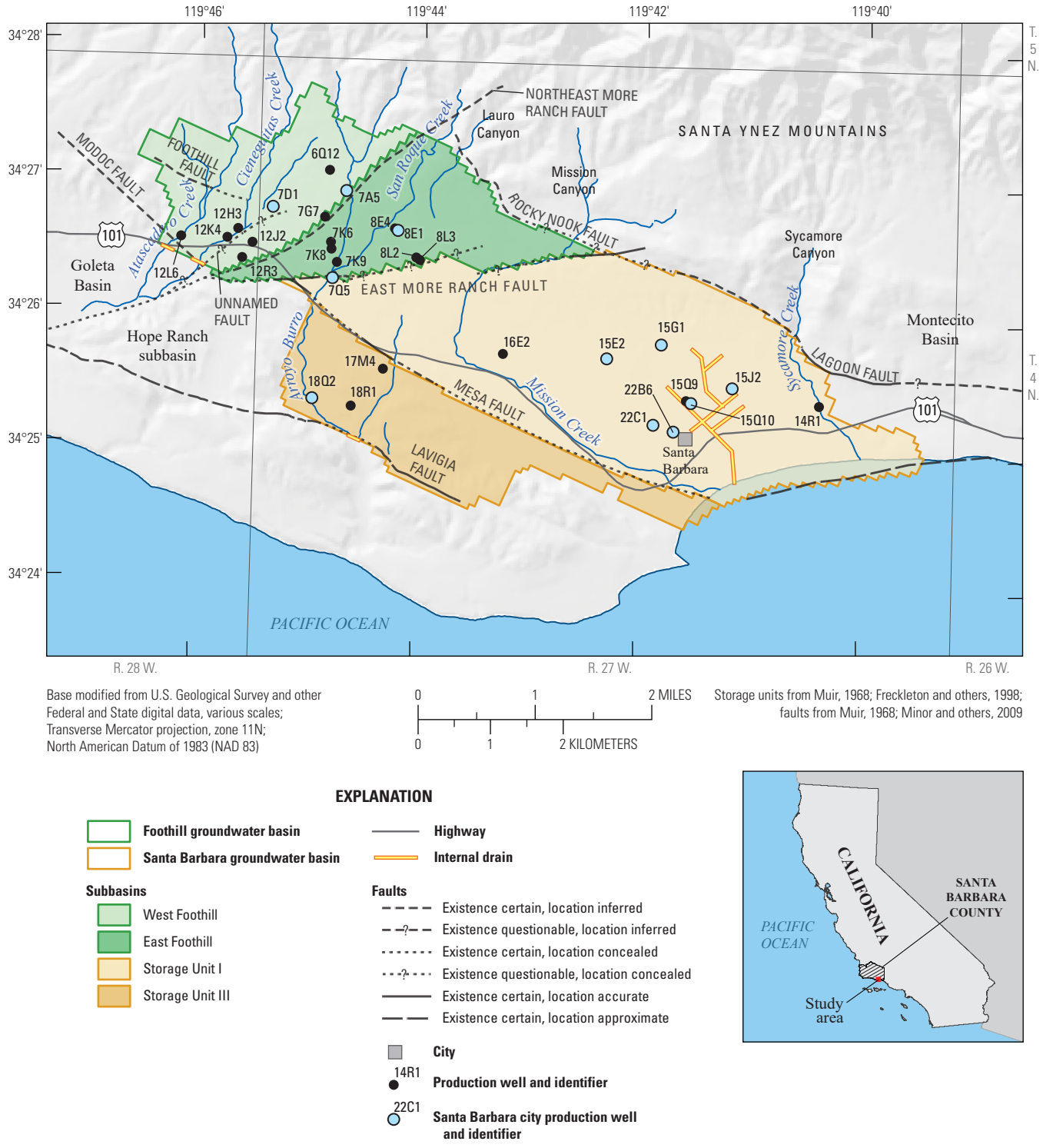

Figure 5. Santa Barbara and Foothill groundwater subbasins, creeks, faults, production wells, and drains, Santa Barbara, California.

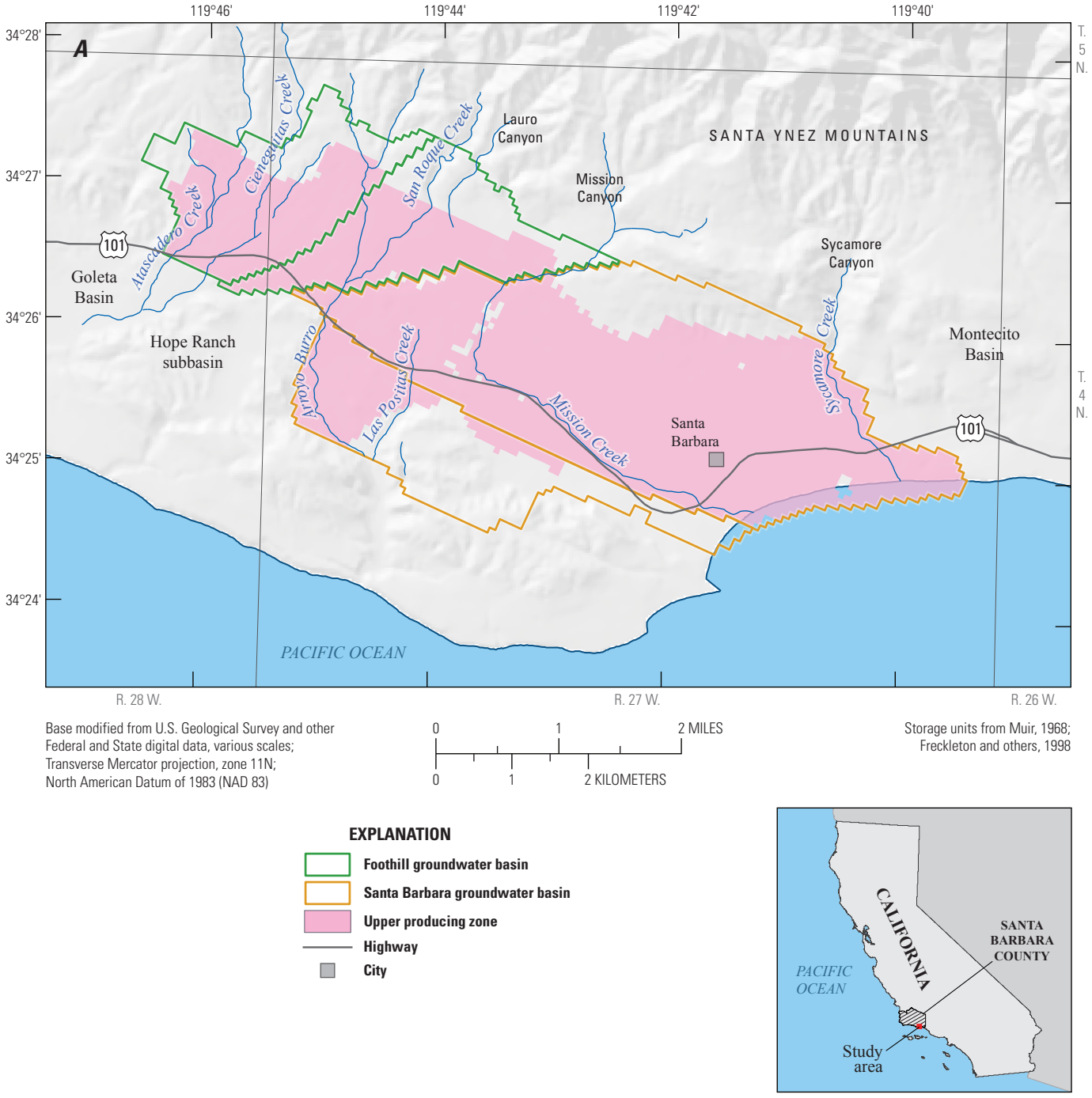

Figure 6. Lateral extent of the upper, middle, and lower producing zones in the Santa Barbara and Foothill groundwater basins, Santa Barbara, California: *A*, upper producing zone, *B*, middle producing zone, and *C*, lower producing zone.

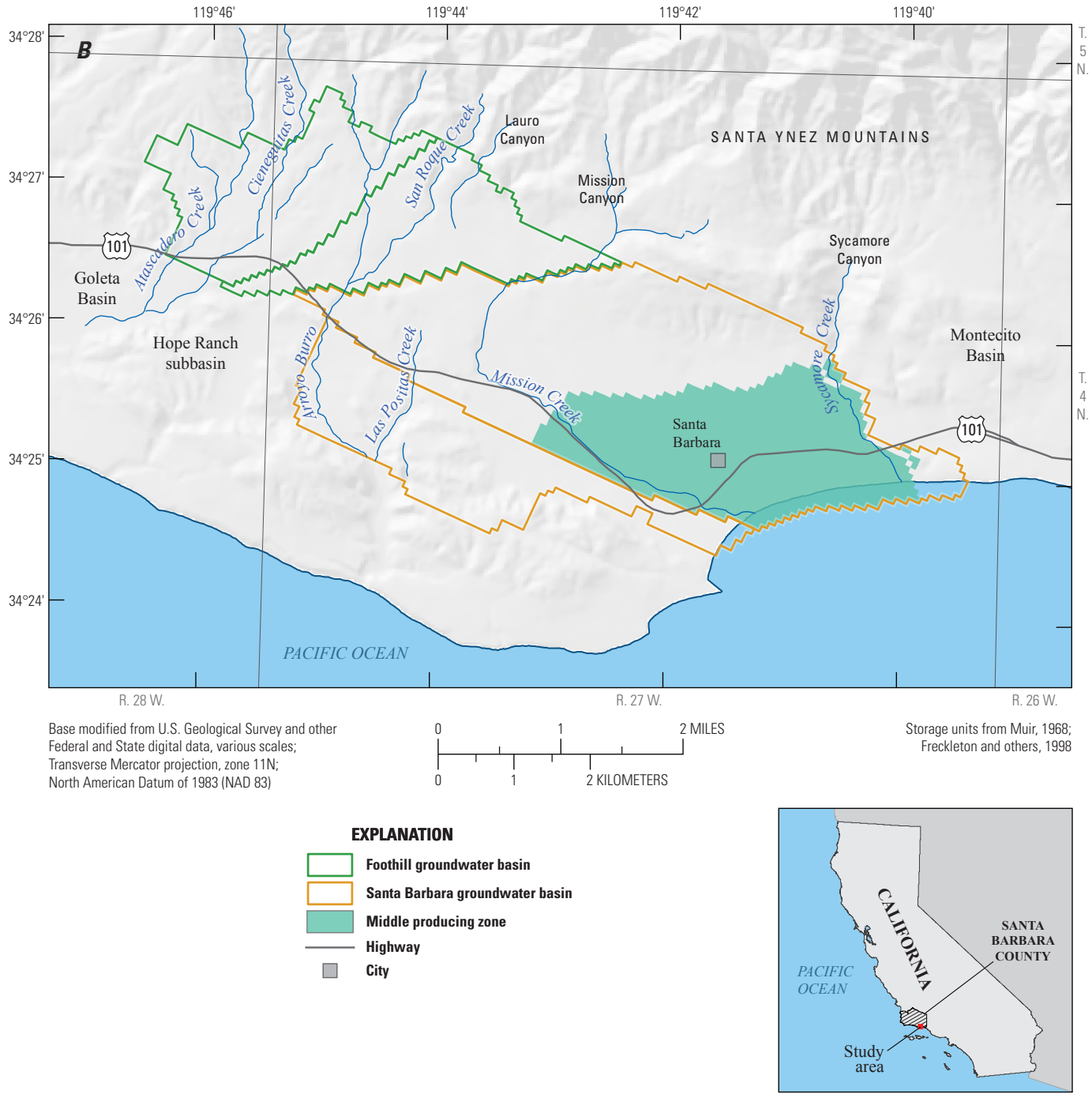

Figure 6. —Continued

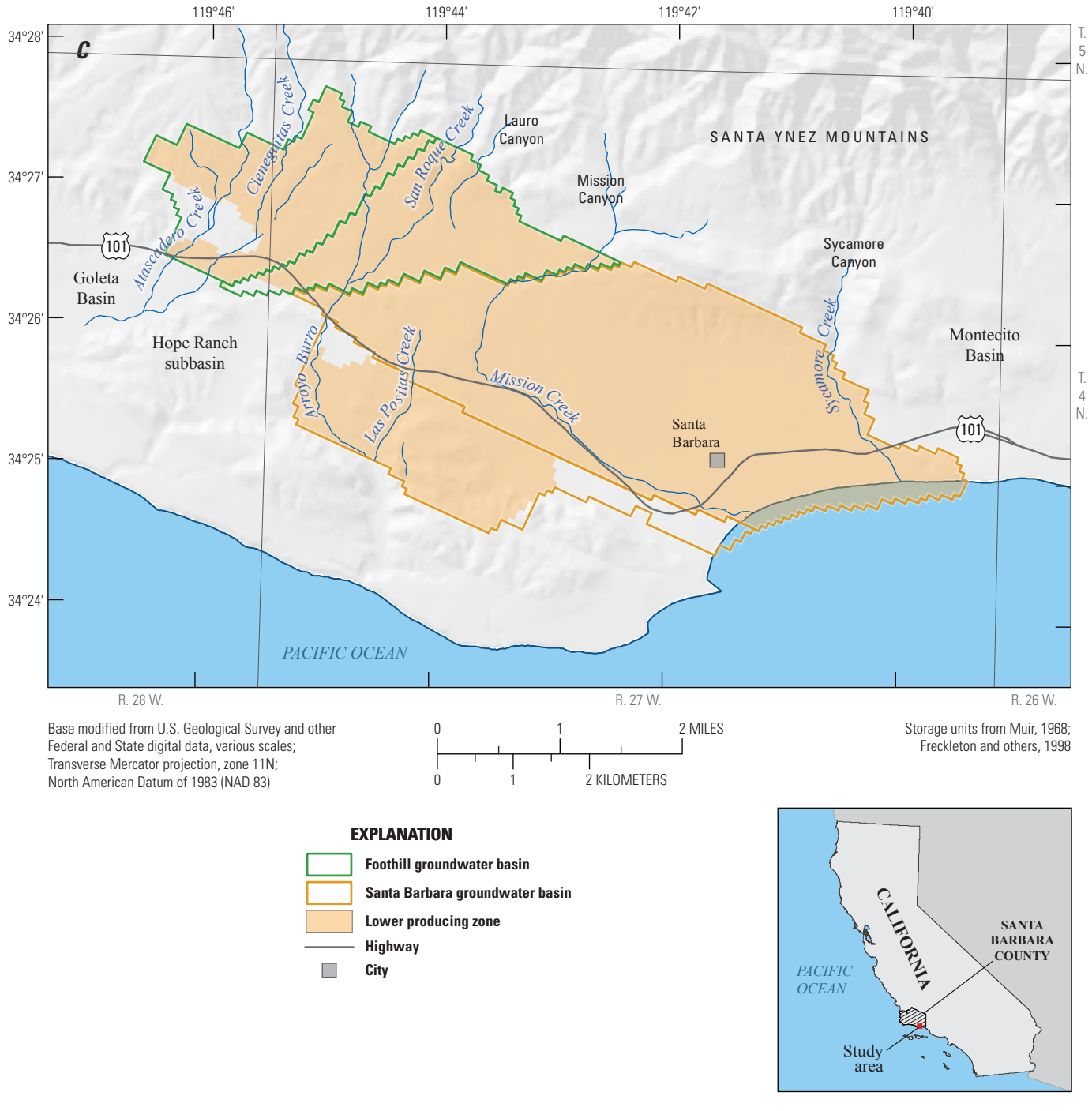

Figure 6. —Continued

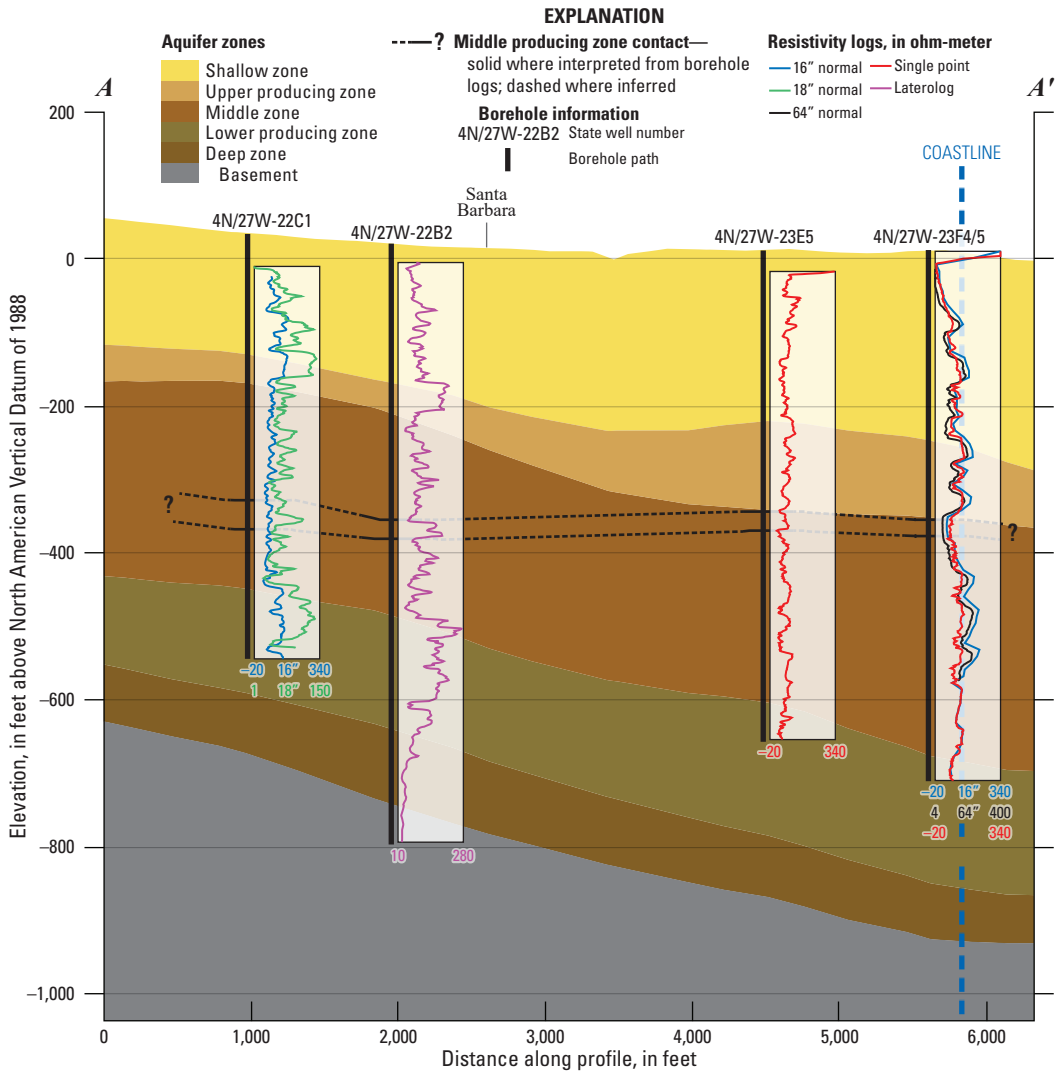

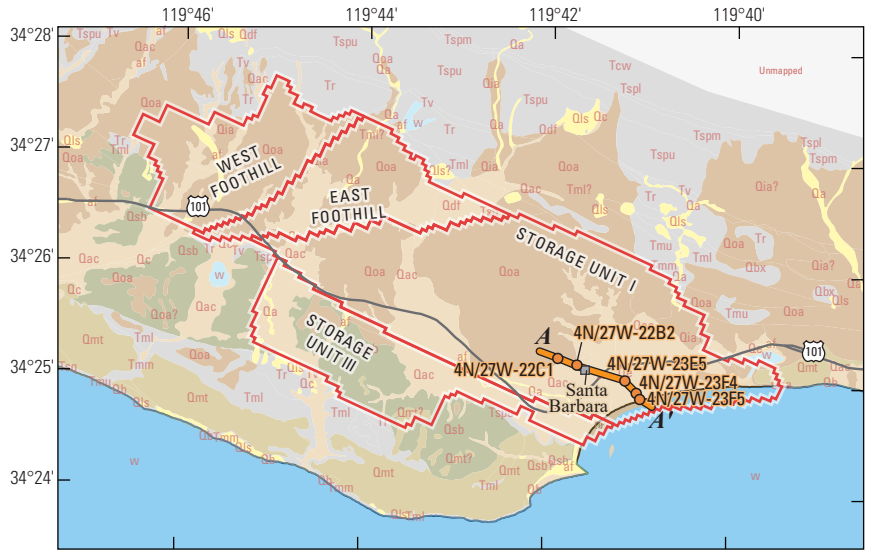

Figure 7. Storage Unit I from the northwest to the southeast coast (from left to right), showing resistivity logs for selected wells and aquifer-zone horizons defined by the hydrogeologic framework model (see chapter B), Santa Barbara groundwater basin, Santa Barbara, California.

Table 1. Velocity-profile testing results for the Corporation Yard well, Santa Barbara, California.

[Pueblo Water Resources, written commun., 2013, table 3. **Abbreviations**: bls, below land surface; ft, feet; gpm, gallons per minute; —, not applicable]

Screen intervals (ft bls)	Thickness (ft)	Percentage of total production				
		Step 1 411 gpm	Step 2 602 gpm	Step 3 817 gpm	Step 4 1,006 gpm	Averages
Upper producing aquifer zone						
190–205	15	3	9	2	12	6
225–270	45	15	14	15	14	14
Subtotal	60	17	23	16	25	21
Middle aquifer zone						
350–395	45	10	9	20	7	12
410–430	20	16	16	18	17	17
450–460	10	3	6	5	6	5
490–510	20	14	11	4	13	10
Subtotal	95	42	42	47	44	44
Lower producing aquifer zone						
580–605	25	15	14	15	16	15
615–655	40	26	21	22	15	21
Subtotal	65	41	35	36	31	36
Total	220	100	100	100	100	—

Resistivity logs for wells 4N/27W-22C1, -22B2, -22A2, and 4N/27W-23E5 display high resistivity readings in the middle zone at the interval around 360 to 380 ft below NAVD 88 (fig. 7), indicating coarser sediments in this interval. Near the coastline, however, wells 4N/27W-23F4 and 4N/27W-23F5 showed low-resistivity readings over the same interval (fig. 7), which could be due to increased salinity or the presence of fine-grained materials. Groundwater samples collected from these wells have higher salinity levels at this interval, indicating that the resistivity drop is likely due to higher salinity levels and not fine-grained material. The higher salinity levels are confined to this narrow interval of coarse-grained materials because there are finer grained materials above and below this interval.

The coarse-grained deposits in the middle zone of Storage Unit I around 360–380 ft below NAVD 88 are defined as the middle producing zone. This analysis is based on the Corporation Yard well velocity survey, resistivity logs, and examination of drillers' logs throughout Storage Unit I, as described in chapter B. The middle producing zone extends from the coastline in Storage Unit I to about 1–2 mi inland (fig. 6*B*), where it pinches out. It appears to terminate at the offshore fault to the southeast and at the Mesa fault to the southwest.

Lower Producing Zone

The lower producing zone, the third main water-bearing unit, consists of medium- to coarse-grained sand with fine gravel. The lower producing zone extends through much of the Santa Barbara and Foothill groundwater basins and thins or pinches out near the Santa Ynez foothills to the north and pinches out in southeastern Storage Unit III (fig. 6*C*). The lower producing zone thickens to about 200 ft from north to south in Storage Unit I (fig. 7).

Deep Zone

In most of the study area, there is a deep zone of fine-grained deposits of variable thickness below the lower producing zone (fig. 7). In general, these deposits have relatively low hydraulic conductivity, are reported to have poor water quality (Martin and Berenbrock, 1986), and are assumed to not be an important source of water.

Pre-Development Recharge and Discharge

The main components of pre-development groundwater recharge and discharge for the Santa Barbara and Foothill groundwater basins are stream (creek) leakage, small-catchment recharge, areal recharge, underflow, and evapotranspiration. Ephemeral creeks originating from the Santa Ynez Mountains pass through the study area and empty into the Pacific Ocean. Creeks in the study area include Mission, Sycamore, Arroyo Burro, San Roque, Cieneguitas, and Atascadero Creeks (fig. 3). Depending on location, creeks can be either a source of groundwater recharge or mechanism of discharge. Martin (1984) identified segments of groundwater recharge and discharge along Mission Creek and estimated net recharge from Mission Creek to be 376 acre-ft/yr on the basis of seepage-loss measurements. Freckleton and others (1998) estimated the long-term, mean groundwater recharge from creeks was about 925 acre-ft/yr, and the steady-state groundwater discharge to creeks was as high as 1,700 acre-ft/yr, yielding a net loss of groundwater to creeks of about 775 acre-ft/yr. Note that Freckleton and others (1998) used MODFLOW's Drain Package (Harbaugh and others, 2000) to simulate the groundwater discharge to creeks and the drain system beneath downtown Santa Barbara, but did not differentiate between these losses; therefore, the groundwater discharge to creeks was probably less than 1,700 acre-ft/yr.

For this study, small-catchment recharge is defined as runoff and underflow from the Santa Ynez Mountains and foothills. Muir (1968) estimated an average of approximately 300 acre-ft/yr of recharge to the Santa Barbara groundwater basin as underflow from the consolidated rocks that form the majority of the boundary between the Santa Barbara groundwater basin and the Santa Ynez foothills.

Areal recharge is the amount of direct infiltration from precipitation in the study area. As stated earlier, the average annual precipitation for the study area is 18.55 in. Not all precipitation that falls in the study area recharges the groundwater basins. A large percentage of precipitation runs off directly to the ocean, predominantly in the urban areas of the city, where much of the area is paved, and water runs through the city's drain system to the ocean. Some of the precipitation that infiltrates the vadose zone is evaporated or is transpired by plants before reaching the groundwater system. Freckleton and others (1998) simulated the total steady-state areal recharge to be about 1,100 acre-ft/yr for the Santa Barbara and Foothill groundwater basins.

Groundwater can leave the basins laterally as underflow across the offshore fault from the Santa Barbara groundwater basin, at Arroyo Burro Creek across the Lavigia fault in Storage Unit III, at Atascadero and Cieneguitas Creeks across the Modoc fault from the Foothill to the Goleta groundwater basin, or from Storage Unit I to the Montecito groundwater basin (fig. 5). Freckleton and others (1998) simulated pre-development discharge across the offshore fault to be about 290 acre-ft/yr and discharge across the Lavigia fault to be about 24 acre-ft/yr. Freckleton and others (1998) did not simulate the flux across the Modoc fault and treated the boundary between Storage Unit I and Montecito groundwater basin as a no-flow boundary; however, no known geologic feature prevents flow between the two basins.

An area of the city of Santa Barbara was originally part of the Santa Barbara Estero, a marshy lagoon (Martin and Berenbrock, 1986). Because artesian groundwater conditions existed before development in much of this part of the basin, groundwater most likely exited the Santa Barbara groundwater basin through evapotranspiration in the Santa Barbara Estero. Martin and Berenbrock (1986) estimated the steady-state groundwater loss to the Estero was about 400 acre-ft/yr.

Post-Development Effects on Groundwater System

Development in the study area has had several effects on groundwater recharge, flow, and discharge. The major effect has been from groundwater pumping; however, development has had other effects as well. Limited groundwater pumpage data were available prior to 1947; records are more complete from 1947 to present. The available data show that groundwater pumpage has varied greatly over the past 85 years (fig. 8). From water year 1949 through water year 1991, there was substantial groundwater pumping in the study area, with pumpage averaging over 1,700 acre-ft/yr for the Santa Barbara and Foothill groundwater basins. For comparison, Freckleton and others (1998) reported that the total simulated outflow from the basins under pre-development conditions was about 2,030 acre-ft/yr. Since water year 1992, groundwater pumping in Storage Unit I has been reduced, with pumpage averaging less than 200 acre-ft/yr. There were three main periods of heavier pumping in the Foothill groundwater basin, from water years 1964 to 1970, 1985 to 1991, and 2008 to 2013 (fig. 8), with pumpage averaging 831, 1,005, and 869 acre-ft/yr, respectively. During dry years, groundwater pumping accounts for a substantial part of the discharge in Santa Barbara and Foothill groundwater basins.

Septic tanks are used for wastewater treatment in the parcels shown in figure 9. These data were provided by the Santa Barbara County Clerk-Recorder-Assessor's Mapping Division. There were 195 single-family residences (SFR), 16 multi-unit dwellings (MUD) with 2–4 units, one rest home, one restaurant, and one retail store with septic systems. Eckenfelder (1980, in table 4.5) reported an average septic-effluent flow of 90 gallons per day (gal/d) for each person in "better subdivisions." This average yields a total septic flowrate of about 65 acre-ft/yr, if one assumes 2.5 residents for each SFR (U.S. Census Bureau, 2017) and 10 people for each MUD, rest home, restaurant, and store (assuming 4 units in each MUD and 2.5 people in each unit).

The land use in the study area is predominantly residential and commercial (fig. 3). Below an elevation of 100 ft, storm sewers, city streets, and buildings prevent much infiltration of rain (Muir, 1968). In addition, the concrete lining of the lower section of Mission Creek has reduced groundwater interaction with the creek. Likewise, a network of drains was installed near land surface to dewater the Santa Barbara Estero area prior to development (fig. 5). This network continues to drain runoff and groundwater to the ocean during storm events.

Pre-Development Groundwater Movement

Martin and Berenbrock (1986) reported that under unpumped conditions (presumably similar to pre-development conditions) groundwater movement in Storage Unit I was generally from the northwest and north toward the Pacific Ocean. Martin and Berenbrock (1986, fig. 3) also indicated that pre-development groundwater movement in the Foothill groundwater basin was to the west-southwest across the Modoc fault. Pre-development groundwater movement in Storage Unit III was easterly toward the Pacific Ocean (Martin and Berenbrock, 1986, fig. 3).

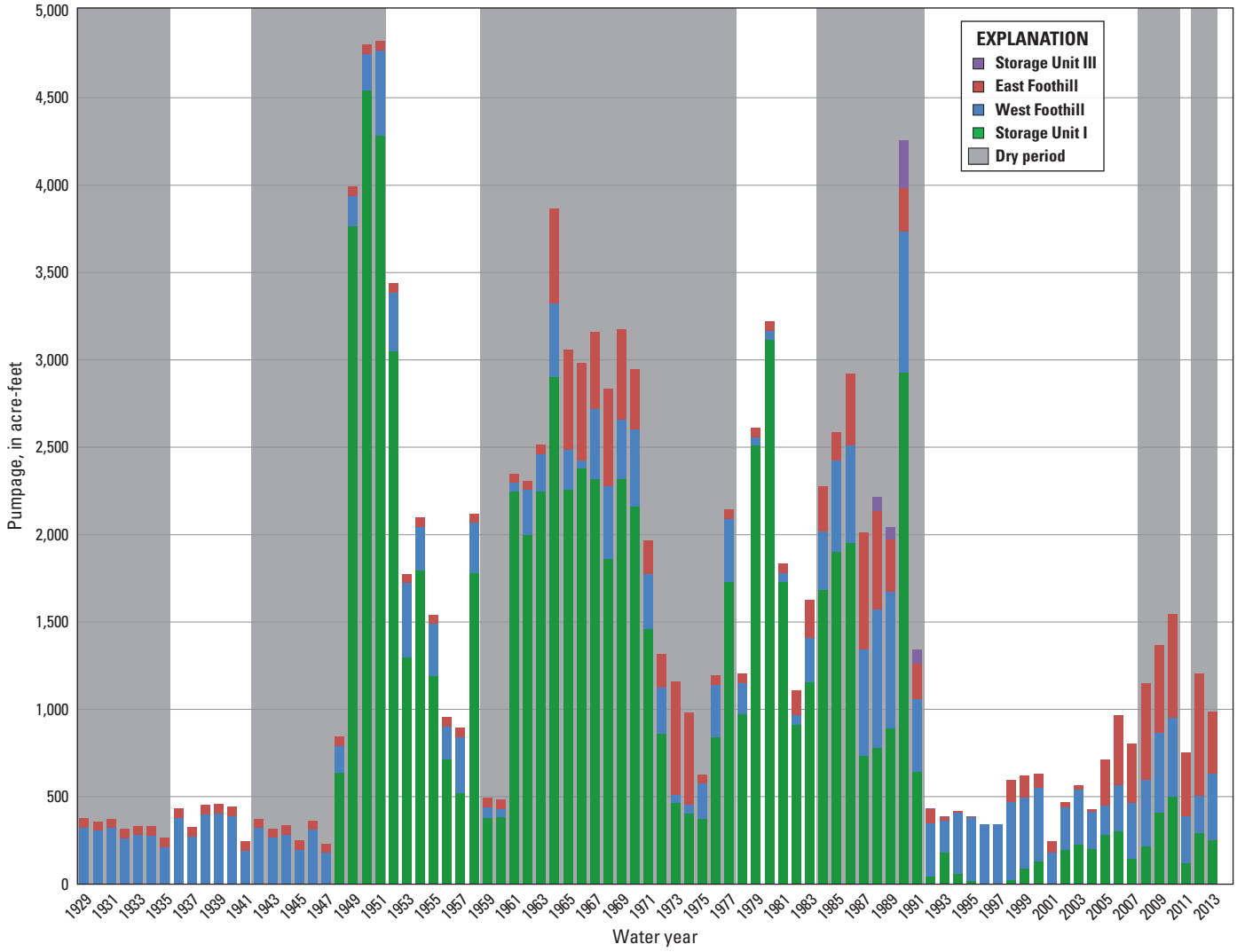

Figure 8. Estimated and reported total annual pumpage in the Santa Barbara and Foothill groundwater basins, water years 1929–2013, Santa Barbara, California.

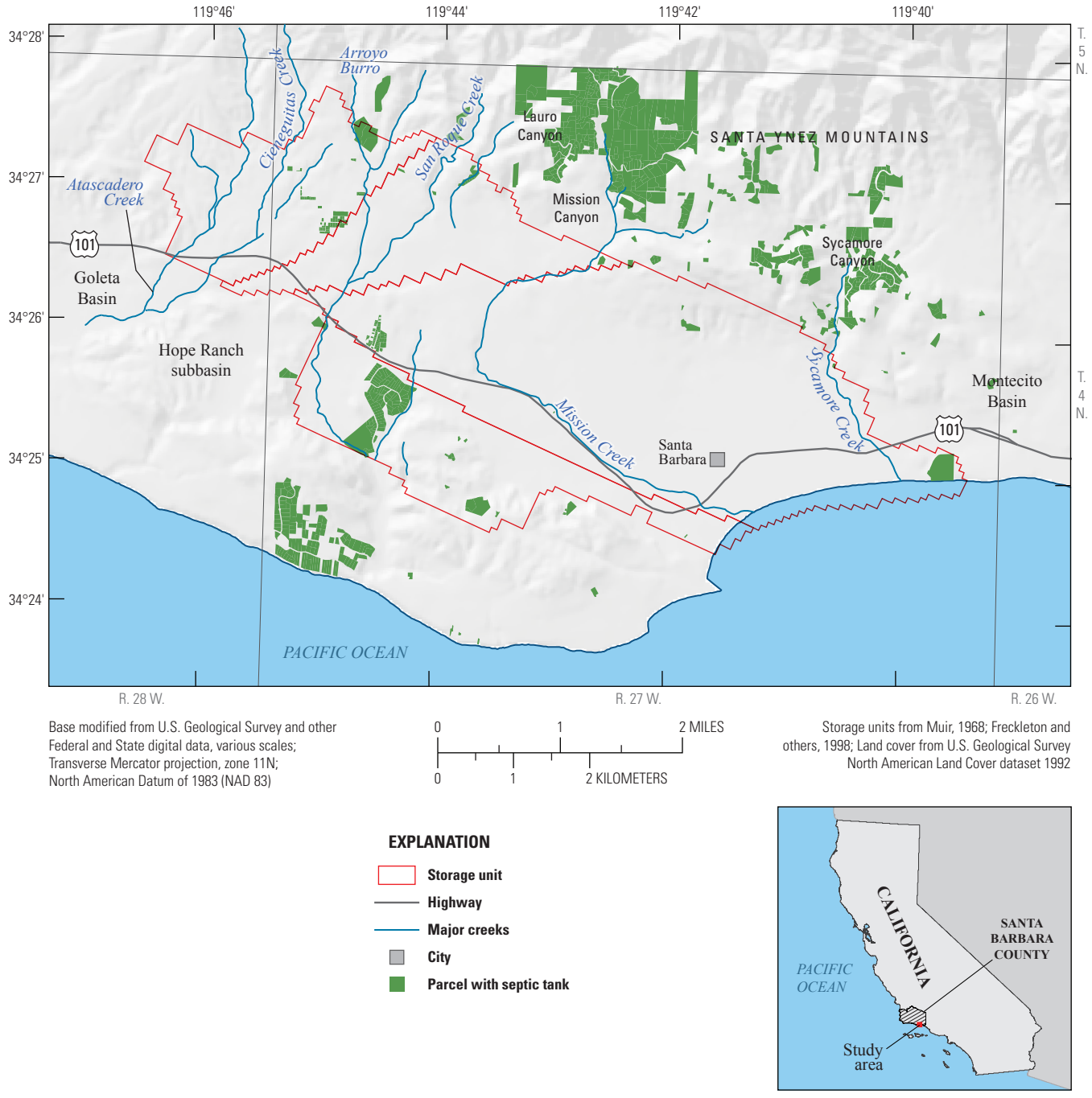

Figure 9. Parcels with septic tanks, Santa Barbara, California (parcel data from Santa Barbara County, Mapping Division, 2011).

Post-Development Groundwater Levels and Movement

The groundwater-level contours of the lower producing zone, based on measured water levels from the summer of 1990, the end of an extended period of high pumping, and from the spring of 1997, after several years of low pumping, are shown in figures 10*A* and *B*, respectively. Water-level data from the lower producing zone were used because of limited data availability for the upper and middle producing zones; also, most groundwater was pumped from the lower producing zone.

The summer of 1990 was the end of a prolonged period of increased pumpage between 1985 and 1990 (fig. 8), when total annual pumping in the study area varied from 2,000 to 4,300 acre-ft/yr. Pumping in the Foothill groundwater basin resulted in water levels as low as about 70 ft above NAVD 88 (fig. 10*A*). Flow directions in Foothill groundwater basin were generally from northeast to southwest, except near production wells, where flow directions were radially inward toward the production well. Pumping in Storage Unit I resulted in water levels as low as 90 ft below NAVD 88 in the vicinity of production wells and in a large area of below sea level water levels in the southeastern part of Storage Unit I (fig. 10*A*). Flow in Storage Unit I was generally from northwest to southeast, except in the southeastern part, where flow directions were radially inward toward the production wells. The radial flow extended through much of the southeastern region of Storage Unit I between the Lagoon and Mesa faults.

In the spring of 1997, the flow direction in Foothill groundwater basin was from northeast to southwest; the highest heads were near the intersection of Mission Creek and Rocky Nook fault and were at least 170 ft above NAVD 88 and could be much higher, and lowest heads were less than 100 ft above NAVD 88 and were near the border of Foothill and Goleta groundwater basins (fig. 10*B*). Flow in Storage Unit I and Storage Unit III was from northwest to southeast; the highest heads were near the intersection of the East More Ranch and Mesa faults, and the lowest heads were near the coast.

Water levels in the Foothill groundwater basin decreased during the late 1980s through the early 1990s, which was followed by a recovery period with increasing water levels from the mid-1990s through 2004, and then by another period of decreasing water levels from 2005 through 2014. Monitoring well 4N/27W-08M6 (located adjacent to well 8M5 in fig. 10) is perforated in the upper producing zone and is in the middle of the East Foothill subbasin about 0.25 mi southwest of the San Roque Park production wells (8E4; table 2) and about 0.4 mi west of the McKenzie production wells (8L2, 8L3; fig. 5). The hydrograph for this well (fig. 11) shows drawdown from the late 1980s through the early 1990s during a period of high pumping from the McKenzie #2 (8L3) well. Water levels dropped below 130 ft during this period. As pumping decreased in this well during the mid-1990s, water levels in 4N/27W-08M6 recovered through 2004, when they peaked close to 180 ft. Beginning in 2005, the San Roque Park #2 (8E4) well started pumping, leading to another period of drawdown through 2015, when water levels dropped below 120 ft.

Monitoring well 4N/28W-12H04 is perforated in the lower producing zone and is in the West Foothill subbasin about 0.2 mi north of La Cumbre Mutual Water Company Well #16 production well (12J2) and about 0.25 mi southwest of the Los Robles production well (7D1). Groundwater levels from this well indicated a similar drawdown and recovery pattern as monitoring well 4N/27W-08M6 (fig. 11).

Water levels in Storage Unit I fluctuated during much of the 1980s, such that water levels declined substantially between the late 1980s and early 1990s in response to groundwater pumping. Water levels started increasing in 1991 and continued to recover through 1999, when they leveled off and then slowly declined through 2014 in the lower part of the basin, compared to a more rapid decline in the upper part of the basin. Well 4N/27W-16C1 is perforated in the lower producing zone and is representative of the inland part of Storage Unit I, upgradient of most of the production wells in Storage Unit I. Water levels in 4N/27W-16C1 fluctuated with pumping between 90 and 105 ft from 1982 to 1988 (fig. 11). Water levels dropped abruptly in 1989 and were at 70 ft by late 1990. Water levels recovered during the 1990s, peaking at about 115 ft in 1999. From 1999 through 2015, water levels declined, and the annual fluctuations in water levels increased.

Well 4N/27W-22A4 is perforated in the lower producing zone between the main production wells in Storage Unit I and the coast. It is representative of the coastal part of Storage Unit I. In general, the water levels for this well were much lower than those measured in the inland part of Storage Unit I, Foothill groundwater basin, and Storage Unit III (fig. 11). During the late 1980s through 1990, water levels fluctuated greatly, varying from 20 ft in 1989 to –80 ft in 1990 (fig. 11). Water levels recovered starting in 1990, peaking at 52 ft in 1996. From 1999 through 2009, water levels generally trended downward to about 25 ft by 2014. Water levels decreased to about –60 ft by late 2016 The below-sea-level water levels in the late 1980s to early 1990s, and again in the mid-2010s, indicate that seawater could have intruded the aquifer during these periods.

Water levels fluctuated more in the inland part of Storage Unit III than in the areas closer to the coast. Water levels at well 4N/27W-18Q4 in the inland part of Storage Unit III, near the Val Verde production well (18Q2), responded to nearby pumping, varying from a low of about 85 ft in 1991 to a high of 102 ft in 2005 (fig. 11). Water levels at well 4N/27W-21F1, downgradient from well 18Q4, were fairly steady between the early 1990s and 2010s, but water levels started to decline after 2010 (fig. 11).

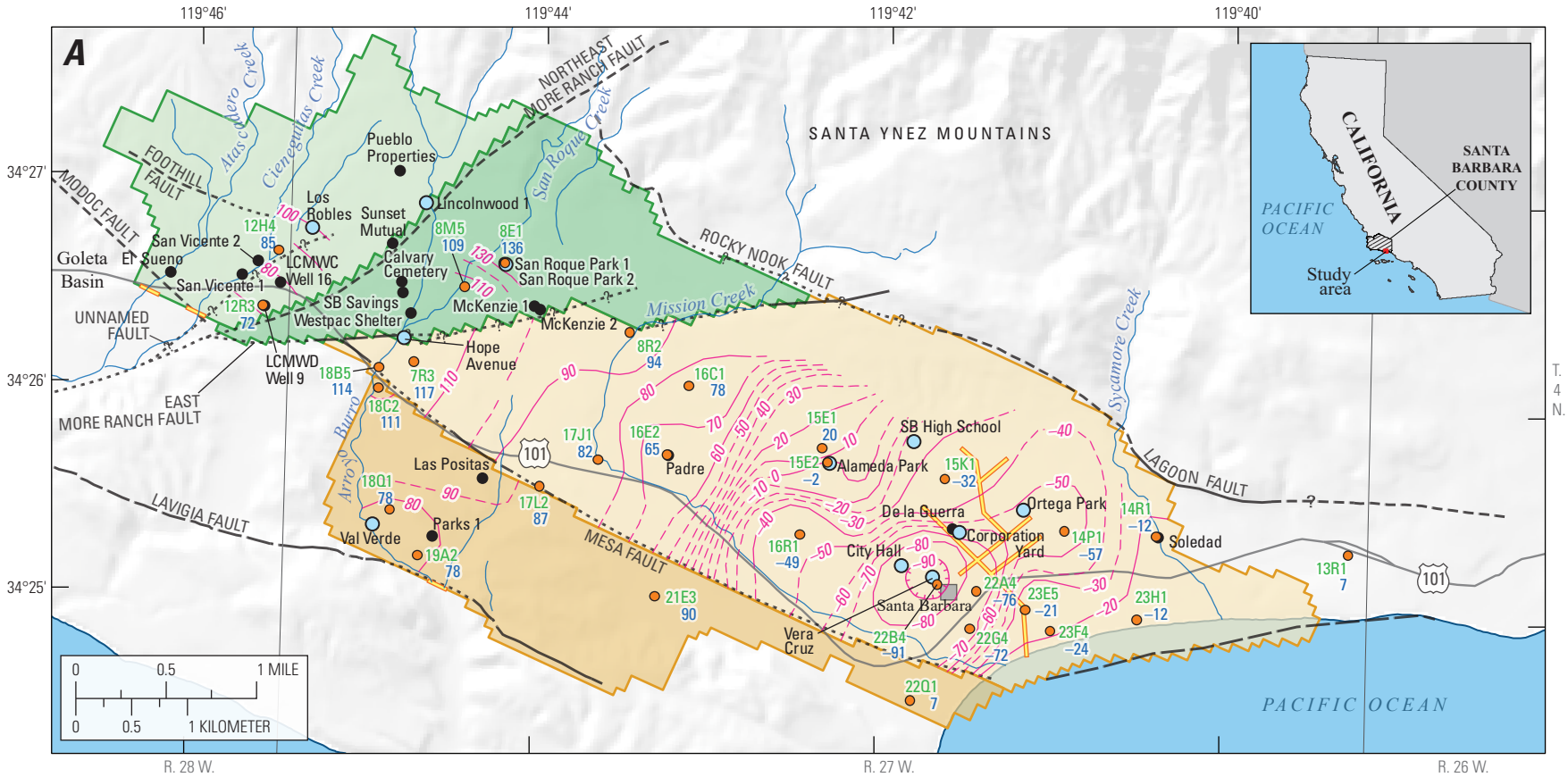

Base modified from U.S. Geological Survey and other Federal and State digital data, various scales; Transverse Mercator projection, zone 11N; North American Datum of 1983 (NAD 83)

Storage units from Muir, 1968; Freckleton and others, 1998; faults from Muir, 1968; Minor and others, 2009

EXPLANATION

- **Foothill groundwater basin**
- **Santa Barbara groundwater basin**

Subbasin

- West Foothill
- East Foothill
- Storage Unit I
- Storage Unit III

Faults

- Existence certain, location inferred
- Existence questionable, location inferred
- Existence certain, location concealed
- Existence questionable, location concealed
- Existence certain, location accurate
- Existence certain, location approximate

- **Water-table contour**—Shows elevation of water table. Location is approximate; dashes where uncertain. Hachures indicate depression. Contour interval 10 feet.
- **Well and identifier**—Top number is abbreviated state well number. Bottom number is elevation of water level, in feet above North American Vertical Datum 1988.

- Padre — **Production well and identifier**
- Vera Cruz — **Santa Barbara city production well and identifier**
- **City**
- **Highway**
- **Internal drain**

Figure 10. Groundwater-level contours of the lower producing zone in the Santa Barbara and Foothill groundwater basins, Santa Barbara, California: *A*, summer 1990, and *B*, spring 1997.

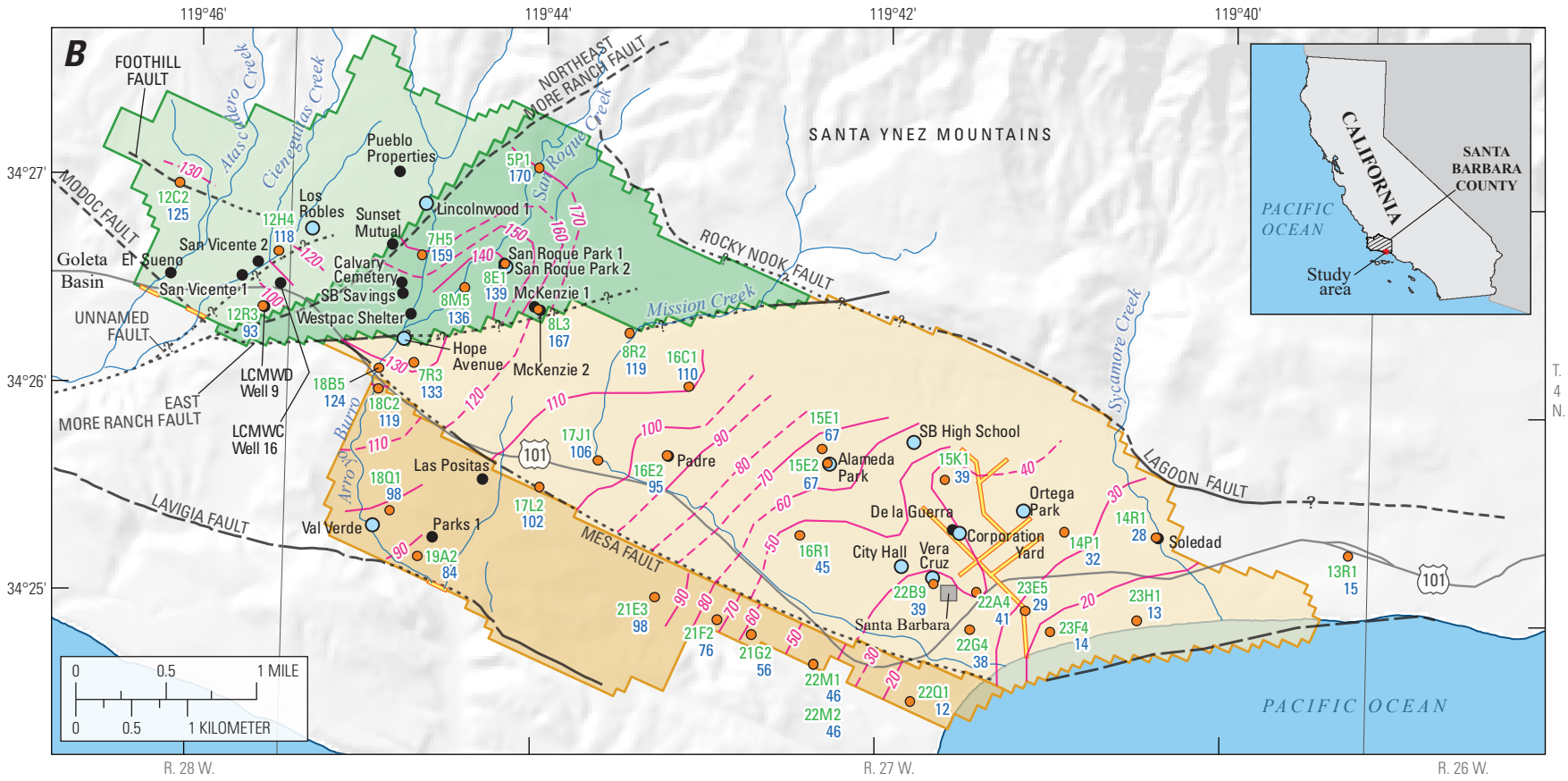

Base modified from U.S. Geological Survey and other Federal and State digital data, various scales; Transverse Mercator projection, zone 11N; North American Datum of 1983 (NAD 83)

Storage units from Muir, 1968; Freckleton and others, 1998; faults from Muir, 1968; Minor and others, 2009

EXPLANATION

- **Foothill groundwater basin**
- **Santa Barbara groundwater basin**

Subbasin

- West Foothill
- East Foothill
- Storage Unit I
- Storage Unit III

Faults

- Existence certain, location inferred
- Existence questionable, location inferred
- Existence certain, location concealed
- Existence questionable, location concealed
- Existence certain, location accurate
- Existence certain, location approximate

Water-table contour—Shows elevation of water table. Location is approximate; dashes where uncertain. Hachures indicate depression. Contour interval 10 feet.

Well and identifier—Top number is abbreviated state well number. Bottom number is elevation of water level, in feet above NAVD 88.

- **Production well and identifier**
- **Santa Barbara city production well and identifier**
- **City**
- **Highway**
- **Internal drain**

Figure 10. —Continued

Table 2. City of Santa Barbara production wells and state well identifiers, Santa Barbara, California.

Common name	State well number
Alameda Park	4N/27W-15E2
City Hall	4N/27W-22C1
Corporation Yard	4N/27W-15Q10
Hope Avenue	4N/27W-07Q5
Lincolnwood 1	4N/27W-07A5
Los Robles	4N/27W-07D1
Ortega Park	4N/27W-15J2
San Roque Park (2)	4N/27W-08E4
Santa Barbara High School	4N/27W-15G1
Val Verde	4N/27W-18Q2
Vera Cruz	4N/27W-22B6

Seawater Intrusion

Because of the Santa Barbara groundwater basin's proximity to the Pacific Ocean and historical pumpage, seawater intrusion has been an important water-quality issue. Fortunately, the risk of seawater intrusion is mitigated by the (previously noted) unnamed offshore fault that truncates the water-bearing deposits of Storage Unit I, which are adjacent to consolidated rocks on the seaward side of the fault. The offshore fault acts as a partial barrier to groundwater movement; however, saltwater at depth in Storage Unit I indicates that saline groundwater can cross the offshore fault (Martin and Berenbrock, 1986).

Several of the city of Santa Barbara's production wells are within a mile of the ocean, including Vera Cruz (22B6), City Hall (22C1), Corporation Yard (15Q10), and Ortega Park (15J2) wells. Between 1985 and 1991, increased pumping rates in these wells caused notable decreases in water levels in the lower producing zone, with heads as low as 90 ft bsl in the vicinity of these wells and more than 10 ft bsl at the coast (fig. 10*A*). Relatively high salinity levels were observed in wells perforated in the middle and lower producing zones along the coast, including wells 4N/27W-23F8, 4N/27W-23F4, 4N/27W-23E5, and 4N/27W-23E1 (figs. 12, 13). Higher salinity levels were not observed at monitoring wells 4N/27W-22G3, 4N/27W-22G4, 4N/27W-22A4 (fig. 13),

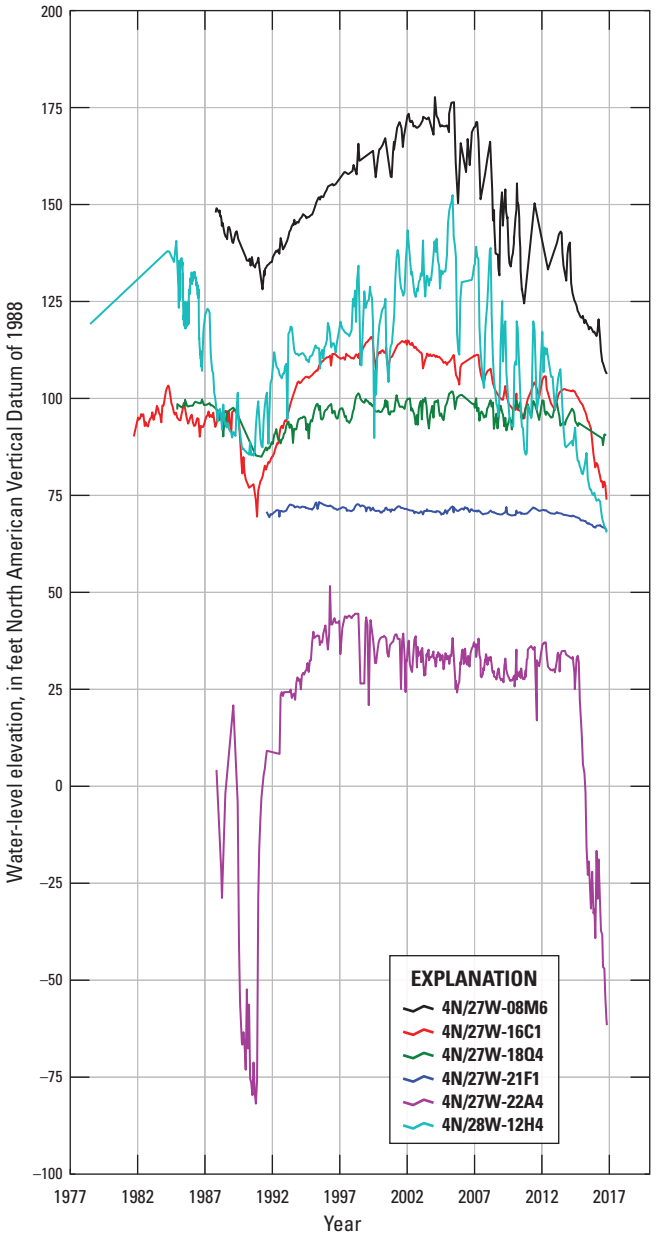

Figure 11. Water-level elevations from selected wells in Storage Unit I, Storage Unit III, and Foothill groundwater basin, Santa Barbara, California.

which are perforated in the middle and lower producing zone and are about 0.5 mi from the coast and 0.25 mi from the production wells (figs. 10*B*, 11). Although elevated chloride concentrations up to 1,600 milligrams per liter (mg/L) were recorded in some of the deeper wells (for example, well 4N/27W-22B8), the elevated chloride concentrations were most likely not from seawater intrusion. The presence of barium and boron in concentrations much greater than those in ocean water indicates that seawater intrusion was not the source of the elevated chloride concentrations in these deeper wells (Martin, 1984).

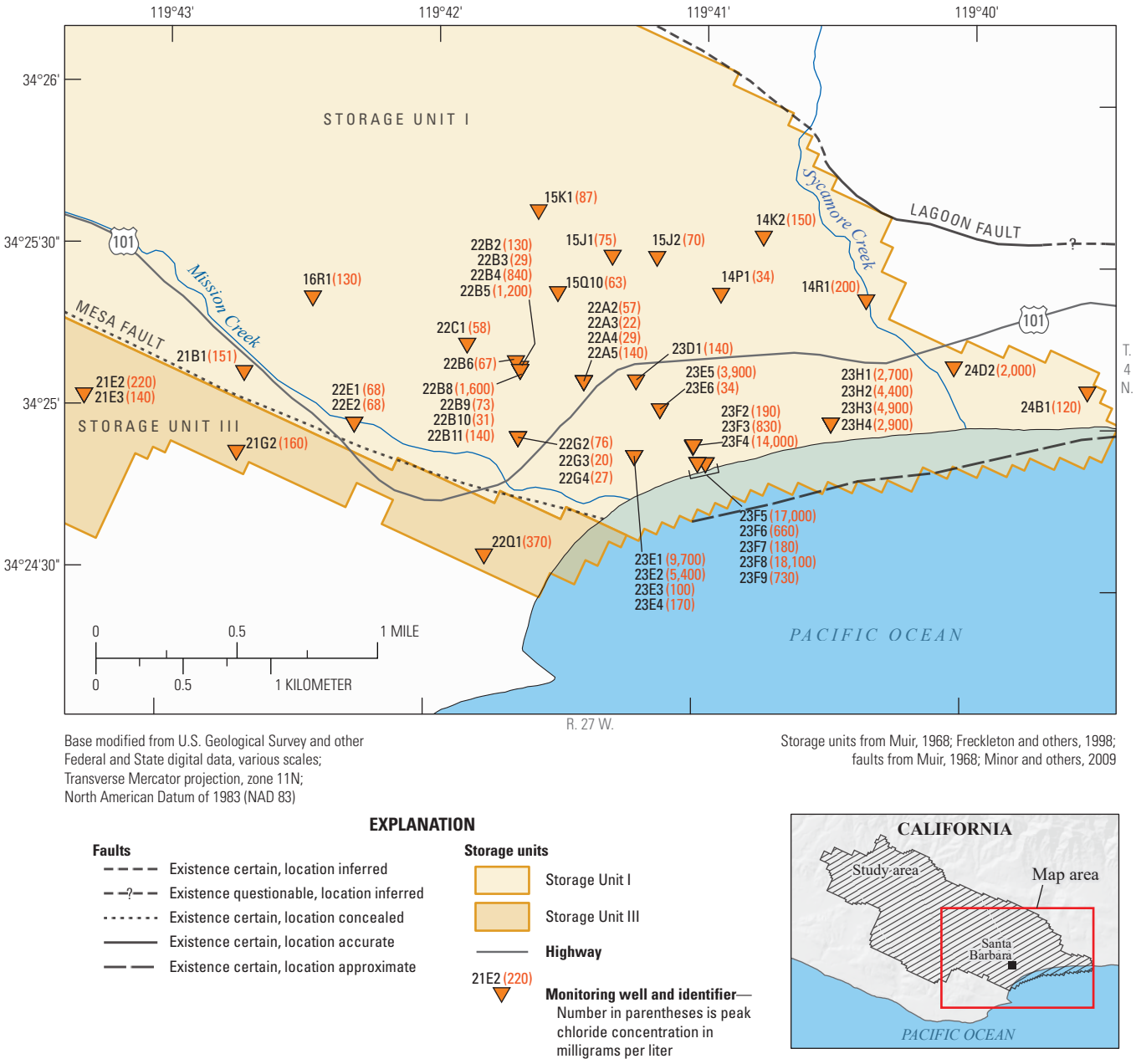

Base modified from U.S. Geological Survey and other Federal and State digital data, various scales; Transverse Mercator projection, zone 11N; North American Datum of 1983 (NAD 83)

Storage units from Muir, 1968; Freckleton and others, 1998; faults from Muir, 1968; Minor and others, 2009

EXPLANATION

Faults

- Existence certain, location inferred
- Existence questionable, location inferred
- Existence certain, location concealed
- Existence certain, location accurate
- Existence certain, location approximate

Storage units

- Storage Unit I
- Storage Unit III

Highway

21E2 (220) **Monitoring well and identifier**—Number in parentheses is peak chloride concentration in milligrams per liter

Figure 12. Locations of coastal monitoring wells with associated peak, measured chloride concentrations, Santa Barbara groundwater basin, Santa Barbara, California.

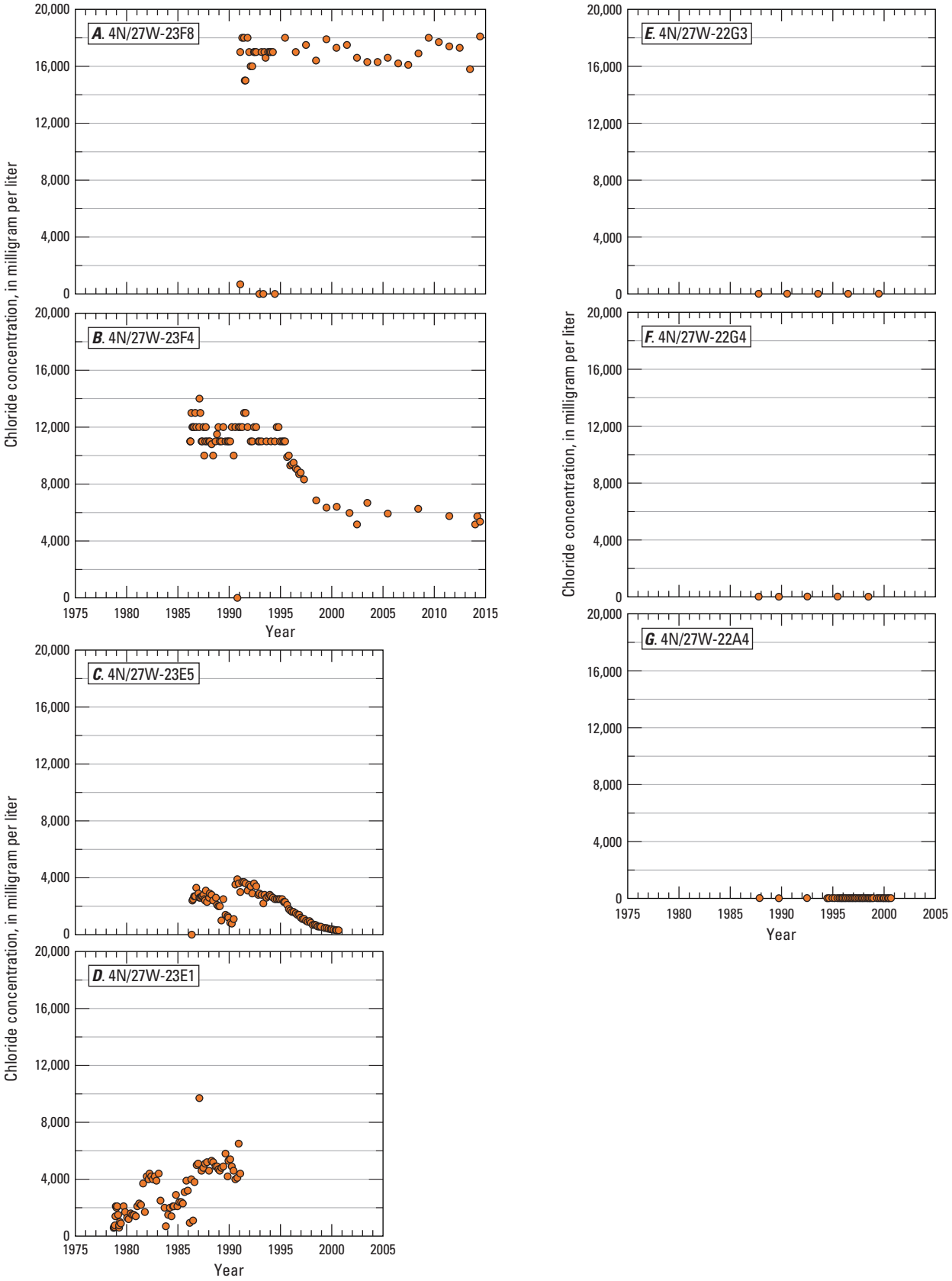

Figure 13. Time-varying chloride concentrations from coastal wells, Santa Barbara groundwater basin, Santa Barbara, California: *A*, 4N/27W-23F8; *B*, 4N/27W-23F4; *C*, 4N/27W-23E5; *D*, 4N/27W-23E1; *E*, 4N/27W-22G3; *F*, 4N/27W-22G4; and *G*, 4N/27W-22A4.

References Cited

City of Santa Barbara, 2015, Water sources: Santa Barbara, Calif., Public Works Department, accessed April 2015 at http://www.santabarbaraca.gov/gov/depts/pw/resources/system/sources/default.asp.

County of Santa Barbara, 2014, Rainfall-daily XLS data: Santa Barbara, Calif., Public Works, Water Resources Division, accessed November 2014 at http://www.countyofsb.org/pwd/pwwater.aspx?id=30042.

Eckenfelder, W.W., Jr., 1980, Principles of water quality management: Boston, CBI Publishing Company, Inc., 717 p.

Freckleton, J.R., 1989, Geohydrology of the Foothill ground-water basin near Santa Barbara, California: U.S. Geological Survey Water-Resources Investigations Report 89–4017, 46 p., https://pubs.er.usgs.gov/publication/wri894017.

Freckleton, J.R., Martin, P., and Nishikawa, T., 1998, Geohydrology of Storage Unit III and a combined flow model of the Santa Barbara and Foothill ground-water basins, Santa Barbara County, California: U.S. Geological Survey Water-Resources Investigations Report 97–4121, 80 p., http://pubs.er.usgs.gov/publication/wri974121.

Harbaugh, A.W., Banta, E.R., Hill, M.C., and McDonald, M.G., 2000, MODFLOW-2000, the U.S. Geological Survey modular ground-water model—User guide to modularization concepts and the ground-water flow process: U.S. Geological Survey Open-File Report 2000–92, 121 p., https://pubs.er.usgs.gov/publication/ofr200092.

Hutchinson, C.B., 1979, Ground-water monitoring at Santa Barbara, California—Phase 1, Coastal monitor-well installation and initial measurements: U.S. Geological Survey Open-File Report 79–923, 36 p., https://pubs.er.usgs.gov/publication/ofr79923.

Martin, P., 1984, Ground-water monitoring at Santa Barbara, California; Phase 2—Effects of pumping on water levels and on water quality in the Santa Barbara ground-water basin: U.S. Geological Survey Water Supply Paper 2197, 31 p., https://pubs.er.usgs.gov/publication/wsp2197.

Martin, P., and Berenbrock, C., 1986, Ground-water monitoring at Santa Barbara, California; Phase 3—Development of a three-dimensional digital ground-water flow model for Storage Unit I of the Santa Barbara ground-water basin: U.S. Geological Survey Water-Resources Investigations Report 86–4103, 58 p., https://pubs.er.usgs.gov/publication/wri864103.

McFadden, M.C., Polinoski, K.G., and Martin, P.M., 1991, Measurement of streamflow gains and losses on Mission Creek at Santa Barbara, California; July and September 1987: U.S. Geological Survey Water-Resources Investigations Report 91–4002, 15 p., https://pubs.er.usgs.gov/publication/wri914002.

Minor, S.A., Kellogg, K.S., Stanley, R.G., Gurrola, L.D., Keller, E.A., and Brandt, T.R., 2009, Geologic map of the Santa Barbara coastal plain area, Santa Barbara County, California: U.S. Geological Survey Scientific Investigations Map 3001, scale 1:25,000, 1 sheet, pamphlet, 38 p., https://pubs.er.usgs.gov/publication/sim3001.

Muir, K.S., 1968, Ground-water reconnaissance of the Santa Barbara-Montecito area, Santa Barbara County, California: U.S. Geological Survey Water Supply Paper 1859–A, 28 p., https://pubs.er.usgs.gov/publication/wsp1859A.

National Weather Service, 2016, Santa Barbara, California (047902) period of record monthly climate summary [1893–2016]: Western Regional Climate Center, accessed November 14, 2016, at http://www.wrcc.dri.edu/cgi-bin/cliMAIN.pl?ca7902.

Nishikawa, T., and Martin, P., 1998, Postaudit of optimal conjunctive use policies, *in* Loucks, E.D., ed., Water Resources in the Urban Environment, Chicago, June 7–10, 1998, Proceedings: Reston, Va., American Society of Civil Engineers, p. 591–596.

U.S. Census Bureau, 2017, Santa Barbara (city), California, QuickFacts: U.S. Census Bureau, accessed May 2017 at https://www.census.gov/quickfacts/table/PST045215/0669070.

U.S. Geological Survey, 2018, Sustainable groundwater management: U.S. Geological Survey, accessed March 2018 at https://ca.water.usgs.gov/sustainable-groundwater-management/.

Chapter B: Overview of Hydrogeologic Framework Model

By Geoffrey Cromwell and Scott E. Boyce

Introduction

This chapter describes the compilation of measured data and the construction of a hydrogeologic-framework model (HFM) of the Santa Barbara and Foothill groundwater basins. The development of the HFM required the compilation and reconciliation of geologic and geophysical data from existing maps, reports, and databases, which were then integrated along with data from recently drilled wells. The goal in developing an HFM is to define the three-dimensional (3D) geometry of the major geologic structures and stratigraphy. This HFM also expresses the variation of properties in each stratigraphic unit in the form of the percentage of coarse-grained deposits (texture). The HFM was developed using EarthVision, a three-dimensional geologic-modeling software package (Dynamic Graphics, Inc., 2015).

Hydrogeology and Structure of the Santa Barbara Study Area

The HFM domain is composed of two separate groundwater basins, Santa Barbara (Hutchinson, 1979) and Foothill (Freckleton, 1989) groundwater basins, which are separated by the East More Ranch fault (fig. 1). Each of the groundwater basins is further subdivided into what can be called subbasins or storage units. The Santa Barbara groundwater basin is subdivided into Storage Unit I and Storage Unit III by the Mesa fault (Muir, 1968), and the Foothill groundwater basin is subdivided into the East and West Foothill subbasins by the Northeast More Ranch fault (see chapter A).

As described in chapter A, the two groundwater basins are composed of stratified unconsolidated deposits. These deposits have been classified in five aquifer zones that represent the overall hydraulic characteristics and depositional history of the unconsolidated material (see fig. 2; table 1). The five aquifer zones are the shallow zone, upper producing zone, middle zone, lower producing zone, and deep zone. Consolidated sedimentary rocks of Tertiary age are beneath the deep zone and also compose parts of the surrounding hills (Martin and Berenbrock, 1986). These consolidated rocks, predominantly marine in origin, are relatively impermeable, except for some sandstone layers and in fractured areas. Because of their low permeability, these consolidated units are considered the basement, or bedrock, of the HFM and form the lower boundary of the groundwater basins.

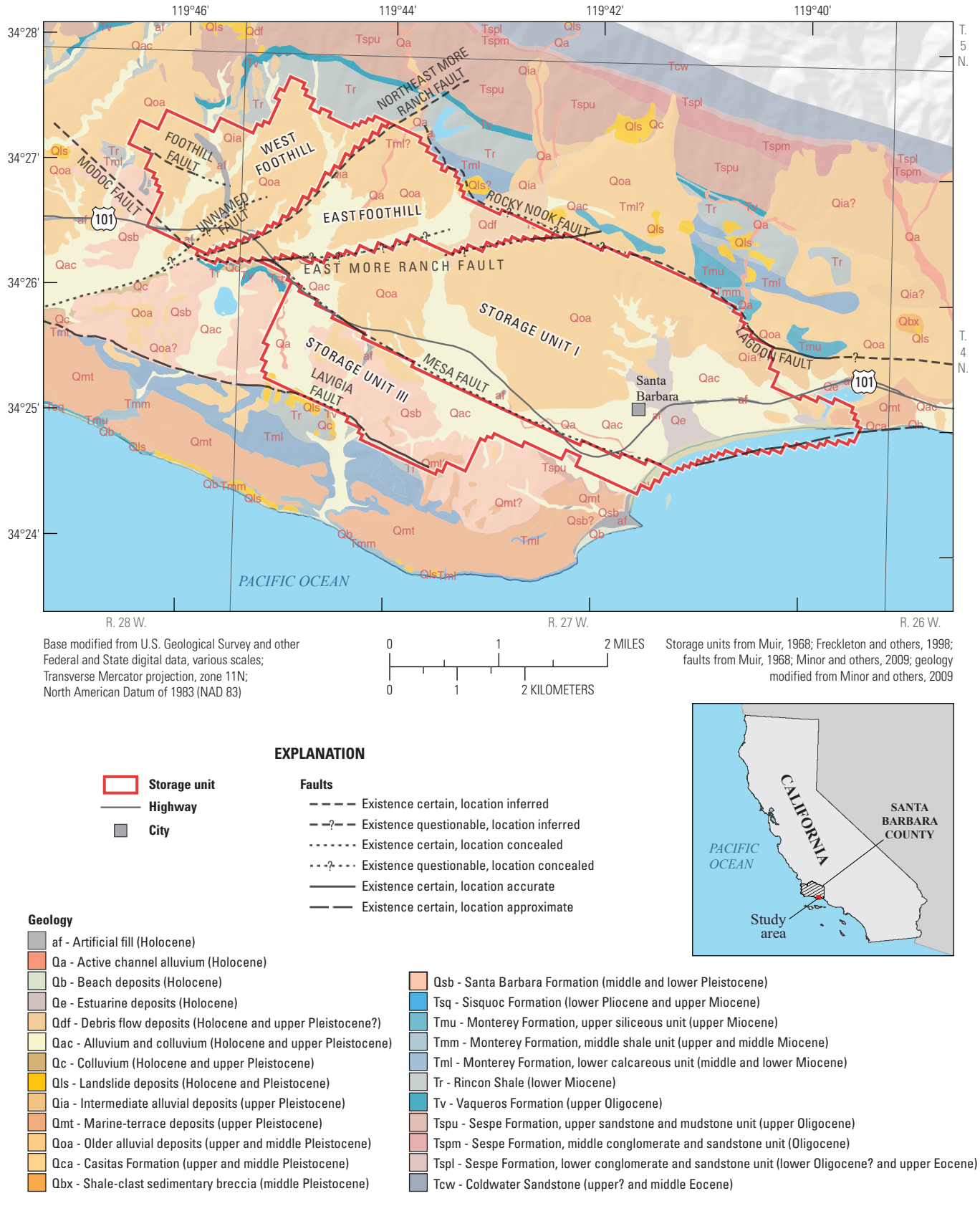

Figure 1. Hydrogeologic framework model domain, subbasins and storage units, and major faults, Santa Barbara and Foothill groundwater basins, Santa Barbara, California.

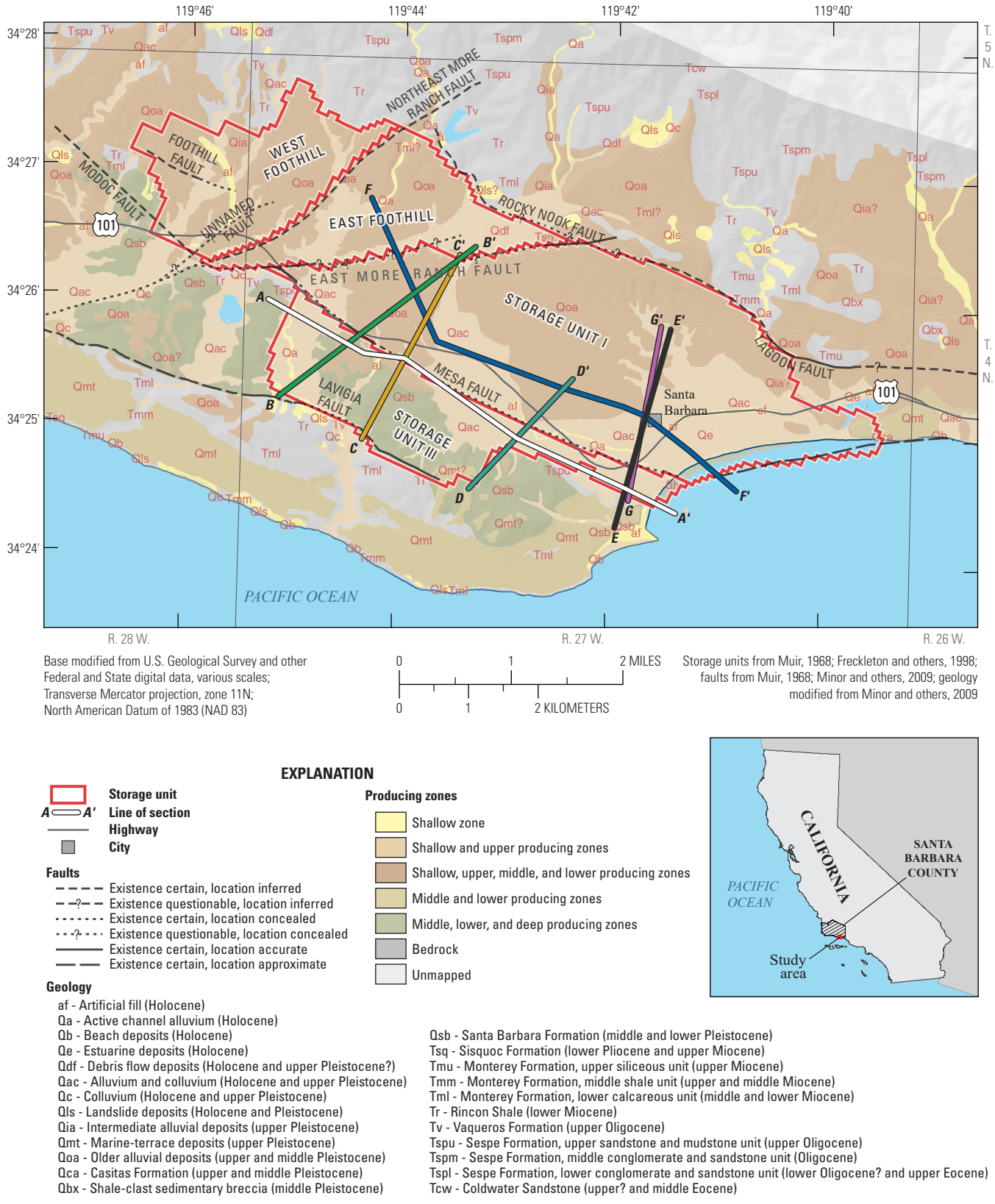

Figure 2. Aquifer-zone groupings organized by mapped geologic units, Santa Barbara and Foothill groundwater basins, California; cross-section lines show locations of previously published cross sections (Freckleton and others, 1998; Martin and Berenbrock, 1986) used in the hydrogeologic framework model.

Table 1. Aquifer-zone groupings listed by mapped geologic unit and age, Santa Barbara and Foothill groundwater basins, California.

[—, not applicable]

Aquifer zone	Geologic unit	Age
Shallow	af, Qa, Qls, Qls?	Holocene
Shallow and upper	Qac, Qb, Qc, Qdf, Qe	Holocene and upper Pleistocene
Shallow, upper, middle, and lower	Qca, Qia, Qia?, Qoa	Upper and middle Pleistocene
Middle and lower	Qmt, Qmt?	Upper Pleistocene
Middle, lower, and deep	Qsb	Middle and lower Pleistocene
Bedrock	Tsq, Tml, Tmm, Tmu, Tr, Tv, Tspu, Tspm, Tspl, Tcw	Miocene, Oligocene, and Eocene

Construction of the Hydrogeologic Framework Model

The HFM has two main parts: (1) a geometric framework model showing the stratigraphic relationships of the aquifer zones; (2) a textural model detailing physical properties of the aquifer zones within the geometric framework.

Geometric Framework

The geometric framework model quantifies the surficial and subsurface extent of the four subbasins or storage units as defined by major faults, the distribution of consolidated rocks, and the extent and thickness of the five aquifer zones. Subbasin geometry was constructed by compiling and digitizing existing geologic maps, cross sections, textural descriptions from drillers' lithology logs, and geophysical logs. These data sets were interpolated to define the extent and geometry of the subbasins and the thickness of the aquifer zones within them.

Input Data

Previous studies have presented geologic maps and cross sections of the Santa Barbara region. The geologic map used for this study is of the Santa Barbara coastal plain area by Minor and others (2009; fig. 1). This map served as a reference to the location and dip of the major faults and to the surficial extent of the consolidated, Tertiary sedimentary rocks that define much of the HFM boundary. The subsurface extent of the aquifer zones was derived from previously published geologic cross sections and drillers' lithology logs and from geophysical electricity resistivity logs (e-logs) compiled as part of this study. Two sets of previously published geologic cross sections were digitized from Freckleton and others (1998; fig. 2, sections A–A' through E–E') and Martin and Berenbrock (1986; fig. 2, sections F–F' and G–G'). For a more detailed description of these sections, see Freckleton and others (1998) and Martin and Berenbrock (1986).

Drillers' lithology logs and e-logs were compiled from the California Department of Water Resources. Drillers' logs from a total of 159 boreholes in the study area (fig. 3) were obtained and entered in a new digital database containing well-construction information and subsurface-lithology characteristics (following the database design of Burow and others, 2004). Of those 159 boreholes, 40 had geophysical e-logs included with the drillers' lithology log. The deepest boreholes in Storage Unit I, East Foothill, Storage Unit III, and West Foothill had depths of 840, 660, 340, and 490 feet (ft), respectively (table 2).

Structures and Aquifer Zones

The HFM area was formed from a set of independent blocks defined by faults and, therefore, fault blocks that represent geologic materials. In this case, the geologic material consists of Tertiary consolidated rocks that form the bedrock and unconsolidated sedimentary deposits that are divided into five aquifer zones and are stacked chronologically to fill the volume of the HFM.

Fault Blocks

Each of the four subbasins are delineated by faults, some of which are estimated to have substantial vertical offset (Martin and Berenbrock, 1986; Freckleton and others, 1998). To preserve the measured offset across these faults in the HFM, each subbasin was defined as an independent fault block. Using EarthVision software, the elevation of the top of bedrock and each aquifer zone in a particular fault block were calculated independently and then combined to form a single model. This method prevents any aquifer-zone horizon data from one subbasin affecting the horizon data in another subbasin and, thus, preserves the expected geologic offsets between subbasins.

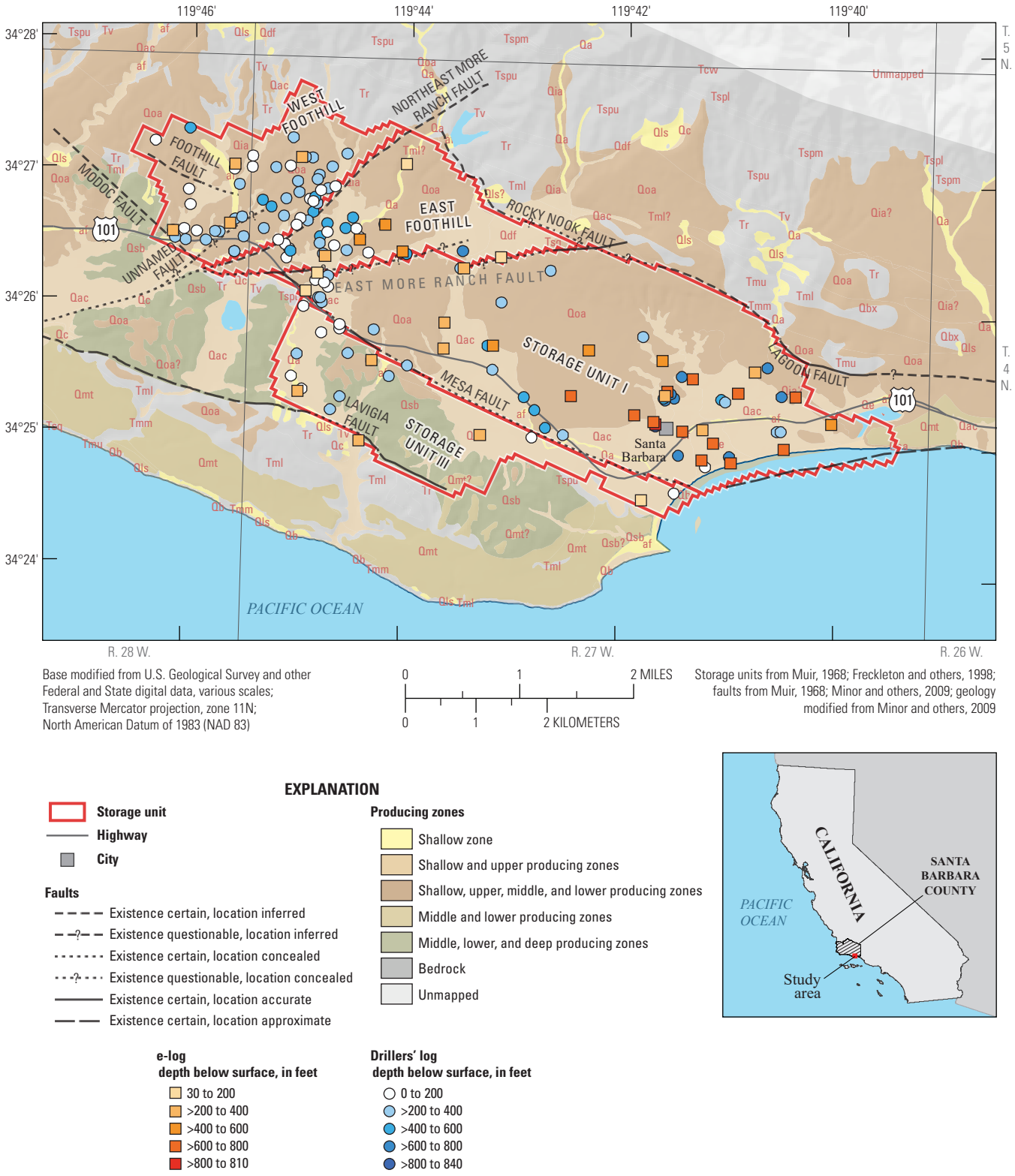

Figure 3. Aquifer-zone groupings with drillers' well logs and geophysical e-logs used in the hydrogeologic framework model for Storage Unit I, Storage Unit III, and the Foothill subbasins, Santa Barbara and Foothill groundwater basins, California.

Table 2. Summary statistics of borehole depths by subbasin, Santa Barbara and Foothill groundwater basins, Santa Barbara, California.

Groundwater subbasin	Depth statistic property, in feet					Count
	Minimum	Maximum	Median	Mean	Standard deviation	
Storage Unit I	5	840	420	452.9	213.7	60
East Foothill	90	660	280	323.8	182.7	29
Storage Unit III	5	340	210	188.6	93.12	18
West Foothill	90	490	245	254.4	99.0	52

Aquifer-Zone and Bedrock-Horizon Modeling

The horizons for the five aquifer zones and the bedrock unit were constructed by interpolating and extrapolating a two-dimensional surface in EarthVision from subsurface data points. EarthVision uses a biharmonic cubic-spline algorithm that uses a minimum-tension (minimum curvature) gridding technique (Dynamic Graphics, Inc., 2015). Grid spacing for bedrock and the aquifer zones is about 328 ft (100 meters) in the X and Y horizontal directions. Artificial control points were added in areas with limited subsurface data (that is, from drillers' logs or geologic cross sections) to improve constraint of horizon interpolations. When input data are sparse, the EarthVision gridding algorithm may extrapolate unreasonably high or low values, and in areas where data show abrupt changes in elevations, the horizon grid interpolation could be unrealistic; the addition of artificial control points helps minimize these effects. Control points also are used in the HFM to force horizon grids to pinch out where a unit is no longer present at depth. EarthVision stacks the aquifer-zone horizon grids in stratigraphic order on top of the bedrock horizon. In this manner, the total thickness of each zone is defined as the difference between the zone horizon and the upper surface of the zone below. Aquifer-zone and bedrock horizons and subsurface data used for horizon-grid interpolation are shown in figure 4.

Recall, there are five aquifer zones: the shallow zone, upper producing zone, middle zone, lower producing zone, and deep zone (see table 1 for a list of the geologic units in each zone). The shallow zone is composed of younger and older alluvium; the upper producing zone is only older alluvium. The middle, lower producing, and deep zones are composed of the Santa Barbara Formation and some older alluvial units. For a detailed discussion about the geology of the five zones, see Martin and Berenbrock (1986) and Freckleton and others (1998). As described in chapter A, near the ocean boundary, there is a small section of relatively high permeability rocks in the middle zone, referred to as the middle producing zone. Although a distinct hydrologic zone, the middle producing zone was not modeled independently, but was included in the HFM as part of the middle zone.

The five aquifer zones were identified by analyzing geophysical e-logs, surficial geologic maps (fig. 1), and published geologic cross sections. The upper contact of each aquifer zone was identified and digitized from geologic cross sections published by Martin and Berenbock (1986) and Freckleton and others (1998). Similarly, geophysical e-logs were digitized and examined, and the upper contact of each zone was identified. The geologic map was used to identify where the aquifer zones outcrop at land surface. The interpolated aquifer-zone horizons and subsurface data points are shown in figure 4*A–E*.

In this study, bedrock is defined as the relatively less-permeable consolidated Tertiary rocks of Miocene age and older. In general, the upper contact of the bedrock unit was identified by the presence of shale (as identified in previous reports or interpreted in drillers' lithology logs and geophysical e-logs) or fine-grained lithologic layers of substantial thickness. Surficial and subsurface bedrock elevations were derived from drillers' lithology logs, geophysical e-logs, surficial geologic maps (fig. 1), and geologic cross sections from previous reports (Martin and Berenbock, 1986; Freckleton and others, 1998). Where bedrock outcrops at land surface, the total aquifer thickness was assumed to be zero. The interpolated bedrock horizon and subsurface data points are shown in figure 4*F*.

Geometric Framework Model Description

A fence diagram of the geometric framework model is shown in figure 5*A*. The cross sections in the fence diagram are the same as those shown in figure 2 (with the exception of G–G'), and with the addition of one cross section (H–H') cutting southwest–northeast through the Foothill groundwater basin and a second cross section (I–I') running northwest–southeast through the entire study area.

Total aquifer thickness, as defined by land surface and top of the bedrock unit, varies considerably across the study area. The thickest part of the aquifer is at the coast, in the southeastern-most part of Storage Unit I, where the total thickness of unconsolidated sediment is about 1,100 ft. Aquifer thickness gradually decreases from southeast to northwest in Storage Unit I to a minimum of about 200 ft along the boundary between the Storage Unit I and the Foothill groundwater basin. In Storage Unit III, the aquifer ranges in thickness from about 200 to 450 ft, except at the southeastern end, where the bedrock unit rises substantially, and only a thin veneer of shallow-zone sediments is present. Total aquifer thickness is relatively constant in the West Foothill and East Foothill subbasins, at about 330 ft and 650 ft, respectively. In the northern section of both subbasins, bedrock rises rapidly in elevation toward land surface, and the thickness of unconsolidated sediments decreases in similar fashion.

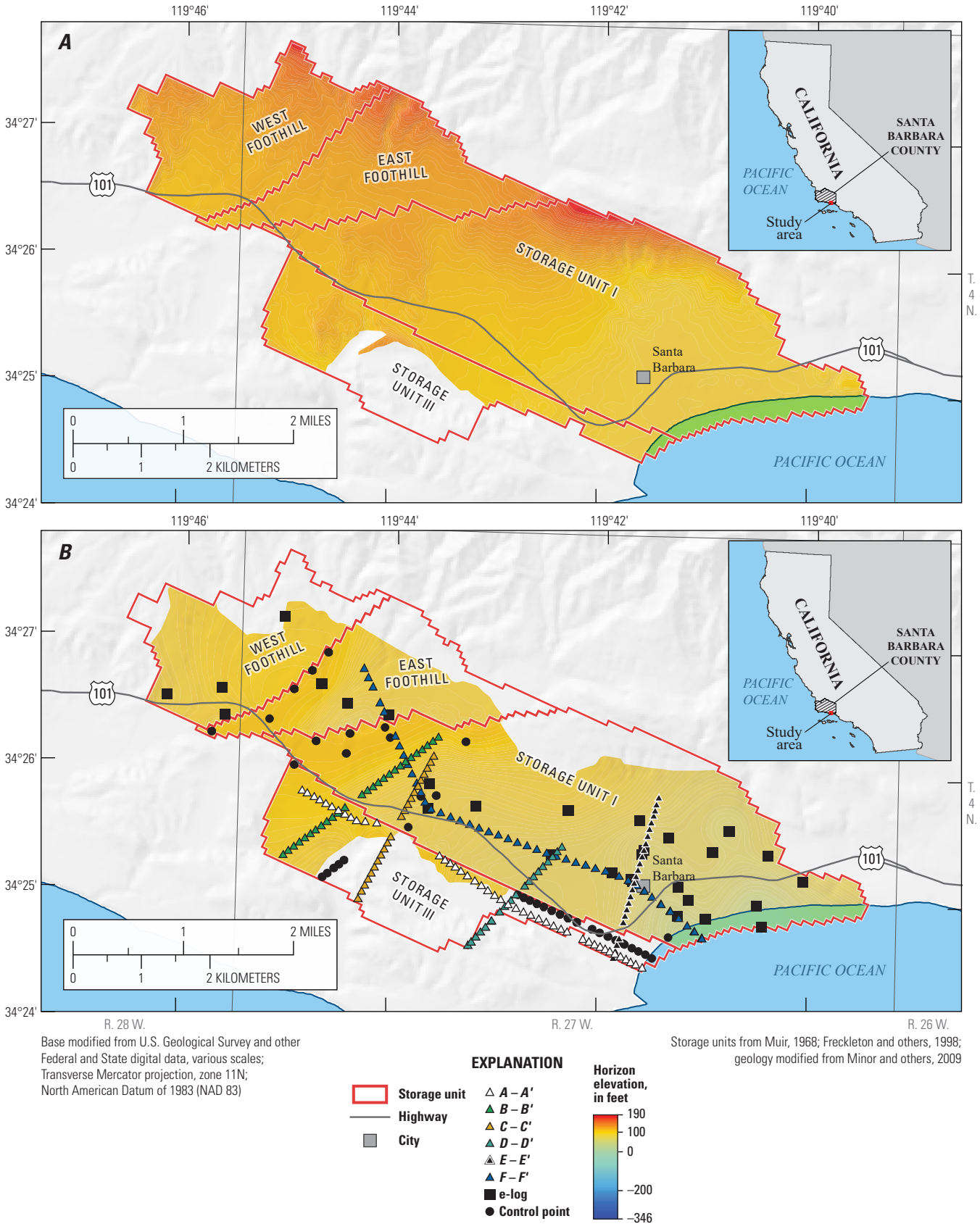

Base modified from U.S. Geological Survey and other Federal and State digital data, various scales; Transverse Mercator projection, zone 11N; North American Datum of 1983 (NAD 83)

Storage units from Muir, 1968; Freckleton and others, 1998; geology modified from Minor and others, 2009

Figure 4. Interpolated elevations of hydrogeologic framework model horizons with subsurface data points, Santa Barbara and Foothill groundwater basins, Santa Barbara, California: *A*, shallow zone; *B*, upper producing zone; *C*, middle zone; *D*, lower producing zone; *E*, deep zone; and *F*, bedrock. Horizon elevation is feet above NAVD 88.

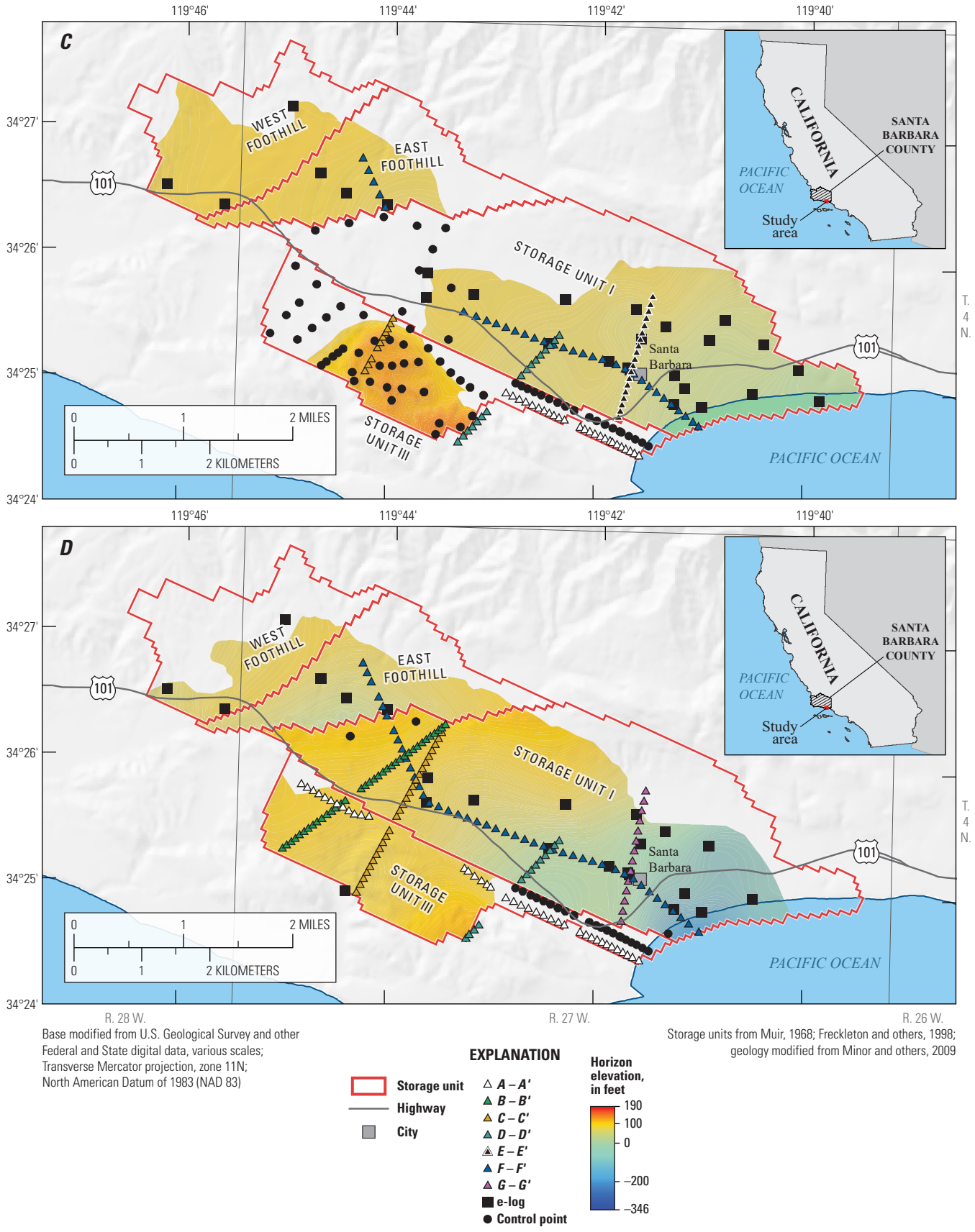

Base modified from U.S. Geological Survey and other Federal and State digital data, various scales; Transverse Mercator projection, zone 11N; North American Datum of 1983 (NAD 83)

Storage units from Muir, 1968; Freckleton and others, 1998; geology modified from Minor and others, 2009

Figure 4. —Continued

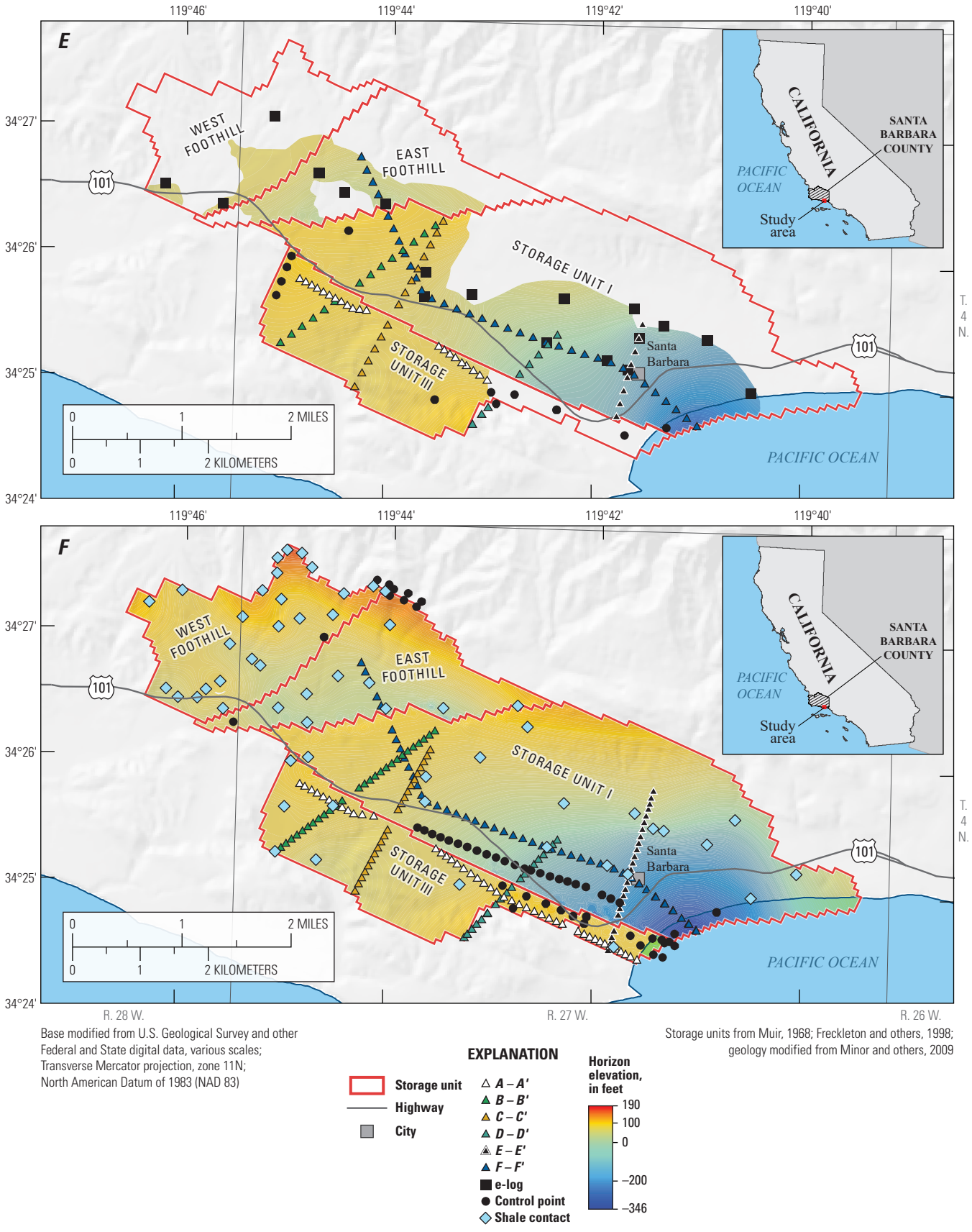

Base modified from U.S. Geological Survey and other Federal and State digital data, various scales; Transverse Mercator projection, zone 11N; North American Datum of 1983 (NAD 83)

Storage units from Muir, 1968; Freckleton and others, 1998; geology modified from Minor and others, 2009

Figure 4. —Continued

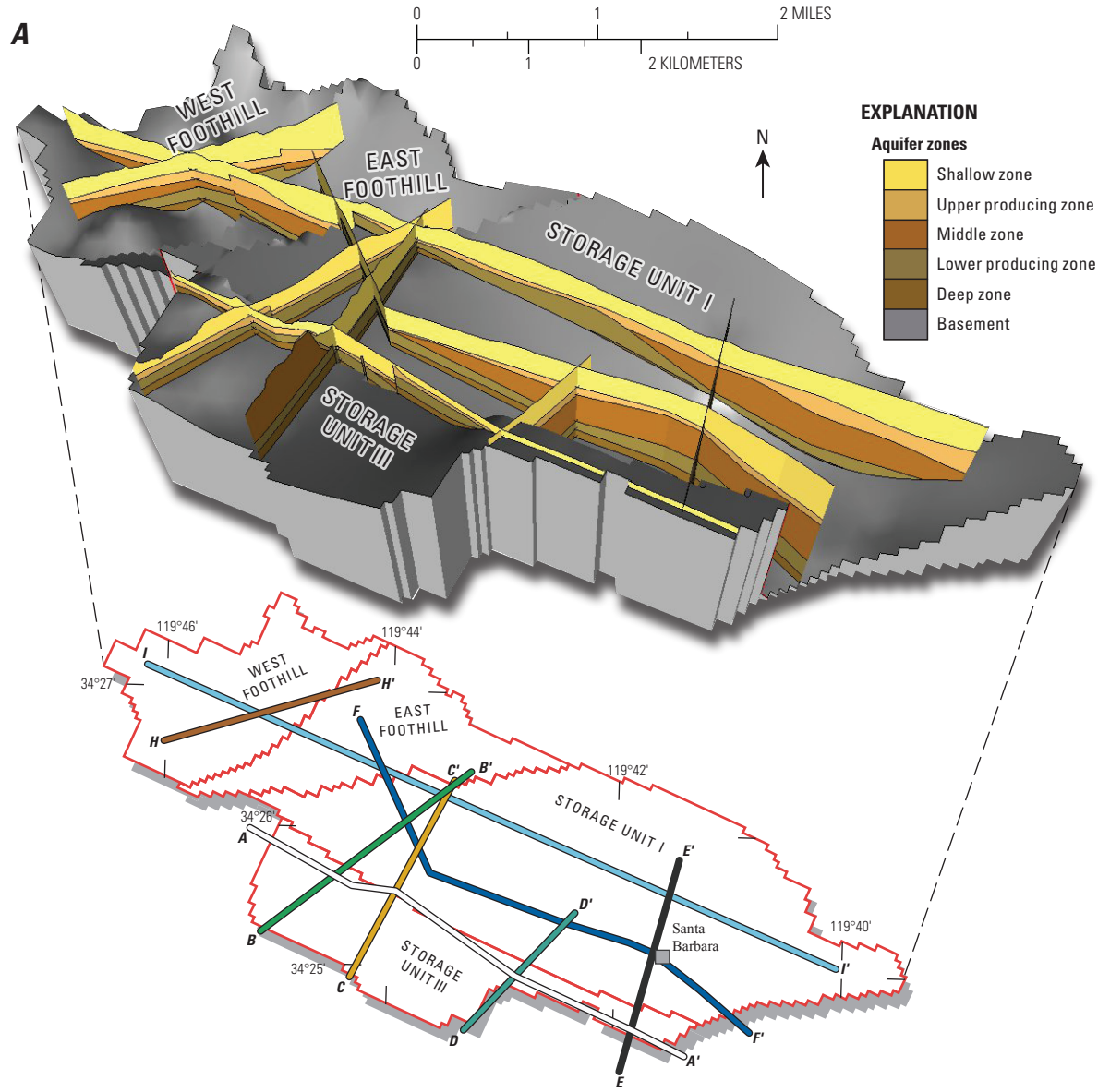

Figure 5. Hydrogeologic framework model results by fence diagram, Santa Barbara and Foothill groundwater basins, Santa Barbara, California: *A*, geometric framework model showing subsurface extent of the five aquifer zones, and *B*, texture model showing the distribution of coarse- and fine-grained material in each aquifer zone, with percent-coarse intervals for drillers' well logs and geophysical e-logs (locations of all logs are also shown on the inset diagram). Fence diagrams shown with five times vertical exaggeration.

In general, all five aquifer zones are present across the study area, with the exception of (1) the middle zone in Storage Units I and III and (2) the upper producing zone and shallow zone in the southeastern section of Storage Unit III. In Storage Unit I, the middle zone pinches out approximately 2–3 miles from the coast, and is absent further inland and in the northwestern part of Storage Unit III. In the southeastern part of Storage Unit III, the Santa Barbara Formation outcrops at land surface; therefore, the younger upper producing zone and shallow zone are absent.

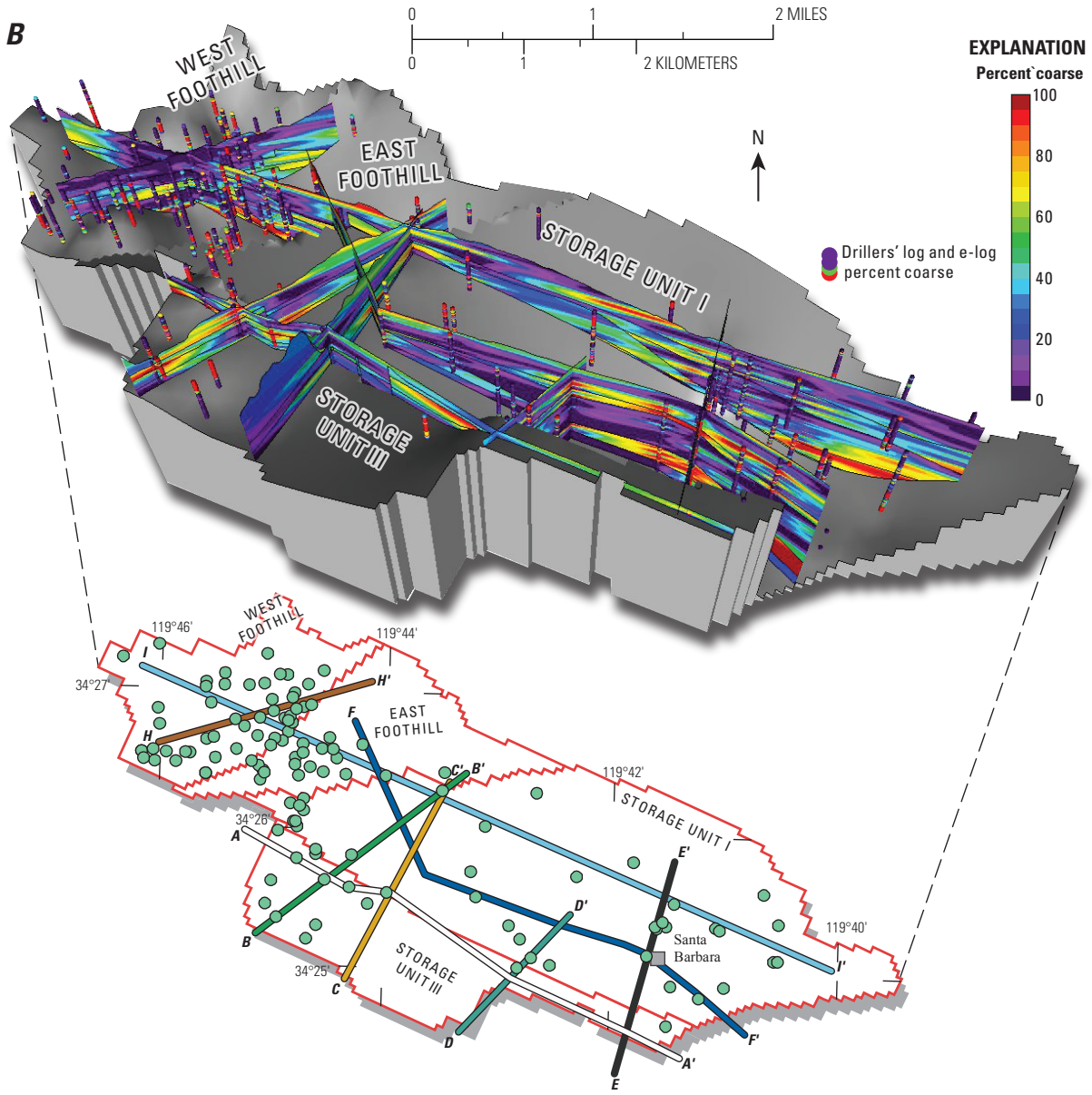

Figure 5. —Continued

Textural Model

The textural model quantifies the lateral and vertical distribution of aquifer materials that affect the rate, and possibly direction, of groundwater flow through the aquifer system. Variability in sediment texture (lithology type and grain size), as identified in drillers' lithology logs and geophysical e-logs, is ultimately a function of the depositional environment and geologic history of the area. An analysis of the spatial variability of lithology and grain size was done for the unconsolidated deposits that compose the five aquifer zones. The interpreted distribution of these textural properties can be used to define the distribution of hydrologic characteristics (such as horizontal and vertical hydraulic conductivity and groundwater storage), which can be used in a numerical groundwater-flow and solute-transport model.

Textural Classification of Borehole Data

In order to describe the spatial variability in textural properties, the drillers' lithologic descriptions and geophysical e-logs were evaluated and classified by texture. Texture is defined as the percentage of coarse-grained sediment present in a specified subsurface-depth interval (Hanson and others, 1990; Laudon and Belitz, 1991; Faunt and others, 2009). Drillers' log depth-interval entries were categorized into 15 main lithology types and assigned one of 8 lithology modifiers (if applicable), resulting in a total of 62 unique lithology classes (table 3). Each of these unique lithology classes was further codified as either "coarse" or "fine" (representing sediment grain size) on the basis of the main lithology type and modifier. In this study, coarse-grained sediment was defined as that consisting principally of sand, gravel, boulders, or cobbles. Fine-grained sediment was defined as that consisting principally of clay, loam, mud, silt, or conglomerate. If either the lithology or its modifier was considered fine-grained, then the overall composition was considered to be fine-grained (for example, silty-sand and sandy-silt were considered fine-grained; table 3).

Geophysical e-logs measure the resistivity of rock and sediment adjacent to a borehole. Typically, greater resistance represents more permeable materials, such as sand; lower resistance indicates clays. However, if seawater is present or the sediments have a high salt concentration the resistance is substantially less, irrespective of the lithology. Combining resistivity values from e-log measurements with descriptions from drillers' logs often provides a more detailed description of borehole lithology. Using the associated drillers' log as a guide, a vertical line was subjectively fitted with the resistivity to the e-log, such that it delineated coarse- (right of the line) and fine- (left of the line) grained materials by depth. An example of this process is shown in figure 6, where a red line is fit across the black resistivity curve until the coarse (shaded) and fine (white) depth intervals generally correspond to the observations in the associated drillers' log.

Table 3. Unique lithology descriptions and modifiers with associated binary coarse or fine classification as identified in drillers' lithology logs, Santa Barbara and Foothill groundwater basins, Santa Barbara, California.

[Descriptions with no associated modifier are indicated by dashes (—) in the appropriate modifier cell.]

Modifier	Lithology	Texture
—	Boulders	Coarse
Clayey	Boulders	Fine
Sandy	Boulders	Coarse
Silty	Boulders	Fine
—	Clay	Fine
Cobbley	Clay	Fine
Gravelly	Clay	Fine
Pebbley	Clay	Fine
Sandy	Clay	Fine
Silty	Clay	Fine
Sticky	Clay	Fine
—	Cobbles	Coarse
Clayey	Cobbles	Fine
Gravelly	Cobbles	Coarse
Sandy	Cobbles	Coarse
—	Conglomerate	Fine
—	Gravel	Coarse
Clayey	Gravel	Fine
Cobbley	Gravel	Coarse
Pebbley	Gravel	Coarse
Sandy	Gravel	Coarse
Silty	Gravel	Fine
—	Hard pan	Fine
Sandy	Hard pan	Fine
Sandy	Loam	Fine
—	Mud	Fine
Sandy	Mud	Fine
Silty	Mud	Fine
Sticky	Mud	Fine
—	Rock	Fine
—	Sand	Coarse
Clayey	Sand	Fine
Cobbley	Sand	Coarse
Gravelly	Sand	Coarse
Muddy	Sand	Fine
Pebbley	Sand	Coarse
Silty	Sand	Fine
Sticky	Sand	Fine
—	Sandstone	Coarse
Clayey	Sandstone	Fine
Cobbley	Sandstone	Coarse
Gravelly	Sandstone	Coarse
Pebbley	Sandstone	Coarse
Sandy	Sandstone	Coarse
—	Shale	Fine
Clayey	Shale	Fine
Cobbley	Shale	Fine
Gravelly	Shale	Fine
Sandy	Shale	Fine
Silty	Shale	Fine
—	Silt	Fine
Clayey	Silt	Fine
Gravelly	Silt	Fine
Sandy	Silt	Fine
Sticky	Silt	Fine
—	Siltstone	Fine
Clayey	Siltstone	Fine
Sandy	Siltstone	Fine
—	Top soil	Coarse
Clayey	Top soil	Fine
Cobbley	Top soil	Coarse
Sandy	Top soil	Coarse

A

WELL LOG

Total depth: 630 feet			**Depth of completed well**: 630 feet
0	–	50	Fine sand
50	–	140	Clay
140	–	148	Sand
148	–	164	Swelling clay
164	–	166	Gravel
166	–	214	Fine sand
214	–	244	Swelling clay
244	–	248	Rock
248	–	294	Swelling clay
294	–	316	Fine sand
316	–	366	Swelling clay
366	–	372	Brown rock
372	–	406	Swelling clay
406	–	408	Rock
408	–	430	Clay
430	–	440	Gravel (waterless)
440	–	510	Clay
510	–	518	Large gravel
518	–	532	Clay
532	–	614	Gravel (rock)
614	–	625	Clay
625	–	630	Gravel

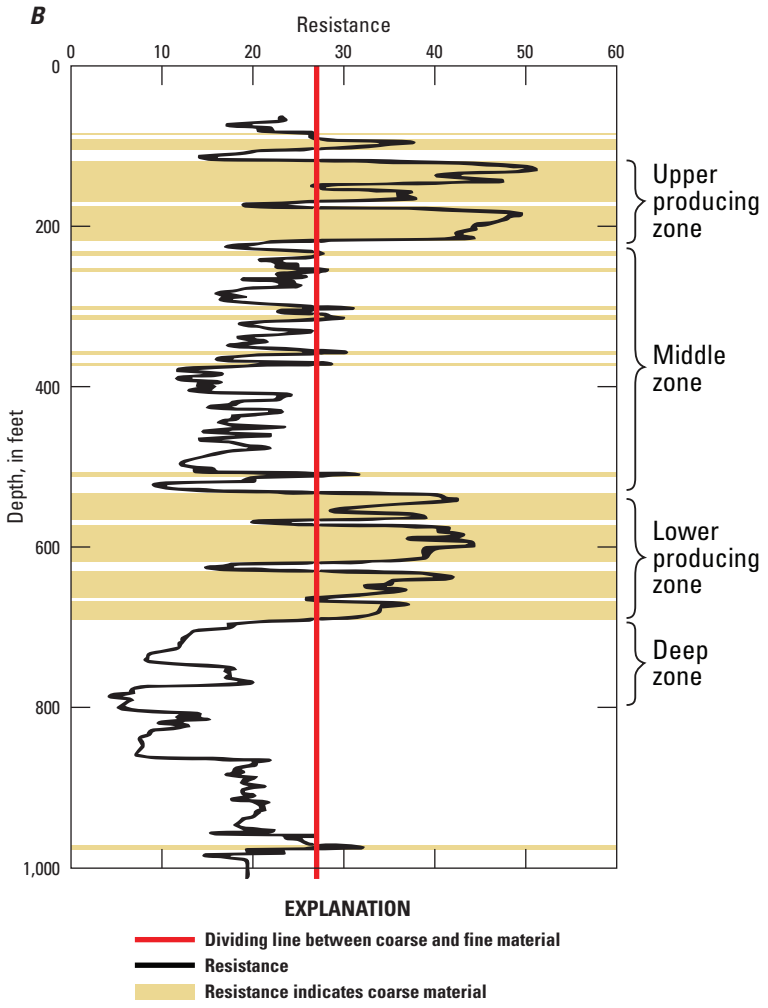

Figure 6. Example of logs from one borehole showing the textural variation and interpretation of borehole sediments with depth: *A*, drillers' lithology log, and *B*, geophysical resistivity e-log.

The percentage of coarse-grained deposits was calculated in 10-ft intervals both for the drillers' lithology logs and for geophysical e-logs. When the drillers' logs and geophysical e-logs were both available for a given borehole, the percent-coarse calculation from the e-log was preferentially used. The percent-coarse distribution for each borehole is shown in figure 5*B* (appendix B–1).

Textural Property Modeling

The three-dimensional distribution of aquifer properties was interpolated from the percent-coarse values for each borehole using the EarthVision software. As stated earlier, the property gridding module in EarthVision uses a biharmonic cubic-spline algorithm. This algorithm is an iterative process that adjusts tension surfaces so that they honor the input data with minimum curvature. The percent-coarse distribution was modeled for each aquifer zone as quantified in the geometric framework model: percent-coarse data from each borehole were partitioned according to the zone they were in, allowing the gridding software to interpolate only the data from within a specific zone. In addition, the faults separating the subbasins act as barriers to interpolation within zones, maintaining fault offsets and modeling textural discontinuities.

Textural Model Description

A fence diagram showing the three-dimensional distribution of aquifer texture is shown in figure 5*B*. The cross-section profile locations, orientation, and vertical exaggeration (5 times) are the same as in figure 5*A*. The spatial pattern of the percentage of coarse-grained texture is heterogeneous in each aquifer zone, although in general, the textures in the upper and lower producing zones yielded higher percent-coarse values than the shallow, middle, and deep zones. Regions with a predominance of very coarse-grained material (greater than 90-percent coarse) are locally important, as indicated by concentrations of high percent coarse for boreholes in the Storage Unit I, Storage Unit III, and East Foothill subbasins. Overall, however, there appeared to be an intermediate predominance of coarse-grained material (30–70-percent coarse) throughout the study area.

Figure 7 shows the relationship between the geometric framework (fig. 7*A*) and textural property (fig. 7*B*) model outputs along a single cross section that cuts through Storage Unit I. Select geophysical resistivity e-logs used to quantify the aquifer-zone horizons and percent-coarse textural values are displayed. These e-logs show the textural variation of each aquifer zone by depth and how the aquifer-zone horizon elevations change along the cross section. The upper and lower producing zones were defined by distinct, high-amplitude increases in the resistivity curves, indicating more permeable, very coarse-grained sedimentary material. This observation is shown in the textural model by a concentration of warm colors in the upper and lower producing zones. Conversely, the shallow, middle, and deep zones were characterized by smaller, low-amplitude shifts in resistivity, indicating less-permeable sediments with a lower percentage of coarse-grained material. These aquifer zones are indicated by cooler colors in figure 7*B*.

The middle producing zone is a thin, areally limited layer of coarse-grained deposits at a depth of about 360–380 ft below NAVD 88 and extending 1–2 miles inland from the coast. Because of its limited areal extent, the middle producing zone was not modeled as an independent layer in the geometric framework model, but is shown in the cross section in figure 7. High-resistivity e-log readings in the middle zone indicate lenses of coarse-grained material, which were identified as the middle producing zone. The exception to this observation was from well 4N/27W-23F05, where a low-resistivity reading was interpreted to be seawater intrusion along the coarse-grained middle producing zone.

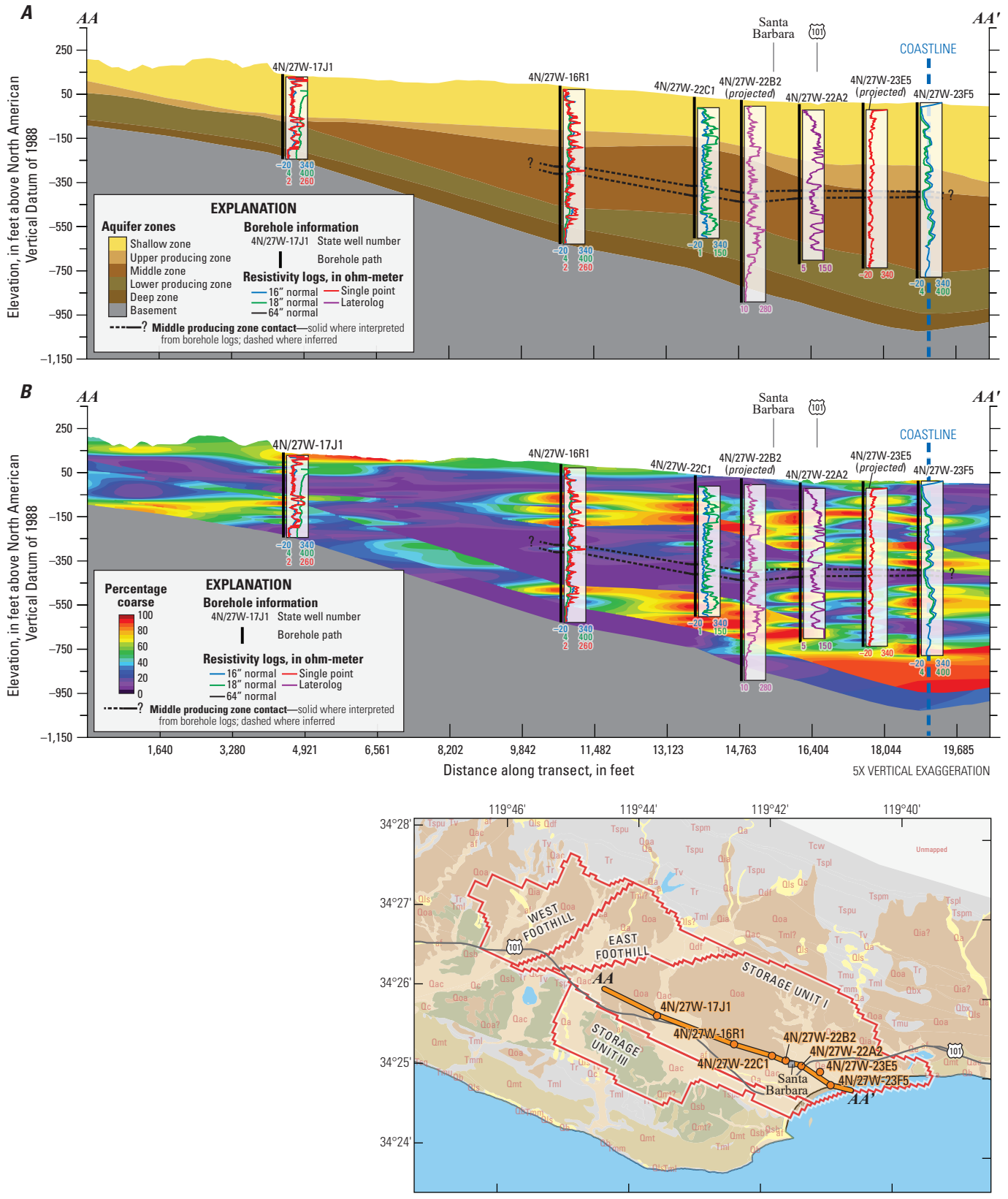

Figure 7. Cross section through the hydrogeologic framework model and geophysical resistivity e-logs shown for select boreholes and approximate extent of the middle producing zone, Santa Barbara and Foothill groundwater basins, Santa Barbara, California: *A*, aquifer-zone horizons in the geometric framework model, and *B*, percent-coarse distributions in each aquifer zone in the textural model.

Summary and Conclusions

This chapter presents an integrated three-dimensional hydrogeologic framework model (HFM) of the Santa Barbara and Foothill groundwater basins. The HFM has two parts: (1) a geometric framework model that quantifies the subsurface extent of the five aquifer zones in the study area with respect to major geologic structures and stratigraphy and (2) a texture model that characterizes the distribution of sedimentary lithology type and grain size in each aquifer zone. The geometric framework model incorporates previously published geologic maps, interpretive geologic cross sections, drillers' lithology descriptions, and geophysical resistivity e-log information in a three-dimensional digital representation of aquifer-zone horizons and major geologic structures. The texture model uses interpreted lithologic information from drillers' lithology logs and e-logs to interpolate the distribution of coarse- and fine-grained material throughout the aquifer zones defined in the geometric framework model.

The aquifer system in the Santa Barbara and Foothill groundwater basins was divided into five stratigraphic aquifer zones made up of unconsolidated sedimentary deposits of Pleistocene age and younger. The five aquifer zones are, from youngest to oldest, the shallow zone, upper producing zone, middle zone, lower producing zone, and deep zone. With few exceptions, the five aquifer zones are present throughout the study area, but vary in thickness between and within subbasins. The two main producing aquifer layers, the upper and lower producing zones, contain considerably more coarse-grained material than the other three zones. Thin lenses of coarse sediments are locally present in the shallow, middle, and deep zones and could be significant in terms of groundwater extraction, such as the middle producing zone in the middle zone.

References Cited

Burow, K.R., Shelton, J.L., Hevesi, J.A., and Weissmann, G.S., 2004, Hydrogeologic characterization of the Modesto area, San Joaquin Valley, California: U.S. Geological Survey Scientific Investigations Report 2004–5232, 54 p., http://pubs.usgs.gov/sir/2004/5232/.

Dynamic Graphics, Inc., 2015, EarthVision, accessed November 24, 2015, at http://www.dgi.com/earthvision/evmain.html.

Faunt, C.C., Belitz, Kenneth, and Hanson, R.T., 2009, Development of a three-dimensional model of sedimentary texture in valley-fill deposits of Central Valley, CA, USA: Hydrogeology Journal, v. 18, p. 625–649, https://doi.org/0.1007/s10040-009-0539-7.

Freckleton, J.R., 1989, Geohydrology of the Foothill ground-water basin near Santa Barbara, California: U.S. Geological Survey Water-Resources Investigations Report 89–4017, 46 p., https://pubs.er.usgs.gov/publication/wri894017.

Freckleton, J.R., Martin, P., Nishikawa, T., 1998, Geohydrology of Storage Unit III and a combined flow model of the Santa Barbara and foothill ground-water basins, Santa Barbara County, California: U.S. Geological Survey Water-Resources Investigations Report 97–4121, 85 p., http://pubs.er.usgs.gov/publication/wri974121.

Hanson, R.T., Anderson, S.R., and Pool, D.R., 1990, Simulation of ground-water flow and potential land subsidence, Avra Valley, Arizona: U.S. Geological Survey Water-Resources Investigations Report 90–4178, 41 p., http://pubs.er.usgs.gov/usgspubs/wri/wri904178.

Hutchinson, C.B., 1979, Ground-water monitoring at Santa Barbara, California—Phase 1, Coastal monitor-well installation and initial measurements: U.S. Geological Survey Open-File Report 79–923, 24 p., https://pubs.er.usgs.gov/publication/ofr79923.

Laudon, J., and Belitz, K., 1991, Texture and depositional history of late Pleistocene-Holocene alluvium in the central part of the western San Joaquin Valley, California: Environmental and Engineering Geoscience, v. 28, no. 1, p. 73–88, https://doi.org/10.2113/ggeosci.xxviii.1.73.

Martin, P., and Berenbrock, C., 1986, Ground-water monitoring at Santa Barbara, California; Phase 3—Development of a three-dimensional digital ground-water flow model for Storage Unit I of the Santa Barbara ground-water basin: U.S. Geological Survey Water-Resources Investigations Report 86–4103, 58 p., https://pubs.er.usgs.gov/publication/wri864103.

Minor, S.A., Kellogg, K.S., Stanley, R.G., Gurrola, L.D., Keller, E.A., and Brandt, T.R., 2009, Geologic map of the Santa Barbara coastal plain area, Santa Barbara County, California: U.S. Geological Survey Scientific Investigations Map 3001, scale 1:25,000, 1 sheet, pamphlet, 38 p., https://pubs.er.usgs.gov/publication/sim3001.

Muir, K.S., 1968, Ground-water reconnaissance of the Santa Barbara-Montecito area, Santa Barbara County, California: Geological Survey Water-Supply Paper 1859–A, p. A1–A28, https://pubs.er.usgs.gov/publication/wsp1859A.

Appendix B–1

Table B1–1. Calculated percent-coarse intervals for all drillers' logs and e-logs used to define textural properties of the hydrogeologic framework model.

[Percent-coarse values are calculated for 10-foot intervals for the entire depth of each borehole. State well number is the state of California well identifier; interval midpoint depth is the midpoint of each 10-foot interval, in feet from top of borehole; PC is the percent-coarse value for each interval; log type defines whether the borehole is a drillers' lithology log (D) or a geophysical e-log (E).]

State well number	Interval midpoint depth (feet)	PC	Log type
4N/27W-6L1	5	18.2	D
4N/27W-6L1	15	0	D
4N/27W-6L1	25	0	D
4N/27W-6L1	35	0	D
4N/27W-6L1	45	0	D
4N/27W-6L1	55	60	D
4N/27W-6L1	65	80	D
4N/27W-6L1	75	80	D
4N/27W-6L1	85	100	D
4N/27W-6L1	95	100	D
4N/27W-6L1	105	100	D
4N/27W-6L1	115	100	D
4N/27W-6L1	125	100	D
4N/27W-6L1	135	100	D
4N/27W-6L1	145	100	D
4N/27W-6L1	155	100	D
4N/27W-6L1	165	100	D
4N/27W-6L1	175	100	D
4N/27W-6L1	185	100	D
4N/27W-6L1	195	100	D
4N/27W-6L1	205	88.9	D
4N/27W-6L1	215	0	D
4N/27W-6L1	225	0	D
4N/27W-6L1	235	0	D
4N/27W-6L1	245	0	D
4N/27W-6L1	255	0	D
4N/27W-6L1	265	0	D
4N/27W-6N1	5	0	D
4N/27W-6N1	15	0	D
4N/27W-6N1	25	0	D
4N/27W-6N1	35	0	D
4N/27W-6N1	45	0	D
4N/27W-6N1	55	0	D
4N/27W-6N1	65	0	D
4N/27W-6N1	75	0	D
4N/27W-6N1	85	60	D
4N/27W-6N1	95	100	D
4N/27W-6N1	105	60	D
4N/27W-6N1	115	0	D
4N/27W-6N1	125	0	D
4N/27W-6N1	135	0	D
4N/27W-6N1	145	0	D
4N/27W-6N1	155	0	D
4N/27W-6N1	165	0	D
4N/27W-6N2	5	0	D
4N/27W-6N2	15	0	D
4N/27W-6N2	25	0	D
4N/27W-6N2	35	80	D
4N/27W-6N2	45	100	D
4N/27W-6N2	55	100	D
4N/27W-6N2	65	100	D
4N/27W-6N2	75	100	D
4N/27W-6N2	85	100	D
4N/27W-6N2	95	100	D
4N/27W-6N2	105	100	D
4N/27W-6N2	115	20	D
4N/27W-6P1	5	18.2	D
4N/27W-6P1	15	0	D
4N/27W-6P1	25	0	D
4N/27W-6P1	35	0	D
4N/27W-6P1	45	0	D
4N/27W-6P1	55	0	D
4N/27W-6P1	65	0	D
4N/27W-6P1	75	0	D
4N/27W-6P1	85	0	D
4N/27W-6P1	95	60	D
4N/27W-6P1	105	100	D
4N/27W-6P1	115	100	D

Table B1–1. Calculated percent-coarse intervals for all drillers' logs and e-logs used to define textural properties of the hydrogeologic framework model.—Continued

[Percent-coarse values are calculated for 10-foot intervals for the entire depth of each borehole. State well number is the state of California well identifier; interval midpoint depth is the midpoint of each 10-foot interval, in feet from top of borehole; PC is the percent-coarse value for each interval; log type defines whether the borehole is a drillers' lithology log (D) or a geophysical e-log (E).]

State well number	Interval midpoint depth (feet)	PC	Log type
4N/27W-6P1	125	100	D
4N/27W-6P1	135	100	D
4N/27W-6P1	145	40	D
4N/27W-6P1	155	100	D
4N/27W-6P1	165	100	D
4N/27W-6P1	175	100	D
4N/27W-6P1	185	77.8	D
4N/27W-6P1	195	45.5	D
4N/27W-6P1	205	22.2	D
4N/27W-6P2	75	0	D
4N/27W-6P2	85	0	D
4N/27W-6P2	95	0	D
4N/27W-6P2	105	0	D
4N/27W-6P2	115	0	D
4N/27W-6P2	125	0	D
4N/27W-6P2	135	0	D
4N/27W-6P2	145	0	D
4N/27W-6P2	155	0	D
4N/27W-6P2	165	0	D
4N/27W-6P2	175	0	D
4N/27W-6P2	185	0	D
4N/27W-6P2	195	0	D
4N/27W-6P2	205	0	D
4N/27W-6P2	215	27.3	D
4N/27W-6P2	225	20	D
4N/27W-6P2	235	0	D
4N/27W-6P2	245	0	D
4N/27W-6Q2	5	81.8	D
4N/27W-6Q2	15	0	D
4N/27W-6Q2	25	0	D
4N/27W-6Q2	35	0	D
4N/27W-6Q2	45	60	D
4N/27W-6Q2	55	0	D
4N/27W-6Q2	65	0	D
4N/27W-6Q2	75	0	D
4N/27W-6Q2	85	0	D
4N/27W-6Q2	95	0	D
4N/27W-6Q2	105	0	D
4N/27W-6Q2	115	0	D
4N/27W-6Q2	125	90	D
4N/27W-6Q2	135	100	D
4N/27W-6Q2	145	50	D
4N/27W-6Q2	155	0	D
4N/27W-6Q2	165	0	D
4N/27W-6Q2	175	70	D
4N/27W-6Q2	185	100	D
4N/27W-6Q2	195	60	D
4N/27W-6Q2	205	88.9	D
4N/27W-6Q2	215	72.7	D
4N/27W-6Q2	225	100	D
4N/27W-6Q2	235	90	D
4N/27W-6Q2	245	90	D
4N/27W-6Q2	255	100	D
4N/27W-6Q11	5	72.7	D
4N/27W-6Q11	15	0	D
4N/27W-6Q11	25	50	D
4N/27W-6Q11	35	100	D
4N/27W-6Q11	45	100	D
4N/27W-6Q11	55	100	D
4N/27W-6Q11	65	100	D
4N/27W-6Q11	75	100	D
4N/27W-6Q11	85	100	D
4N/27W-6Q11	95	100	D
4N/27W-6Q11	105	100	D
4N/27W-6Q11	115	100	D
4N/27W-6Q11	125	90	D
4N/27W-6Q11	135	0	D
4N/27W-6Q11	145	0	D
4N/27W-6Q11	155	0	D
4N/27W-6Q11	165	0	D
4N/27W-6Q11	175	0	D
4N/27W-6Q11	185	0	D
4N/27W-6Q11	195	0	D
4N/27W-6Q11	205	0	D
4N/27W-6Q11	215	0	D
4N/27W-6Q11	225	0	D
4N/27W-6Q11	235	0	D
4N/27W-6Q11	245	0	D

Table B1–1. Calculated percent-coarse intervals for all drillers' logs and e-logs used to define textural properties of the hydrogeologic framework model.—Continued

[Percent-coarse values are calculated for 10-foot intervals for the entire depth of each borehole. State well number is the state of California well identifier; interval midpoint depth is the midpoint of each 10-foot interval, in feet from top of borehole; PC is the percent-coarse value for each interval; log type defines whether the borehole is a drillers' lithology log (D) or a geophysical e-log (E).]

State well number	Interval midpoint depth (feet)	PC	Log type
4N/27W-6Q11	255	0	D
4N/27W-6Q11	265	0	D
4N/27W-6Q11	275	0	D
4N/27W-6Q11	285	0	D
4N/27W-6Q11	295	0	D
4N/27W-6Q11	305	0	D
4N/27W-6Q11	315	90	D
4N/27W-6Q11	325	100	D
4N/27W-6Q11	335	100	D
4N/27W-6Q11	345	100	D
4N/27W-6Q11	355	100	D
4N/27W-6Q11	365	100	D
4N/27W-6Q11	375	100	D
4N/27W-6Q11	385	100	D
4N/27W-6Q11	395	90	D
4N/27W-6R2	5	54.5	D
4N/27W-6R2	15	0	D
4N/27W-6R2	25	0	D
4N/27W-6R2	35	0	D
4N/27W-6R2	45	0	D
4N/27W-6R2	55	0	D
4N/27W-6R2	65	30	D
4N/27W-6R2	75	0	D
4N/27W-6R2	85	0	D
4N/27W-6R2	95	0	D
4N/27W-6R2	105	0	D
4N/27W-6R2	115	0	D
4N/27W-6R2	125	0	D
4N/27W-6R2	135	70	D
4N/27W-6R2	145	30	D
4N/27W-6R2	155	0	D
4N/27W-6R2	165	0	D
4N/27W-6R2	175	0	D
4N/27W-6R2	185	40	D
4N/27W-6R2	195	0	D
4N/27W-6R2	205	88.9	D
4N/27W-6R2	215	100	D
4N/27W-6R2	225	60	D
4N/27W-6R2	235	0	D
4N/27W-6R2	245	0	D
4N/27W-6R2	255	0	D
4N/27W-6R2	265	60	D
4N/27W-6R2	275	100	D
4N/27W-6R2	285	100	D
4N/27W-6R2	295	100	D
4N/27W-6R2	305	20	D
4N/27W-6R3	5	0	D
4N/27W-6R3	15	0	D
4N/27W-6R3	25	0	D
4N/27W-6R3	35	0	D
4N/27W-6R3	45	0	D
4N/27W-6R3	55	0	D
4N/27W-6R3	65	0	D
4N/27W-6R3	75	0	D
4N/27W-6R3	85	0	D
4N/27W-6R3	95	0	D
4N/27W-6R3	105	0	D
4N/27W-6R3	115	80	D
4N/27W-6R3	125	100	D
4N/27W-6R3	135	80	D
4N/27W-6R3	145	50	D
4N/27W-6R3	155	0	D
4N/27W-6R3	165	0	D
4N/27W-6R3	175	10	D
4N/27W-6R3	185	20	D
4N/27W-6R3	195	30	D
4N/27W-6R3	205	100	D
4N/27W-6R3	215	63.6	D
4N/27W-6R3	225	90	D
4N/27W-6R3	235	90	D
4N/27W-6R3	245	100	D
4N/27W-6R3	255	100	D
4N/27W-6R3	265	100	D
4N/27W-7A5	155	0	D
4N/27W-7A5	165	0	D
4N/27W-7A5	175	10	D
4N/27W-7A5	185	44.4	D
4N/27W-7A5	195	0	D

Table B1–1. Calculated percent-coarse intervals for all drillers' logs and e-logs used to define textural properties of the hydrogeologic framework model.—Continued

[Percent-coarse values are calculated for 10-foot intervals for the entire depth of each borehole. State well number is the state of California well identifier; interval midpoint depth is the midpoint of each 10-foot interval, in feet from top of borehole; PC is the percent-coarse value for each interval; log type defines whether the borehole is a drillers' lithology log (D) or a geophysical e-log (E).]

State well number	Interval midpoint depth (feet)	PC	Log type
4N/27W-7A5	205	0	D
4N/27W-7A5	215	0	D
4N/27W-7A5	225	30	D
4N/27W-7A5	235	80	D
4N/27W-7A5	245	22.2	D
4N/27W-7B2	5	9.1	D
4N/27W-7B2	15	0	D
4N/27W-7B2	25	0	D
4N/27W-7B2	35	0	D
4N/27W-7B2	45	0	D
4N/27W-7B2	55	0	D
4N/27W-7B2	65	0	D
4N/27W-7B2	75	0	D
4N/27W-7B2	85	0	D
4N/27W-7B2	95	0	D
4N/27W-7B2	105	0	D
4N/27W-7B2	115	0	D
4N/27W-7B2	125	20	D
4N/27W-7B2	135	40	D
4N/27W-7B2	145	100	D
4N/27W-7B2	155	10	D
4N/27W-7B2	165	0	D
4N/27W-7B2	175	50	D
4N/27W-7B2	185	100	D
4N/27W-7B4	5	9.1	D
4N/27W-7B4	15	0	D
4N/27W-7B4	25	0	D
4N/27W-7B4	35	0	D
4N/27W-7B4	45	30	D
4N/27W-7B4	55	50	D
4N/27W-7B4	65	0	D
4N/27W-7B4	75	0	D
4N/27W-7B4	85	0	D
4N/27W-7B4	95	0	D
4N/27W-7B4	105	0	D
4N/27W-7B4	115	0	D
4N/27W-7B4	125	0	D
4N/27W-7B4	135	70	D
4N/27W-7B4	145	0	D
4N/27W-7B4	155	0	D
4N/27W-7B6	5	18.2	D
4N/27W-7B6	15	0	D
4N/27W-7B6	25	0	D
4N/27W-7B6	35	0	D
4N/27W-7B6	45	0	D
4N/27W-7B6	55	0	D
4N/27W-7B6	65	0	D
4N/27W-7B6	75	0	D
4N/27W-7B6	85	0	D
4N/27W-7B6	95	0	D
4N/27W-7B6	105	10	D
4N/27W-7B6	115	0	D
4N/27W-7B6	125	0	D
4N/27W-7B6	135	0	D
4N/27W-7B6	145	0	D
4N/27W-7B6	155	0	D
4N/27W-7B6	165	0	D
4N/27W-7B6	175	0	D
4N/27W-7B6	185	11.1	D
4N/27W-7B6	195	18.2	D
4N/27W-7B6	205	0	D
4N/27W-7B6	215	0	D
4N/27W-7B6	225	0	D
4N/27W-7B7	5	9.1	D
4N/27W-7B7	15	40	D
4N/27W-7B7	25	0	D
4N/27W-7B7	35	0	D
4N/27W-7B7	45	0	D
4N/27W-7B7	55	0	D
4N/27W-7B7	65	0	D
4N/27W-7B7	75	0	D
4N/27W-7B7	85	0	D
4N/27W-7B7	95	0	D
4N/27W-7B7	105	0	D
4N/27W-7B7	115	0	D
4N/27W-7B7	125	0	D
4N/27W-7B7	135	0	D
4N/27W-7B7	145	0	D

Table B1–1. Calculated percent-coarse intervals for all drillers' logs and e-logs used to define textural properties of the hydrogeologic framework model.—Continued

[Percent-coarse values are calculated for 10-foot intervals for the entire depth of each borehole. State well number is the state of California well identifier; interval midpoint depth is the midpoint of each 10-foot interval, in feet from top of borehole; PC is the percent-coarse value for each interval; log type defines whether the borehole is a drillers' lithology log (D) or a geophysical e-log (E).]

State well number	Interval midpoint depth (feet)	PC	Log type
4N/27W-7B7	155	0	D
4N/27W-7B7	165	0	D
4N/27W-7B7	175	0	D
4N/27W-7B7	185	0	D
4N/27W-7B7	195	0	D
4N/27W-7B7	205	0	D
4N/27W-7B7	215	0	D
4N/27W-7B7	225	40	D
4N/27W-7B7	235	40	D
4N/27W-7B7	245	44.4	D
4N/27W-7B10	5	72.7	D
4N/27W-7B10	15	0	D
4N/27W-7B10	25	0	D
4N/27W-7B10	35	0	D
4N/27W-7B10	45	0	D
4N/27W-7B10	55	0	D
4N/27W-7B10	65	0	D
4N/27W-7B10	75	0	D
4N/27W-7B10	85	0	D
4N/27W-7B10	95	0	D
4N/27W-7B10	105	0	D
4N/27W-7B10	115	0	D
4N/27W-7B10	125	0	D
4N/27W-7B10	135	0	D
4N/27W-7B10	145	90	D
4N/27W-7B10	155	0	D
4N/27W-7B10	165	20	D
4N/27W-7B10	175	0	D
4N/27W-7B10	185	0	D
4N/27W-7B10	195	0	D
4N/27W-7B10	205	0	D
4N/27W-7B10	215	0	D
4N/27W-7B10	225	0	D
4N/27W-7B10	235	0	D
4N/27W-7B10	245	0	D
4N/27W-7B10	255	0	D
4N/27W-7B10	265	0	D
4N/27W-7B10	275	60	D
4N/27W-7B10	285	20	D
4N/27W-7B10	295	81.8	D
4N/27W-7B11	5	100	D
4N/27W-7B11	15	100	D
4N/27W-7B11	25	100	D
4N/27W-7B11	35	100	D
4N/27W-7B11	45	100	D
4N/27W-7B11	55	90	D
4N/27W-7B11	65	0	D
4N/27W-7B11	75	0	D
4N/27W-7B11	85	0	D
4N/27W-7B11	95	0	D
4N/27W-7B11	105	0	D
4N/27W-7B11	115	0	D
4N/27W-7B11	125	0	D
4N/27W-7B11	135	0	D
4N/27W-7B11	145	0	D
4N/27W-7B11	155	0	D
4N/27W-7B11	165	0	D
4N/27W-7B11	175	0	D
4N/27W-7B11	185	0	D
4N/27W-7B11	195	0	D
4N/27W-7B11	205	0	D
4N/27W-7B11	215	0	D
4N/27W-7B11	225	0	D
4N/27W-7B11	235	0	D
4N/27W-7B11	245	0	D
4N/27W-7B11	255	0	D
4N/27W-7B11	265	0	D
4N/27W-7B11	275	0	D
4N/27W-7B11	285	0	D
4N/27W-7B11	295	0	D
4N/27W-7B11	305	0	D
4N/27W-7B11	315	0	D
4N/27W-7B11	325	0	D
4N/27W-7B11	335	0	D
4N/27W-7B11	345	0	D
4N/27W-7B11	355	0	D
4N/27W-7B11	365	0	D
4N/27W-7B11	375	0	D

Table B1–1. Calculated percent-coarse intervals for all drillers' logs and e-logs used to define textural properties of the hydrogeologic framework model.—Continued

[Percent-coarse values are calculated for 10-foot intervals for the entire depth of each borehole. State well number is the state of California well identifier; interval midpoint depth is the midpoint of each 10-foot interval, in feet from top of borehole; PC is the percent-coarse value for each interval; log type defines whether the borehole is a drillers' lithology log (D) or a geophysical e-log (E).]

State well number	Interval midpoint depth (feet)	PC	Log type
4N/27W-7B11	385	0	D
4N/27W-7B11	395	0	D
4N/27W-7B11	405	0	D
4N/27W-7B11	415	0	D
4N/27W-7B11	425	0	D
4N/27W-7B11	435	0	D
4N/27W-7B11	445	0	D
4N/27W-7B11	455	0	D
4N/27W-7B11	465	0	D
4N/27W-7B11	475	0	D
4N/27W-7B11	485	0	D
4N/27W-7C3	5	100	D
4N/27W-7C3	15	30	D
4N/27W-7C3	25	0	D
4N/27W-7C3	35	0	D
4N/27W-7C3	45	0	D
4N/27W-7C3	55	0	D
4N/27W-7C3	65	0	D
4N/27W-7C3	75	0	D
4N/27W-7C3	85	0	D
4N/27W-7C3	95	0	D
4N/27W-7C3	105	0	D
4N/27W-7C3	115	0	D
4N/27W-7C3	125	0	D
4N/27W-7C3	135	0	D
4N/27W-7C3	145	30	D
4N/27W-7C3	155	100	D
4N/27W-7C3	165	100	D
4N/27W-7C3	175	100	D
4N/27W-7C3	185	100	D
4N/27W-7C3	195	36.4	D
4N/27W-7C3	205	0	D
4N/27W-7C3	215	27.3	D
4N/27W-7C3	225	100	D
4N/27W-7C6	5	18.2	D
4N/27W-7C6	15	0	D
4N/27W-7C6	25	0	D
4N/27W-7C6	35	0	D
4N/27W-7C6	45	0	D
4N/27W-7C6	55	0	D
4N/27W-7C6	65	0	D
4N/27W-7C6	75	0	D
4N/27W-7C6	85	0	D
4N/27W-7C6	95	0	D
4N/27W-7C6	105	0	D
4N/27W-7C6	115	0	D
4N/27W-7C6	125	0	D
4N/27W-7C6	135	0	D
4N/27W-7C6	145	0	D
4N/27W-7C6	155	0	D
4N/27W-7C6	165	0	D
4N/27W-7C6	175	0	D
4N/27W-7C6	185	0	D
4N/27W-7C6	195	0	D
4N/27W-7C6	205	0	D
4N/27W-7C6	215	0	D
4N/27W-7C6	225	0	D
4N/27W-7C6	235	0	D
4N/27W-7C6	245	66.7	D
4N/27W-7D1	5	0	D
4N/27W-7D1	15	0	D
4N/27W-7D1	25	0	D
4N/27W-7D1	35	0	D
4N/27W-7D1	45	0	D
4N/27W-7D1	55	0	D
4N/27W-7D1	65	0	D
4N/27W-7D1	75	0	D
4N/27W-7D1	85	0	D
4N/27W-7D1	95	0	D
4N/27W-7D1	105	0	D
4N/27W-7D1	115	0	D
4N/27W-7D1	125	0	D
4N/27W-7D1	135	0	D
4N/27W-7D1	145	0	D
4N/27W-7D1	155	0	D
4N/27W-7D1	165	0	D
4N/27W-7D1	175	0	D
4N/27W-7D1	185	0	D

Table B1–1. Calculated percent-coarse intervals for all drillers' logs and e-logs used to define textural properties of the hydrogeologic framework model.—Continued

[Percent-coarse values are calculated for 10-foot intervals for the entire depth of each borehole. State well number is the state of California well identifier; interval midpoint depth is the midpoint of each 10-foot interval, in feet from top of borehole; PC is the percent-coarse value for each interval; log type defines whether the borehole is a drillers' lithology log (D) or a geophysical e-log (E).]

State well number	Interval midpoint depth (feet)	PC	Log type
4N/27W-7D1	195	0	D
4N/27W-7D1	205	0	D
4N/27W-7D1	215	100	D
4N/27W-7D1	225	100	D
4N/27W-7D1	235	100	D
4N/27W-7D1	245	100	D
4N/27W-7D1	255	90	D
4N/27W-7D1	265	0	D
4N/27W-7D1	275	100	D
4N/27W-7D1	285	100	D
4N/27W-7D1	295	45.5	D
4N/27W-7D1	305	0	D
4N/27W-7D1	315	0	D
4N/27W-7D1	325	0	D
4N/27W-7D1	335	0	D
4N/27W-7D1	345	0	D
4N/27W-7D1	355	0	D
4N/27W-7D1	365	0	D
4N/27W-7D1	375	0	D
4N/27W-7D1	385	0	D
4N/27W-7D1	395	0	D
4N/27W-7D1	405	0	D
4N/27W-7D1	415	0	D
4N/27W-7D1	425	54.5	D
4N/27W-7D1	435	100	D
4N/27W-7D1	445	100	D
4N/27W-7D1	455	100	D
4N/27W-7D1	465	100	D
4N/27W-7D1	475	90	D
4N/27W-7F5	5	0	D
4N/27W-7F5	15	20	D
4N/27W-7F5	25	0	D
4N/27W-7F5	35	0	D
4N/27W-7F5	45	0	D
4N/27W-7F5	55	30	D
4N/27W-7F5	65	20	D
4N/27W-7F5	75	0	D
4N/27W-7F5	85	60	D
4N/27W-7F5	95	10	D
4N/27W-7F5	105	0	D
4N/27W-7F5	115	0	D
4N/27W-7F5	125	0	D
4N/27W-7F5	135	0	D
4N/27W-7F5	145	40	D
4N/27W-7F5	155	40	D
4N/27W-7F10	5	36.4	D
4N/27W-7F10	15	0	D
4N/27W-7F10	25	0	D
4N/27W-7F10	35	0	D
4N/27W-7F10	45	20	D
4N/27W-7F10	55	40	D
4N/27W-7F10	65	0	D
4N/27W-7F10	75	0	D
4N/27W-7F10	85	0	D
4N/27W-7F10	95	0	D
4N/27W-7F10	105	60	D
4N/27W-7F10	115	50	D
4N/27W-7F10	125	0	D
4N/27W-7F10	135	0	D
4N/27W-7F10	145	0	D
4N/27W-7F10	155	0	D
4N/27W-7F10	165	0	D
4N/27W-7F10	175	0	D
4N/27W-7F10	185	0	D
4N/27W-7F10	195	0	D
4N/27W-7F10	205	0	D
4N/27W-7F10	215	0	D
4N/27W-7F10	225	0	D
4N/27W-7F10	235	20	D
4N/27W-7F10	245	0	D
4N/27W-7F10	255	0	D
4N/27W-7F10	265	0	D
4N/27W-7F10	275	0	D
4N/27W-7F10	285	0	D
4N/27W-7F10	295	0	D
4N/27W-7F11	5	9.1	D
4N/27W-7F11	15	0	D
4N/27W-7F11	25	0	D

Table B1–1. Calculated percent-coarse intervals for all drillers' logs and e-logs used to define textural properties of the hydrogeologic framework model.—Continued

[Percent-coarse values are calculated for 10-foot intervals for the entire depth of each borehole. State well number is the state of California well identifier; interval midpoint depth is the midpoint of each 10-foot interval, in feet from top of borehole; PC is the percent-coarse value for each interval; log type defines whether the borehole is a drillers' lithology log (D) or a geophysical e-log (E).]

State well number	Interval midpoint depth (feet)	PC	Log type
4N/27W-7F11	35	0	D
4N/27W-7F11	45	0	D
4N/27W-7F11	55	0	D
4N/27W-7F11	65	0	D
4N/27W-7F11	75	0	D
4N/27W-7F11	85	0	D
4N/27W-7F11	95	0	D
4N/27W-7F11	105	20	D
4N/27W-7F11	115	40	D
4N/27W-7F11	125	10	D
4N/27W-7F11	135	0	D
4N/27W-7F11	145	0	D
4N/27W-7F11	155	0	D
4N/27W-7F11	165	0	D
4N/27W-7F11	175	0	D
4N/27W-7F11	185	0	D
4N/27W-7F11	195	0	D
4N/27W-7F11	205	0	D
4N/27W-7F11	215	0	D
4N/27W-7F11	225	30	D
4N/27W-7F11	235	100	D
4N/27W-7F11	245	100	D
4N/27W-7F11	255	100	D
4N/27W-7F11	265	0	D
4N/27W-7F11	275	80	D
4N/27W-7F11	285	100	D
4N/27W-7F12	5	0	D
4N/27W-7F12	15	0	D
4N/27W-7F12	25	0	D
4N/27W-7F12	35	0	D
4N/27W-7F12	45	0	D
4N/27W-7F12	55	0	D
4N/27W-7F12	65	0	D
4N/27W-7F12	75	0	D
4N/27W-7F12	85	0	D
4N/27W-7F12	95	0	D
4N/27W-7F12	105	0	D
4N/27W-7F12	115	0	D
4N/27W-7F12	125	0	D
4N/27W-7F12	135	0	D
4N/27W-7F12	145	0	D
4N/27W-7F12	155	0	D
4N/27W-7F12	165	0	D
4N/27W-7F12	175	0	D
4N/27W-7F12	185	0	D
4N/27W-7F12	195	0	D
4N/27W-7F12	205	0	D
4N/27W-7F12	215	0	D
4N/27W-7F12	225	0	D
4N/27W-7F12	235	0	D
4N/27W-7F12	245	0	D
4N/27W-7F12	255	0	D
4N/27W-7F12	265	0	D
4N/27W-7F12	275	0	D
4N/27W-7F12	285	0	D
4N/27W-7F12	295	0	D
4N/27W-7F12	305	0	D
4N/27W-7F12	315	0	D
4N/27W-7F12	325	0	D
4N/27W-7F12	335	0	D
4N/27W-7F12	345	0	D
4N/27W-7F12	355	0	D
4N/27W-7F12	365	0	D
4N/27W-7F12	375	0	D
4N/27W-7F12	385	0	D
4N/27W-7F12	395	0	D
4N/27W-7F12	405	0	D
4N/27W-7F12	415	0	D
4N/27W-7F12	425	100	D
4N/27W-7F12	435	100	D
4N/27W-7F12	445	100	D
4N/27W-7F12	455	100	D
4N/27W-7F12	465	100	D
4N/27W-7F12	475	100	D
4N/27W-7F12	485	100	D
4N/27W-7F12	495	40	D
4N/27W-7G1	5	27.3	D
4N/27W-7G1	15	0	D

Table B1–1. Calculated percent-coarse intervals for all drillers' logs and e-logs used to define textural properties of the hydrogeologic framework model.—Continued

[Percent-coarse values are calculated for 10-foot intervals for the entire depth of each borehole. State well number is the state of California well identifier; interval midpoint depth is the midpoint of each 10-foot interval, in feet from top of borehole; PC is the percent-coarse value for each interval; log type defines whether the borehole is a drillers' lithology log (D) or a geophysical e-log (E).]

State well number	Interval midpoint depth (feet)	PC	Log type
4N/27W-7G1	25	0	D
4N/27W-7G1	35	0	D
4N/27W-7G1	45	0	D
4N/27W-7G1	55	0	D
4N/27W-7G1	65	0	D
4N/27W-7G1	75	0	D
4N/27W-7G1	85	0	D
4N/27W-7G1	95	20	D
4N/27W-7G1	105	0	D
4N/27W-7G1	115	20	D
4N/27W-7G1	125	0	D
4N/27W-7G1	135	70	D
4N/27W-7G1	145	60	D
4N/27W-7G1	155	100	D
4N/27W-7G1	165	50	D
4N/27W-7G1	175	60	D
4N/27W-7G1	185	100	D
4N/27W-7G1	195	0	D
4N/27W-7G2	5	81.8	D
4N/27W-7G2	15	0	D
4N/27W-7G2	25	0	D
4N/27W-7G2	35	0	D
4N/27W-7G2	45	10	D
4N/27W-7G2	55	90	D
4N/27W-7G2	65	0	D
4N/27W-7G2	75	0	D
4N/27W-7G2	85	0	D
4N/27W-7G2	95	0	D
4N/27W-7G2	105	0	D
4N/27W-7G2	115	0	D
4N/27W-7G2	125	0	D
4N/27W-7G2	135	0	D
4N/27W-7G2	145	30	D
4N/27W-7G3	5	0	D
4N/27W-7G3	15	0	D
4N/27W-7G3	25	0	D
4N/27W-7G3	35	0	D
4N/27W-7G3	45	0	D
4N/27W-7G3	55	0	D
4N/27W-7G3	65	0	D
4N/27W-7G3	75	0	D
4N/27W-7G3	85	0	D
4N/27W-7G3	95	0	D
4N/27W-7G3	105	0	D
4N/27W-7G3	115	0	D
4N/27W-7G3	125	30	D
4N/27W-7G3	135	40	D
4N/27W-7G3	145	0	D
4N/27W-7G3	155	0	D
4N/27W-7G3	165	10	D
4N/27W-7G3	175	0	D
4N/27W-7G3	185	20	D
4N/27W-7G3	195	0	D
4N/27W-7G3	205	0	D
4N/27W-7G3	215	0	D
4N/27W-7G3	225	0	D
4N/27W-7G3	235	0	D
4N/27W-7G3	245	0	D
4N/27W-7G3	255	0	D
4N/27W-7G3	265	40	D
4N/27W-7G3	275	0	D
4N/27W-7G3	285	0	D
4N/27W-7G3	295	0	D
4N/27W-7G3	305	0	D
4N/27W-7G3	315	0	D
4N/27W-7G3	325	0	D
4N/27W-7G3	335	30	D
4N/27W-7G3	345	30	D
4N/27W-7G3	355	55.6	D
4N/27W-7G6	5	0	D
4N/27W-7G6	15	0	D
4N/27W-7G6	25	0	D
4N/27W-7G6	35	0	D
4N/27W-7G6	45	0	D
4N/27W-7G6	55	0	D
4N/27W-7G6	65	0	D
4N/27W-7G6	75	0	D
4N/27W-7G6	85	0	D

Table B1–1. Calculated percent-coarse intervals for all drillers' logs and e-logs used to define textural properties of the hydrogeologic framework model.—Continued

[Percent-coarse values are calculated for 10-foot intervals for the entire depth of each borehole. State well number is the state of California well identifier; interval midpoint depth is the midpoint of each 10-foot interval, in feet from top of borehole; PC is the percent-coarse value for each interval; log type defines whether the borehole is a drillers' lithology log (D) or a geophysical e-log (E).]

State well number	Interval midpoint depth (feet)	PC	Log type
4N/27W-7G6	95	0	D
4N/27W-7G6	105	0	D
4N/27W-7G6	115	0	D
4N/27W-7G6	125	0	D
4N/27W-7G6	135	0	D
4N/27W-7G6	145	0	D
4N/27W-7G6	155	0	D
4N/27W-7G6	165	0	D
4N/27W-7G6	175	0	D
4N/27W-7G6	185	0	D
4N/27W-7G6	195	0	D
4N/27W-7G6	205	0	D
4N/27W-7G6	215	0	D
4N/27W-7G6	225	0	D
4N/27W-7G6	235	0	D
4N/27W-7G6	245	44.4	D
4N/27W-7G7	5	100	D
4N/27W-7G7	15	100	D
4N/27W-7G7	25	100	D
4N/27W-7G7	35	70	D
4N/27W-7G7	45	10	D
4N/27W-7G7	55	100	D
4N/27W-7G7	65	100	D
4N/27W-7G7	75	90	D
4N/27W-7G7	85	0	D
4N/27W-7G7	95	90	D
4N/27W-7G7	105	100	D
4N/27W-7G7	115	100	D
4N/27W-7G7	125	100	D
4N/27W-7G7	135	50	D
4N/27W-7G7	145	0	D
4N/27W-7G7	155	0	D
4N/27W-7G7	165	30	D
4N/27W-7G7	175	100	D
4N/27W-7G7	185	100	D
4N/27W-7G7	195	100	D
4N/27W-7G7	205	100	D
4N/27W-7G7	215	100	D
4N/27W-7G7	225	100	D
4N/27W-7G7	235	100	D
4N/27W-7G7	245	100	D
4N/27W-7G7	255	100	D
4N/27W-7G7	265	40	D
4N/27W-7G7	275	100	D
4N/27W-7G7	285	100	D
4N/27W-7G7	295	100	D
4N/27W-7G7	305	90	D
4N/27W-7G7	315	0	D
4N/27W-7G7	325	0	D
4N/27W-7G7	335	0	D
4N/27W-7G7	345	0	D
4N/27W-7G7	355	0	D
4N/27W-7G7	365	0	D
4N/27W-7G7	375	100	D
4N/27W-7G7	385	100	D
4N/27W-7G7	395	100	D
4N/27W-7G7	405	100	D
4N/27W-7G7	415	100	D
4N/27W-7G7	425	100	D
4N/27W-7G7	435	100	D
4N/27W-7H3	5	100	D
4N/27W-7H3	15	100	D
4N/27W-7H3	25	60	D
4N/27W-7H3	35	40	D
4N/27W-7H3	45	40	D
4N/27W-7H3	55	100	D
4N/27W-7H3	65	20	D
4N/27W-7H3	75	0	D
4N/27W-7H3	85	0	D
4N/27W-7H3	95	0	D
4N/27W-7H3	105	0	D
4N/27W-7H3	115	0	D
4N/27W-7H3	125	0	D
4N/27W-7H3	135	0	D
4N/27W-7H3	145	0	D
4N/27W-7H3	155	0	D
4N/27W-7H3	165	0	D
4N/27W-7H3	175	0	D

Table B1–1. Calculated percent-coarse intervals for all drillers' logs and e-logs used to define textural properties of the hydrogeologic framework model.—Continued

[Percent-coarse values are calculated for 10-foot intervals for the entire depth of each borehole. State well number is the state of California well identifier; interval midpoint depth is the midpoint of each 10-foot interval, in feet from top of borehole; PC is the percent-coarse value for each interval; log type defines whether the borehole is a drillers' lithology log (D) or a geophysical e-log (E).]

State well number	Interval midpoint depth (feet)	PC	Log type
4N/27W-7H3	185	40	D
4N/27W-7H3	195	100	D
4N/27W-7H3	205	100	D
4N/27W-7H3	215	100	D
4N/27W-7H3	225	100	D
4N/27W-7H3	235	50	D
4N/27W-7H3	245	0	D
4N/27W-7H3	255	0	D
4N/27W-7H3	265	40	D
4N/27W-7H3	275	100	D
4N/27W-7H3	285	80	D
4N/27W-7H3	295	0	D
4N/27W-7H3	305	90	D
4N/27W-7H3	315	100	D
4N/27W-7H3	325	100	D
4N/27W-7H3	335	100	D
4N/27W-7H3	345	100	D
4N/27W-7H3	355	100	D
4N/27W-7H3	365	100	D
4N/27W-7H3	375	100	D
4N/27W-7H3	385	0	D
4N/27W-7H3	395	0	D
4N/27W-7H3	405	0	D
4N/27W-7H3	415	55.6	D
4N/27W-7H3	425	100	D
4N/27W-7H3	435	100	D
4N/27W-7H3	445	100	D
4N/27W-7H3	455	100	D
4N/27W-7H3	465	100	D
4N/27W-7H3	475	100	D
4N/27W-7H3	485	100	D
4N/27W-7H3	495	100	D
4N/27W-7H3	505	100	D
4N/27W-7H3	515	100	D
4N/27W-7H3	525	100	D
4N/27W-7H3	535	100	D
4N/27W-7H3	545	50	D
4N/27W-7J1	5	36.4	D
4N/27W-7J1	15	0	D
4N/27W-7J1	25	0	D
4N/27W-7J1	35	0	D
4N/27W-7J1	45	80	D
4N/27W-7J1	55	100	D
4N/27W-7J1	65	100	D
4N/27W-7J1	75	30	D
4N/27W-7J1	85	0	D
4N/27W-7J1	95	0	D
4N/27W-7J1	105	0	D
4N/27W-7J1	115	0	D
4N/27W-7J1	125	0	D
4N/27W-7J1	135	0	D
4N/27W-7J1	145	0	D
4N/27W-7J1	155	0	D
4N/27W-7J1	165	0	D
4N/27W-7J1	175	60	D
4N/27W-7J1	185	0	D
4N/27W-7J1	195	0	D
4N/27W-7J2	5	100	D
4N/27W-7J2	15	60	D
4N/27W-7J2	25	100	D
4N/27W-7J2	35	100	D
4N/27W-7J2	45	70	D
4N/27W-7J2	55	80	D
4N/27W-7J2	65	60	D
4N/27W-7J2	75	0	D
4N/27W-7J2	85	20	D
4N/27W-7J2	95	0	D
4N/27W-7J2	105	70	D
4N/27W-7J2	115	0	D
4N/27W-7J2	125	0	D
4N/27W-7J2	135	0	D
4N/27W-7J2	145	0	D
4N/27W-7J2	155	0	D
4N/27W-7J2	165	0	D
4N/27W-7J2	175	0	D
4N/27W-7J4	5	100	D
4N/27W-7J4	15	30	D
4N/27W-7J4	25	0	D

Table B1–1. Calculated percent-coarse intervals for all drillers' logs and e-logs used to define textural properties of the hydrogeologic framework model.—Continued

[Percent-coarse values are calculated for 10-foot intervals for the entire depth of each borehole. State well number is the state of California well identifier; interval midpoint depth is the midpoint of each 10-foot interval, in feet from top of borehole; PC is the percent-coarse value for each interval; log type defines whether the borehole is a drillers' lithology log (D) or a geophysical e-log (E).]

State well number	Interval midpoint depth (feet)	PC	Log type
4N/27W-7J4	35	80	D
4N/27W-7J4	45	50	D
4N/27W-7J4	55	0	D
4N/27W-7J4	65	0	D
4N/27W-7J4	75	0	D
4N/27W-7J4	85	0	D
4N/27W-7J4	95	0	D
4N/27W-7J4	105	0	D
4N/27W-7J4	115	40	D
4N/27W-7J4	125	100	D
4N/27W-7J4	135	10	D
4N/27W-7J4	145	10	D
4N/27W-7J4	155	60	D
4N/27W-7J4	165	0	D
4N/27W-7J4	175	90	D
4N/27W-7J4	185	40	D
4N/27W-7J4	195	0	D
4N/27W-7J4	205	0	D
4N/27W-7J4	215	0	D
4N/27W-7J4	225	0	D
4N/27W-7J4	235	0	D
4N/27W-7J4	245	100	D
4N/27W-7J4	255	60	D
4N/27W-7J4	265	0	D
4N/27W-7J4	275	0	D
4N/27W-7J4	285	0	D
4N/27W-7J4	295	0	D
4N/27W-7J4	305	0	D
4N/27W-7J4	315	30	D
4N/27W-7J4	325	30	D
4N/27W-7J4	335	0	D
4N/27W-7J4	345	50	D
4N/27W-7J4	355	33.3	D
4N/27W-7J4	365	0	D
4N/27W-7J4	375	40	D
4N/27W-7J4	385	36.4	D
4N/27W-7J4	395	100	D
4N/27W-7J4	405	100	D
4N/27W-7J4	415	100	D
4N/27W-7J5	5	18.2	D
4N/27W-7J5	15	0	D
4N/27W-7J5	25	0	D
4N/27W-7J5	35	0	D
4N/27W-7J5	45	0	D
4N/27W-7J5	55	0	D
4N/27W-7J5	65	0	D
4N/27W-7J5	75	0	D
4N/27W-7J5	85	0	D
4N/27W-7J5	95	0	D
4N/27W-7J5	105	0	D
4N/27W-7J5	115	0	D
4N/27W-7J5	125	0	D
4N/27W-7J5	135	10	D
4N/27W-7J5	145	40	D
4N/27W-7J5	155	0	D
4N/27W-7J5	165	100	D
4N/27W-7J5	175	50	D
4N/27W-7J5	185	40	D
4N/27W-7J5	195	81.8	D
4N/27W-7J5	205	55.6	D
4N/27W-7J5	215	0	D
4N/27W-7J5	225	0	D
4N/27W-7J5	235	0	D
4N/27W-7J5	245	77.8	D
4N/27W-7J5	255	100	D
4N/27W-7J5	265	100	D
4N/27W-7J5	275	100	D
4N/27W-7J5	285	100	D
4N/27W-7K2	5	36.4	D
4N/27W-7K2	15	0	D
4N/27W-7K2	25	0	D
4N/27W-7K2	35	60	D
4N/27W-7K2	45	0	D
4N/27W-7K2	55	0	D
4N/27W-7K2	65	0	D
4N/27W-7K2	75	0	D
4N/27W-7K2	85	0	D
4N/27W-7K2	95	0	D

Table B1–1. Calculated percent-coarse intervals for all drillers' logs and e-logs used to define textural properties of the hydrogeologic framework model.—Continued

[Percent-coarse values are calculated for 10-foot intervals for the entire depth of each borehole. State well number is the state of California well identifier; interval midpoint depth is the midpoint of each 10-foot interval, in feet from top of borehole; PC is the percent-coarse value for each interval; log type defines whether the borehole is a drillers' lithology log (D) or a geophysical e-log (E).]

State well number	Interval midpoint depth (feet)	PC	Log type
4N/27W-7K2	105	0	D
4N/27W-7K2	115	90	D
4N/27W-7K2	125	0	D
4N/27W-7K2	135	0	D
4N/27W-7K2	145	0	D
4N/27W-7K2	155	10	D
4N/27W-7K2	165	88.9	D
4N/27W-7K2	175	0	D
4N/27W-7K4	5	0	D
4N/27W-7K4	15	0	D
4N/27W-7K4	25	40	D
4N/27W-7K4	35	40	D
4N/27W-7K4	45	10	D
4N/27W-7K4	55	100	D
4N/27W-7K4	65	90	D
4N/27W-7K4	75	10	D
4N/27W-7K4	85	100	D
4N/27W-7K4	95	100	D
4N/27W-7K4	105	60	D
4N/27W-7K4	115	80	D
4N/27W-7K4	125	0	D
4N/27W-7K4	135	0	D
4N/27W-7K4	145	0	D
4N/27W-7K4	155	0	D
4N/27W-7K4	165	0	D
4N/27W-7K4	175	0	D
4N/27W-7K4	185	0	D
4N/27W-7K4	195	0	D
4N/27W-7K4	205	0	D
4N/27W-7K4	215	0	D
4N/27W-7K4	225	0	D
4N/27W-7K4	235	0	D
4N/27W-7K4	245	0	D
4N/27W-7K4	255	0	D
4N/27W-7K4	265	0	D
4N/27W-7K4	275	0	D
4N/27W-7K4	285	0	D
4N/27W-7K6	5	90.9	D
4N/27W-7K6	15	0	D
4N/27W-7K6	25	0	D
4N/27W-7K6	35	0	D
4N/27W-7K6	45	0	D
4N/27W-7K6	55	0	D
4N/27W-7K6	65	0	D
4N/27W-7K6	75	0	D
4N/27W-7K6	85	0	D
4N/27W-7K6	95	0	D
4N/27W-7K6	105	0	D
4N/27W-7K6	115	0	D
4N/27W-7K6	125	0	D
4N/27W-7K6	135	0	D
4N/27W-7K6	145	0	D
4N/27W-7K6	155	0	D
4N/27W-7K6	165	0	D
4N/27W-7K6	175	0	D
4N/27W-7K6	185	0	D
4N/27W-7K6	195	0	D
4N/27W-7K6	205	0	D
4N/27W-7K6	215	0	D
4N/27W-7K6	225	0	D
4N/27W-7K6	235	0	D
4N/27W-7K6	245	0	D
4N/27W-7K6	255	0	D
4N/27W-7K6	265	0	D
4N/27W-7K6	275	0	D
4N/27W-7K6	285	0	D
4N/27W-7K6	295	0	D
4N/27W-7K6	305	0	D
4N/27W-7K6	315	0	D
4N/27W-7K6	325	0	D
4N/27W-7K6	335	0	D
4N/27W-7K6	345	0	D
4N/27W-7K6	355	0	D
4N/27W-7K6	365	0	D
4N/27W-7K6	375	0	D
4N/27W-7K6	385	0	D
4N/27W-7K6	395	60	D
4N/27W-7K6	405	100	D

Table B1–1. Calculated percent-coarse intervals for all drillers' logs and e-logs used to define textural properties of the hydrogeologic framework model.—Continued

[Percent-coarse values are calculated for 10-foot intervals for the entire depth of each borehole. State well number is the state of California well identifier; interval midpoint depth is the midpoint of each 10-foot interval, in feet from top of borehole; PC is the percent-coarse value for each interval; log type defines whether the borehole is a drillers' lithology log (D) or a geophysical e-log (E).]

State well number	Interval midpoint depth (feet)	PC	Log type
4N/27W-7K6	415	100	D
4N/27W-7K6	425	100	D
4N/27W-7K6	435	100	D
4N/27W-7K6	445	100	D
4N/27W-7K6	455	100	D
4N/27W-7K6	465	100	D
4N/27W-7K6	475	100	D
4N/27W-7K6	485	100	D
4N/27W-7K6	495	100	D
4N/27W-7K6	505	100	D
4N/27W-7K6	515	90	D
4N/27W-7K7	5	100	D
4N/27W-7K7	15	100	D
4N/27W-7K7	25	100	D
4N/27W-7K7	35	0	D
4N/27W-7K7	45	0	D
4N/27W-7K7	55	0	D
4N/27W-7K7	65	90	D
4N/27W-7K7	75	100	D
4N/27W-7K7	85	40	D
4N/27W-7K7	95	0	D
4N/27W-7K7	105	0	D
4N/27W-7K7	115	0	D
4N/27W-7K7	125	0	D
4N/27W-7K7	135	0	D
4N/27W-7K7	145	0	D
4N/27W-7K7	155	0	D
4N/27W-7K7	165	0	D
4N/27W-7K7	175	0	D
4N/27W-7K7	185	0	D
4N/27W-7K7	195	0	D
4N/27W-7K7	205	0	D
4N/27W-7K7	215	0	D
4N/27W-7K7	225	0	D
4N/27W-7K7	235	0	D
4N/27W-7K7	245	0	D
4N/27W-7K7	255	0	D
4N/27W-7K7	265	0	D
4N/27W-7K7	275	0	D
4N/27W-7K7	285	0	D
4N/27W-7K7	295	0	D
4N/27W-7K7	305	0	D
4N/27W-7K7	315	0	D
4N/27W-7K7	325	60	D
4N/27W-7K7	335	0	D
4N/27W-7K7	345	0	D
4N/27W-7K7	355	0	D
4N/27W-7K7	365	0	D
4N/27W-7K7	375	0	D
4N/27W-7K7	385	0	D
4N/27W-7K7	395	0	D
4N/27W-7K7	405	0	D
4N/27W-7K7	415	0	D
4N/27W-7K8	5	27.3	D
4N/27W-7K8	15	0	D
4N/27W-7K8	25	0	D
4N/27W-7K8	35	0	D
4N/27W-7K8	45	60	D
4N/27W-7K8	55	80	D
4N/27W-7K8	65	0	D
4N/27W-7K8	75	0	D
4N/27W-7K8	85	0	D
4N/27W-7K8	95	0	D
4N/27W-7K8	105	0	D
4N/27W-7K8	115	20	D
4N/27W-7K8	125	80	D
4N/27W-7K8	135	60	D
4N/27W-7K8	145	100	D
4N/27W-7K8	155	100	D
4N/27W-7K8	165	90	D
4N/27W-7K8	175	60	D
4N/27W-7K8	185	70	D
4N/27W-7K8	195	100	D
4N/27W-7K8	205	100	D
4N/27W-7K8	215	90.9	D
4N/27W-7K8	225	90	D
4N/27W-7K8	235	90	D
4N/27W-7K8	245	100	D

Table B1–1. Calculated percent-coarse intervals for all drillers' logs and e-logs used to define textural properties of the hydrogeologic framework model.—Continued

[Percent-coarse values are calculated for 10-foot intervals for the entire depth of each borehole. State well number is the state of California well identifier; interval midpoint depth is the midpoint of each 10-foot interval, in feet from top of borehole; PC is the percent-coarse value for each interval; log type defines whether the borehole is a drillers' lithology log (D) or a geophysical e-log (E).]

State well number	Interval midpoint depth (feet)	PC	Log type
4N/27W-7K8	255	30	D
4N/27W-7K8	265	50	D
4N/27W-7K8	275	40	D
4N/27W-7K8	285	90	D
4N/27W-7K8	295	45.5	D
4N/27W-7K8	305	30	D
4N/27W-7L1	5	9.1	D
4N/27W-7L1	15	0	D
4N/27W-7L1	25	0	D
4N/27W-7L1	35	0	D
4N/27W-7L1	45	0	D
4N/27W-7L1	55	0	D
4N/27W-7L1	65	0	D
4N/27W-7L1	75	0	D
4N/27W-7L1	85	0	D
4N/27W-7L1	95	0	D
4N/27W-7L1	105	0	D
4N/27W-7L1	115	0	D
4N/27W-7L1	125	0	D
4N/27W-7L1	135	0	D
4N/27W-7L3	5	72.7	D
4N/27W-7L3	15	0	D
4N/27W-7L3	25	0	D
4N/27W-7L3	35	100	D
4N/27W-7L3	45	0	D
4N/27W-7L3	55	0	D
4N/27W-7L3	65	20	D
4N/27W-7L3	75	90	D
4N/27W-7L3	85	0	D
4N/27W-7L3	95	30	D
4N/27W-7L3	105	40	D
4N/27W-7L3	115	0	D
4N/27W-7L4	5	100	D
4N/27W-7L4	15	40	D
4N/27W-7L4	25	10	D
4N/27W-7L4	35	50	D
4N/27W-7L4	45	50	D
4N/27W-7L4	55	90	D
4N/27W-7L4	65	30	D
4N/27W-7L4	75	60	D
4N/27W-7L4	85	10	D
4N/27W-7L4	95	0	D
4N/27W-7L4	105	0	D
4N/27W-7L4	115	0	D
4N/27W-7L4	125	50	D
4N/27W-7L4	135	80	D
4N/27W-7L4	145	60	D
4N/27W-7L4	155	80	D
4N/27W-7L7	5	45.5	D
4N/27W-7L7	15	0	D
4N/27W-7L7	25	20	D
4N/27W-7L7	35	30	D
4N/27W-7L7	45	80	D
4N/27W-7L7	55	100	D
4N/27W-7L7	65	30	D
4N/27W-7L7	75	50	D
4N/27W-7L7	85	0	D
4N/27W-7L7	95	70	D
4N/27W-7L7	105	100	D
4N/27W-7L7	115	100	D
4N/27W-7L7	125	90	D
4N/27W-7L10	5	18.2	D
4N/27W-7L10	15	0	D
4N/27W-7L10	25	0	D
4N/27W-7L10	35	0	D
4N/27W-7L10	45	0	D
4N/27W-7L10	55	0	D
4N/27W-7L10	65	0	D
4N/27W-7L10	75	0	D
4N/27W-7L10	85	0	D
4N/27W-7L10	95	0	D
4N/27W-7L10	105	0	D
4N/27W-7L10	115	0	D
4N/27W-7L10	125	0	D
4N/27W-7L10	135	0	D
4N/27W-7L10	145	0	D
4N/27W-7L10	155	0	D
4N/27W-7L10	165	0	D

Table B1–1. Calculated percent-coarse intervals for all drillers' logs and e-logs used to define textural properties of the hydrogeologic framework model.—Continued

[Percent-coarse values are calculated for 10-foot intervals for the entire depth of each borehole. State well number is the state of California well identifier; interval midpoint depth is the midpoint of each 10-foot interval, in feet from top of borehole; PC is the percent-coarse value for each interval; log type defines whether the borehole is a drillers' lithology log (D) or a geophysical e-log (E).]

State well number	Interval midpoint depth (feet)	PC	Log type
4N/27W-7L10	175	0	D
4N/27W-7L10	185	0	D
4N/27W-7L10	195	9.1	D
4N/27W-7L10	205	66.7	D
4N/27W-7L10	215	0	D
4N/27W-7L10	225	0	D
4N/27W-7L10	235	0	D
4N/27W-7L10	245	0	D
4N/27W-7L10	255	0	D
4N/27W-7L10	265	0	D
4N/27W-7L10	275	0	D
4N/27W-7L10	285	0	D
4N/27W-7L10	295	100	D
4N/27W-7L10	305	100	D
4N/27W-7L10	315	100	D
4N/27W-7L10	325	100	D
4N/27W-7L10	335	100	D
4N/27W-7L10	345	30	D
4N/27W-7L10	355	0	D
4N/27W-7L10	365	0	D
4N/27W-7L10	375	0	D
4N/27W-7L10	385	100	D
4N/27W-7L10	395	100	D
4N/27W-7L10	405	100	D
4N/27W-7L10	415	100	D
4N/27W-7L10	425	100	D
4N/27W-7L10	435	100	D
4N/27W-7L10	445	100	D
4N/27W-7L10	455	100	D
4N/27W-7L10	465	100	D
4N/27W-7L10	475	100	D
4N/27W-7L10	485	100	D
4N/27W-7L10	495	100	D
4N/27W-7L10	505	100	D
4N/27W-7L10	515	100	D
4N/27W-7L10	525	40	D
4N/27W-7L10	535	0	D
4N/27W-7L10	545	0	D
4N/27W-7L10	555	0	D
4N/27W-7L10	565	0	D
4N/27W-7L10	575	0	D
4N/27W-7L10	585	0	D
4N/27W-7M1	5	0	D
4N/27W-7M1	15	0	D
4N/27W-7M1	25	0	D
4N/27W-7M1	35	0	D
4N/27W-7M1	45	0	D
4N/27W-7M1	55	0	D
4N/27W-7M1	65	0	D
4N/27W-7M1	75	40	D
4N/27W-7M1	85	0	D
4N/27W-7M1	95	0	D
4N/27W-7M1	105	0	D
4N/27W-7M1	115	0	D
4N/27W-7M1	125	0	D
4N/27W-7M1	135	0	D
4N/27W-7M1	145	0	D
4N/27W-7M1	155	0	D
4N/27W-7M1	165	50	D
4N/27W-7M1	175	20	D
4N/27W-7M1	185	0	D
4N/27W-7M1	195	0	D
4N/27W-7M1	205	0	D
4N/27W-7M1	215	0	D
4N/27W-7M1	225	0	D
4N/27W-7M1	235	0	D
4N/27W-7Q1	45	60	D
4N/27W-7Q1	55	10	D
4N/27W-7Q1	65	44.4	D
4N/27W-7Q1	75	0	D
4N/27W-7Q1	85	0	D
4N/27W-7Q1	95	60	D
4N/27W-7Q1	105	90	D
4N/27W-7Q1	115	0	D
4N/27W-7Q1	125	55.6	D
4N/27W-7Q1	135	50	D
4N/27W-7Q1	145	45.5	D
4N/27W-7Q1	155	10	D

Table B1–1. Calculated percent-coarse intervals for all drillers' logs and e-logs used to define textural properties of the hydrogeologic framework model.—Continued

[Percent-coarse values are calculated for 10-foot intervals for the entire depth of each borehole. State well number is the state of California well identifier; interval midpoint depth is the midpoint of each 10-foot interval, in feet from top of borehole; PC is the percent-coarse value for each interval; log type defines whether the borehole is a drillers' lithology log (D) or a geophysical e-log (E).]

State well number	Interval midpoint depth (feet)	PC	Log type
4N/27W-7Q1	165	100	D
4N/27W-7Q1	175	100	D
4N/27W-7Q1	185	50	D
4N/27W-7Q1	195	0	D
4N/27W-7Q2	5	100	D
4N/27W-7Q2	15	100	D
4N/27W-7Q2	25	90	D
4N/27W-7Q2	35	90	D
4N/27W-7Q2	45	10	D
4N/27W-7Q2	55	50	D
4N/27W-7Q2	65	0	D
4N/27W-7Q2	75	54.5	D
4N/27W-7Q2	85	100	D
4N/27W-7Q2	95	100	D
4N/27W-7Q2	105	50	D
4N/27W-7Q2	115	100	D
4N/27W-7Q2	125	100	D
4N/27W-7Q2	135	100	D
4N/27W-7Q2	145	90.9	D
4N/27W-7Q2	155	0	D
4N/27W-7Q3	5	54.5	D
4N/27W-7Q3	15	90	D
4N/27W-7Q3	25	80	D
4N/27W-7Q3	35	0	D
4N/27W-7Q3	45	0	D
4N/27W-7Q3	55	10	D
4N/27W-7Q3	65	100	D
4N/27W-7Q3	75	100	D
4N/27W-7Q3	85	100	D
4N/27W-7Q3	95	100	D
4N/27W-7Q3	105	100	D
4N/27W-7Q3	115	20	D
4N/27W-7Q3	125	100	D
4N/27W-7Q3	135	100	D
4N/27W-7Q3	145	100	D
4N/27W-7Q3	155	100	D
4N/27W-7Q3	165	100	D
4N/27W-7Q3	175	100	D
4N/27W-7Q3	185	100	D
4N/27W-7Q3	195	72.7	D
4N/27W-7Q3	205	0	D
4N/27W-7Q3	215	54.5	D
4N/27W-7R3	45	0	D
4N/27W-7R3	55	0	D
4N/27W-7R3	65	0	D
4N/27W-7R3	75	9.1	D
4N/27W-7R3	85	100	D
4N/27W-7R3	95	100	D
4N/27W-7R3	105	90	D
4N/27W-7R3	115	0	D
4N/27W-7R3	125	0	D
4N/27W-7R3	135	100	D
4N/27W-7R3	145	100	D
4N/27W-7R3	155	90	D
4N/27W-7R3	165	0	D
4N/27W-7R3	175	100	D
4N/27W-7R3	185	100	D
4N/27W-7R3	195	90.9	D
4N/27W-7R3	205	0	D
4N/27W-7R3	215	0	D
4N/27W-7R3	225	0	D
4N/27W-8E4	5	100	D
4N/27W-8E4	15	100	D
4N/27W-8E4	25	100	D
4N/27W-8E4	35	100	D
4N/27W-8E4	45	100	D
4N/27W-8E4	55	100	D
4N/27W-8E4	65	100	D
4N/27W-8E4	75	100	D
4N/27W-8E4	85	100	D
4N/27W-8E4	95	100	D
4N/27W-8E4	105	100	D
4N/27W-8E4	115	90	D
4N/27W-8E4	125	0	D
4N/27W-8E4	135	0	D
4N/27W-8E4	145	0	D
4N/27W-8E4	155	10	D
4N/27W-8E4	165	100	D

Table B1–1. Calculated percent-coarse intervals for all drillers' logs and e-logs used to define textural properties of the hydrogeologic framework model.—Continued

[Percent-coarse values are calculated for 10-foot intervals for the entire depth of each borehole. State well number is the state of California well identifier; interval midpoint depth is the midpoint of each 10-foot interval, in feet from top of borehole; PC is the percent-coarse value for each interval; log type defines whether the borehole is a drillers' lithology log (D) or a geophysical e-log (E).]

State well number	Interval midpoint depth (feet)	PC	Log type
4N/27W-8E4	175	90	D
4N/27W-8E4	185	0	D
4N/27W-8E4	195	0	D
4N/27W-8E4	205	0	D
4N/27W-8E4	215	0	D
4N/27W-8E4	225	0	D
4N/27W-8E4	235	0	D
4N/27W-8E4	245	0	D
4N/27W-8E4	255	0	D
4N/27W-8E4	265	0	D
4N/27W-8E4	275	0	D
4N/27W-8E4	285	0	D
4N/27W-8E4	295	100	D
4N/27W-8E4	305	100	D
4N/27W-8E4	315	100	D
4N/27W-8E4	325	90	D
4N/27W-8E4	335	0	D
4N/27W-8E4	345	0	D
4N/27W-8E4	355	0	D
4N/27W-8E4	365	0	D
4N/27W-8E4	375	0	D
4N/27W-8E4	385	9.1	D
4N/27W-8E4	395	100	D
4N/27W-8E4	405	100	D
4N/27W-8E4	415	100	D
4N/27W-8E4	425	9.1	D
4N/27W-8E4	435	100	D
4N/27W-8E4	445	100	D
4N/27W-8E4	455	100	D
4N/27W-8E4	465	90	D
4N/27W-8E4	475	0	D
4N/27W-8E4	485	0	D
4N/27W-8E4	495	0	D
4N/27W-8E4	505	0	D
4N/27W-8E4	515	0	D
4N/27W-8E4	525	10	D
4N/27W-8E4	535	100	D
4N/27W-8E4	545	100	D
4N/27W-8E4	555	100	D
4N/27W-8E4	565	0	D
4N/27W-8E4	575	0	D
4N/27W-8E4	585	0	D
4N/27W-8E4	595	0	D
4N/27W-8J1	5	100	D
4N/27W-8J1	15	100	D
4N/27W-8J1	25	100	D
4N/27W-8J1	35	100	D
4N/27W-8J1	45	90	D
4N/27W-8J1	55	0	D
4N/27W-8J1	65	30	D
4N/27W-8J1	75	90	D
4N/27W-8J1	85	0	D
4N/27W-8J1	95	0	D
4N/27W-8J1	105	50	D
4N/27W-8J1	115	0	D
4N/27W-8J1	125	0	D
4N/27W-8J1	135	0	D
4N/27W-8J1	145	0	D
4N/27W-8J1	155	0	D
4N/27W-8J1	165	0	D
4N/27W-8J1	175	90	D
4N/27W-8J1	185	11.1	D
4N/27W-8J1	195	30	D
4N/27W-8J1	205	60	D
4N/27W-8J1	215	45.5	D
4N/27W-8J1	225	30	D
4N/27W-8J1	235	40	D
4N/27W-8J1	245	0	D
4N/27W-8J1	255	50	D
4N/27W-8J1	265	40	D
4N/27W-8J1	275	0	D
4N/27W-8J1	285	0	D
4N/27W-8J1	295	54.5	D
4N/27W-8J1	305	10	D
4N/27W-8J1	315	0	D
4N/27W-8J1	325	40	D
4N/27W-8J1	335	30	D
4N/27W-8J1	345	66.7	D

Table B1–1. Calculated percent-coarse intervals for all drillers' logs and e-logs used to define textural properties of the hydrogeologic framework model.—Continued

[Percent-coarse values are calculated for 10-foot intervals for the entire depth of each borehole. State well number is the state of California well identifier; interval midpoint depth is the midpoint of each 10-foot interval, in feet from top of borehole; PC is the percent-coarse value for each interval; log type defines whether the borehole is a drillers' lithology log (D) or a geophysical e-log (E).]

State well number	Interval midpoint depth (feet)	PC	Log type
4N/27W-8J1	355	50	D
4N/27W-8J1	365	0	D
4N/27W-8J1	375	90	D
4N/27W-8J1	385	100	D
4N/27W-8J1	395	40	D
4N/27W-8J1	405	20	D
4N/27W-8J1	415	77.8	D
4N/27W-8J1	425	0	D
4N/27W-8J1	435	0	D
4N/27W-8J1	445	0	D
4N/27W-8J1	455	0	D
4N/27W-8J1	465	0	D
4N/27W-8J1	475	0	D
4N/27W-8J1	485	0	D
4N/27W-8J1	495	20	D
4N/27W-8J1	505	20	D
4N/27W-8J1	515	100	D
4N/27W-8J1	525	100	D
4N/27W-8J1	535	100	D
4N/27W-8J1	545	100	D
4N/27W-8J1	555	100	D
4N/27W-8J1	565	40	D
4N/27W-8J1	575	0	D
4N/27W-8J1	585	0	D
4N/27W-8J1	595	0	D
4N/27W-8J1	605	0	D
4N/27W-8J1	615	0	D
4N/27W-8J1	625	0	D
4N/27W-8J1	635	0	D
4N/27W-8J1	645	100	D
4N/27W-8J1	655	80	D
4N/27W-8J1	665	50	D
4N/27W-8L3	65	0	D
4N/27W-8L3	75	0	D
4N/27W-8L3	85	0	D
4N/27W-8L3	95	0	D
4N/27W-8L3	105	0	D
4N/27W-8L3	115	0	D
4N/27W-8L3	125	0	D
4N/27W-8L3	135	0	D
4N/27W-8L3	145	0	D
4N/27W-8L3	155	0	D
4N/27W-8L3	165	0	D
4N/27W-8L3	175	0	D
4N/27W-8L3	185	0	D
4N/27W-8L3	195	0	D
4N/27W-8L3	205	0	D
4N/27W-8L3	215	0	D
4N/27W-8L3	225	0	D
4N/27W-8L3	235	0	D
4N/27W-8L3	245	0	D
4N/27W-8L3	255	0	D
4N/27W-8L3	265	0	D
4N/27W-8L3	275	0	D
4N/27W-8L3	285	0	D
4N/27W-8L3	295	0	D
4N/27W-8L3	305	0	D
4N/27W-8L3	315	0	D
4N/27W-8L3	325	0	D
4N/27W-8L3	335	0	D
4N/27W-8L3	345	0	D
4N/27W-8L3	355	0	D
4N/27W-8L3	365	0	D
4N/27W-8L3	375	0	D
4N/27W-8L3	385	0	D
4N/27W-8L3	395	0	D
4N/27W-8L3	405	0	D
4N/27W-8L3	415	0	D
4N/27W-8L3	425	0	D
4N/27W-8L3	435	0	D
4N/27W-8L3	445	0	D
4N/27W-8L3	455	0	D
4N/27W-8L3	465	0	D
4N/27W-8L3	475	0	D
4N/27W-8L3	485	0	D
4N/27W-8L3	495	0	D
4N/27W-8L3	505	0	D
4N/27W-8L3	515	0	D

Table B1–1. Calculated percent-coarse intervals for all drillers' logs and e-logs used to define textural properties of the hydrogeologic framework model.—Continued

[Percent-coarse values are calculated for 10-foot intervals for the entire depth of each borehole. State well number is the state of California well identifier; interval midpoint depth is the midpoint of each 10-foot interval, in feet from top of borehole; PC is the percent-coarse value for each interval; log type defines whether the borehole is a drillers' lithology log (D) or a geophysical e-log (E).]

State well number	Interval midpoint depth (feet)	PC	Log type
4N/27W-8L3	525	0	D
4N/27W-8L3	535	0	D
4N/27W-8L3	545	50	D
4N/27W-8L3	555	100	D
4N/27W-8L3	565	100	D
4N/27W-8L3	575	0	D
4N/27W-8L3	585	0	D
4N/27W-8L3	595	0	D
4N/27W-8L3	605	0	D
4N/27W-8L3	615	0	D
4N/27W-8L3	625	0	D
4N/27W-8M1	5	100	D
4N/27W-8M1	15	10	D
4N/27W-8M1	25	0	D
4N/27W-8M1	35	0	D
4N/27W-8M1	45	0	D
4N/27W-8M1	55	0	D
4N/27W-8M1	65	0	D
4N/27W-8M1	75	0	D
4N/27W-8M1	85	0	D
4N/27W-8M1	95	0	D
4N/27W-8M1	105	0	D
4N/27W-8M1	115	0	D
4N/27W-8M1	125	0	D
4N/27W-8M1	135	0	D
4N/27W-8M3	5	9.1	D
4N/27W-8M3	15	0	D
4N/27W-8M3	25	0	D
4N/27W-8M3	35	0	D
4N/27W-8M3	45	0	D
4N/27W-8M3	55	0	D
4N/27W-8M3	65	0	D
4N/27W-8M3	75	0	D
4N/27W-8M3	85	0	D
4N/27W-8M3	95	0	D
4N/27W-8M3	105	0	D
4N/27W-8M3	115	0	D
4N/27W-8M3	125	0	D
4N/27W-8M3	135	0	D
4N/27W-8M3	145	0	D
4N/27W-8M3	155	0	D
4N/27W-8M3	165	0	D
4N/27W-8M3	175	0	D
4N/27W-8M3	185	80	D
4N/27W-8R1	5	100	D
4N/27W-8R1	15	100	D
4N/27W-8R1	25	50	D
4N/27W-8R1	35	0	D
4N/27W-8R1	45	30	D
4N/27W-8R1	55	100	D
4N/27W-8R1	65	70	D
4N/27W-8R1	75	100	D
4N/27W-8R1	85	50	D
4N/27W-8R1	95	0	D
4N/27W-8R1	105	0	D
4N/27W-8R1	115	0	D
4N/27W-8R1	125	0	D
4N/27W-8R1	135	0	D
4N/27W-8R1	145	0	D
4N/27W-8R1	155	0	D
4N/27W-8R1	165	0	D
4N/27W-8R1	175	0	D
4N/27W-8R1	185	100	D
4N/27W-8R1	195	100	D
4N/27W-8R1	205	100	D
4N/27W-8R1	215	100	D
4N/27W-8R1	225	90	D
4N/27W-8R1	235	0	D
4N/27W-8R1	245	0	D
4N/27W-8R1	255	0	D
4N/27W-9Q1	5	0	D
4N/27W-9Q1	15	0	D
4N/27W-9Q1	25	0	D
4N/27W-9Q1	35	60	D
4N/27W-9Q1	45	100	D
4N/27W-9Q1	55	10	D
4N/27W-9Q1	65	0	D
4N/27W-9Q1	75	0	D

Table B1–1. Calculated percent-coarse intervals for all drillers' logs and e-logs used to define textural properties of the hydrogeologic framework model.—Continued

[Percent-coarse values are calculated for 10-foot intervals for the entire depth of each borehole. State well number is the state of California well identifier; interval midpoint depth is the midpoint of each 10-foot interval, in feet from top of borehole; PC is the percent-coarse value for each interval; log type defines whether the borehole is a drillers' lithology log (D) or a geophysical e-log (E).]

State well number	Interval midpoint depth (feet)	PC	Log type
4N/27W-9Q1	85	0	D
4N/27W-9Q1	95	0	D
4N/27W-9Q1	105	0	D
4N/27W-9Q1	115	0	D
4N/27W-9Q1	125	0	D
4N/27W-9Q1	135	0	D
4N/27W-9Q1	145	0	D
4N/27W-9Q1	155	0	D
4N/27W-9Q1	165	0	D
4N/27W-9Q1	175	0	D
4N/27W-9Q1	185	0	D
4N/27W-9Q1	195	0	D
4N/27W-9Q1	205	0	D
4N/27W-9Q1	215	0	D
4N/27W-9Q1	225	0	D
4N/27W-9Q1	235	0	D
4N/27W-9Q1	245	0	D
4N/27W-9Q1	255	0	D
4N/27W-14K1	5	45.5	D
4N/27W-14K1	15	0	D
4N/27W-14K1	25	0	D
4N/27W-14K1	35	0	D
4N/27W-14K1	45	0	D
4N/27W-14K1	55	0	D
4N/27W-14K1	65	0	D
4N/27W-14K1	75	0	D
4N/27W-14K1	85	0	D
4N/27W-14K1	95	0	D
4N/27W-14K1	105	0	D
4N/27W-14K1	115	0	D
4N/27W-14K1	125	0	D
4N/27W-14K1	135	0	D
4N/27W-14K1	145	0	D
4N/27W-14K1	155	0	D
4N/27W-14K1	165	0	D
4N/27W-14K1	175	0	D
4N/27W-14K1	185	0	D
4N/27W-14K1	195	0	D
4N/27W-14K1	205	0	D
4N/27W-14K1	215	0	D
4N/27W-14K1	225	0	D
4N/27W-14K1	235	0	D
4N/27W-14K1	245	10	D
4N/27W-14K1	255	100	D
4N/27W-14K1	265	100	D
4N/27W-14K1	275	100	D
4N/27W-14K1	285	100	D
4N/27W-14K1	295	100	D
4N/27W-14K1	305	100	D
4N/27W-14K1	315	100	D
4N/27W-14K1	325	100	D
4N/27W-14K1	335	100	D
4N/27W-14K1	345	100	D
4N/27W-14K1	355	100	D
4N/27W-14K1	365	100	D
4N/27W-14K1	375	100	D
4N/27W-14K1	385	100	D
4N/27W-14K1	395	100	D
4N/27W-14K1	405	100	D
4N/27W-14K1	415	100	D
4N/27W-14K1	425	100	D
4N/27W-14K1	435	100	D
4N/27W-14K1	445	100	D
4N/27W-14K1	455	100	D
4N/27W-14K1	465	100	D
4N/27W-14K1	475	100	D
4N/27W-14K1	485	100	D
4N/27W-14K1	495	100	D
4N/27W-14K1	505	100	D
4N/27W-14K1	515	100	D
4N/27W-14K1	525	100	D
4N/27W-14K1	535	100	D
4N/27W-14K1	545	100	D
4N/27W-14K1	555	100	D
4N/27W-14K1	565	0	D
4N/27W-14K1	575	0	D
4N/27W-14K1	585	0	D
4N/27W-14K1	595	0	D

Table B1–1. Calculated percent-coarse intervals for all drillers' logs and e-logs used to define textural properties of the hydrogeologic framework model.—Continued

[Percent-coarse values are calculated for 10-foot intervals for the entire depth of each borehole. State well number is the state of California well identifier; interval midpoint depth is the midpoint of each 10-foot interval, in feet from top of borehole; PC is the percent-coarse value for each interval; log type defines whether the borehole is a drillers' lithology log (D) or a geophysical e-log (E).]

State well number	Interval midpoint depth (feet)	PC	Log type
4N/27W-14K1	605	0	D
4N/27W-14K1	615	0	D
4N/27W-14K1	625	0	D
4N/27W-14K1	635	0	D
4N/27W-14K1	645	0	D
4N/27W-14N1	5	100	D
4N/27W-14N1	15	50	D
4N/27W-14N1	25	0	D
4N/27W-14N1	35	0	D
4N/27W-14N1	45	0	D
4N/27W-14N1	55	0	D
4N/27W-14N1	65	0	D
4N/27W-14N1	75	0	D
4N/27W-14N1	85	0	D
4N/27W-14N1	95	0	D
4N/27W-14N1	105	0	D
4N/27W-14N1	115	0	D
4N/27W-14N1	125	0	D
4N/27W-14N1	135	10	D
4N/27W-14N1	145	100	D
4N/27W-14N1	155	90	D
4N/27W-14N1	165	60	D
4N/27W-14N1	175	70	D
4N/27W-14N1	185	0	D
4N/27W-14N1	195	0	D
4N/27W-14N1	205	0	D
4N/27W-14N1	215	0	D
4N/27W-14N1	225	0	D
4N/27W-14N1	235	0	D
4N/27W-14N1	245	0	D
4N/27W-14N1	255	0	D
4N/27W-14N1	265	0	D
4N/27W-14N1	275	50	D
4N/27W-14N1	285	20	D
4N/27W-14N1	295	0	D
4N/27W-14N1	305	0	D
4N/27W-14N1	315	0	D
4N/27W-14N1	325	0	D
4N/27W-14N1	335	0	D
4N/27W-14N1	345	0	D
4N/27W-14N1	355	0	D
4N/27W-14N1	365	0	D
4N/27W-14N1	375	0	D
4N/27W-14N1	385	0	D
4N/27W-14N1	395	0	D
4N/27W-14N1	405	0	D
4N/27W-14N1	415	0	D
4N/27W-14N1	425	0	D
4N/27W-14N1	435	0	D
4N/27W-14N1	445	0	D
4N/27W-14N1	455	0	D
4N/27W-14N1	465	0	D
4N/27W-14N1	475	0	D
4N/27W-14N1	485	0	D
4N/27W-14P2	5	0	D
4N/27W-14P2	15	0	D
4N/27W-14P2	25	0	D
4N/27W-14P2	35	0	D
4N/27W-14P2	45	0	D
4N/27W-14P2	55	0	D
4N/27W-14P2	65	0	D
4N/27W-14P2	75	0	D
4N/27W-14P2	85	0	D
4N/27W-14P2	95	0	D
4N/27W-14P2	105	0	D
4N/27W-14P2	115	0	D
4N/27W-14P2	125	0	D
4N/27W-14P2	135	0	D
4N/27W-14P2	145	0	D
4N/27W-14P2	155	0	D
4N/27W-14P2	165	0	D
4N/27W-14P2	175	0	D
4N/27W-14P2	185	0	D
4N/27W-14P2	195	0	D
4N/27W-14P2	205	0	D
4N/27W-14P2	215	0	D
4N/27W-14P2	225	0	D
4N/27W-14P2	235	0	D

Table B1–1. Calculated percent-coarse intervals for all drillers' logs and e-logs used to define textural properties of the hydrogeologic framework model.—Continued

[Percent-coarse values are calculated for 10-foot intervals for the entire depth of each borehole. State well number is the state of California well identifier; interval midpoint depth is the midpoint of each 10-foot interval, in feet from top of borehole; PC is the percent-coarse value for each interval; log type defines whether the borehole is a drillers' lithology log (D) or a geophysical e-log (E).]

State well number	Interval midpoint depth (feet)	PC	Log type
4N/27W-14P2	245	0	D
4N/27W-14P2	255	0	D
4N/27W-14P2	265	0	D
4N/27W-14P2	275	0	D
4N/27W-14P2	285	0	D
4N/27W-14P2	295	0	D
4N/27W-14P2	305	0	D
4N/27W-14Q1	5	100	D
4N/27W-14Q1	15	100	D
4N/27W-14Q1	25	100	D
4N/27W-14Q1	35	100	D
4N/27W-14Q1	45	100	D
4N/27W-14Q1	55	100	D
4N/27W-14Q1	65	100	D
4N/27W-14Q1	75	90.9	D
4N/27W-14Q1	85	0	D
4N/27W-14Q1	95	54.5	D
4N/27W-14Q1	105	100	D
4N/27W-14Q1	115	100	D
4N/27W-14Q1	125	100	D
4N/27W-14Q1	135	0	D
4N/27W-14Q1	145	0	D
4N/27W-14Q1	155	0	D
4N/27W-14Q1	165	0	D
4N/27W-14Q1	175	0	D
4N/27W-14Q1	185	0	D
4N/27W-14Q1	195	0	D
4N/27W-14Q1	205	0	D
4N/27W-14Q1	215	0	D
4N/27W-14Q1	225	0	D
4N/27W-14Q1	235	0	D
4N/27W-14Q1	245	0	D
4N/27W-14Q1	255	0	D
4N/27W-14Q1	265	0	D
4N/27W-14Q1	275	0	D
4N/27W-14Q1	285	100	D
4N/27W-14Q1	295	100	D
4N/27W-14Q1	305	100	D
4N/27W-14Q1	315	100	D
4N/27W-14Q1	325	100	D
4N/27W-14Q1	335	100	D
4N/27W-14Q1	345	100	D
4N/27W-14Q1	355	100	D
4N/27W-14Q1	365	100	D
4N/27W-14Q1	375	100	D
4N/27W-14Q1	385	100	D
4N/27W-14Q1	395	100	D
4N/27W-14Q1	405	100	D
4N/27W-14Q1	415	100	D
4N/27W-14Q1	425	100	D
4N/27W-14Q1	435	100	D
4N/27W-14Q1	445	100	D
4N/27W-14Q1	455	100	D
4N/27W-14Q1	465	100	D
4N/27W-14Q1	475	100	D
4N/27W-14Q1	485	100	D
4N/27W-14Q1	495	100	D
4N/27W-14Q1	505	100	D
4N/27W-14Q1	515	100	D
4N/27W-14Q1	525	100	D
4N/27W-14Q1	535	100	D
4N/27W-14Q1	545	90	D
4N/27W-14Q1	555	0	D
4N/27W-14Q1	565	60	D
4N/27W-14Q1	575	100	D
4N/27W-14Q1	585	100	D
4N/27W-14Q1	595	100	D
4N/27W-14Q1	605	100	D
4N/27W-14Q1	615	100	D
4N/27W-14Q1	625	100	D
4N/27W-14Q1	635	100	D
4N/27W-14Q1	645	100	D
4N/27W-14Q1	655	100	D
4N/27W-14Q1	665	100	D
4N/27W-14Q1	675	100	D
4N/27W-14Q1	685	100	D
4N/27W-15E2	5	0	D
4N/27W-15E2	15	0	D

Table B1–1. Calculated percent-coarse intervals for all drillers' logs and e-logs used to define textural properties of the hydrogeologic framework model.—Continued

[Percent-coarse values are calculated for 10-foot intervals for the entire depth of each borehole. State well number is the state of California well identifier; interval midpoint depth is the midpoint of each 10-foot interval, in feet from top of borehole; PC is the percent-coarse value for each interval; log type defines whether the borehole is a drillers' lithology log (D) or a geophysical e-log (E).]

State well number	Interval midpoint depth (feet)	PC	Log type
4N/27W-15E2	25	0	D
4N/27W-15E2	35	0	D
4N/27W-15E2	45	10	D
4N/27W-15E2	55	100	D
4N/27W-15E2	65	100	D
4N/27W-15E2	75	100	D
4N/27W-15E2	85	100	D
4N/27W-15E2	95	90.9	D
4N/27W-15E2	105	0	D
4N/27W-15E2	115	0	D
4N/27W-15E2	125	0	D
4N/27W-15E2	135	0	D
4N/27W-15E2	145	0	D
4N/27W-15E2	155	0	D
4N/27W-15E2	165	0	D
4N/27W-15E2	175	100	D
4N/27W-15E2	185	100	D
4N/27W-15E2	195	100	D
4N/27W-15E2	205	100	D
4N/27W-15E2	215	100	D
4N/27W-15E2	225	100	D
4N/27W-15E2	235	100	D
4N/27W-15E2	245	100	D
4N/27W-15E2	255	90	D
4N/27W-15E2	265	0	D
4N/27W-15E2	275	0	D
4N/27W-15E2	285	100	D
4N/27W-15E2	295	100	D
4N/27W-15E2	305	100	D
4N/27W-15E2	315	100	D
4N/27W-15E2	325	100	D
4N/27W-15E2	335	100	D
4N/27W-15E2	345	100	D
4N/27W-15E2	355	90	D
4N/27W-15E2	365	0	D
4N/27W-15E2	375	0	D
4N/27W-15E2	385	0	D
4N/27W-15E2	395	0	D
4N/27W-15E2	405	0	D
4N/27W-15E2	415	0	D
4N/27W-15E2	425	54.5	D
4N/27W-15E2	435	100	D
4N/27W-15E2	445	100	D
4N/27W-15E2	455	100	D
4N/27W-15E2	465	100	D
4N/27W-15E2	475	90	D
4N/27W-15E2	485	0	D
4N/27W-15E2	495	0	D
4N/27W-15E2	505	0	D
4N/27W-15E2	515	0	D
4N/27W-15E2	525	0	D
4N/27W-15G1	5	100	D
4N/27W-15G1	15	100	D
4N/27W-15G1	25	100	D
4N/27W-15G1	35	90	D
4N/27W-15G1	45	0	D
4N/27W-15G1	55	0	D
4N/27W-15G1	65	0	D
4N/27W-15G1	75	0	D
4N/27W-15G1	85	0	D
4N/27W-15G1	95	0	D
4N/27W-15G1	105	0	D
4N/27W-15G1	115	0	D
4N/27W-15G1	125	0	D
4N/27W-15G1	135	0	D
4N/27W-15G1	145	0	D
4N/27W-15G1	155	0	D
4N/27W-15G1	165	0	D
4N/27W-15G1	175	0	D
4N/27W-15G1	185	0	D
4N/27W-15G1	195	0	D
4N/27W-15G1	205	0	D
4N/27W-15G1	215	100	D
4N/27W-15G1	225	100	D
4N/27W-15G1	235	100	D
4N/27W-15G1	245	100	D
4N/27W-15G1	255	100	D
4N/27W-15G1	265	0	D

Table B1–1. Calculated percent-coarse intervals for all drillers' logs and e-logs used to define textural properties of the hydrogeologic framework model.—Continued

[Percent-coarse values are calculated for 10-foot intervals for the entire depth of each borehole. State well number is the state of California well identifier; interval midpoint depth is the midpoint of each 10-foot interval, in feet from top of borehole; PC is the percent-coarse value for each interval; log type defines whether the borehole is a drillers' lithology log (D) or a geophysical e-log (E).]

State well number	Interval midpoint depth (feet)	PC	Log type
4N/27W-15G1	275	0	D
4N/27W-15G1	285	0	D
4N/27W-15G1	295	100	D
4N/27W-15G1	305	90	D
4N/27W-15J2	5	9.1	D
4N/27W-15J2	15	0	D
4N/27W-15J2	25	0	D
4N/27W-15J2	35	20	D
4N/27W-15J2	45	0	D
4N/27W-15J2	55	0	D
4N/27W-15J2	65	0	D
4N/27W-15J2	75	80	D
4N/27W-15J2	85	20	D
4N/27W-15J2	95	90	D
4N/27W-15J2	105	100	D
4N/27W-15J2	115	50	D
4N/27W-15J2	125	0	D
4N/27W-15J2	135	0	D
4N/27W-15J2	145	0	D
4N/27W-15J2	155	0	D
4N/27W-15J2	165	0	D
4N/27W-15J2	175	0	D
4N/27W-15J2	185	0	D
4N/27W-15J2	195	45.5	D
4N/27W-15J2	205	100	D
4N/27W-15J2	215	18.2	D
4N/27W-15J2	225	0	D
4N/27W-15J2	235	0	D
4N/27W-15J2	245	10	D
4N/27W-15J2	255	100	D
4N/27W-15J2	265	10	D
4N/27W-15J2	275	0	D
4N/27W-15J2	285	0	D
4N/27W-15J2	295	0	D
4N/27W-15J2	305	0	D
4N/27W-15J2	315	0	D
4N/27W-15J2	325	30	D
4N/27W-15J2	335	0	D
4N/27W-15J2	345	0	D
4N/27W-15J2	355	0	D
4N/27W-15J2	365	0	D
4N/27W-15J2	375	0	D
4N/27W-15J2	385	0	D
4N/27W-15J2	395	0	D
4N/27W-15J2	405	0	D
4N/27W-15J2	415	0	D
4N/27W-15J2	425	0	D
4N/27W-15J2	435	30	D
4N/27W-15J2	445	0	D
4N/27W-15J2	455	0	D
4N/27W-15J2	465	0	D
4N/27W-15J2	475	0	D
4N/27W-15J2	485	0	D
4N/27W-15J2	495	0	D
4N/27W-15J2	505	0	D
4N/27W-15J2	515	0	D
4N/27W-15J2	525	50	D
4N/27W-15J2	535	20	D
4N/27W-15J2	545	0	D
4N/27W-15J2	555	0	D
4N/27W-15J2	565	0	D
4N/27W-15J2	575	0	D
4N/27W-15J2	585	0	D
4N/27W-15J2	595	27.3	D
4N/27W-15J2	605	0	D
4N/27W-15J2	615	0	D
4N/27W-15J2	625	0	D
4N/27W-15Q1	5	0	D
4N/27W-15Q1	15	0	D
4N/27W-15Q1	25	0	D
4N/27W-15Q1	35	0	D
4N/27W-15Q1	45	0	D
4N/27W-15Q1	55	0	D
4N/27W-15Q1	65	0	D
4N/27W-15Q1	75	0	D
4N/27W-15Q1	85	40	D
4N/27W-15Q1	95	22.2	D
4N/27W-15Q1	105	63.6	D

Table B1–1. Calculated percent-coarse intervals for all drillers' logs and e-logs used to define textural properties of the hydrogeologic framework model.—Continued

[Percent-coarse values are calculated for 10-foot intervals for the entire depth of each borehole. State well number is the state of California well identifier; interval midpoint depth is the midpoint of each 10-foot interval, in feet from top of borehole; PC is the percent-coarse value for each interval; log type defines whether the borehole is a drillers' lithology log (D) or a geophysical e-log (E).]

State well number	Interval midpoint depth (feet)	PC	Log type
4N/27W-15Q1	115	100	D
4N/27W-15Q1	125	20	D
4N/27W-15Q1	135	0	D
4N/27W-15Q1	145	20	D
4N/27W-15Q1	155	90	D
4N/27W-15Q1	165	50	D
4N/27W-15Q1	175	80	D
4N/27W-15Q1	185	100	D
4N/27W-15Q1	195	27.3	D
4N/27W-15Q1	205	0	D
4N/27W-15Q1	215	36.4	D
4N/27W-15Q1	225	100	D
4N/27W-15Q1	235	100	D
4N/27W-15Q1	245	100	D
4N/27W-15Q1	255	40	D
4N/27W-15Q1	265	30	D
4N/27W-15Q1	275	30	D
4N/27W-15Q1	285	0	D
4N/27W-15Q1	295	0	D
4N/27W-15Q1	305	0	D
4N/27W-15Q1	315	0	D
4N/27W-15Q1	325	30	D
4N/27W-15Q1	335	0	D
4N/27W-15Q1	345	0	D
4N/27W-15Q1	355	0	D
4N/27W-15Q1	365	0	D
4N/27W-15Q1	375	10	D
4N/27W-15Q1	385	80	D
4N/27W-15Q1	395	30	D
4N/27W-15Q1	405	0	D
4N/27W-15Q1	415	11.1	D
4N/27W-15Q1	425	0	D
4N/27W-15Q7	5	0	D
4N/27W-15Q7	15	0	D
4N/27W-15Q7	25	0	D
4N/27W-15Q7	35	0	D
4N/27W-15Q7	45	0	D
4N/27W-15Q7	55	0	D
4N/27W-15Q7	65	0	D
4N/27W-15Q7	75	0	D
4N/27W-15Q7	85	0	D
4N/27W-15Q7	95	0	D
4N/27W-15Q7	105	0	D
4N/27W-15Q7	115	0	D
4N/27W-15Q7	125	0	D
4N/27W-15Q7	135	0	D
4N/27W-15Q7	145	0	D
4N/27W-15Q7	155	0	D
4N/27W-15Q7	165	0	D
4N/27W-15Q7	175	0	D
4N/27W-15Q7	185	0	D
4N/27W-15Q7	195	0	D
4N/27W-15Q7	205	0	D
4N/27W-15Q7	215	54.5	D
4N/27W-15Q7	225	0	D
4N/27W-15Q7	235	90	D
4N/27W-15Q7	245	100	D
4N/27W-15Q7	255	100	D
4N/27W-15Q7	265	100	D
4N/27W-15Q7	275	70	D
4N/27W-15Q7	285	0	D
4N/27W-15Q7	295	0	D
4N/27W-15Q7	305	0	D
4N/27W-15Q7	315	0	D
4N/27W-15Q7	325	0	D
4N/27W-15Q7	335	0	D
4N/27W-15Q7	345	0	D
4N/27W-15Q7	355	0	D
4N/27W-15Q7	365	0	D
4N/27W-15Q7	375	0	D
4N/27W-15Q7	385	0	D
4N/27W-15Q7	395	0	D
4N/27W-15Q7	405	0	D
4N/27W-15Q7	415	0	D
4N/27W-15Q7	425	0	D
4N/27W-15Q7	435	0	D
4N/27W-15Q7	445	0	D
4N/27W-15Q7	455	0	D

Table B1–1. Calculated percent-coarse intervals for all drillers' logs and e-logs used to define textural properties of the hydrogeologic framework model.—Continued

[Percent-coarse values are calculated for 10-foot intervals for the entire depth of each borehole. State well number is the state of California well identifier; interval midpoint depth is the midpoint of each 10-foot interval, in feet from top of borehole; PC is the percent-coarse value for each interval; log type defines whether the borehole is a drillers' lithology log (D) or a geophysical e-log (E).]

State well number	Interval midpoint depth (feet)	PC	Log type
4N/27W-15Q7	465	0	D
4N/27W-15Q7	475	0	D
4N/27W-15Q7	485	0	D
4N/27W-15Q7	495	0	D
4N/27W-15Q7	505	0	D
4N/27W-15Q7	515	0	D
4N/27W-15Q7	525	0	D
4N/27W-15Q7	535	0	D
4N/27W-15Q7	545	0	D
4N/27W-15Q7	555	0	D
4N/27W-15Q7	565	0	D
4N/27W-15Q7	575	0	D
4N/27W-15Q7	585	0	D
4N/27W-15Q7	595	0	D
4N/27W-15Q7	605	0	D
4N/27W-15Q7	615	0	D
4N/27W-15Q7	625	10	D
4N/27W-15Q7	635	100	D
4N/27W-15Q7	645	60	D
4N/27W-15Q7	655	0	D
4N/27W-15Q7	665	0	D
4N/27W-15Q7	675	10	D
4N/27W-15Q7	685	100	D
4N/27W-15Q7	695	100	D
4N/27W-15Q7	705	100	D
4N/27W-15Q7	715	100	D
4N/27W-15Q7	725	100	D
4N/27W-15Q7	735	30	D
4N/27W-15Q7	745	70	D
4N/27W-15Q7	755	100	D
4N/27W-15Q7	765	100	D
4N/27W-15Q7	775	70	D
4N/27W-15Q10	5	0	D
4N/27W-15Q10	15	0	D
4N/27W-15Q10	25	0	D
4N/27W-15Q10	35	30	D
4N/27W-15Q10	45	0	D
4N/27W-15Q10	55	40	D
4N/27W-15Q10	65	0	D
4N/27W-15Q10	75	0	D
4N/27W-15Q10	85	0	D
4N/27W-15Q10	95	20	D
4N/27W-15Q10	105	100	D
4N/27W-15Q10	115	30	D
4N/27W-15Q10	125	0	D
4N/27W-15Q10	135	0	D
4N/27W-15Q10	145	0	D
4N/27W-15Q10	155	30	D
4N/27W-15Q10	165	0	D
4N/27W-15Q10	175	0	D
4N/27W-15Q10	185	0	D
4N/27W-15Q10	195	0	D
4N/27W-15Q10	205	0	D
4N/27W-15Q10	215	0	D
4N/27W-15Q10	225	0	D
4N/27W-15Q10	235	90	D
4N/27W-15Q10	245	100	D
4N/27W-15Q10	255	100	D
4N/27W-15Q10	265	100	D
4N/27W-15Q10	275	0	D
4N/27W-15Q10	285	0	D
4N/27W-15Q10	295	0	D
4N/27W-15Q10	305	0	D
4N/27W-15Q10	315	0	D
4N/27W-15Q10	325	0	D
4N/27W-15Q10	335	0	D
4N/27W-15Q10	345	10	D
4N/27W-15Q10	355	30	D
4N/27W-15Q10	365	0	D
4N/27W-15Q10	375	0	D
4N/27W-15Q10	385	10	D
4N/27W-15Q10	395	90	D
4N/27W-15Q10	405	0	D
4N/27W-15Q10	415	22.2	D
4N/27W-15Q10	425	63.6	D
4N/27W-15Q10	435	0	D
4N/27W-15Q10	445	0	D
4N/27W-15Q10	455	0	D

Table B1–1. Calculated percent-coarse intervals for all drillers' logs and e-logs used to define textural properties of the hydrogeologic framework model.—Continued

[Percent-coarse values are calculated for 10-foot intervals for the entire depth of each borehole. State well number is the state of California well identifier; interval midpoint depth is the midpoint of each 10-foot interval, in feet from top of borehole; PC is the percent-coarse value for each interval; log type defines whether the borehole is a drillers' lithology log (D) or a geophysical e-log (E).]

State well number	Interval midpoint depth (feet)	PC	Log type
4N/27W-15Q10	465	10	D
4N/27W-15Q10	475	40	D
4N/27W-15Q10	485	0	D
4N/27W-15Q10	495	0	D
4N/27W-15Q10	505	0	D
4N/27W-15Q10	515	0	D
4N/27W-15Q10	525	0	D
4N/27W-15Q10	535	0	D
4N/27W-15Q10	545	0	D
4N/27W-15Q10	555	0	D
4N/27W-15Q10	565	0	D
4N/27W-15Q10	575	0	D
4N/27W-15Q10	585	0	D
4N/27W-15Q10	595	0	D
4N/27W-15Q10	605	0	D
4N/27W-15Q10	615	30	D
4N/27W-15Q10	625	100	D
4N/27W-15Q10	635	60	D
4N/27W-15Q10	645	100	D
4N/27W-15Q10	655	40	D
4N/27W-15Q10	665	50	D
4N/27W-15Q10	675	0	D
4N/27W-15R1	5	100	D
4N/27W-15R1	15	100	D
4N/27W-15R1	25	100	D
4N/27W-15R1	35	100	D
4N/27W-15R1	45	100	D
4N/27W-15R1	55	100	D
4N/27W-15R1	65	100	D
4N/27W-15R1	75	100	D
4N/27W-15R1	85	100	D
4N/27W-15R1	95	100	D
4N/27W-15R1	105	100	D
4N/27W-15R1	115	100	D
4N/27W-15R1	125	100	D
4N/27W-15R1	135	100	D
4N/27W-15R1	145	100	D
4N/27W-15R1	155	100	D
4N/27W-15R1	165	100	D
4N/27W-15R1	175	100	D
4N/27W-15R1	185	100	D
4N/27W-15R1	195	100	D
4N/27W-15R1	205	100	D
4N/27W-15R1	215	100	D
4N/27W-15R1	225	100	D
4N/27W-15R1	235	100	D
4N/27W-15R1	245	100	D
4N/27W-15R1	255	100	D
4N/27W-15R1	265	100	D
4N/27W-15R1	275	100	D
4N/27W-15R1	285	100	D
4N/27W-15R1	295	100	D
4N/27W-15R1	305	100	D
4N/27W-15R1	315	100	D
4N/27W-15R1	325	100	D
4N/27W-15R1	335	100	D
4N/27W-15R1	345	100	D
4N/27W-15R1	355	100	D
4N/27W-15R1	365	10	D
4N/27W-15R1	375	0	D
4N/27W-15R1	385	0	D
4N/27W-15R1	395	0	D
4N/27W-15R1	405	0	D
4N/27W-15R1	415	88.9	D
4N/27W-15R1	425	100	D
4N/27W-15R1	435	100	D
4N/27W-15R1	445	100	D
4N/27W-15R1	455	100	D
4N/27W-15R1	465	100	D
4N/27W-15R1	475	100	D
4N/27W-15R1	485	100	D
4N/27W-15R1	495	100	D
4N/27W-15R1	505	100	D
4N/27W-15R1	515	100	D
4N/27W-15R1	525	100	D
4N/27W-15R1	535	100	D
4N/27W-15R1	545	100	D
4N/27W-15R1	555	100	D

Table B1–1. Calculated percent-coarse intervals for all drillers' logs and e-logs used to define textural properties of the hydrogeologic framework model.—Continued

[Percent-coarse values are calculated for 10-foot intervals for the entire depth of each borehole. State well number is the state of California well identifier; interval midpoint depth is the midpoint of each 10-foot interval, in feet from top of borehole; PC is the percent-coarse value for each interval; log type defines whether the borehole is a drillers' lithology log (D) or a geophysical e-log (E).]

State well number	Interval midpoint depth (feet)	PC	Log type
4N/27W-15R1	565	100	D
4N/27W-15R1	575	100	D
4N/27W-15R1	585	100	D
4N/27W-15R1	595	100	D
4N/27W-15R1	605	100	D
4N/27W-15R1	615	100	D
4N/27W-15R1	625	100	D
4N/27W-15R1	635	100	D
4N/27W-15R1	645	100	D
4N/27W-15R1	655	100	D
4N/27W-15R1	665	100	D
4N/27W-15R1	675	100	D
4N/27W-15R1	685	100	D
4N/27W-15R1	695	100	D
4N/27W-16C1	5	0	D
4N/27W-16C1	15	0	D
4N/27W-16C1	25	0	D
4N/27W-16C1	35	10	D
4N/27W-16C1	45	100	D
4N/27W-16C1	55	100	D
4N/27W-16C1	65	90	D
4N/27W-16C1	75	0	D
4N/27W-16C1	85	0	D
4N/27W-16C1	95	0	D
4N/27W-16C1	105	0	D
4N/27W-16C1	115	0	D
4N/27W-16C1	125	0	D
4N/27W-16C1	135	0	D
4N/27W-16C1	145	0	D
4N/27W-16C1	155	0	D
4N/27W-16C1	165	0	D
4N/27W-16C1	175	0	D
4N/27W-16C1	185	0	D
4N/27W-16C1	195	0	D
4N/27W-16C1	205	0	D
4N/27W-16C1	215	9.1	D
4N/27W-16C1	225	90	D
4N/27W-16C1	235	0	D
4N/27W-16C1	245	0	D
4N/27W-16C1	255	0	D
4N/27W-16C1	265	50	D
4N/27W-16C1	275	50	D
4N/27W-16C1	285	0	D
4N/27W-16C1	295	9.1	D
4N/27W-16C1	305	100	D
4N/27W-16C1	315	90	D
4N/27W-16C1	325	0	D
4N/27W-16C1	335	0	D
4N/27W-16C1	345	0	D
4N/27W-16E2	5	100	D
4N/27W-16E2	15	100	D
4N/27W-16E2	25	90	D
4N/27W-16E2	35	0	D
4N/27W-16E2	45	10	D
4N/27W-16E2	55	100	D
4N/27W-16E2	65	100	D
4N/27W-16E2	75	100	D
4N/27W-16E2	85	100	D
4N/27W-16E2	95	90.9	D
4N/27W-16E2	105	0	D
4N/27W-16E2	115	0	D
4N/27W-16E2	125	0	D
4N/27W-16E2	135	100	D
4N/27W-16E2	145	0	D
4N/27W-16E2	155	0	D
4N/27W-16E2	165	0	D
4N/27W-16E2	175	0	D
4N/27W-16E2	185	0	D
4N/27W-16E2	195	9.1	D
4N/27W-16E2	205	100	D
4N/27W-16E2	215	90.9	D
4N/27W-16E2	225	0	D
4N/27W-16E2	235	0	D
4N/27W-16E2	245	0	D
4N/27W-16E2	255	0	D
4N/27W-16E2	265	0	D
4N/27W-16E2	275	0	D
4N/27W-16E2	285	100	D

Table B1–1. Calculated percent-coarse intervals for all drillers' logs and e-logs used to define textural properties of the hydrogeologic framework model.—Continued

[Percent-coarse values are calculated for 10-foot intervals for the entire depth of each borehole. State well number is the state of California well identifier; interval midpoint depth is the midpoint of each 10-foot interval, in feet from top of borehole; PC is the percent-coarse value for each interval; log type defines whether the borehole is a drillers' lithology log (D) or a geophysical e-log (E).]

State well number	Interval midpoint depth (feet)	PC	Log type
4N/27W-16E2	295	100	D
4N/27W-16E2	305	100	D
4N/27W-16E2	315	90	D
4N/27W-16E2	325	10	D
4N/27W-16E2	335	90	D
4N/27W-16E2	345	0	D
4N/27W-16E2	355	0	D
4N/27W-16E2	365	0	D
4N/27W-16E2	375	0	D
4N/27W-16E2	385	0	D
4N/27W-16E2	395	40	D
4N/27W-16E2	405	0	D
4N/27W-16E2	415	0	D
4N/27W-16E2	425	0	D
4N/27W-16M1	5	100	D
4N/27W-16M1	15	50	D
4N/27W-16M1	25	30	D
4N/27W-16M1	35	0	D
4N/27W-16M1	45	0	D
4N/27W-16M1	55	0	D
4N/27W-16M1	65	0	D
4N/27W-16M1	75	0	D
4N/27W-16M1	85	0	D
4N/27W-16M1	95	0	D
4N/27W-16M1	105	0	D
4N/27W-16M1	115	0	D
4N/27W-16M1	125	0	D
4N/27W-16M1	135	0	D
4N/27W-16M1	145	0	D
4N/27W-16M1	155	30	D
4N/27W-16M1	165	0	D
4N/27W-16M1	175	0	D
4N/27W-16M1	185	0	D
4N/27W-16M1	195	0	D
4N/27W-16M1	205	0	D
4N/27W-16M1	215	36.4	D
4N/27W-16M1	225	0	D
4N/27W-16M1	235	0	D
4N/27W-16M1	245	0	D
4N/27W-16M1	255	0	D
4N/27W-16M1	265	0	D
4N/27W-16M1	275	0	D
4N/27W-16M1	285	20	D
4N/27W-16M1	295	54.5	D
4N/27W-16M1	305	0	D
4N/27W-16M1	315	0	D
4N/27W-16M1	325	0	D
4N/27W-16M1	335	0	D
4N/27W-16M1	345	0	D
4N/27W-16M1	355	0	D
4N/27W-16P1	5	36.4	D
4N/27W-16P1	15	100	D
4N/27W-16P1	25	70	D
4N/27W-16P1	35	0	D
4N/27W-16P1	45	0	D
4N/27W-16P1	55	0	D
4N/27W-16P1	65	0	D
4N/27W-16P1	75	54.5	D
4N/27W-16P1	85	0	D
4N/27W-16P1	95	0	D
4N/27W-16P1	105	0	D
4N/27W-16P1	115	0	D
4N/27W-16P1	125	0	D
4N/27W-16P1	135	0	D
4N/27W-16P1	145	0	D
4N/27W-16P1	155	0	D
4N/27W-16P1	165	0	D
4N/27W-16P1	175	0	D
4N/27W-16P1	185	40	D
4N/27W-16P1	195	36.4	D
4N/27W-16P1	205	0	D
4N/27W-16P1	215	0	D
4N/27W-16P1	225	40	D
4N/27W-16P1	235	0	D
4N/27W-16P1	245	0	D
4N/27W-16P1	255	0	D
4N/27W-16P1	265	0	D
4N/27W-16P1	275	0	D

Table B1–1. Calculated percent-coarse intervals for all drillers' logs and e-logs used to define textural properties of the hydrogeologic framework model.—Continued

[Percent-coarse values are calculated for 10-foot intervals for the entire depth of each borehole. State well number is the state of California well identifier; interval midpoint depth is the midpoint of each 10-foot interval, in feet from top of borehole; PC is the percent-coarse value for each interval; log type defines whether the borehole is a drillers' lithology log (D) or a geophysical e-log (E).]

State well number	Interval midpoint depth (feet)	PC	Log type
4N/27W-16P1	285	0	D
4N/27W-16P1	295	0	D
4N/27W-16P1	305	0	D
4N/27W-16P1	315	0	D
4N/27W-16P1	325	0	D
4N/27W-16P1	335	0	D
4N/27W-16P1	345	0	D
4N/27W-16P1	355	0	D
4N/27W-16P1	365	0	D
4N/27W-16P1	375	0	D
4N/27W-16P1	385	0	D
4N/27W-16P1	395	20	D
4N/27W-16P1	405	0	D
4N/27W-16P1	415	0	D
4N/27W-16P1	425	18.2	D
4N/27W-16P1	435	0	D
4N/27W-16P1	445	0	D
4N/27W-16P1	455	0	D
4N/27W-16P1	465	50	D
4N/27W-16P1	475	50	D
4N/27W-16P1	485	0	D
4N/27W-16P1	495	0	D
4N/27W-16P1	505	0	D
4N/27W-16P1	515	0	D
4N/27W-17E1	5	100	D
4N/27W-17E1	15	100	D
4N/27W-17E1	25	50	D
4N/27W-17E1	35	0	D
4N/27W-17E1	45	0	D
4N/27W-17E1	55	0	D
4N/27W-17E1	65	0	D
4N/27W-17E1	75	0	D
4N/27W-17E1	85	0	D
4N/27W-17E1	95	0	D
4N/27W-17E1	105	10	D
4N/27W-17E1	115	0	D
4N/27W-17E1	125	0	D
4N/27W-17E1	135	0	D
4N/27W-17E1	145	0	D
4N/27W-17E1	155	0	D
4N/27W-17E1	165	0	D
4N/27W-17E1	175	0	D
4N/27W-17E1	185	0	D
4N/27W-17E1	195	0	D
4N/27W-17E1	205	0	D
4N/27W-17E1	215	0	D
4N/27W-17E1	225	0	D
4N/27W-17E1	235	0	D
4N/27W-17E1	245	90	D
4N/27W-17E1	255	100	D
4N/27W-17E1	265	100	D
4N/27W-17E1	275	100	D
4N/27W-17E1	285	100	D
4N/27W-17L1	5	100	D
4N/27W-17L1	15	100	D
4N/27W-17L1	25	100	D
4N/27W-17L1	35	40	D
4N/27W-17L1	45	0	D
4N/27W-17L1	55	0	D
4N/27W-17L1	65	0	D
4N/27W-17L1	75	0	D
4N/27W-17L1	85	40	D
4N/27W-17L1	95	100	D
4N/27W-17L1	105	90	D
4N/27W-17L1	115	0	D
4N/27W-17L1	125	0	D
4N/27W-17L1	135	100	D
4N/27W-17L1	145	36.4	D
4N/27W-17L1	155	0	D
4N/27W-17L1	165	0	D
4N/27W-17L1	175	0	D
4N/27W-17L1	185	0	D
4N/27W-17L1	195	100	D
4N/27W-17L1	205	11.1	D
4N/27W-17L1	215	0	D
4N/27W-17L1	225	0	D
4N/27W-17L1	235	0	D
4N/27W-17L1	245	0	D

Table B1–1. Calculated percent-coarse intervals for all drillers' logs and e-logs used to define textural properties of the hydrogeologic framework model.—Continued

[Percent-coarse values are calculated for 10-foot intervals for the entire depth of each borehole. State well number is the state of California well identifier; interval midpoint depth is the midpoint of each 10-foot interval, in feet from top of borehole; PC is the percent-coarse value for each interval; log type defines whether the borehole is a drillers' lithology log (D) or a geophysical e-log (E).]

State well number	Interval midpoint depth (feet)	PC	Log type
4N/27W-17L1	255	70	D
4N/27W-17L1	265	100	D
4N/27W-17L1	275	100	D
4N/27W-17L2	25	0	D
4N/27W-17L2	25	0	D
4N/27W-17L2	35	0	D
4N/27W-17L2	35	0	D
4N/27W-17L2	45	50	D
4N/27W-17L2	45	50	D
4N/27W-17L2	55	100	D
4N/27W-17L2	55	100	D
4N/27W-17L2	65	30	D
4N/27W-17L2	65	30	D
4N/27W-17L2	75	0	D
4N/27W-17L2	75	0	D
4N/27W-17L2	85	0	D
4N/27W-17L2	85	0	D
4N/27W-17L2	95	0	D
4N/27W-17L2	95	0	D
4N/27W-17L2	105	0	D
4N/27W-17L2	105	0	D
4N/27W-17L2	115	0	D
4N/27W-17L2	115	0	D
4N/27W-17L2	125	0	D
4N/27W-17L2	125	0	D
4N/27W-17L2	135	0	D
4N/27W-17L2	135	0	D
4N/27W-17L2	145	0	D
4N/27W-17L2	145	0	D
4N/27W-17L2	155	0	D
4N/27W-17L2	155	0	D
4N/27W-17L2	165	45.5	D
4N/27W-17L2	165	45.5	D
4N/27W-17L2	175	50	D
4N/27W-17L2	175	50	D
4N/27W-17L2	185	50	D
4N/27W-17L2	185	50	D
4N/27W-17L2	195	50	D
4N/27W-17L2	195	50	D
4N/27W-17L2	205	50	D
4N/27W-17L2	205	50	D
4N/27W-17L2	215	52.4	D
4N/27W-17L2	215	52.4	D
4N/27W-17L2	225	21.1	D
4N/27W-17L2	225	21.1	D
4N/27W-17L2	235	0	D
4N/27W-17L2	235	0	D
4N/27W-17L2	245	5	D
4N/27W-17L2	245	5	D
4N/27W-17L2	255	20	D
4N/27W-17L2	255	20	D
4N/27W-17L2	265	30	D
4N/27W-17L2	265	30	D
4N/27W-17L2	275	45	D
4N/27W-17L2	275	45	D
4N/27W-17L2	285	0	D
4N/27W-17L2	285	0	D
4N/27W-17L2	295	47.6	D
4N/27W-17L2	295	47.6	D
4N/27W-17L2	305	21.1	D
4N/27W-17L2	305	21.1	D
4N/27W-17L2	315	0	D
4N/27W-17L2	315	0	D
4N/27W-17L2	325	35	D
4N/27W-17L2	325	35	D
4N/27W-17L2	335	25	D
4N/27W-17L2	335	25	D
4N/27W-17L2	345	42.9	D
4N/27W-17L2	345	42.9	D
4N/27W-17L2	355	5	D
4N/27W-17L2	355	5	D
4N/27W-17L2	365	0	D
4N/27W-17L2	365	0	D
4N/27W-17M4	5	36.4	D
4N/27W-17M4	15	0	D
4N/27W-17M4	25	0	D
4N/27W-17M4	35	0	D
4N/27W-17M4	45	0	D

Table B1–1. Calculated percent-coarse intervals for all drillers' logs and e-logs used to define textural properties of the hydrogeologic framework model.—Continued

[Percent-coarse values are calculated for 10-foot intervals for the entire depth of each borehole. State well number is the state of California well identifier; interval midpoint depth is the midpoint of each 10-foot interval, in feet from top of borehole; PC is the percent-coarse value for each interval; log type defines whether the borehole is a drillers' lithology log (D) or a geophysical e-log (E).]

State well number	Interval midpoint depth (feet)	PC	Log type
4N/27W-17M4	55	0	D
4N/27W-17M4	65	0	D
4N/27W-17M4	75	0	D
4N/27W-17M4	85	0	D
4N/27W-17M4	95	0	D
4N/27W-17M4	105	0	D
4N/27W-17M4	115	30	D
4N/27W-17M4	125	100	D
4N/27W-17M4	135	100	D
4N/27W-17M4	145	100	D
4N/27W-17M4	155	100	D
4N/27W-17M4	165	100	D
4N/27W-17M4	175	100	D
4N/27W-17M4	185	50	D
4N/27W-17M4	195	0	D
4N/27W-17M4	205	0	D
4N/27W-17M4	215	0	D
4N/27W-17M4	225	0	D
4N/27W-17M4	235	0	D
4N/27W-17M4	245	0	D
4N/27W-17M4	255	0	D
4N/27W-17M4	265	0	D
4N/27W-17M4	275	0	D
4N/27W-18B1	5	72.7	D
4N/27W-18B1	15	10	D
4N/27W-18B1	25	100	D
4N/27W-18B1	35	90	D
4N/27W-18B1	45	0	D
4N/27W-18B1	55	0	D
4N/27W-18B1	65	0	D
4N/27W-18B1	75	0	D
4N/27W-18B1	85	0	D
4N/27W-18B1	95	0	D
4N/27W-18B1	105	0	D
4N/27W-18B1	115	0	D
4N/27W-18B1	125	0	D
4N/27W-18B1	135	0	D
4N/27W-18B1	145	9.1	D
4N/27W-18B1	155	100	D
4N/27W-18B1	165	100	D
4N/27W-18B1	175	100	D
4N/27W-18B1	185	80	D
4N/27W-18B1	195	100	D
4N/27W-18B1	205	22.2	D
4N/27W-18B1	215	100	D
4N/27W-18B1	225	80	D
4N/27W-18B1	235	100	D
4N/27W-18B1	245	100	D
4N/27W-18B3	5	45.5	D
4N/27W-18B3	15	100	D
4N/27W-18B3	25	90	D
4N/27W-18B3	35	0	D
4N/27W-18B3	45	0	D
4N/27W-18B3	55	0	D
4N/27W-18B3	65	0	D
4N/27W-18B3	75	0	D
4N/27W-18B3	85	0	D
4N/27W-18B3	95	0	D
4N/27W-18B3	105	0	D
4N/27W-18B3	115	0	D
4N/27W-18B3	125	0	D
4N/27W-18B3	135	0	D
4N/27W-18B3	145	0	D
4N/27W-18B3	155	60	D
4N/27W-18B3	165	100	D
4N/27W-18B3	175	100	D
4N/27W-18B3	185	100	D
4N/27W-18B3	195	100	D
4N/27W-18B3	205	100	D
4N/27W-18B3	215	100	D
4N/27W-18B3	225	100	D
4N/27W-18B3	235	100	D
4N/27W-18B3	245	90	D
4N/27W-18B4	5	100	D
4N/27W-18B4	15	90	D
4N/27W-18B4	25	0	D
4N/27W-18B4	35	0	D
4N/27W-18B4	45	0	D

Table B1–1. Calculated percent-coarse intervals for all drillers' logs and e-logs used to define textural properties of the hydrogeologic framework model.—Continued

[Percent-coarse values are calculated for 10-foot intervals for the entire depth of each borehole. State well number is the state of California well identifier; interval midpoint depth is the midpoint of each 10-foot interval, in feet from top of borehole; PC is the percent-coarse value for each interval; log type defines whether the borehole is a drillers' lithology log (D) or a geophysical e-log (E).]

State well number	Interval midpoint depth (feet)	PC	Log type
4N/27W-18B4	55	0	D
4N/27W-18B4	65	0	D
4N/27W-18B4	75	0	D
4N/27W-18B4	85	0	D
4N/27W-18B4	95	10	D
4N/27W-18B4	105	100	D
4N/27W-18B4	115	100	D
4N/27W-18B4	125	100	D
4N/27W-18B4	135	100	D
4N/27W-18B4	145	100	D
4N/27W-18B4	155	100	D
4N/27W-18B4	165	100	D
4N/27W-18B4	175	100	D
4N/27W-18B4	185	100	D
4N/27W-18B4	195	90.9	D
4N/27W-18B4	205	0	D
4N/27W-18B4	215	0	D
4N/27W-18B4	225	0	D
4N/27W-18B4	235	0	D
4N/27W-18B4	245	0	D
4N/27W-18C1	25	0	D
4N/27W-18C1	35	0	D
4N/27W-18C1	45	100	D
4N/27W-18C1	55	100	D
4N/27W-18C1	65	100	D
4N/27W-18C1	75	100	D
4N/27W-18C1	85	100	D
4N/27W-18C1	95	100	D
4N/27W-18C1	105	100	D
4N/27W-18C1	115	100	D
4N/27W-18C1	125	100	D
4N/27W-18C1	135	100	D
4N/27W-18C1	145	100	D
4N/27W-18C1	155	100	D
4N/27W-18G1	5	0	D
4N/27W-18G1	15	0	D
4N/27W-18G1	25	0	D
4N/27W-18G1	35	0	D
4N/27W-18G1	45	0	D
4N/27W-18G1	55	0	D
4N/27W-18G1	65	55.6	D
4N/27W-18G1	75	9.1	D
4N/27W-18G1	85	0	D
4N/27W-18G1	95	0	D
4N/27W-18G1	105	0	D
4N/27W-18G1	115	0	D
4N/27W-18G1	125	22.2	D
4N/27W-18G1	135	100	D
4N/27W-18G1	145	100	D
4N/27W-18G1	155	90	D
4N/27W-18H1	5	100	D
4N/27W-18H1	15	10	D
4N/27W-18H1	25	0	D
4N/27W-18H1	35	0	D
4N/27W-18H1	45	0	D
4N/27W-18H1	55	0	D
4N/27W-18H1	65	33.3	D
4N/27W-18H1	75	9.1	D
4N/27W-18H1	85	30	D
4N/27W-18H1	95	0	D
4N/27W-18H1	105	0	D
4N/27W-18H1	115	30	D
4N/27W-18H1	125	100	D
4N/27W-18H1	135	20	D
4N/27W-18H1	145	0	D
4N/27W-18H1	155	70	D
4N/27W-18H2	5	0	D
4N/27W-18H2	15	0	D
4N/27W-18H2	25	0	D
4N/27W-18H2	35	0	D
4N/27W-18H2	45	60	D
4N/27W-18H2	55	100	D
4N/27W-18H2	65	100	D
4N/27W-18H2	75	100	D
4N/27W-18H2	85	100	D
4N/27W-18H2	95	100	D
4N/27W-18H2	105	100	D
4N/27W-18H2	115	90	D

Table B1–1. Calculated percent-coarse intervals for all drillers' logs and e-logs used to define textural properties of the hydrogeologic framework model.—Continued

[Percent-coarse values are calculated for 10-foot intervals for the entire depth of each borehole. State well number is the state of California well identifier; interval midpoint depth is the midpoint of each 10-foot interval, in feet from top of borehole; PC is the percent-coarse value for each interval; log type defines whether the borehole is a drillers' lithology log (D) or a geophysical e-log (E).]

State well number	Interval midpoint depth (feet)	PC	Log type
4N/27W-18H2	125	0	D
4N/27W-18H2	135	0	D
4N/27W-18H2	145	9.1	D
4N/27W-18H2	155	100	D
4N/27W-18H2	165	100	D
4N/27W-18J1	5	0	D
4N/27W-18J1	15	10	D
4N/27W-18J1	25	100	D
4N/27W-18J1	35	100	D
4N/27W-18J1	45	100	D
4N/27W-18J1	55	100	D
4N/27W-18J1	65	10	D
4N/27W-18J1	75	10	D
4N/27W-18J1	85	100	D
4N/27W-18J1	95	100	D
4N/27W-18J1	105	100	D
4N/27W-18J1	115	80	D
4N/27W-18J1	125	0	D
4N/27W-18J1	135	100	D
4N/27W-18J1	145	90	D
4N/27W-18J1	155	0	D
4N/27W-18J1	165	0	D
4N/27W-18J1	175	0	D
4N/27W-18J1	185	0	D
4N/27W-18J1	195	0	D
4N/27W-18J1	205	0	D
4N/27W-18J1	215	0	D
4N/27W-18J1	225	0	D
4N/27W-18J1	235	0	D
4N/27W-18J1	245	0	D
4N/27W-18J1	255	0	D
4N/27W-18J1	265	0	D
4N/27W-18J1	275	0	D
4N/27W-18J1	285	80	D
4N/27W-18L1	5	72.7	D
4N/27W-18L1	15	0	D
4N/27W-18L1	25	0	D
4N/27W-18L1	35	0	D
4N/27W-18L1	45	30	D
4N/27W-18L1	55	0	D
4N/27W-18L1	65	0	D
4N/27W-18L1	75	0	D
4N/27W-18L1	85	44.4	D
4N/27W-18L1	95	100	D
4N/27W-18L1	105	100	D
4N/27W-18L1	115	100	D
4N/27W-18L1	125	100	D
4N/27W-18L1	135	60	D
4N/27W-18L1	145	18.2	D
4N/27W-18L1	155	0	D
4N/27W-18L1	165	88.9	D
4N/27W-18L1	175	10	D
4N/27W-18L1	185	100	D
4N/27W-18L1	195	0	D
4N/27W-18L1	205	55.6	D
4N/27W-18L1	215	100	D
4N/27W-18L1	225	100	D
4N/27W-18L1	235	60	D
4N/27W-18P2	5	0	D
4N/27W-18P2	15	0	D
4N/27W-18P2	25	0	D
4N/27W-18P2	35	0	D
4N/27W-18P2	45	0	D
4N/27W-18P2	55	0	D
4N/27W-18P2	65	0	D
4N/27W-18P2	75	0	D
4N/27W-18P2	85	0	D
4N/27W-18P2	95	81.8	D
4N/27W-18P2	105	0	D
4N/27W-18P2	115	90	D
4N/27W-18P2	125	100	D
4N/27W-18P2	135	100	D
4N/27W-18P2	145	100	D
4N/27W-18P2	155	50	D
4N/27W-18P2	165	11.1	D
4N/27W-18P2	175	0	D
4N/27W-18P2	185	0	D
4N/27W-18Q2	5	100	D

Table B1–1. Calculated percent-coarse intervals for all drillers' logs and e-logs used to define textural properties of the hydrogeologic framework model.—Continued

[Percent-coarse values are calculated for 10-foot intervals for the entire depth of each borehole. State well number is the state of California well identifier; interval midpoint depth is the midpoint of each 10-foot interval, in feet from top of borehole; PC is the percent-coarse value for each interval; log type defines whether the borehole is a drillers' lithology log (D) or a geophysical e-log (E).]

State well number	Interval midpoint depth (feet)	PC	Log type
4N/27W-18Q2	15	100	D
4N/27W-18Q2	25	100	D
4N/27W-18Q2	35	90	D
4N/27W-18Q2	45	0	D
4N/27W-18Q2	55	60	D
4N/27W-18Q2	65	100	D
4N/27W-18Q2	75	100	D
4N/27W-18Q2	85	100	D
4N/27W-18Q2	95	100	D
4N/27W-18Q2	105	100	D
4N/27W-18Q2	115	100	D
4N/27W-18Q2	125	100	D
4N/27W-18Q2	135	100	D
4N/27W-18Q2	145	100	D
4N/27W-18Q2	155	100	D
4N/27W-18Q2	165	100	D
4N/27W-18Q2	175	100	D
4N/27W-18R1	5	100	D
4N/27W-18R1	15	100	D
4N/27W-18R1	25	100	D
4N/27W-18R1	35	100	D
4N/27W-18R1	45	100	D
4N/27W-18R1	55	100	D
4N/27W-18R1	65	100	D
4N/27W-18R1	75	100	D
4N/27W-18R1	85	100	D
4N/27W-18R1	95	100	D
4N/27W-18R1	105	100	D
4N/27W-18R1	115	100	D
4N/27W-18R1	125	100	D
4N/27W-18R1	135	100	D
4N/27W-18R1	145	100	D
4N/27W-18R1	155	40	D
4N/27W-18R1	165	0	D
4N/27W-18R1	175	0	D
4N/27W-18R1	185	0	D
4N/27W-18R1	195	0	D
4N/27W-18R1	205	0	D
4N/27W-18R1	215	0	D
4N/27W-18R1	225	0	D
4N/27W-18R1	235	0	D
4N/27W-19A1	5	100	D
4N/27W-19A1	15	100	D
4N/27W-19A1	25	100	D
4N/27W-19A1	35	100	D
4N/27W-19A1	45	100	D
4N/27W-19A1	55	100	D
4N/27W-19A1	65	100	D
4N/27W-19A1	75	100	D
4N/27W-19A1	85	55.6	D
4N/27W-19A1	95	54.5	D
4N/27W-19A1	105	0	D
4N/27W-19A1	115	0	D
4N/27W-19A1	125	0	D
4N/27W-19A1	135	0	D
4N/27W-19A1	145	0	D
4N/27W-19A1	155	10	D
4N/27W-19A1	165	0	D
4N/27W-19A1	175	0	D
4N/27W-19A1	185	0	D
4N/27W-19A1	195	0	D
4N/27W-19A1	205	0	D
4N/27W-19A1	215	0	D
4N/27W-19A1	225	0	D
4N/27W-19A1	235	0	D
4N/27W-19A1	245	0	D
4N/27W-19A1	255	0	D
4N/27W-19A1	265	0	D
4N/27W-19A1	275	0	D
4N/27W-19A1	285	0	D
4N/27W-19A1	295	0	D
4N/27W-19A1	305	0	D
4N/27W-19A1	315	0	D
4N/27W-19A1	325	0	D
4N/27W-19A1	335	0	D
4N/27W-19A1	345	0	D
4N/27W-21B1	5	100	D
4N/27W-21B1	15	100	D

Table B1–1. Calculated percent-coarse intervals for all drillers' logs and e-logs used to define textural properties of the hydrogeologic framework model.—Continued

[Percent-coarse values are calculated for 10-foot intervals for the entire depth of each borehole. State well number is the state of California well identifier; interval midpoint depth is the midpoint of each 10-foot interval, in feet from top of borehole; PC is the percent-coarse value for each interval; log type defines whether the borehole is a drillers' lithology log (D) or a geophysical e-log (E).]

State well number	Interval midpoint depth (feet)	PC	Log type
4N/27W-21B1	25	0	D
4N/27W-21B1	35	0	D
4N/27W-21B1	45	0	D
4N/27W-21B1	55	0	D
4N/27W-21B1	65	77.8	D
4N/27W-21B1	75	0	D
4N/27W-21B1	85	0	D
4N/27W-21B1	95	0	D
4N/27W-21B1	105	70	D
4N/27W-21B1	115	100	D
4N/27W-21B1	125	100	D
4N/27W-21B1	135	10	D
4N/27W-21B1	145	0	D
4N/27W-21B1	155	0	D
4N/27W-21B1	165	0	D
4N/27W-21B1	175	30	D
4N/27W-21B1	185	0	D
4N/27W-21B1	195	0	D
4N/27W-21B1	205	0	D
4N/27W-21B1	215	100	D
4N/27W-21B1	225	20	D
4N/27W-21B1	235	0	D
4N/27W-21B1	245	0	D
4N/27W-21B1	255	30	D
4N/27W-21B1	265	90	D
4N/27W-21B1	275	22.2	D
4N/27W-21B1	285	20	D
4N/27W-21B1	295	0	D
4N/27W-21B1	305	50	D
4N/27W-21B1	315	100	D
4N/27W-21B1	325	100	D
4N/27W-21B1	335	100	D
4N/27W-21B1	345	100	D
4N/27W-21B1	355	100	D
4N/27W-21B1	365	100	D
4N/27W-21B1	375	100	D
4N/27W-21B1	385	100	D
4N/27W-21B1	395	100	D
4N/27W-21B1	405	100	D
4N/27W-21B1	415	100	D
4N/27W-21B1	425	100	D
4N/27W-21B1	435	100	D
4N/27W-21B1	445	100	D
4N/27W-21B2	5	0	D
4N/27W-21B2	15	0	D
4N/27W-21B2	25	0	D
4N/27W-21B2	35	0	D
4N/27W-21B2	45	0	D
4N/27W-21B2	55	0	D
4N/27W-21B2	65	0	D
4N/27W-21B2	75	0	D
4N/27W-21B2	85	0	D
4N/27W-21B2	95	0	D
4N/27W-21B2	105	0	D
4N/27W-21B2	115	0	D
4N/27W-21B2	125	0	D
4N/27W-21B2	135	0	D
4N/27W-21B2	145	0	D
4N/27W-21B2	155	0	D
4N/27W-21B2	165	44.4	D
4N/27W-21B2	175	0	D
4N/27W-21B2	185	0	D
4N/27W-21B2	195	45.5	D
4N/27W-21B2	205	44.4	D
4N/27W-21B2	215	9.1	D
4N/27W-21B2	225	0	D
4N/27W-21B2	235	0	D
4N/27W-21B2	245	0	D
4N/27W-21B2	255	0	D
4N/27W-21B2	265	40	D
4N/27W-21B2	275	0	D
4N/27W-21B2	285	0	D
4N/27W-21B2	295	0	D
4N/27W-21B2	305	0	D
4N/27W-21B2	315	0	D
4N/27W-21B2	325	0	D
4N/27W-21B2	335	0	D
4N/27W-21B2	345	0	D

Table B1–1. Calculated percent-coarse intervals for all drillers' logs and e-logs used to define textural properties of the hydrogeologic framework model.—Continued

[Percent-coarse values are calculated for 10-foot intervals for the entire depth of each borehole. State well number is the state of California well identifier; interval midpoint depth is the midpoint of each 10-foot interval, in feet from top of borehole; PC is the percent-coarse value for each interval; log type defines whether the borehole is a drillers' lithology log (D) or a geophysical e-log (E).]

State well number	Interval midpoint depth (feet)	PC	Log type
4N/27W-21B2	355	0	D
4N/27W-21B2	365	0	D
4N/27W-21B2	375	0	D
4N/27W-21B2	385	0	D
4N/27W-21B2	395	0	D
4N/27W-21B2	405	0	D
4N/27W-21B2	415	0	D
4N/27W-21B2	425	0	D
4N/27W-21B2	435	0	D
4N/27W-21B2	445	0	D
4N/27W-21B2	455	0	D
4N/27W-21B2	465	0	D
4N/27W-21B2	475	0	D
4N/27W-21B2	485	0	D
4N/27W-21B2	495	0	D
4N/27W-21B2	505	0	D
4N/27W-21B2	515	0	D
4N/27W-21B2	525	0	D
4N/27W-21B2	535	0	D
4N/27W-21B2	545	0	D
4N/27W-21B2	555	10	D
4N/27W-21B2	565	90	D
4N/27W-21B2	575	50	D
4N/27W-21B2	585	0	D
4N/27W-21B2	595	0	D
4N/27W-21G3	5	0	D
4N/27W-21G3	15	40	D
4N/27W-21H1	5	100	D
4N/27W-21H1	15	60	D
4N/27W-21H1	25	30	D
4N/27W-21H1	35	50	D
4N/27W-21H1	45	0	D
4N/27W-21H1	55	0	D
4N/27W-21H1	65	11.1	D
4N/27W-21H1	75	100	D
4N/27W-21H1	85	55.6	D
4N/27W-21H1	95	0	D
4N/27W-21H1	105	20	D
4N/27W-21H1	115	80	D
4N/27W-21H1	125	0	D
4N/27W-21H1	135	0	D
4N/27W-21H1	145	0	D
4N/27W-21H1	155	0	D
4N/27W-21H1	165	0	D
4N/27W-21H1	175	60	D
4N/27W-21H1	185	0	D
4N/27W-21H1	195	0	D
4N/27W-21H1	205	0	D
4N/27W-21H1	215	0	D
4N/27W-21H1	225	0	D
4N/27W-21H1	235	0	D
4N/27W-21H1	245	0	D
4N/27W-21H1	255	0	D
4N/27W-21H1	265	0	D
4N/27W-21H1	275	0	D
4N/27W-21H1	285	0	D
4N/27W-21H1	295	100	D
4N/27W-21H1	305	40	D
4N/27W-21H1	315	0	D
4N/27W-21H1	325	0	D
4N/27W-21H1	335	0	D
4N/27W-21H1	345	0	D
4N/27W-21H1	355	0	D
4N/27W-21H1	365	0	D
4N/27W-21H1	375	44.4	D
4N/27W-21H1	385	100	D
4N/27W-21H1	395	60	D
4N/27W-22B7	5	0	D
4N/27W-22B7	15	0	D
4N/27W-22B7	25	0	D
4N/27W-22B7	35	0	D
4N/27W-22B7	45	0	D
4N/27W-22B7	55	0	D
4N/27W-22B7	65	0	D
4N/27W-22B7	75	0	D
4N/27W-22B7	85	0	D
4N/27W-22B7	95	50	D
4N/27W-22B7	105	100	D

Table B1–1. Calculated percent-coarse intervals for all drillers' logs and e-logs used to define textural properties of the hydrogeologic framework model.—Continued

[Percent-coarse values are calculated for 10-foot intervals for the entire depth of each borehole. State well number is the state of California well identifier; interval midpoint depth is the midpoint of each 10-foot interval, in feet from top of borehole; PC is the percent-coarse value for each interval; log type defines whether the borehole is a drillers' lithology log (D) or a geophysical e-log (E).]

State well number	Interval midpoint depth (feet)	PC	Log type
4N/27W-22B7	115	100	D
4N/27W-22B7	125	100	D
4N/27W-22B7	135	100	D
4N/27W-22B7	145	100	D
4N/27W-22B7	155	100	D
4N/27W-22B7	165	100	D
4N/27W-22B7	175	100	D
4N/27W-22B7	185	100	D
4N/27W-22B7	195	100	D
4N/27W-22B7	205	100	D
4N/27W-22B7	215	100	D
4N/27W-22B7	225	100	D
4N/27W-22B7	235	100	D
4N/27W-22B7	245	100	D
4N/27W-22B7	255	100	D
4N/27W-22B7	265	100	D
4N/27W-22B7	275	40	D
4N/27W-22B7	285	0	D
4N/27W-22B7	295	0	D
4N/27W-22B7	305	0	D
4N/27W-22B7	315	0	D
4N/27W-22B7	325	0	D
4N/27W-22B7	335	0	D
4N/27W-22B7	345	0	D
4N/27W-22B7	355	0	D
4N/27W-22B7	365	10	D
4N/27W-22B7	375	100	D
4N/27W-22B7	385	100	D
4N/27W-22B7	395	100	D
4N/27W-22B7	405	100	D
4N/27W-22B7	415	100	D
4N/27W-22B7	425	90.9	D
4N/27W-22B7	435	0	D
4N/27W-22B7	445	10	D
4N/27W-22B7	455	100	D
4N/27W-22B7	465	90	D
4N/27W-22B7	475	0	D
4N/27W-22B7	485	0	D
4N/27W-22B7	495	0	D
4N/27W-22B7	505	0	D
4N/27W-22B7	515	0	D
4N/27W-22B7	525	0	D
4N/27W-22B7	535	0	D
4N/27W-22B7	545	0	D
4N/27W-22B7	555	0	D
4N/27W-22B7	565	0	D
4N/27W-22B7	575	0	D
4N/27W-22B7	585	70	D
4N/27W-22B7	595	100	D
4N/27W-22B7	605	100	D
4N/27W-22B7	615	100	D
4N/27W-22B7	625	100	D
4N/27W-22B7	635	100	D
4N/27W-22B7	645	100	D
4N/27W-22B7	655	100	D
4N/27W-22B7	665	100	D
4N/27W-22B7	675	100	D
4N/27W-22B7	685	100	D
4N/27W-22B7	695	100	D
4N/27W-22B7	705	100	D
4N/27W-22B7	715	100	D
4N/27W-22B7	725	100	D
4N/27W-22B7	735	100	D
4N/27W-22B7	745	100	D
4N/27W-22B7	755	100	D
4N/27W-22B7	765	100	D
4N/27W-22B7	775	100	D
4N/27W-22B7	785	100	D
4N/27W-22B7	795	90	D
4N/27W-22B7	805	0	D
4N/27W-22B7	815	0	D
4N/27W-22B7	825	0	D
4N/27W-22B7	835	0	D
4N/27W-22B7	845	0	D
4N/27W-22G4	5	100	D
4N/27W-22G4	15	100	D
4N/27W-22G4	25	100	D
4N/27W-22G4	35	40	D

Table B1–1. Calculated percent-coarse intervals for all drillers' logs and e-logs used to define textural properties of the hydrogeologic framework model.—Continued

[Percent-coarse values are calculated for 10-foot intervals for the entire depth of each borehole. State well number is the state of California well identifier; interval midpoint depth is the midpoint of each 10-foot interval, in feet from top of borehole; PC is the percent-coarse value for each interval; log type defines whether the borehole is a drillers' lithology log (D) or a geophysical e-log (E).]

State well number	Interval midpoint depth (feet)	PC	Log type
4N/27W-22G4	45	0	D
4N/27W-22G4	55	0	D
4N/27W-22G4	65	0	D
4N/27W-22G4	75	63.6	D
4N/27W-22G4	85	0	D
4N/27W-22G4	95	0	D
4N/27W-22G4	105	0	D
4N/27W-22G4	115	0	D
4N/27W-22G4	125	90	D
4N/27W-22G4	135	50	D
4N/27W-22G4	145	100	D
4N/27W-22G4	155	100	D
4N/27W-22G4	165	100	D
4N/27W-22G4	175	100	D
4N/27W-22G4	185	100	D
4N/27W-22G4	195	81.8	D
4N/27W-22G4	205	100	D
4N/27W-22G4	215	54.5	D
4N/27W-22G4	225	10	D
4N/27W-22G4	235	40	D
4N/27W-22G4	245	0	D
4N/27W-22G4	255	0	D
4N/27W-22G4	265	0	D
4N/27W-22G4	275	0	D
4N/27W-22G4	285	0	D
4N/27W-22G4	295	0	D
4N/27W-22G4	305	0	D
4N/27W-22G4	315	0	D
4N/27W-22G4	325	0	D
4N/27W-22G4	335	0	D
4N/27W-22G4	345	0	D
4N/27W-22G4	355	0	D
4N/27W-22G4	365	0	D
4N/27W-22G4	375	0	D
4N/27W-22G4	385	0	D
4N/27W-22G4	395	0	D
4N/27W-22G4	405	0	D
4N/27W-22G4	415	0	D
4N/27W-22G4	425	0	D
4N/27W-22G4	435	0	D
4N/27W-22G4	445	0	D
4N/27W-22G4	455	0	D
4N/27W-22G4	465	0	D
4N/27W-22G4	475	0	D
4N/27W-22G4	485	0	D
4N/27W-22G4	495	60	D
4N/27W-22G4	505	100	D
4N/27W-22G4	515	100	D
4N/27W-22G4	525	100	D
4N/27W-22G4	535	90	D
4N/27W-22G4	545	0	D
4N/27W-22G4	555	10	D
4N/27W-22G4	565	100	D
4N/27W-22G4	575	100	D
4N/27W-22G4	585	0	D
4N/27W-22G4	595	0	D
4N/27W-22G4	605	0	D
4N/27W-22G4	615	0	D
4N/27W-22G4	625	0	D
4N/27W-22G4	635	0	D
4N/27W-22G4	645	0	D
4N/27W-22G4	655	10	D
4N/27W-22G4	665	100	D
4N/27W-22G4	675	100	D
4N/27W-22G4	685	100	D
4N/27W-22G4	695	100	D
4N/27W-22G4	705	100	D
4N/27W-22G4	715	100	D
4N/27W-22G4	725	100	D
4N/27W-22G4	735	100	D
4N/27W-22J1	5	0	D
4N/27W-23A1	5	90.9	D
4N/27W-23A1	15	0	D
4N/27W-23A1	25	0	D
4N/27W-23A1	35	0	D
4N/27W-23A1	45	0	D
4N/27W-23A1	55	0	D
4N/27W-23A1	65	0	D

Table B1–1. Calculated percent-coarse intervals for all drillers' logs and e-logs used to define textural properties of the hydrogeologic framework model.—Continued

[Percent-coarse values are calculated for 10-foot intervals for the entire depth of each borehole. State well number is the state of California well identifier; interval midpoint depth is the midpoint of each 10-foot interval, in feet from top of borehole; PC is the percent-coarse value for each interval; log type defines whether the borehole is a drillers' lithology log (D) or a geophysical e-log (E).]

State well number	Interval midpoint depth (feet)	PC	Log type
4N/27W-23A1	75	0	D
4N/27W-23A1	85	0	D
4N/27W-23A1	95	0	D
4N/27W-23A1	105	0	D
4N/27W-23A1	115	0	D
4N/27W-23A1	125	0	D
4N/27W-23A1	135	0	D
4N/27W-23A1	145	0	D
4N/27W-23A1	155	0	D
4N/27W-23A1	165	0	D
4N/27W-23A1	175	0	D
4N/27W-23A1	185	0	D
4N/27W-23A1	195	0	D
4N/27W-23A1	205	0	D
4N/27W-23A1	215	0	D
4N/27W-23A1	225	0	D
4N/27W-23A1	235	0	D
4N/27W-23A1	245	0	D
4N/27W-23A1	255	80	D
4N/27W-23A1	265	100	D
4N/27W-23A1	275	100	D
4N/27W-23A1	285	100	D
4N/27W-23A1	295	45.5	D
4N/27W-23A1	305	0	D
4N/27W-23A1	315	0	D
4N/27W-23A2	5	0	D
4N/27W-23A2	15	0	D
4N/27W-23A2	25	0	D
4N/27W-23A2	35	0	D
4N/27W-23A2	45	0	D
4N/27W-23A2	55	0	D
4N/27W-23A2	65	0	D
4N/27W-23A2	75	0	D
4N/27W-23A2	85	0	D
4N/27W-23A2	95	0	D
4N/27W-23A2	105	90.9	D
4N/27W-23A2	115	100	D
4N/27W-23A2	125	30	D
4N/27W-23A2	135	0	D
4N/27W-23A2	145	0	D
4N/27W-23A2	155	0	D
4N/27W-23A2	165	0	D
4N/27W-23A2	175	0	D
4N/27W-23A2	185	11.1	D
4N/27W-23A2	195	100	D
4N/27W-23A2	205	100	D
4N/27W-23A2	215	100	D
4N/27W-23A2	225	100	D
4N/27W-23A2	235	20	D
4N/27W-23A2	245	60	D
4N/27W-23A2	255	100	D
4N/27W-23A2	265	40	D
4N/27W-23A2	275	30	D
4N/27W-23A2	285	100	D
4N/27W-23A2	295	100	D
4N/27W-23F4	5	0	D
4N/27W-23F4	15	0	D
4N/27W-23F4	25	0	D
4N/27W-23F4	35	0	D
4N/27W-23F4	45	0	D
4N/27W-23F4	55	10	D
4N/27W-23F4	65	100	D
4N/27W-23F4	75	100	D
4N/27W-23F4	85	100	D
4N/27W-23F4	95	100	D
4N/27W-23F4	105	90	D
4N/27W-23F4	115	0	D
4N/27W-23F4	125	0	D
4N/27W-23F4	135	0	D
4N/27W-23F4	145	10	D
4N/27W-23F4	155	100	D
4N/27W-23F4	165	100	D
4N/27W-23F4	175	100	D
4N/27W-23F4	185	40	D
4N/27W-23F4	195	0	D
4N/27W-23F4	205	0	D
4N/27W-23F4	215	0	D
4N/27W-23F4	225	0	D

Table B1–1. Calculated percent-coarse intervals for all drillers' logs and e-logs used to define textural properties of the hydrogeologic framework model.—Continued

[Percent-coarse values are calculated for 10-foot intervals for the entire depth of each borehole. State well number is the state of California well identifier; interval midpoint depth is the midpoint of each 10-foot interval, in feet from top of borehole; PC is the percent-coarse value for each interval; log type defines whether the borehole is a drillers' lithology log (D) or a geophysical e-log (E).]

State well number	Interval midpoint depth (feet)	PC	Log type
4N/27W-23F4	235	0	D
4N/27W-23F4	245	0	D
4N/27W-23F4	255	0	D
4N/27W-23F4	265	10	D
4N/27W-23F4	275	100	D
4N/27W-23F4	285	100	D
4N/27W-23F4	295	100	D
4N/27W-23F4	305	90	D
4N/27W-23F4	315	0	D
4N/27W-23F4	325	0	D
4N/27W-23F4	335	0	D
4N/27W-23F4	345	10	D
4N/27W-23F4	355	100	D
4N/27W-23F4	365	100	D
4N/27W-23F4	375	90	D
4N/27W-23F4	385	0	D
4N/27W-23F4	395	0	D
4N/27W-23F4	405	0	D
4N/27W-23F4	415	0	D
4N/27W-23F4	425	0	D
4N/27W-23F4	435	0	D
4N/27W-23F4	445	0	D
4N/27W-23F4	455	0	D
4N/27W-23F4	465	0	D
4N/27W-23F4	475	60	D
4N/27W-23F4	485	100	D
4N/27W-23F4	495	40	D
4N/27W-23F4	505	0	D
4N/27W-23F4	515	0	D
4N/27W-23F4	525	50	D
4N/27W-23F4	535	100	D
4N/27W-23F4	545	100	D
4N/27W-23F4	555	100	D
4N/27W-23F4	565	100	D
4N/27W-23F4	575	0	D
4N/27W-23F4	585	100	D
4N/27W-23F4	595	90.9	D
4N/27W-23F4	605	0	D
4N/27W-23F4	615	0	D
4N/27W-23F4	625	0	D
4N/27W-23F4	635	0	D
4N/27W-23F4	645	0	D
4N/27W-23F4	655	0	D
4N/27W-23F4	665	0	D
4N/27W-23F4	675	0	D
4N/27W-23F4	685	0	D
4N/27W-23F4	695	100	D
4N/27W-23F4	705	100	D
4N/27W-23F4	715	100	D
4N/27W-23F4	725	100	D
4N/27W-23F4	735	100	D
4N/27W-23F4	745	100	D
4N/27W-23F4	755	100	D
4N/27W-23F4	765	100	D
4N/27W-23F4	775	90	D
4N/27W-23F4	785	0	D
4N/27W-23M1	5	100	D
4N/28W-1L1	5	18.2	D
4N/28W-1L1	15	0	D
4N/28W-1L1	25	0	D
4N/28W-1L1	35	0	D
4N/28W-1L1	45	0	D
4N/28W-1L1	55	10	D
4N/28W-1L1	65	70	D
4N/28W-1L1	75	0	D
4N/28W-1L1	85	0	D
4N/28W-1L1	95	0	D
4N/28W-1L1	105	0	D
4N/28W-1L1	115	10	D
4N/28W-1L1	125	100	D
4N/28W-1L1	135	0	D
4N/28W-1L1	145	0	D
4N/28W-1L1	155	0	D
4N/28W-1L1	165	10	D
4N/28W-1L1	175	100	D
4N/28W-1L1	185	100	D
4N/28W-1L1	195	100	D
4N/28W-1L1	205	44.4	D

Table B1–1. Calculated percent-coarse intervals for all drillers' logs and e-logs used to define textural properties of the hydrogeologic framework model.—Continued

[Percent-coarse values are calculated for 10-foot intervals for the entire depth of each borehole. State well number is the state of California well identifier; interval midpoint depth is the midpoint of each 10-foot interval, in feet from top of borehole; PC is the percent-coarse value for each interval; log type defines whether the borehole is a drillers' lithology log (D) or a geophysical e-log (E).]

State well number	Interval midpoint depth (feet)	PC	Log type
4N/28W-1L1	215	54.5	D
4N/28W-1L1	225	100	D
4N/28W-1L1	235	100	D
4N/28W-1L1	245	100	D
4N/28W-1L1	255	100	D
4N/28W-1L1	265	100	D
4N/28W-1L1	275	100	D
4N/28W-1L1	285	100	D
4N/28W-1L1	295	100	D
4N/28W-1L1	305	100	D
4N/28W-1L1	315	100	D
4N/28W-1L1	325	100	D
4N/28W-1L1	335	100	D
4N/28W-1L1	345	100	D
4N/28W-1L1	355	100	D
4N/28W-1L1	365	100	D
4N/28W-1L1	375	100	D
4N/28W-1L1	385	100	D
4N/28W-1L1	395	90	D
4N/28W-1L1	405	0	D
4N/28W-1L1	415	0	D
4N/28W-1L1	425	100	D
4N/28W-1L1	435	100	D
4N/28W-1L1	445	100	D
4N/28W-1L1	455	100	D
4N/28W-1L1	465	100	D
4N/28W-1N2	5	36.4	D
4N/28W-1N2	15	0	D
4N/28W-1N2	25	0	D
4N/28W-1N2	35	0	D
4N/28W-1N2	45	0	D
4N/28W-1N2	55	0	D
4N/28W-1N2	65	0	D
4N/28W-1N2	75	0	D
4N/28W-1N2	85	0	D
4N/28W-1N2	95	0	D
4N/28W-1N2	105	0	D
4N/28W-1N2	115	0	D
4N/28W-1N2	125	0	D
4N/28W-1N2	135	0	D
4N/28W-1N2	145	0	D
4N/28W-1N2	155	0	D
4N/28W-1N2	165	40	D
4N/28W-1N2	175	30	D
4N/28W-1N2	185	0	D
4N/28W-1R1	5	0	D
4N/28W-1R1	15	0	D
4N/28W-1R1	25	0	D
4N/28W-1R1	35	0	D
4N/28W-1R1	45	0	D
4N/28W-1R1	55	0	D
4N/28W-1R1	65	0	D
4N/28W-1R1	75	0	D
4N/28W-1R1	85	0	D
4N/28W-1R1	95	0	D
4N/28W-1R1	105	0	D
4N/28W-1R1	115	0	D
4N/28W-1R1	125	0	D
4N/28W-1R1	135	0	D
4N/28W-1R1	145	0	D
4N/28W-1R1	155	0	D
4N/28W-1R1	165	0	D
4N/28W-1R1	175	0	D
4N/28W-1R1	185	0	D
4N/28W-1R2	25	0	D
4N/28W-1R2	35	0	D
4N/28W-1R2	45	0	D
4N/28W-1R2	55	0	D
4N/28W-1R2	65	0	D
4N/28W-1R2	75	0	D
4N/28W-1R2	85	0	D
4N/28W-1R2	95	10	D
4N/28W-1R2	105	70	D
4N/28W-1R2	115	0	D
4N/28W-1R2	125	0	D
4N/28W-1R2	135	0	D
4N/28W-1R2	145	0	D
4N/28W-1R2	155	10	D

Table B1–1. Calculated percent-coarse intervals for all drillers' logs and e-logs used to define textural properties of the hydrogeologic framework model.—Continued

[Percent-coarse values are calculated for 10-foot intervals for the entire depth of each borehole. State well number is the state of California well identifier; interval midpoint depth is the midpoint of each 10-foot interval, in feet from top of borehole; PC is the percent-coarse value for each interval; log type defines whether the borehole is a drillers' lithology log (D) or a geophysical e-log (E).]

State well number	Interval midpoint depth (feet)	PC	Log type
4N/28W-1R2	165	22.2	D
4N/28W-1R2	175	0	D
4N/28W-1R2	185	0	D
4N/28W-1R2	195	0	D
4N/28W-1R2	205	0	D
4N/28W-1R2	215	0	D
4N/28W-1R2	225	0	D
4N/28W-1R2	235	0	D
4N/28W-1R2	245	0	D
4N/28W-1R2	255	0	D
4N/28W-1R2	265	0	D
4N/28W-1R2	275	0	D
4N/28W-1R2	285	0	D
4N/28W-12A1	5	72.7	D
4N/28W-12A1	15	0	D
4N/28W-12A1	25	0	D
4N/28W-12A1	35	0	D
4N/28W-12A1	45	0	D
4N/28W-12A1	55	0	D
4N/28W-12A1	65	0	D
4N/28W-12A1	75	0	D
4N/28W-12A1	85	0	D
4N/28W-12A1	95	0	D
4N/28W-12A1	105	0	D
4N/28W-12A1	115	0	D
4N/28W-12A1	125	0	D
4N/28W-12A1	135	0	D
4N/28W-12A1	145	0	D
4N/28W-12A1	155	0	D
4N/28W-12A1	165	0	D
4N/28W-12A1	175	0	D
4N/28W-12A1	185	0	D
4N/28W-12A1	195	0	D
4N/28W-12A1	205	0	D
4N/28W-12A1	215	0	D
4N/28W-12A1	225	40	D
4N/28W-12A1	235	0	D
4N/28W-12A1	245	0	D
4N/28W-12A1	255	0	D
4N/28W-12A1	265	0	D
4N/28W-12A1	275	0	D
4N/28W-12A1	285	0	D
4N/28W-12A1	295	0	D
4N/28W-12A1	305	0	D
4N/28W-12A1	315	10	D
4N/28W-12A1	325	80	D
4N/28W-12A1	335	0	D
4N/28W-12A1	345	0	D
4N/28W-12A1	355	70	D
4N/28W-12A1	365	0	D
4N/28W-12A1	375	40	D
4N/28W-12A1	385	0	D
4N/28W-12A1	395	0	D
4N/28W-12C4	5	36.4	D
4N/28W-12C4	15	100	D
4N/28W-12C4	25	100	D
4N/28W-12C4	35	100	D
4N/28W-12C4	45	100	D
4N/28W-12C4	55	100	D
4N/28W-12C4	65	20	D
4N/28W-12C4	75	0	D
4N/28W-12C4	85	0	D
4N/28W-12C4	95	0	D
4N/28W-12F1	5	0	D
4N/28W-12F1	15	0	D
4N/28W-12F1	25	80	D
4N/28W-12F1	35	0	D
4N/28W-12F1	45	0	D
4N/28W-12F1	55	0	D
4N/28W-12F1	65	0	D
4N/28W-12F1	75	0	D
4N/28W-12F1	85	0	D
4N/28W-12F1	95	0	D
4N/28W-12F1	105	0	D
4N/28W-12F2	5	0	D
4N/28W-12F2	15	0	D
4N/28W-12F2	25	0	D
4N/28W-12F2	35	0	D

Table B1–1. Calculated percent-coarse intervals for all drillers' logs and e-logs used to define textural properties of the hydrogeologic framework model.—Continued

[Percent-coarse values are calculated for 10-foot intervals for the entire depth of each borehole. State well number is the state of California well identifier; interval midpoint depth is the midpoint of each 10-foot interval, in feet from top of borehole; PC is the percent-coarse value for each interval; log type defines whether the borehole is a drillers' lithology log (D) or a geophysical e-log (E).]

State well number	Interval midpoint depth (feet)	PC	Log type
4N/28W-12F2	45	0	D
4N/28W-12F2	55	40	D
4N/28W-12F2	65	22.2	D
4N/28W-12F2	75	0	D
4N/28W-12F2	85	0	D
4N/28W-12F2	95	0	D
4N/28W-12H1	5	0	D
4N/28W-12H1	15	0	D
4N/28W-12H1	25	0	D
4N/28W-12H1	35	0	D
4N/28W-12H1	45	0	D
4N/28W-12H1	55	0	D
4N/28W-12H1	65	0	D
4N/28W-12H1	75	0	D
4N/28W-12H1	85	0	D
4N/28W-12H1	95	0	D
4N/28W-12H1	105	0	D
4N/28W-12H1	115	0	D
4N/28W-12H1	125	0	D
4N/28W-12H1	135	40	D
4N/28W-12H1	145	72.7	D
4N/28W-12H1	155	30	D
4N/28W-12H1	165	100	D
4N/28W-12H1	175	100	D
4N/28W-12H1	185	40	D
4N/28W-12H1	195	100	D
4N/28W-12H1	205	22.2	D
4N/28W-12H1	215	0	D
4N/28W-12H1	225	0	D
4N/28W-12H1	235	0	D
4N/28W-12H1	245	0	D
4N/28W-12H4	5	0	D
4N/28W-12H4	15	0	D
4N/28W-12H4	25	0	D
4N/28W-12H4	35	0	D
4N/28W-12H4	45	10	D
4N/28W-12H4	55	100	D
4N/28W-12H4	65	100	D
4N/28W-12H4	75	9.1	D
4N/28W-12H4	85	0	D
4N/28W-12H4	95	0	D
4N/28W-12H4	105	0	D
4N/28W-12H4	115	0	D
4N/28W-12H4	125	0	D
4N/28W-12H4	135	0	D
4N/28W-12H4	145	0	D
4N/28W-12H4	155	10	D
4N/28W-12H4	165	100	D
4N/28W-12H4	175	30	D
4N/28W-12H4	185	0	D
4N/28W-12H4	195	9.1	D
4N/28W-12H4	205	100	D
4N/28W-12H4	215	100	D
4N/28W-12H4	225	100	D
4N/28W-12H4	235	100	D
4N/28W-12H4	245	100	D
4N/28W-12H4	255	100	D
4N/28W-12H4	265	100	D
4N/28W-12H4	275	100	D
4N/28W-12H4	285	30	D
4N/28W-12H4	295	0	D
4N/28W-12H4	305	0	D
4N/28W-12H4	315	0	D
4N/28W-12J2	5	100	D
4N/28W-12J2	15	100	D
4N/28W-12J2	25	100	D
4N/28W-12J2	35	100	D
4N/28W-12J2	45	100	D
4N/28W-12J2	55	100	D
4N/28W-12J2	65	100	D
4N/28W-12J2	75	100	D
4N/28W-12J2	85	70	D
4N/28W-12J2	95	0	D
4N/28W-12J2	105	0	D
4N/28W-12J2	115	0	D
4N/28W-12J2	125	0	D
4N/28W-12J2	135	0	D
4N/28W-12J2	145	0	D

Table B1–1. Calculated percent-coarse intervals for all drillers' logs and e-logs used to define textural properties of the hydrogeologic framework model.—Continued

[Percent-coarse values are calculated for 10-foot intervals for the entire depth of each borehole. State well number is the state of California well identifier; interval midpoint depth is the midpoint of each 10-foot interval, in feet from top of borehole; PC is the percent-coarse value for each interval; log type defines whether the borehole is a drillers' lithology log (D) or a geophysical e-log (E).]

State well number	Interval midpoint depth (feet)	PC	Log type
4N/28W-12J2	155	10	D
4N/28W-12J2	165	100	D
4N/28W-12J2	175	100	D
4N/28W-12J2	185	100	D
4N/28W-12J2	195	100	D
4N/28W-12J2	205	100	D
4N/28W-12J2	215	100	D
4N/28W-12J2	225	100	D
4N/28W-12J2	235	100	D
4N/28W-12J2	245	100	D
4N/28W-12J2	255	100	D
4N/28W-12J2	265	100	D
4N/28W-12J2	275	100	D
4N/28W-12J2	285	100	D
4N/28W-12J2	295	100	D
4N/28W-12K1	5	90.9	D
4N/28W-12K1	15	0	D
4N/28W-12K1	25	90	D
4N/28W-12K1	35	100	D
4N/28W-12K1	45	100	D
4N/28W-12K1	55	100	D
4N/28W-12K1	65	100	D
4N/28W-12K1	75	30	D
4N/28W-12K1	85	20	D
4N/28W-12K1	95	45.5	D
4N/28W-12K1	105	0	D
4N/28W-12K1	115	0	D
4N/28W-12K1	125	55.6	D
4N/28W-12K1	135	100	D
4N/28W-12K1	145	90.9	D
4N/28W-12K1	155	0	D
4N/28W-12K1	165	0	D
4N/28W-12K1	175	0	D
4N/28W-12K1	185	80	D
4N/28W-12K1	195	0	D
4N/28W-12K1	205	0	D
4N/28W-12K1	215	0	D
4N/28W-12K1	225	0	D
4N/28W-12K1	235	10	D
4N/28W-12K1	245	60	D
4N/28W-12K1	255	10	D
4N/28W-12K1	265	55.6	D
4N/28W-12K1	275	30	D
4N/28W-12K1	285	80	D
4N/28W-12K2	5	100	D
4N/28W-12K2	15	50	D
4N/28W-12K2	25	0	D
4N/28W-12K2	35	0	D
4N/28W-12K2	45	0	D
4N/28W-12K2	55	0	D
4N/28W-12K2	65	0	D
4N/28W-12K2	75	0	D
4N/28W-12K2	85	0	D
4N/28W-12K2	95	0	D
4N/28W-12K2	105	0	D
4N/28W-12K2	115	0	D
4N/28W-12K2	125	0	D
4N/28W-12K2	135	0	D
4N/28W-12K2	145	0	D
4N/28W-12K2	155	0	D
4N/28W-12K2	165	0	D
4N/28W-12K2	175	10	D
4N/28W-12K2	185	100	D
4N/28W-12K2	195	45.5	D
4N/28W-12K2	205	0	D
4N/28W-12K2	215	0	D
4N/28W-12K2	225	0	D
4N/28W-12K2	235	0	D
4N/28W-12K2	245	0	D
4N/28W-12K2	255	0	D
4N/28W-12K2	265	0	D
4N/28W-12K2	275	0	D
4N/28W-12K2	285	0	D
4N/28W-12K3	5	0	D
4N/28W-12K3	15	0	D
4N/28W-12K3	25	0	D
4N/28W-12K3	35	0	D
4N/28W-12K3	45	0	D

Table B1–1. Calculated percent-coarse intervals for all drillers' logs and e-logs used to define textural properties of the hydrogeologic framework model.—Continued

[Percent-coarse values are calculated for 10-foot intervals for the entire depth of each borehole. State well number is the state of California well identifier; interval midpoint depth is the midpoint of each 10-foot interval, in feet from top of borehole; PC is the percent-coarse value for each interval; log type defines whether the borehole is a drillers' lithology log (D) or a geophysical e-log (E).]

State well number	Interval midpoint depth (feet)	PC	Log type
4N/28W-12K3	55	0	D
4N/28W-12K3	65	0	D
4N/28W-12K3	75	0	D
4N/28W-12K3	85	0	D
4N/28W-12K3	95	90	D
4N/28W-12K4	5	0	D
4N/28W-12K4	15	0	D
4N/28W-12K4	25	0	D
4N/28W-12K4	35	0	D
4N/28W-12K4	45	0	D
4N/28W-12K4	55	0	D
4N/28W-12K4	65	0	D
4N/28W-12K4	75	0	D
4N/28W-12K4	85	0	D
4N/28W-12K4	95	0	D
4N/28W-12K4	105	0	D
4N/28W-12K4	115	0	D
4N/28W-12K4	125	0	D
4N/28W-12K4	135	0	D
4N/28W-12K4	145	0	D
4N/28W-12K4	155	10	D
4N/28W-12K4	165	100	D
4N/28W-12K4	175	100	D
4N/28W-12K4	185	100	D
4N/28W-12K4	195	100	D
4N/28W-12K4	205	100	D
4N/28W-12K4	215	9.1	D
4N/28W-12K4	225	100	D
4N/28W-12K4	235	90	D
4N/28W-12K4	245	0	D
4N/28W-12K4	255	0	D
4N/28W-12K4	265	0	D
4N/28W-12K4	275	0	D
4N/28W-12L1	5	0	D
4N/28W-12L1	15	0	D
4N/28W-12L1	25	0	D
4N/28W-12L1	35	0	D
4N/28W-12L1	45	0	D
4N/28W-12L1	55	0	D
4N/28W-12L1	65	0	D
4N/28W-12L1	75	0	D
4N/28W-12L1	85	0	D
4N/28W-12L1	95	0	D
4N/28W-12L1	105	0	D
4N/28W-12L1	115	0	D
4N/28W-12L1	125	0	D
4N/28W-12L1	135	60	D
4N/28W-12L1	145	100	D
4N/28W-12L1	155	100	D
4N/28W-12L1	165	100	D
4N/28W-12L1	175	100	D
4N/28W-12L1	185	100	D
4N/28W-12L1	195	100	D
4N/28W-12L1	205	100	D
4N/28W-12L1	215	100	D
4N/28W-12L1	225	100	D
4N/28W-12L1	235	100	D
4N/28W-12L1	245	100	D
4N/28W-12L1	255	100	D
4N/28W-12L2	35	0	D
4N/28W-12L2	45	0	D
4N/28W-12L2	55	0	D
4N/28W-12L2	65	44.4	D
4N/28W-12L2	75	20	D
4N/28W-12L2	85	0	D
4N/28W-12L2	95	0	D
4N/28W-12L2	105	40	D
4N/28W-12L2	115	0	D
4N/28W-12L2	125	0	D
4N/28W-12L2	135	100	D
4N/28W-12L2	145	100	D
4N/28W-12L2	155	100	D
4N/28W-12L2	165	100	D
4N/28W-12L2	175	100	D
4N/28W-12L2	185	100	D
4N/28W-12L4	5	0	D
4N/28W-12L4	15	0	D
4N/28W-12L4	25	0	D

Table B1–1. Calculated percent-coarse intervals for all drillers' logs and e-logs used to define textural properties of the hydrogeologic framework model.—Continued

[Percent-coarse values are calculated for 10-foot intervals for the entire depth of each borehole. State well number is the state of California well identifier; interval midpoint depth is the midpoint of each 10-foot interval, in feet from top of borehole; PC is the percent-coarse value for each interval; log type defines whether the borehole is a drillers' lithology log (D) or a geophysical e-log (E).]

State well number	Interval midpoint depth (feet)	PC	Log type
4N/28W-12L4	35	0	D
4N/28W-12L4	45	0	D
4N/28W-12L4	55	0	D
4N/28W-12L4	65	0	D
4N/28W-12L4	75	0	D
4N/28W-12L4	85	0	D
4N/28W-12L4	95	0	D
4N/28W-12L4	105	0	D
4N/28W-12L4	115	0	D
4N/28W-12L4	125	0	D
4N/28W-12L4	135	0	D
4N/28W-12L4	145	0	D
4N/28W-12L4	155	0	D
4N/28W-12L4	165	0	D
4N/28W-12L4	175	0	D
4N/28W-12L4	185	0	D
4N/28W-12L4	195	0	D
4N/28W-12L4	205	0	D
4N/28W-12L4	215	9.1	D
4N/28W-12L4	225	10	D
4N/28W-12L4	235	0	D
4N/28W-12L4	245	0	D
4N/28W-12L4	255	0	D
4N/28W-12L4	265	0	D
4N/28W-12L4	275	11.1	D
4N/28W-12L4	285	40	D
4N/28W-12L4	295	0	D
4N/28W-12L4	305	0	D
4N/28W-12L4	315	0	D
4N/28W-12L4	325	0	D
4N/28W-12L4	335	90	D
4N/28W-12L4	345	40	D
4N/28W-12L4	355	0	D
4N/28W-12L4	365	80	D
4N/28W-12L4	375	66.7	D
4N/28W-12L4	385	0	D
4N/28W-12L4	395	0	D
4N/28W-12L5	5	72.7	D
4N/28W-12L5	15	0	D
4N/28W-12L5	25	0	D
4N/28W-12L5	35	0	D
4N/28W-12L5	45	0	D
4N/28W-12L5	55	0	D
4N/28W-12L5	65	0	D
4N/28W-12L5	75	0	D
4N/28W-12L5	85	0	D
4N/28W-12L5	95	0	D
4N/28W-12L5	105	0	D
4N/28W-12L5	115	0	D
4N/28W-12L5	125	0	D
4N/28W-12L5	135	30	D
4N/28W-12L5	145	100	D
4N/28W-12L5	155	100	D
4N/28W-12L5	165	100	D
4N/28W-12L5	175	100	D
4N/28W-12L5	185	100	D
4N/28W-12L5	195	100	D
4N/28W-12L5	205	100	D
4N/28W-12L5	215	100	D
4N/28W-12L5	225	90	D
4N/28W-12L5	235	0	D
4N/28W-12R1	5	27.3	D
4N/28W-12R1	15	0	D
4N/28W-12R1	25	0	D
4N/28W-12R1	35	0	D
4N/28W-12R1	45	0	D
4N/28W-12R1	55	40	D
4N/28W-12R1	65	0	D
4N/28W-12R1	75	0	D
4N/28W-12R1	85	0	D
4N/28W-12R1	95	0	D
4N/28W-12R1	105	80	D
4N/28W-12R1	115	60	D
4N/28W-12R1	125	0	D
4N/28W-12R1	135	0	D
4N/28W-12R1	145	0	D
4N/28W-12R1	155	0	D
4N/28W-12R1	165	0	D

Table B1–1. Calculated percent-coarse intervals for all drillers' logs and e-logs used to define textural properties of the hydrogeologic framework model.—Continued

[Percent-coarse values are calculated for 10-foot intervals for the entire depth of each borehole. State well number is the state of California well identifier; interval midpoint depth is the midpoint of each 10-foot interval, in feet from top of borehole; PC is the percent-coarse value for each interval; log type defines whether the borehole is a drillers' lithology log (D) or a geophysical e-log (E).]

State well number	Interval midpoint depth (feet)	PC	Log type
4N/28W-12R1	175	0	D
4N/28W-12R1	185	0	D
4N/28W-12R1	195	0	D
4N/28W-12R1	205	55.6	D
4N/28W-12R1	215	100	D
4N/28W-12R1	225	40	D
4N/28W-12R1	235	0	D
4N/28W-12R1	245	100	D
4N/28W-12R1	255	100	D
4N/28W-12R1	265	100	D
4N/28W-12R1	275	0	D
4N/28W-12R1	285	0	D
4N/28W-12R1	295	63.6	D
4N/28W-12R1	305	0	D
4N/28W-12R1	315	0	D
4N/28W-12R1	325	0	D
4N/28W-12R1	335	0	D
4N/28W-12R1	345	0	D
4N/28W-12R1	355	0	D
4N/28W-12R2	5	100	D
4N/28W-12R2	15	100	D
4N/28W-12R2	25	40	D
4N/28W-12R2	35	0	D
4N/28W-12R2	45	0	D
4N/28W-12R2	55	0	D
4N/28W-12R2	65	0	D
4N/28W-12R2	75	0	D
4N/28W-12R2	85	50	D
4N/28W-12R2	95	100	D
4N/28W-12R2	105	40	D
4N/28W-12R2	115	0	D
4N/28W-12R2	125	0	D
4N/28W-12R2	135	0	D
4N/28W-12R2	145	0	D
4N/28W-12R2	155	0	D
4N/28W-12R2	165	0	D
4N/28W-12R2	175	0	D
4N/28W-12R2	185	0	D
4N/28W-12R2	195	0	D
4N/28W-12R2	205	55.6	D
4N/28W-12R2	215	100	D
4N/28W-12R2	225	100	D
4N/28W-12R2	235	100	D
4N/28W-12R2	245	100	D
4N/28W-12R2	255	100	D
4N/28W-12R2	265	100	D
4N/28W-12R2	275	0	D
4N/28W-12R2	285	90	D
4N/28W-12R2	295	100	D
4N/28W-12R2	305	100	D
4N/28W-12R2	315	60	D
4N/28W-12R2	325	100	D
4N/27W-8M6	45	0	E
4N/27W-8M6	55	0	E
4N/27W-8M6	65	0	E
4N/27W-8M6	75	0	E
4N/27W-8M6	85	0	E
4N/27W-8M6	95	0	E
4N/27W-8M6	105	0	E
4N/27W-8M6	115	0	E
4N/27W-8M6	125	0	E
4N/27W-8M6	135	0	E
4N/27W-8M6	145	90	E
4N/27W-8M6	155	0	E
4N/27W-8M6	165	0	E
4N/27W-8M6	175	0	E
4N/27W-8M6	185	0	E
4N/27W-8M6	195	0	E
4N/27W-8M6	205	0	E
4N/27W-8M6	215	0	E
4N/27W-8M6	225	0	E
4N/27W-8M6	235	0	E
4N/27W-8M6	245	20	E
4N/27W-8M6	255	0	E
4N/27W-8M6	265	70	E
4N/27W-8M6	275	90	E
4N/27W-8M6	285	0	E
4N/27W-8M6	295	0	E

Table B1–1. Calculated percent-coarse intervals for all drillers' logs and e-logs used to define textural properties of the hydrogeologic framework model.—Continued

[Percent-coarse values are calculated for 10-foot intervals for the entire depth of each borehole. State well number is the state of California well identifier; interval midpoint depth is the midpoint of each 10-foot interval, in feet from top of borehole; PC is the percent-coarse value for each interval; log type defines whether the borehole is a drillers' lithology log (D) or a geophysical e-log (E).]

State well number	Interval midpoint depth (feet)	PC	Log type
4N/27W-8M6	305	60	E
4N/27W-8M6	315	90	E
4N/27W-8M6	325	0	E
4N/27W-8M6	335	0	E
4N/27W-8M6	345	20	E
4N/27W-8M6	355	0	E
4N/27W-8M6	365	70	E
4N/27W-8M6	375	80	E
4N/27W-8M6	385	100	E
4N/27W-8M6	395	100	E
4N/27W-8M6	405	60	E
4N/27W-8M6	415	0	E
4N/27W-8M6	425	0	E
4N/27W-8M6	435	0	E
4N/27W-8M6	445	0	E
4N/27W-8M6	455	0	E
4N/27W-8M6	465	0	E
4N/27W-8M6	475	0	E
4N/27W-8M6	485	0	E
4N/27W-8M6	495	0	E
4N/27W-8M6	505	0	E
4N/27W-8M6	515	0	E
4N/27W-8M6	525	0	E
4N/27W-8M6	535	70	E
4N/27W-8M6	545	100	E
4N/27W-8M6	555	100	E
4N/27W-8M6	565	100	E
4N/27W-8M6	575	100	E
4N/27W-8M6	585	50	E
4N/27W-22A2	35	0	E
4N/27W-22A2	45	0	E
4N/27W-22A2	55	0	E
4N/27W-22A2	65	0	E
4N/27W-22A2	75	0	E
4N/27W-22A2	85	0	E
4N/27W-22A2	95	0	E
4N/27W-22A2	105	0	E
4N/27W-22A2	115	0	E
4N/27W-22A2	125	0	E
4N/27W-22A2	135	80	E
4N/27W-22A2	145	100	E
4N/27W-22A2	155	100	E
4N/27W-22A2	165	100	E
4N/27W-22A2	175	100	E
4N/27W-22A2	185	100	E
4N/27W-22A2	195	70	E
4N/27W-22A2	205	60	E
4N/27W-22A2	215	80	E
4N/27W-22A2	225	70	E
4N/27W-22A2	235	100	E
4N/27W-22A2	245	30	E
4N/27W-22A2	255	0	E
4N/27W-22A2	265	60	E
4N/27W-22A2	275	100	E
4N/27W-22A2	285	100	E
4N/27W-22A2	295	100	E
4N/27W-22A2	305	40	E
4N/27W-22A2	315	0	E
4N/27W-22A2	325	0	E
4N/27W-22A2	335	0	E
4N/27W-22A2	345	0	E
4N/27W-22A2	355	0	E
4N/27W-22A2	365	60	E
4N/27W-22A2	375	100	E
4N/27W-22A2	385	60	E
4N/27W-22A2	395	0	E
4N/27W-22A2	405	0	E
4N/27W-22A2	415	0	E
4N/27W-22A2	425	0	E
4N/27W-22A2	435	0	E
4N/27W-22A2	445	0	E
4N/27W-22A2	455	0	E
4N/27W-22A2	465	0	E
4N/27W-22A2	475	20	E
4N/27W-22A2	485	40	E
4N/27W-22A2	495	20	E
4N/27W-22A2	505	100	E
4N/27W-22A2	515	100	E

Table B1–1. Calculated percent-coarse intervals for all drillers' logs and e-logs used to define textural properties of the hydrogeologic framework model.—Continued

[Percent-coarse values are calculated for 10-foot intervals for the entire depth of each borehole. State well number is the state of California well identifier; interval midpoint depth is the midpoint of each 10-foot interval, in feet from top of borehole; PC is the percent-coarse value for each interval; log type defines whether the borehole is a drillers' lithology log (D) or a geophysical e-log (E).]

State well number	Interval midpoint depth (feet)	PC	Log type
4N/27W-22A2	525	100	E
4N/27W-22A2	535	100	E
4N/27W-22A2	545	10	E
4N/27W-22A2	555	0	E
4N/27W-22A2	565	50	E
4N/27W-22A2	575	100	E
4N/27W-22A2	585	40	E
4N/27W-22A2	595	0	E
4N/27W-22A2	605	0	E
4N/27W-22A2	615	0	E
4N/27W-22A2	625	80	E
4N/27W-22A2	635	20	E
4N/27W-22A2	645	0	E
4N/27W-22A2	655	0	E
4N/27W-22A2	665	100	E
4N/27W-22A2	675	100	E
4N/27W-22A2	685	100	E
4N/27W-22A2	695	100	E
4N/27W-18Q4	25	0	E
4N/27W-18Q4	35	0	E
4N/27W-18Q4	45	0	E
4N/27W-18Q4	55	10	E
4N/27W-18Q4	65	100	E
4N/27W-18Q4	75	100	E
4N/27W-18Q4	85	100	E
4N/27W-18Q4	95	100	E
4N/27W-18Q4	105	100	E
4N/27W-18Q4	115	80	E
4N/27W-18Q4	125	0	E
4N/27W-18Q4	135	0	E
4N/27W-18Q4	145	0	E
4N/27W-18Q4	155	0	E
4N/27W-18Q4	165	0	E
4N/27W-18Q4	175	0	E
4N/27W-18Q4	185	0	E
4N/27W-18Q4	195	0	E
4N/27W-18Q4	205	0	E
4N/27W-18Q4	215	0	E
4N/27W-18Q4	225	0	E
4N/27W-18Q4	235	0	E
4N/28W-12L6	35	0	E
4N/28W-12L6	45	0	E
4N/28W-12L6	55	0	E
4N/28W-12L6	65	0	E
4N/28W-12L6	75	0	E
4N/28W-12L6	85	0	E
4N/28W-12L6	95	0	E
4N/28W-12L6	105	0	E
4N/28W-12L6	115	0	E
4N/28W-12L6	125	0	E
4N/28W-12L6	135	0	E
4N/28W-12L6	145	0	E
4N/28W-12L6	155	0	E
4N/28W-12L6	165	0	E
4N/28W-12L6	175	40	E
4N/28W-12L6	185	90	E
4N/28W-12L6	195	0	E
4N/28W-12L6	205	0	E
4N/28W-12L6	215	0	E
4N/28W-12L6	225	0	E
4N/28W-12L6	235	0	E
4N/28W-12L6	245	0	E
4N/28W-12L6	255	0	E
4N/28W-12L6	265	0	E
4N/28W-12L6	275	10	E
4N/28W-12L6	285	30	E
4N/28W-12L6	295	100	E
4N/28W-12L6	305	100	E
4N/28W-12L6	315	80	E
4N/28W-12L6	325	0	E
4N/28W-12L6	335	30	E
4N/28W-12L6	345	100	E
4N/28W-12L6	355	100	E
4N/28W-12L6	365	100	E
4N/28W-12L6	375	70	E
4N/28W-12L6	385	0	E
4N/27W-24D2	55	0	E
4N/27W-24D2	65	0	E

Table B1–1. Calculated percent-coarse intervals for all drillers' logs and e-logs used to define textural properties of the hydrogeologic framework model.—Continued

[Percent-coarse values are calculated for 10-foot intervals for the entire depth of each borehole. State well number is the state of California well identifier; interval midpoint depth is the midpoint of each 10-foot interval, in feet from top of borehole; PC is the percent-coarse value for each interval; log type defines whether the borehole is a drillers' lithology log (D) or a geophysical e-log (E).]

State well number	Interval midpoint depth (feet)	PC	Log type
4N/27W-24D2	75	0	E
4N/27W-24D2	85	0	E
4N/27W-24D2	95	0	E
4N/27W-24D2	105	0	E
4N/27W-24D2	115	0	E
4N/27W-24D2	125	0	E
4N/27W-24D2	135	0	E
4N/27W-24D2	145	0	E
4N/27W-24D2	155	40	E
4N/27W-24D2	165	0	E
4N/27W-24D2	175	0	E
4N/27W-24D2	185	0	E
4N/27W-24D2	195	0	E
4N/27W-24D2	205	40	E
4N/27W-24D2	215	100	E
4N/27W-24D2	225	100	E
4N/27W-24D2	235	70	E
4N/27W-24D2	245	0	E
4N/27W-24D2	255	20	E
4N/27W-24D2	265	50	E
4N/27W-24D2	275	90	E
4N/27W-24D2	285	30	E
4N/27W-24D2	295	0	E
4N/27W-24D2	305	40	E
4N/27W-24D2	315	20	E
4N/27W-24D2	325	0	E
4N/27W-24D2	335	60	E
4N/27W-24D2	345	100	E
4N/27W-24D2	355	0	E
4N/27W-24D2	365	50	E
4N/27W-24D2	375	0	E
4N/27W-24D2	385	0	E
4N/27W-24D2	395	0	E
4N/27W-24D2	405	0	E
4N/27W-24D2	415	90	E
4N/27W-24D2	425	100	E
4N/27W-24D2	435	100	E
4N/27W-24D2	445	70	E
4N/27W-24D2	455	100	E
4N/27W-24D2	465	90	E
4N/27W-24D2	475	0	E
4N/27W-24D2	485	0	E
4N/27W-24D2	495	0	E
4N/27W-24D2	505	0	E
4N/27W-23H1	115	0	E
4N/27W-23H1	125	30	E
4N/27W-23H1	135	100	E
4N/27W-23H1	145	70	E
4N/27W-23H1	155	0	E
4N/27W-23H1	165	0	E
4N/27W-23H1	175	0	E
4N/27W-23H1	185	0	E
4N/27W-23H1	195	0	E
4N/27W-23H1	205	0	E
4N/27W-23H1	215	0	E
4N/27W-23H1	225	0	E
4N/27W-23H1	235	0	E
4N/27W-23H1	245	0	E
4N/27W-23H1	255	0	E
4N/27W-23H1	265	30	E
4N/27W-23H1	275	90	E
4N/27W-23H1	285	60	E
4N/27W-23H1	295	0	E
4N/27W-23H1	305	80	E
4N/27W-23H1	315	30	E
4N/27W-23H1	325	0	E
4N/27W-23H1	335	0	E
4N/27W-23H1	345	0	E
4N/27W-23H1	355	0	E
4N/27W-23H1	365	0	E
4N/27W-23H1	375	0	E
4N/27W-23H1	385	80	E
4N/27W-23H1	395	30	E
4N/27W-23H1	405	20	E
4N/27W-23H1	415	80	E
4N/27W-23H1	425	50	E
4N/27W-23H1	435	0	E
4N/27W-23H1	445	20	E

Table B1–1. Calculated percent-coarse intervals for all drillers' logs and e-logs used to define textural properties of the hydrogeologic framework model.—Continued

[Percent-coarse values are calculated for 10-foot intervals for the entire depth of each borehole. State well number is the state of California well identifier; interval midpoint depth is the midpoint of each 10-foot interval, in feet from top of borehole; PC is the percent-coarse value for each interval; log type defines whether the borehole is a drillers' lithology log (D) or a geophysical e-log (E).]

State well number	Interval midpoint depth (feet)	PC	Log type
4N/27W-23H1	455	30	E
4N/27W-23H1	465	20	E
4N/27W-23H1	475	0	E
4N/27W-23H1	485	20	E
4N/27W-23H1	495	50	E
4N/27W-23H1	505	100	E
4N/27W-23H1	515	20	E
4N/27W-23H1	525	0	E
4N/27W-23H1	535	100	E
4N/27W-23H1	545	100	E
4N/27W-23H1	555	100	E
4N/27W-23H1	565	100	E
4N/27W-23H1	575	100	E
4N/27W-23H1	585	100	E
4N/27W-23H1	595	30	E
4N/27W-23H1	605	0	E
4N/27W-23H1	615	50	E
4N/27W-23H1	625	40	E
4N/27W-23H1	635	100	E
4N/27W-23H1	645	40	E
4N/27W-23H1	655	90	E
4N/27W-23H1	665	30	E
4N/27W-23H1	675	50	E
4N/27W-23H1	685	100	E
4N/27W-23H1	695	100	E
4N/27W-23H1	705	100	E
4N/27W-23H1	715	100	E
4N/27W-23H1	725	100	E
4N/27W-23H1	735	100	E
4N/27W-23F5	5	100	E
4N/27W-23F5	15	50	E
4N/27W-23F5	25	0	E
4N/27W-23F5	35	0	E
4N/27W-23F5	45	0	E
4N/27W-23F5	55	0	E
4N/27W-23F5	65	0	E
4N/27W-23F5	75	0	E
4N/27W-23F5	85	0	E
4N/27W-23F5	95	0	E
4N/27W-23F5	105	0	E
4N/27W-23F5	115	0	E
4N/27W-23F5	125	0	E
4N/27W-23F5	135	0	E
4N/27W-23F5	145	0	E
4N/27W-23F5	155	0	E
4N/27W-23F5	165	40	E
4N/27W-23F5	175	90	E
4N/27W-23F5	185	100	E
4N/27W-23F5	195	100	E
4N/27W-23F5	205	30	E
4N/27W-23F5	215	70	E
4N/27W-23F5	225	40	E
4N/27W-23F5	235	0	E
4N/27W-23F5	245	100	E
4N/27W-23F5	255	10	E
4N/27W-23F5	265	0	E
4N/27W-23F5	275	0	E
4N/27W-23F5	285	100	E
4N/27W-23F5	295	100	E
4N/27W-23F5	305	100	E
4N/27W-23F5	315	80	E
4N/27W-23F5	325	50	E
4N/27W-23F5	335	100	E
4N/27W-23F5	345	90	E
4N/27W-23F5	355	0	E
4N/27W-23F5	365	100	E
4N/27W-23F5	375	100	E
4N/27W-23F5	385	100	E
4N/27W-23F5	395	70	E
4N/27W-23F5	405	0	E
4N/27W-23F5	415	0	E
4N/27W-23F5	425	0	E
4N/27W-23F5	435	0	E
4N/27W-23F5	445	0	E
4N/27W-23F5	455	0	E
4N/27W-23F5	465	0	E
4N/27W-23F5	475	50	E
4N/27W-23F5	485	80	E

Table B1–1. Calculated percent-coarse intervals for all drillers' logs and e-logs used to define textural properties of the hydrogeologic framework model.—Continued

[Percent-coarse values are calculated for 10-foot intervals for the entire depth of each borehole. State well number is the state of California well identifier; interval midpoint depth is the midpoint of each 10-foot interval, in feet from top of borehole; PC is the percent-coarse value for each interval; log type defines whether the borehole is a drillers' lithology log (D) or a geophysical e-log (E).]

State well number	Interval midpoint depth (feet)	PC	Log type
4N/27W-23F5	495	100	E
4N/27W-23F5	505	70	E
4N/27W-23F5	515	80	E
4N/27W-23F5	525	60	E
4N/27W-23F5	535	100	E
4N/27W-23F5	545	100	E
4N/27W-23F5	555	100	E
4N/27W-23F5	565	100	E
4N/27W-23F5	575	100	E
4N/27W-23F5	585	40	E
4N/27W-23F5	595	40	E
4N/27W-23F5	605	100	E
4N/27W-23F5	615	100	E
4N/27W-23F5	625	40	E
4N/27W-23F5	635	0	E
4N/27W-23F5	645	10	E
4N/27W-23F5	655	60	E
4N/27W-23F5	665	100	E
4N/27W-23F5	675	100	E
4N/27W-23F5	685	100	E
4N/27W-23F5	695	100	E
4N/27W-23F5	705	40	E
4N/27W-23F5	715	60	E
4N/27W-23F5	725	100	E
4N/27W-23F5	735	100	E
4N/27W-23F5	745	100	E
4N/27W-23F5	755	100	E
4N/27W-23F5	765	100	E
4N/27W-23F5	775	100	E
4N/27W-23F5	785	100	E
4N/27W-23E6	35	100	E
4N/27W-23E6	45	60	E
4N/27W-23E6	55	20	E
4N/27W-23E6	65	10	E
4N/27W-23E6	75	100	E
4N/27W-23E6	85	100	E
4N/27W-23E6	95	100	E
4N/27W-23E6	105	70	E
4N/27W-23E6	115	100	E
4N/27W-23E6	125	0	E
4N/27W-23E6	135	80	E
4N/27W-23E6	145	100	E
4N/27W-23E6	155	100	E
4N/27W-23E6	165	20	E
4N/27W-23E6	175	0	E
4N/27W-23E6	185	0	E
4N/27W-23E6	195	0	E
4N/27W-23E6	205	0	E
4N/27W-23E6	215	0	E
4N/27W-23E6	225	30	E
4N/27W-23E6	235	30	E
4N/27W-23E6	245	0	E
4N/27W-23E6	255	90	E
4N/27W-23E6	265	100	E
4N/27W-23E6	275	100	E
4N/27W-23E6	285	20	E
4N/27W-23E6	295	40	E
4N/27W-23E6	305	70	E
4N/27W-23E6	315	100	E
4N/27W-23E6	325	70	E
4N/27W-23E6	335	60	E
4N/27W-23E6	345	100	E
4N/27W-23E6	355	10	E
4N/27W-23E6	365	0	E
4N/27W-23E6	375	60	E
4N/27W-23E6	385	40	E
4N/27W-23E6	395	0	E
4N/27W-23E6	405	0	E
4N/27W-23E6	415	60	E
4N/27W-23E6	425	0	E
4N/27W-23E6	435	0	E
4N/27W-23E6	445	60	E
4N/27W-23E6	455	0	E
4N/27W-23E6	465	0	E
4N/27W-23E6	475	0	E
4N/27W-23E6	485	0	E
4N/27W-23E6	495	0	E
4N/27W-23E6	505	100	E

Table B1–1. Calculated percent-coarse intervals for all drillers' logs and e-logs used to define textural properties of the hydrogeologic framework model.—Continued

[Percent-coarse values are calculated for 10-foot intervals for the entire depth of each borehole. State well number is the state of California well identifier; interval midpoint depth is the midpoint of each 10-foot interval, in feet from top of borehole; PC is the percent-coarse value for each interval; log type defines whether the borehole is a drillers' lithology log (D) or a geophysical e-log (E).]

State well number	Interval midpoint depth (feet)	PC	Log type
4N/27W-23E6	515	100	E
4N/27W-23E6	525	100	E
4N/27W-23E6	535	0	E
4N/27W-23E6	545	0	E
4N/27W-23E6	555	80	E
4N/27W-23E6	565	60	E
4N/27W-23E6	575	0	E
4N/27W-23E6	585	0	E
4N/27W-23E6	595	0	E
4N/27W-23E6	605	40	E
4N/27W-23E6	615	100	E
4N/27W-23E6	625	70	E
4N/27W-23E6	635	0	E
4N/27W-23E6	645	30	E
4N/27W-23E6	655	100	E
4N/27W-23E6	665	100	E
4N/27W-23E6	675	40	E
4N/27W-23E6	685	0	E
4N/27W-23E6	695	0	E
4N/27W-23E6	705	50	E
4N/27W-23E6	715	0	E
4N/27W-23E6	725	0	E
4N/27W-23E1	45	0	E
4N/27W-23E1	55	0	E
4N/27W-23E1	65	0	E
4N/27W-23E1	75	0	E
4N/27W-23E1	85	10	E
4N/27W-23E1	95	50	E
4N/27W-23E1	105	0	E
4N/27W-23E1	115	0	E
4N/27W-23E1	125	0	E
4N/27W-23E1	135	100	E
4N/27W-23E1	145	100	E
4N/27W-23E1	155	100	E
4N/27W-23E1	165	100	E
4N/27W-23E1	175	80	E
4N/27W-23E1	185	0	E
4N/27W-23E1	195	0	E
4N/27W-23E1	205	0	E
4N/27W-23E1	215	10	E
4N/27W-23E1	225	100	E
4N/27W-23E1	235	20	E
4N/27W-23E1	245	0	E
4N/27W-23E1	255	70	E
4N/27W-23E1	265	100	E
4N/27W-23E1	275	100	E
4N/27W-23E1	285	50	E
4N/27W-23E1	295	0	E
4N/27W-23E1	305	0	E
4N/27W-23E1	315	0	E
4N/27W-23E1	325	0	E
4N/27W-23E1	335	70	E
4N/27W-23E1	345	100	E
4N/27W-23E1	355	100	E
4N/27W-23E1	365	100	E
4N/27W-23E1	375	70	E
4N/27W-23E1	385	0	E
4N/27W-23E1	395	0	E
4N/27W-23E1	405	0	E
4N/27W-23E1	415	0	E
4N/27W-23E1	425	0	E
4N/27W-23E1	435	0	E
4N/27W-23E1	445	10	E
4N/27W-23E1	455	50	E
4N/27W-23E1	465	0	E
4N/27W-23E1	475	0	E
4N/27W-23E1	485	0	E
4N/27W-23E1	495	0	E
4N/27W-23E1	505	50	E
4N/27W-23E1	515	100	E
4N/27W-23E1	525	20	E
4N/27W-23E1	535	0	E
4N/27W-23E1	545	70	E
4N/27W-23E1	555	30	E
4N/27W-23E1	565	0	E
4N/27W-23E1	575	0	E
4N/27W-23E1	585	50	E
4N/27W-23E1	595	100	E

Table B1–1. Calculated percent-coarse intervals for all drillers' logs and e-logs used to define textural properties of the hydrogeologic framework model.—Continued

[Percent-coarse values are calculated for 10-foot intervals for the entire depth of each borehole. State well number is the state of California well identifier; interval midpoint depth is the midpoint of each 10-foot interval, in feet from top of borehole; PC is the percent-coarse value for each interval; log type defines whether the borehole is a drillers' lithology log (D) or a geophysical e-log (E).]

State well number	Interval midpoint depth (feet)	PC	Log type
4N/27W-23E1	605	30	E
4N/27W-23E1	615	0	E
4N/27W-23E1	625	20	E
4N/27W-23E1	635	100	E
4N/27W-23E1	645	50	E
4N/27W-23E1	655	0	E
4N/27W-23E1	665	0	E
4N/27W-23E1	675	0	E
4N/27W-23E1	685	0	E
4N/27W-23E1	695	0	E
4N/27W-23E1	705	0	E
4N/27W-23E1	715	0	E
4N/27W-23E1	725	0	E
4N/27W-23E1	735	0	E
4N/27W-23E1	745	0	E
4N/27W-23E1	755	0	E
4N/27W-23E1	765	0	E
4N/27W-23E1	775	100	E
4N/27W-23E1	785	80	E
4N/27W-23E1	795	0	E
4N/27W-23E1	805	10	E
4N/27W-23E1	815	100	E
4N/27W-23E1	825	10	E
4N/27W-23D1	15	0	E
4N/27W-23D1	25	0	E
4N/27W-23D1	35	0	E
4N/27W-23D1	45	0	E
4N/27W-23D1	55	0	E
4N/27W-23D1	65	0	E
4N/27W-23D1	75	0	E
4N/27W-23D1	85	0	E
4N/27W-23D1	95	80	E
4N/27W-23D1	105	50	E
4N/27W-23D1	115	20	E
4N/27W-23D1	125	100	E
4N/27W-23D1	135	100	E
4N/27W-23D1	145	90	E
4N/27W-23D1	155	0	E
4N/27W-23D1	165	0	E
4N/27W-23D1	175	30	E
4N/27W-23D1	185	80	E
4N/27W-23D1	195	0	E
4N/27W-23D1	205	0	E
4N/27W-23D1	215	0	E
4N/27W-23D1	225	60	E
4N/27W-23D1	235	0	E
4N/27W-23D1	245	40	E
4N/27W-23D1	255	100	E
4N/27W-23D1	265	100	E
4N/27W-23D1	275	30	E
4N/27W-23D1	285	60	E
4N/27W-23D1	295	60	E
4N/27W-23D1	305	0	E
4N/27W-23D1	315	0	E
4N/27W-23D1	325	100	E
4N/27W-23D1	335	100	E
4N/27W-23D1	345	100	E
4N/27W-23D1	355	100	E
4N/27W-23D1	365	50	E
4N/27W-23D1	375	0	E
4N/27W-23D1	385	0	E
4N/27W-22Q1	25	70	E
4N/27W-22Q1	35	100	E
4N/27W-22Q1	45	20	E
4N/27W-22Q1	55	20	E
4N/27W-22B2	35	0	E
4N/27W-22B2	45	0	E
4N/27W-22B2	55	0	E
4N/27W-22B2	65	0	E
4N/27W-22B2	75	0	E
4N/27W-22B2	85	0	E
4N/27W-22B2	95	40	E
4N/27W-22B2	105	30	E
4N/27W-22B2	115	30	E
4N/27W-22B2	125	30	E
4N/27W-22B2	135	40	E
4N/27W-22B2	145	0	E
4N/27W-22B2	155	0	E

Table B1–1. Calculated percent-coarse intervals for all drillers' logs and e-logs used to define textural properties of the hydrogeologic framework model.—Continued

[Percent-coarse values are calculated for 10-foot intervals for the entire depth of each borehole. State well number is the state of California well identifier; interval midpoint depth is the midpoint of each 10-foot interval, in feet from top of borehole; PC is the percent-coarse value for each interval; log type defines whether the borehole is a drillers' lithology log (D) or a geophysical e-log (E).]

State well number	Interval midpoint depth (feet)	PC	Log type
4N/27W-22B2	165	0	E
4N/27W-22B2	175	20	E
4N/27W-22B2	185	0	E
4N/27W-22B2	195	40	E
4N/27W-22B2	205	30	E
4N/27W-22B2	215	100	E
4N/27W-22B2	225	100	E
4N/27W-22B2	235	100	E
4N/27W-22B2	245	100	E
4N/27W-22B2	255	30	E
4N/27W-22B2	265	0	E
4N/27W-22B2	275	0	E
4N/27W-22B2	285	0	E
4N/27W-22B2	295	0	E
4N/27W-22B2	305	0	E
4N/27W-22B2	315	50	E
4N/27W-22B2	325	0	E
4N/27W-22B2	335	60	E
4N/27W-22B2	345	0	E
4N/27W-22B2	355	50	E
4N/27W-22B2	365	60	E
4N/27W-22B2	375	0	E
4N/27W-22B2	385	0	E
4N/27W-22B2	395	0	E
4N/27W-22B2	405	0	E
4N/27W-22B2	415	0	E
4N/27W-22B2	425	100	E
4N/27W-22B2	435	100	E
4N/27W-22B2	445	30	E
4N/27W-22B2	455	0	E
4N/27W-22B2	465	50	E
4N/27W-22B2	475	100	E
4N/27W-22B2	485	30	E
4N/27W-22B2	495	50	E
4N/27W-22B2	505	0	E
4N/27W-22B2	515	0	E
4N/27W-22B2	525	40	E
4N/27W-22B2	535	0	E
4N/27W-22B2	545	0	E
4N/27W-22B2	555	0	E
4N/27W-22B2	565	50	E
4N/27W-22B2	575	100	E
4N/27W-22B2	585	100	E
4N/27W-22B2	595	100	E
4N/27W-22B2	605	100	E
4N/27W-22B2	615	100	E
4N/27W-22B2	625	100	E
4N/27W-22B2	635	100	E
4N/27W-22B2	645	100	E
4N/27W-22B2	655	100	E
4N/27W-22B2	665	100	E
4N/27W-22B2	675	100	E
4N/27W-22B2	685	90	E
4N/27W-22B2	695	0	E
4N/27W-22B2	705	80	E
4N/27W-22B2	715	100	E
4N/27W-22B2	725	80	E
4N/27W-22B2	735	0	E
4N/27W-22B2	745	0	E
4N/27W-22B2	755	0	E
4N/27W-22B2	765	0	E
4N/27W-22B2	775	0	E
4N/27W-22B2	785	0	E
4N/27W-22B2	795	0	E
4N/27W-22B2	805	0	E
4N/27W-22B2	815	0	E
4N/27W-22B2	825	0	E
4N/27W-22B2	835	0	E
4N/27W-22B2	845	0	E
4N/27W-21E1	25	30	E
4N/27W-21E1	35	100	E
4N/27W-21E1	45	100	E
4N/27W-21E1	55	100	E
4N/27W-21E1	65	100	E
4N/27W-21E1	75	100	E
4N/27W-21E1	85	80	E
4N/27W-21E1	95	100	E
4N/27W-21E1	105	100	E

Table B1–1. Calculated percent-coarse intervals for all drillers' logs and e-logs used to define textural properties of the hydrogeologic framework model.—Continued

[Percent-coarse values are calculated for 10-foot intervals for the entire depth of each borehole. State well number is the state of California well identifier; interval midpoint depth is the midpoint of each 10-foot interval, in feet from top of borehole; PC is the percent-coarse value for each interval; log type defines whether the borehole is a drillers' lithology log (D) or a geophysical e-log (E).]

State well number	Interval midpoint depth (feet)	PC	Log type
4N/27W-21E1	115	100	E
4N/27W-21E1	125	100	E
4N/27W-21E1	135	100	E
4N/27W-21E1	145	100	E
4N/27W-21E1	155	100	E
4N/27W-21E1	165	100	E
4N/27W-21E1	175	70	E
4N/27W-21E1	185	80	E
4N/27W-21E1	195	80	E
4N/27W-21E1	205	100	E
4N/27W-21E1	215	70	E
4N/27W-21E1	225	30	E
4N/27W-21E1	235	0	E
4N/27W2-E1	75	0	E
4N/27W2-E1	85	0	E
4N/27W2-E1	95	0	E
4N/27W2-E1	105	0	E
4N/27W2-E1	115	0	E
4N/27W2-E1	125	0	E
4N/27W2-E1	135	0	E
4N/27W2-E1	145	0	E
4N/27W2-E1	155	0	E
4N/27W2-E1	165	20	E
4N/27W2-E1	175	100	E
4N/27W2-E1	185	100	E
4N/27W2-E1	195	60	E
4N/27W2-E1	205	0	E
4N/27W2-E1	215	0	E
4N/27W2-E1	225	20	E
4N/27W2-E1	235	100	E
4N/27W2-E1	245	100	E
4N/27W2-E1	255	100	E
4N/27W2-E1	265	100	E
4N/27W2-E1	275	60	E
4N/27W2-E1	285	60	E
4N/27W2-E1	295	100	E
4N/27W2-E1	305	100	E
4N/27W2-E1	315	100	E
4N/27W2-E1	325	100	E
4N/27W2-E1	335	10	E
4N/27W2-E1	345	0	E
4N/27W-18B5	25	60	E
4N/27W-18B5	35	0	E
4N/27W-18B5	45	0	E
4N/27W-18B5	55	30	E
4N/27W-18B5	65	40	E
4N/27W-18B5	75	80	E
4N/27W-18B5	85	20	E
4N/27W-18B5	95	0	E
4N/27W-17M1	25	0	E
4N/27W-17M1	35	0	E
4N/27W-17M1	45	0	E
4N/27W-17M1	55	20	E
4N/27W-17M1	65	0	E
4N/27W-17M1	75	0	E
4N/27W-17M1	85	70	E
4N/27W-17M1	95	100	E
4N/27W-17M1	105	100	E
4N/27W-17M1	115	100	E
4N/27W-17M1	125	100	E
4N/27W-17M1	135	100	E
4N/27W-17M1	145	100	E
4N/27W-17M1	155	100	E
4N/27W-17M1	165	100	E
4N/27W-17M1	175	100	E
4N/27W-17M1	185	100	E
4N/27W-17M1	195	100	E
4N/27W-17M1	205	100	E
4N/27W-17M1	215	100	E
4N/27W-17M1	225	100	E
4N/27W-17M1	235	100	E
4N/27W-17M1	245	100	E
4N/27W-17M1	255	20	E
4N/27W-17M1	265	50	E
4N/27W-17M1	275	100	E
4N/27W-17J1	25	87.5	E
4N/27W-17J1	35	60	E
4N/27W-17J1	45	50	E

Table B1–1. Calculated percent-coarse intervals for all drillers' logs and e-logs used to define textural properties of the hydrogeologic framework model.—Continued

[Percent-coarse values are calculated for 10-foot intervals for the entire depth of each borehole. State well number is the state of California well identifier; interval midpoint depth is the midpoint of each 10-foot interval, in feet from top of borehole; PC is the percent-coarse value for each interval; log type defines whether the borehole is a drillers' lithology log (D) or a geophysical e-log (E).]

State well number	Interval midpoint depth (feet)	PC	Log type
4N/27W-17J1	55	70	E
4N/27W-17J1	65	0	E
4N/27W-17J1	75	20	E
4N/27W-17J1	85	100	E
4N/27W-17J1	95	30	E
4N/27W-17J1	105	0	E
4N/27W-17J1	115	0	E
4N/27W-17J1	125	0	E
4N/27W-17J1	135	0	E
4N/27W-17J1	145	20	E
4N/27W-17J1	155	0	E
4N/27W-17J1	165	0	E
4N/27W-17J1	175	0	E
4N/27W-17J1	185	0	E
4N/27W-17J1	195	30	E
4N/27W-17J1	205	90	E
4N/27W-17J1	215	30	E
4N/27W-17J1	225	100	E
4N/27W-17J1	235	100	E
4N/27W-17J1	245	0	E
4N/27W-17J1	255	30	E
4N/27W-17J1	265	50	E
4N/27W-17J1	275	80	E
4N/27W-17J1	285	0	E
4N/27W-17J1	295	0	E
4N/27W-17J1	305	60	E
4N/27W-17J1	315	70	E
4N/27W-17J1	325	0	E
4N/27W-17J1	335	0	E
4N/27W-17J1	345	0	E
4N/27W-17J1	355	0	E
4N/27W-17J1	365	0	E
4N/27W-17H1	45	70	E
4N/27W-17H1	55	30	E
4N/27W-17H1	65	0	E
4N/27W-17H1	75	20	E
4N/27W-17H1	85	0	E
4N/27W-17H1	95	50	E
4N/27W-17H1	105	0	E
4N/27W-17H1	115	40	E
4N/27W-17H1	125	0	E
4N/27W-17H1	135	0	E
4N/27W-17H1	145	90	E
4N/27W-17H1	155	60	E
4N/27W-17H1	165	80	E
4N/27W-17H1	175	70	E
4N/27W-17H1	185	0	E
4N/27W-17H1	195	70	E
4N/27W-17H1	205	100	E
4N/27W-17H1	215	100	E
4N/27W-17H1	225	40	E
4N/27W-17H1	235	60	E
4N/27W-17H1	245	100	E
4N/27W-17H1	255	100	E
4N/27W-17H1	265	100	E
4N/27W-17H1	275	100	E
4N/27W-17H1	285	100	E
4N/27W-17H1	295	50	E
4N/27W-17H1	305	10	E
4N/27W-17H1	315	50	E
4N/27W-17H1	325	30	E
4N/27W-16R1	65	57.1	E
4N/27W-16R1	75	100	E
4N/27W-16R1	85	100	E
4N/27W-16R1	95	100	E
4N/27W-16R1	105	100	E
4N/27W-16R1	115	100	E
4N/27W-16R1	125	100	E
4N/27W-16R1	135	100	E
4N/27W-16R1	145	100	E
4N/27W-16R1	155	100	E
4N/27W-16R1	165	100	E
4N/27W-16R1	175	100	E
4N/27W-16R1	185	100	E
4N/27W-16R1	195	100	E
4N/27W-16R1	205	100	E
4N/27W-16R1	215	100	E
4N/27W-16R1	225	100	E

Table B1–1. Calculated percent-coarse intervals for all drillers' logs and e-logs used to define textural properties of the hydrogeologic framework model.—Continued

[Percent-coarse values are calculated for 10-foot intervals for the entire depth of each borehole. State well number is the state of California well identifier; interval midpoint depth is the midpoint of each 10-foot interval, in feet from top of borehole; PC is the percent-coarse value for each interval; log type defines whether the borehole is a drillers' lithology log (D) or a geophysical e-log (E).]

State well number	Interval midpoint depth (feet)	PC	Log type
4N/27W-16R1	235	30	E
4N/27W-16R1	245	100	E
4N/27W-16R1	255	100	E
4N/27W-16R1	265	100	E
4N/27W-16R1	275	100	E
4N/27W-16R1	285	80	E
4N/27W-16R1	295	0	E
4N/27W-16R1	305	0	E
4N/27W-16R1	315	0	E
4N/27W-16R1	325	80	E
4N/27W-16R1	335	100	E
4N/27W-16R1	345	90	E
4N/27W-16R1	355	0	E
4N/27W-16R1	365	20	E
4N/27W-16R1	375	100	E
4N/27W-16R1	385	100	E
4N/27W-16R1	395	0	E
4N/27W-16R1	405	0	E
4N/27W-16R1	415	0	E
4N/27W-16R1	425	0	E
4N/27W-16R1	435	0	E
4N/27W-16R1	445	0	E
4N/27W-16R1	455	0	E
4N/27W-16R1	465	0	E
4N/27W-16R1	475	0	E
4N/27W-16R1	485	0	E
4N/27W-16R1	495	0	E
4N/27W-16R1	505	0	E
4N/27W-16R1	515	0	E
4N/27W-16R1	525	0	E
4N/27W-16R1	535	0	E
4N/27W-16R1	545	0	E
4N/27W-16R1	555	50	E
4N/27W-16R1	565	100	E
4N/27W-16R1	575	100	E
4N/27W-16R1	585	70	E
4N/27W-16R1	595	0	E
4N/27W-16R1	605	10	E
4N/27W-16R1	615	0	E
4N/27W-16R1	625	0	E
4N/27W-16R1	635	0	E
4N/27W-16R1	645	0	E
4N/27W-16R1	655	0	E
4N/27W-16R1	665	0	E
4N/27W-16R1	675	0	E
4N/27W-16R1	685	0	E
4N/27W-16R1	695	0	E
4N/27W-16R1	705	0	E
4N/27W-16E1	35	100	E
4N/27W-16E1	45	50	E
4N/27W-16E1	55	70	E
4N/27W-16E1	65	100	E
4N/27W-16E1	75	70	E
4N/27W-16E1	85	100	E
4N/27W-16E1	95	30	E
4N/27W-16E1	105	20	E
4N/27W-16E1	115	70	E
4N/27W-16E1	125	0	E
4N/27W-16E1	135	80	E
4N/27W-16E1	145	0	E
4N/27W-16E1	155	30	E
4N/27W-16E1	165	0	E
4N/27W-16E1	175	0	E
4N/27W-16E1	185	0	E
4N/27W-16E1	195	0	E
4N/27W-16E1	205	70	E
4N/27W-16E1	215	100	E
4N/27W-16E1	225	100	E
4N/27W-16E1	235	60	E
4N/27W-16E1	245	30	E
4N/27W-16E1	255	20	E
4N/27W-16E1	265	80	E
4N/27W-16E1	275	10	E
4N/27W-16E1	285	0	E
4N/27W-16E1	295	60	E
4N/27W-16E1	305	50	E
4N/27W-16E1	315	0	E
4N/27W-16E1	325	0	E

Table B1–1. Calculated percent-coarse intervals for all drillers' logs and e-logs used to define textural properties of the hydrogeologic framework model.—Continued

[Percent-coarse values are calculated for 10-foot intervals for the entire depth of each borehole. State well number is the state of California well identifier; interval midpoint depth is the midpoint of each 10-foot interval, in feet from top of borehole; PC is the percent-coarse value for each interval; log type defines whether the borehole is a drillers' lithology log (D) or a geophysical e-log (E).]

State well number	Interval midpoint depth (feet)	PC	Log type
4N/27W-16E1	335	80	E
4N/27W-16E1	345	100	E
4N/27W-16E1	355	100	E
4N/27W-16E1	365	100	E
4N/27W-16E1	375	100	E
4N/27W-16E1	385	100	E
4N/27W-16E1	395	100	E
4N/27W-16E1	405	100	E
4N/27W-16E1	415	100	E
4N/27W-16E1	425	100	E
4N/27W-16E1	435	20	E
4N/27W-15Q9	25	0	E
4N/27W-15Q9	35	0	E
4N/27W-15Q9	45	0	E
4N/27W-15Q9	55	0	E
4N/27W-15Q9	65	40	E
4N/27W-15Q9	75	0	E
4N/27W-15Q9	85	0	E
4N/27W-15Q9	95	0	E
4N/27W-15Q9	105	0	E
4N/27W-15Q9	115	0	E
4N/27W-15Q9	125	0	E
4N/27W-15Q9	135	10	E
4N/27W-15Q9	145	60	E
4N/27W-15Q9	155	40	E
4N/27W-15Q9	165	10	E
4N/27W-15Q9	175	0	E
4N/27W-15Q9	185	0	E
4N/27W-15Q9	195	70	E
4N/27W-15Q9	205	20	E
4N/27W-15Q9	215	40	E
4N/27W-15Q9	225	20	E
4N/27W-15Q9	235	100	E
4N/27W-15Q9	245	100	E
4N/27W-15Q9	255	100	E
4N/27W-15Q9	265	80	E
4N/27W-15Q9	275	0	E
4N/27W-15Q9	285	20	E
4N/27W-15Q9	295	0	E
4N/27W-15Q9	305	0	E
4N/27W-15Q9	315	0	E
4N/27W-15Q9	325	20	E
4N/27W-15Q9	335	0	E
4N/27W-15Q9	345	0	E
4N/27W-15Q9	355	0	E
4N/27W-15Q9	365	70	E
4N/27W-15Q9	375	80	E
4N/27W-15Q9	385	100	E
4N/27W-15Q9	395	80	E
4N/27W-15Q9	405	40	E
4N/27W-15Q9	415	100	E
4N/27W-15Q9	425	10	E
4N/27W-15Q9	435	0	E
4N/27W-15Q9	445	0	E
4N/27W-15Q9	455	0	E
4N/27W-15Q9	465	0	E
4N/27W-15Q9	475	0	E
4N/27W-15Q9	485	0	E
4N/27W-15Q9	495	100	E
4N/27W-15Q9	505	20	E
4N/27W-15Q9	515	0	E
4N/27W-15Q9	525	0	E
4N/27W-15Q9	535	0	E
4N/27W-15Q9	545	0	E
4N/27W-15Q9	555	0	E
4N/27W-15Q9	565	0	E
4N/27W-15Q9	575	0	E
4N/27W-15Q9	585	30	E
4N/27W-15Q9	595	100	E
4N/27W-15Q9	605	0	E
4N/27W-15Q9	615	0	E
4N/27W-15Q9	625	20	E
4N/27W-15Q9	635	0	E
4N/27W-15Q9	645	100	E
4N/27W-15Q9	655	100	E
4N/27W-15Q9	665	70	E
4N/27W-15Q9	675	0	E
4N/27W-15Q9	685	0	E

Table B1–1. Calculated percent-coarse intervals for all drillers' logs and e-logs used to define textural properties of the hydrogeologic framework model.—Continued

[Percent-coarse values are calculated for 10-foot intervals for the entire depth of each borehole. State well number is the state of California well identifier; interval midpoint depth is the midpoint of each 10-foot interval, in feet from top of borehole; PC is the percent-coarse value for each interval; log type defines whether the borehole is a drillers' lithology log (D) or a geophysical e-log (E).]

State well number	Interval midpoint depth (feet)	PC	Log type
4N/27W-15Q9	695	20	E
4N/27W-15Q9	705	60	E
4N/27W-15Q8	45	0	E
4N/27W-15Q8	55	0	E
4N/27W-15Q8	65	30	E
4N/27W-15Q8	75	100	E
4N/27W-15Q8	85	100	E
4N/27W-15Q8	95	0	E
4N/27W-15Q8	105	0	E
4N/27W-15Q8	115	0	E
4N/27W-15Q8	125	0	E
4N/27W-15Q8	135	0	E
4N/27W-15Q8	145	0	E
4N/27W-15Q8	155	10	E
4N/27W-15Q8	165	30	E
4N/27W-15Q8	175	0	E
4N/27W-15Q8	185	0	E
4N/27W-15Q8	195	0	E
4N/27W-15Q8	205	0	E
4N/27W-15Q8	215	90	E
4N/27W-15Q8	225	100	E
4N/27W-15Q8	235	100	E
4N/27W-15Q8	245	70	E
4N/27W-15K1	75	33.3	E
4N/27W-15K1	85	80	E
4N/27W-15K1	95	40	E
4N/27W-15K1	105	60	E
4N/27W-15K1	115	100	E
4N/27W-15K1	125	100	E
4N/27W-15K1	135	100	E
4N/27W-15K1	145	90	E
4N/27W-15K1	155	0	E
4N/27W-15K1	165	0	E
4N/27W-15K1	175	90	E
4N/27W-15K1	185	50	E
4N/27W-15K1	195	0	E
4N/27W-15K1	205	60	E
4N/27W-15K1	215	90	E
4N/27W-15K1	225	100	E
4N/27W-15K1	235	20	E
4N/27W-15K1	245	0	E
4N/27W-15K1	255	0	E
4N/27W-15K1	265	0	E
4N/27W-15K1	275	0	E
4N/27W-15K1	285	0	E
4N/27W-15K1	295	10	E
4N/27W-15K1	305	70	E
4N/27W-15K1	315	100	E
4N/27W-15K1	325	100	E
4N/27W-15K1	335	100	E
4N/27W-15K1	345	100	E
4N/27W-15K1	355	30	E
4N/27W-15K1	365	0	E
4N/27W-15K1	375	0	E
4N/27W-15K1	385	0	E
4N/27W-15K1	395	0	E
4N/27W-15K1	405	0	E
4N/27W-15K1	415	0	E
4N/27W-15K1	425	60	E
4N/27W-15K1	435	100	E
4N/27W-15K1	445	100	E
4N/27W-15K1	455	100	E
4N/27W-15K1	465	0	E
4N/27W-15K1	475	0	E
4N/27W-15J1	25	0	E
4N/27W-15J1	35	0	E
4N/27W-15J1	45	0	E
4N/27W-15J1	55	30	E
4N/27W-15J1	65	40	E
4N/27W-15J1	75	0	E
4N/27W-15J1	85	0	E
4N/27W-15J1	95	0	E
4N/27W-15J1	105	100	E
4N/27W-15J1	115	0	E
4N/27W-15J1	125	0	E
4N/27W-15J1	135	0	E
4N/27W-15J1	145	10	E
4N/27W-15J1	155	40	E

Table B1–1. Calculated percent-coarse intervals for all drillers' logs and e-logs used to define textural properties of the hydrogeologic framework model.—Continued

[Percent-coarse values are calculated for 10-foot intervals for the entire depth of each borehole. State well number is the state of California well identifier; interval midpoint depth is the midpoint of each 10-foot interval, in feet from top of borehole; PC is the percent-coarse value for each interval; log type defines whether the borehole is a drillers' lithology log (D) or a geophysical e-log (E).]

State well number	Interval midpoint depth (feet)	PC	Log type
4N/27W-15J1	165	80	E
4N/27W-15J1	175	0	E
4N/27W-15J1	185	30	E
4N/27W-15J1	195	100	E
4N/27W-15J1	205	90	E
4N/27W-15J1	215	0	E
4N/27W-15J1	225	0	E
4N/27W-15J1	235	0	E
4N/27W-15J1	245	0	E
4N/27W-15J1	255	0	E
4N/27W-15J1	265	0	E
4N/27W-15J1	275	30	E
4N/27W-15J1	285	60	E
4N/27W-15J1	295	0	E
4N/27W-15J1	305	0	E
4N/27W-15J1	315	0	E
4N/27W-15J1	325	30	E
4N/27W-15J1	335	0	E
4N/27W-15J1	345	0	E
4N/27W-15J1	355	0	E
4N/27W-15J1	365	40	E
4N/27W-15J1	375	100	E
4N/27W-15J1	385	50	E
4N/27W-15J1	395	0	E
4N/27W-15J1	405	20	E
4N/27W-15J1	415	30	E
4N/27W-15J1	425	0	E
4N/27W-15J1	435	0	E
4N/27W-15J1	445	20	E
4N/27W-15J1	455	0	E
4N/27W-15J1	465	30	E
4N/27W-15J1	475	70	E
4N/27W-15J1	485	0	E
4N/27W-15J1	495	0	E
4N/27W-15J1	505	20	E
4N/27W-15J1	515	100	E
4N/27W-15J1	525	30	E
4N/27W-15J1	535	100	E
4N/27W-15J1	545	100	E
4N/27W-15J1	555	80	E
4N/27W-15J1	565	60	E
4N/27W-15J1	575	0	E
4N/27W-15J1	585	80	E
4N/27W-15J1	595	0	E
4N/27W-15J1	605	0	E
4N/27W-15J1	615	0	E
4N/27W-15J1	625	0	E
4N/27W-15E1	75	100	E
4N/27W-15E1	85	100	E
4N/27W-15E1	95	100	E
4N/27W-15E1	105	100	E
4N/27W-15E1	115	100	E
4N/27W-15E1	125	100	E
4N/27W-15E1	135	100	E
4N/27W-15E1	145	40	E
4N/27W-15E1	155	0	E
4N/27W-15E1	165	0	E
4N/27W-15E1	175	80	E
4N/27W-15E1	185	20	E
4N/27W-15E1	195	10	E
4N/27W-15E1	205	80	E
4N/27W-15E1	215	90	E
4N/27W-15E1	225	90	E
4N/27W-15E1	235	0	E
4N/27W-15E1	245	0	E
4N/27W-15E1	255	0	E
4N/27W-15E1	265	0	E
4N/27W-15E1	275	50	E
4N/27W-15E1	285	80	E
4N/27W-15E1	295	0	E
4N/27W-15E1	305	0	E
4N/27W-15E1	315	0	E
4N/27W-15E1	325	0	E
4N/27W-15E1	335	0	E
4N/27W-15E1	345	40	E
4N/27W-15E1	355	0	E
4N/27W-15E1	365	80	E
4N/27W-15E1	375	0	E

Table B1–1. Calculated percent-coarse intervals for all drillers' logs and e-logs used to define textural properties of the hydrogeologic framework model.—Continued

[Percent-coarse values are calculated for 10-foot intervals for the entire depth of each borehole. State well number is the state of California well identifier; interval midpoint depth is the midpoint of each 10-foot interval, in feet from top of borehole; PC is the percent-coarse value for each interval; log type defines whether the borehole is a drillers' lithology log (D) or a geophysical e-log (E).]

State well number	Interval midpoint depth (feet)	PC	Log type
4N/27W-15E1	385	10	E
4N/27W-15E1	395	30	E
4N/27W-15E1	405	0	E
4N/27W-15E1	415	30	E
4N/27W-15E1	425	10	E
4N/27W-15E1	435	100	E
4N/27W-15E1	445	30	E
4N/27W-15E1	455	100	E
4N/27W-15E1	465	100	E
4N/27W-15E1	475	100	E
4N/27W-15E1	485	70	E
4N/27W-15E1	495	0	E
4N/27W-15E1	505	0	E
4N/27W-15E1	515	0	E
4N/27W-14R1	25	0	E
4N/27W-14R1	35	40	E
4N/27W-14R1	45	0	E
4N/27W-14R1	55	0	E
4N/27W-14R1	65	0	E
4N/27W-14R1	75	0	E
4N/27W-14R1	85	40	E
4N/27W-14R1	95	80	E
4N/27W-14R1	105	50	E
4N/27W-14R1	115	20	E
4N/27W-14R1	125	0	E
4N/27W-14R1	135	0	E
4N/27W-14R1	145	0	E
4N/27W-14R1	155	0	E
4N/27W-14R1	165	0	E
4N/27W-14R1	175	0	E
4N/27W-14R1	185	0	E
4N/27W-14R1	195	0	E
4N/27W-14R1	205	0	E
4N/27W-14R1	215	0	E
4N/27W-14R1	225	0	E
4N/27W-14R1	235	0	E
4N/27W-14R1	245	0	E
4N/27W-14R1	255	60	E
4N/27W-14R1	265	0	E
4N/27W-14R1	275	0	E
4N/27W-14R1	285	20	E
4N/27W-14R1	295	50	E
4N/27W-14R1	305	20	E
4N/27W-14R1	315	40	E
4N/27W-14R1	325	30	E
4N/27W-14R1	335	60	E
4N/27W-14R1	345	100	E
4N/27W-14R1	355	20	E
4N/27W-14R1	365	0	E
4N/27W-14R1	375	0	E
4N/27W-14R1	385	20	E
4N/27W-14R1	395	0	E
4N/27W-14R1	405	0	E
4N/27W-14R1	415	0	E
4N/27W-14R1	425	0	E
4N/27W-14R1	435	100	E
4N/27W-14R1	445	10	E
4N/27W-14R1	455	20	E
4N/27W-14R1	465	0	E
4N/27W-14R1	475	20	E
4N/27W-14R1	485	100	E
4N/27W-14R1	495	100	E
4N/27W-14R1	505	20	E
4N/27W-14R1	515	30	E
4N/27W-14R1	525	30	E
4N/27W-14R1	535	0	E
4N/27W-14R1	545	10	E
4N/27W-14R1	555	70	E
4N/27W-14R1	565	100	E
4N/27W-14R1	575	60	E
4N/27W-14R1	585	50	E
4N/27W-14R1	595	100	E
4N/27W-14R1	605	100	E
4N/27W-14R1	615	100	E
4N/27W-14R1	625	90	E
4N/27W-14R1	635	70	E
4N/27W-14R1	645	100	E
4N/27W-14R1	655	100	E

Table B1–1. Calculated percent-coarse intervals for all drillers' logs and e-logs used to define textural properties of the hydrogeologic framework model.—Continued

[Percent-coarse values are calculated for 10-foot intervals for the entire depth of each borehole. State well number is the state of California well identifier; interval midpoint depth is the midpoint of each 10-foot interval, in feet from top of borehole; PC is the percent-coarse value for each interval; log type defines whether the borehole is a drillers' lithology log (D) or a geophysical e-log (E).]

State well number	Interval midpoint depth (feet)	PC	Log type
4N/27W-7K9	35	0	E
4N/27W-7K9	45	0	E
4N/27W-7K9	55	0	E
4N/27W-7K9	65	0	E
4N/27W-7K9	75	30	E
4N/27W-7K9	85	90	E
4N/27W-7K9	95	30	E
4N/27W-7K9	105	100	E
4N/27W-7K9	115	90	E
4N/27W-7K9	125	30	E
4N/27W-7K9	135	90	E
4N/27W-7K9	145	40	E
4N/27W-7K9	155	0	E
4N/27W-7K9	165	0	E
4N/27W-7K9	175	0	E
4N/27W-7K9	185	0	E
4N/27W-7K9	195	0	E
4N/27W-7K9	205	0	E
4N/27W-7K9	215	0	E
4N/27W-7K9	225	0	E
4N/27W-7K9	235	0	E
4N/27W-7K9	245	0	E
4N/27W-7K9	255	0	E
4N/27W-7K9	265	0	E
4N/27W-7K9	275	0	E
4N/27W-7K9	285	0	E
4N/27W-7K9	295	30	E
4N/27W-7K9	305	0	E
4N/27W-7K9	315	0	E
4N/27W-7K9	325	10	E
4N/27W-7K9	335	70	E
4N/27W-7K9	345	90	E
4N/27W-14P1	135	0	E
4N/27W-14P1	145	0	E
4N/27W-14P1	155	0	E
4N/27W-14P1	165	0	E
4N/27W-14P1	175	0	E
4N/27W-14P1	185	0	E
4N/27W-14P1	195	20	E
4N/27W-14P1	205	60	E
4N/27W-14P1	215	90	E
4N/27W-14P1	225	10	E
4N/27W-14P1	235	60	E
4N/27W-14P1	245	0	E
4N/27W-14P1	255	0	E
4N/27W-14P1	265	40	E
4N/27W-14P1	275	100	E
4N/27W-14P1	285	100	E
4N/27W-14P1	295	60	E
4N/27W-14P1	305	0	E
4N/27W-14P1	315	0	E
4N/27W-14P1	325	0	E
4N/27W-14P1	335	70	E
4N/27W-14P1	345	40	E
4N/27W-14P1	355	100	E
4N/27W-14P1	365	70	E
4N/27W-14P1	375	20	E
4N/27W-14P1	385	0	E
4N/27W-14P1	395	0	E
4N/27W-14P1	405	0	E
4N/27W-14P1	415	0	E
4N/27W-14P1	425	30	E
4N/27W-14P1	435	10	E
4N/27W-14P1	445	0	E
4N/27W-14P1	455	0	E
4N/27W-14P1	465	20	E
4N/27W-14P1	475	70	E
4N/27W-14P1	485	0	E
4N/27W-14P1	495	50	E
4N/27W-14P1	505	40	E
4N/27W-14P1	515	0	E
4N/27W-14P1	525	30	E
4N/27W-14P1	535	20	E
4N/27W-14P1	545	0	E
4N/27W-14P1	555	20	E
4N/27W-14P1	565	0	E
4N/27W-14P1	575	50	E
4N/27W-14P1	585	0	E

Table B1–1. Calculated percent-coarse intervals for all drillers' logs and e-logs used to define textural properties of the hydrogeologic framework model.—Continued

[Percent-coarse values are calculated for 10-foot intervals for the entire depth of each borehole. State well number is the state of California well identifier; interval midpoint depth is the midpoint of each 10-foot interval, in feet from top of borehole; PC is the percent-coarse value for each interval; log type defines whether the borehole is a drillers' lithology log (D) or a geophysical e-log (E).]

State well number	Interval midpoint depth (feet)	PC	Log type
4N/27W-14P1	595	0	E
4N/27W-14P1	605	0	E
4N/27W-14P1	615	50	E
4N/27W-14P1	625	70	E
4N/27W-14P1	635	20	E
4N/27W-14P1	645	30	E
4N/27W-14P1	655	20	E
4N/27W-14P1	665	0	E
4N/27W-14P1	675	100	E
4N/27W-14P1	685	100	E
4N/27W-14P1	695	90	E
4N/27W-14P1	705	100	E
4N/27W-14P1	715	100	E
4N/27W-14P1	725	100	E
4N/27W-14P1	735	100	E
4N/27W-14P1	745	100	E
4N/27W-14P1	755	100	E
4N/27W-14P1	765	70	E
4N/27W-14P1	775	30	E
4N/27W-14K2	65	0	E
4N/27W-14K2	75	80	E
4N/27W-14K2	85	100	E
4N/27W-14K2	95	40	E
4N/27W-14K2	105	0	E
4N/27W-14K2	115	0	E
4N/27W-14K2	125	0	E
4N/27W-14K2	135	0	E
4N/27W-14K2	145	0	E
4N/27W-14K2	155	0	E
4N/27W-14K2	165	0	E
4N/27W-14K2	175	0	E
4N/27W-14K2	185	0	E
4N/27W-14K2	195	0	E
4N/27W-14K2	205	0	E
4N/27W-14K2	215	0	E
4N/27W-14K2	225	0	E
4N/27W-14K2	235	0	E
4N/27W-14K2	245	0	E
4N/27W-14K2	255	0	E
4N/27W-14K2	265	20	E
4N/27W-14K2	275	100	E
4N/27W-14K2	285	100	E
4N/27W-14K2	295	100	E
4N/27W-14K2	305	100	E
4N/27W-14K2	315	30	E
4N/27W-14K2	325	0	E
4N/27W-14K2	335	0	E
4N/27W-14K2	345	20	E
4N/27W-14K2	355	100	E
4N/27W-14K2	365	100	E
4N/27W-14K2	375	0	E
4N/27W-14K2	385	0	E
4N/27W-14K2	395	0	E
4N/27W-14K2	405	0	E
4N/27W-14K2	415	0	E
4N/27W-14K2	425	0	E
4N/27W-14K2	435	0	E
4N/27W-9M1	25	50	E
4N/27W-9M1	35	30	E
4N/27W-9M1	45	80	E
4N/27W-9M1	55	20	E
4N/27W-9M1	65	20	E
4N/27W-9M1	75	100	E
4N/27W-9M1	85	10	E
4N/27W-9M1	95	90	E
4N/27W-9M1	105	40	E
4N/27W-9M1	115	0	E
4N/27W-9M1	125	0	E
4N/27W-9M1	135	0	E
4N/27W-9M1	145	0	E
4N/27W-9M1	155	0	E
4N/27W-9M1	165	0	E
4N/27W-9M1	175	0	E
4N/27W-8R2	25	0	E
4N/27W-8R2	35	0	E
4N/27W-8R2	45	40	E
4N/27W-8R2	55	100	E
4N/27W-8R2	65	40	E

Table B1–1. Calculated percent-coarse intervals for all drillers' logs and e-logs used to define textural properties of the hydrogeologic framework model.—Continued

[Percent-coarse values are calculated for 10-foot intervals for the entire depth of each borehole. State well number is the state of California well identifier; interval midpoint depth is the midpoint of each 10-foot interval, in feet from top of borehole; PC is the percent-coarse value for each interval; log type defines whether the borehole is a drillers' lithology log (D) or a geophysical e-log (E).]

State well number	Interval midpoint depth (feet)	PC	Log type
4N/27W-8R2	75	90	E
4N/27W-8R2	85	60	E
4N/27W-8R2	95	0	E
4N/27W-8R2	105	0	E
4N/27W-8R2	115	0	E
4N/27W-8R2	125	0	E
4N/27W-8R2	135	0	E
4N/27W-8R2	145	40	E
4N/27W-8R2	155	100	E
4N/27W-8R2	165	100	E
4N/27W-8R2	175	100	E
4N/27W-8R2	185	100	E
4N/27W-8R2	195	20	E
4N/27W-8R2	205	0	E
4N/27W-8R2	215	70	E
4N/27W-8R2	225	0	E
4N/27W-8R2	235	30	E
4N/27W-8R2	245	0	E
4N/27W-8E1	85	71.4	E
4N/27W-8E1	95	0	E
4N/27W-8E1	105	0	E
4N/27W-8E1	115	0	E
4N/27W-8E1	125	0	E
4N/27W-8E1	135	0	E
4N/27W-8E1	145	20	E
4N/27W-8E1	155	80	E
4N/27W-8E1	165	0	E
4N/27W-8E1	175	0	E
4N/27W-8E1	185	0	E
4N/27W-8E1	195	0	E
4N/27W-8E1	205	0	E
4N/27W-8E1	215	0	E
4N/27W-8E1	225	0	E
4N/27W-8E1	235	0	E
4N/27W-8E1	245	10	E
4N/27W-8E1	255	80	E
4N/27W-8E1	265	30	E
4N/27W-8E1	275	0	E
4N/27W-8E1	285	40	E
4N/27W-8E1	295	50	E
4N/27W-8E1	305	100	E
4N/27W-8E1	315	100	E
4N/27W-8E1	325	80	E
4N/27W-8E1	335	30	E
4N/27W-8E1	345	10	E
4N/27W-8E1	355	20	E
4N/27W-8E1	365	20	E
4N/27W-8E1	375	50	E
4N/27W-8E1	385	0	E
4N/27W-8E1	395	0	E
4N/27W-8E1	405	0	E
4N/27W-8E1	415	0	E
4N/27W-8E1	425	0	E
4N/27W-8E1	435	90	E
4N/27W-8E1	445	100	E
4N/27W-8E1	455	90	E
4N/27W-8E1	465	0	E
4N/27W-8E1	475	0	E
4N/27W-8E1	485	0	E
4N/27W-8E1	495	0	E
4N/27W-8E1	505	0	E
4N/27W-8E1	515	50	E
4N/27W-8E1	525	80	E
4N/27W-8E1	535	70	E
4N/27W-8E1	545	0	E
4N/27W-8E1	555	0	E
4N/27W-8E1	565	30	E
4N/27W-8E1	575	0	E
4N/27W-8E1	585	0	E
4N/27W-8E1	595	0	E
4N/27W-8E1	605	0	E
4N/27W-6Q12	75	42.9	E
4N/27W-6Q12	85	100	E
4N/27W-6Q12	95	60	E
4N/27W-6Q12	105	70	E
4N/27W-6Q12	115	100	E
4N/27W-6Q12	125	70	E
4N/27W-6Q12	135	0	E

Table B1–1. Calculated percent-coarse intervals for all drillers' logs and e-logs used to define textural properties of the hydrogeologic framework model.—Continued

[Percent-coarse values are calculated for 10-foot intervals for the entire depth of each borehole. State well number is the state of California well identifier; interval midpoint depth is the midpoint of each 10-foot interval, in feet from top of borehole; PC is the percent-coarse value for each interval; log type defines whether the borehole is a drillers' lithology log (D) or a geophysical e-log (E).]

State well number	Interval midpoint depth (feet)	PC	Log type
4N/27W-6Q12	145	0	E
4N/27W-6Q12	155	0	E
4N/27W-6Q12	165	0	E
4N/27W-6Q12	175	0	E
4N/27W-6Q12	185	0	E
4N/27W-6Q12	195	0	E
4N/27W-6Q12	205	0	E
4N/27W-6Q12	215	50	E
4N/27W-6Q12	225	100	E
4N/27W-6Q12	235	100	E
4N/27W-6Q12	245	100	E
4N/27W-6Q12	255	0	E
4N/27W-6Q12	265	0	E
4N/27W-6Q12	275	60	E
4N/27W-6Q12	285	100	E
4N/27W-6Q12	295	100	E
4N/27W-6Q12	305	0	E
4N/27W-6Q12	315	0	E
4N/27W-5P1	15	44.4	E
4N/27W-5P1	25	10	E
4N/27W-5P1	35	0	E
4N/27W-5P1	45	0	E
4N/27W-5P1	55	0	E
4N/27W-5P1	65	0	E
4N/27W-5P1	75	0	E
4N/27W-5P1	85	50	E
4N/27W-5P1	95	10	E
4N/27W-5P1	105	10	E
4N/27W-5P1	115	100	E
4N/27W-5P1	125	100	E
4N/27W-5P1	135	50	E
4N/27W-5P1	145	10	E
4N/27W-5P1	155	100	E
4N/27W-5P1	165	80	E
4N/27W-5P1	175	10	E
4N/28W-12H3	5	0	E
4N/28W-12H3	15	0	E
4N/28W-12H3	25	0	E
4N/28W-12H3	35	0	E
4N/28W-12H3	45	0	E
4N/28W-12H3	55	20	E
4N/28W-12H3	65	0	E
4N/28W-12H3	75	30	E
4N/28W-12H3	85	50	E
4N/28W-12H3	95	60	E
4N/28W-12H3	105	50	E
4N/28W-12H3	115	50	E
4N/28W-12H3	125	0	E
4N/28W-12H3	135	20	E
4N/28W-12H3	145	30	E
4N/28W-12H3	155	70	E
4N/28W-12H3	165	100	E
4N/28W-12H3	175	50	E
4N/28W-12H3	185	30	E
4N/28W-12H3	195	60	E
4N/28W-12H3	205	0	E
4N/28W-12H3	215	20	E
4N/28W-12H3	225	60	E
4N/28W-12H3	235	30	E
4N/28W-12H3	245	0	E
4N/27W-1R1	35	0	E
4N/27W-1R1	45	0	E
4N/27W-1R1	55	0	E
4N/27W-1R1	65	40	E
4N/27W-1R1	75	0	E
4N/27W-1R1	85	10	E
4N/27W-1R1	95	70	E
4N/27W-1R1	105	100	E
4N/27W-1R1	115	50	E
4N/27W-1R1	125	50	E
4N/27W-1R1	135	50	E
4N/27W-1R1	145	40	E
4N/27W-1R1	155	100	E
4N/27W-1R1	165	40	E
4N/27W-1R1	175	80	E
4N/27W-1R1	185	0	E
4N/27W-1R1	195	0	E
4N/27W-1R1	205	0	E

Table B1–1. Calculated percent-coarse intervals for all drillers' logs and e-logs used to define textural properties of the hydrogeologic framework model.—Continued

[Percent-coarse values are calculated for 10-foot intervals for the entire depth of each borehole. State well number is the state of California well identifier; interval midpoint depth is the midpoint of each 10-foot interval, in feet from top of borehole; PC is the percent-coarse value for each interval; log type defines whether the borehole is a drillers' lithology log (D) or a geophysical e-log (E).]

State well number	Interval midpoint depth (feet)	PC	Log type
4N/27W-1R1	215	0	E
4N/27W-1R1	225	0	E
4N/27W-1R1	235	0	E
4N/27W-1R1	245	0	E
4N/27W-1R1	255	0	E
4N/27W-1R1	265	0	E
4N/27W-1R1	275	0	E
4N/27W-1R1	285	0	E
4N/27W-7Q5	25	0	E
4N/27W-7Q5	35	0	E
4N/27W-7Q5	45	0	E
4N/27W-7Q5	55	20	E
4N/27W-7Q5	65	60	E
4N/27W-7Q5	75	0	E
4N/27W-7Q5	85	20	E
4N/27W-7Q5	95	0	E
4N/27W-7Q5	105	0	E
4N/27W-7Q5	115	0	E
4N/27W-7Q5	125	0	E
4N/27W-7Q5	135	0	E
4N/27W-7Q5	145	0	E
4N/27W-7Q5	155	50	E
4N/27W-7Q5	165	100	E
4N/27W-7Q5	175	50	E
4N/27W-7Q5	185	10	E
4N/27W-7Q5	195	0	E
4N/27W-22C1	65	0	E
4N/27W-22C1	75	0	E
4N/27W-22C1	85	10	E
4N/27W-22C1	95	90	E
4N/27W-22C1	105	40	E
4N/27W-22C1	115	20	E
4N/27W-22C1	125	100	E
4N/27W-22C1	135	100	E
4N/27W-22C1	145	90	E
4N/27W-22C1	155	100	E
4N/27W-22C1	165	90	E
4N/27W-22C1	175	40	E
4N/27W-22C1	185	100	E
4N/27W-22C1	195	100	E
4N/27W-22C1	205	100	E
4N/27W-22C1	215	80	E
4N/27W-22C1	225	0	E
4N/27W-22C1	235	40	E
4N/27W-22C1	245	0	E
4N/27W-22C1	255	40	E
4N/27W-22C1	265	0	E
4N/27W-22C1	275	0	E
4N/27W-22C1	285	0	E
4N/27W-22C1	295	0	E
4N/27W-22C1	305	50	E
4N/27W-22C1	315	60	E
4N/27W-22C1	325	0	E
4N/27W-22C1	335	0	E
4N/27W-22C1	345	0	E
4N/27W-22C1	355	40	E
4N/27W-22C1	365	0	E
4N/27W-22C1	375	20	E
4N/27W-22C1	385	0	E
4N/27W-22C1	395	0	E
4N/27W-22C1	405	0	E
4N/27W-22C1	415	0	E
4N/27W-22C1	425	0	E
4N/27W-22C1	435	0	E
4N/27W-22C1	445	0	E
4N/27W-22C1	455	0	E
4N/27W-22C1	465	0	E
4N/27W-22C1	475	0	E
4N/27W-22C1	485	0	E
4N/27W-22C1	495	0	E
4N/27W-22C1	505	20	E
4N/27W-22C1	515	10	E
4N/27W-22C1	525	0	E
4N/27W-22C1	535	80	E
4N/27W-22C1	545	100	E
4N/27W-22C1	555	100	E
4N/27W-22C1	565	60	E
4N/27W-22C1	575	80	E

Table B1–1. Calculated percent-coarse intervals for all drillers' logs and e-logs used to define textural properties of the hydrogeologic framework model.—Continued

[Percent-coarse values are calculated for 10-foot intervals for the entire depth of each borehole. State well number is the state of California well identifier; interval midpoint depth is the midpoint of each 10-foot interval, in feet from top of borehole; PC is the percent-coarse value for each interval; log type defines whether the borehole is a drillers' lithology log (D) or a geophysical e-log (E).]

State well number	Interval midpoint depth (feet)	PC	Log type
4N/27W-22C1	585	100	E
4N/27W-22C1	595	100	E
4N/27W-22C1	605	100	E
4N/27W-22C1	615	90	E
4N/27W-22C1	625	0	E
4N/27W-22C1	635	100	E
4N/27W-22C1	645	100	E
4N/27W-22C1	655	100	E
4N/27W-22C1	665	60	E
4N/27W-22C1	675	100	E
4N/27W-22C1	685	100	E
4N/27W-22C1	695	0	E
4N/27W-22C1	705	0	E
4N/27W-22C1	715	0	E
4N/27W-22C1	725	0	E
4N/27W-22C1	735	0	E
4N/27W-22C1	745	0	E
4N/27W-22C1	755	0	E
4N/27W-22C1	765	0	E
4N/27W-22C1	775	0	E
4N/27W-22B6	55	0	E
4N/27W-22B6	65	0	E
4N/27W-22B6	75	0	E
4N/27W-22B6	85	0	E
4N/27W-22B6	95	0	E
4N/27W-22B6	105	0	E
4N/27W-22B6	115	0	E
4N/27W-22B6	125	0	E
4N/27W-22B6	135	0	E
4N/27W-22B6	145	0	E
4N/27W-22B6	155	0	E
4N/27W-22B6	165	0	E
4N/27W-22B6	175	20	E
4N/27W-22B6	185	0	E
4N/27W-22B6	195	0	E
4N/27W-22B6	205	40	E
4N/27W-22B6	215	100	E
4N/27W-22B6	225	100	E
4N/27W-22B6	235	100	E
4N/27W-22B6	245	50	E
4N/27W-22B6	255	0	E
4N/27W-22B6	265	0	E
4N/27W-22B6	275	0	E
4N/27W-22B6	285	0	E
4N/27W-22B6	295	0	E
4N/27W-22B6	305	0	E
4N/27W-22B6	315	0	E
4N/27W-22B6	325	0	E
4N/27W-22B6	335	0	E
4N/27W-22B6	345	0	E
4N/27W-22B6	355	0	E
4N/27W-22B6	365	0	E
4N/27W-22B6	375	0	E
4N/27W-22B6	385	0	E
4N/27W-22B6	395	0	E
4N/27W-22B6	405	0	E
4N/27W-22B6	415	90	E
4N/27W-22B6	425	100	E
4N/27W-22B6	435	40	E
4N/27W-22B6	445	0	E
4N/27W-22B6	455	0	E
4N/27W-22B6	465	50	E
4N/27W-22B6	475	50	E
4N/27W-22B6	485	0	E
4N/27W-22B6	495	0	E
4N/27W-22B6	505	0	E
4N/27W-22B6	515	40	E
4N/27W-22B6	525	0	E
4N/27W-22B6	535	0	E
4N/27W-22B6	545	0	E
4N/27W-22B6	555	30	E
4N/27W-22B6	565	100	E
4N/27W-22B6	575	100	E
4N/27W-22B6	585	50	E
4N/27W-22B6	595	40	E
4N/27W-22B6	605	100	E
4N/27W-22B6	615	100	E
4N/27W-22B6	625	80	E

Table B1–1. Calculated percent-coarse intervals for all drillers' logs and e-logs used to define textural properties of the hydrogeologic framework model.—Continued

[Percent-coarse values are calculated for 10-foot intervals for the entire depth of each borehole. State well number is the state of California well identifier; interval midpoint depth is the midpoint of each 10-foot interval, in feet from top of borehole; PC is the percent-coarse value for each interval; log type defines whether the borehole is a drillers' lithology log (D) or a geophysical e-log (E).]

State well number	Interval midpoint depth (feet)	PC	Log type
4N/27W-22B6	635	70	E
4N/27W-22B6	645	100	E
4N/27W-22B6	655	100	E
4N/27W-22B6	665	100	E
4N/27W-22B6	675	100	E
4N/27W-22B6	685	30	E
4N/27W-8L2	85	100	E
4N/27W-8L2	95	100	E
4N/27W-8L2	105	100	E
4N/27W-8L2	115	80	E
4N/27W-8L2	125	100	E
4N/27W-8L2	135	20	E
4N/27W-8L2	145	60	E
4N/27W-8L2	155	100	E
4N/27W-8L2	165	100	E
4N/27W-8L2	175	100	E
4N/27W-8L2	185	100	E
4N/27W-8L2	195	100	E
4N/27W-8L2	205	100	E
4N/27W-8L2	215	40	E
4N/27W-8L2	225	0	E
4N/27W-8L2	235	0	E
4N/27W-8L2	245	0	E
4N/27W-8L2	255	0	E
4N/27W-8L2	265	50	E
4N/27W-8L2	275	100	E
4N/27W-8L2	285	100	E
4N/27W-8L2	295	100	E
4N/27W-8L2	305	100	E
4N/27W-8L2	315	100	E
4N/27W-8L2	325	100	E
4N/27W-8L2	335	100	E
4N/27W-8L2	345	10	E
4N/27W-8L2	355	0	E
4N/27W-8L2	365	0	E
4N/27W-8L2	375	0	E
4N/27W-8L2	385	0	E
4N/27W-8L2	395	0	E
4N/27W-8L2	405	70	E
4N/27W-8L2	415	100	E
4N/27W-8L2	425	40	E
4N/27W-8L2	435	0	E
4N/27W-8L2	445	0	E
4N/27W-8L2	455	0	E
4N/27W-8L2	465	10	E
4N/27W-8L2	475	100	E
4N/27W-8L2	485	100	E
4N/27W-8L2	495	100	E
4N/27W-8L2	505	80	E
4N/27W-8L2	515	0	E
4N/27W-8L2	525	60	E
4N/27W-8L2	535	100	E
4N/27W-8L2	545	100	E
4N/27W-8L2	555	60	E
4N/27W-8L2	565	100	E
4N/27W-8L2	575	100	E
4N/27W-8L2	585	100	E
4N/27W-8L2	595	100	E
4N/27W-8L2	605	100	E
4N/27W-8L2	615	100	E
4N/27W-8L2	625	70	E
4N/27W-8L2	635	0	E

Chapter C: Numerical Model of Groundwater Flow and Solute Transport

By Scott R. Paulinski

Introduction

The city of Santa Barbara is interested in simulating seawater intrusion under various water-management scenarios, estimating the sustainability of the groundwater basins, and determining optimal strategies to manage the groundwater basins. The existing U.S. Geological Survey (USGS) Santa Barbara groundwater-flow model by Freckleton and others (1998) simulates flow in the Santa Barbara and Foothill groundwater basins from 1978 to 1992. To simulate seawater intrusion into the Santa Barbara groundwater basin and evaluate various management strategies for the Santa Barbara groundwater basin, updates to the existing model were necessary, including the simulation of salinity transport and of variable-density flow and an extension of the timeframe of the model. A new model was developed, the Santa Barbara Flow and Transport Model (SBFTM), to simulate variable-density flow and transport from 1929 through 2013. The SBFTM was then used to determine optimal solutions for various water-management scenarios and estimate the sustainability of the groundwater basins.

Groundwater Model Development

A three-dimensional groundwater-flow and solute-transport model of the Santa Barbara and Foothill groundwater basins was developed using SEAWAT (Langevin and others, 2008). SEAWAT is a groundwater-flow and solute-transport simulation code that is based on MODFLOW-2000 (Harbaugh and others, 2000) and MT3DMS (Zheng and Wang, 1999; Zheng, 2006). Two versions of the SBFTM were constructed: an initial-condition model and a simulation-period transient model. The initial-condition model is a long-term transient model that simulates flow and solute-transport conditions during a period of lesser anthropogenic influences leading up to the start of the simulation-period transient model. A steady-state simulation would not suffice for determining these initial conditions, because the solute-transport computations require transience to determine concentration distribution. The simulation-period transient model simulates flow and transport conditions from 1929 through 2013. The flow and transport models use the SEAWAT packages listed in table 1.

The SBFTM was constructed in three steps. First, a hydrogeologic framework model (HFM) was constructed based on previous studies and available hydrologic, geologic, and geophysical data for the basin. As described in chapter B, the HFM has two parts: a geometric model that describes the extent and thickness of the hydrogeologic units and a textural model that defines the properties of these units. Next, this HFM was partitioned into the layers and cells of the groundwater-flow model. Finally, the available hydrologic observation and stress data were compiled and used to construct and calibrate the SBFTM.

Spatial and Temporal Discretization

The SBFTM is spatially discretized on a grid with 58 rows, 152 columns, and 56 layers (fig. 1) with 113,072 active cells. The model grid was rotated by 25 degrees clockwise from true north to align with the dominant direction of flow in Storage Unit I. The horizontal discretization is 250 by 250 feet (ft), and the vertical discretization is spatially variable; most model cells are approximately 20 ft thick. The coordinates of the four corners for the model grid are presented in table 2. The 56 model layers were necessary to replicate the horizontal variability in constituent transport reasonably and follow the contours of the land surface. They do not represent specific geologic layers, hydrogeologic units, or water-bearing units. Properties from the various hydrogeologic units and textural distribution in the HFM were used to populate the flow and transport model.

To simulate predevelopment conditions (no stresses), groundwater flow and solute transport were simulated for 10,000 years with 10-year time steps to allow the flow and concentration fields to equilibrate to the specified initial and boundary conditions. No pumpage data were available prior to 1929, and it was assumed that pumping prior to 1929 had a minor effect on the study area hydrology; therefore, it was assumed that 1929 represented predevelopment conditions.

Table 1. SEAWAT Version 4 packages and processes used with the Santa Barbara flow and transport model, Santa Barbara, California.

Package, process, or program name	Function	Reference
	Processes and solver	
Global (GLO) and groundwater flow (GWF) processes of MODFLOW-2000	Setup and solve equations simulating a basic ground-water flow model.	McDonald and Harbaugh, 1988; Harbaugh and others, 2000; Hill and others, 2000
Preconditioned conjugate-gradient package (PCG)	Solves the groundwater flow equations.	Hill, 1990; Harbaugh and others, 2000
Generalized conjugate-gradient solver package (GCG) of MT3DMS	Setup and solve equations simulating a basic ground-water transport model.	Zheng and Wang, 1999
Variable-density flow (VDF) process of SEAWAT	Setup and solve the variable-density ground-water flow equation.	Langevin and others, 2008
	Files	
Name file (name)	Controls the capabilities of SEAWAT (MODFLOW-2000 and MT3DMS) utilized during a simulation.	Harbaugh and others, 2000
Output control option (OC)	Used to output head, drawdown, and budget information for specified time periods.	Harbaugh and others, 2000
Global file	Output file for information that applied to the model simulation as a whole.	Harbaugh and others, 2000
List file	Output file for allocation information, values used by the GWF process, and calculated results such as head, drawdown, and the water budget.	Harbaugh and others, 2000
	Discretization	
Basic package (BAS6)	Defines the initial conditions and some of the boundary conditions.	Harbaugh and others, 2000
Discretization package (DIS)	Defines how the model is spatially and temporally broken up into model cells, time steps, and stress periods.	Harbaugh and others, 2000
Basic transport package (BTN)	Defines the initial conditions, some boundary conditions, and how the model is spatially and temporally broken up into model cells, time steps, and stress periods.	Zheng and Wang, 1999
Multiplier package (MULT)	Defines multiplier arrays for calculation of model properties.	Harbaugh and others, 2000
Zones (ZONE)	Defines zones to distinguish different parts of the model.	Harbaugh and others, 2000
	Aquifer properties	
Layer property flow package (LPF)	Calculates the conductance between cell centers.	Harbaugh and others, 2000
Hydrologic flow barriers (HFB6)	Simulates a groundwater barrier using a hydraulic conductance between two adjacent cells.	Harbaugh and others, 2000
	Solute transport	
Advection package (ADV)	Defines how advective flow is simulated.	Zheng and Wang, 1999
Dispersion package (DSP)	Defines how dispersion and molecular diffusion is simulated.	Zheng and Wang, 1999
Sink and source mixing package (SSM)	Defines the sources of solute and the solute concentration from each source.	Zheng and Wang, 1999
	Boundary conditions	
General head boundaries (GHB)	Head-dependent boundary condition to allow groundwater to flow into or out of the model.	Harbaugh and others, 2000
	Recharge and discharge	
Well (WEL)	Simulates a specified flux to individual cells.	Harbaugh and others, 2000
River (RIV)	Simulates a head-dependent flux boundary at specified cells.	Harbaugh and others, 2000
Drain (DRN)	Simulates a head dependent flux boundary at specified cells. The flux from the drain drops to zero when the head in the cell falls below a threshold.	Harbaugh and others, 2000
Recharge (RCH)	Simulates a specified flux distributed over the top of the model.	Harbaugh and others, 2000
	Output, observations, and sensitivity	
Head observations (HOB)	Defines the head observation and weight by layer(s), row, column, and time.	Hill and others, 2000
Transport observation (TOB)	Defines the solute concentration and weight by layer(s), row, column, and time.	Zheng, 2010

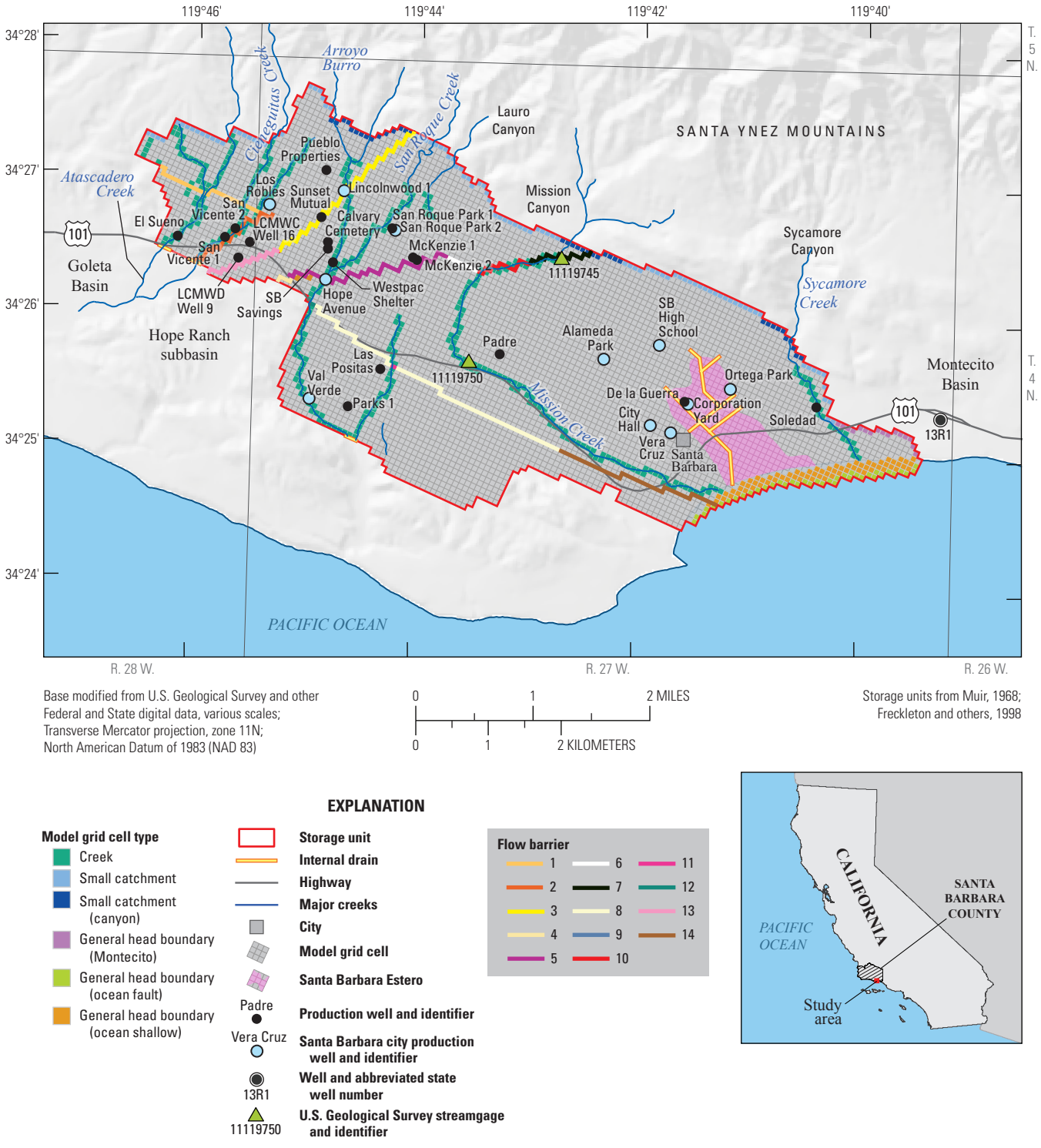

Figure 1. Distribution of flow barriers, general-head boundaries, drains, small-catchment recharge, and creek recharge in the Santa Barbara flow and transport model, Santa Barbara, California.

Table 2. Coordinates of the Santa Barbara Flow and Transport Model grid, Santa Barbara, California.

[NAD 1983, North American Datum of 1983; UTM, Universal Transverse Mercator]

Corner of model grid	Model coordinates X (column)	Model coordinates Y (row)	NAD 1983 UTM zone 11N X (meters)	NAD 1983 UTM zone 11N Y (meters)
Northeast	1	1	245,775	3,817,516
Northwest	1	58	243,907	3,813,510
Southeast	152	1	256,272	3,812,621
Southwest	152	58	254,405	3,808,615

The transient simulation represented 1929–2013 conditions; however, the primary focus was 1972–2013 because of superior data availability (in terms of reported stresses and measured data). The transient SBFTM was temporally discretized into 43 1-year stress periods from 1929 to 1971 and an additional 504 1-month stress periods from 1972 to 2013. One-year stress periods were used from 1929 to 1971 because of limited pumpage data during these years. One-month stress periods were chosen from 1972 to 2013 to simulate monthly and seasonal changes in pumpage and recharge.

Boundary Conditions

Model boundary conditions mathematically define the interaction of the SBFTM domain with hydrologic conditions outside of the SBFTM boundaries. For the groundwater-flow model, two types of boundary conditions were used: head dependent and specified flux.

Head-dependent boundaries include creeks, internal drains, and general-head boundaries (fig. 1). Creeks are discussed in the "Simulated Groundwater Recharge" section.

As described in chapter A, groundwater can leave Storage Unit III laterally as underflow at Arroyo Burro across the Lavigia fault or at Atascadero and Cieneguitas Creeks across the Modoc fault from Foothill to Goleta groundwater basin. Following Freckleton and others (1998), drain boundaries were used to simulate flow across the Lavigia and Modoc faults (figs. 1, B–1). Drains were also used to simulate groundwater flow into the Santa Barbara Estero.

The general-head boundary (GHB) package was used to simulate flow across the offshore fault along the coastal boundary (ocean-fault and shallow-ocean GHBs) and simulate flow between the Santa Ynez Mountains and Storage Unit I near the coast (Montecito GHB). The SBFTM extends laterally 500–900 ft to the offshore fault on the eastern edge of Storage Unit I. The ocean-fault and shallow-ocean GHBs simulate flow between the Pacific Ocean and the groundwater system. The ocean-fault GHB is on the vertical face of the southeastern boundary with the Pacific Ocean, and the shallow-ocean GHB is on the top model layer that extends throughout the offshore model area. The head at the ocean-fault GHB remains constant at sea level throughout the simulation. When using GHB in SEAWAT, the GHB seawater heads are set at the measured or assumed elevation and SEAWAT adjusts the head to address the greater density of seawater. The shallow-ocean GHB has a constant head at sea level, and a single conductance parameter is used.

The Montecito GHB simulates flow between the mountains and Storage Unit I and is on the southeastern part of the northeast boundary of the study area. It has varying head values based on observation data from well 4N/27W-13R1 (fig. 1).

Specified-flux boundaries also include no-flow boundaries. No-flow boundary conditions were used to simulate the lateral model boundary where not simulated by head-dependent boundaries or recharge. In addition, the base of the model, at the contact with a relatively low-permeability shale (see chapter B), was simulated as a no-flow boundary.

For the solute-transport model, chloride concentrations are associated with the flow boundaries. Appropriate chloride concentrations were specified at the general-head and specified-flux boundaries for any inflowing water (for example, a standard seawater value of 19,000 milligrams per liter at the ocean boundary).

Simulated Groundwater Recharge

Sources of inflow to the groundwater system include small-catchment recharge, leakage from creeks, underflow from neighboring basins, areal recharge, and septic-tank effluent. Small-catchment recharge was simulated on the north–northeast edge of the SBFTM (fig. 2) by injecting water into model layers 1 and 2 in the highlighted areas shown in figure 2. The fluxes were estimated as explained in the "Model Calibration Approach" section of this chapter. Small-catchment recharge segments were simulated along the north–northeast boundary of the SBFTM by using the well (WEL) package to inject water at a constant rate into the model cells bordering the foothills (fig. 2). Small-catchment recharge segments were aligned with the canyons to simulate the recharge rates from different canyons.

Creeks were simulated using the river (RIV) package (Harbaugh and others, 2000). The RIV package was used because the constituent-transport option in SEAWAT does not support other MODFLOW stream-routing packages (Langevin and others, 2008). Simulated creeks include Sycamore, Mission, San Roque, Arroyo Burro, Cieneguitas, and Atascadero creeks (fig. 1). Stage, creek-bed conductance, and creek-bed elevation are specified for the RIV package. The creek-bed elevations were based on a 10-m digital-elevation model of the study area. The RIV package allows fluxes to enter or leave the groundwater system as a function of creek stage and groundwater level. If the creek stage is higher than the groundwater level, then creek water recharges the groundwater system. If the creek stage is lower than the groundwater level, then groundwater discharges to the creek.

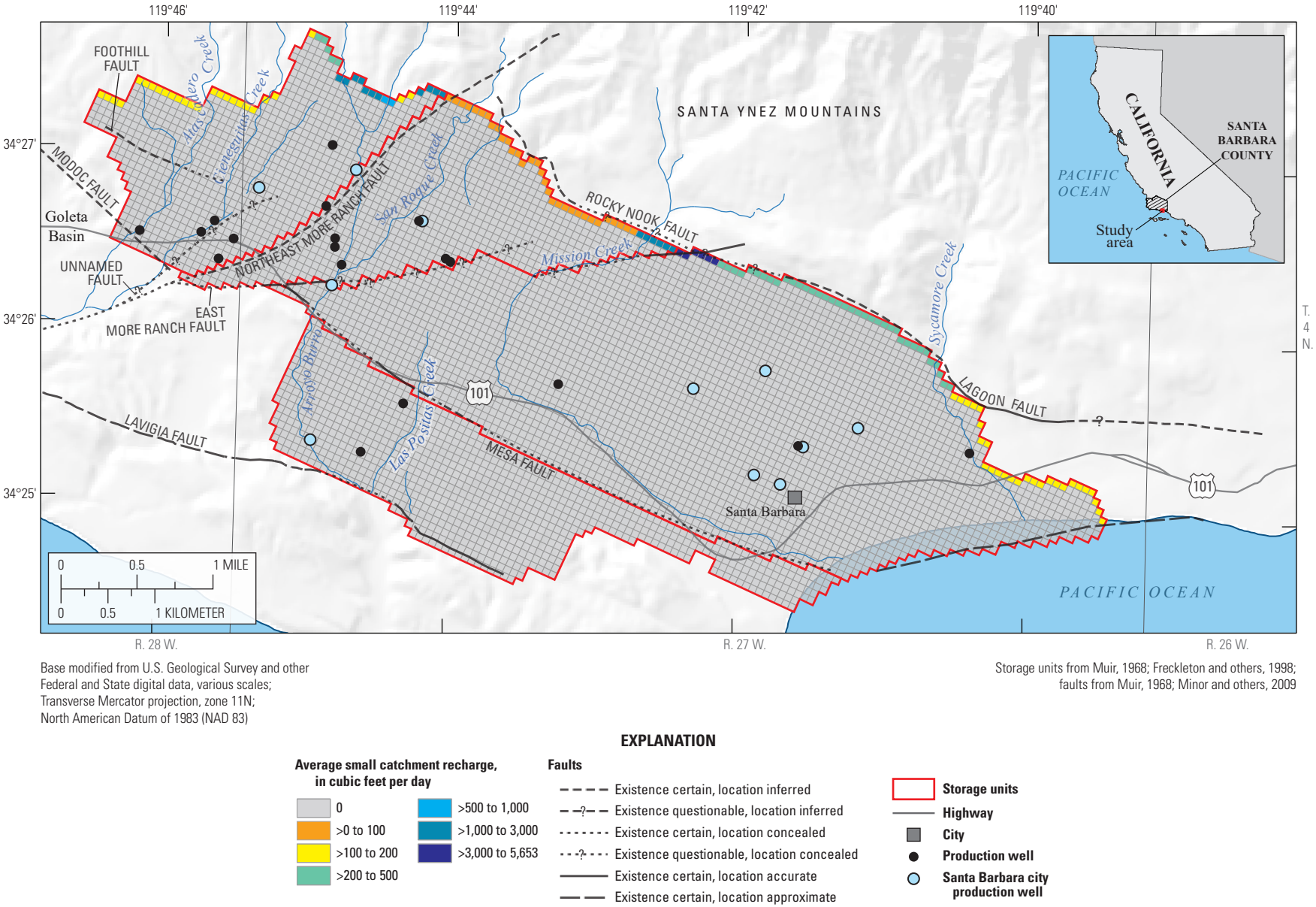

Figure 2. Rates of small-catchment recharge for the Santa Barbara flow and transport model, Santa Barbara, California.

The creeks were defined by multiple segments. Creek stage and creek-bed conductance parameters were allowed to vary during model calibration among creek segments in the model area. Creek stage for all the creek segments was initially estimated using the average of the reported Mission Creek stage data (11119745, Mission Creek at Rocky Nook Park) from 1997 to 2013 (U.S. Geological Survey, 2013). Creek stage was assumed to be constant throughout the simulation period. Final values of creek-stage and creek-bed conductance for each creek segment were both determined by parameter estimation.

Areal recharge represents direct infiltration to the groundwater system throughout the active model domain and is simulated using the recharge (RCH) package (Harbaugh and others, 2000). Areal recharge was estimated on the basis of a percentage of monthly precipitation data from the Parameter-elevation Regressions on Independent Slopes Model (PRISM; Daly and Bryant, 2013), soil permeability (U.S. Department of Agriculture, 2008), and parcel land-use data (California Department of Water Resources, 1996). PRISM uses climate stations and topography to estimate precipitation amounts on a 2.5 mi (4-kilometer) grid throughout the United States. A land-use map was used to define paved, partially paved, and unpaved areas. Soil maps were used to define areas of high, medium, and low permeability and impermeable soils. Based on these classifications of land use and soil, four infiltration zones were identified that range from low (infiltration zone 1) to high infiltration (infiltration zone 4; fig. 3*A*). Infiltration zone 1 represents areas with low-permeability soils that are partially paved. Infiltration zone 2 represents areas with lower to moderate-permeability soils that are minimally to moderately paved. Infiltration zone 3 represents areas with moderate to high permeability soils that are minimally to moderately paved. Infiltration zone 4 represents areas with high-permeability soils that are unpaved. Paved areas and areas with impermeable soils were not included in infiltration zones 1–4, and no infiltration was assigned to these areas. Each infiltration zone was assigned a percentage of infiltration for precipitation, which was determined by parameter estimation. Each topmost active model cell in an infiltration zone was assigned a monthly precipitation rate, and the total recharge rate in a given model cell was determined by multiplying the monthly precipitation rate for that cell by the infiltration zone's infiltration percentage.

Septic-tank recharge was simulated using the RCH package and addressed by defining a fifth infiltration zone (fig. 3*B*). Data for parcels with septic systems were provided by the Santa Barbara County Clerk-Recorder-Assessor's Mapping Division. Septic recharge was applied to all top-most model cells containing parcels where there was septic-system usage.

The map of parcels with septic systems was overlaid onto the model grid, showing 255 acres in the model area with septic systems. Note that this value is greater than the area of the parcels that the septic systems occupy (about 156 acres) because if a parcel overlaid part of a model cell, the entire model cell was included in the area. The parcel map also indicated there were 195 single-family residences (SFR), 16 multi-unit dwellings (MUD) with 2–4 units, one rest home, one restaurant, and one retail store with septic systems. As described in chapter A, assuming 2.5 residents per SFR (U.S. Census Bureau, 2017), 10 residents per MUD, and a septic-effluent rate of 90 gallons per day per person yields a total septic flow rate of about 65 acre-feet per year (acre-ft/yr). Further assuming the model-grid area of 255 acres, yields a flux rate of 7.0E-04 feet per day (ft/d). The initial septic flux rate was assumed to equal 3.3E-03 ft/d, and the final septic flux rate was determined by parameter estimation.

Simulated Groundwater Discharge

Groundwater outflow is primarily from groundwater pumping, underflow, discharge to streams and drains, and evapotranspiration. With the exception of available measurements of pumpage for public supply, flow rates for these components of groundwater outflow were relatively unknown and were simulated as part of this study.

Groundwater pumpage was simulated using the WEL package (Harbaugh and others, 2000). A total of 29 production wells are simulated in the SBFTM (fig. 1). Well location, construction, and production data were obtained from the USGS National Water Information System (NWIS) database and the city's records (Kelley Dyer, City of Santa Barbara, personal commun., 2013). Pumpage data from individual wells were used to estimate pumpage on an annual basis from 1929 to 1971 and on a monthly basis from 1972 to 2013. Total groundwater production in the Santa Barbara and Foothill groundwater basins was highly variable between 1972 and 2008 (fig. A–8). Total groundwater pumpage varied from less than 500 acre-ft/yr during typical years to more than 3,000 acre-ft/yr during dry years. The percentage of pumpage for a single production well extracted from each model cell the well perforates was calculated using equation 1:

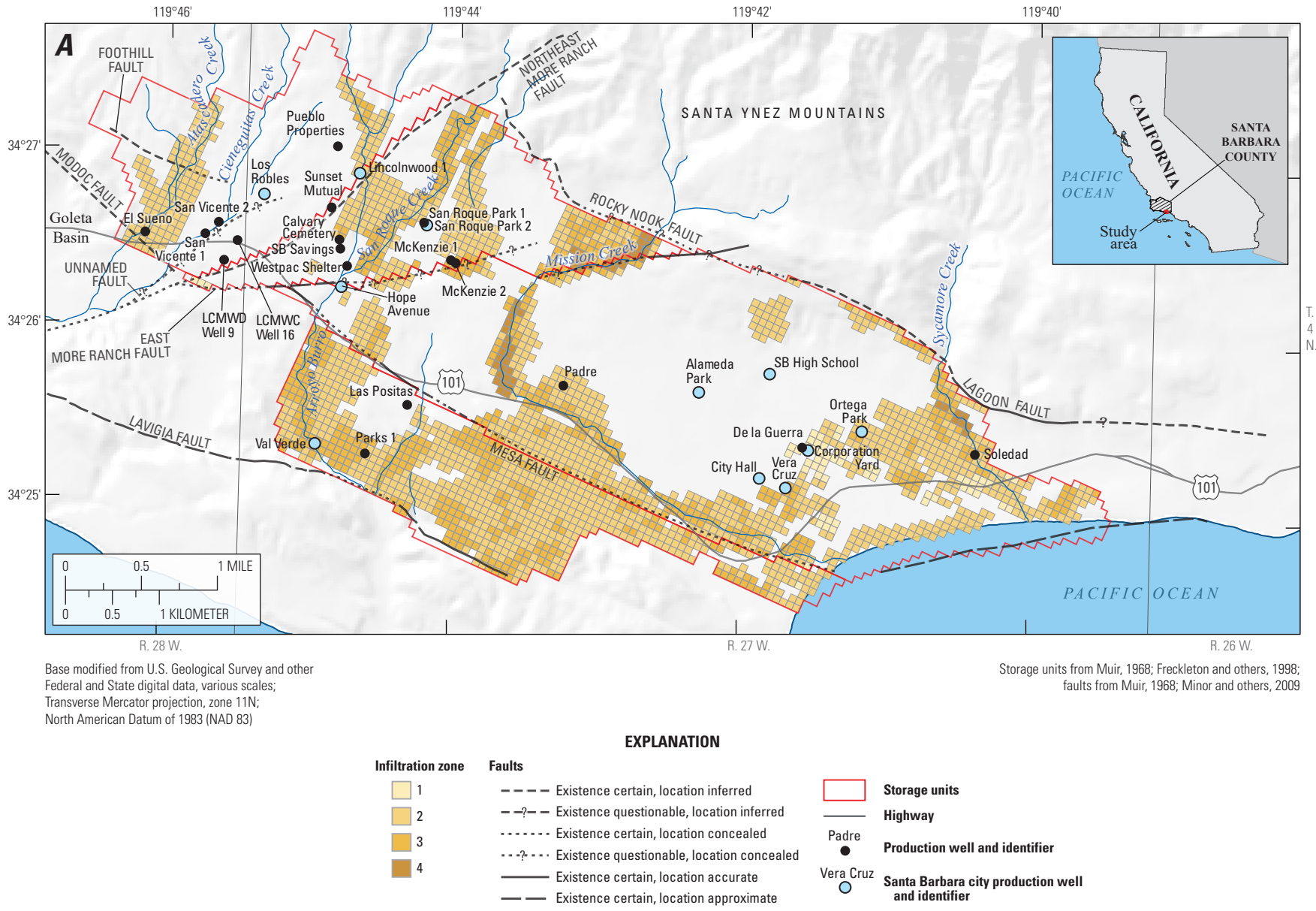

Base modified from U.S. Geological Survey and other Federal and State digital data, various scales; Transverse Mercator projection, zone 11N; North American Datum of 1983 (NAD 83)

Storage units from Muir, 1968; Freckleton and others, 1998; faults from Muir, 1968; Minor and others, 2009

EXPLANATION

Infiltration zone
- 1
- 2
- 3
- 4

Faults
- Existence certain, location inferred
- Existence questionable, location inferred
- Existence certain, location concealed
- Existence questionable, location concealed
- Existence certain, location accurate
- Existence certain, location approximate

- **Storage units**
- **Highway**
- Padre — **Production well and identifier**
- Vera Cruz — **Santa Barbara city production well and identifier**

Figure 3. Areas of potential groundwater recharge for the Santa Barbara flow and transport model, Santa Barbara, California: *A*, infiltration zones and *B*, septic-recharge parcels.

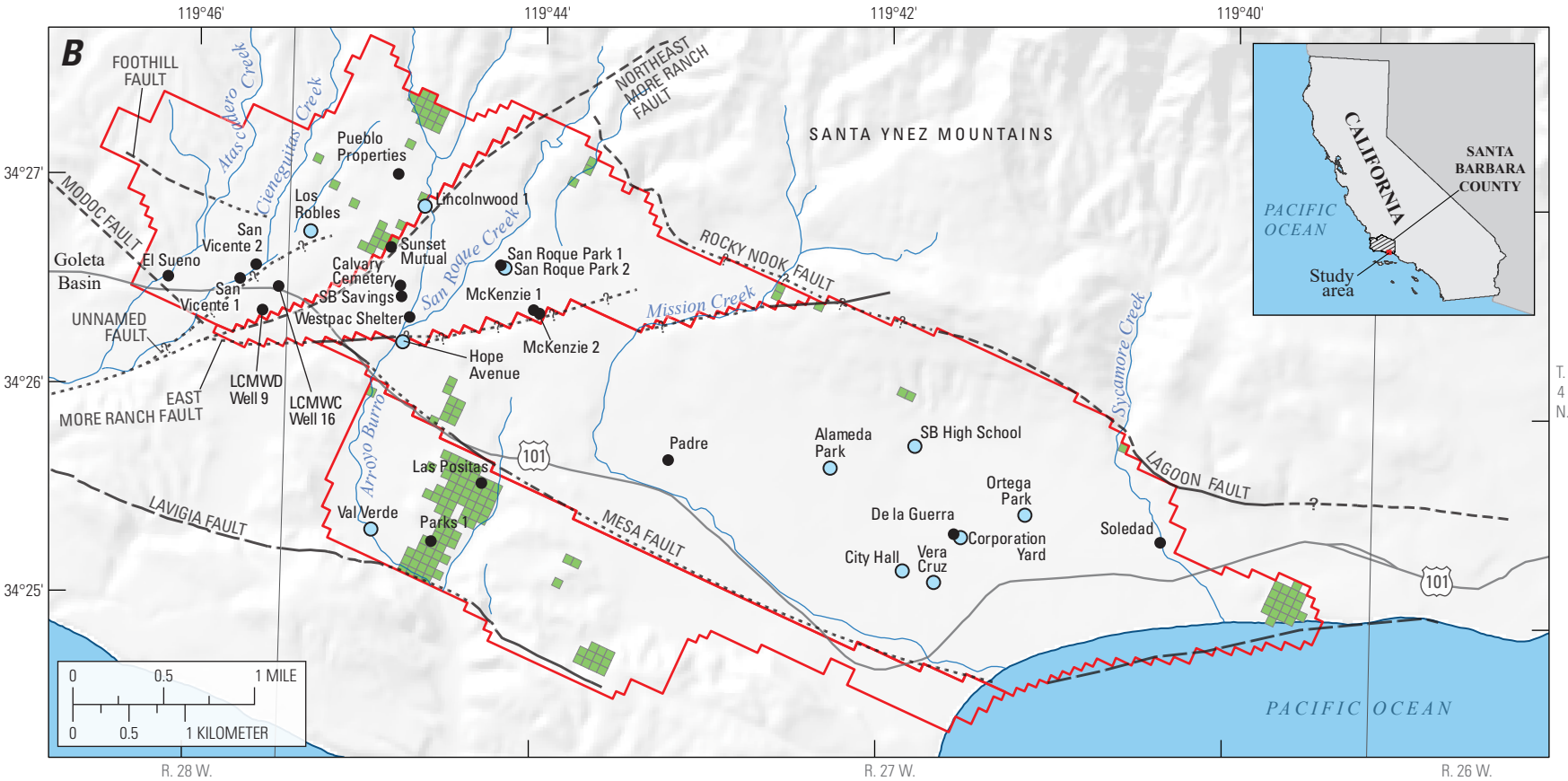

Base modified from U.S. Geological Survey and other Federal and State digital data, various scales; Transverse Mercator projection, zone 11N; North American Datum of 1983 (NAD 83)

Storage units from Muir, 1968; Freckleton and others, 1998; faults from Muir, 1968; Minor and others, 2009

EXPLANATION

Faults

- Existence certain, location inferred
- Existence questionable, location inferred
- Existence certain, location concealed
- Existence questionable, location concealed
- Existence certain, location accurate
- Existence certain, location approximate

- **Storage units**
- **Septic recharge zone**
- **Highway**
- Padre — **Production well and identifier**
- Vera Cruz — **Santa Barbara city production well and identifier**

Figure 3. —Continued

$$Pct_{cell} = \left(HGLF_{zone} \times HK_{cell} \times SL_{cell}\right) / \left(\sum_{i=1}^{n}\left(HGLF_i \times HK_i \times SL_i\right)\right) \quad (1)$$

where

Pct_{cell} is the percentage of pumpage extracted from a given model cell,

$HGLF_{zone}$ is a parameter assigned to each hydrogeologic zone (that is, the shallow zone, upper producing zone, and so on, as described in chapter A) that contains the model cell,

HK_{cell} is the hydraulic conductivity at the well in a given model cell,

SL_{cell} is the length of the perforated interval in a given model cell,

$HGLF_i$ is a multiplier for model cell i (allowed to range from 1E-5 to 10 in Storage Unit I and from 0.1 to 10 in Foothill and Storage Unit III) that allows fine tuning of the vertical pumping distribution (this estimate was updated iteratively during calibration as the hydraulic conductivity was estimated),

HK_i is the hydraulic conductivity at the well for model cell i,

SL_i is the length of the perforated interval for model cell i,

n is the total number of cells connected to the perforated interval of the well.

Basin outflows through creek channels and the city's drain system are simulated using the drain (DRN) package (Harbaugh and others, 2000). Outflow from the Foothill to the Goleta groundwater basin across the Modoc fault was assumed to be mostly along the Atascadero and Cieneguitas Creek deposits, and outflow from Storage Unit III across the Lavigia fault was assumed to be mostly along the Arroyo Burro and Las Positas Creek deposits (fig. 1). Drain head values along these creeks were initially assigned based on nearby well observations; final drain head values were determined by parameter estimation. The manmade drains installed by the city in Storage Unit I to drain the Estero were simulated based on Freckleton and others (1998). Drain head values for manmade drains installed by the city were defined by the drain elevation. Drain conductance values for creeks and the city's drain system were both determined by model calibration.

Aquifer Properties

Aquifer properties used in the simulation were horizontal and vertical hydraulic conductivity, specific storage, conductance across horizontal-flow barriers, and the constituent transport parameters porosity, dispersivity, and diffusion. Percentage of coarse-grained sediment from the texture model was used to define hydraulic conductivity and specific storage. The locations of the horizontal-flow barriers were determined by fault locations reported by Minor and others (2009). Porosity and dispersivity were estimated by parameter estimation and allowed to vary within reasonable limits.

Model Parameterization

To aid in the calibration of the hydraulic properties and boundary conditions in the model, the four groundwater subbasins were divided into regions, subregions, and areas (figs. 4–6). The subbasins were divided into five regions (fig. 4); each region was assigned different hydraulic conductivity ranges. The regions were divided into 14 subregions (fig. 5), which were used to improve the representation of different depositional environments and were based on the geography and geology of the study area, including proximity to stream channels, mountains, and the coast. Each subregion was assigned different multipliers, which were estimated during model calibration. Finally, the model domain was divided into coastal and inland areas (fig. 6), where each area was assigned layer-wise multipliers, which were estimated during model calibration. The coastal area (fig. 6) was parameterized separately from the rest of Storage Unit I because some shallow, low-permeability areas are limited to the flatter areas of the coastal plain; therefore, the coastal and inland areas have different layer-wise multipliers. For example, assume a hydraulic conductivity value for region i, in subregion j, in the coastal area; therefore, the hydraulic conductivity (HK) value for layer k is as follows:

$$HK_k = HK_i \times m_j \times m_{ck} \quad (2)$$

where

m_j is the multiplier for subregion j, and

m_{ck} is the coastal multiplier for layer k.

Hydrogeologic Units

The Santa Barbara and Foothill groundwater basins contain two main high-permeability hydrogeologic units: the upper and lower producing zones (fig. 7). Near the coast, Storage Unit I markedly thickens and contains the additional middle producing zone that does not extend inland into the other subbasins, as discussed in chapters A and B (fig. A–6). As stated earlier, the SBFTM simulates the transport of chloride due to seawater intrusion in Storage Unit I, which requires a relatively high level of model detail; therefore, the hydrogeologic units were defined in greater detail for Storage Unit I than for Storage Unit III and the Foothill subbasins.

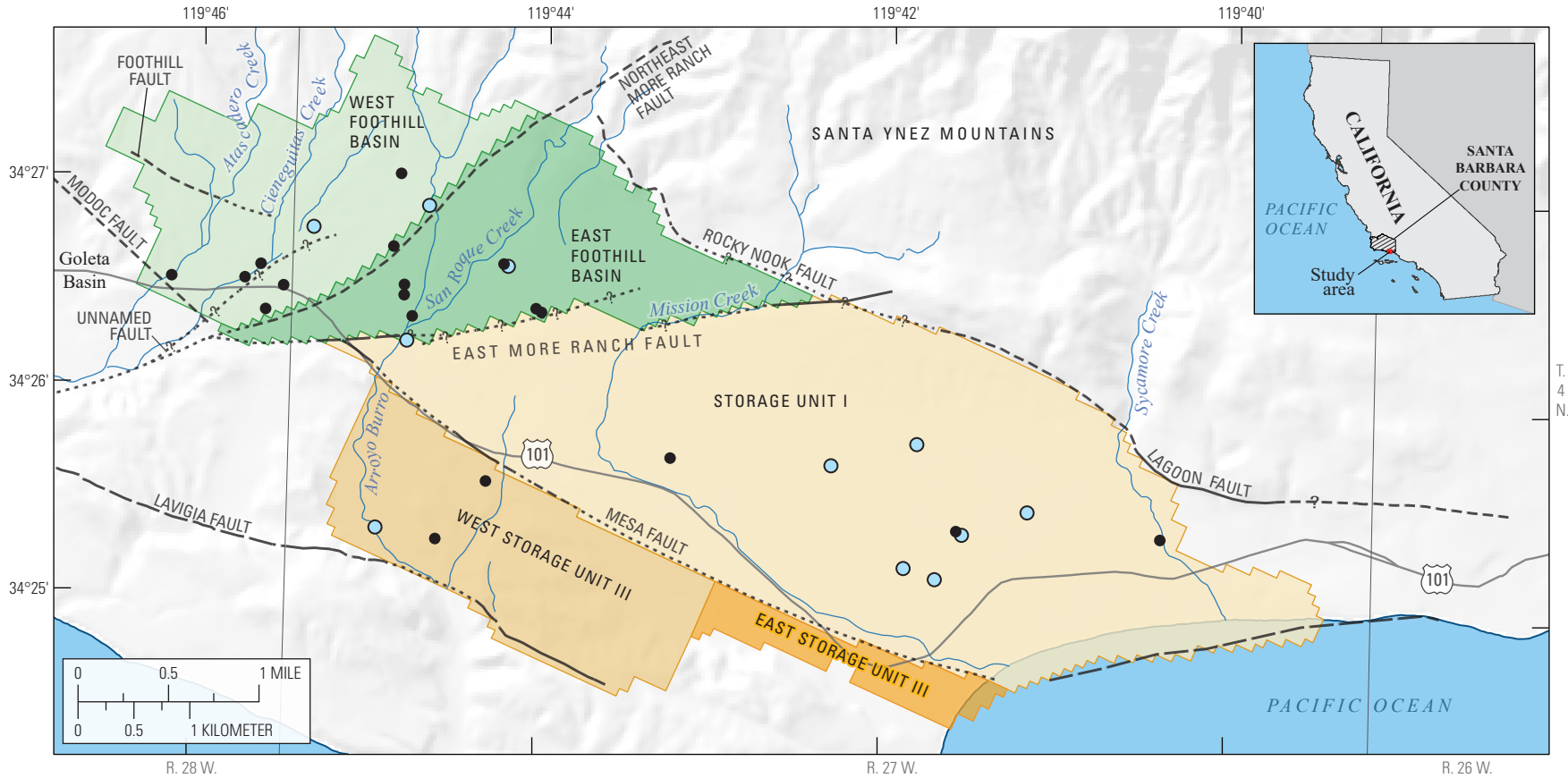

Base modified from U.S. Geological Survey and other Federal and State digital data, various scales; Transverse Mercator projection, zone 11N; North American Datum of 1983 (NAD 83)

Storage units from Muir, 1968; Freckleton and others, 1998; faults from Muir, 1968; Minor and others, 2009

EXPLANATION

Model regions
- West Foothill Basin
- East Foothill Basin
- Storage Unit I
- West Storage Unit III
- East Storage Unit III

Faults
- Existence certain, location inferred
- Existence questionable, location inferred
- Existence certain, location concealed
- Existence questionable, location concealed
- Existence certain, location accurate
- Existence certain, location approximate

- **Highway**
- **Production well**
- **Santa Barbara city production well**

Figure 4. Five regions used in the Santa Barbara flow and transport model, Santa Barbara, California.

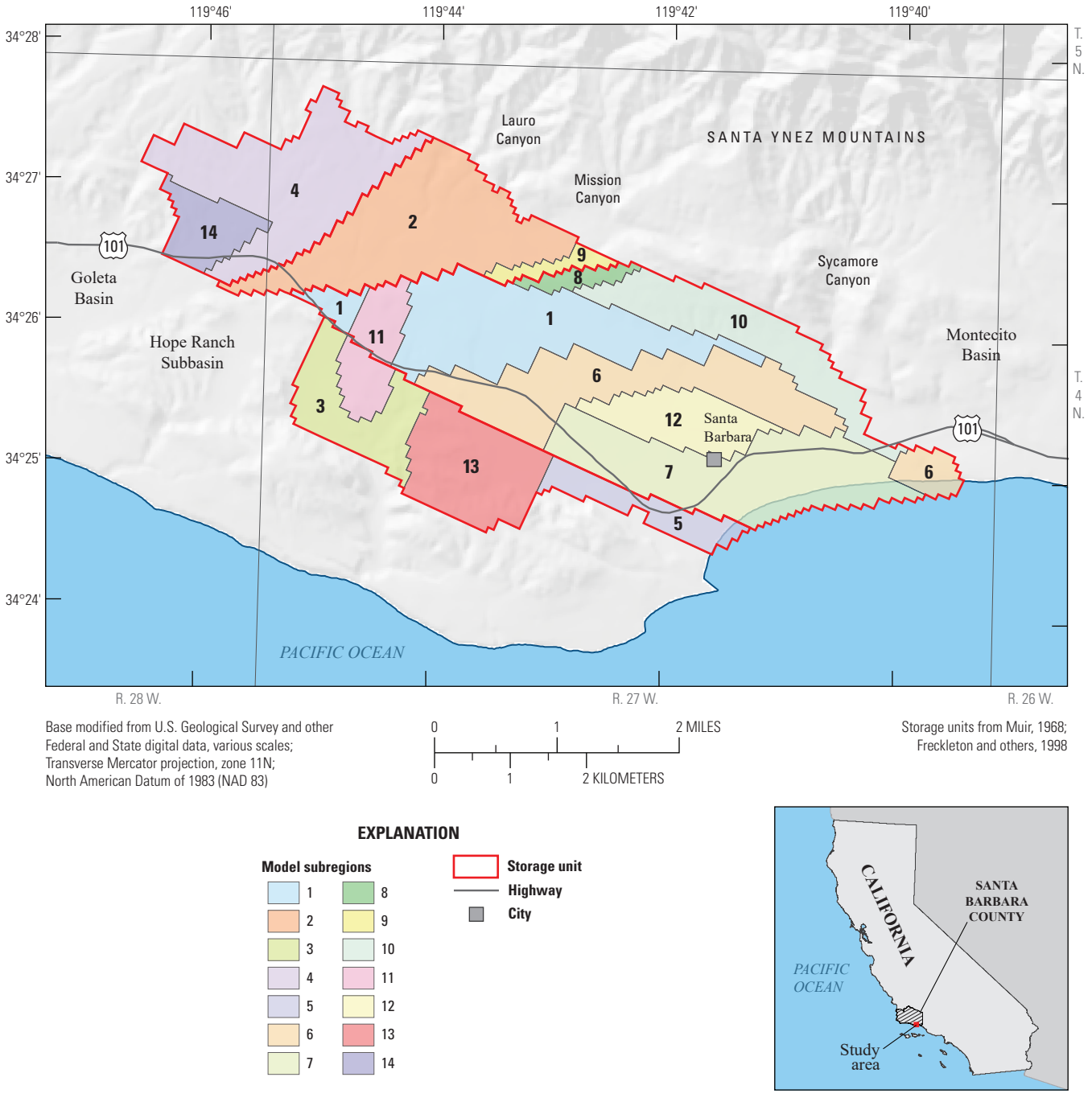

Figure 5. The 14 subregions used in the Santa Barbara flow and transport model, Santa Barbara, California.

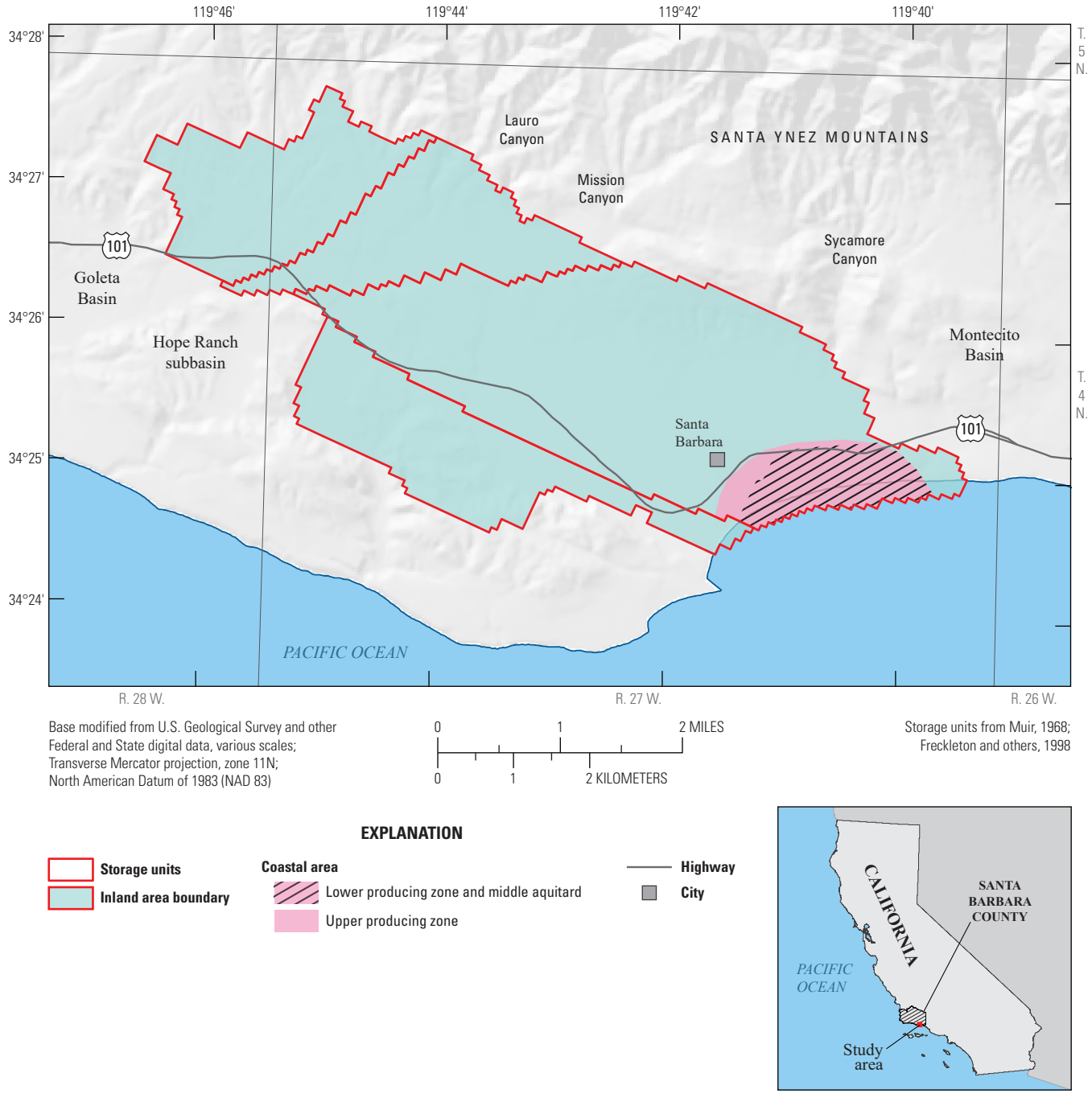

Figure 6. The two areas used in the Santa Barbara flow and transport model, Santa Barbara, California.

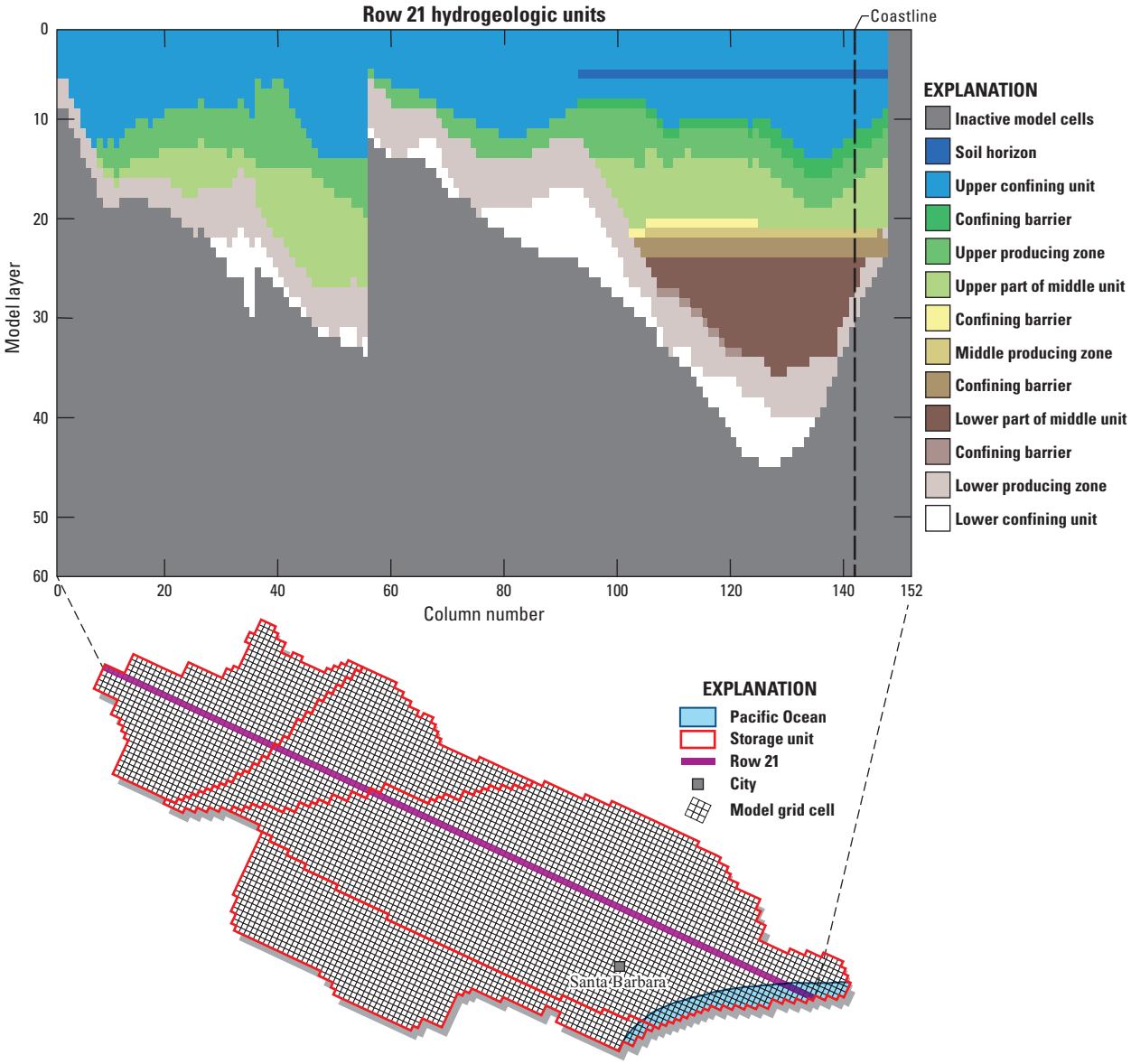

Figure 7. Hydrogeologic units defined for the Santa Barbara flow and transport model, Santa Barbara, California.

Hydraulic and Transport Properties

Hydraulic properties include hydraulic conductivity of the aquifer; conductance of faults, GHBs, and drains; creek-bed conductance; and aquifer storage. Transport properties include porosity, dispersivity, and diffusion.

Hydraulic Conductivity

Hydraulic conductivity was estimated using the sediment texture defined in the HFM (chapter B) by regions, subregions, areas, and creek channels. The hydraulic conductivity for each groundwater-model cell was calculated using the percentage of coarse-grained material from the HFM (see chapter B). The calculation of hydraulic conductivity for the horizontal and vertical directions was done using the power mean. Using this mean, the hydraulic conductivity of the textural end members, representing the coarsest and finest materials, was used in conjunction with the percentage of coarse-grained material in each cell to calculate the overall hydraulic conductivity in each direction. Different lithologic end-member hydraulic conductivities were used for each region (table 3). Initial horizontal hydraulic conductivities were calculated using arithmetic averaging, and initial vertical hydraulic conductivities were calculated using a power approximating the geometric mean. These initial texture-based horizontal and vertical hydraulic-conductivity values were calculated using equations 3 and 4, respectively:

$$HK_{texture} = PC \times K_{cx} + PF \times K_{fx} \quad (3)$$

$$VK_{texture} = \left(K_{ck}^{-1} \times PC + K_{fx}^{-1} \times PF \right)^{-1} \quad (4)$$

where

K_{cx} is the coarse hydraulic-conductivity end member;

K_{fx} is the fine hydraulic-conductivity end member;

PC is the percentage of coarse sediment in a given model cell, expressed as a fraction; and

PF is the percentage of fine sediment in a given model cell, expressed as a fraction.

The texture-based hydraulic-conductivity values were adjusted during model calibration by multipliers defined for each subregion, area, and hydrogeologic unit. The horizontal and vertical hydraulic-conductivity values for specific subregion, area, and hydrogeologic unit combinations were defined by equations 5 and 6:

$$HK_{srl} = HK_{texture} \times HKSRM \times HKLM \quad (5)$$

$$VK_{srl} = VK_{texture} \times VKSRM \times VKLM \quad (6)$$

where

HKSRM and *VKSRM* are multipliers for the horizontal and vertical hydraulic conductivity, respectively, applied to each subregion, and

HKLM and *VKLM* are the horizontal and vertical hydraulic conductivity multipliers, respectively, applied to each hydrogeologic unit. Note that HKLM and VKLM are also functions of area (coastal or inland).

Relatively coarse creek beds are thought to exist in the upper Mission and Sycamore Creeks that were not captured in the textural model because of a lack of borehole data for the creek beds. To simulate the coarse-grained material in these creek beds, a scalar multiplier was applied to the HK and VK in all model layers in creek-infiltration zones. This implicitly assumes that the creek channel has not moved over time and that the coarse-grained material extends vertically beneath the creek bed to the water table.

Conductance Properties

Conductance properties affect the flow across faults, GHBs, and drains. Flow across creek beds is affected by creek-bed conductance and stage; these are discussed in the following section.

On the basis of previous work and water-level offsets, the Mesa, East More Ranch, Northeast More Ranch, unnamed, and Foothill faults are thought to restrict groundwater flow (fig. 8). Accordingly, these faults are simulated using the horizontal-flow barrier (HFB) package (Hsieh and Freckleton, 1993). An HFB is a low-permeability feature that is used to restrict flow across the simulated barrier with a specified hydraulic-characteristic term. The lower the hydraulic characteristic, the greater the effect of the barrier. The East More Ranch, Mesa, Northeast More Ranch, and Foothill faults were divided into segments, and a separate hydraulic-characteristic parameter was estimated for each segment. The unnamed fault and the Foothill fault each have a single hydraulic-characteristic value for the entire length of the fault. In order to simulate increased flow across faults intersected by coarse fluvial deposits, separate hydraulic-characteristic parameters were assigned to the upper model cells at the intersection of faults and major creeks.

The ocean-fault GHB was simulated using seven conductance parameters defined by hydrogeologic zone: one for each of the three producing zones and four for the zones between, above, and below the producing zones. The shallow-ocean GHB was assigned a single conductance parameter. The Montecito GHB was assigned three conductance parameters, one for the middle producing zone, one for all model layers above it, and one for all model layers below it.

As was previously described, there are two general sets of drains: the Santa Barbara city drains and the creek-underflow drains for Arroyo Burro, Atascadero, and Cienguitas Creeks. One conductance parameter was used for the Santa Barbara city drain, and two conductance parameters were used for each creek underflow drain—one parameter for the upper layers and one for the lower layers.

Creek Properties

There are two properties that govern whether and how much a creek gains or loses water: creek-bed conductance and creek stage. Model cells of the stream type (fig. 1) were divided into segments along most creeks, and each segment was assigned a separate value for creek-bed conductance (table 3). In addition, each creek segment was assigned a parameter for the stage of the creek, which was fixed for the entire simulation.

Table 3. Calibrated groundwater flow and solute transport model parameter values, Santa Barbara flow and transport model, Santa Barbara, California.

[/day, per day; ft, foot; ft^2, square foot; GHB, general-head boundary package; HK, horizontal hydraulic conductivity; Rd., road; St., street; VK, vertical hydraulic conductivity; —, not applicable]

Parameter name	Group	Subgroup	Description	Calibrated value	Lower bound	Upper bound	Preliminary value	Units
ab_t_t	streamk	Creek conductance adjustment parameter	Las Positas Creek	3.91E–04	1.08E–04	1.08E+04	1.23E+00	ft^2/day
ab_w_t	streamk	Creek conductance adjustment parameter	Arroyo Burro Creek between Northridge and San Roque Creek junctions	4.57E–05	1.08E–05	1.08E+04	3.33E+02	ft^2/day
ab_we_t	streamk	Creek conductance adjustment parameter	Northridge Creek	5.37E+01	1.08E–04	1.08E+04	6.39E+01	ft^2/day
ab_ww_t	streamk	Creek conductance adjustment parameter	Upstream Arroyo Burro Creek upstream of Northridge Creek junction	4.73E+01	1.08E–04	1.08E+04	1.11E+02	ft^2/day
abcynrchmt	rch	Small catchment recharge multiplier	Small catchment recharge Arroyo Burro Creek area	2.20E+00	1.00E–05	2.50E+00	5.59E–02	—
arroyo_br_t	streamk	Creek conductance adjustment parameter	Arroyo Burro Creek from San Roque Creek to about 0.7 miles south of San Roque Creek junction	1.54E–03	1.08E–04	1.08E+04	9.61E+01	ft^2/day
arroyobrs_t	streamk	Creek conductance adjustment parameter	Downstream portion of Arroy Burro Creak to edge of model	3.56E–01	1.08E–04	1.08E+04	3.56E–01	ft^2/day
arryob_s	rivers	Creek stage adjustment parameter	Upstream Arroyo Burro Creek upstream of Northridge Creek junction	4.64E–01	3.28E–06	3.28E+00	1.38E–04	ft
arryoc_s	rivers	Creek stage adjustment parameter	Arroyo Burro Creek between Northridge and San Roque Creek junctions	4.64E–01	3.28E–06	3.28E+00	1.38E–04	ft
arryod_s	rivers	Creek stage adjustment parameter	Arroyo Burro Creek from San Roque Creek to about 0.7 miles south of San Roque Creek junction	4.64E–01	3.28E–06	3.28E+00	1.38E–04	ft
arryol_s	rivers	Creek stage adjustment parameter	Downstream portion of Arroy Burro Creak to edge of model	4.64E–01	3.28E–06	3.28E+00	1.38E–04	ft
atas_e_t	streamk	Creek conductance adjustment parameter	Upstream Atascadero Creek upstream of Via Chaparral Creek junction	3.04E+01	1.08E–04	1.08E+04	1.12E+00	ft^2/day
atas_t_t	streamk	Creek conductance adjustment parameter	La Paloma Creek	2.51E–05	1.08E–05	1.08E+04	6.43E+01	ft^2/day
atas_w_t	streamk	Creek conductance adjustment parameter	Via Chaparral Creek	2.67E–05	1.08E–05	1.08E+04	2.20E+00	ft^2/day
atasca_s	rivers	Creek stage adjustment parameter	Upstream Atascadero Creek upstream of Via Chaparral Creek junction	4.61E–01	3.28E–06	4.92E+00	1.87E–01	ft
atascadero_t	streamk	Creek conductance adjustment parameter	Atascadero Creek downstream of Via Chaparral Creek junction	8.11E+00	1.08E–04	1.08E+04	1.12E+00	ft^2/day
atascb_s	rivers	Creek stage adjustment parameter	Atascadero Creek downstream of Via Chaparral Creek junction	4.60E–01	3.28E–06	3.28E+00	6.22E–02	ft
atasel	streamk	Creek conductance adjustment parameter	Where Atascadero and Via Chaparral Creek closely parallel one another up to junction	9.73E+00	1.08E–04	1.08E+04	1.15E–04	ft^2/day

Table 3. Calibrated groundwater flow and solute transport model parameter values, Santa Barbara flow and transport model, Santa Barbara, California.—Continued

[/day, per day; ft, foot; ft^2, square foot; GHB, general-head boundary package; HK, horizontal hydraulic conductivity; Rd., road; St., street; VK, vertical hydraulic conductivity; —, not applicable]

Parameter name	Group	Subgroup	Description	Calibrated value	Lower bound	Upper bound	Preliminary value	Units
cien_e_t	streamk	Creek conductance adjustment parameter	Eastern fork of Cieneguitas Creek	6.06E+00	1.08E–04	1.08E+04	1.14E+00	ft^2/day
cien_w_t	streamk	Creek conductance adjustment parameter	Western fork of Cieneguitas Creek	5.50E+01	1.08E–04	1.08E+04	2.64E+01	ft^2/day
cienee_s	rivers	Creek stage adjustment parameter	Eastern fork of Cieneguitas Creek	4.82E–01	3.28E–06	3.28E+00	1.87E–01	ft
cieneguita_t	streamk	Creek conductance adjustment parameter	Cieneguitas Creek downstream of fork	3.94E–05	1.08E–05	1.08E+04	1.24E–01	ft^2/day
cienel_s	rivers	Creek stage adjustment parameter	Cieneguitas Creek downstream of fork	4.82E–01	3.28E–06	3.28E+00	3.94E–02	ft
cieneu_s	rivers	Creek stage adjustment parameter	Western fork of Cieneguitas Creek	4.82E–01	3.28E–06	3.28E+00	3.94E–02	ft
disp	dispersion	Longitudinal dispersivity	Shallow	6.56E+00	4.00E–02	2.50E+02	2.80E+03	ft
dispdp	dispersion	Longitudinal dispersivity	Deep	4.92E+01	4.00E–02	2.50E+02	6.56E+00	ft
draincond	otherk	Drain conductance	City drain conductance	3.70E+02	1.08E–02	1.08E+04	2.73E+01	ft^2/day
drainfha	otherk	Drain conductance	Atascadero Creek drain conductance shallow	1.27E+00	1.08E–04	1.08E+04	1.31E–03	ft^2/day
drainfhadp	otherk	Drain conductance	Atascadero Creek drain conductance deep	1.56E+01	1.08E–02	1.08E+04	3.11E+00	ft^2/day
drainfhc	otherk	Drain conductance	Cieneguitas Creek drain conductance shallow	5.57E–01	1.08E–04	1.08E+04	1.31E–04	ft^2/day
drainfhcdp	otherk	Drain conductance	Cieneguitas Creek drain conductance deep	5.84E+00	1.08E–02	1.08E+04	3.08E–01	ft^2/day
drainsu3	otherk	Drain conductance	Arroyo Burro Creek drain conductance	2.47E+01	1.08E–02	1.08E+04	2.41E+02	ft^2/day
e_more_1	faultk	Fault conductance	East More Ranch fault between western edge of model and 101 freeway	7.49E–08	1.00E–08	1.00E+00	2.23E–04	/day
e_more_2	faultk	Fault conductance	East More Ranch fault between 101 freeway and State Street	5.21E–08	1.00E–08	1.00E+02	1.42E–04	/day
e_more_3	faultk	Fault conductance	East More Ranch fault between State Street and Mission Creek	1.13E–08	1.00E–08	1.00E+00	5.39E–05	/day
e_more_4a	faultk	Fault conductance	East More Ranch fault following Mission Creek northeast of the Mission	8.61E–05	1.00E–07	1.00E+00	1.56E–05	/day
e_more_4b	faultk	Fault conductance	East More Ranch fault following Mission Creek west of the Mission	2.64E–06	1.00E–07	1.00E+00	1.56E–05	/day
e_more_wr	faultk	Fault conductance	East More Ranch fault at Arroyo Burro Creek	1.00E+01	1.00E–07	1.00E+01	1.00E+01	/day
fhdrainhd	other_hd	Drain head	Atascadero and Cieneguitas Creek drain head	–1.32E–02	–6.55E+01	1.64E+02	–1.32E–02	ft
foothillrd	faultk	Fault conductance	Foothill fault	1.04E–04	1.00E–07	1.00E+00	2.63E–05	/day
htransd	dispersion	Horizontal transverse dispersivity	Horizontal shallow	1.64E–02	1.64E–02	1.64E+00	2.76E–01	ft
htransddp	dispersion	Horizontal transverse dispersivity	Horizontal deep	1.64E+00	1.64E–01	1.64E+01	1.64E+00	ft

Table 3. Calibrated groundwater flow and solute transport model parameter values, Santa Barbara flow and transport model, Santa Barbara, California.—Continued

[/day, per day; ft, foot; ft², square foot; GHB, general-head boundary package; HK, horizontal hydraulic conductivity; Rd., road; St., street; VK, vertical hydraulic conductivity; —, not applicable]

Parameter name	Group	Subgroup	Description	Calibrated value	Lower bound	Upper bound	Preliminary value	Units
ic_pmp_mac	rch	Early 20th century pumping multiplier	Early 20th century pumping multiplier	2.00E–01	1.00E–02	8.00E–01	8.00E–01	—
kc1	aquiferk	HK/VK end member	Coarse end member for Storage Unit I	8.58E+00	3.28E–02	3.28E+03	6.62E+00	ft/day
kc2	aquiferk	HK/VK end member	Coarse end member for East Foothill Subbasin	3.97E+00	3.28E–02	3.28E+03	3.67E+02	ft/day
kc3	aquiferk	HK/VK end member	Coarse end member for Storage Unit III West	3.44E+00	3.28E–02	3.28E+03	5.76E+00	ft/day
kc4	aquiferk	HK/VK end member	Coarse end member for West Foothill Subbasin	6.61E+00	3.28E–02	3.28E+03	7.34E+01	ft/day
kc5	aquiferk	HK/VK end member	Coarse end member for Storage Unit III East	2.62E–01	3.28E–02	3.28E+03	3.51E+01	ft/day
kf1	aquiferk	HK/VK end member	Fine end member for Storage Unit I	2.33E–02	3.28E–05	3.28E+00	1.86E–03	ft/day
kf2	aquiferk	HK/VK end member	Fine end member for East Foothill Subbasin	3.85E–03	3.28E–05	3.28E+00	3.12E–03	ft/day
kf3	aquiferk	HK/VK end member	Fine end member for Storage Unit III West	2.86E–03	3.28E–05	3.28E+00	2.67E–03	ft/day
kf4	aquiferk	HK/VK end member	Fine end member for West Foothill Subbasin	1.68E–02	3.28E–05	3.28E+00	1.64E–03	ft/day
kf5	aquiferk	HK/VK end member	Fine end member for Storage Unit III East	1.47E–03	3.28E–05	3.28E+00	4.90E–03	ft/day
lapalo_s	rivers	Creek stage adjustment parameter	La Paloma Creek	4.72E–01	3.28E–06	3.28E+00	6.23E–02	ft
laspos_s	rivers	Creek stage adjustment parameter	Las Positas Creek	4.60E–01	3.28E–06	3.28E+00	1.48E–01	ft
lauro_t	streamk	Creek conductance adjustment parameter	Lauro Canyon Creek	5.26E–04	1.08E–04	1.08E+04	6.64E+01	ft²/day
lauroc_s	rivers	Creek stage adjustment parameter	Lauro Canyon Creek	4.85E–01	3.28E–06	3.28E+00	3.38E–02	ft
mc_1_4_t	streamk	Creek conductance adjustment parameter	Upstream segment of Mission Creek near northern boundary of model to just north of the Mission	2.44E+02	1.08E–02	1.08E+03	5.48E+02	ft²/day
mc_4_6_t	streamk	Creek conductance adjustment parameter	Mission Creek just north of the Mission to State St.	1.72E+02	1.08E–02	1.08E+04	2.73E+02	ft²/day
mc_6_7_t	streamk	Creek conductance adjustment parameter	Mission Creek from State St. to where it runs parallel to 101 freeway	6.43E+01	1.08E–02	1.08E+04	3.12E+00	ft²/day
mc_7_8_t	streamk	Creek conductance adjustment parameter	Mission Creek parallel to 101 freeway upstream of Micheltorena St.	1.98E+00	1.08E–05	1.08E+04	5.84E+01	ft²/day
mc_8_11_t	streamk	Creek conductance adjustment parameter	Mission Creek parallel to 101 freeway downstream of Micheltorena St.	2.15E+02	1.08E–02	1.08E+04	9.37E+00	ft²/day
mcynftrmlt	rch	Small catchment recharge multiplier	Small catchment recharge Mission Canyon area Storage Unit I	6.51E+00	1.00E–05	4.00E+01	1.56E+01	—
mcynrchmlt	rch	Small catchment recharge multiplier	Small catchment recharge Mission Canyon area Foothill subbasin	1.26E+01	1.00E–05	4.00E+01	2.06E+01	—
mesa	faultk	Fault conductance	Mesa fault west of Anapamu St.	2.08E–05	1.00E–07	1.00E+00	6.08E–05	/day
mesa_ab	faultk	Fault conductance	Mesa fault at Arroyo Burro Creek	2.25E+00	1.00E–07	5.00E+00	2.25E+00	/day

Table 3. Calibrated groundwater flow and solute transport model parameter values, Santa Barbara flow and transport model, Santa Barbara, California.—Continued

[/day, per day; ft, foot; ft^2, square foot; GHB, general-head boundary package; HK, horizontal hydraulic conductivity; Rd., road; St., street; VK, vertical hydraulic conductivity; —, not applicable]

Parameter name	Group	Subgroup	Description	Calibrated value	Lower bound	Upper bound	Preliminary value	Units
mesa_lp	faultk	Fault conductance	Mesa fault at Las Positas Creek	3.05E–01	1.00E–07	5.00E+00	3.05E–01	/day
mesal	faultk	Fault conductance	Mesa fault east of Anapamu St.	5.08E–04	1.00E–07	1.00E+00	5.08E–04	/day
missinit	rivers	Creek stage adjustment parameter	Base Creek water level above ground surface for all creeks	4.93E–01	3.28E–01	6.56E+00	2.65E–01	ft
missnb_s	rivers	Creek stage adjustment parameter	Upstream segment of Mission Creek near northern boundary of model to just north of the Mission	3.28E–05	3.28E–06	1.64E+00	2.56E–05	ft
missnc_s	rivers	Creek stage adjustment parameter	Mission Creek just north of the Mission to State St.	2.53E–02	3.28E–06	1.64E+00	2.56E–05	ft
missnd_s	rivers	Creek stage adjustment parameter	Mission Creek from State St. to where it runs parallel to 101 freeway	2.53E–02	3.28E–06	1.64E+00	2.56E–05	ft
missne_s	rivers	Creek stage adjustment parameter	Mission Creek parallel to 101 freeway upstream of Micheltorena St.	2.53E–02	3.28E–06	1.64E+00	2.56E–05	ft
missnf_s	rivers	Creek stage adjustment parameter	Mission Creek parallel to 101 freeway downstream of Micheltorena St.	2.53E–02	3.28E–06	1.64E+00	2.56E–05	ft
montecito	otherk	General head boundary conductance	Montecito GHB conductance shallow	1.61E+01	1.08E–05	1.08E+04	1.49E+02	ft^2/day
montecitol	otherk	General head boundary conductance	Montecito GHB conductance deep	1.61E+01	1.08E–05	1.08E+04	1.49E+02	ft^2/day
montecitom	otherk	General head boundary conductance	Montecito GHB conductance middle producing zone	1.08E–02	1.08E–05	1.08E+04	1.49E+02	ft^2/day
mpc	fact	Mobile porosity end member	Shallow coarse	1.00E–01	5.00E–02	3.50E–01	3.50E–01	—
mpclower	fact	Mobile porosity end member	Deep coarse	7.00E–02	5.00E–02	3.50E–01	7.00E–02	—
mpcmid	fact	Mobile porosity end member	Middle coarse	3.50E–01	5.00E–02	3.50E–01	2.00E–01	—
mpf	fact	Mobile porosity end member	Shallow fine	5.00E–02	1.00E–03	1.50E–01	5.78E–02	—
mpflower	fact	Mobile porosity end member	Deep fine	4.00E–02	1.00E–03	1.50E–01	4.00E–02	—
mpfmid	fact	Mobile porosity end member	Middle fine	2.00E–01	1.00E–03	1.50E–01	1.00E–01	—
mtnrchmult	rch	Small catchment recharge multiplier	Small catchment recharge multiplier	1.00E–05	1.00E–05	7.50E–01	1.07E–01	—
n_more	faultk	Fault conductance	North More Ranch fault	1.12E–05	1.00E–07	1.00E+00	4.71E–04	/day
ne_more	faultk	Fault conductance	Northeast More Ranch fault north of Calle Real Rd.	7.59E–04	1.00E–07	1.00E+00	2.24E–04	/day
ne_mores	faultk	Fault conductance	Northeast More Ranch fault south of Calle Real Rd.	2.16E–04	1.00E–07	1.00E+00	1.16E–04	/day
norrb_s	rivers	Creek stage adjustment parameter	Northridge Creek	4.87E–01	3.28E–06	4.92E+00	2.26E–02	ft
oceancond1	otherk	General head boundary conductance	Ocean GHB conductance upper confining layer across offshore fault	2.34E–04	1.08E–05	1.08E+04	2.41E+03	ft^2/day
oceancond2	otherk	General head boundary conductance	Ocean GHB conductance upper producing zone across offshore fault	1.14E–02	1.08E–05	1.08E+04	2.17E+03	ft^2/day
oceancond3	otherk	General head boundary conductance	Ocean GHB conductance middle confining layer below middle producing zone across offshore fault	1.63E–01	1.08E–05	1.08E+04	9.95E–01	ft^2/day

Table 3. Calibrated groundwater flow and solute transport model parameter values, Santa Barbara flow and transport model, Santa Barbara, California.—Continued

[/day, per day; ft, foot; ft², square foot; GHB, general-head boundary package; HK, horizontal hydraulic conductivity; Rd., road; St., street; VK, vertical hydraulic conductivity; —, not applicable]

Parameter name	Group	Subgroup	Description	Calibrated value	Lower bound	Upper bound	Preliminary value	Units
oceancond4	otherk	General head boundary conductance	Ocean GHB conductance lower producing zone across offshore fault	1.94E+00	1.08E–02	1.08E+04	8.00E–01	ft²/day
oceancond5	otherk	General head boundary conductance	Ocean GHB conductance lower confining layer across offshore fault	3.94E–05	1.08E–05	1.08E+04	4.41E–05	ft²/day
oceancond6	otherk	General head boundary conductance	Ocean GHB conductance middle producing zone across offshore fault	3.23E+02	1.08E–03	1.08E+04	1.01E+00	ft²/day
oceancond7	otherk	General head boundary conductance	Ocean GHB conductance shallow zone across offshore fault	1.08E–01	1.08E–03	1.08E+04	5.47E+02	ft²/day
oceanconds	otherk	General head boundary conductance	Ocean GHB conductance offshore ocean to ground	1.55E+01	1.08E–03	1.08E+04	1.62E+01	ft²/day
pcrivfac	aquiferk	HK/VK multiplier	Multiplier for HK/VK at upper Mission Creek river bed	3.65E+01	1.00E–01	1.00E+02	4.94E+01	—
pow	fact	VK power function for end members	Power function exponent	–1.0	–1.0	–1.00E–02	—	—
rainrch1abs	rch	Areal recharge parameter	Rain recharge for infiltration zone 1	7.22E–05	3.28E–05	3.28E+00	7.61E–03	ft/day
rainrch2add	rch	Areal recharge parameter	Additional rain recharge for infiltration zone 2	3.28E–03	3.28E–03	3.28E+00	1.93E–02	ft/day
rainrch3add	rch	Areal recharge parameter	Additional rain recharge for infiltration zone 3	3.30E–03	3.28E–03	3.28E+00	7.89E–03	ft/day
rainrch4add	rch	Areal recharge parameter	Additional rain recharge for infiltration zone 4	1.03E–02	3.28E–03	3.28E+00	1.08E+00	ft/day
sanroque_t	streamk	Creek conductance adjustment parameter	San Roque Creek	1.01E–03	1.08E–04	1.08E+04	4.30E+01	ft²/day
sanrql_s	rivers	Creek stage adjustment parameter	San Roque Creek	2.04E–01	3.28E–06	4.92E+00	5.39E–02	ft
scynrchmlt	rch	Small catchment recharge multiplier	Small catchment recharge Sycamore Canyon area	1.41E+00	1.00E–05	2.00E+01	5.42E+00	—
septicrchabs	rch	Septic recharge parameter	Septic recharge	7.58E–04	3.28E–10	8.20E–03	3.28E–03	ft/day
sscstcs	ss	Specific storage end member	Specific storage coarse end member coastal area	1.05E–05	10.00E–07	10.00E–04	1.21E–05	/ft
sscstfn	ss	Specific storage end member	Specific storage fine end member coastal area	2.40E–04	10.00E–07	10.00E–02	3.46E–04	/ft
sszon10cs	ss	Specific storage end member	Specific storage coarse end member subregion 10	1.91E–06	10.00E–07	10.00E–04	10.00E–07	/ft
sszon10fn	ss	Specific storage end member	Specific storage fine end member subregion 10	3.79E–05	10.00E–07	10.00E–02	3.95E–05	/ft
sszon1acs	ss	Specific storage end member	Specific storage coarse end member subregions 1, 8, and 11	7.38E–07	10.00E–07	10.00E–04	1.96E–06	/ft
sszon1afn	ss	Specific storage end member	Specific storage fine end member subregions 1, 8, and 11	7.76E–06	10.00E–07	10.00E–02	4.69E–06	/ft
sszon1bcs	ss	Specific storage end member	Specific storage coarse end member subregion 6	2.51E–06	10.00E–07	10.00E–04	1.30E–06	/ft
sszon1bfn	ss	Specific storage end member	Specific storage fine end member subregion 6	2.91E–05	10.00E–07	10.00E–02	1.49E–05	/ft
sszon1ccs	ss	Specific storage end member	Specific storage coarse end member subregion 7	3.05E–07	3.05E–07	10.00E–04	3.05E–07	/ft
sszon1cfn	ss	Specific storage end member	Specific storage fine end member subregion 7	10.00E–07	10.00E–07	10.00E–02	1.02E–06	/ft

Table 3. Calibrated groundwater flow and solute transport model parameter values, Santa Barbara flow and transport model, Santa Barbara, California.—Continued

[/day, per day; ft, foot; ft^2, square foot; GHB, general-head boundary package; HK, horizontal hydraulic conductivity; Rd., road; St., street; VK, vertical hydraulic conductivity; —, not applicable]

Parameter name	Group	Subgroup	Description	Calibrated value	Lower bound	Upper bound	Preliminary value	Units
sszon2cs	ss	Specific storage end member	Specific storage coarse end member subregions 2 and 9	4.19E–07	3.05E–07	10.00E–04	2.00E–05	/ft
sszon2fn	ss	Specific storage end member	Specific storage fine end member subregions 2 and 9	2.57E–05	10.00E–07	10.00E–02	5.91E–04	/ft
sszon3cs	ss	Specific storage end member	Specific storage coarse end member subregions 3 and 13	3.90E–07	3.90E–07	10.00E–04	4.23E–07	/ft
sszon3fn	ss	Specific storage end member	Specific storage fine end member subregions 3 and 13	1.01E–04	10.00E–07	10.00E–02	1.05E–04	/ft
sszon4cs	ss	Specific storage end member	Specific storage coarse end member subregions 4 and 14	2.35E–05	10.00E–07	10.00E–04	1.36E–06	/ft
sszon4fn	ss	Specific storage end member	Specific storage fine end member subregions 4 and 14	1.29E–04	10.00E–07	10.00E–02	3.19E–05	/ft
sszon5cs	ss	Specific storage end member	Specific storage coarse end member subregion 5	10.00E–07	10.00E–07	10.00E–04	10.00E–07	/ft
sszon5fn	ss	Specific storage end member	Specific storage fine end member subregion 5	2.52E–05	10.00E–07	10.00E–02	2.49E–05	/ft
sszonpmpcs	ss	Specific storage end member	Specific storage coarse end member subregion 12	1.60E–06	3.90E–07	10.00E–04	9.87E–06	/ft
sszonpmpfn	ss	Specific storage end member	Specific storage fine end member subregion 12	1.69E–05	10.00E–07	10.00E–04	4.67E–05	/ft
strcondinit	streamk	Creek conductance adjustment parameter	Base Creek conductance for all creeks	8.19E+00	1.08E–01	1.08E+02	2.15E–01	ft^2/day
sufrlhk	aquiferk	HK/VK regional multiplier	Storage Unit Four lower HK	1	0.001	100	1	—
sufrlvk	aquiferk	HK/VK regional multiplier	Storage Unit Four lower VK	0.001	0.001	100	0.001	—
sufrrchmlt	rch	Small catchment recharge multiplier	Small catchment recharge multiplier West Foothill Subbasin	3.03E–01	1.00E–05	2.50E+00	2.03E–01	—
suoneadt	aquiferk	HK/VK regional/layer multiplier	Subregion 1 lower confining layer	1.00E+03	1.00E–03	1.00E+05	1.00E+03	—
suoneahkm	aquiferk	HK/VK regional multiplier	Subregion 1 HK	3.41E+00	1.00E–03	1.00E+01	8.00E–01	—
suonealp	aquiferk	HK/VK regional/layer multiplier	Subregion 1 lower producing zone	2.00E+00	1.00E–03	1.00E+01	2.00E+00	—
suoneamp	aquiferk	HK/VK regional/layer multiplier	Subregion 1 middle producing zone	1.00E+00	1.00E–03	1.00E+01	1.00E+00	—
suoneaup	aquiferk	HK/VK regional/layer multiplier	Subregion 1 upper producing zone	1.00E+00	1.00E–03	1.00E+01	1.00E+00	—
suoneauth	aquiferk	HK/VK regional/layer multiplier	Subregion 1 upper confining layer HK	1.00E–02	1.00E–03	1.00E+02	1.00E–02	—
suoneautv	aquiferk	HK/VK regional/layer multiplier	Subregion 1 upper confining layer VK	1.00E+00	1.00E–03	1.00E+02	5.00E+01	—
suoneavkm	aquiferk	HK/VK regional multiplier	Subregion 1 VK	9.91E–01	1.00E–03	1.00E+01	9.99E–01	—
suonebdt	aquiferk	HK/VK regional/layer multiplier	Subregion 6 lower confining layer	1.00E+03	1.00E–03	1.00E+05	1.00E+03	—
suonebhkm	aquiferk	HK/VK regional multiplier	Subregion 6 HK	9.52E–01	1.00E–03	1.00E+01	1.38E+00	—
suoneblp	aquiferk	HK/VK regional/layer multiplier	Subregion 6 lower producing zone	8.00E–01	1.00E–03	1.00E+01	1.00E+00	—
suonebmp	aquiferk	HK/VK regional/layer multiplier	Subregion 6 middle producing zone	1.00E+00	1.00E–03	1.00E+01	1.00E+00	—

Table 3. Calibrated groundwater flow and solute transport model parameter values, Santa Barbara flow and transport model, Santa Barbara, California.—Continued

[/day, per day; ft, foot; ft^2, square foot; GHB, general-head boundary package; HK, horizontal hydraulic conductivity; Rd., road; St., street; VK, vertical hydraulic conductivity; —, not applicable]

Parameter name	Group	Subgroup	Description	Calibrated value	Lower bound	Upper bound	Preliminary value	Units
suonebup	aquiferk	HK/VK regional/layer multiplier	Subregion 6 upper producing zone	3.00E–01	1.00E–03	1.00E+01	3.00E–01	—
suonebuth	aquiferk	HK/VK regional/layer multiplier	Subregion 6 upper confining layer HK	1.00E+00	1.00E–03	1.00E+02	1.00E+00	—
suonebutv	aquiferk	HK/VK regional/layer multiplier	Subregion 6 upper confining layer VK	1.00E+00	1.00E–03	1.00E+02	1.00E+00	—
suonebvkm	aquiferk	HK/VK regional multiplier	Subregion 6 VK	1.08E+00	1.00E–03	1.00E+01	1.11E+00	—
suonecdt	aquiferk	HK/VK regional/layer multiplier	Subregion 7 lower confining layer	1.00E+03	1.00E–03	1.00E+05	1.00E+03	—
suonechkm	aquiferk	HK/VK regional multiplier	Subregion 7 HK	1.29E+00	1.00E–03	1.00E+01	1.50E+00	—
suoneclp	aquiferk	HK/VK regional/layer multiplier	Subregion 7 lower producing zone	6.00E–02	1.00E–03	1.00E+01	1.00E–01	—
suonecmp	aquiferk	HK/VK regional/layer multiplier	Subregion 7 middle producing zone	1.20E–01	1.00E–03	1.00E+01	1.00E–01	—
suonecup	aquiferk	HK/VK regional/layer multiplier	Subregion 7 upper producing zone	1.60E+00	1.00E–03	1.00E+01	1.60E+00	—
suonecuth	aquiferk	HK/VK regional/layer multiplier	Subregion 7 upper confining layer HK	1.00E+00	1.00E–03	1.00E+02	1.00E+00	—
suonecutv	aquiferk	HK/VK regional/layer multiplier	Subregion 7 upper confining layer VK	1.00E+00	1.00E–03	1.00E+02	1.00E+00	—
suonecvkm	aquiferk	HK/VK regional multiplier	Subregion 7 VK	1.35E+00	1.00E–03	1.00E+01	1.27E+00	—
suonemchk	aquiferk	HK/VK regional multiplier	Subregion 8 HK	6.71E+00	1.00E–03	1.00E+02	4.68E+00	—
suonemcvk	aquiferk	HK/VK regional multiplier	Subregion 8 VK	6.07E+00	1.00E–03	1.00E+02	4.87E+00	—
suonemtlp	aquiferk	HK/VK regional/layer multiplier	Subregion 8 lower producing zone	1.00E+00	1.00E–03	1.00E+01	1.00E–01	—
suonenehk	aquiferk	HK/VK regional multiplier	Subregion 6 HK	1.11E+00	1.00E–03	1.00E+02	1.40E+00	—
suonenevk	aquiferk	HK/VK regional multiplier	Subregion 6 VK	9.16E+00	1.00E–03	1.00E+02	1.04E+01	—
suonenwhk	aquiferk	HK/VK regional multiplier	Subregion 10 HK	1.00E–01	1.00E–03	1.00E+02	1.00E–01	—
suonenwvk	aquiferk	HK/VK regional multiplier	Subregion 10 VK	1.00E–01	1.00E–03	1.00E+02	1.00E–01	—
suonepdt	aquiferk	HK/VK regional/layer multiplier	Subregion 12 lower confining layer	1.00E+03	1.00E–03	1.00E+05	1.00E+03	—
suoneplp	aquiferk	HK/VK regional/layer multiplier	Subregion 12 lower producing zone	1.40E+00	1.00E–03	1.00E+01	1.40E+00	—
suonepmp	aquiferk	HK/VK regional/layer multiplier	Subregion 12 middle producing zone	2.00E+00	1.00E–03	1.00E+01	1.40E+00	—
suonepumphk	aquiferk	HK/VK regional multiplier	Subregion 12 HK	8.99E+00	1.00E–03	1.00E+01	8.99E+00	—
suonepumpvk	aquiferk	HK/VK regional multiplier	Subregion 12 VK	1.08E+00	1.00E–03	1.00E+01	1.08E+00	—
suonepup	aquiferk	HK/VK regional/layer multiplier	Subregion 12 upper producing zone	1.00E+00	1.00E–03	1.00E+01	1.00E+00	—
suoneputh	aquiferk	HK/VK regional/layer multiplier	Subregion 12 upper confining layer HK	1.00E+00	1.00E–03	1.00E+02	1.00E+00	—
suoneputv	aquiferk	HK/VK regional/layer multiplier	Subregion 12 upper confining layer VK	1.00E+00	1.00E–03	1.00E+02	1.00E+00	—
suonerchmlt	rch	Small catchment recharge multiplier	Small catchment recharge multiplier Storage Unit I	9.03E–01	1.00E–05	2.50E+00	1.99E+00	—
suonezegt	rch	Layer pumping adjustment factor	Storage Unit I pumping adjustment factor middle confining layer below middle producing zone	1.00E–04	1.00E–04	1.00E+01	2.20E–04	—
suonezetn	rch	Layer pumping adjustment factor	Storage Unit I pumping adjustment factor confining layer immediately above lower producing zone	1.00E–04	1.00E–04	1.00E+01	1.00E–04	—

Table 3. Calibrated groundwater flow and solute transport model parameter values, Santa Barbara flow and transport model, Santa Barbara, California.—Continued

[/day, per day; ft, foot; ft^2, square foot; GHB, general-head boundary package; HK, horizontal hydraulic conductivity; Rd., road; St., street; VK, vertical hydraulic conductivity; —, not applicable]

Parameter name	Group	Subgroup	Description	Calibrated value	Lower bound	Upper bound	Preliminary value	Units
suonezfive	rch	Layer pumping adjustment factor	Storage Unit I pumping adjustment factor lower confining layer	1.00E–04	1.00E–04	1.00E+01	1.00E–04	—
suonezfour	rch	Layer pumping adjustment factor	Storage Unit I pumping adjustment factor lower producing zone	3.99E+00	1.00E–04	1.00E+01	4.09E+00	—
suonezhdrd	rch	Layer pumping adjustment factor	Storage Unit I pumping adjustment factor confining layer immediately above upper producing zone	1.00E–04	1.00E–04	1.00E+01	1.00E–04	—
suoneznine	rch	Layer pumping adjustment factor	Storage Unit I pumping adjustment factor soil horizon confining layer	1.00E–04	1.00E–04	1.00E+01	1.00E–04	—
suonezone	rch	Layer pumping adjustment factor	Storage Unit I pumping adjustment factor upper confining layer	1.00E–05	1.00E–05	1.00E+01	1.00E–05	—
suonezsix	rch	Layer pumping adjustment factor	Storage Unit I pumping adjustment factor middle producing zone	4.13E+00	1.00E–02	1.00E+01	1.10E+00	—
suonezsvn	rch	Layer pumping adjustment factor	Storage Unit I pumping adjustment factor confining layer immediately below middle producing zone	1.00E–04	1.00E–04	1.00E+01	1.00E–04	—
suonezthree	rch	Layer pumping adjustment factor	Storage Unit I pumping adjustment factor middle confining layer above middle producing zone	1.00E–01	1.00E–04	1.00E+01	1.00E–04	—
suoneztwo	rch	Layer pumping adjustment factor	Storage Unit I pumping adjustment factor upper producing zone	3.25E+00	1.00E–02	1.00E+01	2.10E+00	—
suthehk	aquiferk	HK/VK regional multiplier	Subregion 13 HK	1.00E–01	1.00E–03	1.00E+02	1.00E–01	—
suthevk	aquiferk	HK/VK regional multiplier	Subregion 13 VK	1.00E–01	1.00E–03	1.00E+02	1.00E–01	—
suttfzfive	rch	Layer pumping adjustment factor	Storage Unit III and Foothill Basin pumping adjustment factor lower confining layer	1.00E+00	1.00E–01	1.00E+01	4.38E–01	—
suttfzfour	rch	Layer pumping adjustment factor	Storage Unit III and Foothill Basin pumping adjustment factor lower producing zone	1.10E+01	1.00E–01	1.00E+01	2.01E+00	—
suttfzone	rch	Layer pumping adjustment factor	Storage Unit III and Foothill Basin pumping adjustment factor upper confining layer	6.04E–01	1.00E–01	1.00E+01	4.70E–01	—
suttfzthree	rch	Layer pumping adjustment factor	Storage Unit III and Foothill Basin pumping adjustment factor middle confining layer	1.00E+00	1.00E–01	1.00E+01	4.05E–01	—
suttfztwo	rch	Layer pumping adjustment factor	Storage Unit III and Foothill Basin pumping adjustment factor upper producing zone	3.02E+00	1.00E–01	1.00E+01	1.05E+00	—
sutwolp	aquiferk	HK/VK regional/layer multiplier	Subregion 2 lower producing zone	1.00E+00	1.00E–03	1.00E+01	1.00E+00	—
sutwomchk	aquiferk	HK/VK regional multiplier	Subregion 9 HK	2.08E+01	1.00E–03	1.00E+02	2.96E+01	—
sutwomcvk	aquiferk	HK/VK regional multiplier	Subregion 9 VK	2.13E+00	1.00E–03	1.00E+02	3.04E+00	—
sutwouth	aquiferk	HK/VK regional/layer multiplier	Subregion 2 upper confining layer HK	1.00E–03	1.00E–03	1.00E+02	1.00E–03	—
sutwoutv	aquiferk	HK/VK regional/layer multiplier	Subregion 2 lower confining layer VK	2.00E+00	1.00E–03	1.00E+02	2.00E+00	—

Table 3. Calibrated groundwater flow and solute transport model parameter values, Santa Barbara flow and transport model, Santa Barbara, California.—Continued

[/day, per day; ft, foot; ft², square foot; GHB, general-head boundary package; HK, horizontal hydraulic conductivity; Rd., road; St., street; VK, vertical hydraulic conductivity; —, not applicable]

Parameter name	Group	Subgroup	Description	Calibrated value	Lower bound	Upper bound	Preliminary value	Units
sycacl_s	rivers	Creek stage adjustment parameter	Sycamore Canyon Creek	4.61E–01	3.28E–06	3.28E+00	6.07E–02	ft
sycamore_t	streamk	Creek conductance adjustment parameter	Sycamore Canyon Creek	1.07E+00	1.00E–05	1.00E+03	8.97E–01	—
sycoast	ss	Specific yield simulated value	Specific yield coastal area	1.60E–01	5.00E–02	3.50E–01	1.95E–01	—
syzon10	ss	Specific yield simulated value	Specific yield subregion 10	1.79E–01	5.00E–02	3.50E–01	1.97E–01	—
syzon1a	ss	Specific yield simulated value	Specific yield subregions 1, 8, and 11	4.18E–02	1.00E–02	3.50E–01	1.02E–01	—
syzon1b	ss	Specific yield simulated value	Specific yield subregion 6 and 12	5.69E–02	5.00E–02	3.50E–01	1.64E–01	—
syzon1c	ss	Specific yield simulated value	Specific yield subregion 7	8.12E–02	5.00E–02	3.50E–01	5.63E–02	—
syzon2	ss	Specific yield simulated value	Specific yield subregions 2 and 9	1.07E–02	1.00E–02	3.50E–01	1.72E–02	—
syzon3	ss	Specific yield simulated value	Specific yield subregions 3 and 13	1.10E–01	1.00E–02	3.50E–01	1.18E–02	—
syzon4	ss	Specific yield simulated value	Specific yield subregions 4 and 14	2.71E–02	5.00E–03	3.50E–01	3.05E–02	—
syzon5	ss	Specific yield simulated value	Specific yield subregion 5	1.43E–01	5.00E–02	3.50E–01	1.46E–01	—
viacha_s	rivers	Creek stage adjustment parameter	Via Chaparral Creek	4.75E–01	3.28E–06	3.28E+00	3.86E–02	ft
vtransd	dispersion	Vertical transverse dispersivity	Vertical shallow	3.28E–04	1.64E–04	1.64E–01	2.98E–02	ft
vtransddp	dispersion	Vertical transverse dispersivity	Vertical deep	1.64E–01	1.64E–04	1.64E–01	3.28E–02	ft
zoneegtym	aquiferk	HK/VK layer multiplier	Storage Unit I coastal confining layer between middle and lower producing zone HK	4.83E–01	1.00E–01	1.00E+02	2.41E+00	—
zoneegtyvm	aquiferk	HK/VK layer multiplier	Storage Unit I coastal confining layer between middle and lower producing zone VK	5.00E–02	1.00E–05	1.00E+01	1.69E+00	—
zoneeightm	aquiferk	HK/VK layer multiplier	Storage Unit I non-coastal confining layer between middle and lower producing zone HK	5.05E–01	1.00E–05	1.00E+01	5.36E–01	—
zoneeightvm	aquiferk	HK/VK layer multiplier	Storage Unit I non-coastal confining layer between middle and lower producing zone VK	4.98E–01	1.00E–05	1.00E+00	4.90E–01	—
zoneetnm	aquiferk	HK/VK layer multiplier	Storage Unit I bottom of confining layer between middle and lower producing zone HK	7.82E–04	1.00E–06	1.00E+01	8.25E–05	—
zoneetnvm	aquiferk	HK/VK layer multiplier	Storage Unit I bottom of confining layer between middle and lower producing zone VK	7.82E–04	1.00E–06	1.00E+01	7.82E–04	—
zonefiveam	aquiferk	HK/VK layer multiplier	Foothill basin and Storage Unit III lower confining layer below lower producing zone HK	1.08E–01	1.00E–03	1.00E+01	4.21E–01	—
zonefivem	aquiferk	HK/VK layer multiplier	Storage Unit I lower confining layer below lower producing zone HK	1.00E–05	1.00E–05	1.00E+00	2.16E–01	—
zonefivevm	aquiferk	HK/VK layer multiplier	Storage Unit I lower confining layer below lower producing zone VK	1.00E–05	1.00E–05	1.00E+00	1.00E–05	—

Table 3. Calibrated groundwater flow and solute transport model parameter values, Santa Barbara flow and transport model, Santa Barbara, California.—Continued

[/day, per day; ft, foot; ft^2, square foot; GHB, general-head boundary package; HK, horizontal hydraulic conductivity; Rd., road; St., street; VK, vertical hydraulic conductivity; —, not applicable]

Parameter name	Group	Subgroup	Description	Calibrated value	Lower bound	Upper bound	Preliminary value	Units
zonefouram	aquiferk	HK/VK layer multiplier	Foothill basin and Storage Unit III lower producing zone HK	3.89E+00	1.00E+00	1.00E+01	2.72E+00	—
zonefourm	aquiferk	HK/VK layer multiplier	Storage Unit I non-coastal lower producing zone HK	1.00E+00	1.00E+00	1.00E+01	1.20E+00	—
zonefrsu2	aquiferk	HK/VK layer multiplier	Foothill basin lower producing zone HK	8.00E–02	1.00E–05	1.00E+01	1.20E+00	—
zonefrtym	aquiferk	HK/VK layer multiplier	Storage Unit I coastal lower producing zone HK	1.70E–01	1.00E+00	1.00E+02	1.62E+01	—
zonefrtyvm	aquiferk	HK/VK layer multiplier	Storage Unit I coastal lower producing zone VK	3.08E–02	1.00E–02	1.00E+02	1.02E+01	—
zoneninem	aquiferk	HK/VK layer multiplier	Storage Unit I non-coastal upper confining layer soil surface HK	7.50E–02	1.00E–05	1.00E+00	7.77E–03	—
zoneninevm	aquiferk	HK/VK layer multiplier	Storage Unit I non-coastal upper confining layer soil surface VK	7.50E–02	1.00E–05	1.00E+00	7.50E–02	—
zonenintym	aquiferk	HK/VK layer multiplier	Storage Unit I coastal upper confining layer soil surface HK	7.50E–02	1.00E–05	1.00E+00	7.50E–02	—
zonenintyvm	aquiferk	HK/VK layer multiplier	Storage Unit I coastal upper confining layer soil surface VK	7.50E–02	1.00E–05	1.00E+00	7.50E–02	—
zoneohdrm	aquiferk	HK/VK layer multiplier	Storage Unit I bottom of upper confining layer HK	6.53E–04	1.00E–04	1.00E+01	7.45E–04	—
zoneohdrom	aquiferk	HK/VK layer multiplier	Upper confining layer at Mission Creek HK	1.00E+01	1.00E–04	1.00E+01	1.00E+01	—
zoneoneam	aquiferk	HK/VK layer multiplier	Foothill Basin and Storage Unit III upper confining layer HK	2.71E+00	1.00E–03	5.00E+00	2.00E–01	—
zoneonem	aquiferk	HK/VK layer multiplier	Storage Unit I upper confining layer HK	7.41E–01	1.00E–03	1.00E+00	1.05E–01	—
zoneonevm	aquiferk	HK/VK layer multiplier	Storage Unit I upper confining layer VK	7.02E–01	1.00E–05	1.00E+00	1.31E–01	—
zoneothsm	aquiferk	HK/VK layer multiplier	Storage Unit I coastal bottom of upper confining layer HK	9.76E–04	1.00E–04	1.00E+01	1.07E–02	—
zonesevenm	aquiferk	HK/VK layer multiplier	Storage Unit I non-coastal confining layer directly below middle producing zone HK	5.34E–05	1.00E–06	1.00E+01	7.31E–03	—
zonesevenvm	aquiferk	HK/VK layer multiplier	Storage Unit I non-coastal confining layer directly below middle producing zone VK	5.34E–05	1.00E–06	1.00E+01	5.34E–05	—
zonesixm	aquiferk	HK/VK layer multiplier	Storage Unit I non-coastal middle producing zone HK	8.17E–01	1.00E–01	1.00E+01	1.26E+00	—
zonesixvm	aquiferk	HK/VK layer multiplier	Storage Unit I non-coastal middle producing zone VK	8.17E–01	1.00E–01	1.00E+01	8.17E–01	—
zonesvtym	aquiferk	HK/VK layer multiplier	Storage Unit I coastal confining layer directly below middle producing zone HK	1.09E–01	1.00E–06	1.00E+02	1.09E–02	—
zonesvtyvm	aquiferk	HK/VK layer multiplier	Storage Unit I coastal confining layer directly below middle producing zone VK	3.52E–04	1.00E–06	1.10E+01	3.52E–04	—

Table 3. Calibrated groundwater flow and solute transport model parameter values, Santa Barbara flow and transport model, Santa Barbara, California.—Continued

[/day, per day; ft, foot; ft^2, square foot; GHB, general-head boundary package; HK, horizontal hydraulic conductivity; Rd., road; St., street; VK, vertical hydraulic conductivity; —, not applicable]

Parameter name	Group	Subgroup	Description	Calibrated value	Lower bound	Upper bound	Preliminary value	Units
zonesxhdm	aquiferk	HK/VK layer multiplier	Storage Unit I coastal middle producing zone HK	1.00E+00	1.00E–02	1.00E+01	1.62E+00	—
zonesxhdvm	aquiferk	HK/VK layer multiplier	Storage Unit I coastal middle producing zone VK	1.00E–05	1.00E–06	1.00E+01	1.00E–04	—
zonesxtym	aquiferk	HK/VK layer multiplier	Storage Unit I western edge of middle producing zone HK	1.00E–02	1.00E–03	1.00E+01	1.00E–02	—
zonesxtyom	aquiferk	HK/VK layer multiplier	Storage Unit I eastern edge of middle producing zone HK	1.00E–05	1.00E–06	1.00E+01	1.00E–05	—
zonesxtyvm	aquiferk	HK/VK layer multiplier	Storage Unit I western edge of middle producing zone VK	1.00E–02	1.00E–03	1.00E+01	1.00E–02	—
zonetenm	aquiferk	HK/VK layer multiplier	Storage Unit I coastal upper zone above upper producing zone HK	4.74E+00	1.00E–01	1.00E+01	4.99E+00	—
zonetenvm	aquiferk	HK/VK layer multiplier	Storage Unit I coastal upper zone above upper producing zone VK	4.55E+00	1.00E–01	1.00E+01	4.31E+00	—
zonethd	aquiferk	HK/VK layer multiplier	Storage Unit I non-coastal confining layer directly above middle producing zone VK	1.00E–01	1.00E–05	1.00E+00	5.00E–03	—
zonethreeam	aquiferk	HK/VK layer multiplier	Foothill Basin and Storage Unit III middle confining layer HK	3.00E–01	1.00E–05	1.00E+00	7.49E–01	—
zonethreem	aquiferk	HK/VK layer multiplier	Storage Unit I non-coastal middle zone above middle producing zone HK	3.01E–01	1.00E–03	1.00E+00	1.10E–01	—
zonethreevm	aquiferk	HK/VK layer multiplier	Storage Unit I non-coastal middle zone above middle producing zone VK	3.01E–01	1.00E–03	1.00E+00	3.01E–01	—
zonethrsu2	aquiferk	HK/VK layer multiplier	Foothill Basin middle confining layer HK	6.33E–03	1.00E–05	1.00E+00	1.33E–02	—
zonethtym	aquiferk	HK/VK layer multiplier	Storage Unit I coastal middle zone above middle producing zone HK	5.74E–02	1.00E–06	1.00E+01	4.38E–01	—
zonethtyvm	aquiferk	HK/VK layer multiplier	Storage Unit I coastal middle zone above middle producing zone VK	2.74E–02	1.00E–06	1.00E+01	1.07E–06	—
zonetwoam	aquiferk	HK/VK layer multiplier	Foothill Basin and Storage Unit III upper producing zone HK	5.45E+00	1.00E+00	1.00E+01	2.76E+00	—
zonetwom	aquiferk	HK/VK layer multiplier	Storage Unit I non-coastal upper producing zone HK	1.30E+00	8.50E–01	1.00E+01	1.37E+00	—
zonetwosu2	aquiferk	HK/VK layer multiplier	Foothill Basin upper producing zone HK	5.00E+00	1.00E–05	1.00E+01	1.37E+00	—

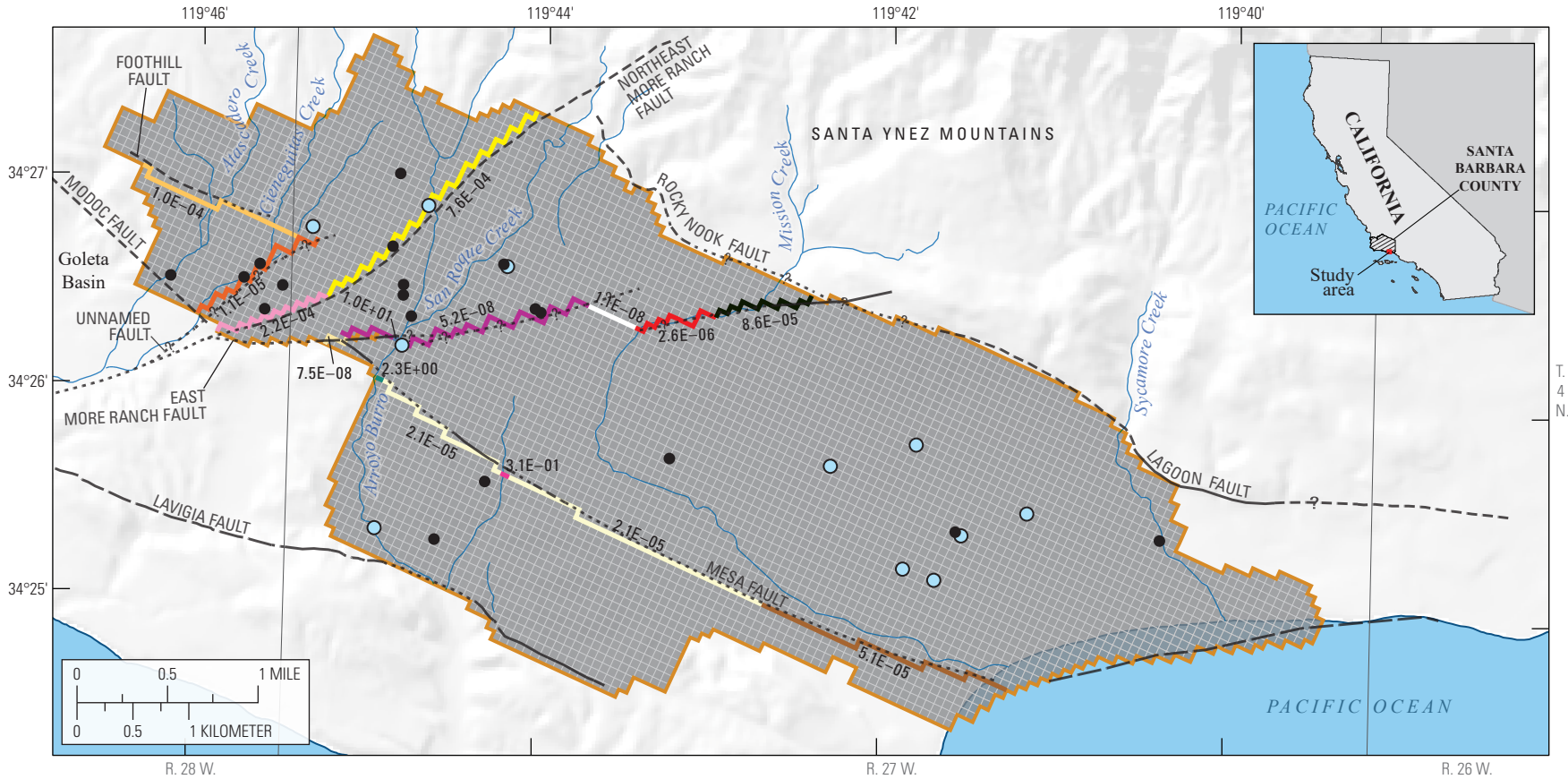

Base modified from U.S. Geological Survey and other Federal and State digital data, various scales; Transverse Mercator projection, zone 11N; North American Datum of 1983 (NAD 83)

Storage units from Muir, 1968; Freckleton and others, 1998; faults from Muir, 1968; Minor and others, 2009

Figure 8. Calibrated horizontal-flow-barrier hydraulic-characteristic values (per day), Santa Barbara flow and transport model, Santa Barbara, California.

Storage Properties

Specific storage (SS) was estimated for each subregion and area using the textural model. The percentage of coarse- and fine-grained material in each groundwater-model cell from the HFM (see chapter B) was used to define specific-storage values. Specific storage was calculated using weighted averaging, as shown in equation 7:

$$SS_{texture} = PC \times SS_{cx} + PF \times SS_{fx} \quad (7)$$

where

PC and PF are the percentage of coarse and fine sediment in a given model percentage, expressed as a fraction, of course and fine sediment, respectively, in a given model cell, and

SS_{cx} and SS_{fx} are the coarse and fine specific-storage end members, respectively, by subregion.

To simulate unconfined conditions, the specific-storage values of the uppermost layer of the SBFTM were estimated separately. The specific-storage values for each cell in the topmost layer were defined by specific yield (SY) divided by the thickness of the model cell and were not based on the HFM. A separate specific-yield value was estimated for each subregion (see parameter group "ss" in table 3).

Solute-Transport Properties

Each source of recharge in the SBFTM was assigned a chloride concentration to represent the salinity. Precipitation, small-catchment recharge, stream recharge, septic recharge, and flow across the Montecito GHB were considered freshwater recharge and were assigned a chloride concentration of 100 milligrams per liter (mg/L), which is typical of fresh water (Goldman and Horne, 1983). Recharge across the ocean GHB was considered to be seawater and assigned a chloride concentration representative of seawater: 19,000 mg/L (Langevin and others, 2008).

Three additional aquifer properties are needed to simulate solute transport: porosity, dispersivity, and diffusion. Porosity values (P) for each model cell were approximated using the percentage of coarse and fine sediments in that model cell. Different textural end-member porosity values (P_{cx} and P_{fx}) were used for the lower producing zone, the middle producing zone, and the rest of the SBFTM. Similar to storage values, porosity was calculated using weighted averages (equation 7).

The three components of dispersivity (longitudinal, horizontal transverse, and vertical transverse) were defined for two dispersivity zones: an upper dispersivity zone consisting of model layers 1–27 and a lower dispersivity zone consisting of model layers 28–56. The upper dispersivity zone includes the upper and middle producing zones, which, on the basis of numerical testing, had different transport properties than the lower producing zone. The lower dispersivity zone included the deeper part of the middle zone and the lower producing zone. The dispersivity values were estimated separately by trial-and-error for the upper and lower dispersivity zones. The final, calibrated dispersivity values are presented in table 3. Diffusion (representing molecular effects) was defined as a constant value, 9.30E-04 ft^2/d, typical of alluvial sediments throughout the SBFTM area (Freeze and Cherry, 1979).

Model Calibration Approach

The SBFTM was calibrated in two parts: predevelopment and transient. Model calibration of the predevelopment and transient models was done in sequence and simultaneously using measured data described in the next section. As mentioned previously, to simulate predevelopment conditions (no stresses), groundwater flow and solute transport were simulated for 10,000 years to allow the flow and concentration fields to equilibrate to specified initial and boundary conditions in 10-year time steps. Calibration of the predevelopment conditions was accomplished by varying small-catchment recharge, creek-bed conductance and stage, areal recharge, drain conductance, general-head boundary conductance, hydraulic conductivity, flow-barrier conductance, porosity, dispersivity, and diffusion. As mentioned earlier, the transient simulation represents the period from 1929 to 2013; however, the focus of the transient calibration was the period from 1972 to 2013. In addition to the predevelopment parameters listed above, specific storage, specific yield, the vertical distribution of pumpage, and septic recharge were also varied.

Calibration of the SBFTM was accomplished using a combination of automated and trial-and-error methods. Initially, PEST (Doherty, 2010) was used for automated calibration of the flow and transport parameters. In addition, PEST was used to assess the sensitivities of parameters used in the parameter-estimation process. During the preliminary calibration process, it was found that PEST did not estimate the transport parameters well; this could be related to the highly nonlinear nature of the density-dependent groundwater flow and transport problem. Therefore, automated calibration was primarily used to calibrate the groundwater-flow component of the SBFTM and trial-and-error calibration was used to calibrate the solute-transport component of the SBFTM. Bounds on model parameters were set to keep parameters within a realistic range of values.

Hydraulic properties were checked for unrealistic values during calibration. Groundwater budgets were regularly examined during the calibration process, and budget components were compared with previously published results (for example, Freckleton and others, 1998).

Measured Data

Five types of observation data were used during model calibration: water levels, changes in water levels (drawdowns), chloride concentrations, changes in chloride concentrations (figs. 8, 9), and published infiltration rates along segments of Mission Creek. The SBFTM was calibrated to 24,884 water-level observations from 75 wells and to 1,064 chloride-concentration observations from 52 wells. Water-level observations were used to compute changes in water levels for each stress period for each well. Similarly, chloride-concentration observations were used to calculate the changes in chloride concentrations. Water-level observations, computed water-level changes, chloride-concentration observations, and computed chloride-concentration changes were compared with simulated results. Infiltration rates along segments of Mission Creek estimated by McFadden and others (1987) also were used in the calibration process (fig. 9).

Selection of Well Data

Water-level and chloride data were reviewed for consistency and accuracy before use as model-observation data. Data points that were inconsistent with other data points or trends and appeared to be in error were removed, as were data collected from wells at or very near a production well and recorded while the production well was active. In addition, water-level data from wells perforated in the shallow zone (a perched aquifer) were not included because the SBFTM was not designed to simulate a perched aquifer. Likewise, chloride data were reviewed with water-level data to determine if and when well casings had corroded to the point of failure. Chloride and water-level data that were thought to be influenced by failed well casings were excluded; for example, water levels from wells 4N/27W-09Q1 and 4N/27W-09M1 (fig. 9) were not used.

Water-Level Data

For model calibration, water-level data were needed that were representative of the main aquifer conditions and distributed spatially and temporally throughout the simulated subbasins—vertically through the upper, middle, and lower producing zones and temporally during the key transient calibration period (1972–2013). Water-level data were distributed at 75 geographic locations throughout Storage Unit I, Storage Unit III, and East and West Foothill subbasins (fig. 9). Multiple-completion wells recording groundwater levels at multiple depths were present at 22 of the 75 geographic well locations. Water-level data from these wells included the entire main simulation period from 1972 to 2013; however, water-level data prior to 1975 were available for only a few of these wells.

Chloride-Concentration Data

To calibrate the SBHTM for seawater intrusion, chloride-concentration data measured in Storage Unit I were used. Specifically, data were available from between the coast and the City Hall, Vera Cruz, Corporation Yard, De la Guerra, and Ortega Park production wells in the upper, middle, and lower producing zones (fig. 10). Chloride data from eight key well clusters recorded chloride concentrations at various depths. Four of the clusters (4N/27W-23F02–04, 4N/27W-23F05–08, 4N/27W-23E01–04, and 4N/27W-23E05–06) are near the coast; two of the clusters (4N/27W-22A02–05 and 4N/27W-22G02–04) are between the production wells and the coast, about 0.5 miles (mi) from the coast and 0.25 mi from the production wells. The last two clusters (4N/27W-22B02–05 and 4N/27W-22B08–11) are near the Vera Cruz production well (fig. 10).

The SBFTM was not designed to simulate the flow of chlorides from the underlying bedrock to the lower producing zone. As stated in chapter A, higher chloride concentrations in wells 4N/27W-22B04, 05, and 08 were likely due to pumping from the Vera Cruz production well drawing saline water from the underlying shale. The SBFTM was, therefore, not calibrated to these particular measured chloride concentrations.

Model Parameters

A total of 254 parameters were used in the SBFTM to define horizontal and vertical hydraulic conductivity; specific storage; specific yield; the pumping distribution of individual wells by layer; the conductance of horizontal-flow barriers, general-head boundaries, drains, and creeks; stream stage; drain elevation; areal and septic recharge infiltration rates; dispersivity; and porosity. In general, all 254 parameters were estimated; however, some were fixed during the course of calibration.

Table 3 contains the calibrated model-parameter values used in the SBFTM. Parameters in table 3 are grouped into eight types: hydraulic conductivity, storage, conductance, head or stage, pumpage distribution, recharge, porosity, and dispersivity.

Parameters affecting the hydraulic and transport properties and the vertical distribution of pumping were described earlier. In addition to these parameters, those affecting small-catchment recharge, areal recharge, and early pumpage were estimated.

As discussed in the "Simulated Groundwater Recharge" section, small-catchment recharge was divided into seven segments based on topography (fig. 2) and was estimated by scaling parameters for each small-catchment segment along the northern model border with the Santa Ynez Mountains (table 3). Recharge was determined by parameter estimation, and the initial recharge amounts were based on Freckleton and others (1998). The initial recharge amounts were modified using a segment multiplier, which was determined by parameter estimation.

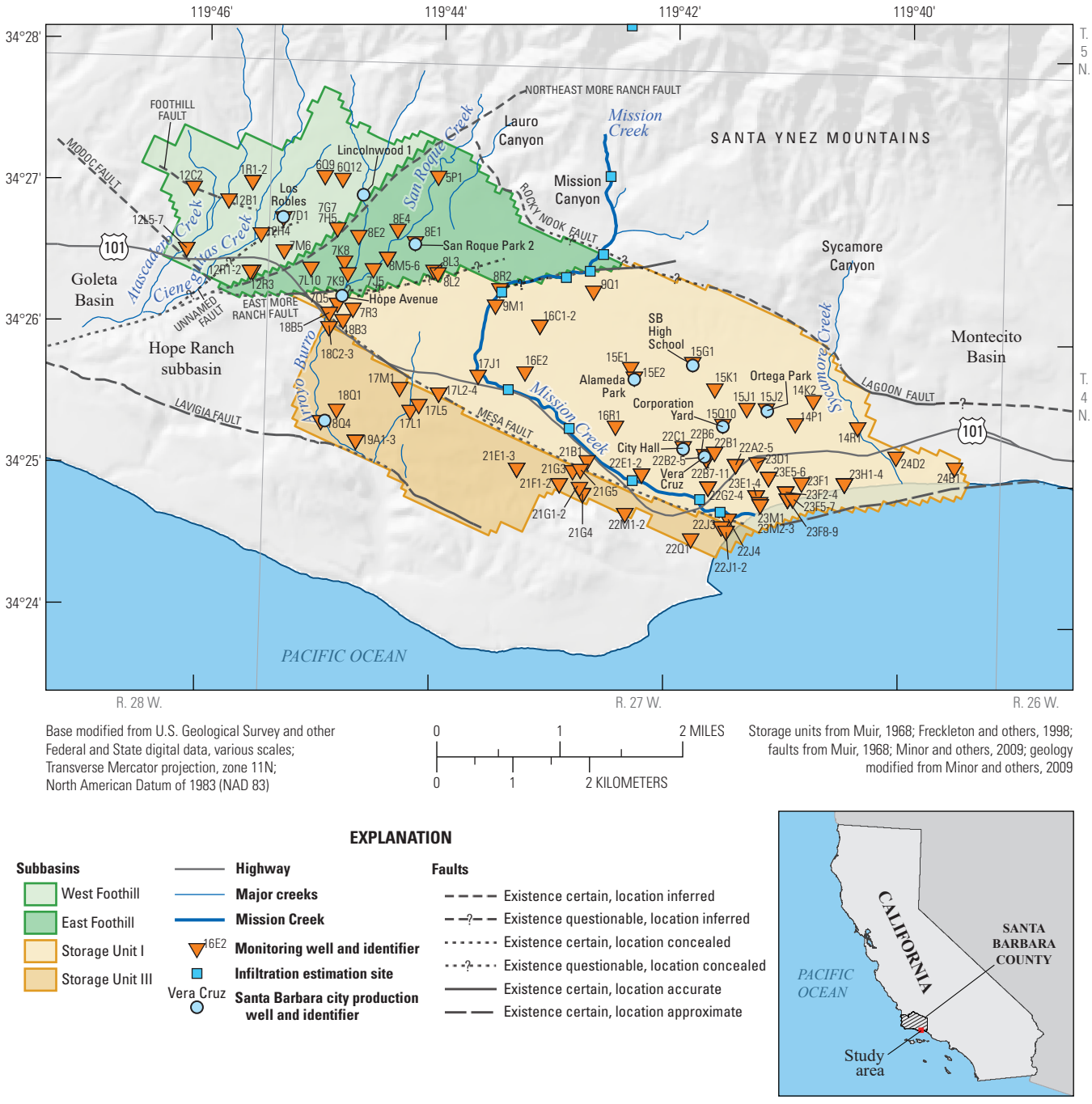

Figure 9. Monitoring wells with available water-level data and Mission Creek segments where infiltration rates were estimated by McFadden and others (1987), Santa Barbara and Foothill groundwater basins, Santa Barbara, California.

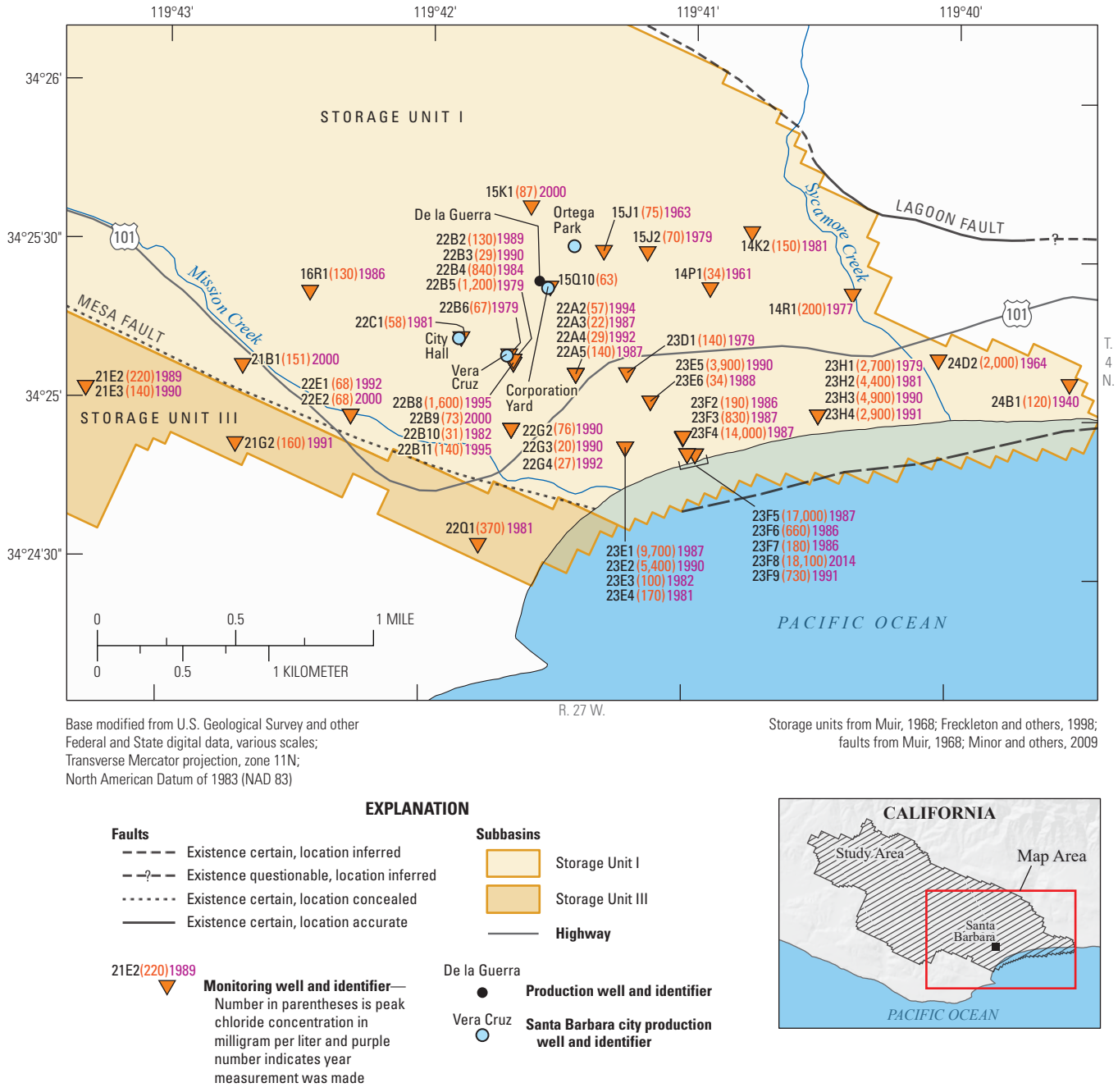

Base modified from U.S. Geological Survey and other Federal and State digital data, various scales; Transverse Mercator projection, zone 11N; North American Datum of 1983 (NAD 83)

Storage units from Muir, 1968; Freckleton and others, 1998; faults from Muir, 1968; Minor and others, 2009

EXPLANATION

Faults
- Existence certain, location inferred
- Existence questionable, location inferred
- Existence certain, location concealed
- Existence certain, location accurate

Subbasins
- Storage Unit I
- Storage Unit III
- **Highway**

21E2(220)1989 — **Monitoring well and identifier**— Number in parentheses is peak chloride concentration in milligram per liter and purple number indicates year measurement was made

De la Guerra — **Production well and identifier**

Vera Cruz — **Santa Barbara city production well and identifier**

Figure 10. Monitoring wells with chloride concentration data near the coast of the city of Santa Barbara, California.

Areal recharge infiltration rates for four infiltration zones were simulated using four parameters that control the infiltration percentage of precipitation in each zone. The range for the calibrated areal recharge parameters was 7.22E-05–1.69E-02 ft/d (table 3). Note that in table 3, the recharge flux rates for infiltration zones 2–4 are cumulative. For example, the recharge flux rate for infiltration zone 4 equals rainrch1abs +rainrch2add+rainrch3add+rainrch4add.

Septic recharge was simulated using a single multiplier as a parameter. The calibrated septic recharge parameter was 7.58E-04 ft/d (table 3), which equals a total flow rate of about 71 acre-ft/yr. This flow rate is greater than the previously calculated septic recharge of 65 acre-ft/yr; however, this value did not include the unknown recharge from the rest home, restaurant, or retail store. Therefore, 71 acre-ft/yr was considered to be a reasonable estimate.

Before 1971, the pumpage data were incomplete. Total model-area pumpage was often known, but the amount of pumpage from each production well could not always be deduced. One of these cases was from 1964 to 1971, when only the McKenzie #1 and De La Guerra production wells were in operation. A single parameter was used to distribute pumpage between the McKenzie #1 and De La Guerra wells during these years. The parameter was constrained such that the total pumpage between these two wells equaled the known total pumpage.

Sensitivity Analysis

PEST calculates an objective function value based on the sum of squared differences between measured and simulated results (Doherty, 2010). The sensitivity process in PEST calculates the change of the objective function as each parameter is varied. The sensitivity of the simulated results to a parameter is determined by the amount the objective function changes when that parameter is varied incrementally; the more the objective function changes, the more sensitive the objective function is to that parameter. Composite scaled sensitivity (CSS) values were used to show relative sensitivity; the definition and derivation are described in Doherty (2010). Note that the solute-transport parameters resulting from trial-and-error calibration were included in the sensitivity analysis.

The sensitivity analysis indicated that, in general, the SBFTM is sensitive to recharge-related parameters (fig. 11*A*). Specifically, the SBFTM is most sensitive to parameters controlling the amount of small-catchment recharge (parameter mtnrchmult) and areal recharge (parameter rainrch1abs; fig. 11*A*). The SBFTM is also sensitive to parameters controlling stream-recharge rates and pumping distribution.

The CSS values for simulated hydraulic head and drawdowns are presented in figures 11*B* and *C*, respectively. The hydraulic heads and drawdowns were sensitive to the same parameters (for example, small catchment, areal, and creeks); however, the drawdown CSS values were less than the hydraulic head CSS values. Because drawdown is a quantity expressing change (difference in initial and final head) and hydraulic head is an absolute quantity, it is not surprising that drawdown was less sensitive to the parameterization of the model.

The CSS values for simulated chloride concentrations and changes in simulated chloride concentrations are presented in figures 11*D* and *E*, respectively. The chloride concentrations and changes in concentrations were sensitive to the same parameters (for example, recharge-related and pumpage-distribution parameters), and the three most sensitive parameters for each had very similar CSS values. For the less sensitive parameters, however, the CSS values for the chloride concentrations were greater than those for the change in chloride concentrations, for the same reason as was explained in the previous paragraph for hydraulic head and drawdown.

Of the solute-transport parameters, simulated chloride concentrations and changes in chloride concentrations were most sensitive to porosity (figs. 11*D, E*). Specifically, the simulated values were more sensitive to the porosity of coarse-grained sediments (parameters mpclower and mpc in figs. 11*D, E*) than to that of fine sediment (parameter mpf) because pumping in the coarse-grained layers draws seawater landward. Dispersivity parameters were generally less sensitive than the porosity parameters; deep longitudinal dispersivity (parameter dispdp) was the most sensitive dispersivity parameter, with a CSS value of 1.39 (fig. 11*D*).

Figure 11*F* presents the CSS values for the simulated values overall and for four of the simulated variables or their derivatives: hydraulic head, change in hydraulic head, chloride concentration, and change in chloride concentration; sensitivity scores were grouped by parameter type (horizontal axis). It is misleading to compare the CSS values within a parameter group because the CSS values are functions of the simulated values. Simulated chloride concentrations were as high as 19,000 mg/L, whereas simulated hydraulic head values might be in the hundreds; therefore, the CSS values for chloride were greater than those for hydraulic head. For comparative purposes, the CSS values in a parameter group were divided by the greatest value in order to normalize the CSS values (fig. 12). The most sensitive parameter groups were fault conductance, creek stage, creek conductance, and specific storage related (fig. 12). The least sensitive parameter groups were transport related (dispersion and porosity; fig. 12).

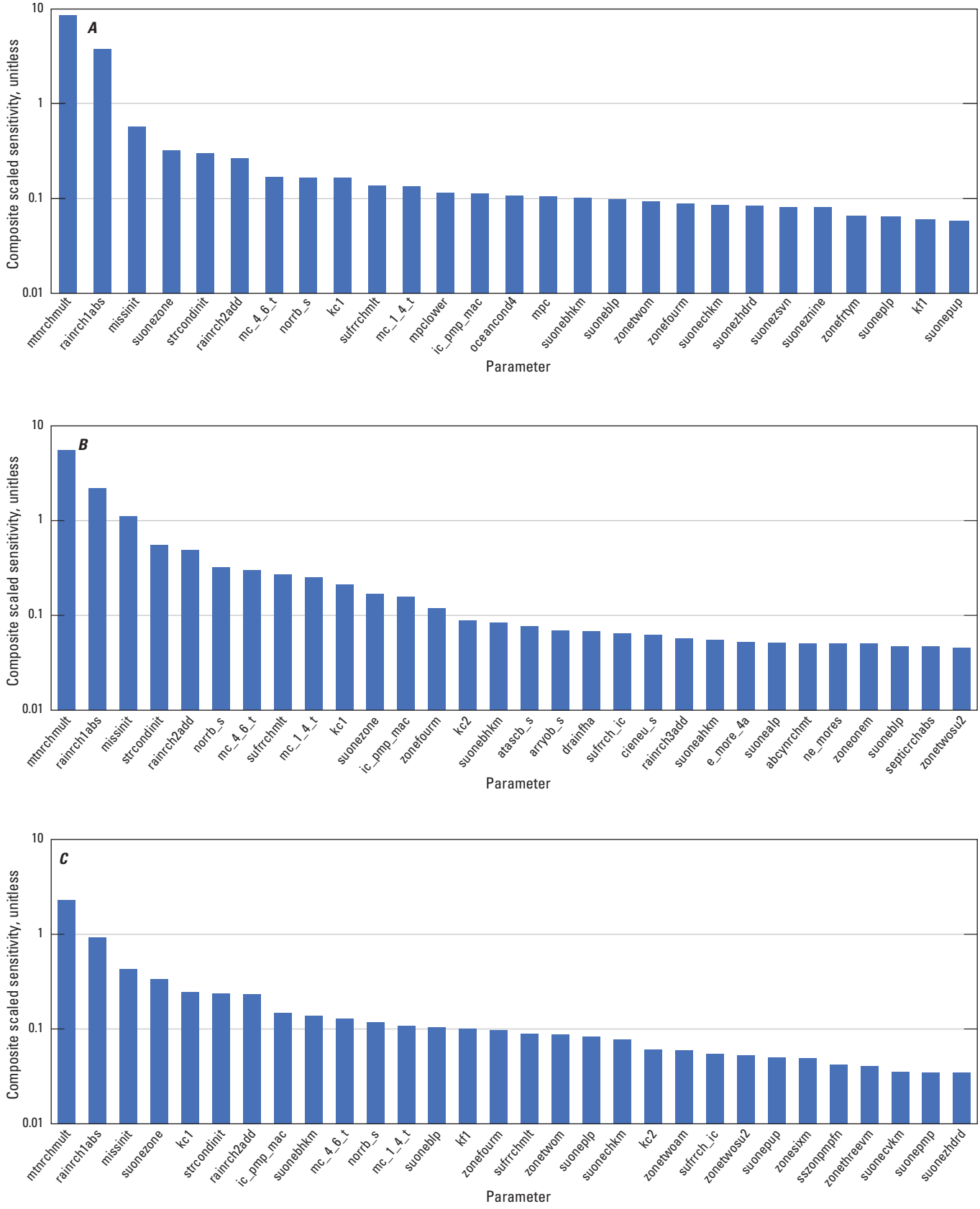

Figure 11. Composite scaled sensitivity values for the Santa Barbara flow and transport model, Santa Barbara, California: *A*, all simulated values; *B*, hydraulic head; *C*, drawdown; *D*, chloride concentration; *E*, change in chloride concentration; and *F*, grouped by parameter type.

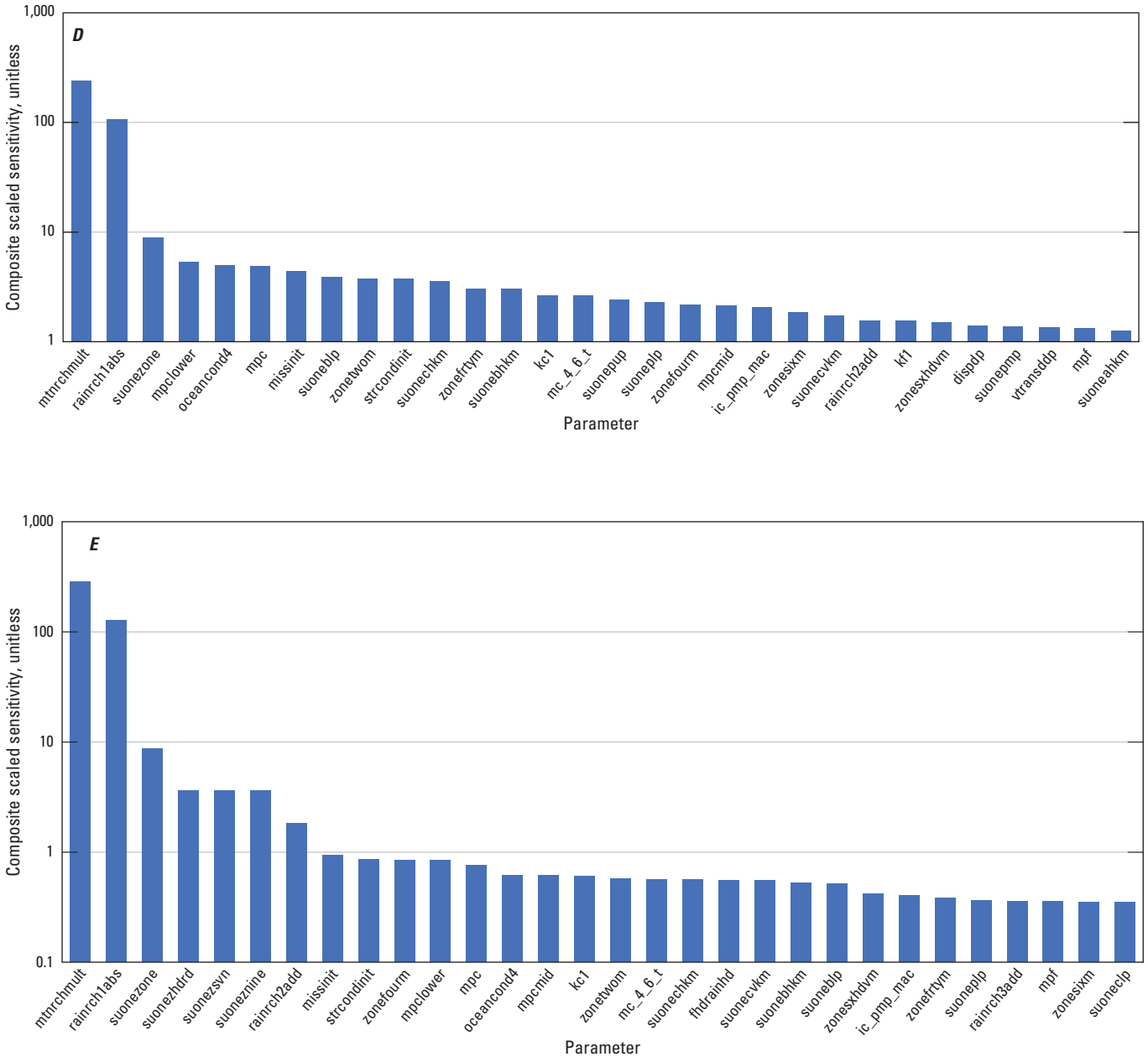

Figure 11. —Continued

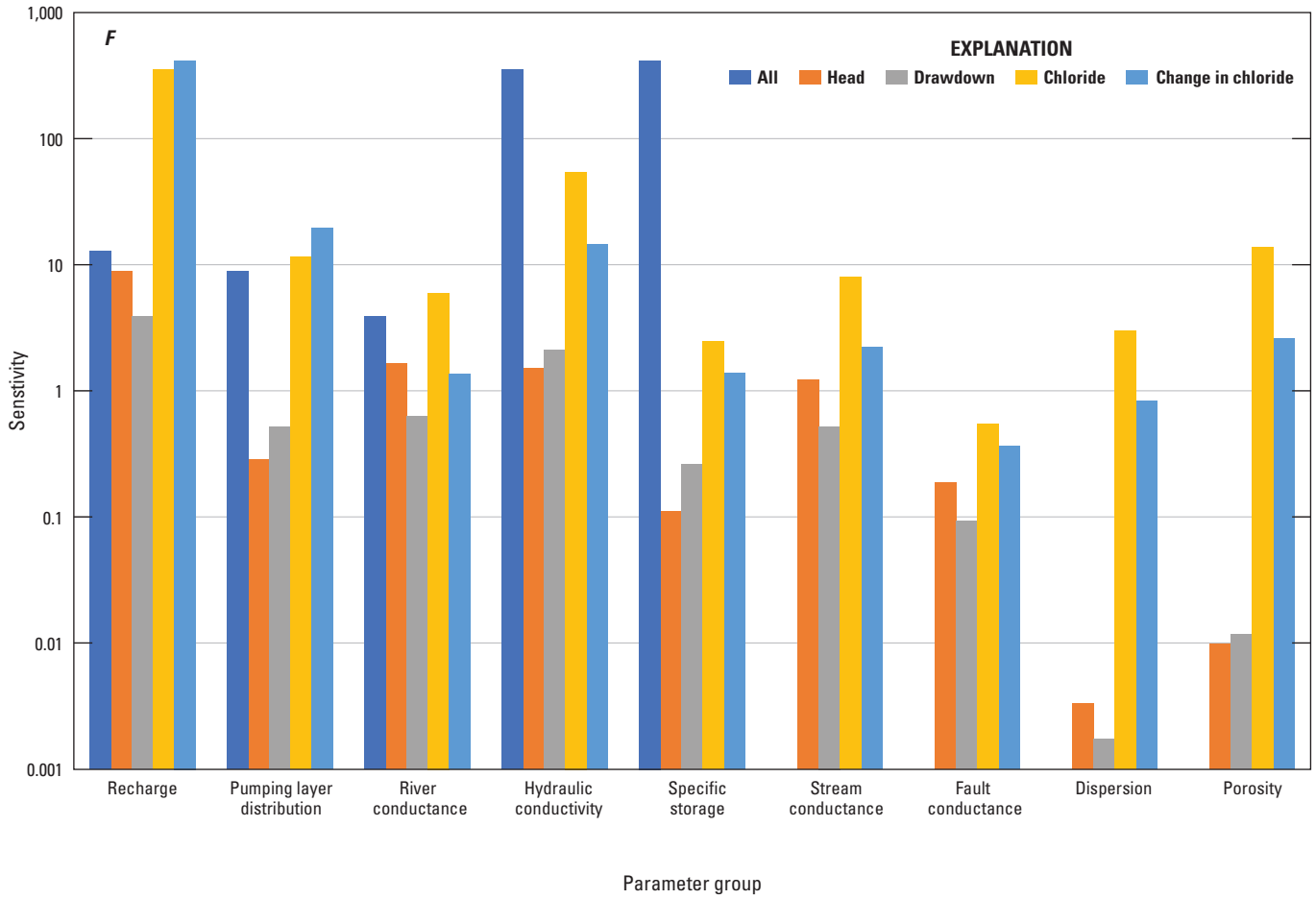

Figure 11. —Continued

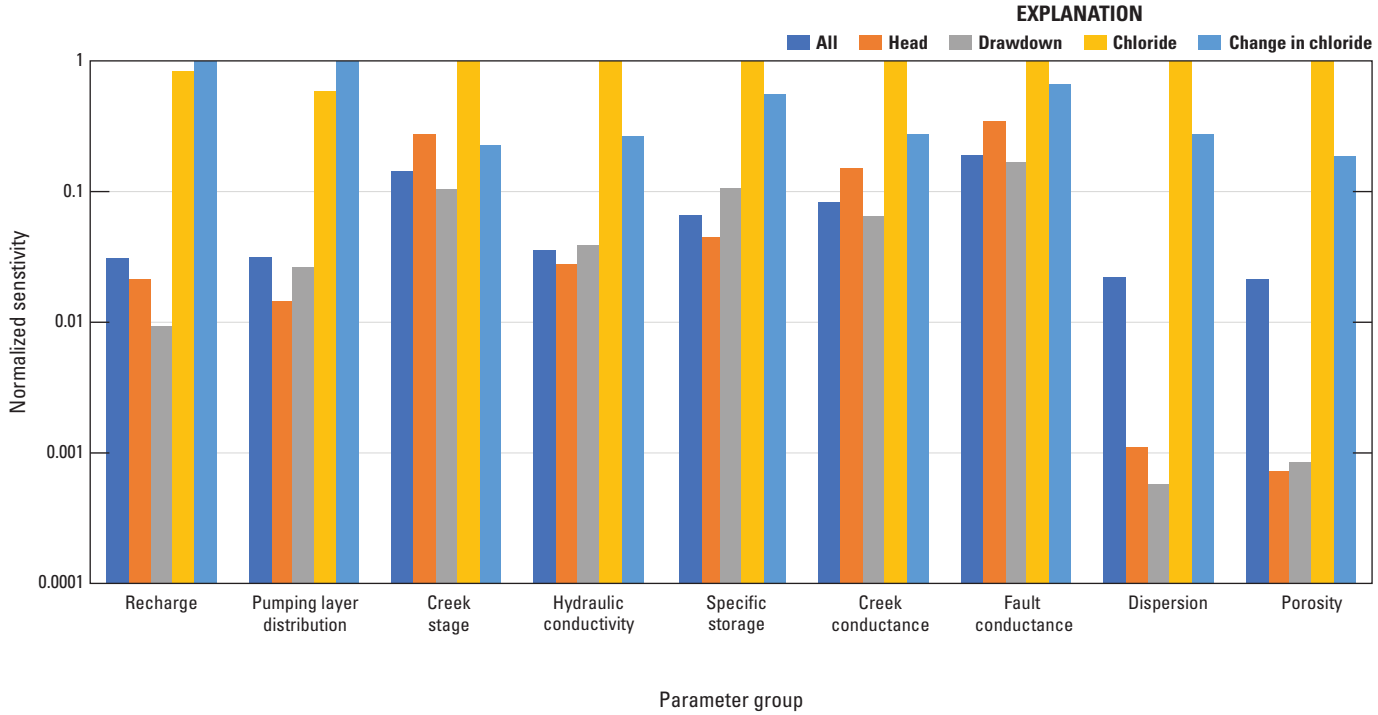

Figure 12. Normalized composite scaled sensitivity values, grouped by parameter types for all simulated values, hydraulic head, drawdown, chloride concentration, and change in chloride concentration, Santa Barbara flow and transport model, Santa Barbara, California.

Simulation Results

Hydraulic-conductivity and storage values were not estimated directly through parameter estimation. Values for these flow parameters were calculated using the extent of the parameter range and multipliers. A brief discussion regarding these parameters follows.

The majority of calibrated hydraulic conductivities ranged from about 10^{2} to about 10^{-5} ft/d (fig. 13). Horizontal hydraulic conductivities had a median value of 1.02 ft/d and were concentrated over a narrow range; more than 74 percent were between 0.5 and 50.0 ft/d. Vertical hydraulic conductivities had a median value of 0.02 ft/d and were also concentrated over a narrow range; more than 56 percent were between 0.005 and 0.5 ft/d. The median anisotropy ratio of vertical to horizontal hydraulic conductivity was 0.03.

Land subsidence has not been detected in the Santa Barbara area. If the estimated storage values indicate land subsidence, therefore, the estimated storage values are not reasonable (Devin L. Galloway, U.S. Geological Survey, written commun., 2015). The SBFTM results were used to estimate land-surface subsidence due to compaction on the basis of water-level drawdowns and specific-storage values. Subsidence was calculated to verify that the model calibrated specific-storage values were realistic for the Santa Barbara groundwater basin, where no land-surface subsidence has been detected. Compaction (Δb) was calculated using equation 8 (Devin L. Galloway, U.S. Geological Survey, written commun, 2015):

$$\Delta b = -S_{sk} \times b \times \Delta h \qquad (8)$$

where

S_{sk} is skeletal specific storage,
b is layer thickness, and
Δh is drawdown in head.

Equation 8 was used to estimate compaction in areas of the SBFTM where drawdowns due to pumping were large. Maximum estimated compaction was approximately 1 inch during the simulation period. Land-surface subsidence has not been detected in the study area; however, an inch of compaction might or might not be detected by geodetic surveys. Therefore, the subsidence estimates based on SBFTM parameter values and simulation results were consistent with no detected subsidence.

Groundwater Budget

Figure 14 shows the simulated annual hydrologic budgets for the entire model area and the subbasins for two different simulation periods. In general, the budgets for 1929 to 1971 are based on annual stress periods and the budgets for 1972 to 2013 are based on monthly stress periods. The SBFTM hydrologic budget for the entire model area from 1929 to 1971 is shown in figure 14*A*, and the budget for the entire model area from 1972 to 2013 is shown in figure 14*B*. Simulated recharge was mostly from small catchments and creeks; there was only a small amount of areal recharge, and recharge across the offshore fault was limited to times of heavy pumping (figs. 14*A, B*). Small-catchment recharge was the primary source of recharge during wetter periods, when there is little pumping; net creek recharge was relatively low because of higher groundwater levels, which resulted in discharge from the groundwater system to the creeks (figs. 14*A, B*). During times of relatively high pumping rates, usually during dry years, creek leakage was the primary source of recharge. Note that it was assumed that the creek stages (that is, the depth of the creek above the creek bed) were always greater than zero; therefore, the creeks are a constant source of water in the model.

Between 1929 and 1971 discharge due to pumping varied greatly (fig. 14*A*). Pumping rates generally were higher during drier periods and lower during wetter periods (fig. 14*A*). There was a net loss in storage from 1929 to 1946 because of a small amount of pumping (fig. 15). Pumpage in the Santa Barbara and Foothill basins increased after 1947, particularly during dry periods (fig. 14*A*). From 1949 to 1952, heavy pumpage resulted in a loss of about 9,200 acre-ft from storage (fig. 15). Pumpage decreased between 1953 and 1960, resulting in about 2,900 acre-ft of storage being recovered. Higher pumpage resumed from 1961 to 1971, resulting in an additional loss of 8,300 acre-ft from storage.

A general decrease in pumpage from 1972 to 1983 in comparison with the previous eight years (figs. 14*A*, *B*) resulted in the recovery of about 6,200 acre-ft of storage, which was then lost because of heavy pumping between 1984 and 1990 (figs. 14*B,* 15). From 1991 to 2006, pumpage was greatly reduced in general, leading to the recovery of over 10,800 acre-ft of storage. Pumping increased generally from 2007 to 2013, resulting in a loss of over 2,900 acre-ft of storage. Overall, groundwater pumping resulted in a net loss of about 11,400 acre-ft of groundwater storage between 1929 and 2013 (fig. 15).

From 1929 to 1971, the majority of water entering the SBFTM was from creek and small catchment recharge, and the majority of the water leaving the SBFTM was from pumping, discharge to creeks (baseflow), and drains (table 4*A*). In addition, about 37 percent of the total pumpage was loss from storage. From 1972 to 2013, the majority of water entering the SBFTM was from creek and small catchment recharge, and the majority of the water leaving the SBFTM was from pumping, discharge to creeks (baseflow), and drains (table 4*B*). In addition, the reduction in pumpage during this period resulted in about 7,800 acre-ft of water being added to storage. During July 1990, a month when approximately 705 acre-ft of groundwater was pumped in the study area, pumpage was much greater than all sources of recharge combined, and about 382 acre-ft of water was removed from storage; therefore, storage accounted for about 54 percent of groundwater pumpage (table 4*C*).

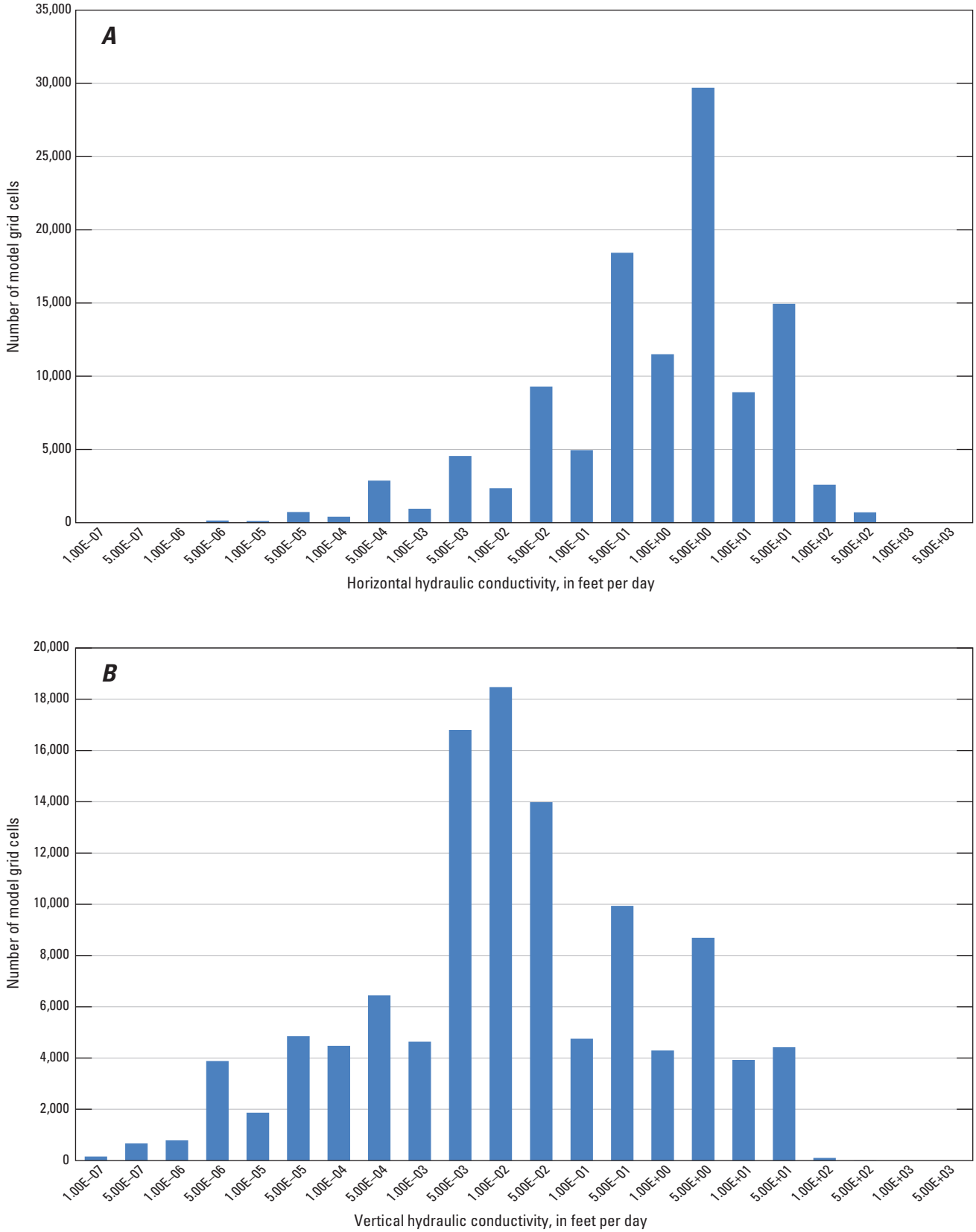

Figure 13. Distribution of hydraulic conductivity values used in the Santa Barbara flow and transport model, Santa Barbara, California: *A*, horizontal, and *B*, vertical.

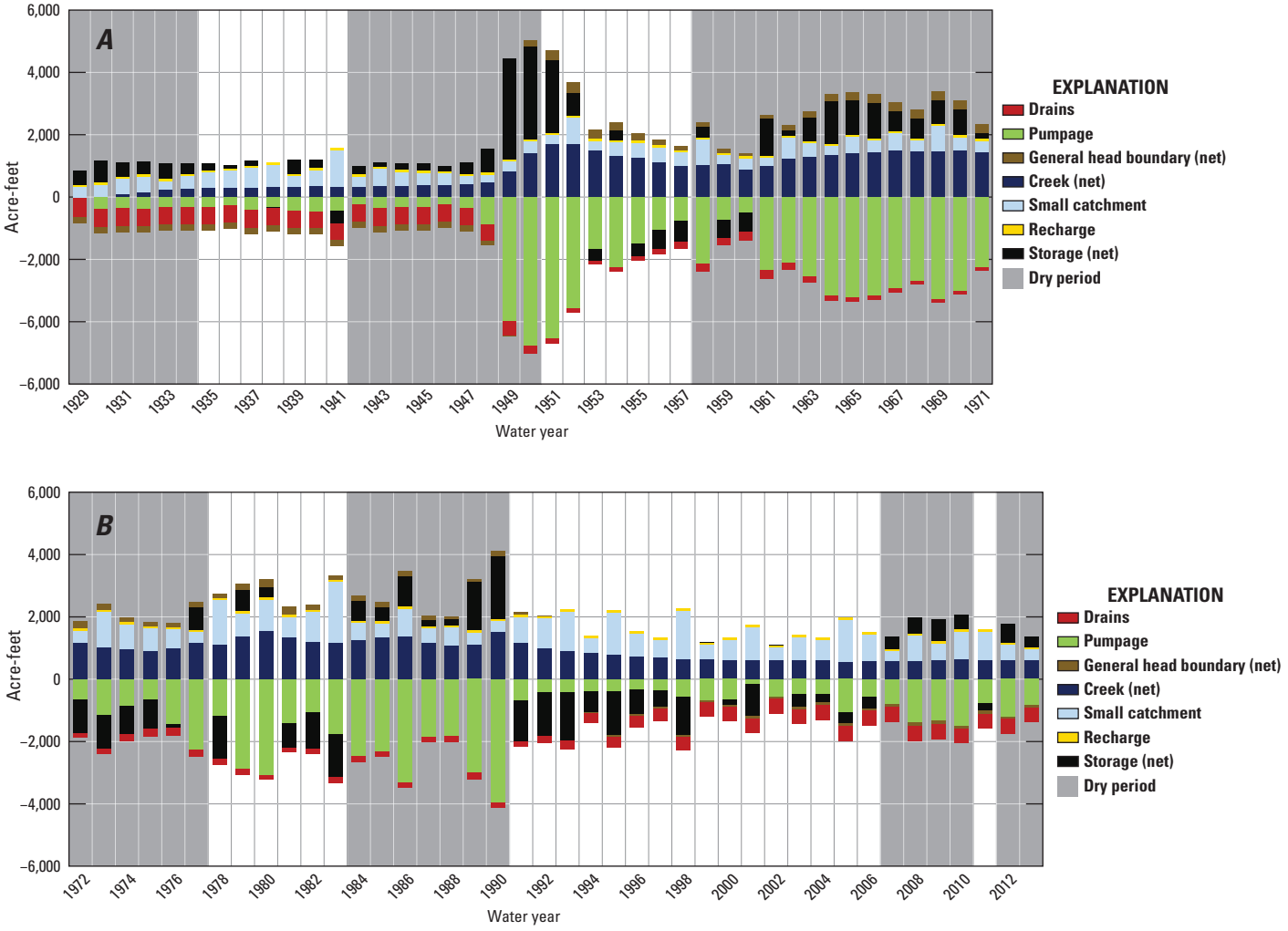

Figure 14. Simulated annual hydrologic budget for two simulation periods, Santa Barbara flow and transport model, Santa Barbara, California: *A*, entire model area, 1929–71; *B*, entire model area, 1972–2013; *C*, Storage Unit I, 1929–71; *D*, Storage Unit I, 1972–2013; *E*, Storage Unit III, 1929–71; *F*, Storage Unit III, 1972–2013; *G*, East Foothill subbasin, 1929–71; *H*, East Foothill subbasin, 1972–2013; *I*, West Foothill subbasin, 1929–71; and *J*, West Foothill subbasin, 1972–2013.

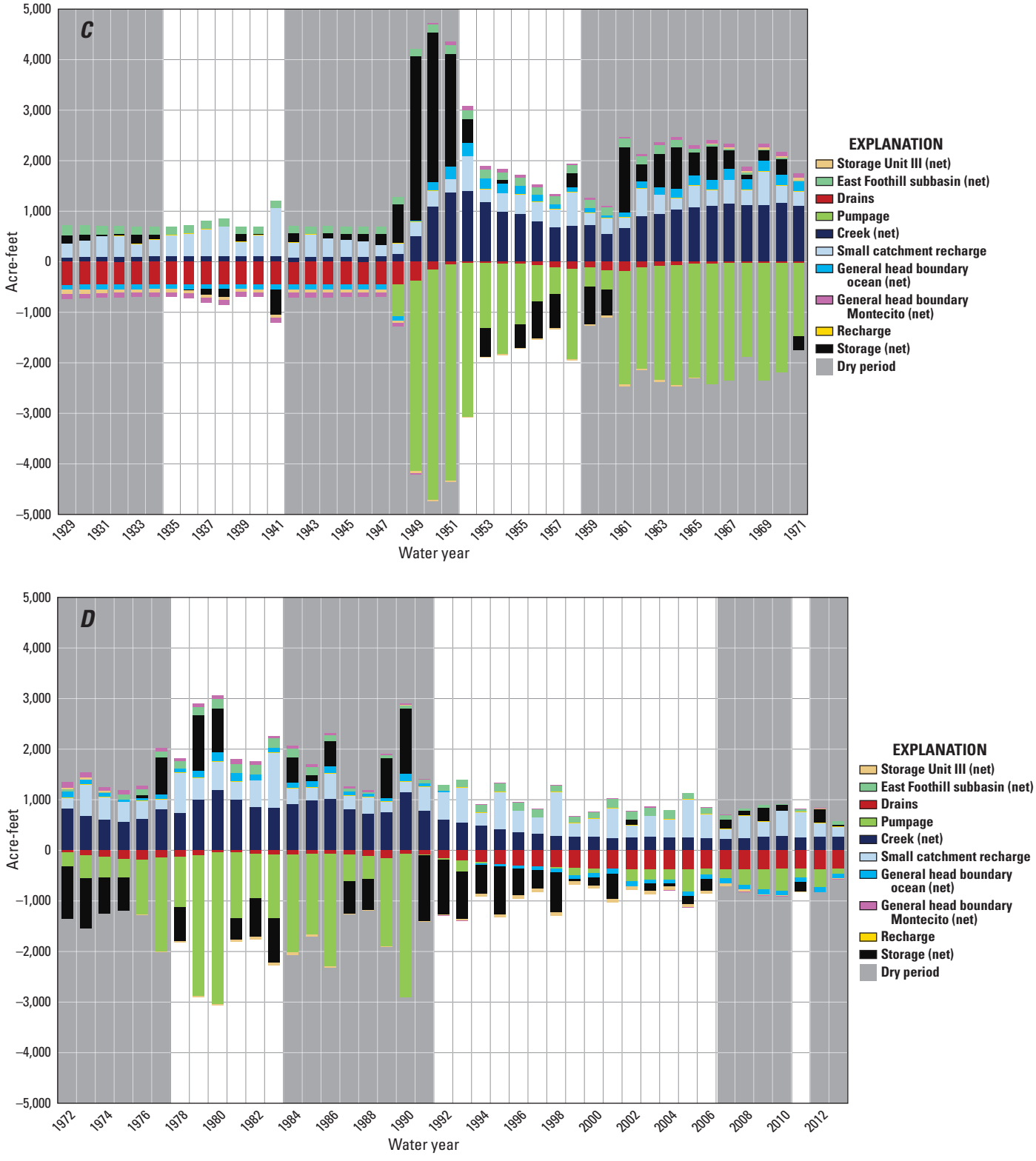

Figure 14. —Continued

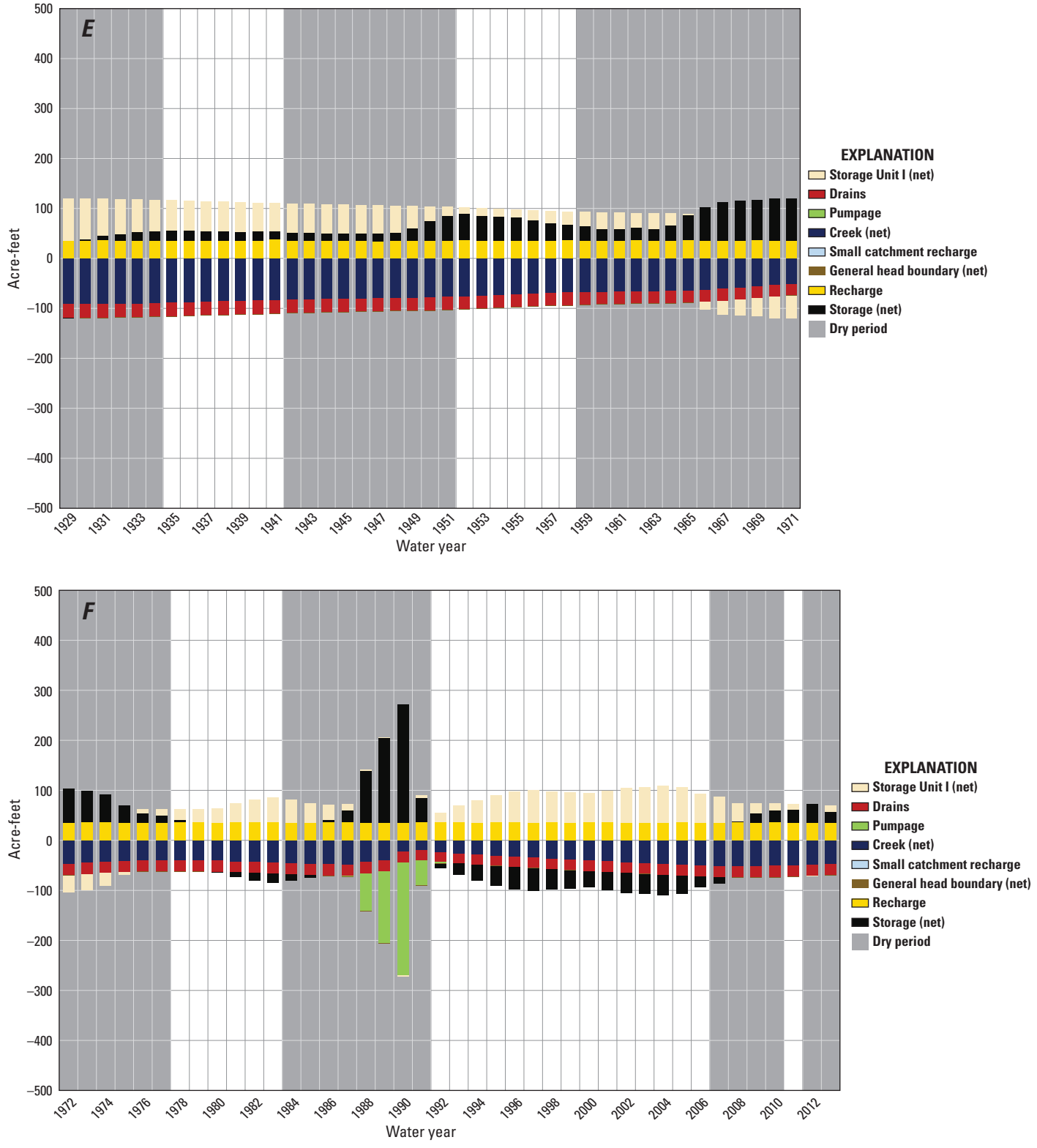

Figure 14. —Continued

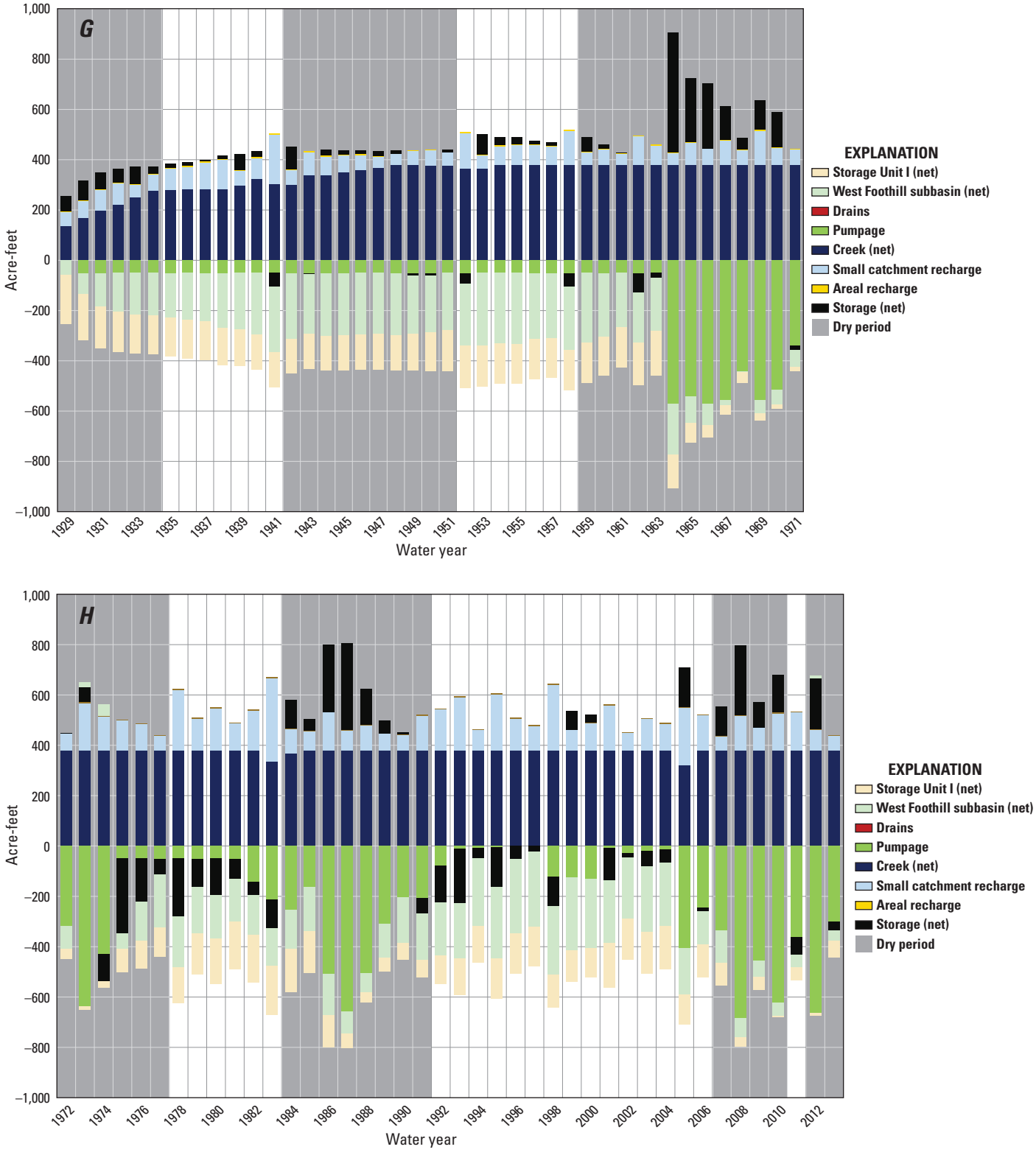

Figure 14. —Continued

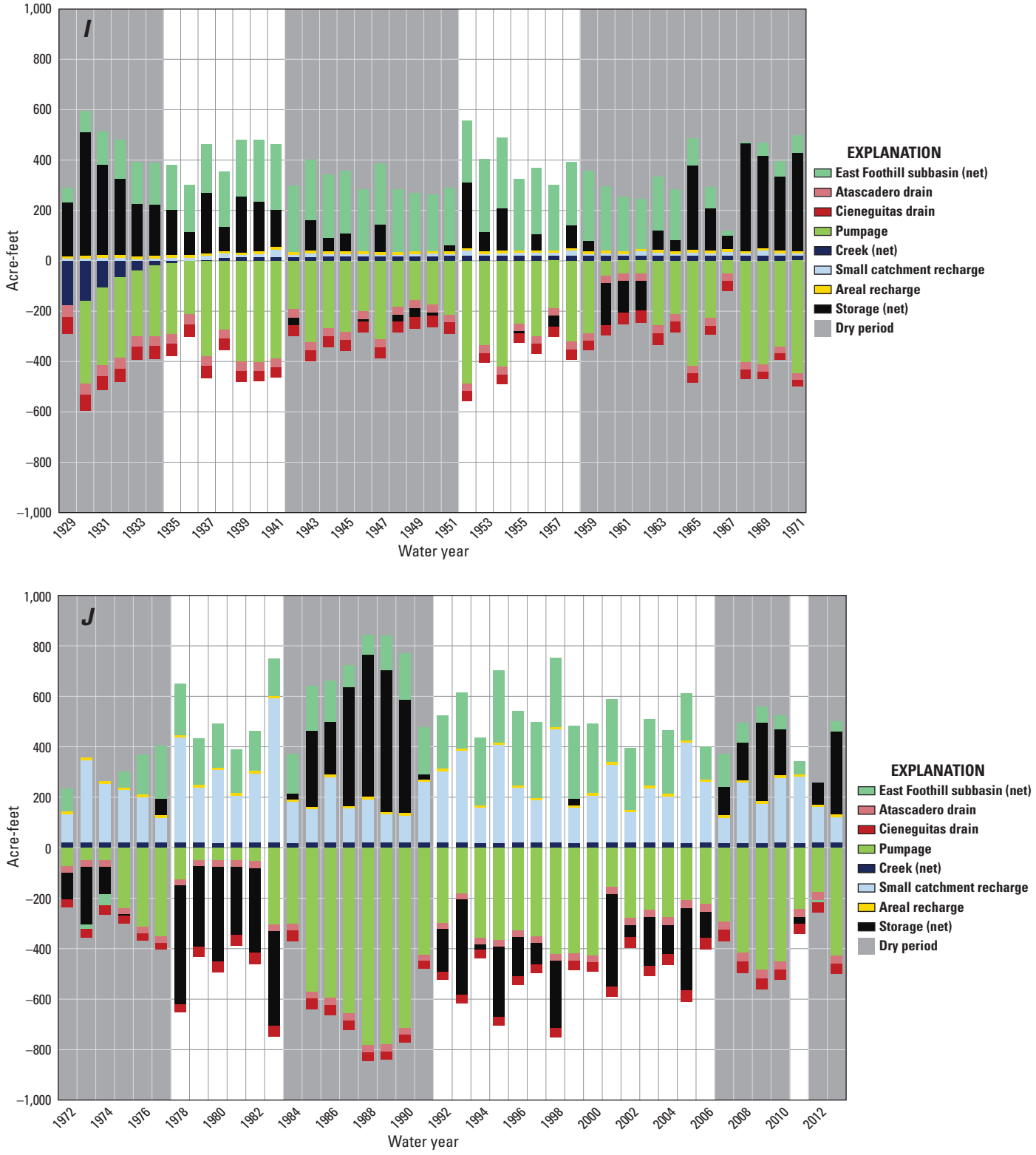

Figure 14. —Continued

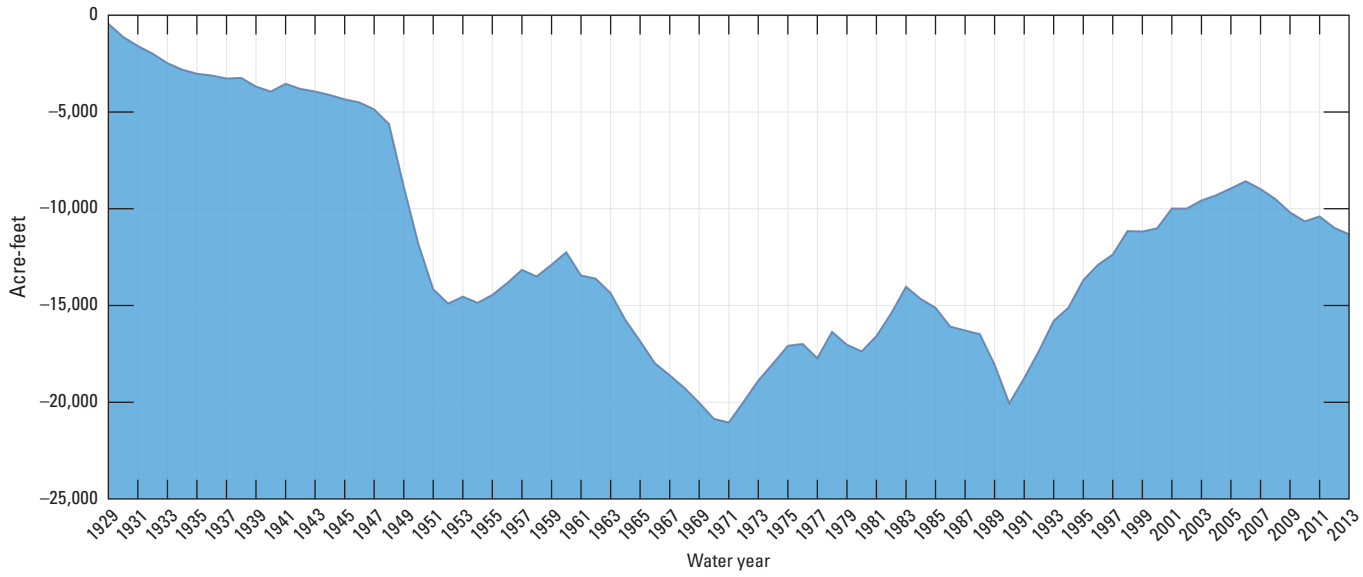

Figure 15. Simulated cumulative change in groundwater storage, 1929–2013, Santa Barbara flow and transport model, Santa Barbara, California.

Table 4*A*. Simulated cumulative groundwater budget, 1929–71, Santa Barbara flow and transport model, Santa Barbara, California.

	Total volume of water, in acre-feet, 1929–71						
	Storage	**Wells**	**Drains**	**Recharge**	**General-head boundary**	**Creek**	**Small catchment**
In	65,018	0	0	5,485	10,353	111,215	40,528
Out	22,527	131,311	31,357	0	8,230	39,363	0
Change	42,491	–131,311	–31,357	5,485	2,123	71,852	40,528
Mass balance	42,491–131,311–31,357+5,485+2,123+71,852+40,528 = –189						

Table 4*B*. Simulated cumulative groundwater budget, 1972–2013, Santa Barbara flow and transport model, Santa Barbara, California.

	Total volume of water, in acre-feet, 1972–2013						
	Storage	**Wells**	**Drains**	**Recharge**	**General-head boundary**	**Creek**	**Small catchment**
In	68,679	0	0	5,320	7,182	106,763	65,761
Out	85,537	106,307	26,833	0	4,615	30,456	0
Change	–16,858	–106,307	–26,833	5,320	2,567	76,307	65,761
Mass balance	–16,858–106,307–26,833+5,320+2,567+76,307+65,761 = –41						

Table 4*C*. Simulated water budget, July 1990, Santa Barbara flow and transport model, Santa Barbara, California.

	Total volume of water, in acre-feet, July 1990						
	Storage	**Wells**	**Drains**	**Recharge**	**General-head boundary**	**Creek**	**Small catchment**
In	399	0	0	10	32	278	47
Out	18	705	25	0	3	16	0
Change	382	–705	–25	10	29	262	47
Mass balance	382–705–25+10+29+262+47 = –1						

The SBFTM hydrologic budget from 1929 to 1971 by subbasin is shown in figures 14*C*, *E*, *G*, and *I*. The SBFTM hydrologic budget from 1972 to 2013 by subbasin is shown in figures 14*D*, *F*, *H*, and *J*. The hydrologic budget for Storage Unit I is shown in figures 14*C* and *D*. The primary sources of recharge were small catchment recharge and net inflow from creeks, although during times of high pumping (for example, 1950 in fig. 14*C*) water removed from groundwater storage was the primary source of water to the groundwater system. In addition to pumping, the primary groundwater discharges were drains and water added to storage.

The hydrologic budget for Storage Unit III is shown in figures 14*E* and *F* (note the much lower values than Storage Unit I). There were three sources of recharge to Storage Unit III: inflow from Storage Unit I, net inflow from groundwater storage, and surface recharge (precipitation), but during times of low inflow from Storage Unit I or outflow to Storage Unit I, water removed from groundwater storage was the primary source of water to the groundwater system (fig. 14*E*). The primary discharge sinks were net creek discharge and outflow from the subbasin (drains).

The hydrologic budget for East Foothill subbasin is shown in figures 14*G* and *H*. The primary sources of recharge were net creek inflow and small catchment recharge. The primary discharge sinks were pumpage (after 1964) and net discharge to Storage Unit I and West Foothill subbasin.

The hydrologic budget for West Foothill subbasin is shown in figures 14*I* and *J*. The primary sources of recharge were net inflow from East Foothill subbasin, inflow from groundwater storage, and small catchment recharge. The primary discharge sinks were pumpage, groundwater added to storage, and outflow from the subbasin (drains).

Simulated Groundwater Flow and Movement

In order to examine changes in hydraulic conditions related to pumpage, the simulated hydraulic heads for initial conditions (1929) and July 1990 were examined for each producing zone. July 1990 was the end of an extended period of high pumping in Storage Unit I and moderate pumping in the Foothill groundwater basin.

In the upper producing zone, the simulated initial-condition hydraulic heads indicated that groundwater in the Foothill groundwater basin generally flowed from the Mission and Lauro Canyons west and southwest toward the southwest corner of the basin and across the Modoc fault to the Goleta groundwater basin (fig. 16*A*). Groundwater also flowed to the Santa Barbara groundwater basin by moving across the East More Ranch fault at Arroyo Burro and, to a limited extent, across other parts of the fault as well. In Storage Unit I, groundwater generally flowed east from the East More Ranch fault toward the Pacific Ocean (fig. 16*A*). Note that the simulated hydraulic heads near the ocean in Storage Unit I were higher than sea level; therefore, with the exception of density effects, seawater would not intrude under these hydraulic conditions. In Storage Unit III, groundwater generally flowed to the southeast (fig. 16*A*).

The middle producing zone only exists in Storage Unit I. The contours of simulated initial-condition hydraulic head indicated that groundwater flowed east toward the Pacific Ocean (fig. 16*B*).

In the lower producing zone, the simulated initial-condition hydraulic heads indicate that groundwater in the Foothill groundwater basin generally flowed from the Mission and Lauro Canyons west and southwest toward the southwest corner of the basin (fig. 16*C*). Unlike the upper producing zone, the lower producing zone was not simulated as connecting hydraulically to the Goleta groundwater basin; therefore, groundwater did not cross into the Goleta groundwater basin, as it did in the upper producing zone. In Storage Unit I, groundwater generally flowed east from the East More Ranch fault toward the Pacific Ocean (fig. 16*C*). In Storage Unit III, groundwater generally flowed to the southeast, except where it deflects more southward along creek channels (fig. 16*C*).

Contours of simulated July 1990 hydraulic heads for the upper, middle, and lower producing zones are shown in figure 17. In general, the simulated July 1990 hydraulic heads were much lower than the initial conditions as a result of groundwater pumping. There was a simulated groundwater low in all three producing zones in Storage Unit I near the Ortega Park production well (fig. 17). In addition, there was a groundwater low in the lower producing zone only in the West Foothill subbasin near the Los Robles production well (fig. 17*C*). Simulated July 1990 hydraulic heads in all three producing zones were below sea level in the coastal area of Storage Unit I; therefore, seawater intrusion in the producing zones was possible.

In the upper producing zone, the simulated July 1990 hydraulic heads indicated that groundwater in the Foothill groundwater basin generally flowed from the Mission and Lauro Canyons west and southwest toward the southwest corner of the basin and across the Modoc fault to the Goleta groundwater basin (fig. 17*A*). In Storage Unit I, the simulated July 1990 hydraulic heads indicated that groundwater flowed east toward the groundwater low near the Ortega Park production well (fig. 17*A*). In Storage Unit III, the simulated July 1990 hydraulic heads indicated that groundwater flowed south toward a groundwater low near the Val Verde production well (fig. 17*A*).

Again, the middle producing zone only exists in Storage Unit I. The simulated results indicated that groundwater flowed radially toward the groundwater low near the Ortega Park production well (fig. 17*B*).

In the lower producing zone, the simulated July 1990 hydraulic heads indicated that groundwater in the West Foothill subbasin flowed radially toward the groundwater low near the Los Robles production well (fig. 17*C*). In the East Foothill subbasin, groundwater flowed west and southwest. In Storage Unit I, groundwater flowed east from the East More Ranch fault, then radially toward the groundwater low (fig. 17*C*). In Storage Unit III, groundwater generally flowed south toward a low near the Val Verde production well (fig. 17*C*).

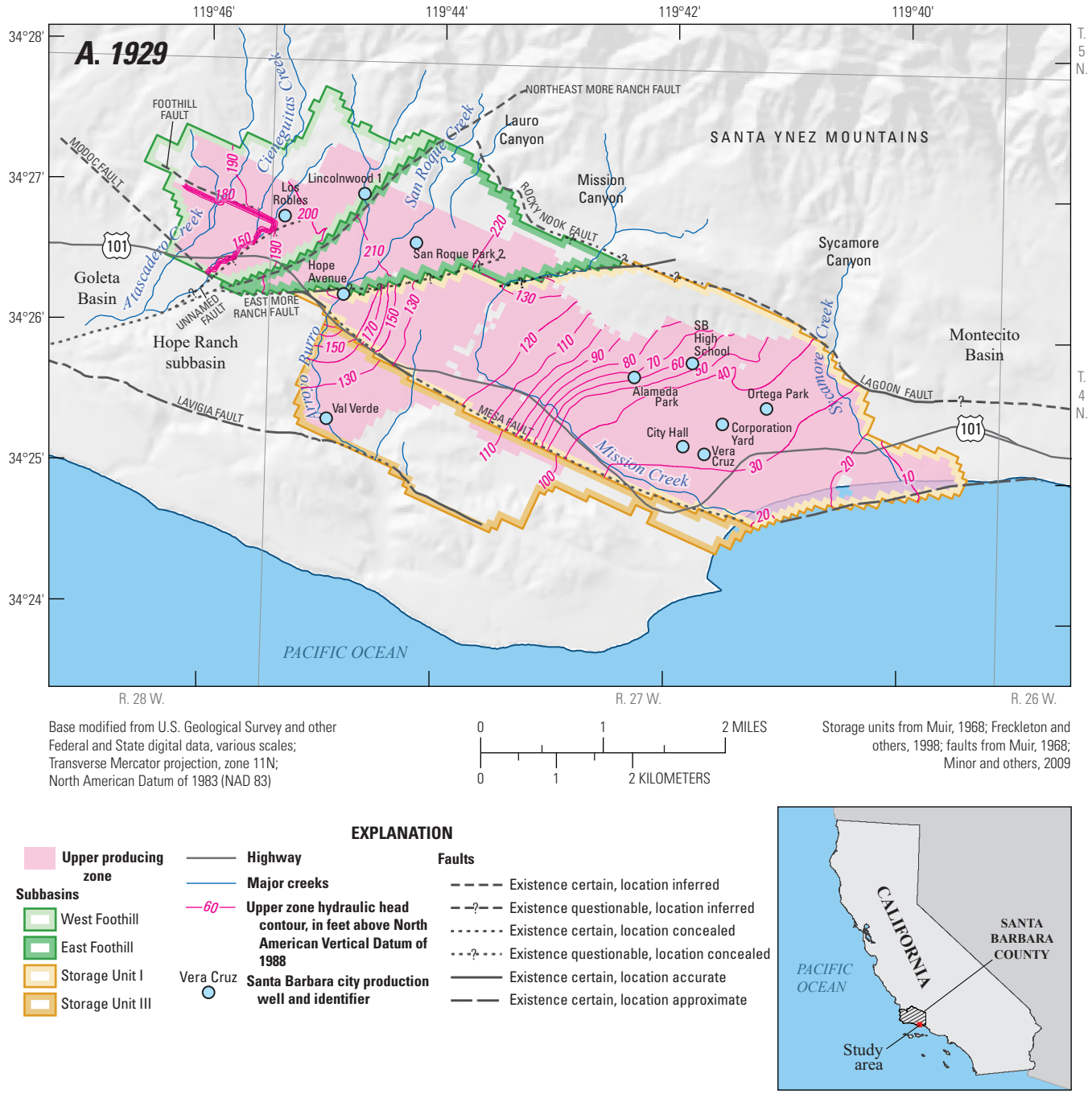

Base modified from U.S. Geological Survey and other Federal and State digital data, various scales; Transverse Mercator projection, zone 11N; North American Datum of 1983 (NAD 83)

0 1 2 MILES

0 1 2 KILOMETERS

Storage units from Muir, 1968; Freckleton and others, 1998; faults from Muir, 1968; Minor and others, 2009

EXPLANATION

- Upper producing zone
- Subbasins
  - West Foothill
  - East Foothill
  - Storage Unit I
  - Storage Unit III
- Highway
- Major creeks
- 60 — Upper zone hydraulic head contour, in feet above North American Vertical Datum of 1988
- Vera Cruz — Santa Barbara city production well and identifier
- Faults
  - Existence certain, location inferred
  - Existence questionable, location inferred
  - Existence certain, location concealed
  - Existence questionable, location concealed
  - Existence certain, location accurate
  - Existence certain, location approximate

Figure 16. Contours of simulated initial-condition (average 1929) hydraulic head for producing zones of the Santa Barbara groundwater basin, California: *A*, upper; *B*, middle; and *C*, lower.

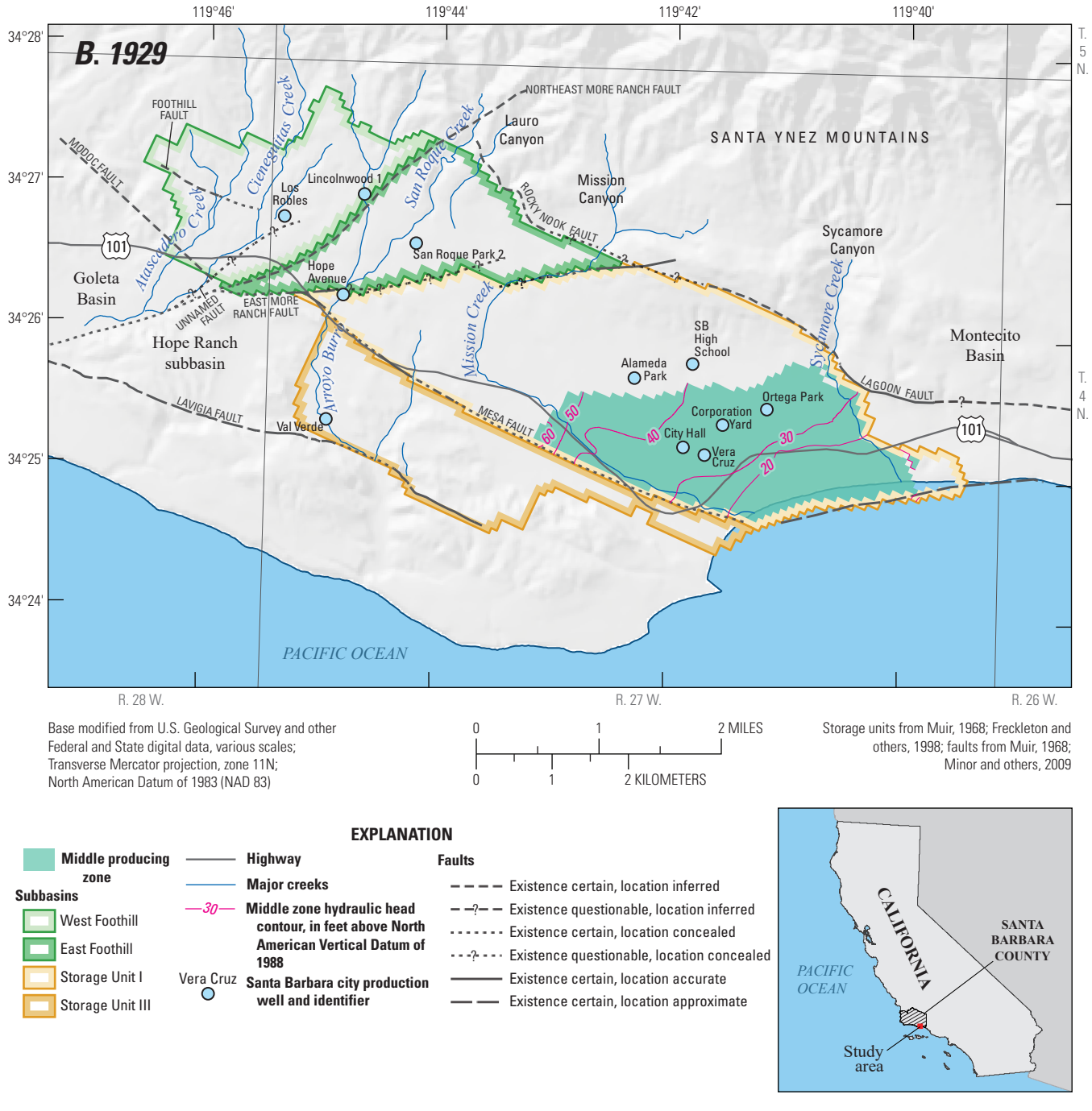

Figure 16. —Continued

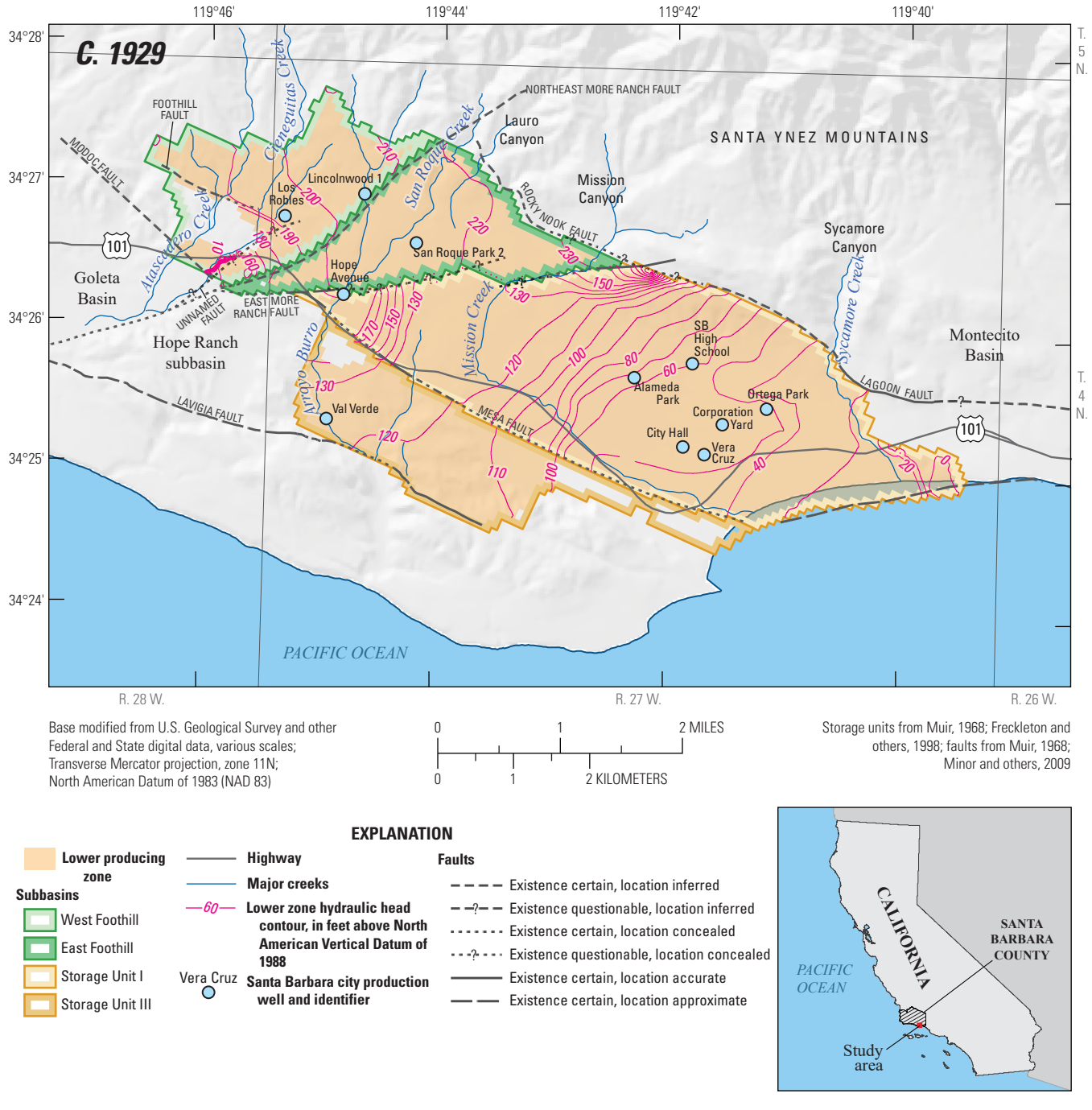

Figure 16. —Continued

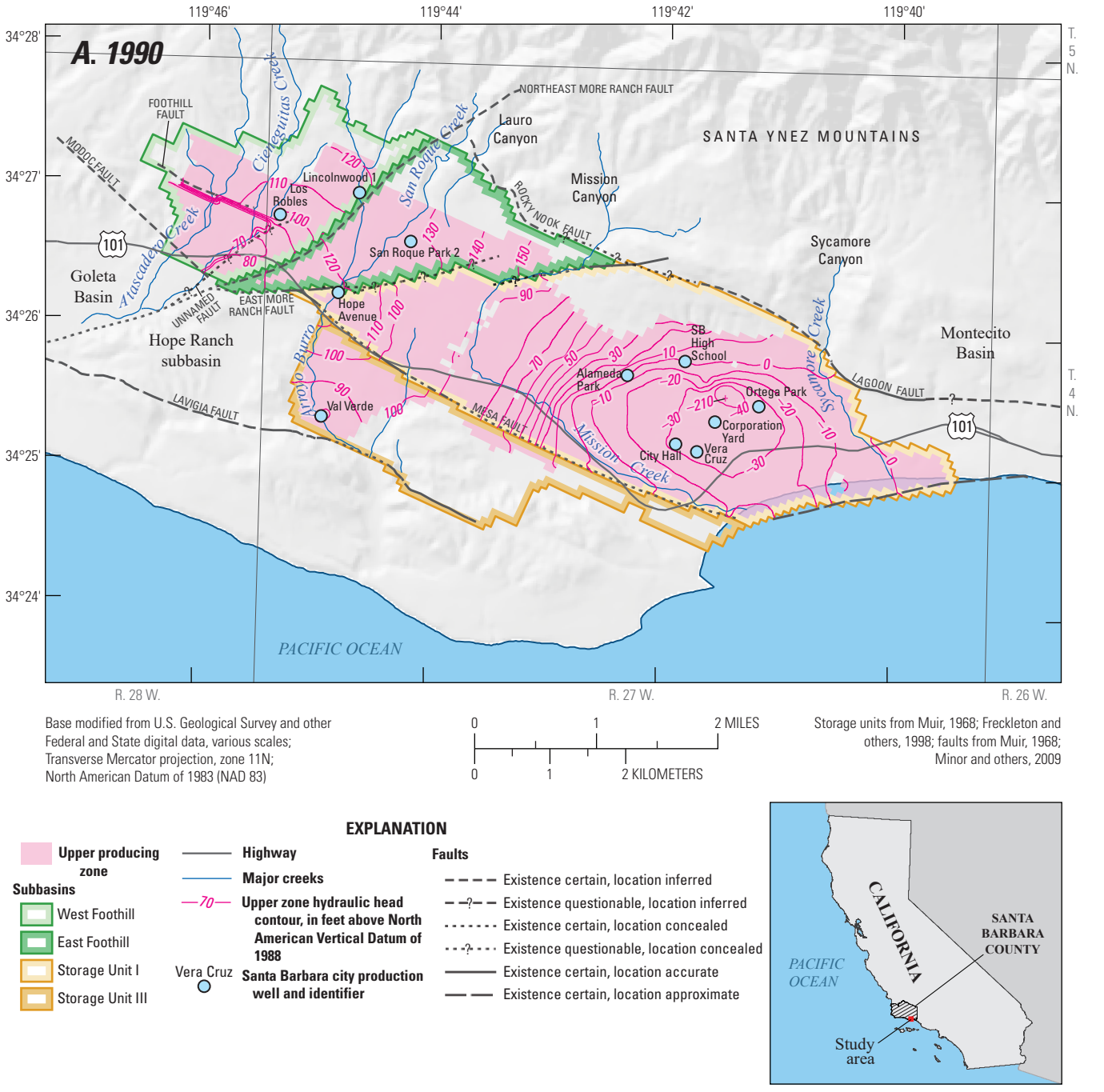

Figure 17. Contours of simulated July 1990 hydraulic head for the producing zones of the Santa Barbara groundwater basin, California: *A*, upper; *B*, middle; and *C*, lower.

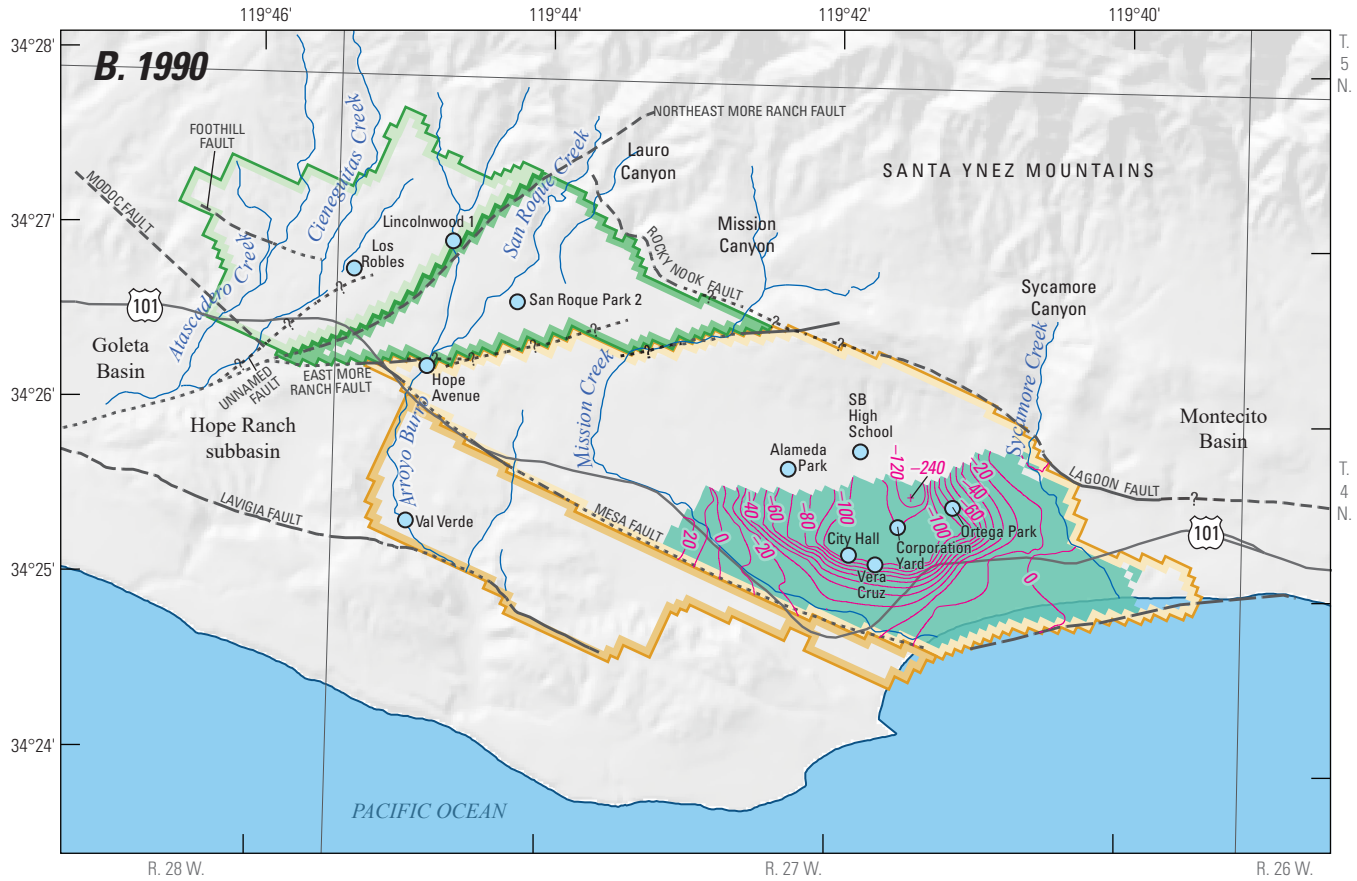

Base modified from U.S. Geological Survey and other Federal and State digital data, various scales; Transverse Mercator projection, zone 11N; North American Datum of 1983 (NAD 83)

0 1 2 MILES
0 1 2 KILOMETERS

Storage units from Muir, 1968; Freckleton and others, 1998; faults from Muir, 1968; Minor and others, 2009

EXPLANATION

- Middle producing zone
- Subbasins
  - West Foothill
  - East Foothill
  - Storage Unit I
  - Storage Unit III
- Highway
- Major creeks
- 20 — Middle zone hydraulic head contour, in feet above North American Vertical Datum of 1988
- Vera Cruz — Santa Barbara city production well and identifier
- Faults
  - Existence certain, location inferred
  - Existence questionable, location inferred
  - Existence certain, location concealed
  - Existence questionable, location concealed
  - Existence certain, location accurate
  - Existence certain, location approximate

Figure 17. —Continued

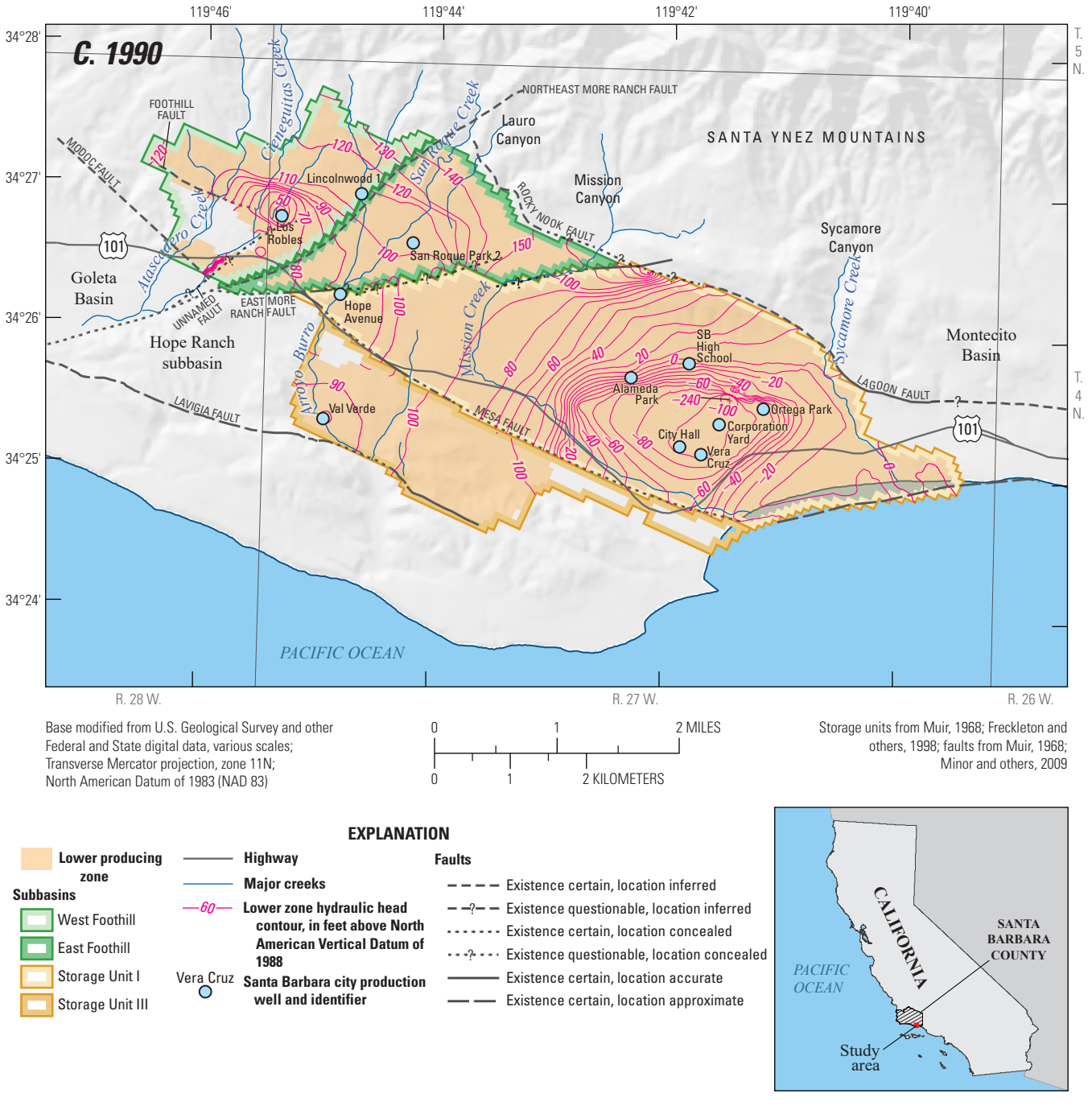

Figure 17. —Continued

In order to examine changes in hydraulic conditions related to pumpage, the simulated hydraulic-head drawdown between initial conditions (1929) and July 1990 was plotted and is shown in figure 18. There were pumping depressions in all three producing zones. In the upper, middle, and lower producing zones, there was a pumping depression near the Ortega Park production well in Storage Unit I (figs. 18*A–C*). In the lower producing zone, there was an additional pumping depression in the West Foothill subbasin near the Los Robles production well (fig. 18*C*).

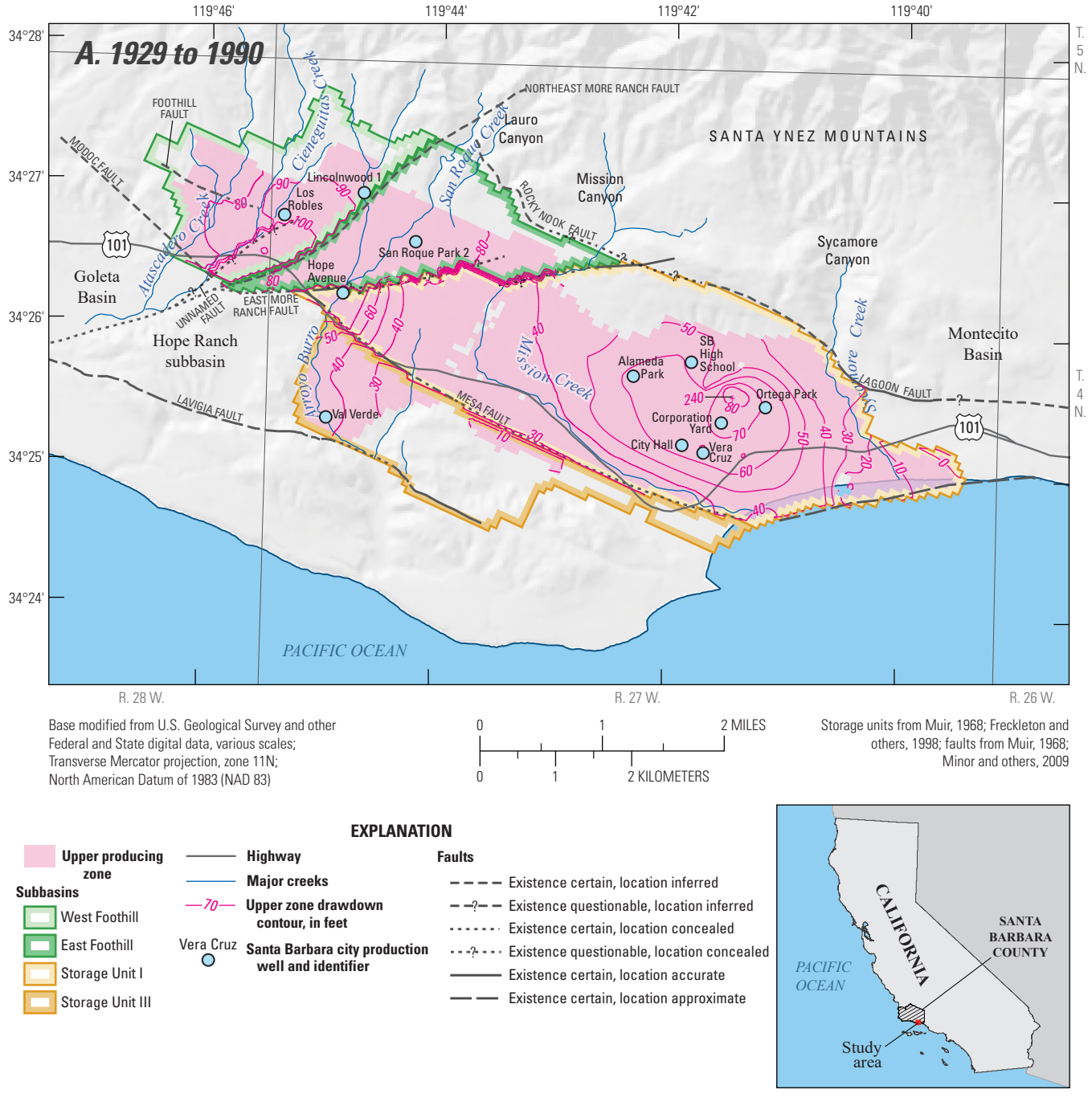

Figure 18. Contours of simulated drawdown between average 1929 and July 1990 hydraulic heads for the producing zones of the Santa Barbara groundwater basin, California: *A*, upper; *B*, middle; and *C*, lower.

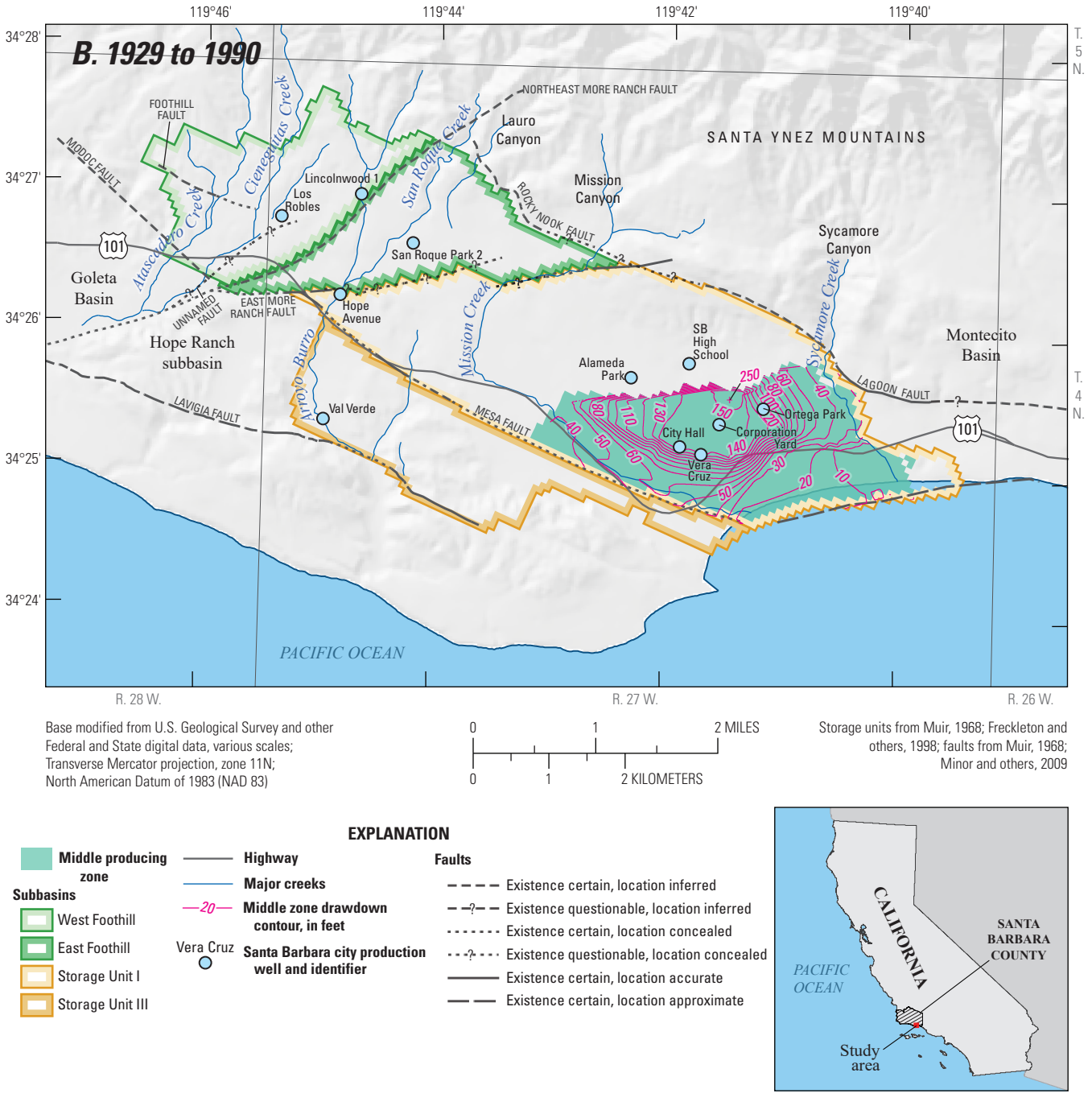

Base modified from U.S. Geological Survey and other Federal and State digital data, various scales; Transverse Mercator projection, zone 11N; North American Datum of 1983 (NAD 83)

0 1 2 MILES

0 1 2 KILOMETERS

Storage units from Muir, 1968; Freckleton and others, 1998; faults from Muir, 1968; Minor and others, 2009

EXPLANATION

- Middle producing zone
- Subbasins
  - West Foothill
  - East Foothill
  - Storage Unit I
  - Storage Unit III
- Highway
- Major creeks
- —20— Middle zone drawdown contour, in feet
- Vera Cruz Santa Barbara city production well and identifier
- Faults
  - Existence certain, location inferred
  - Existence questionable, location inferred
  - Existence certain, location concealed
  - Existence questionable, location concealed
  - Existence certain, location accurate
  - Existence certain, location approximate

Figure 18. —Continued

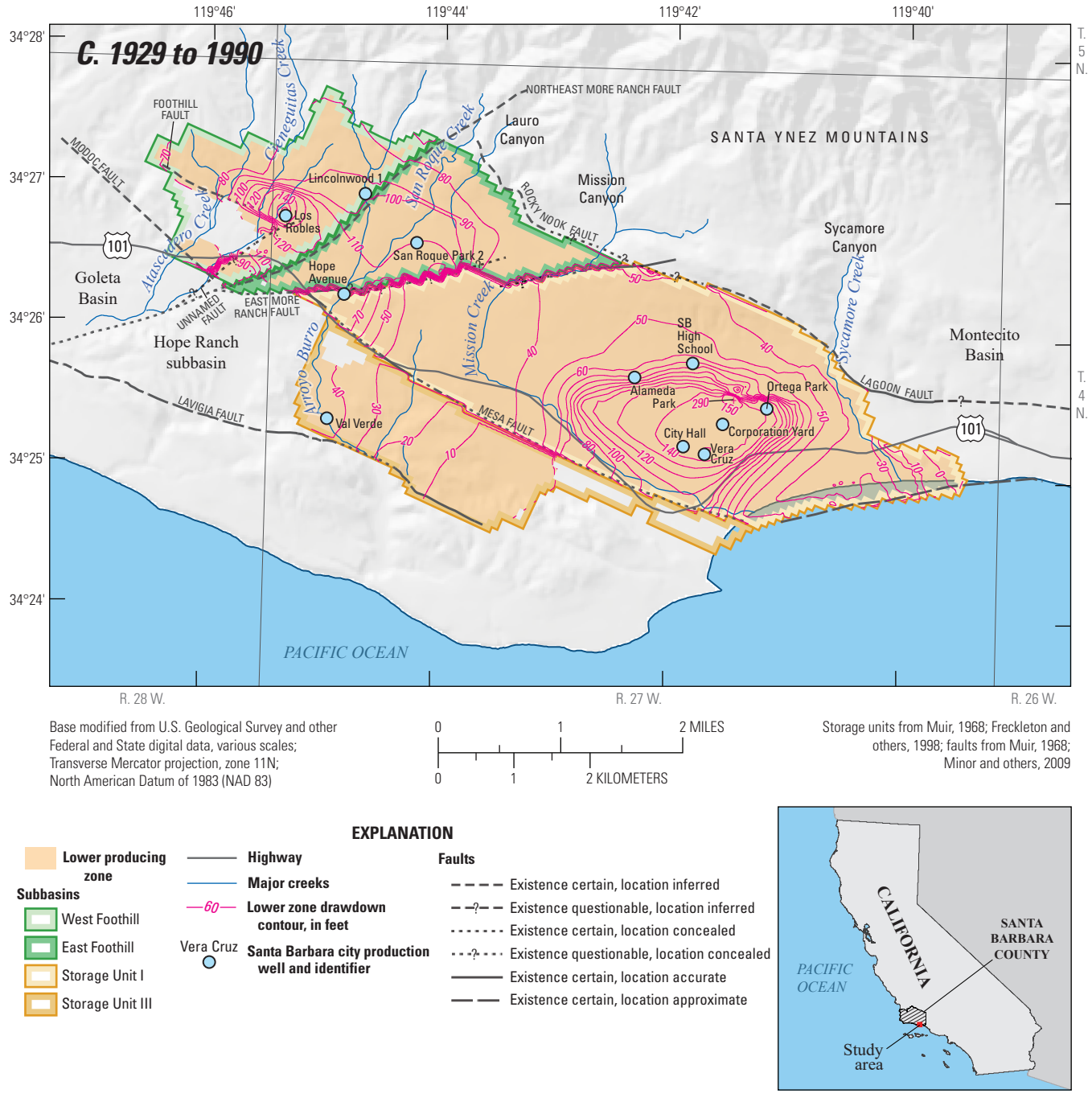

Figure 18. —Continued

Simulated Hydrographs

Several wells were selected as representative of conditions, and changes in conditions, in the four subbasins. The simulated hydraulic heads and corresponding measured water levels at selected wells in West Foothill subbasin, East Foothill subbasin, Storage Unit III, and Storage Unit I are shown in figures 19*A–D*, respectively. To show vertical hydraulic gradients, where possible, water levels are shown in each of the producing zones. Each of the subbasins are discussed in following sections.

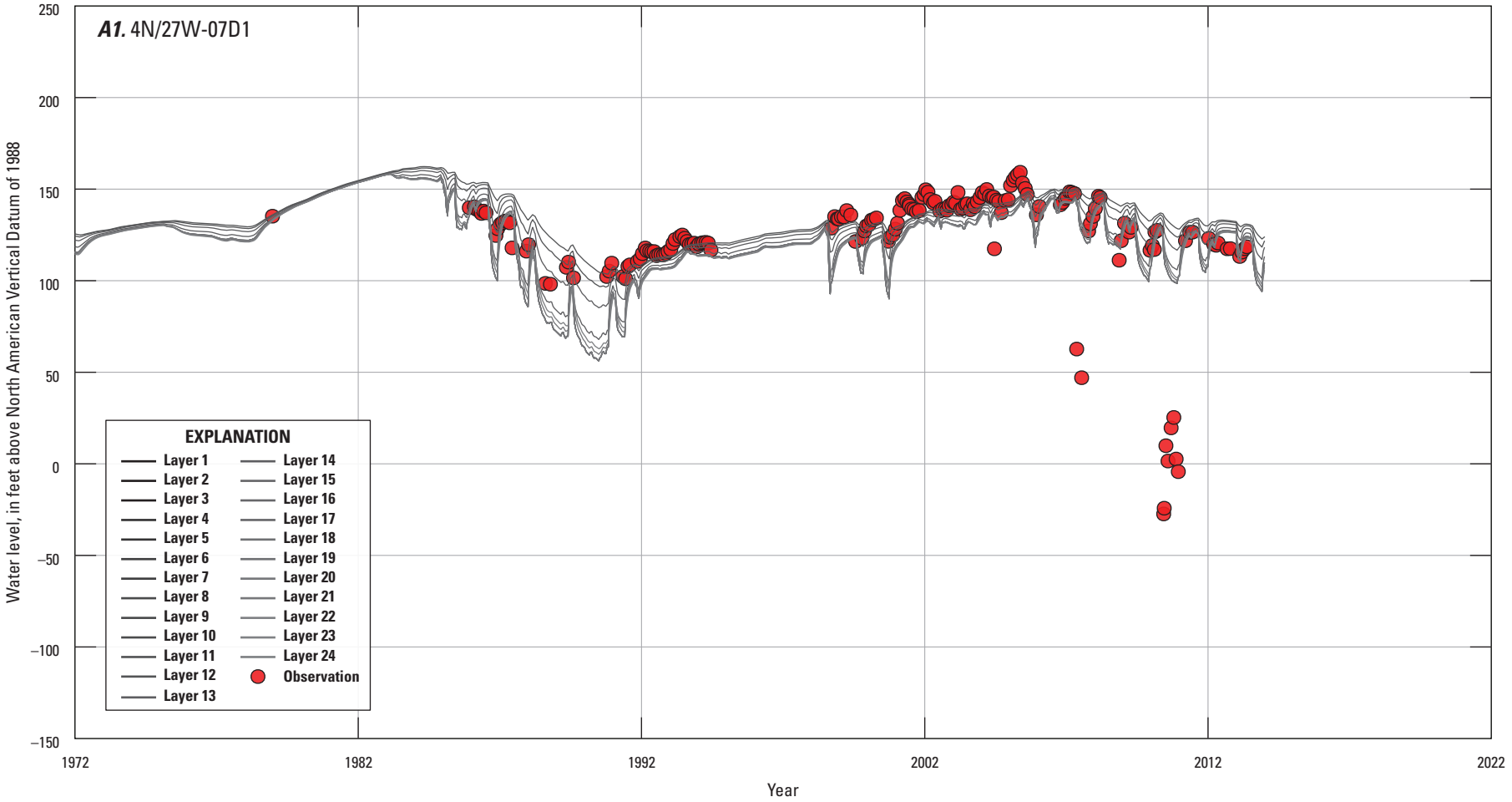

Figure 19. Simulated hydraulic heads and measured water levels for selected wells in the Santa Barbara groundwater basin, California, by subbasin: *A*, West Foothill subbasin; *B*, East Foothill subbasin; *C*, Storage Unit III; and *D*, Storage Unit I.

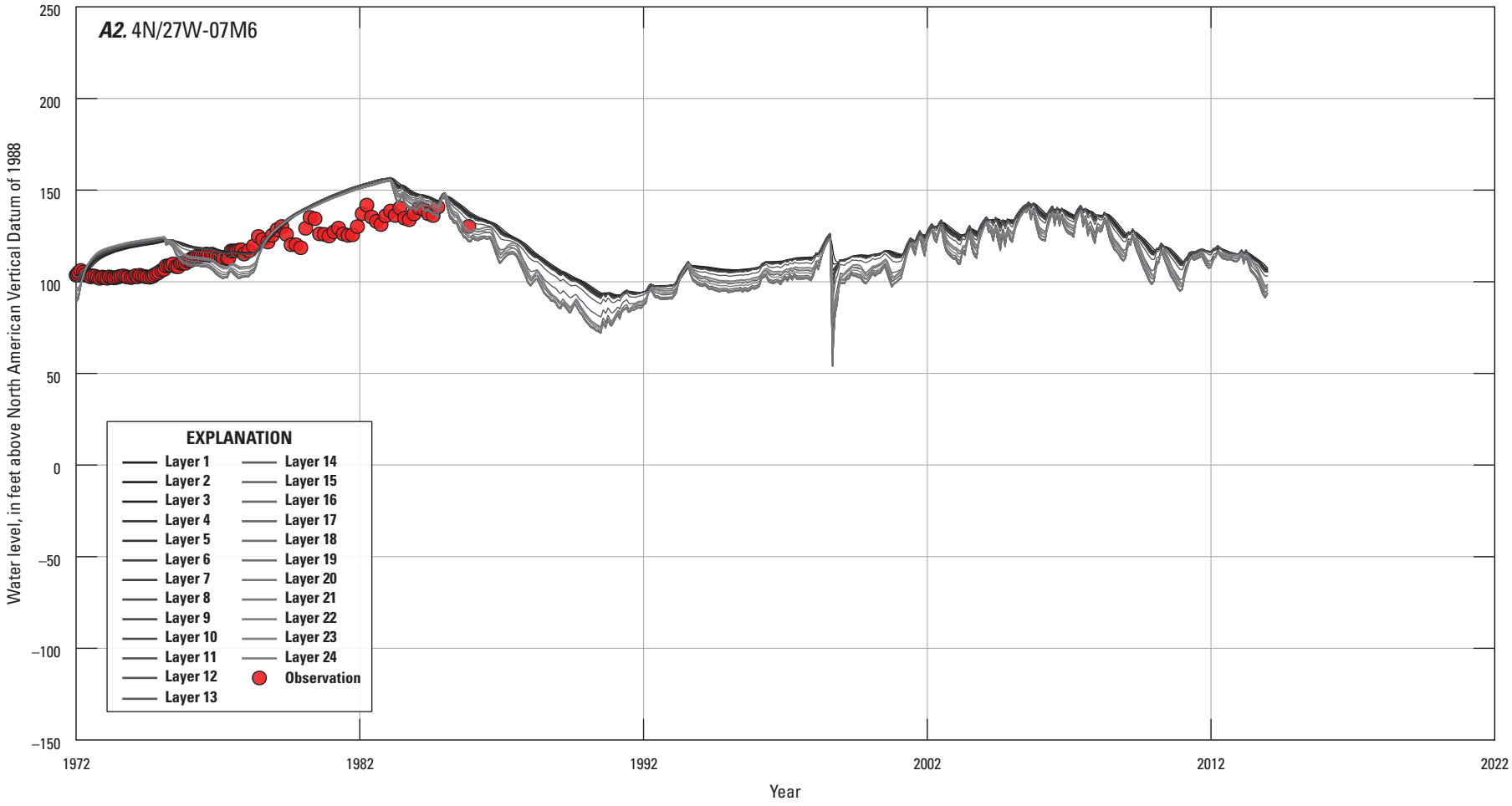

Figure 19. —Continued

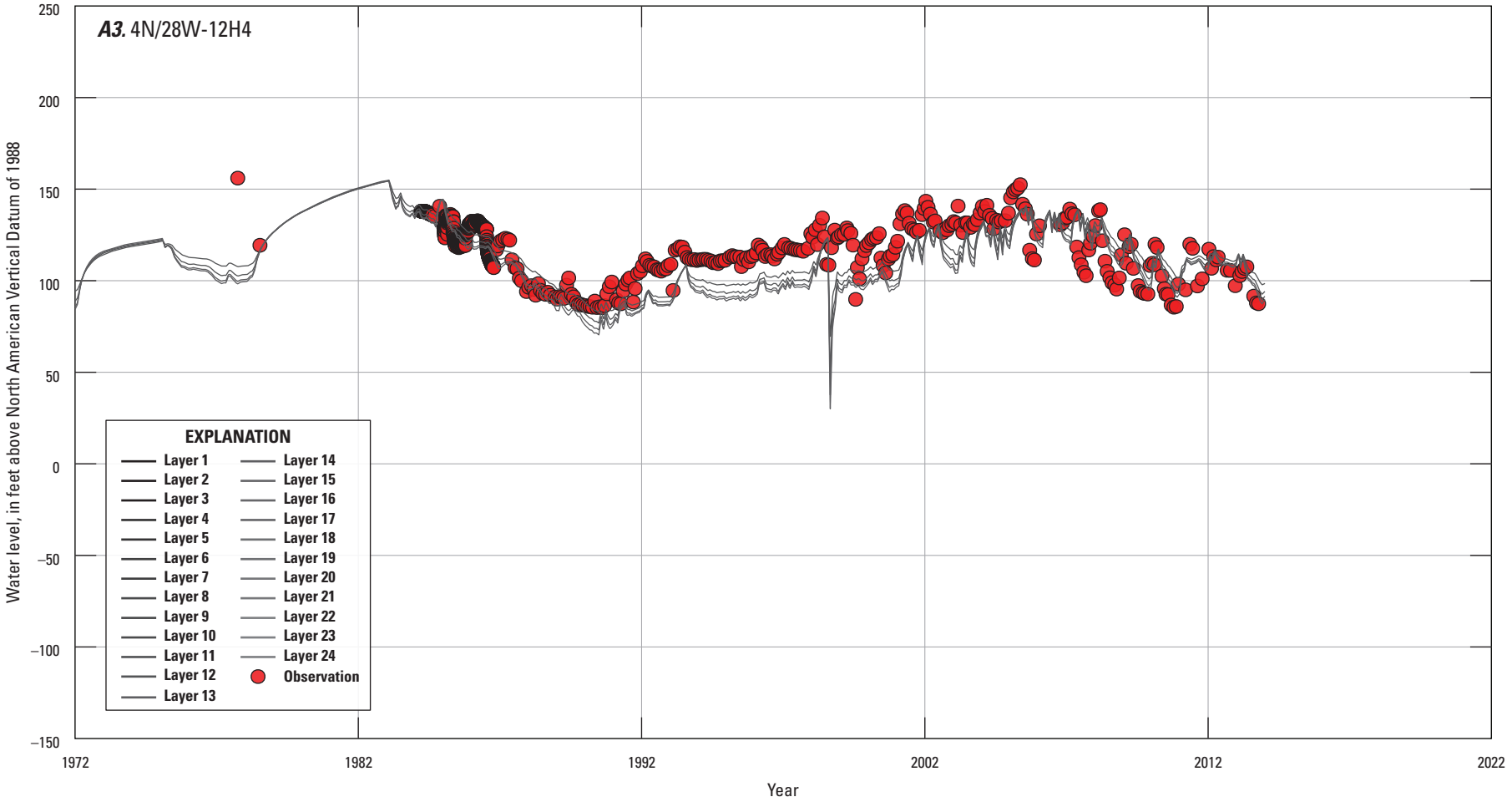

Figure 19. —Continued

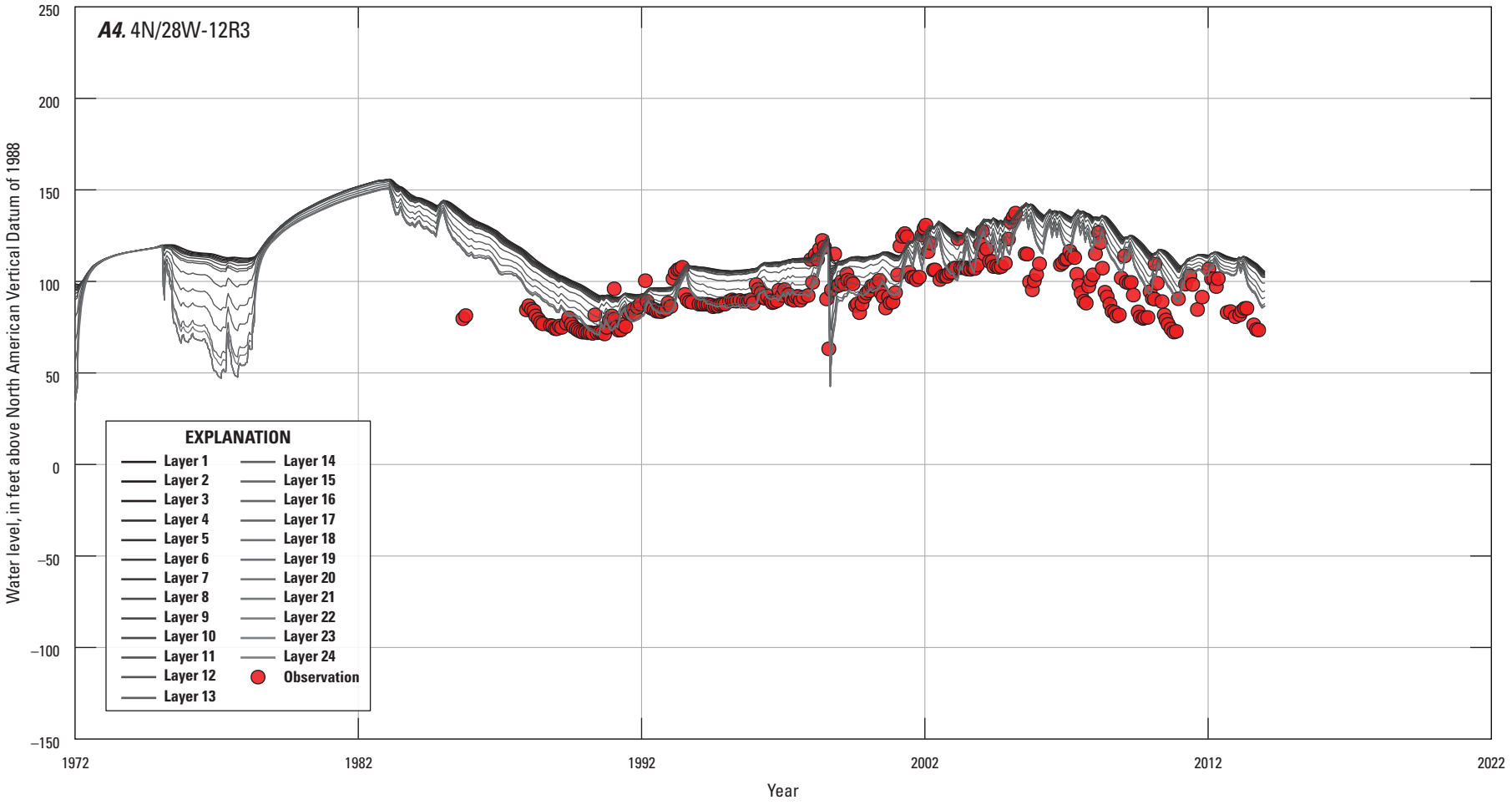

Figure 19. —Continued

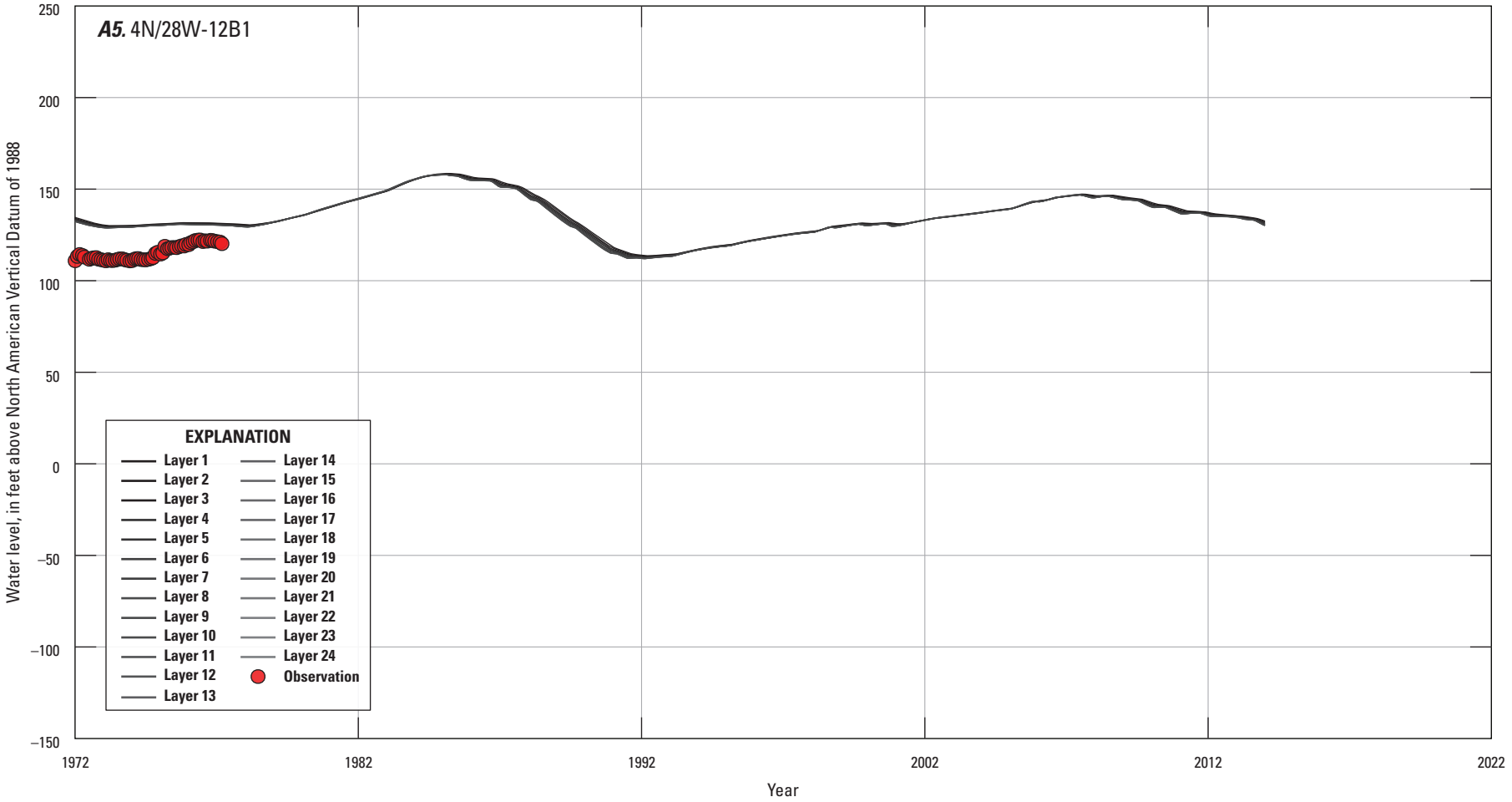

Figure 19. —Continued

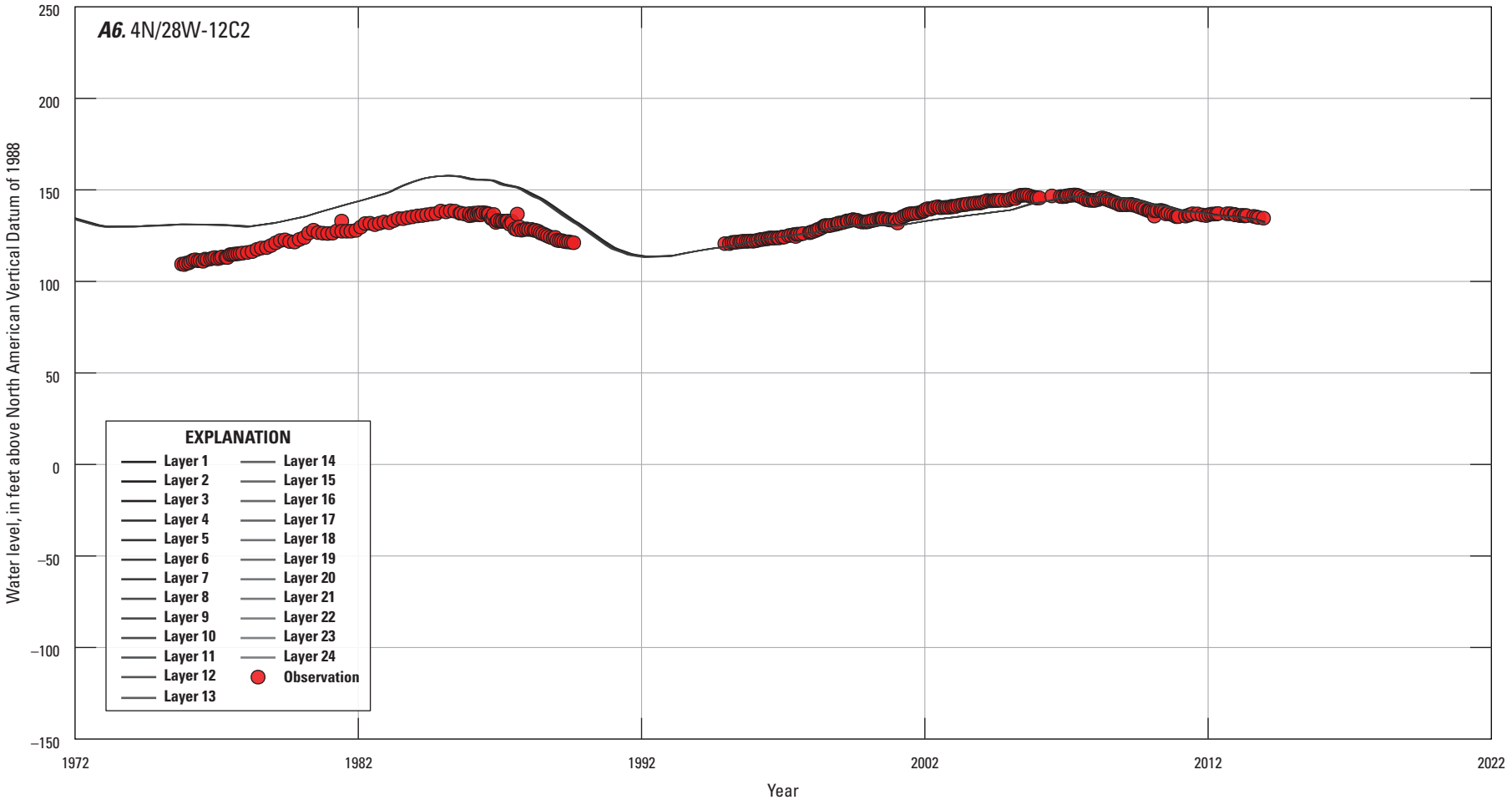

Figure 19. —Continued

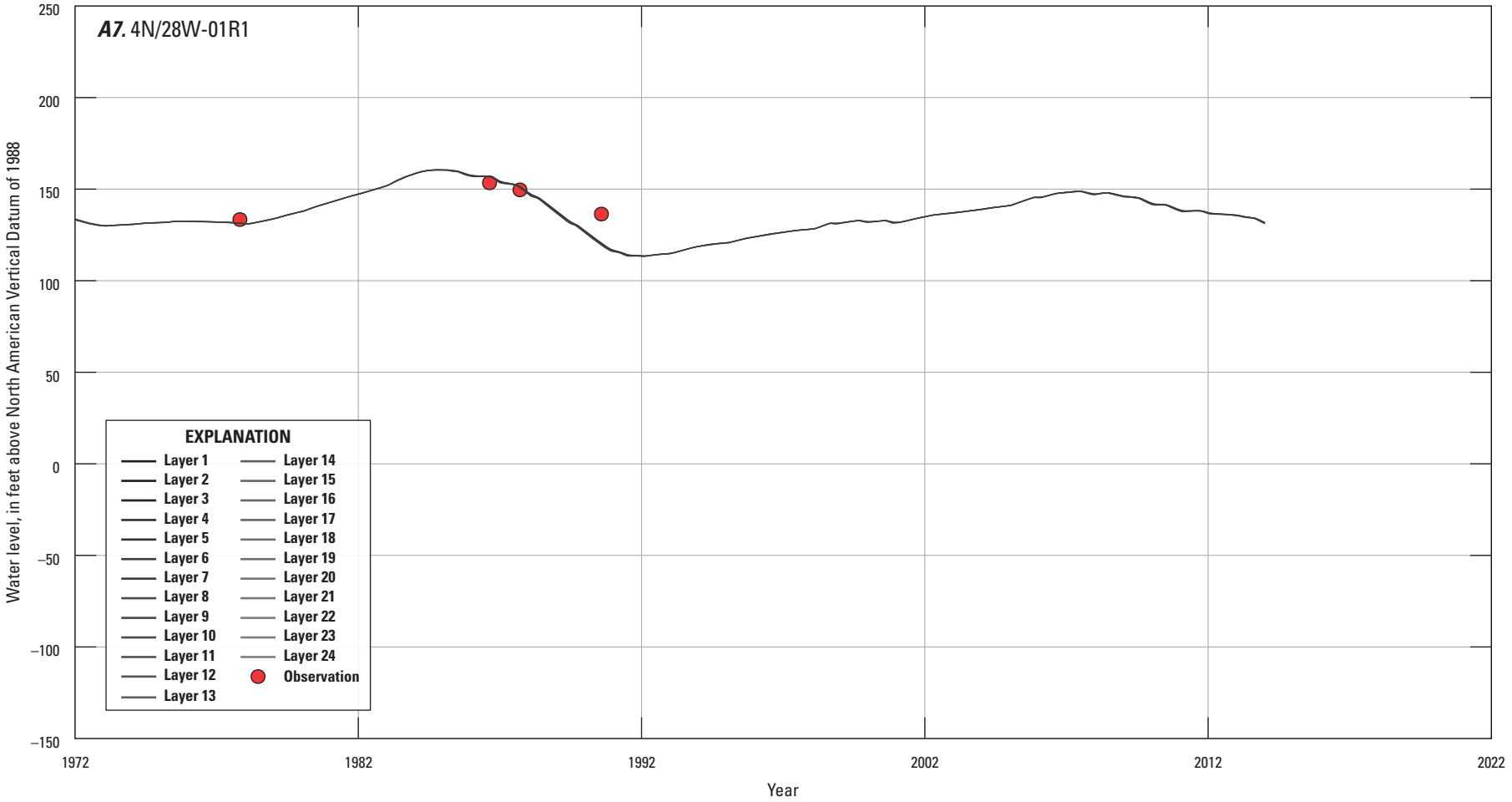

Figure 19. —Continued

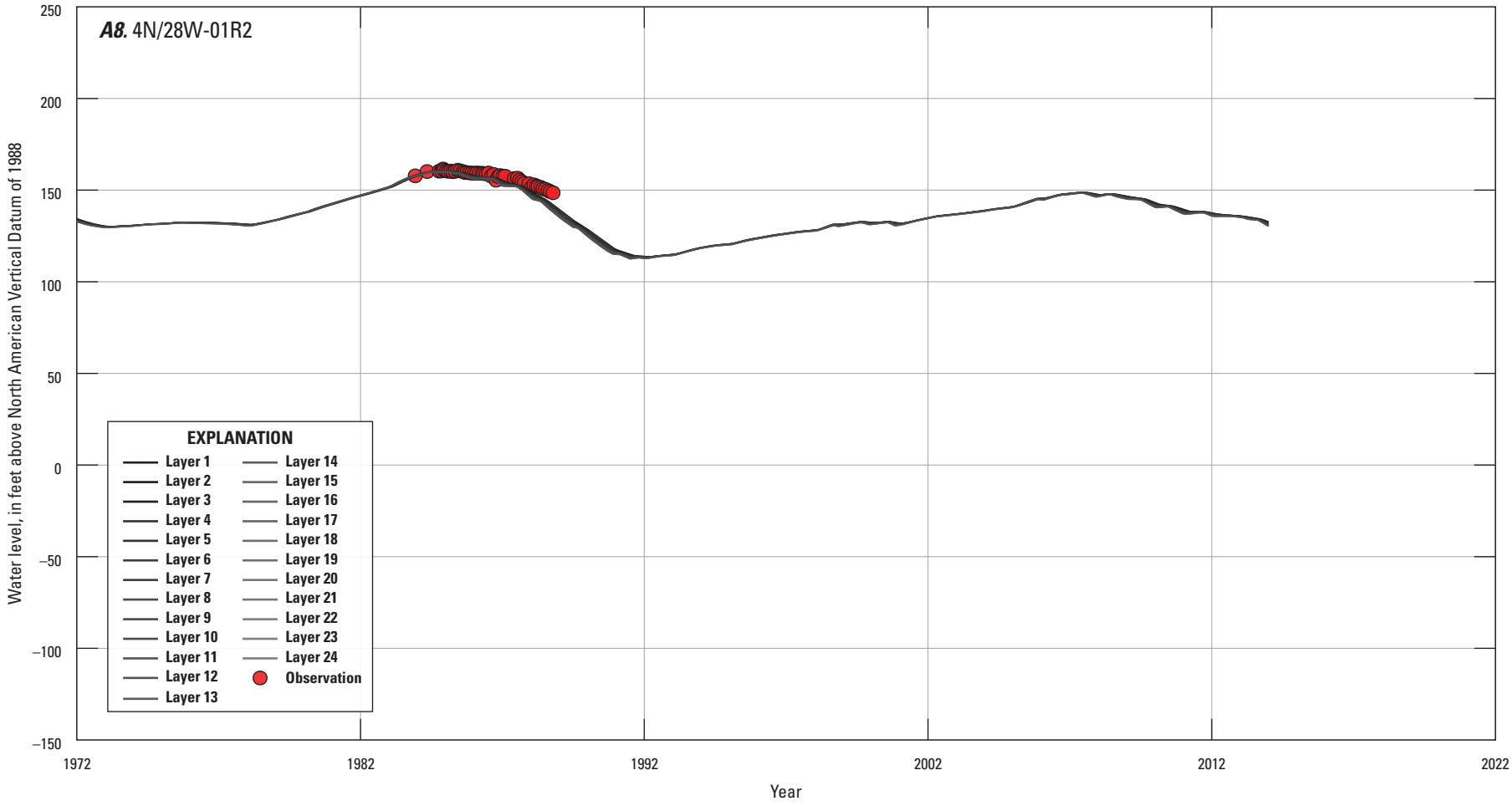

Figure 19. —Continued

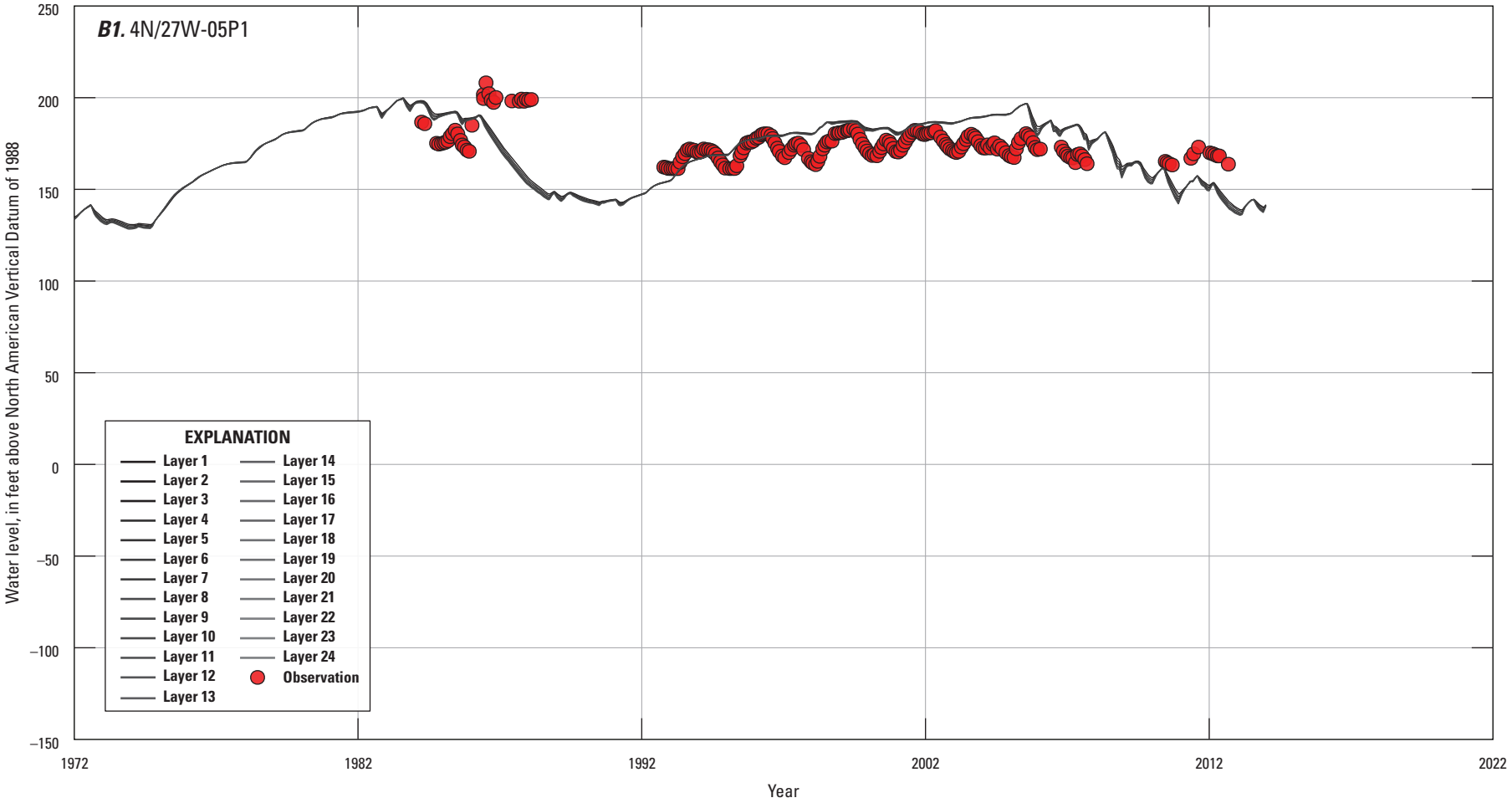

Figure 19. —Continued

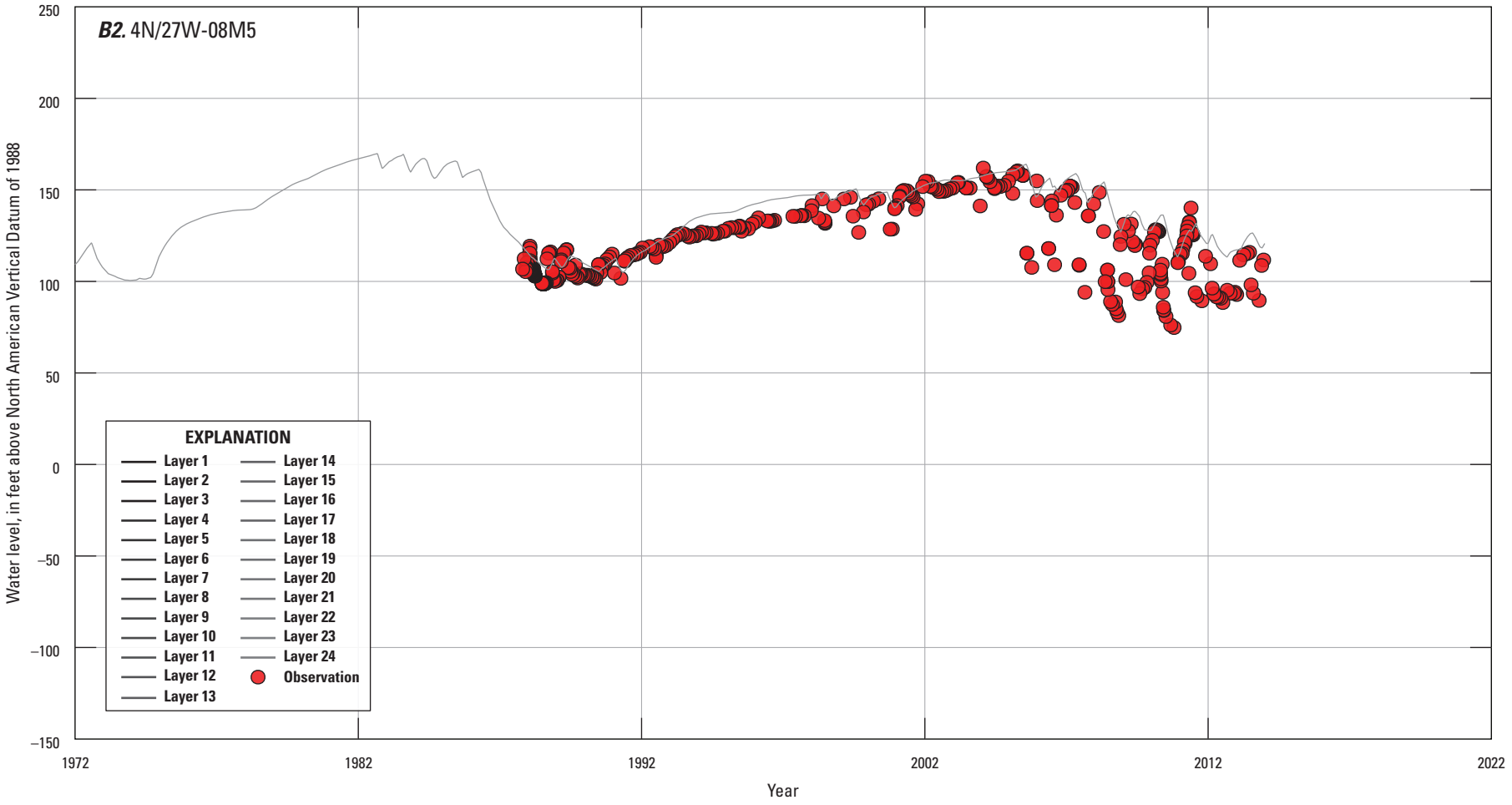

Figure 19. —Continued

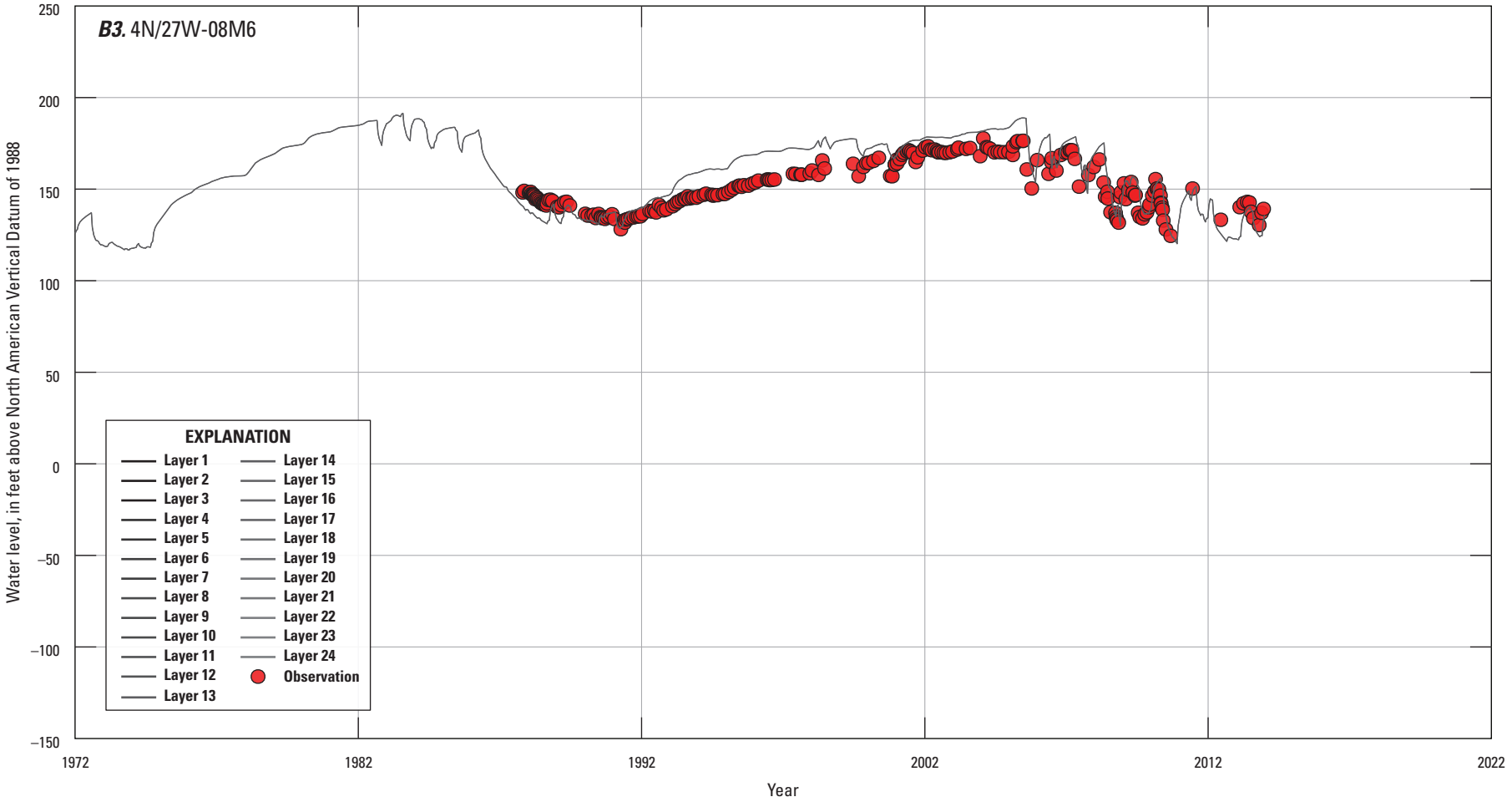

Figure 19. —Continued

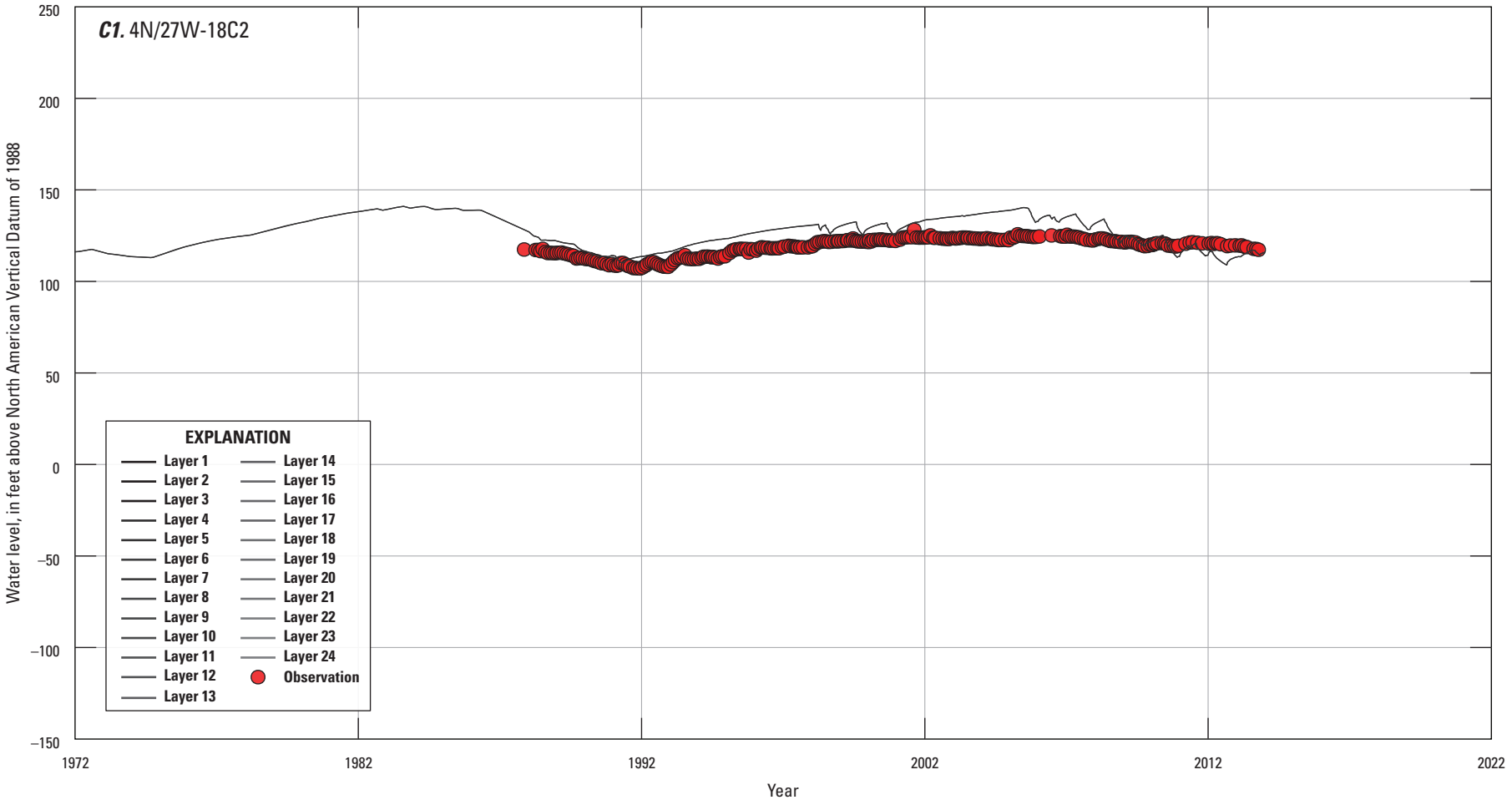

Figure 19. —Continued

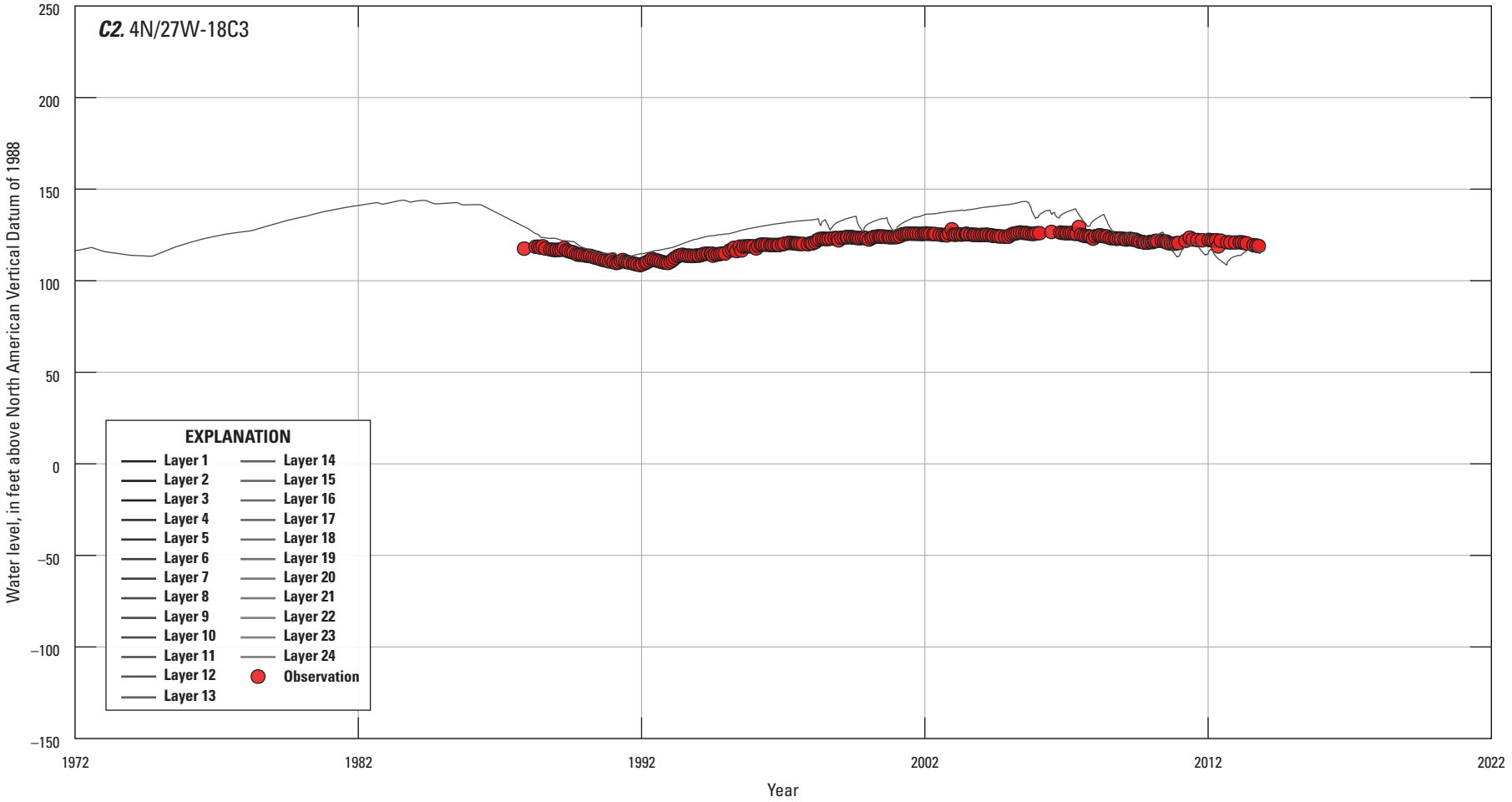

Figure 19. —Continued

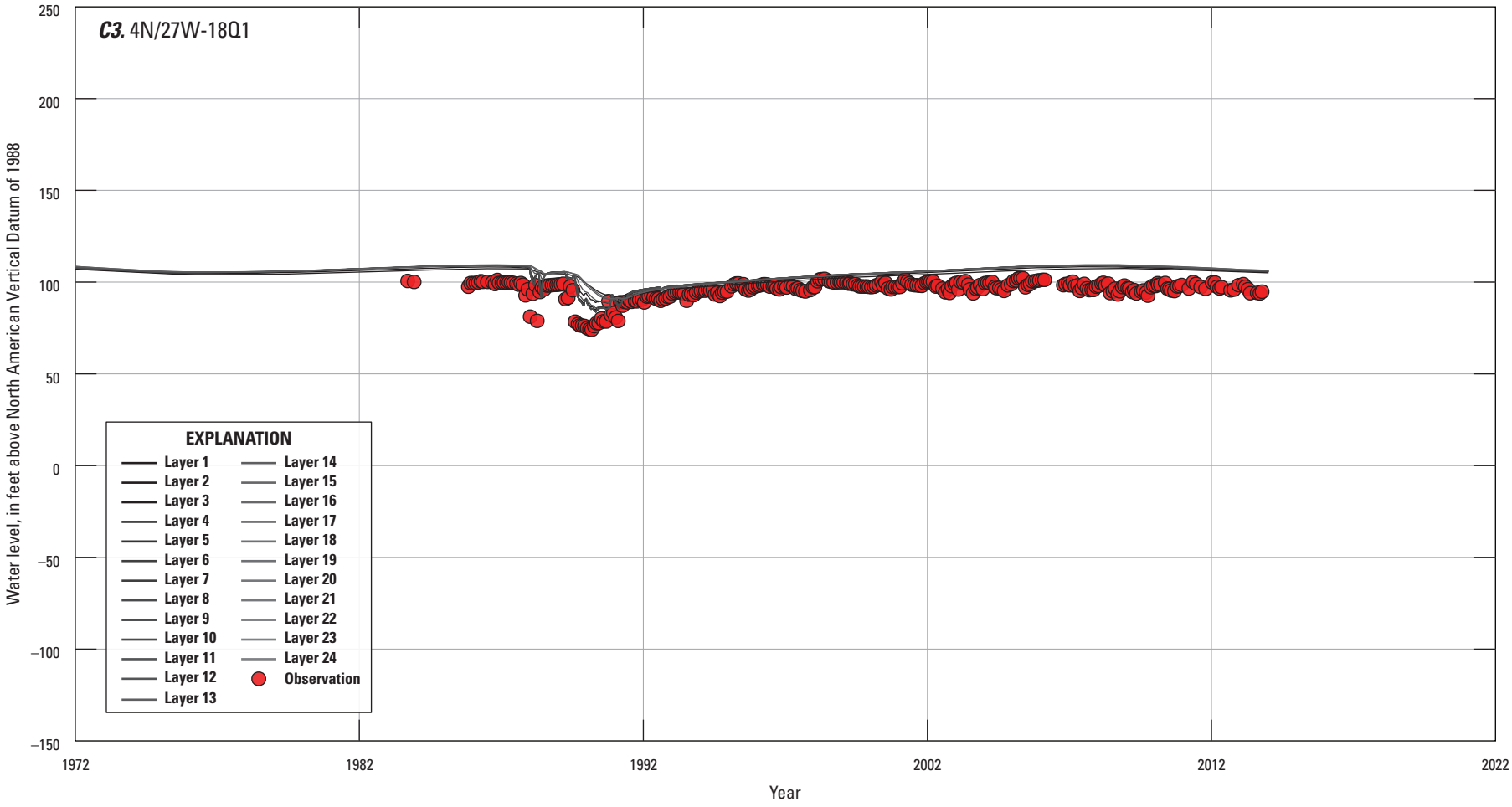

Figure 19. —Continued

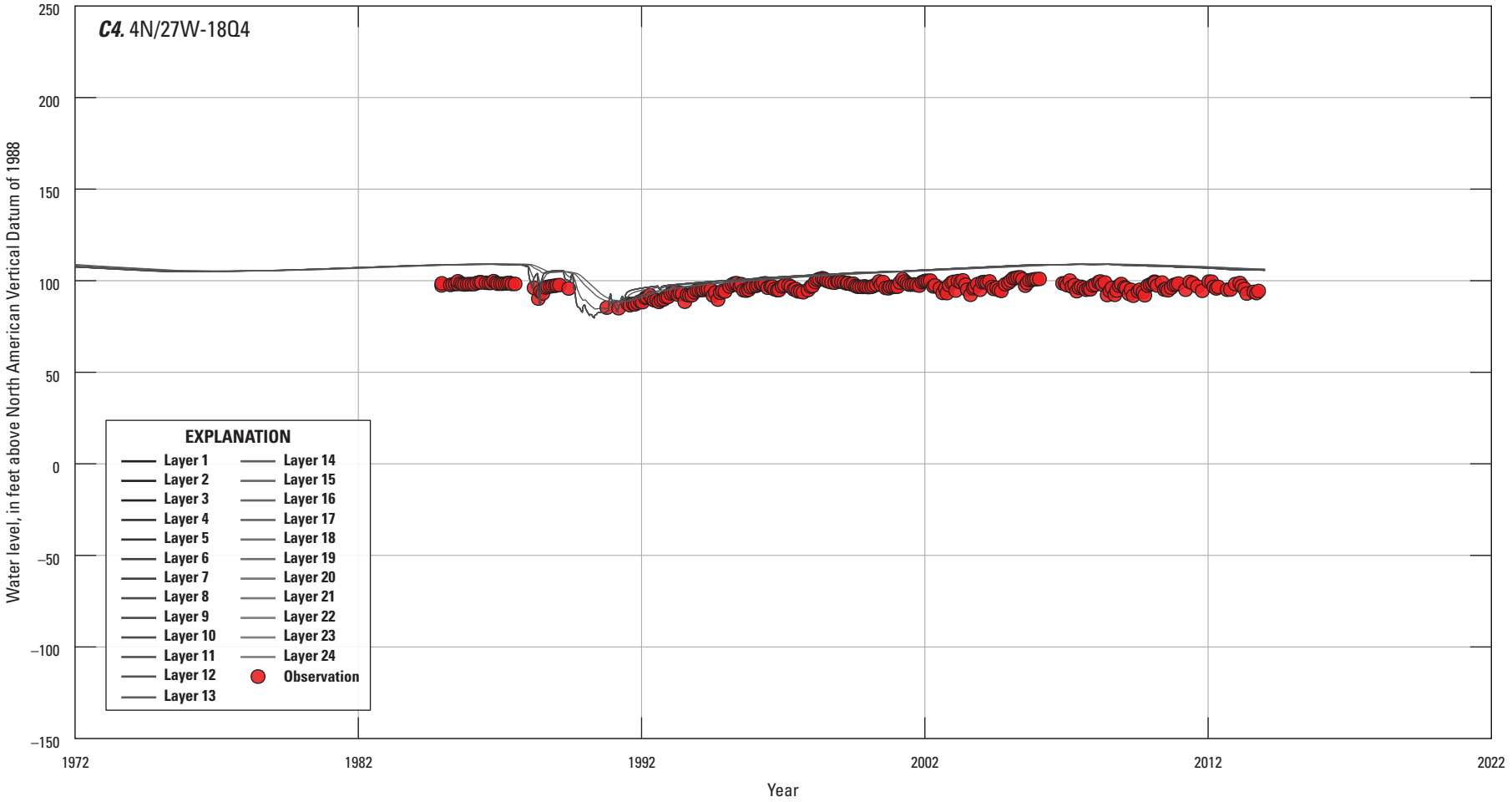

Figure 19. —Continued

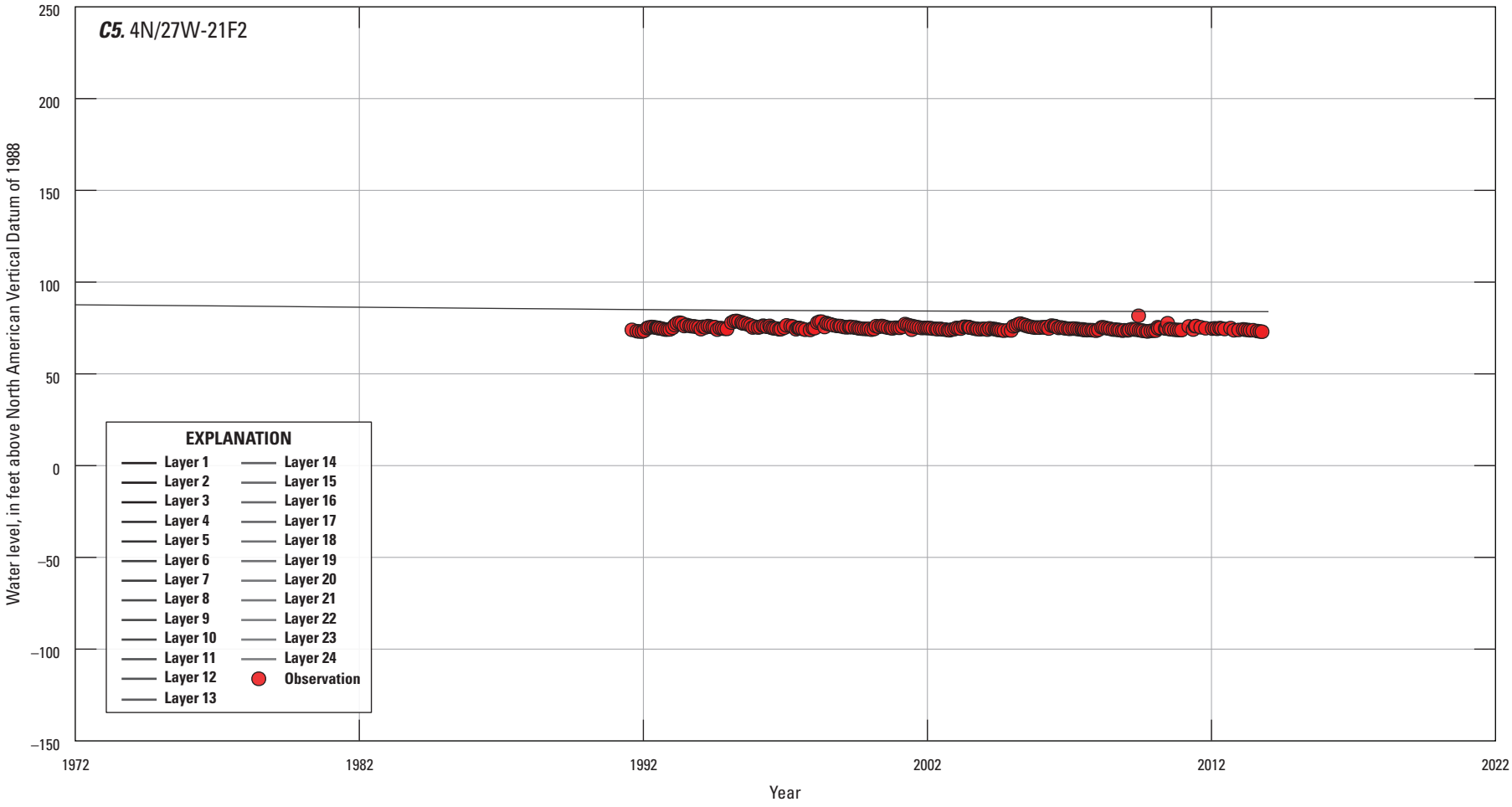

Figure 19. —Continued

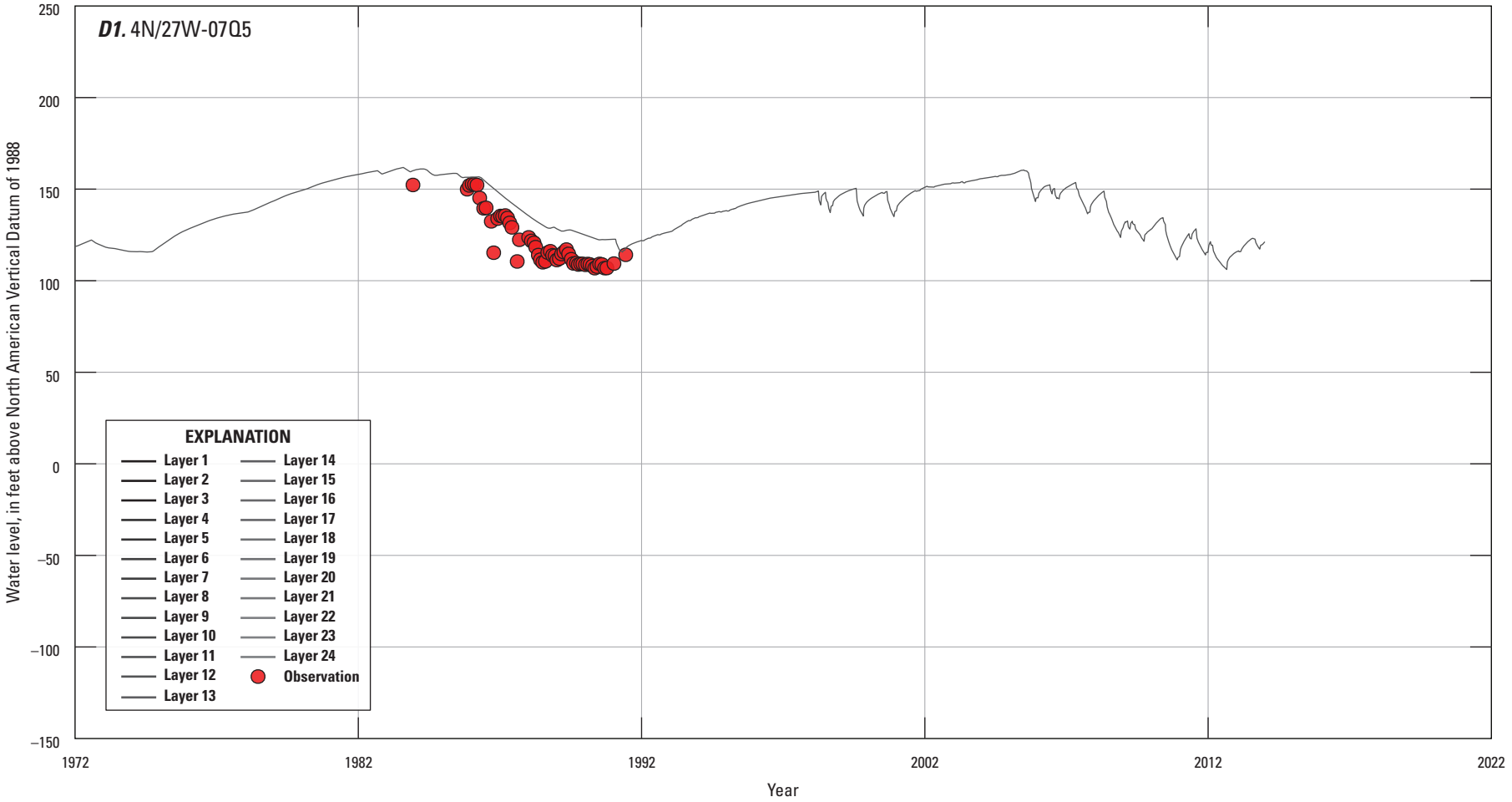

Figure 19. —Continued

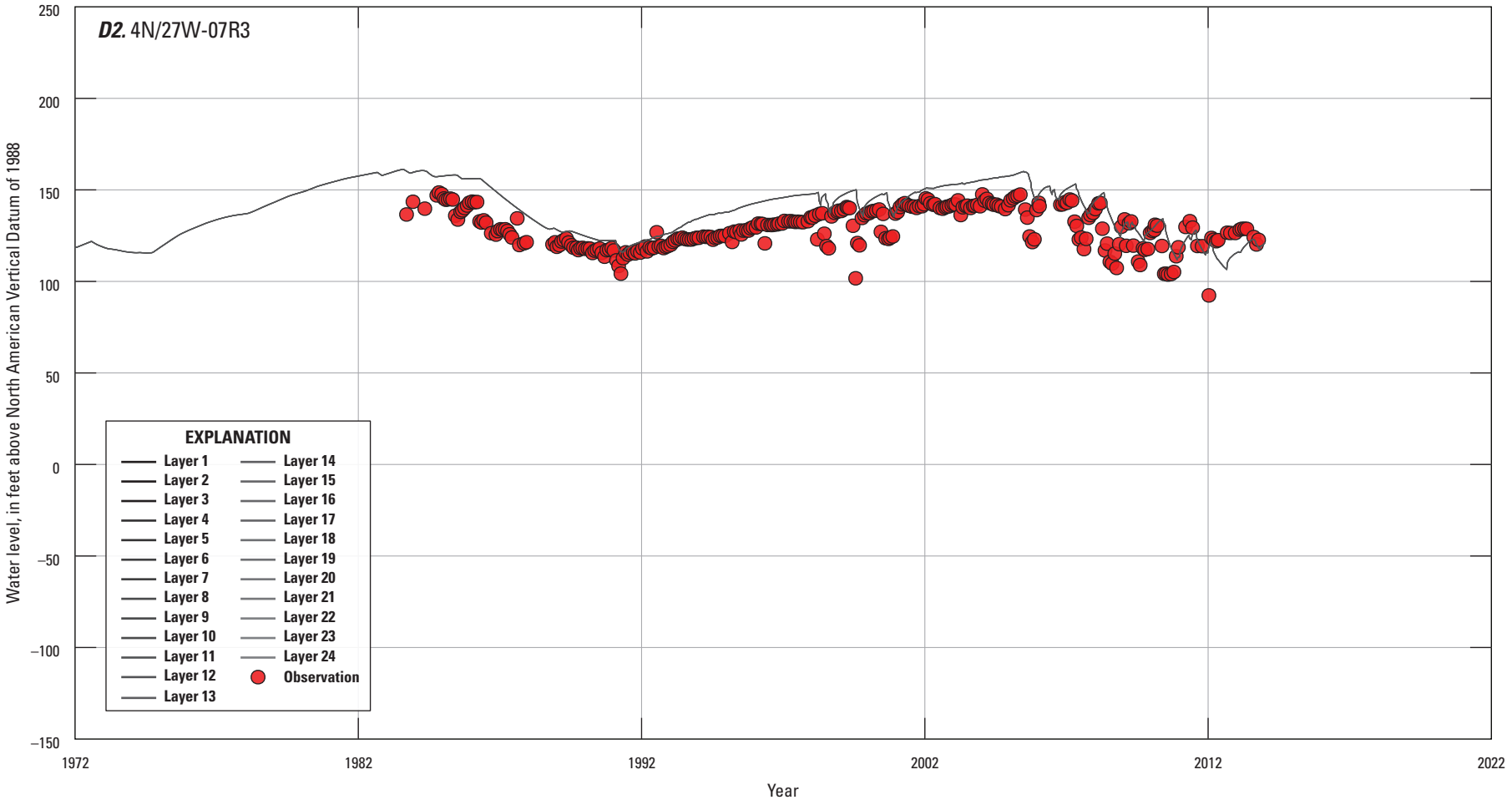

Figure 19. —Continued

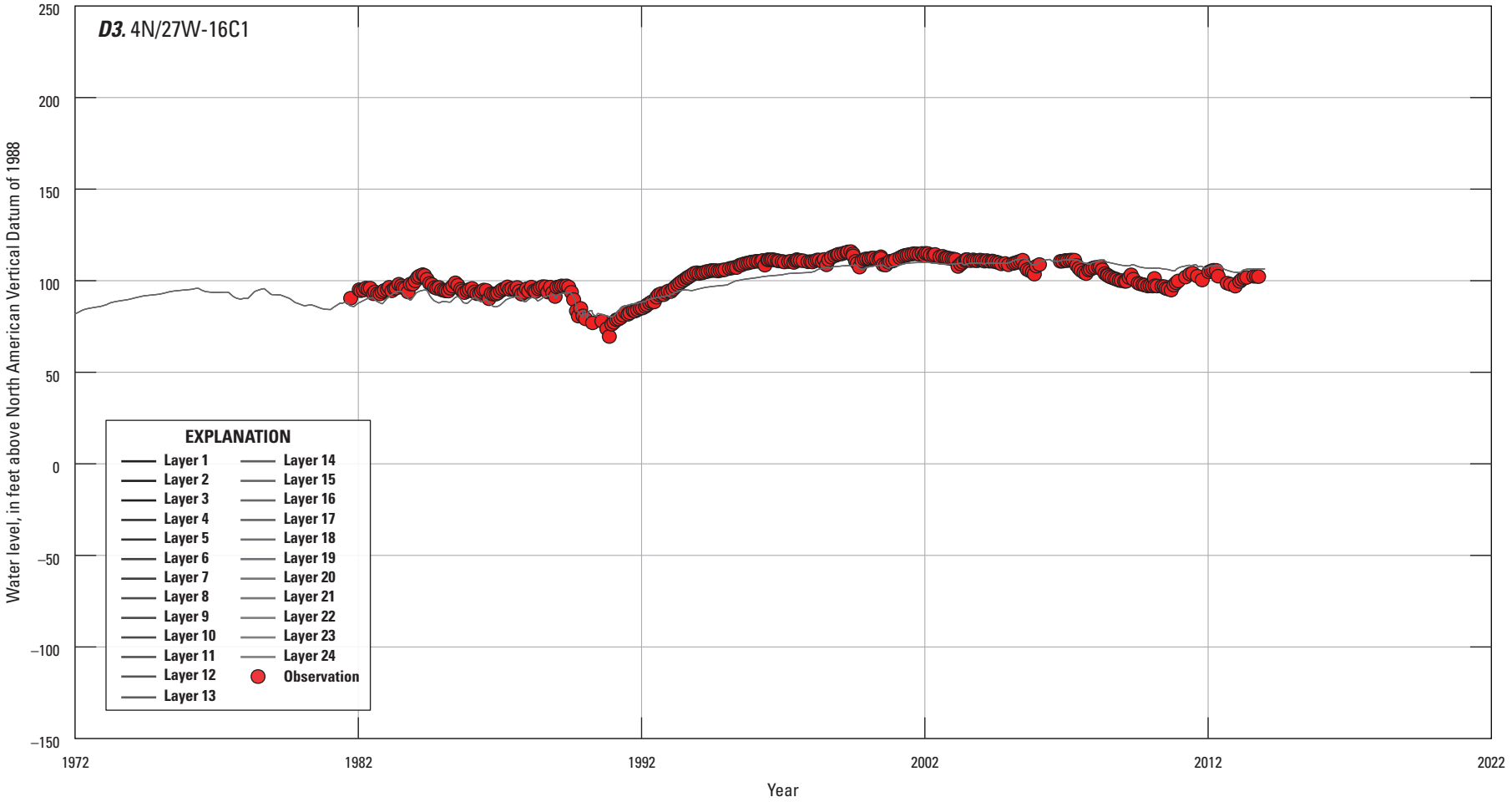

Figure 19. —Continued

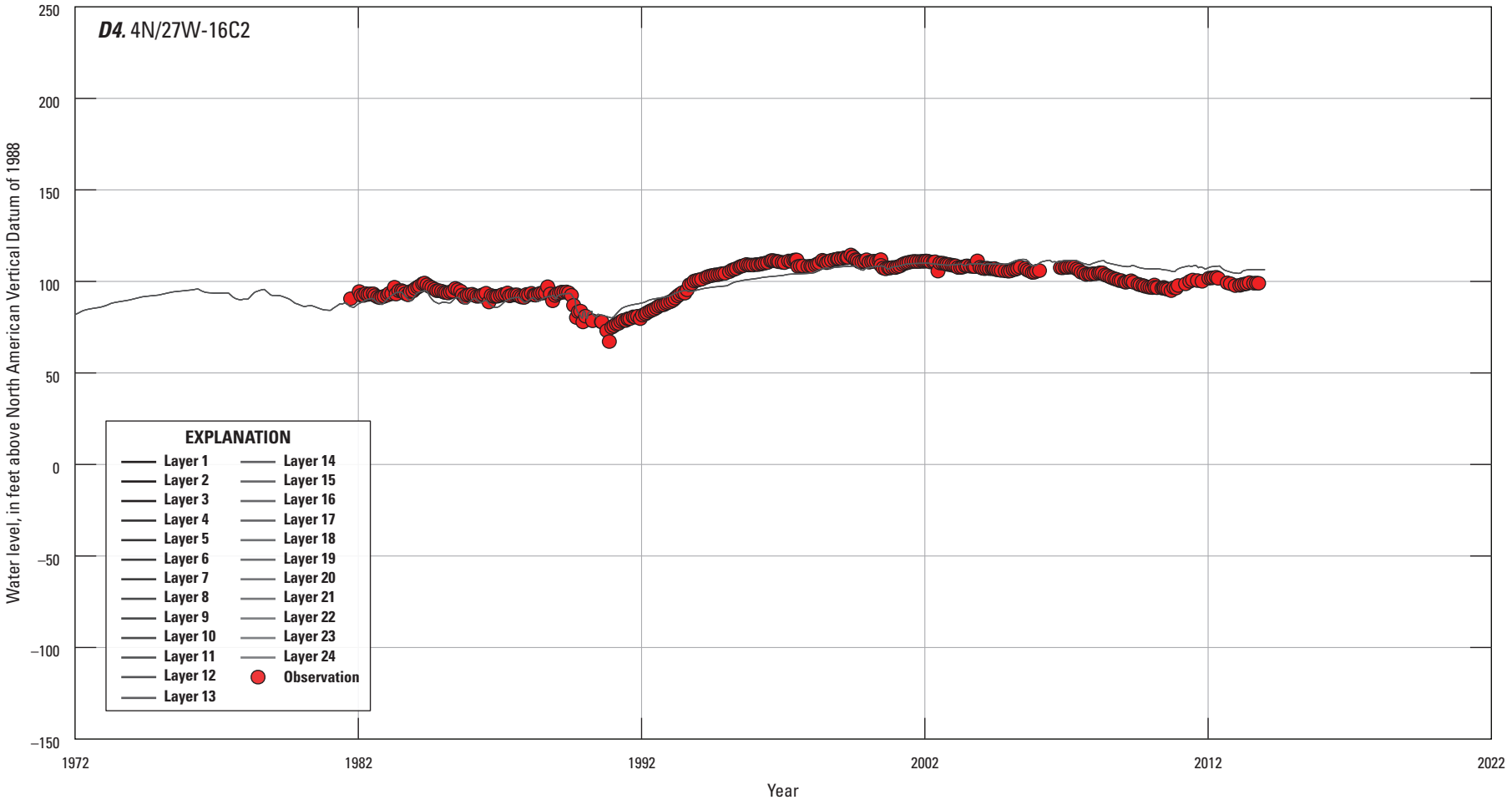

Figure 19. —Continued

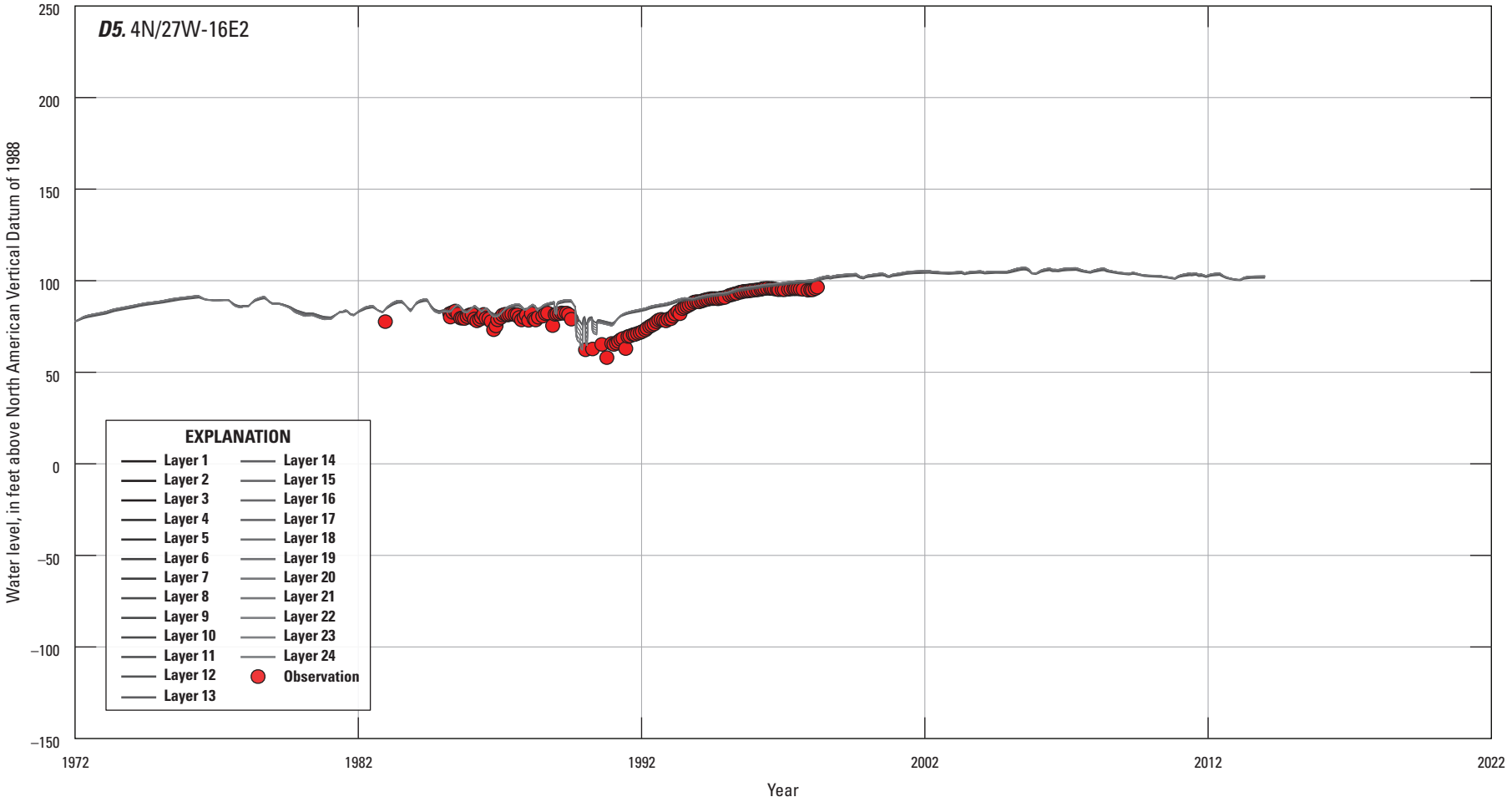

Figure 19. —Continued

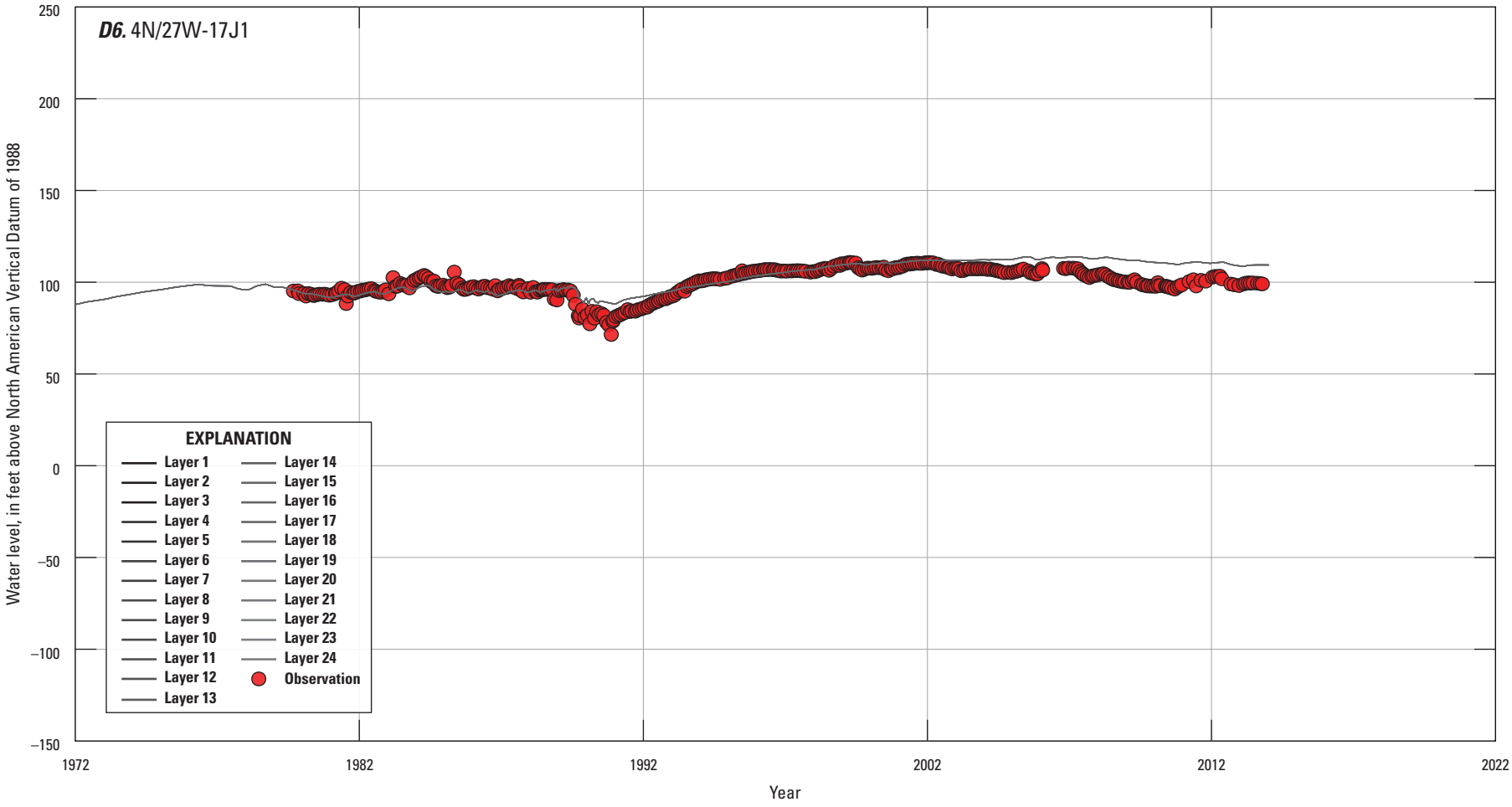

Figure 19. —Continued

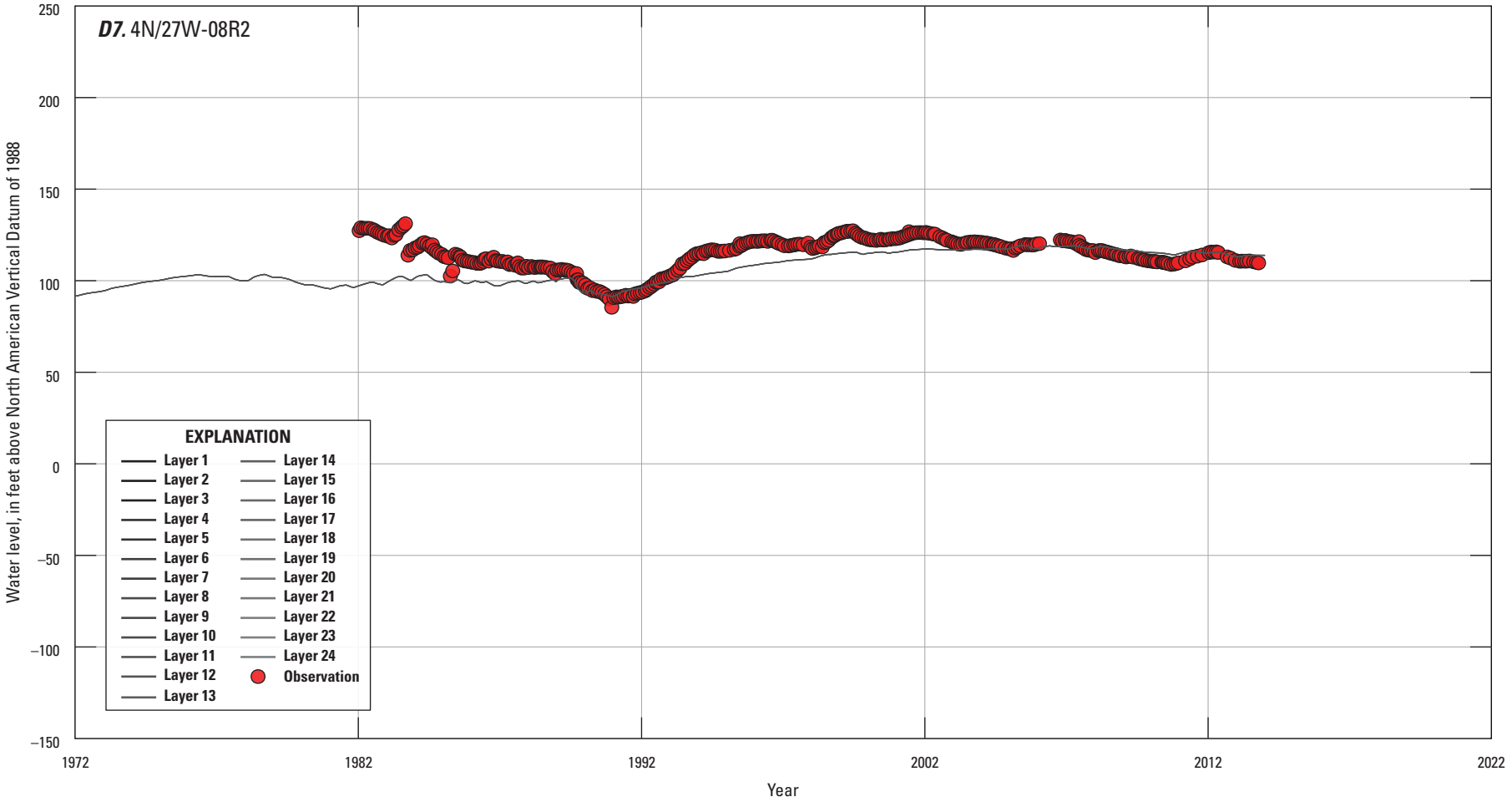

Figure 19. —Continued

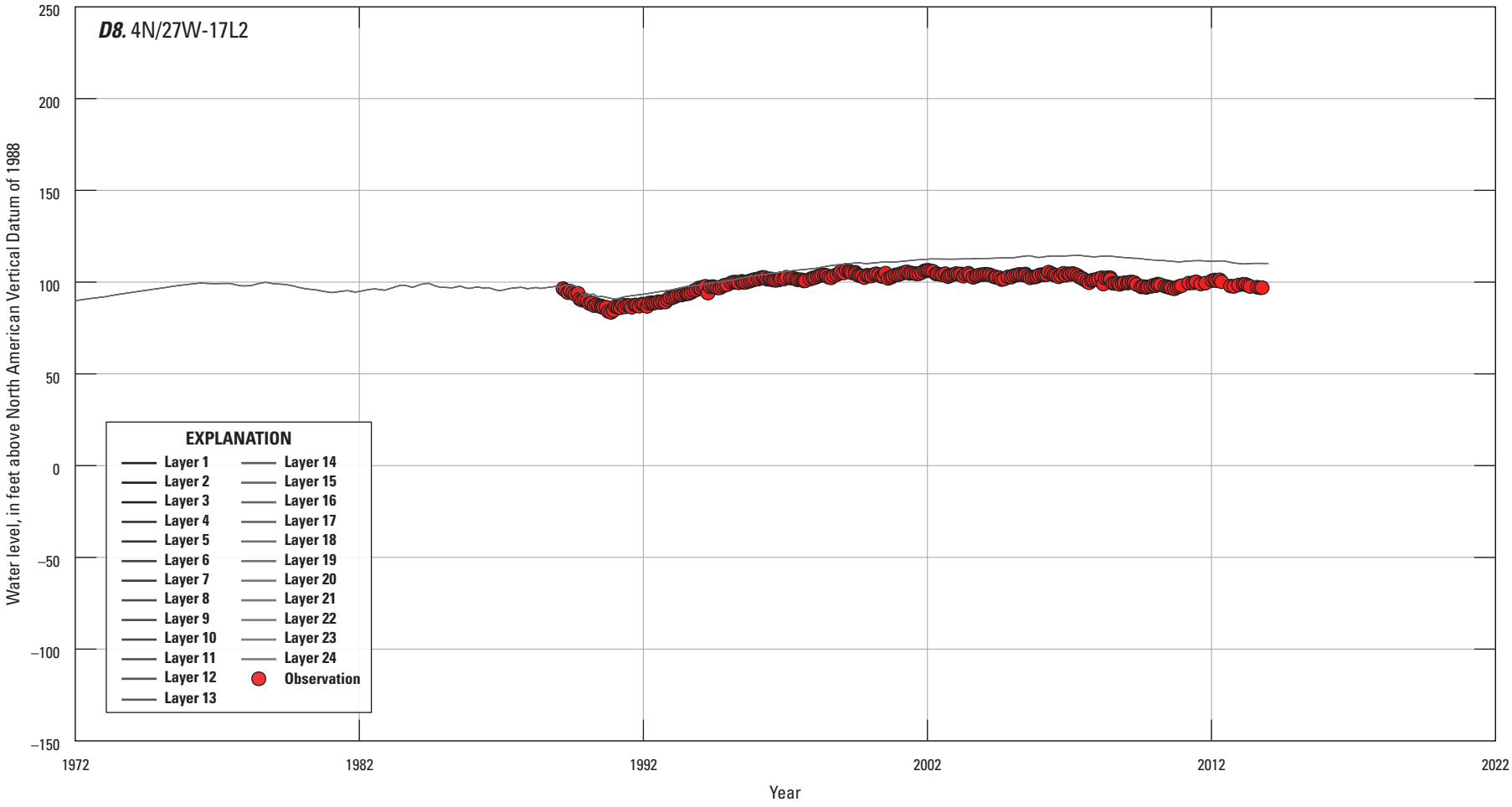

Figure 19. —Continued

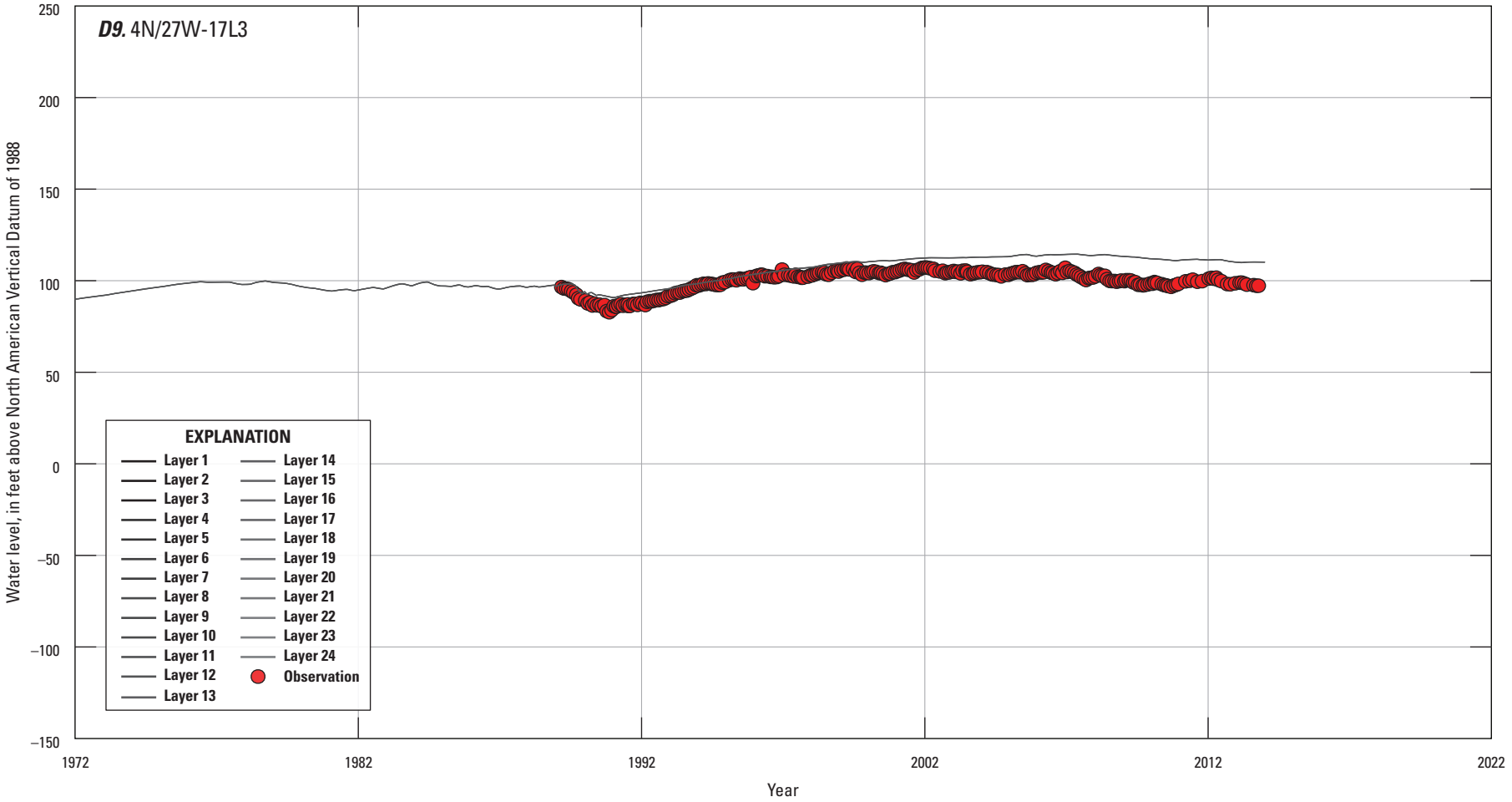

Figure 19. —Continued

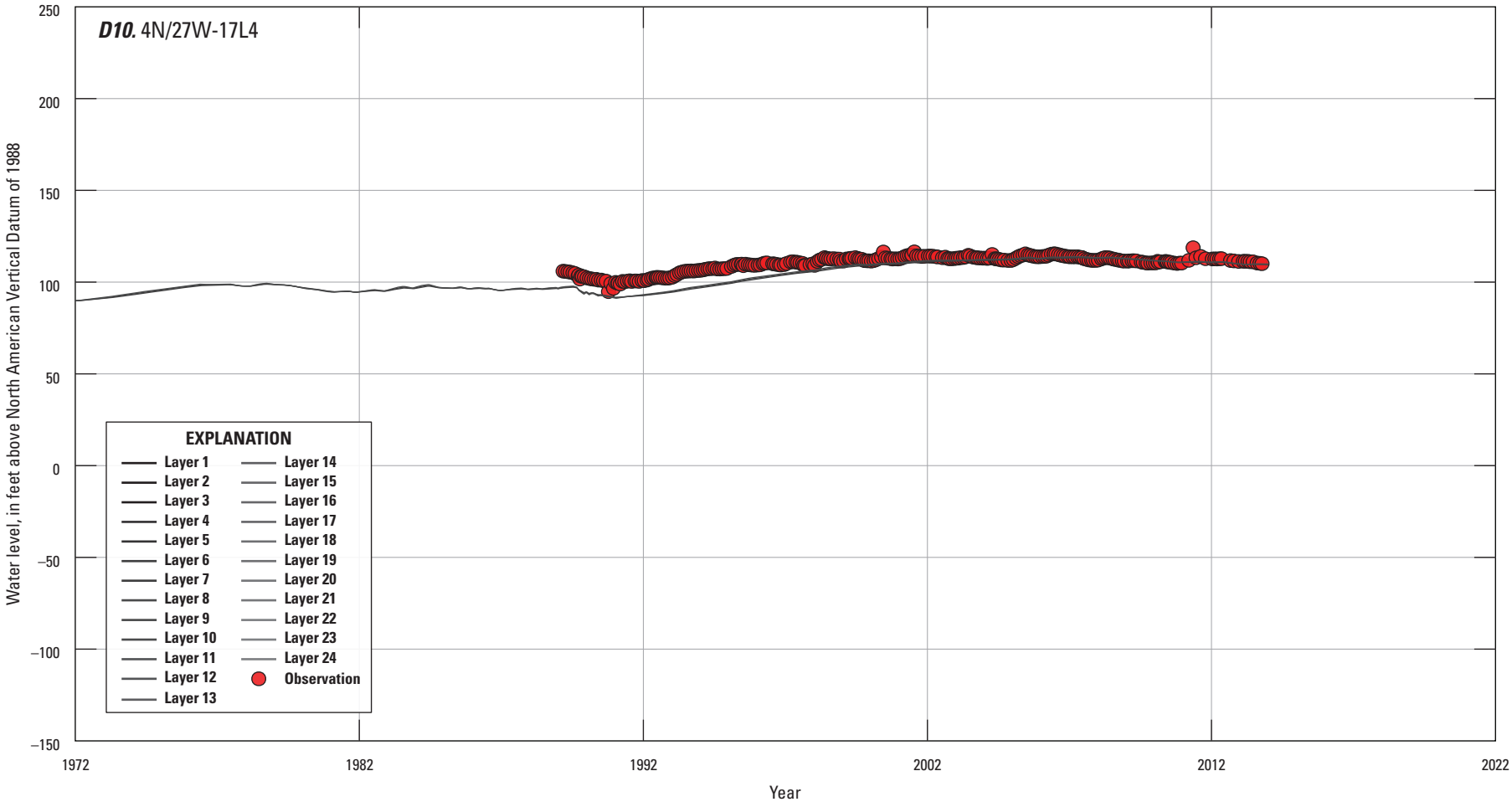

Figure 19. —Continued

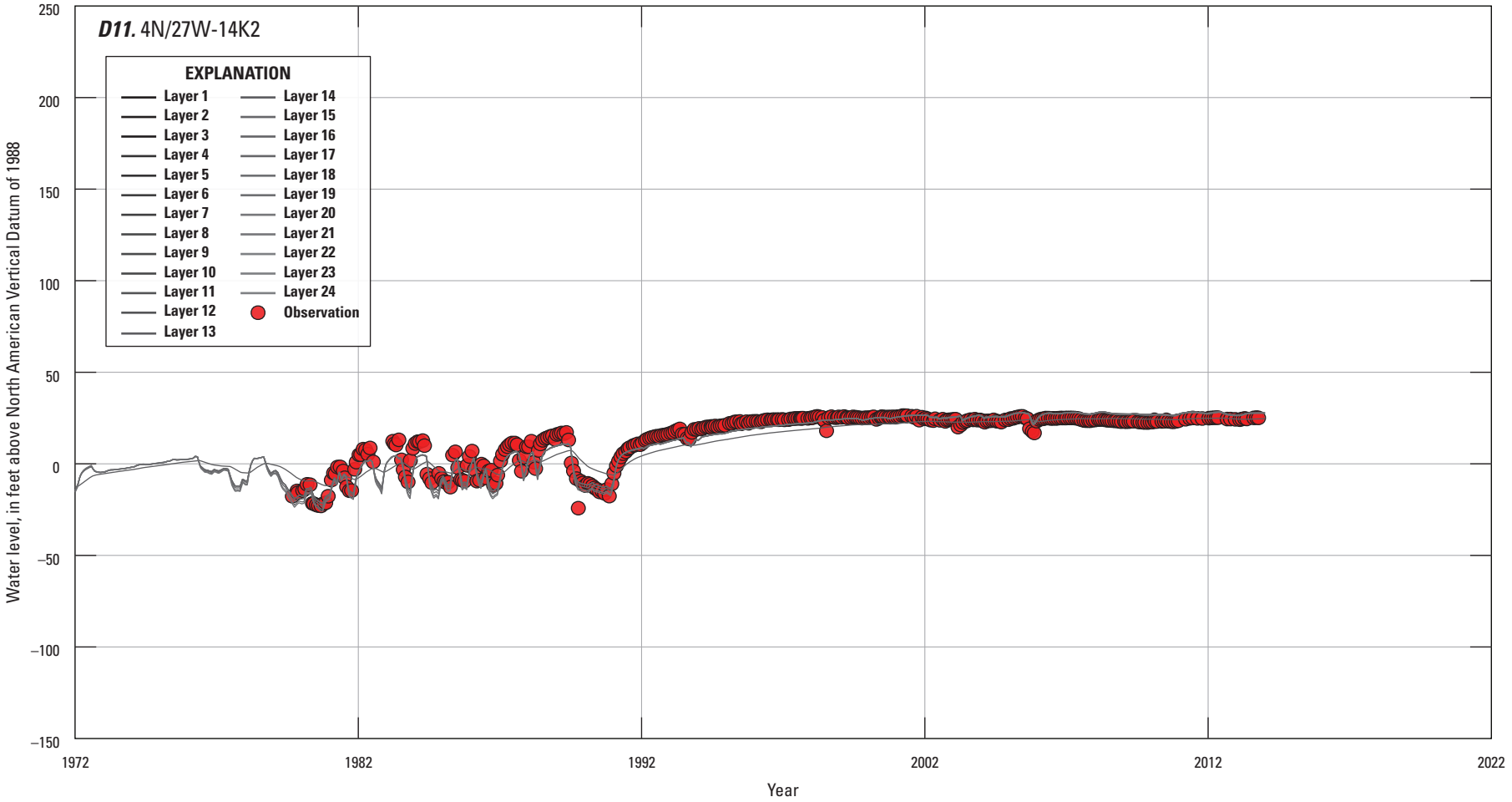

Figure 19. —Continued

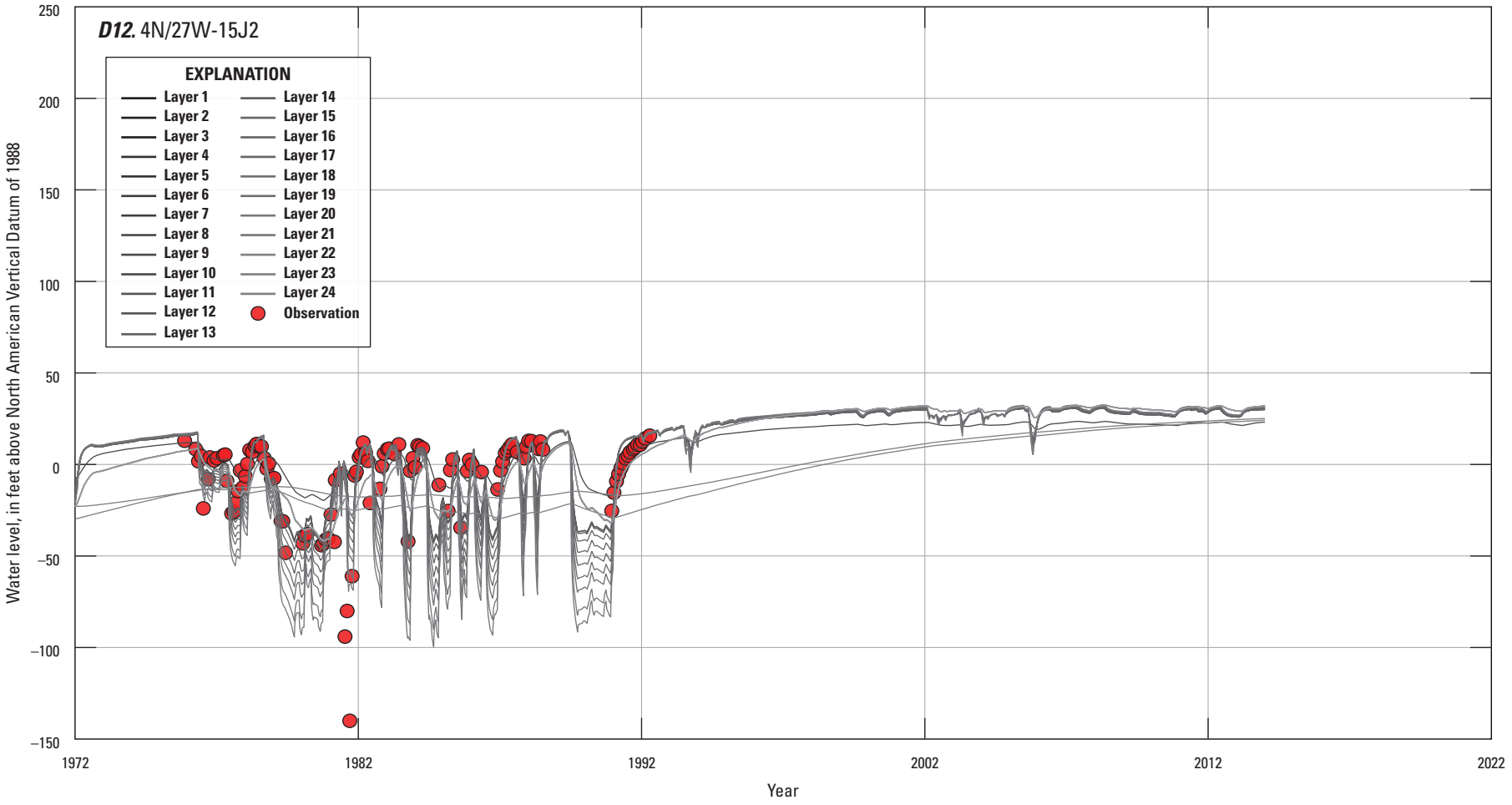

Figure 19. —Continued

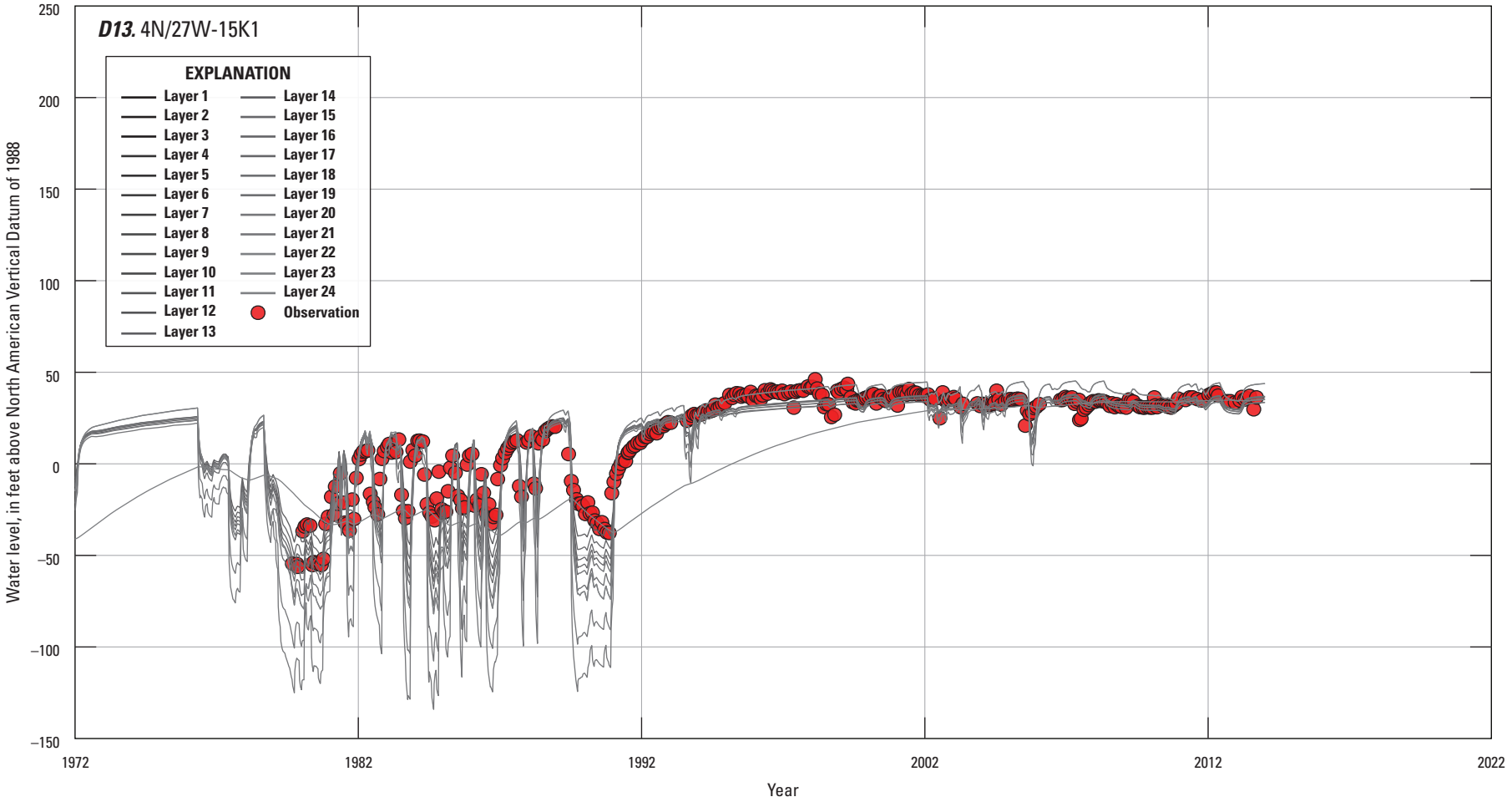

Figure 19. —Continued

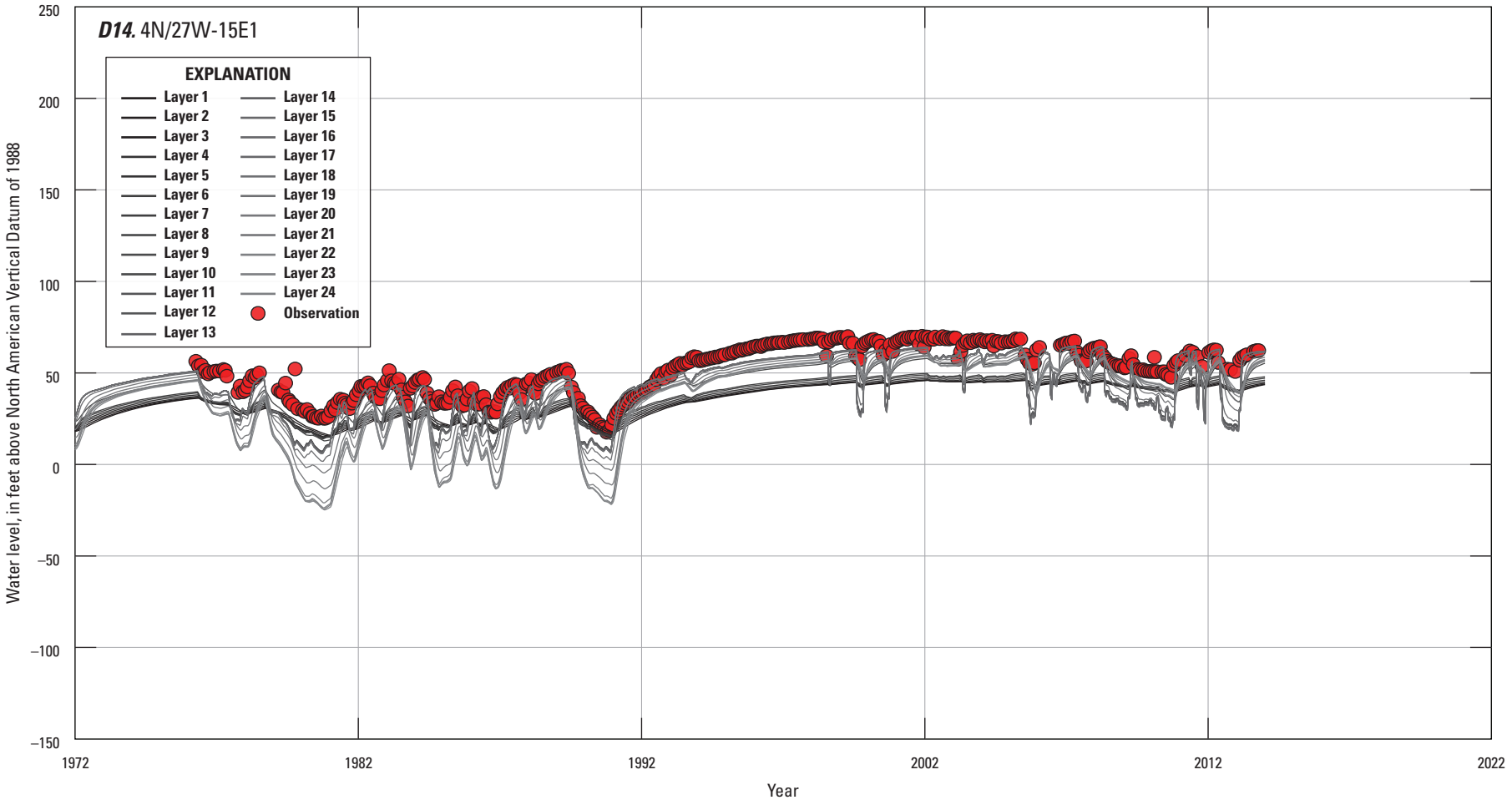

Figure 19. —Continued

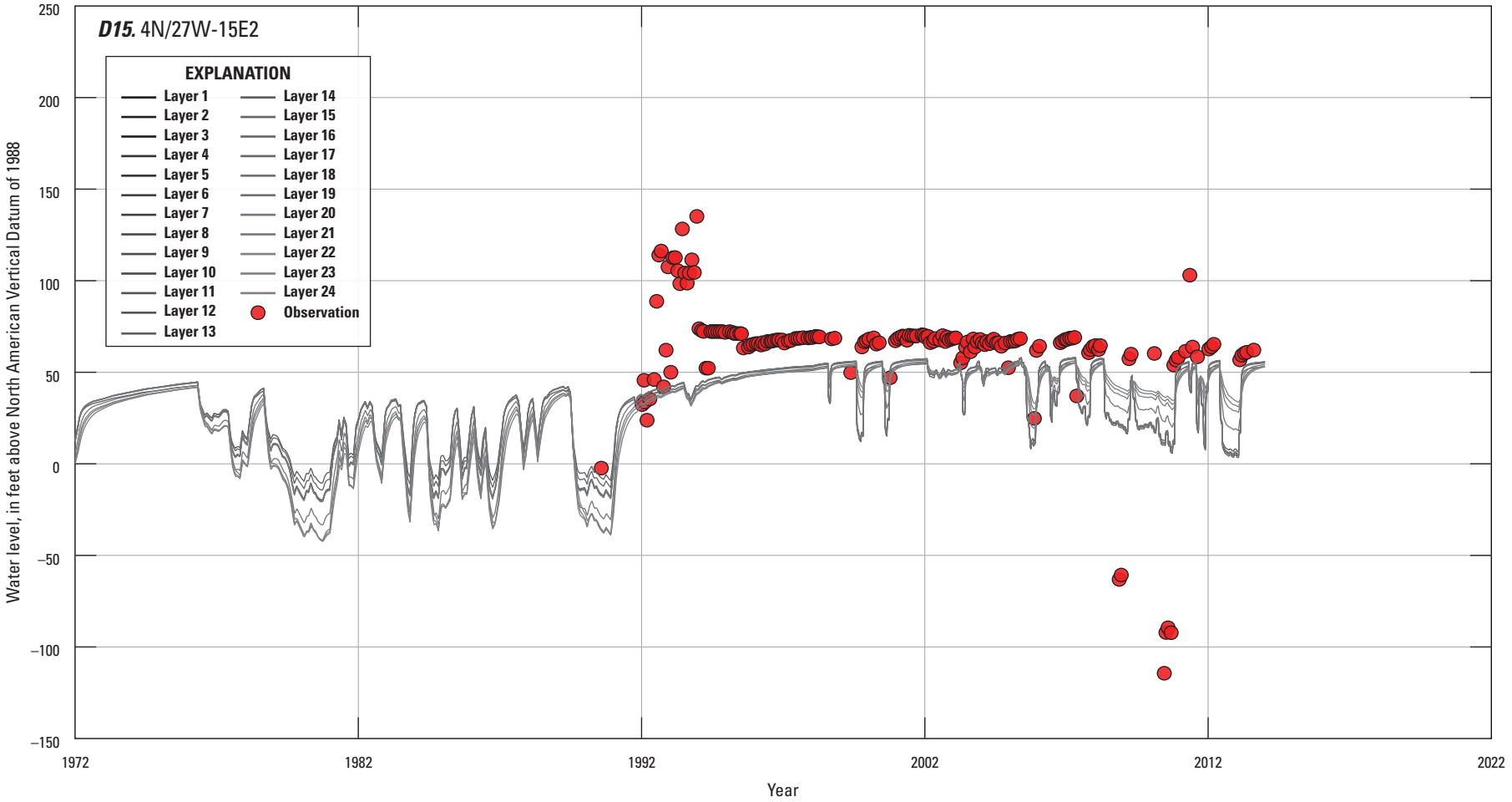

Figure 19. —Continued

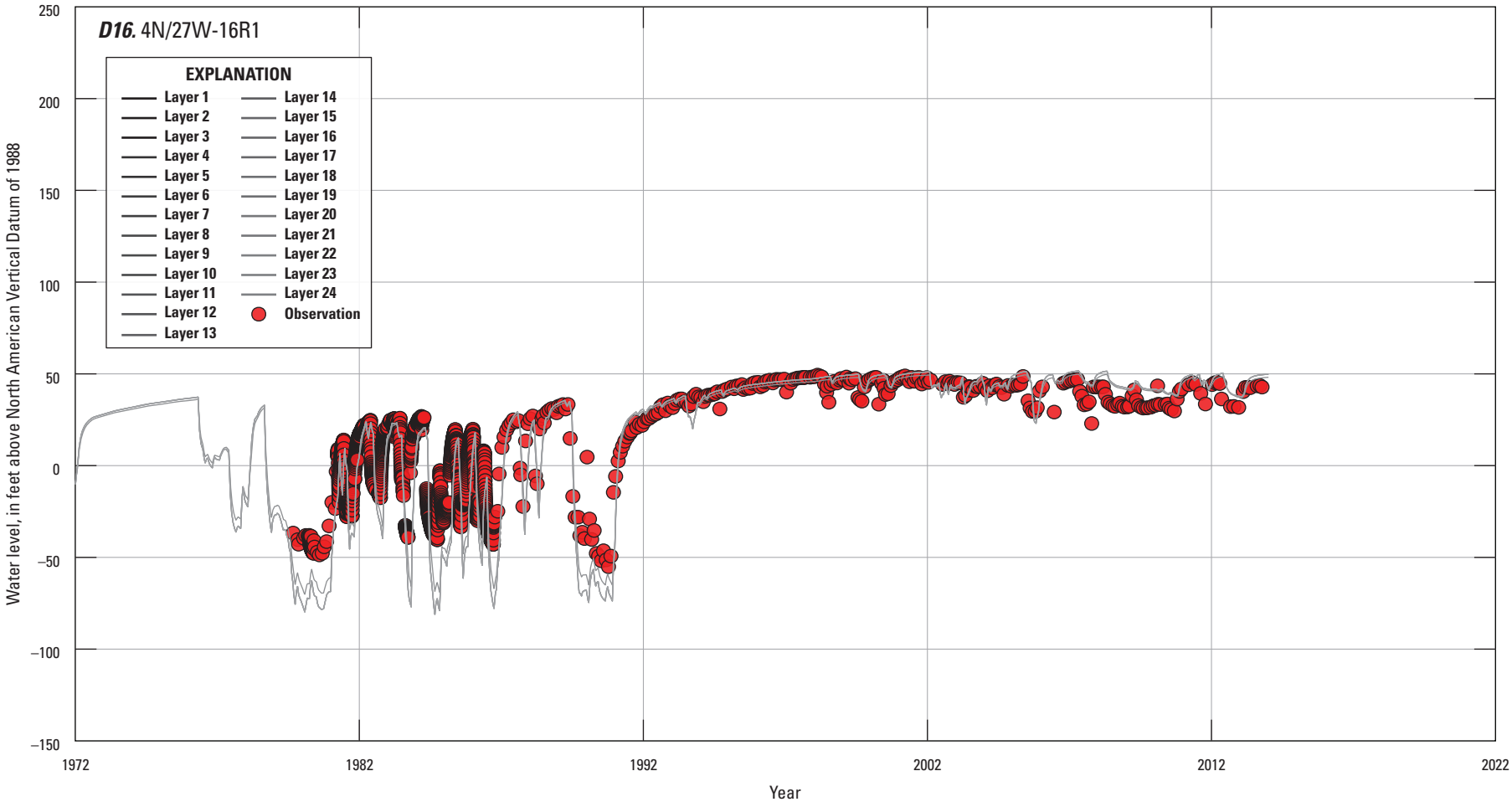

Figure 19. —Continued

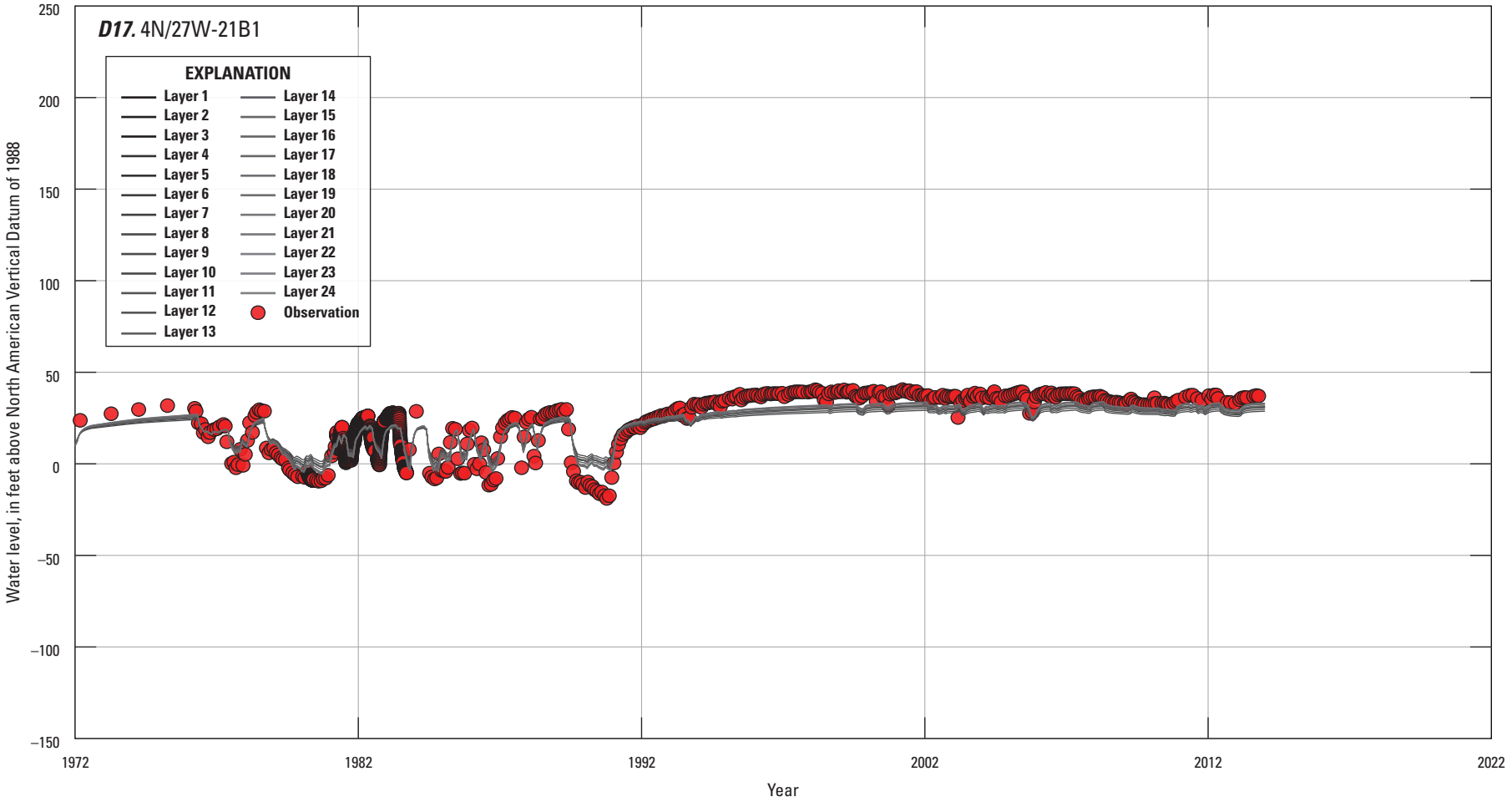

Figure 19. —Continued

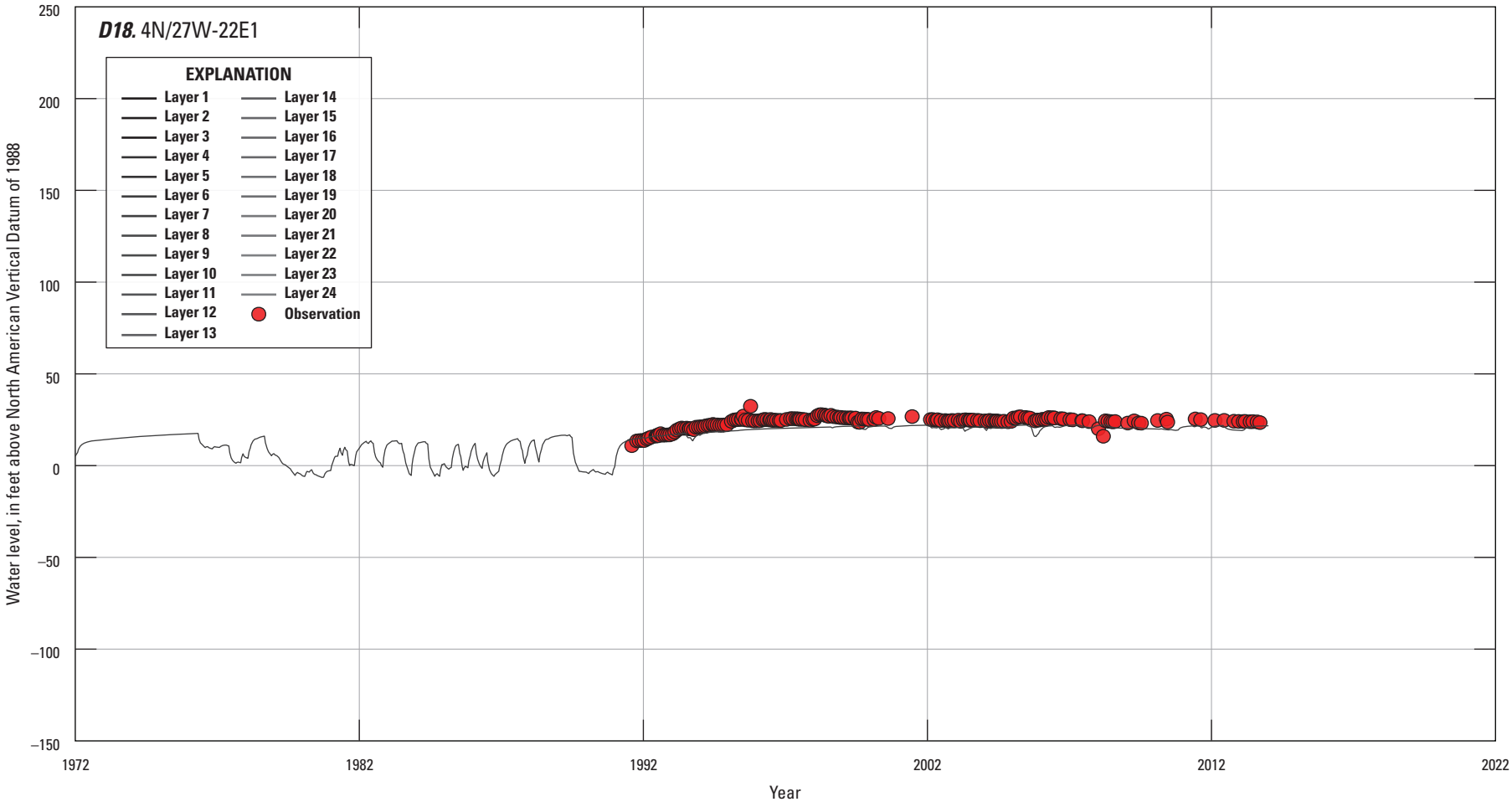

Figure 19. —Continued

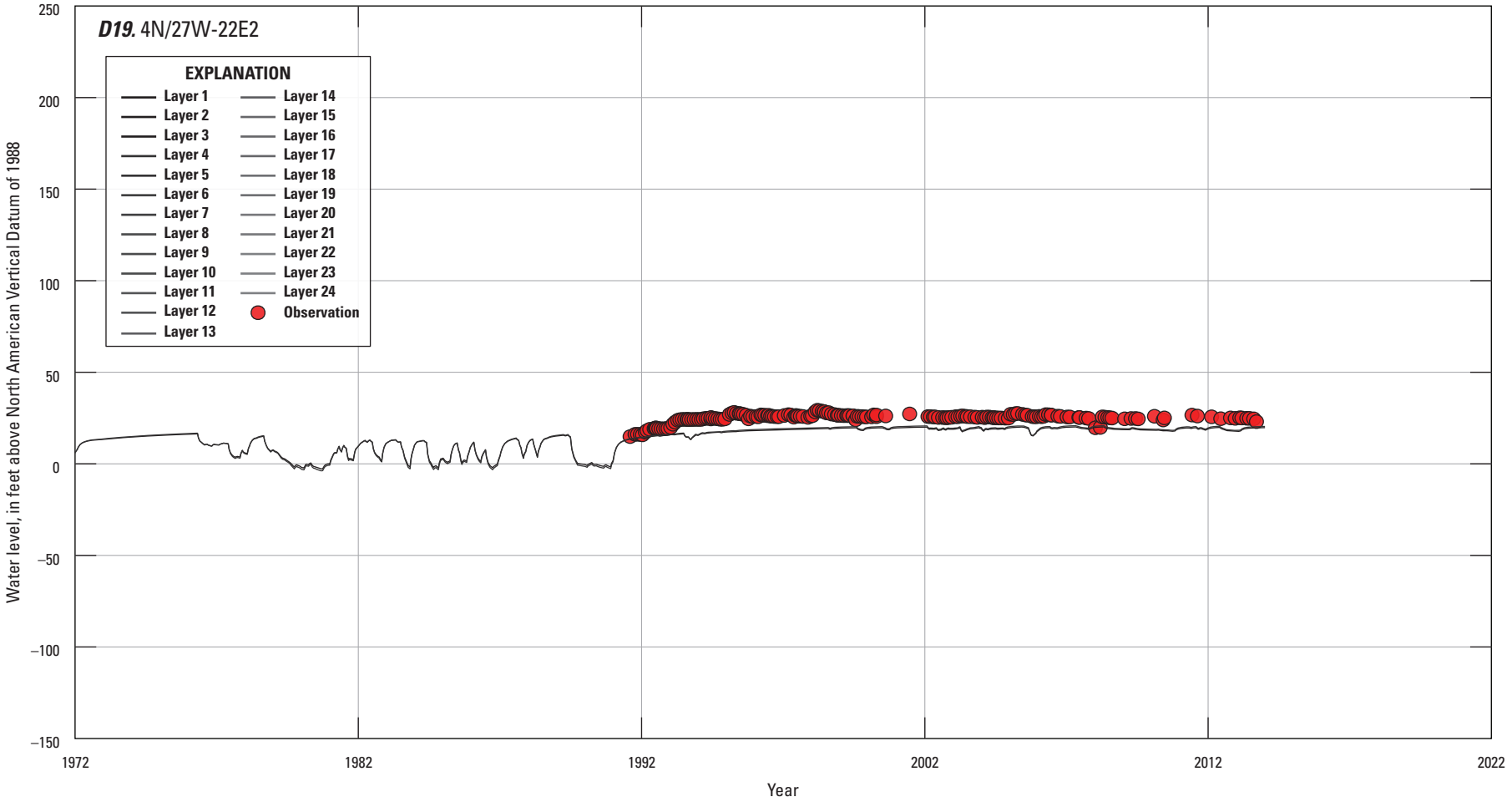

Figure 19. —Continued

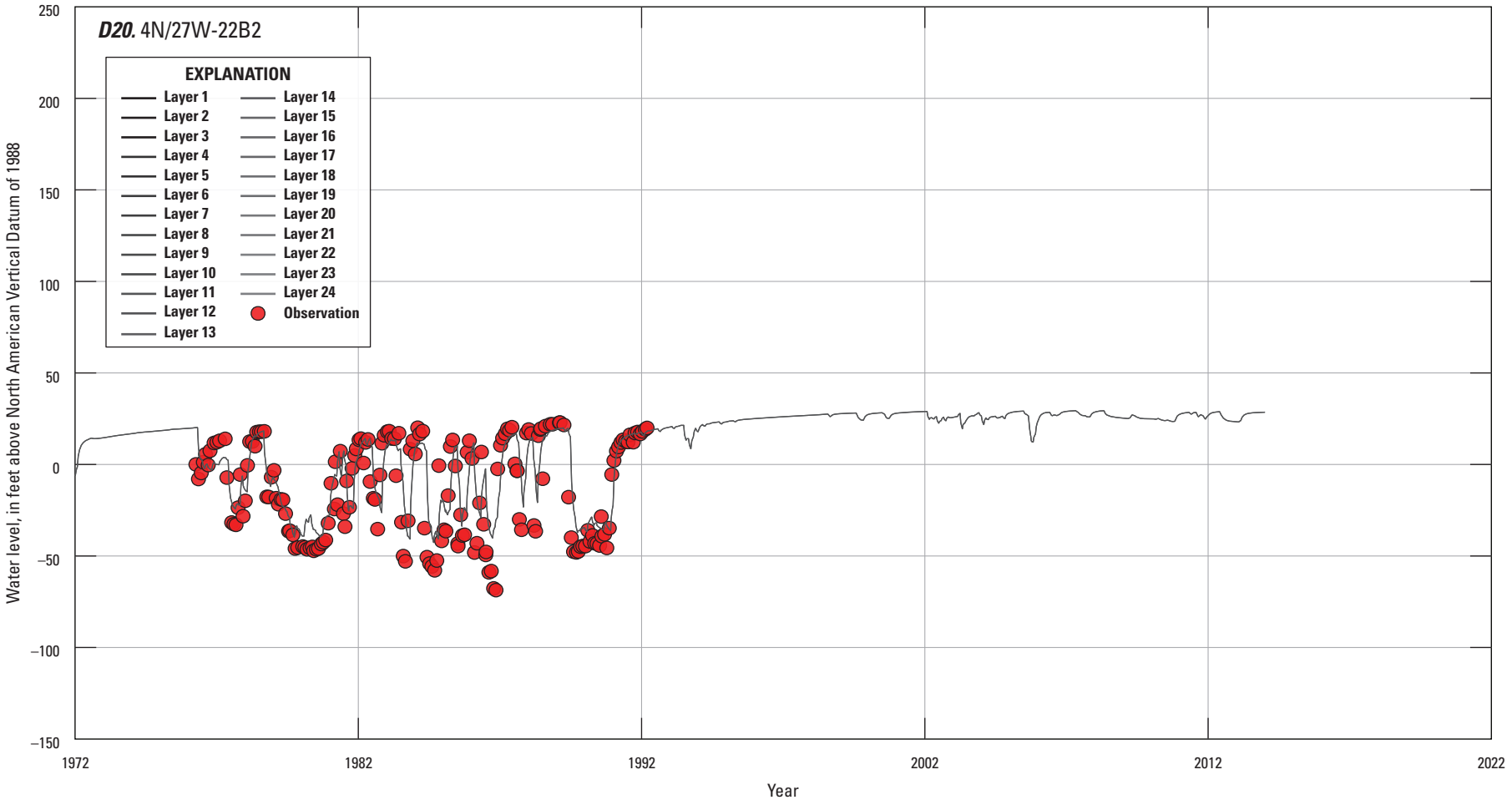

Figure 19. —Continued

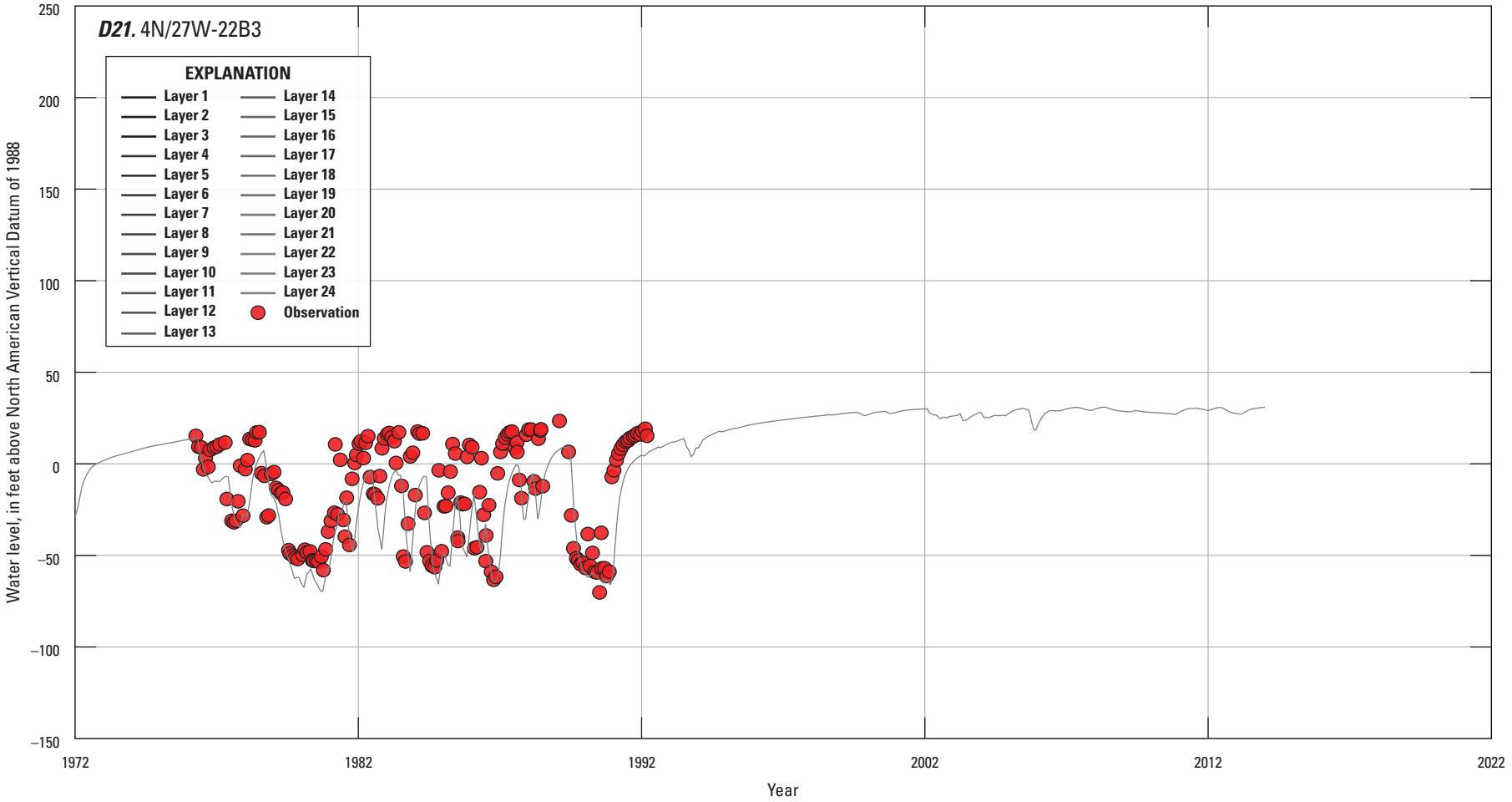

Figure 19. —Continued

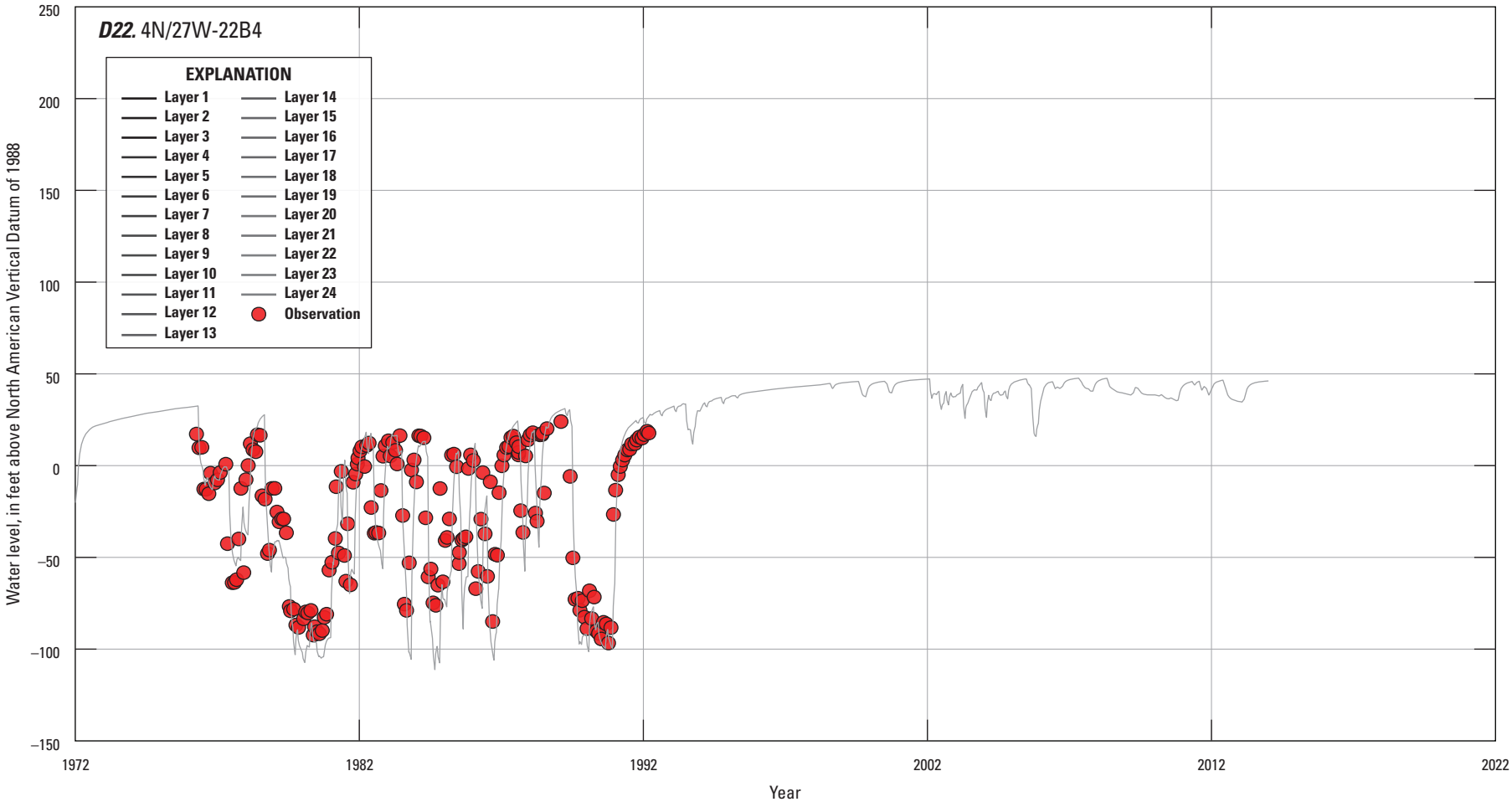

Figure 19. —Continued

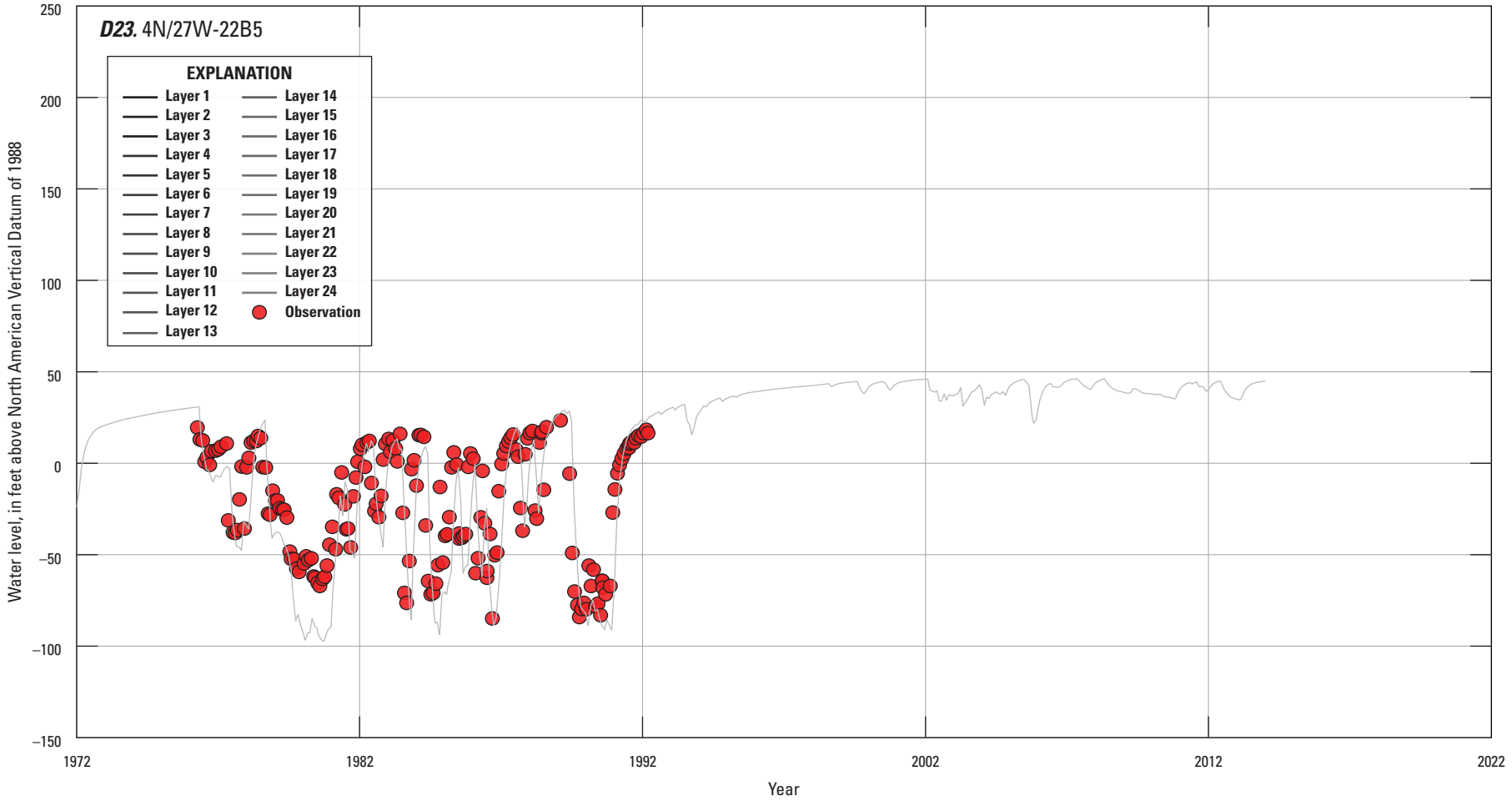

Figure 19. —Continued

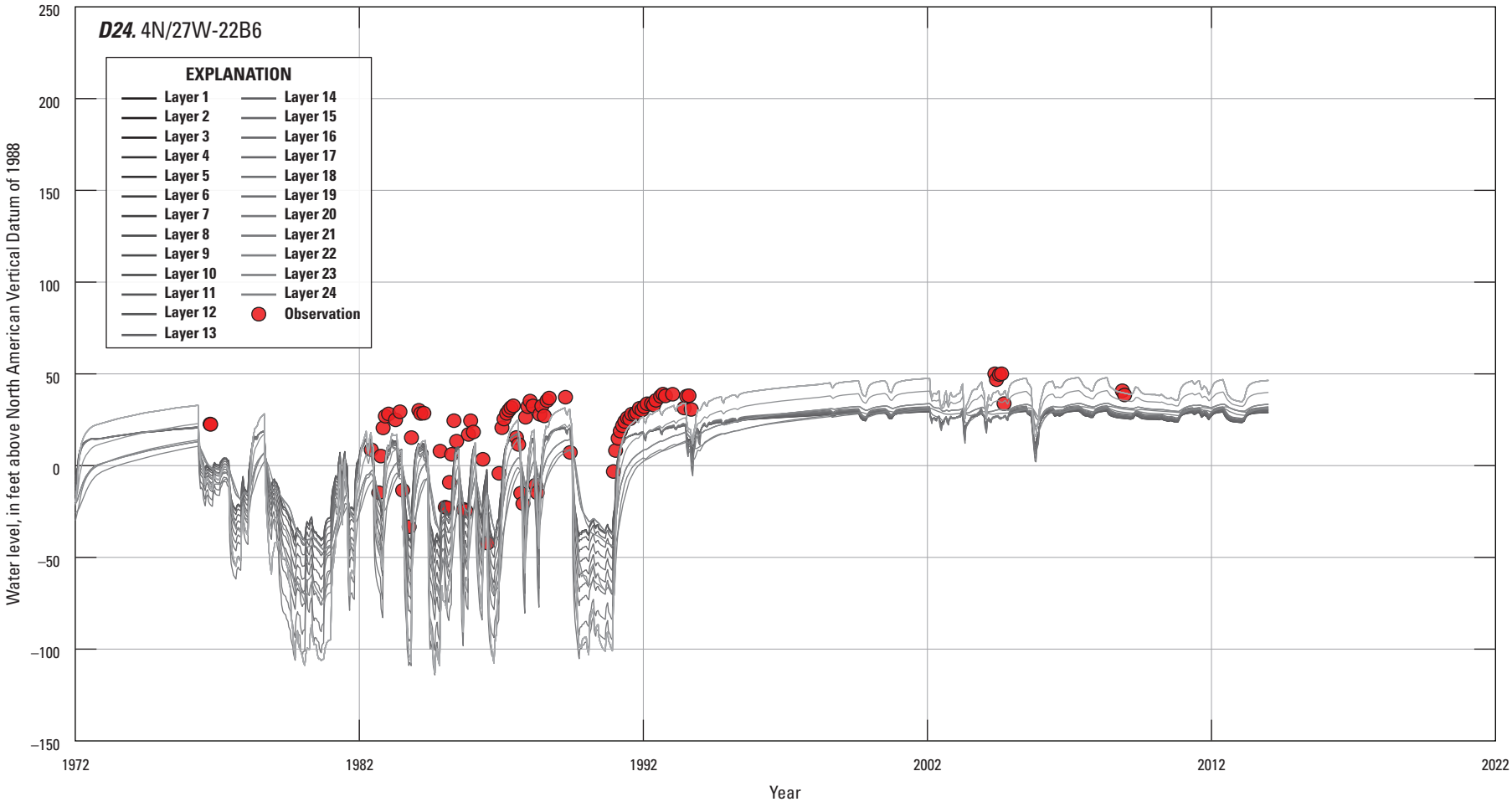

Figure 19. —Continued

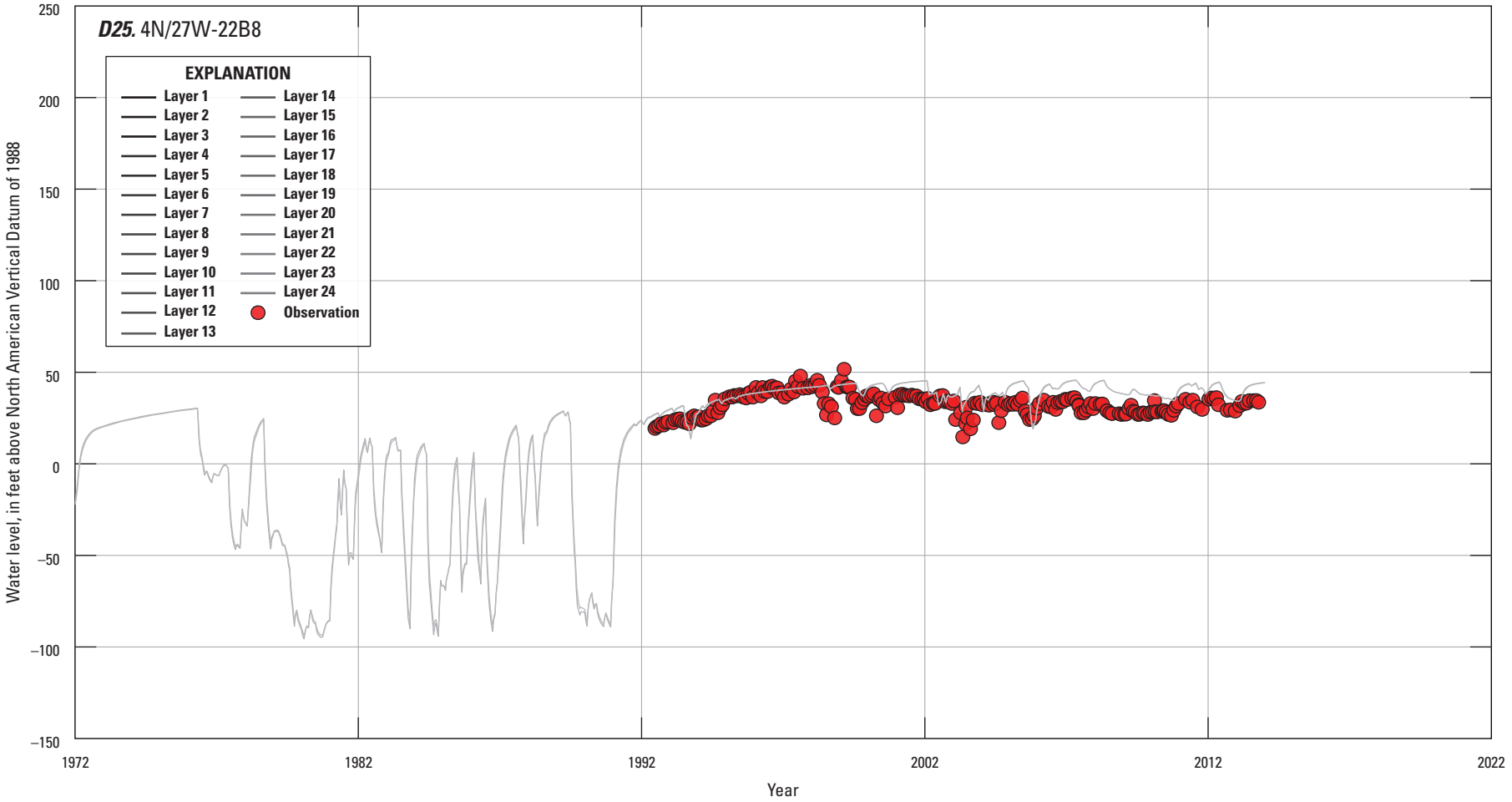

Figure 19. —Continued

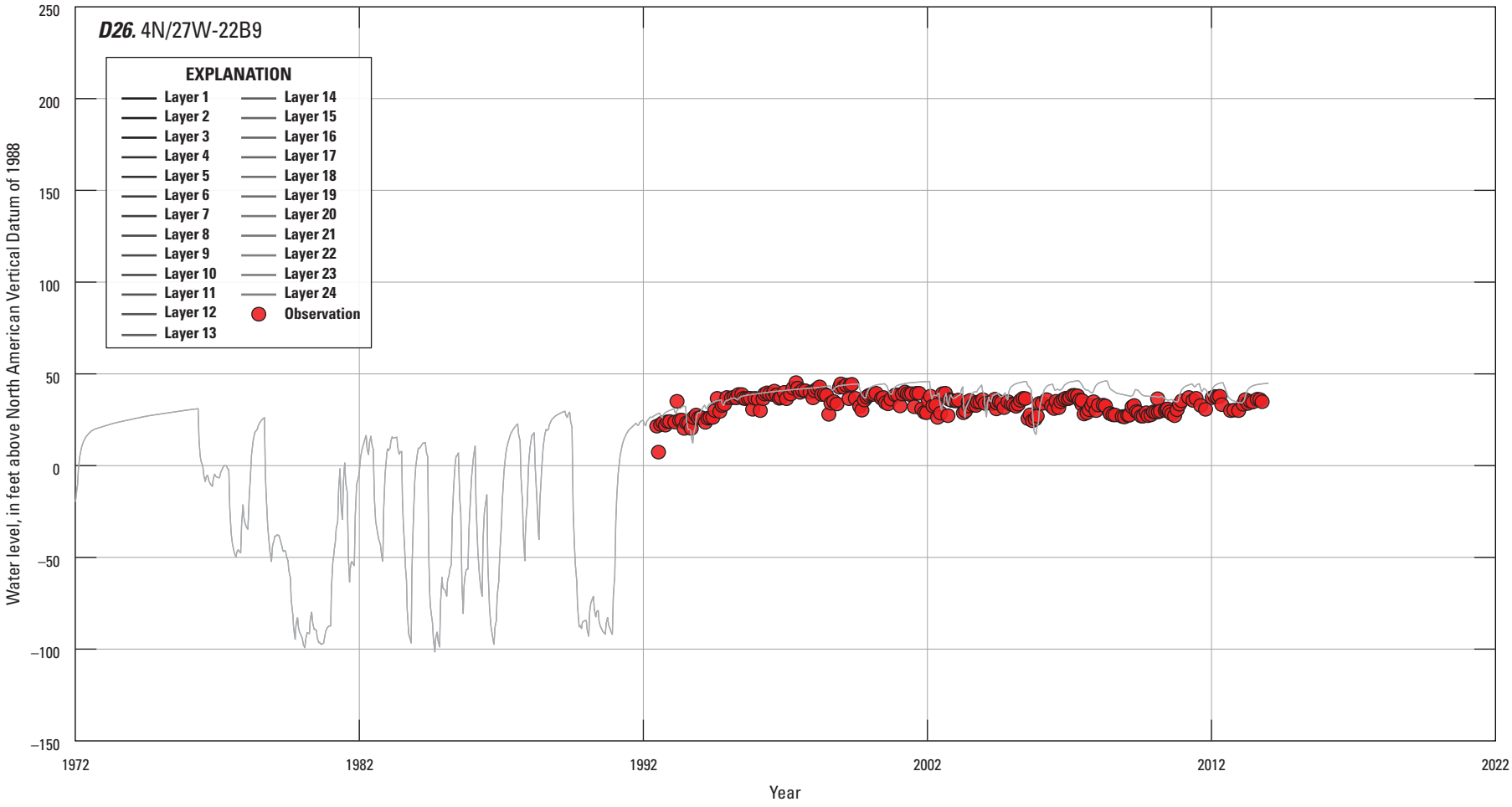

Figure 19. —Continued

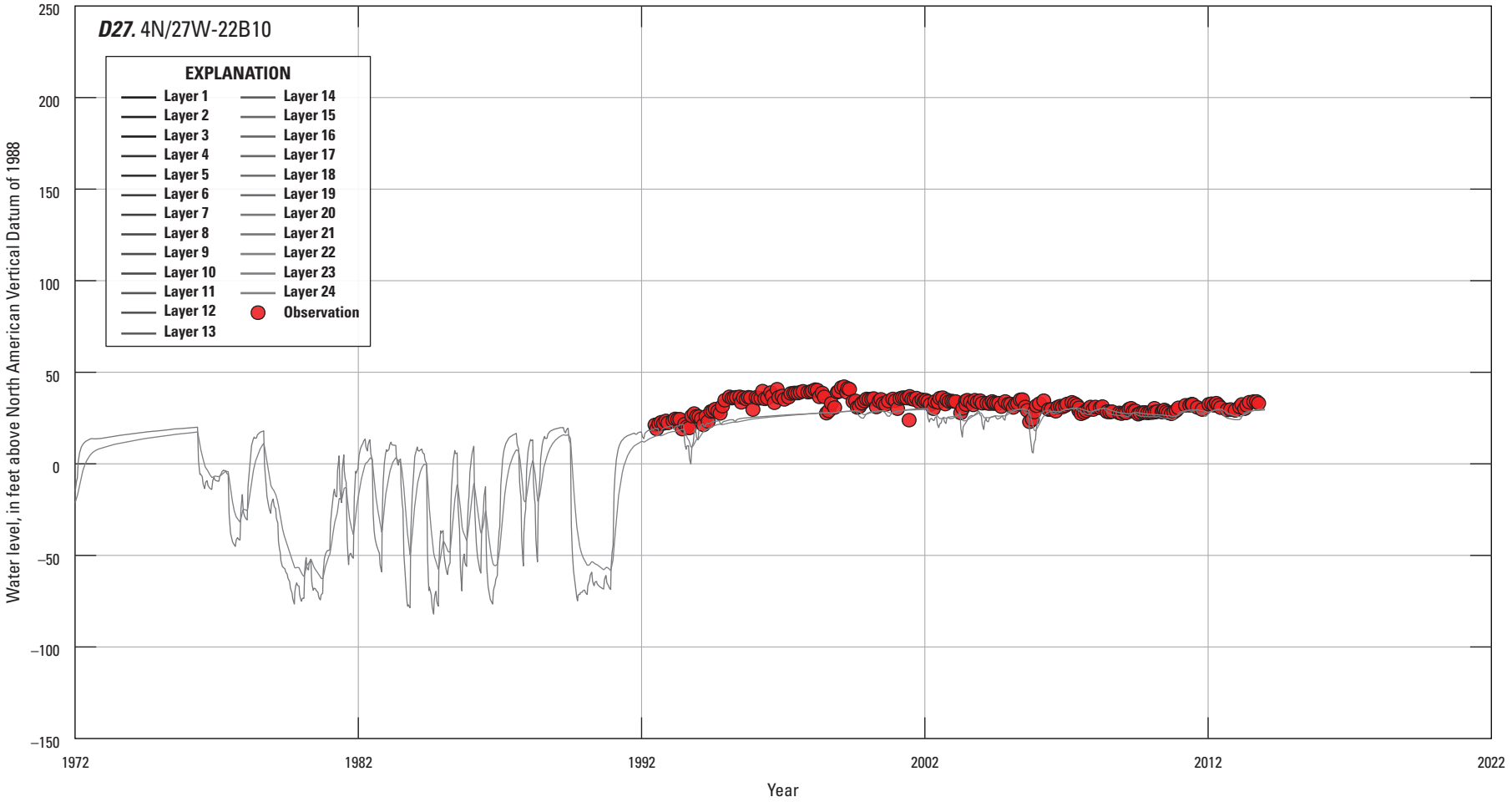

Figure 19. —Continued

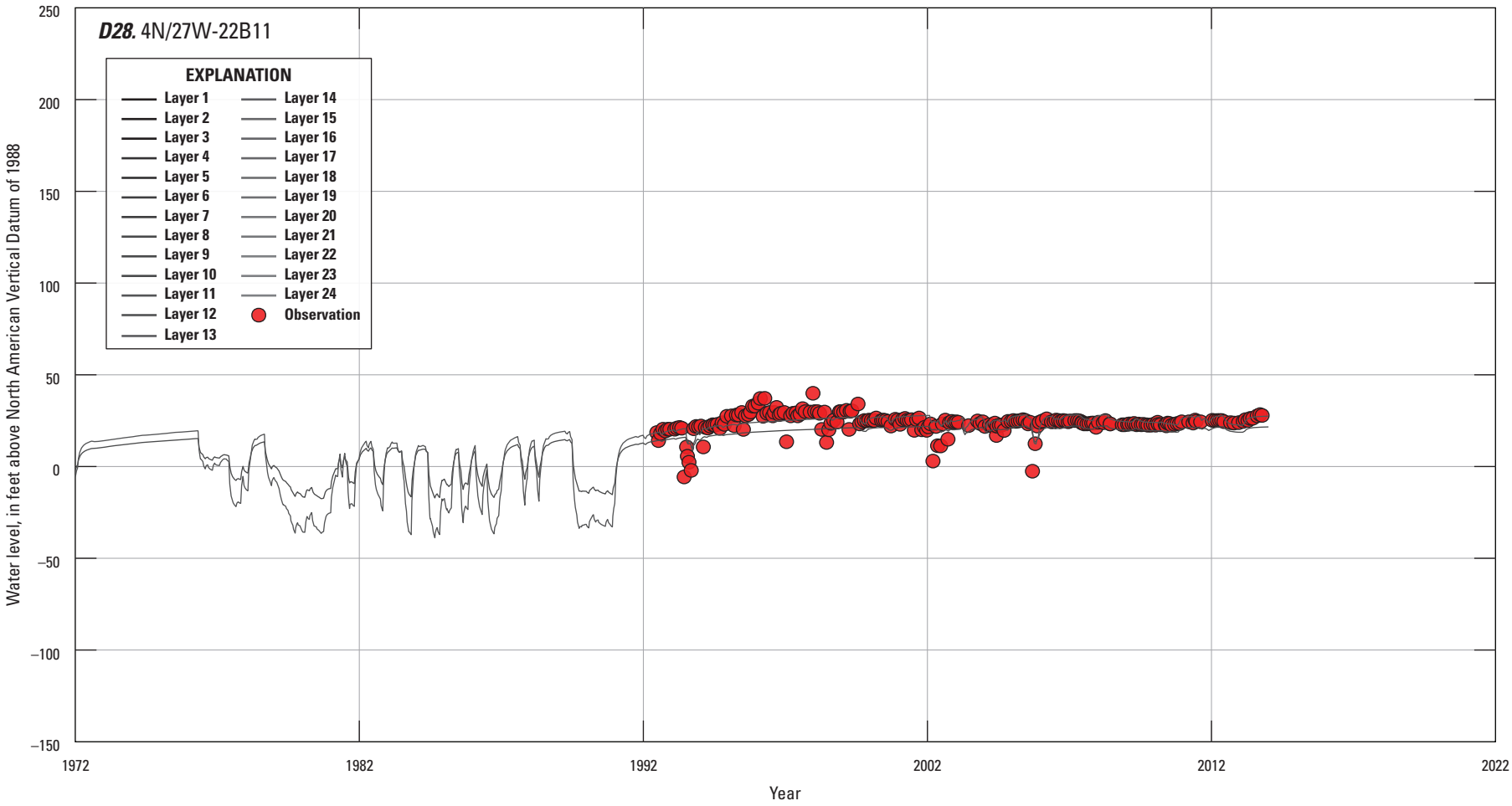

Figure 19. —Continued

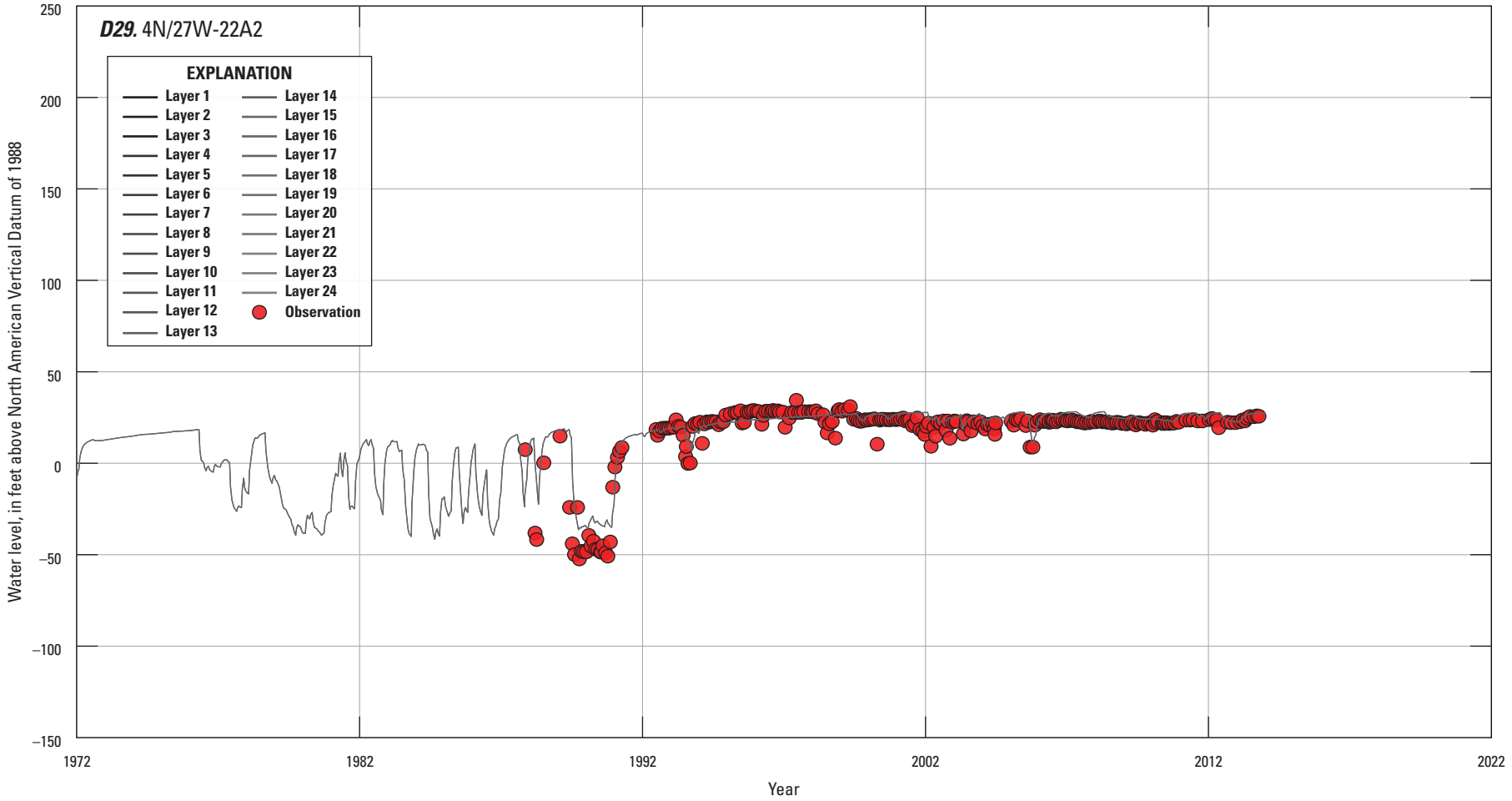

Figure 19. —Continued

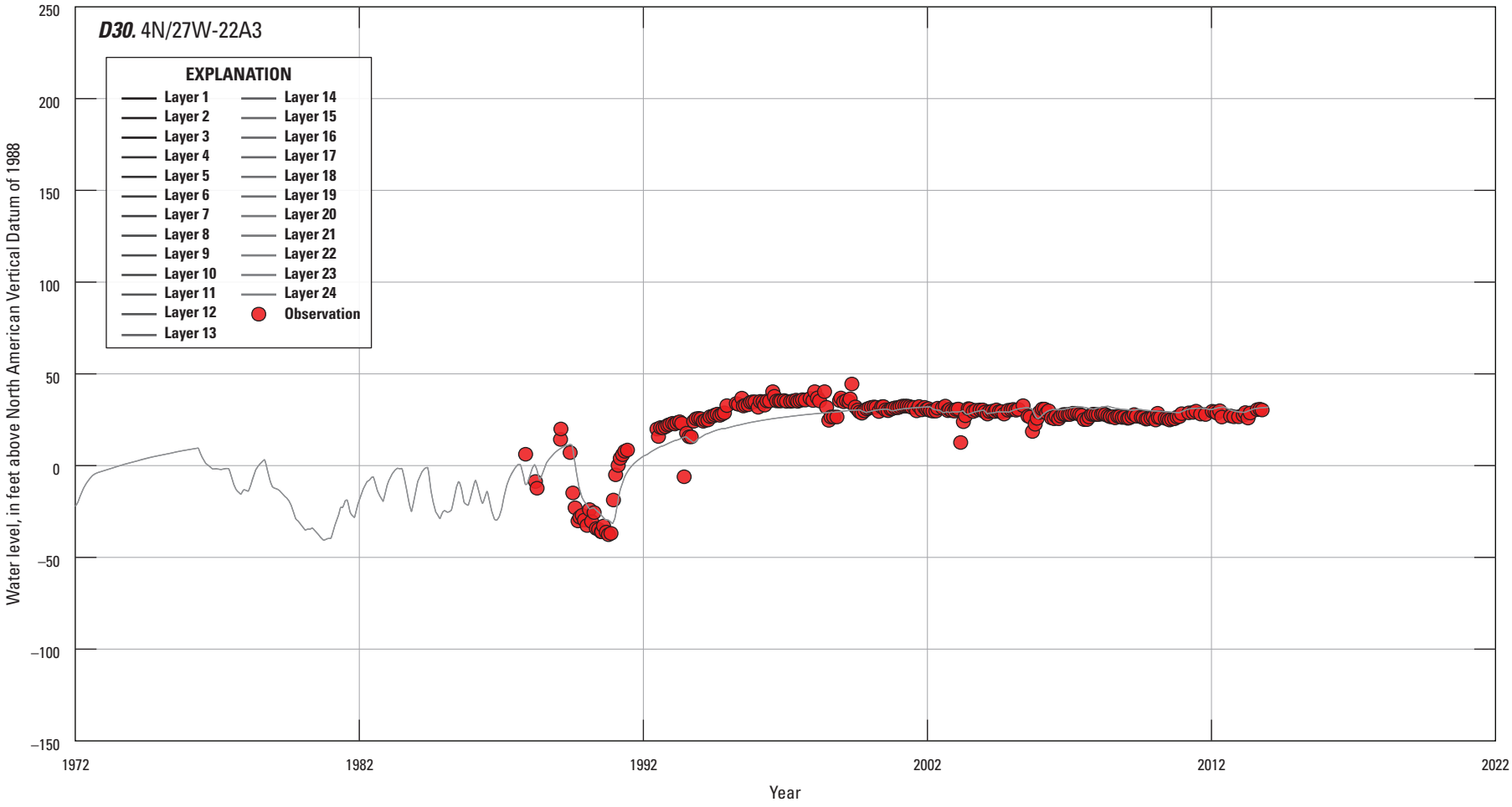

Figure 19. —Continued

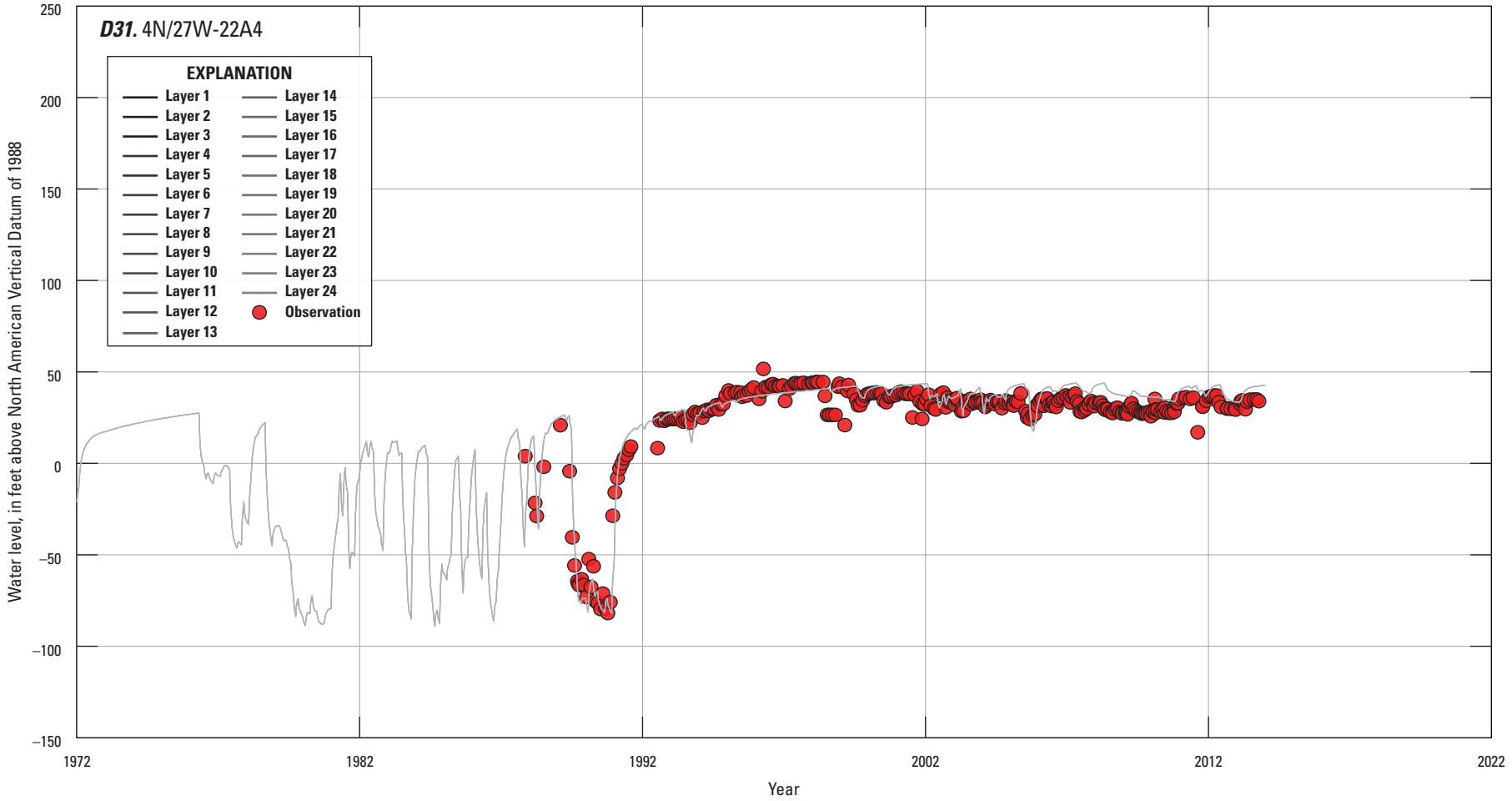

Figure 19. —Continued

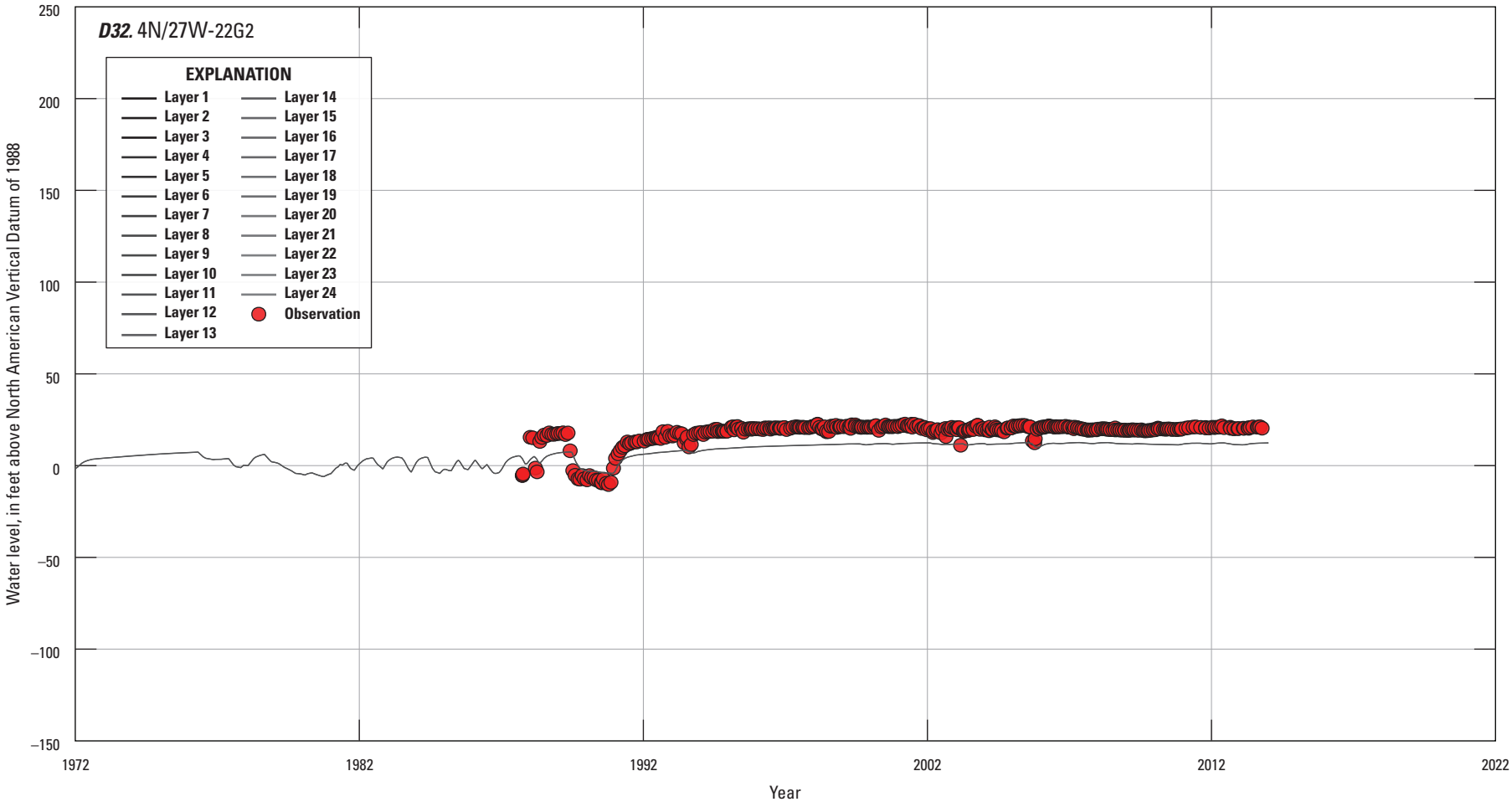

Figure 19. —Continued

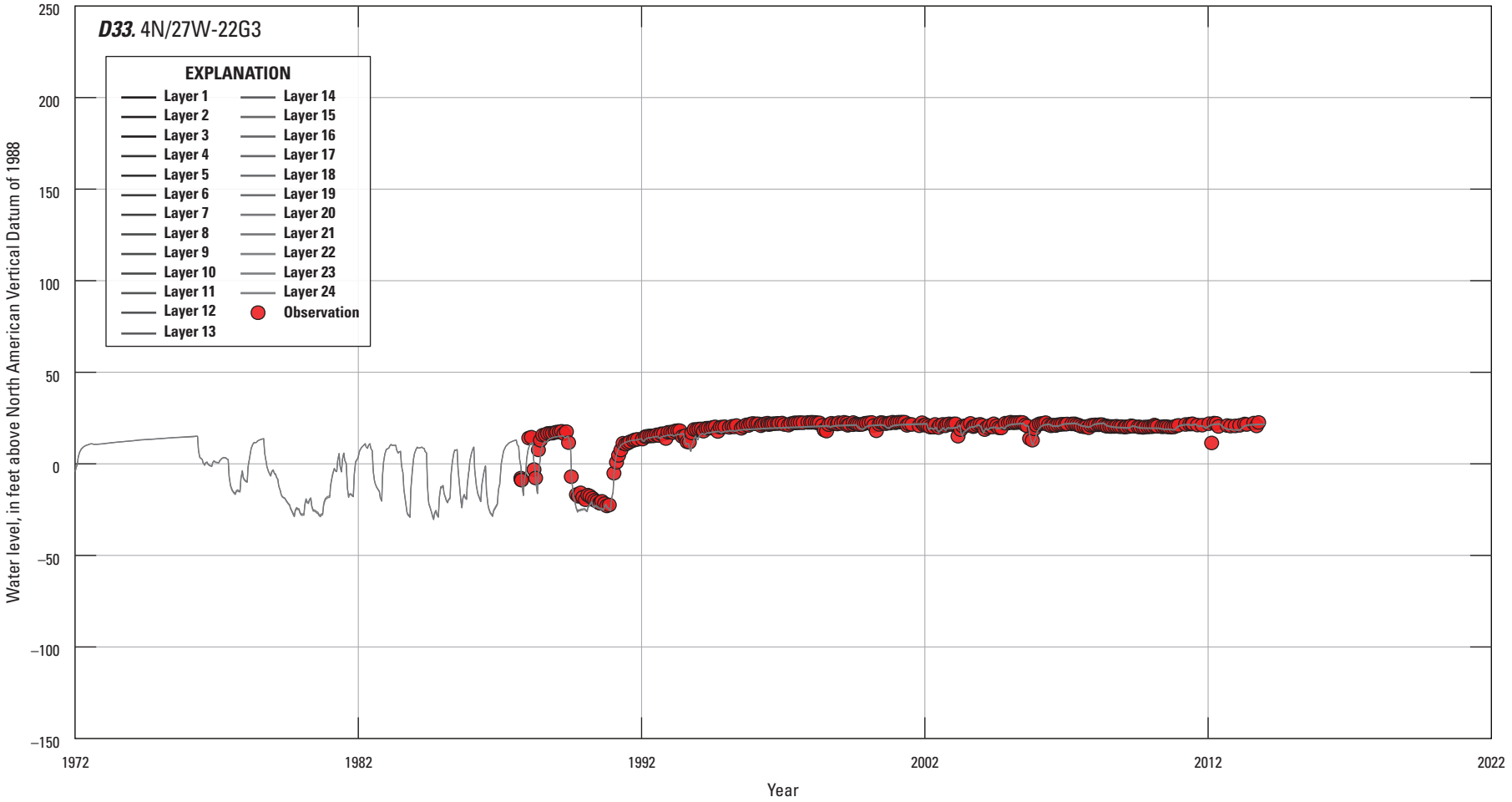

Figure 19. —Continued

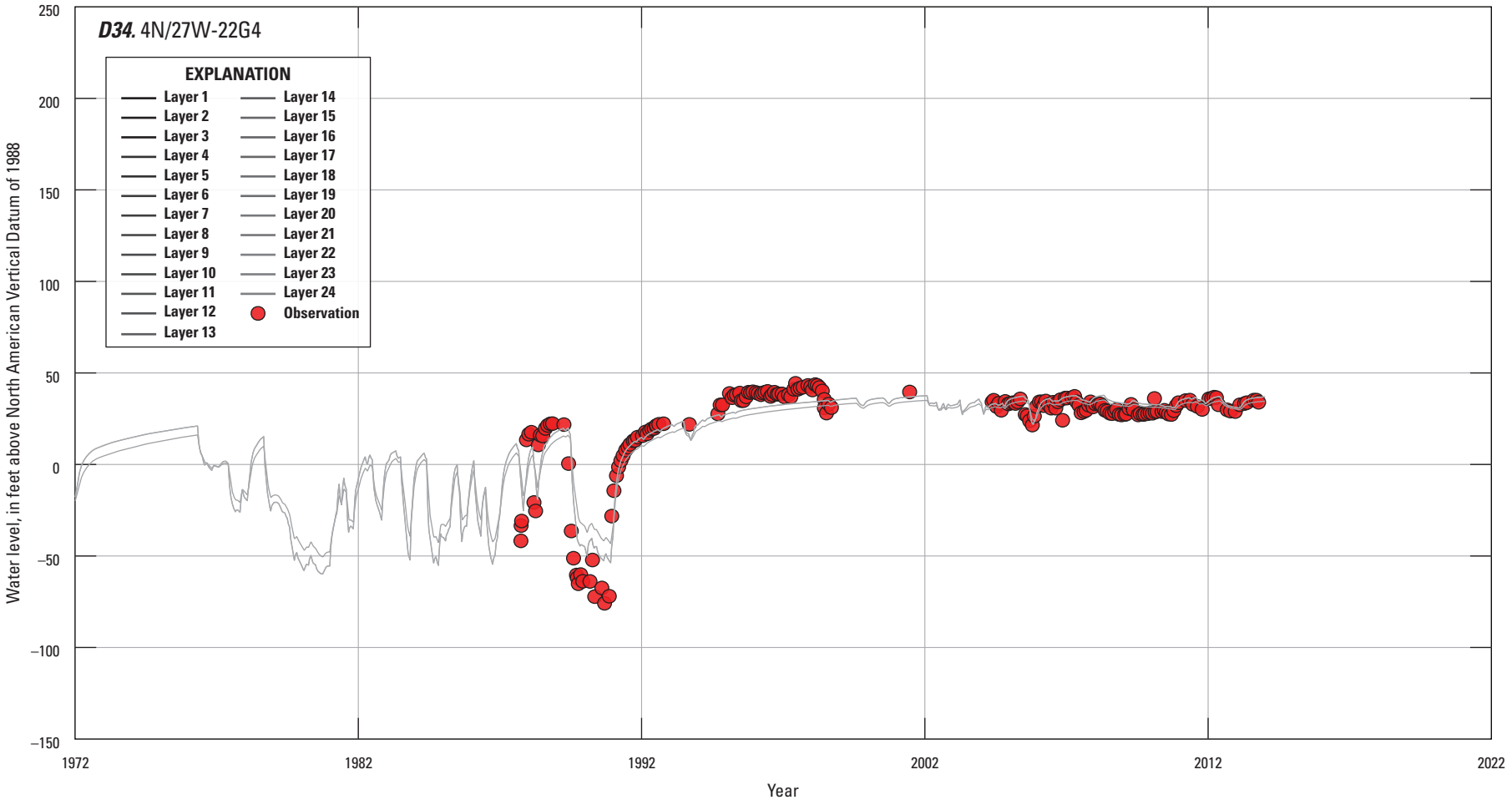

Figure 19. —Continued

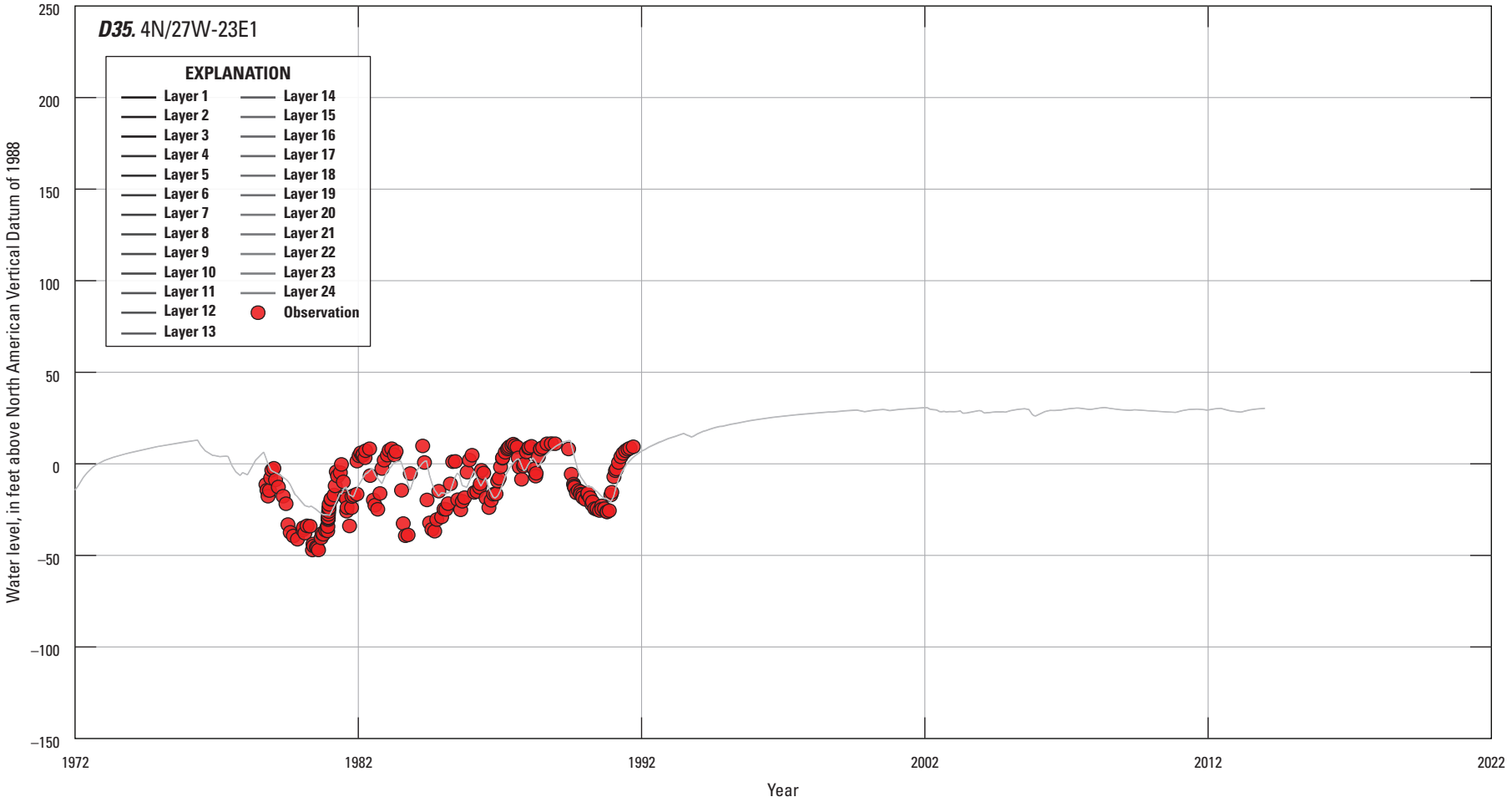

Figure 19. —Continued

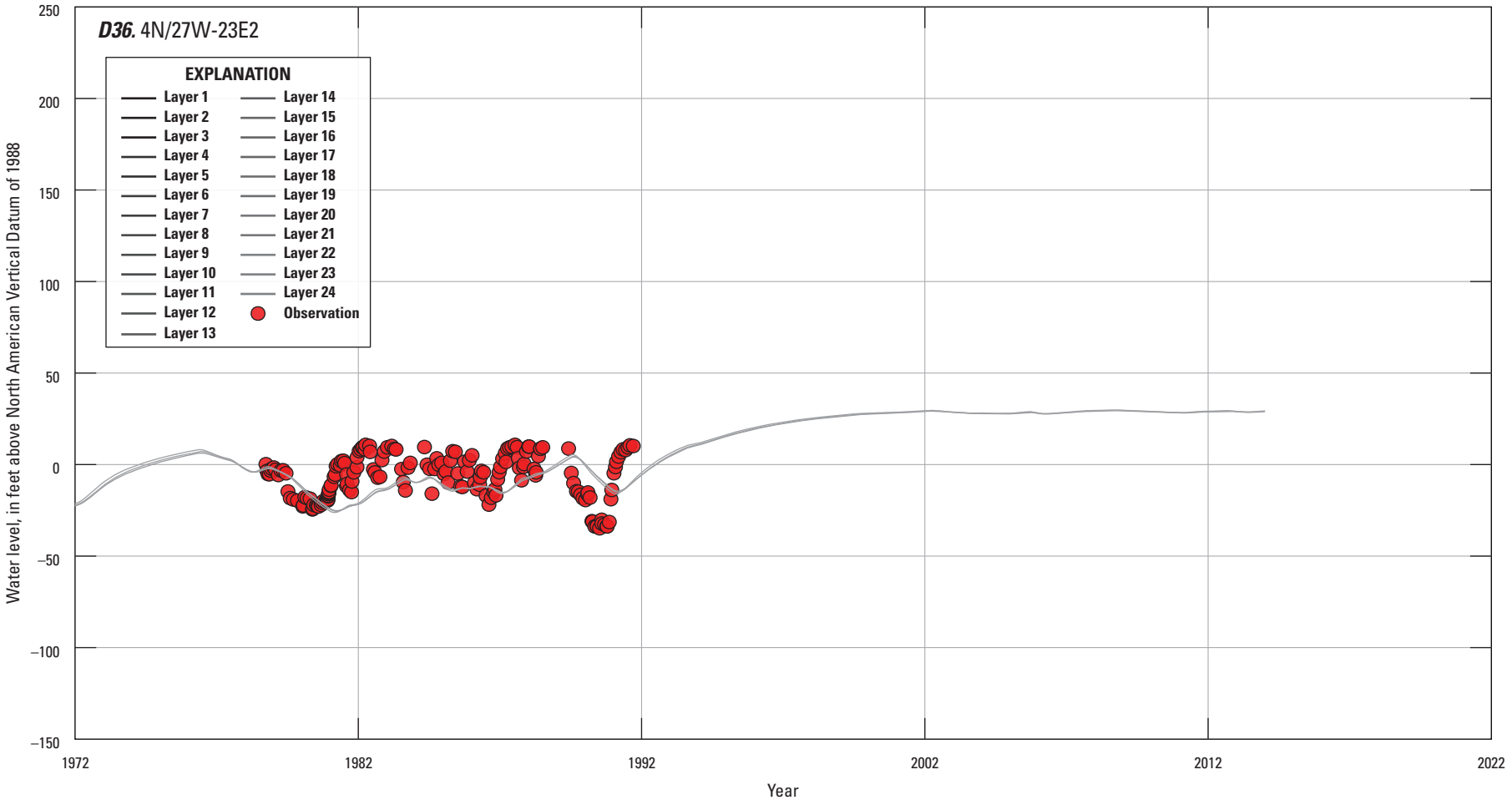

Figure 19. —Continued

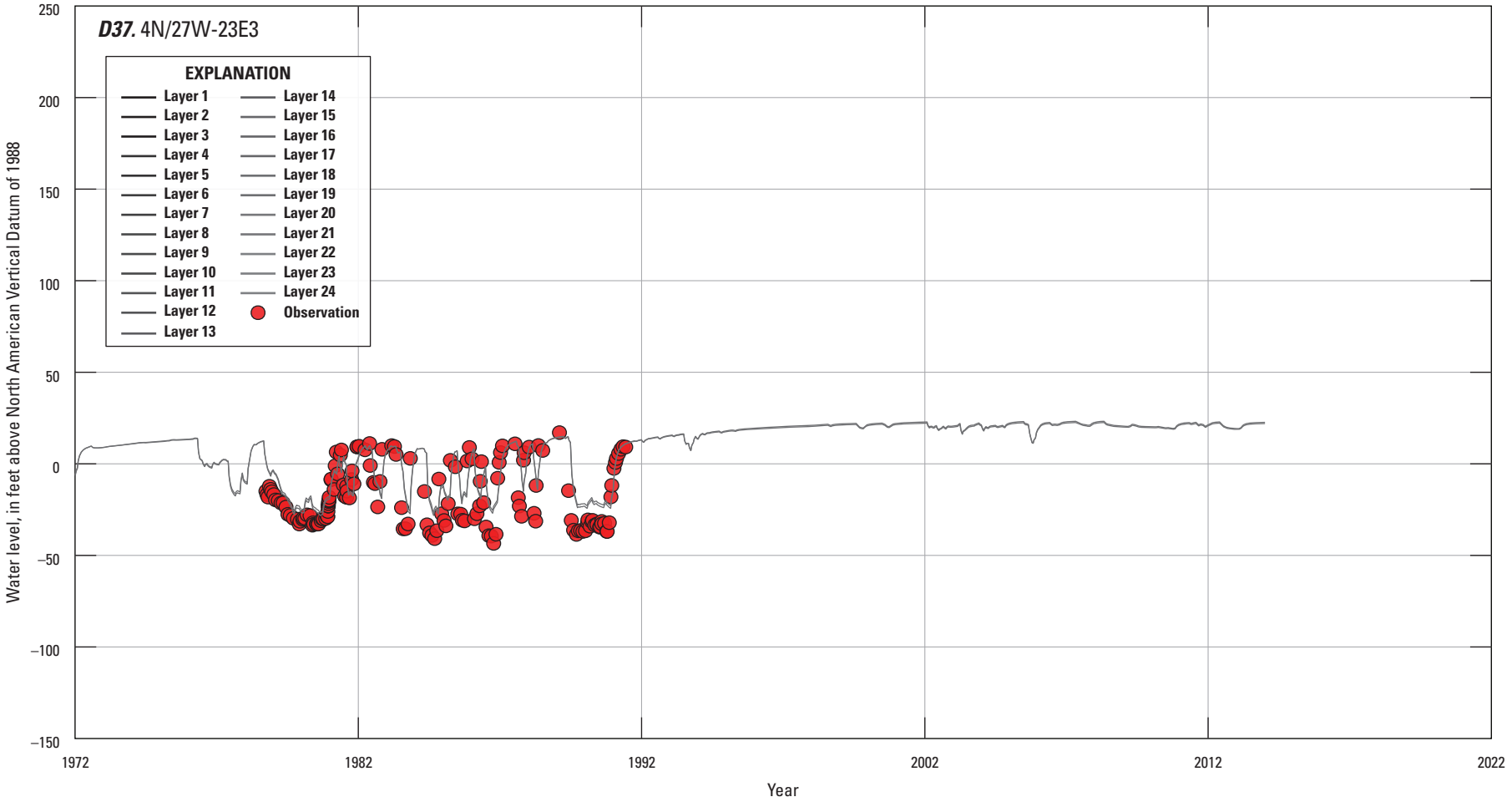

Figure 19. —Continued

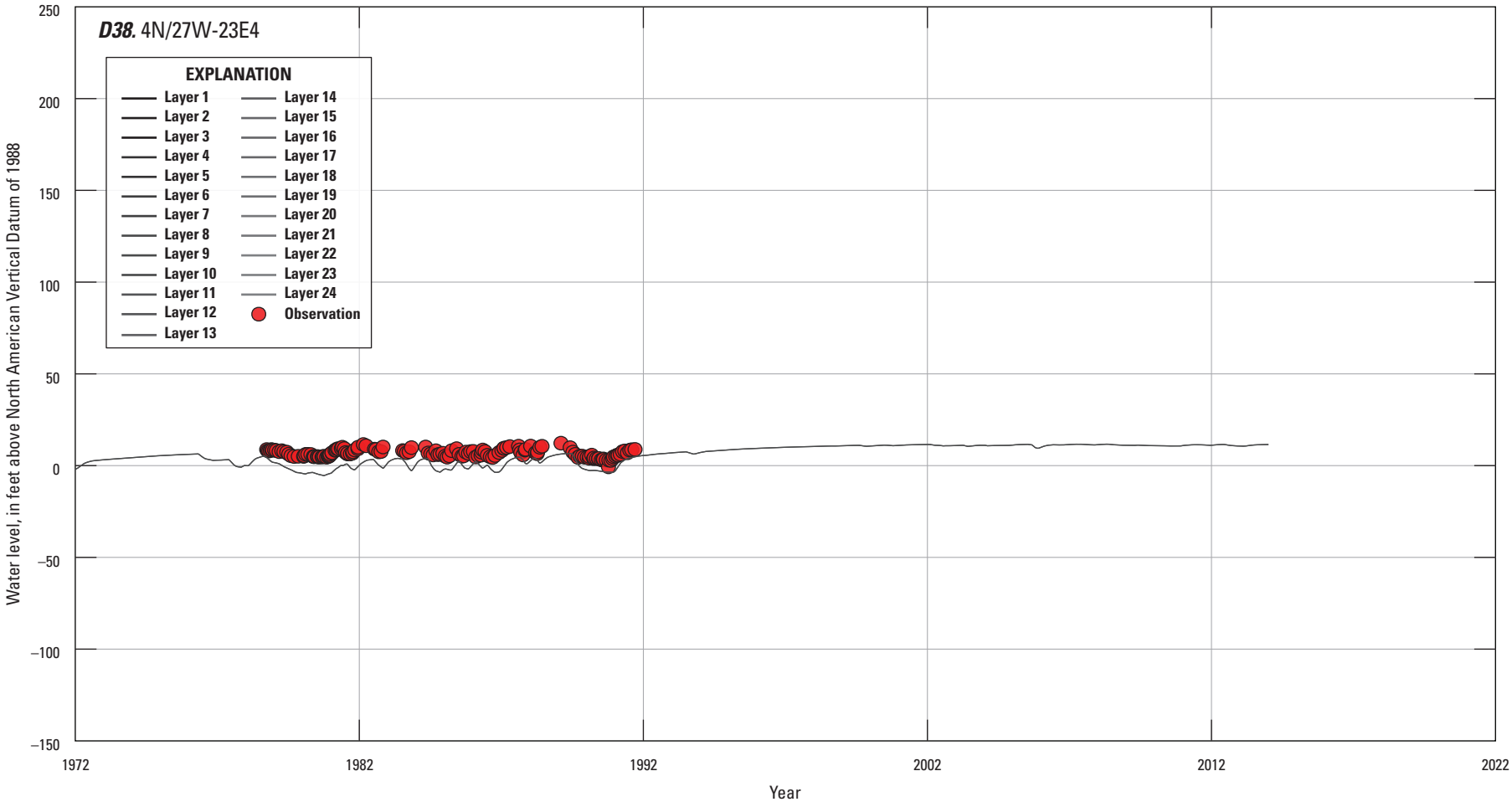

Figure 19. —Continued

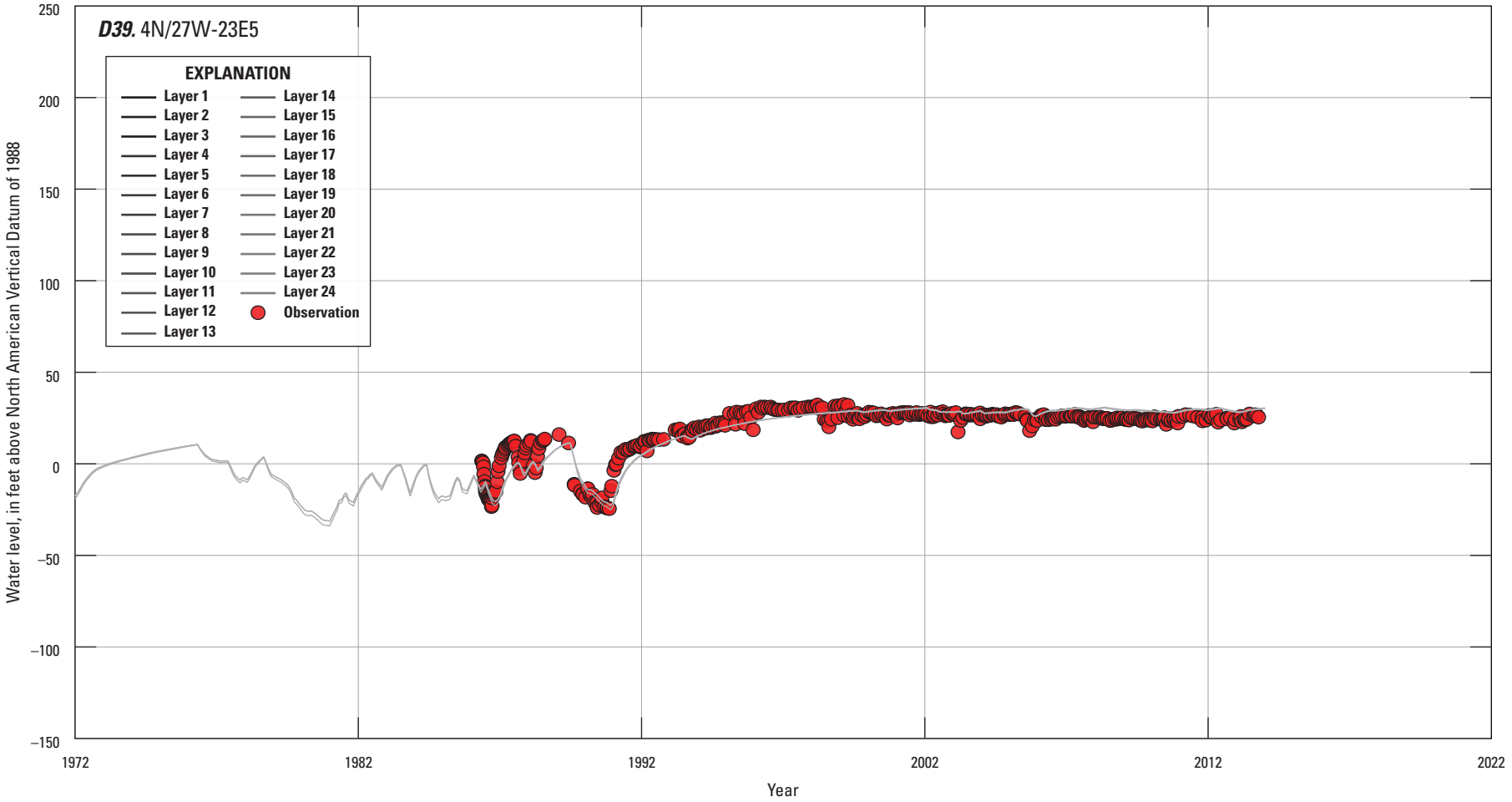

Figure 19. —Continued

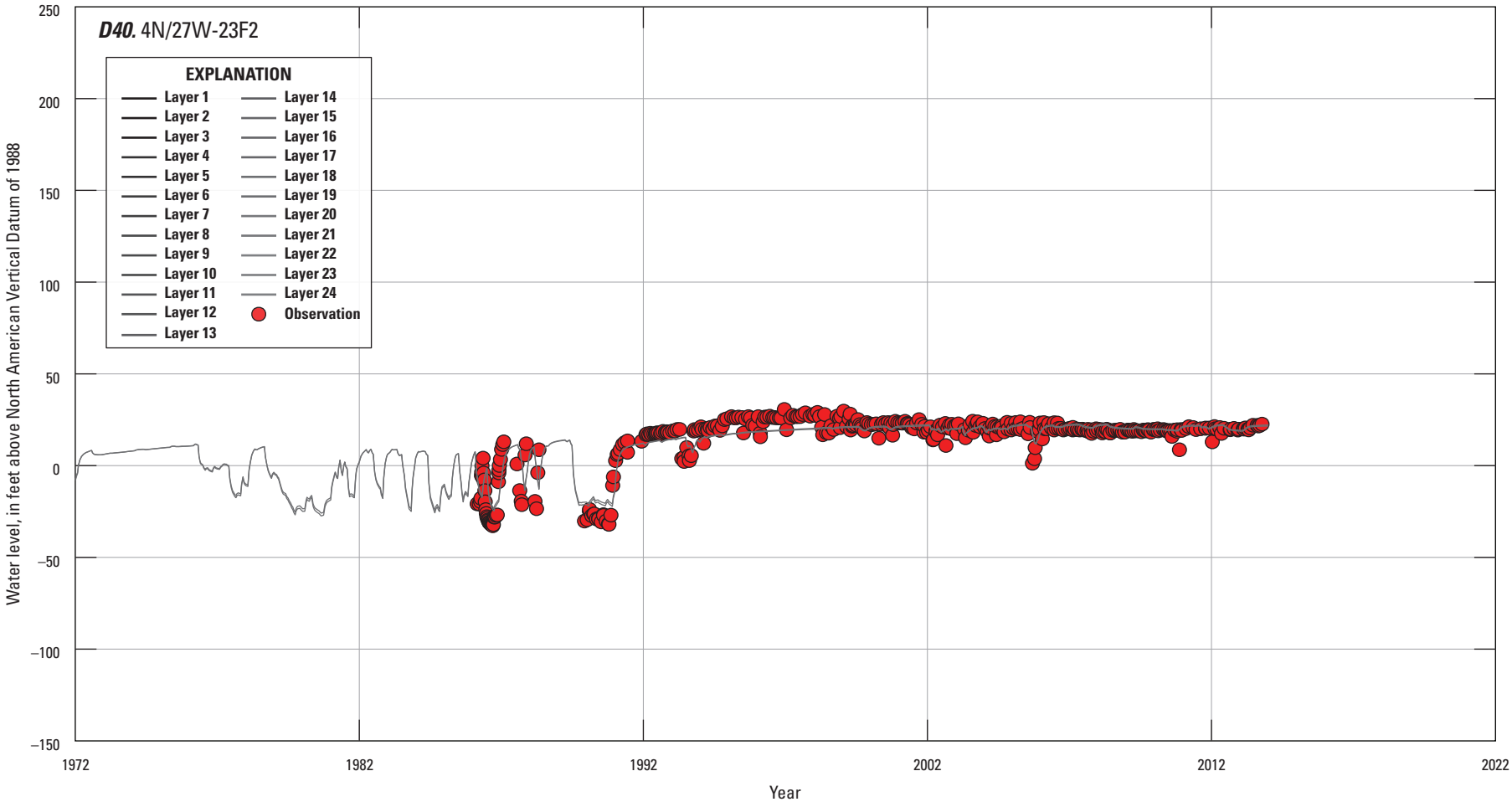

Figure 19. —Continued

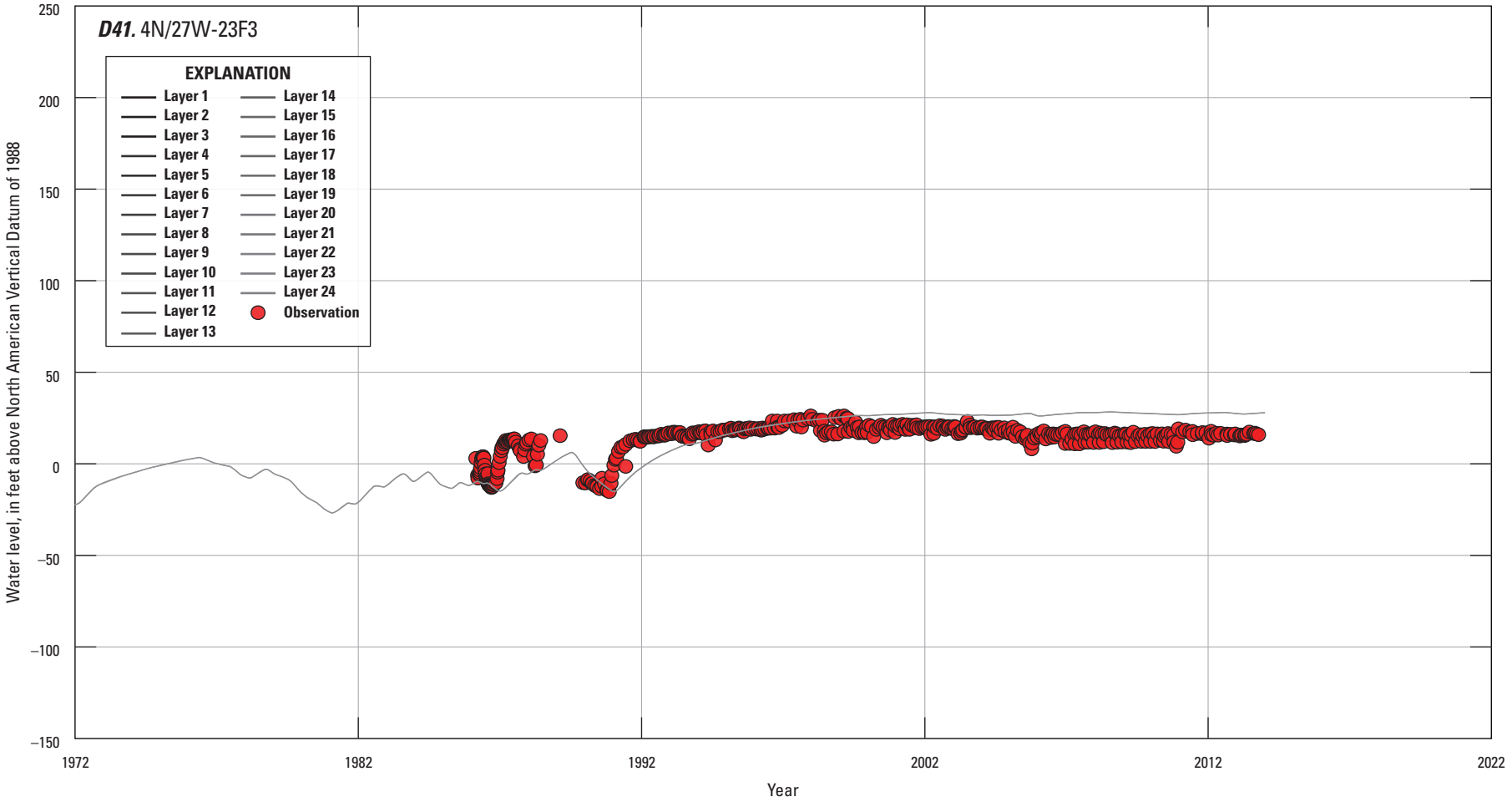

Figure 19. —Continued

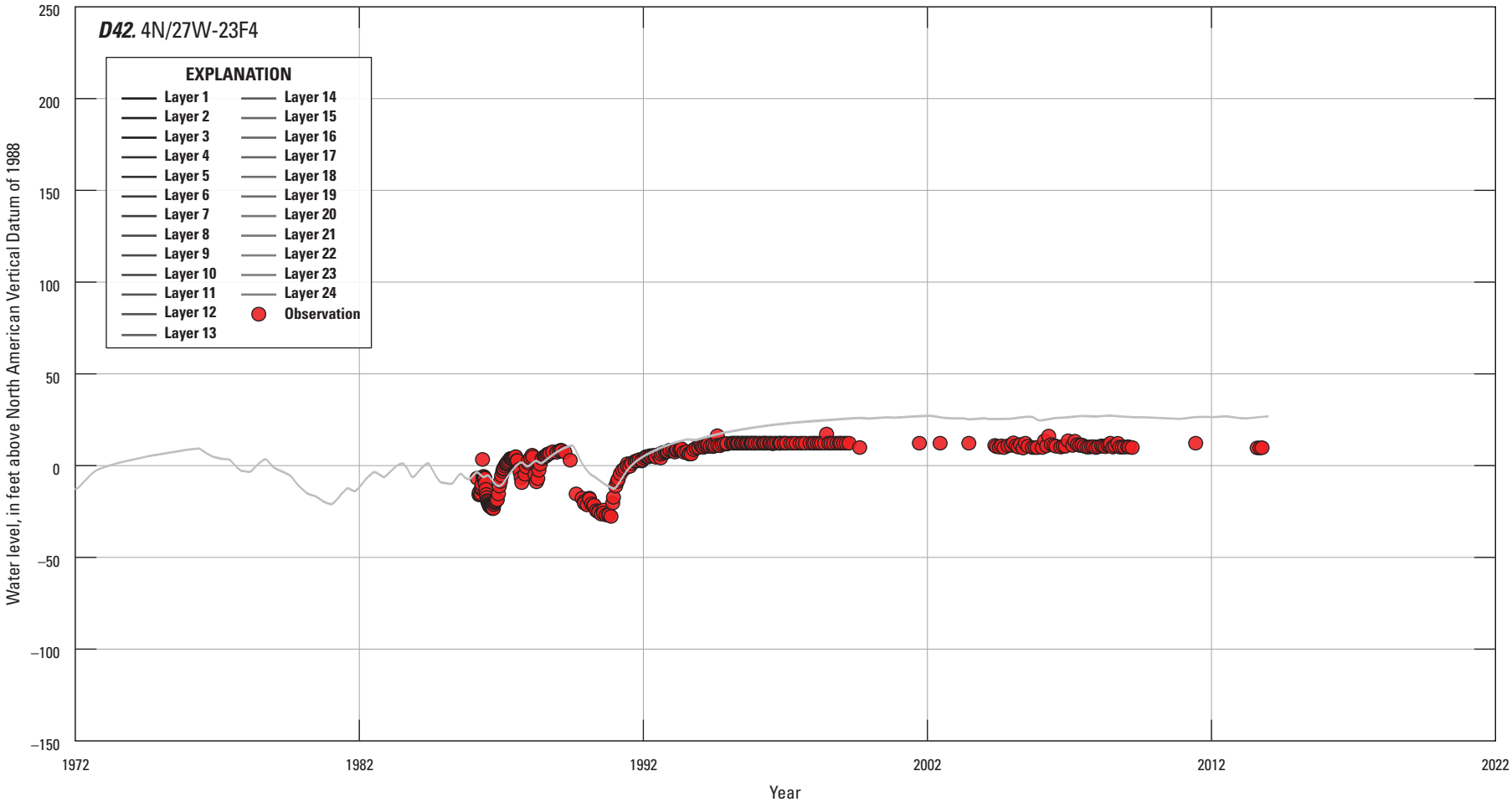

Figure 19. —Continued

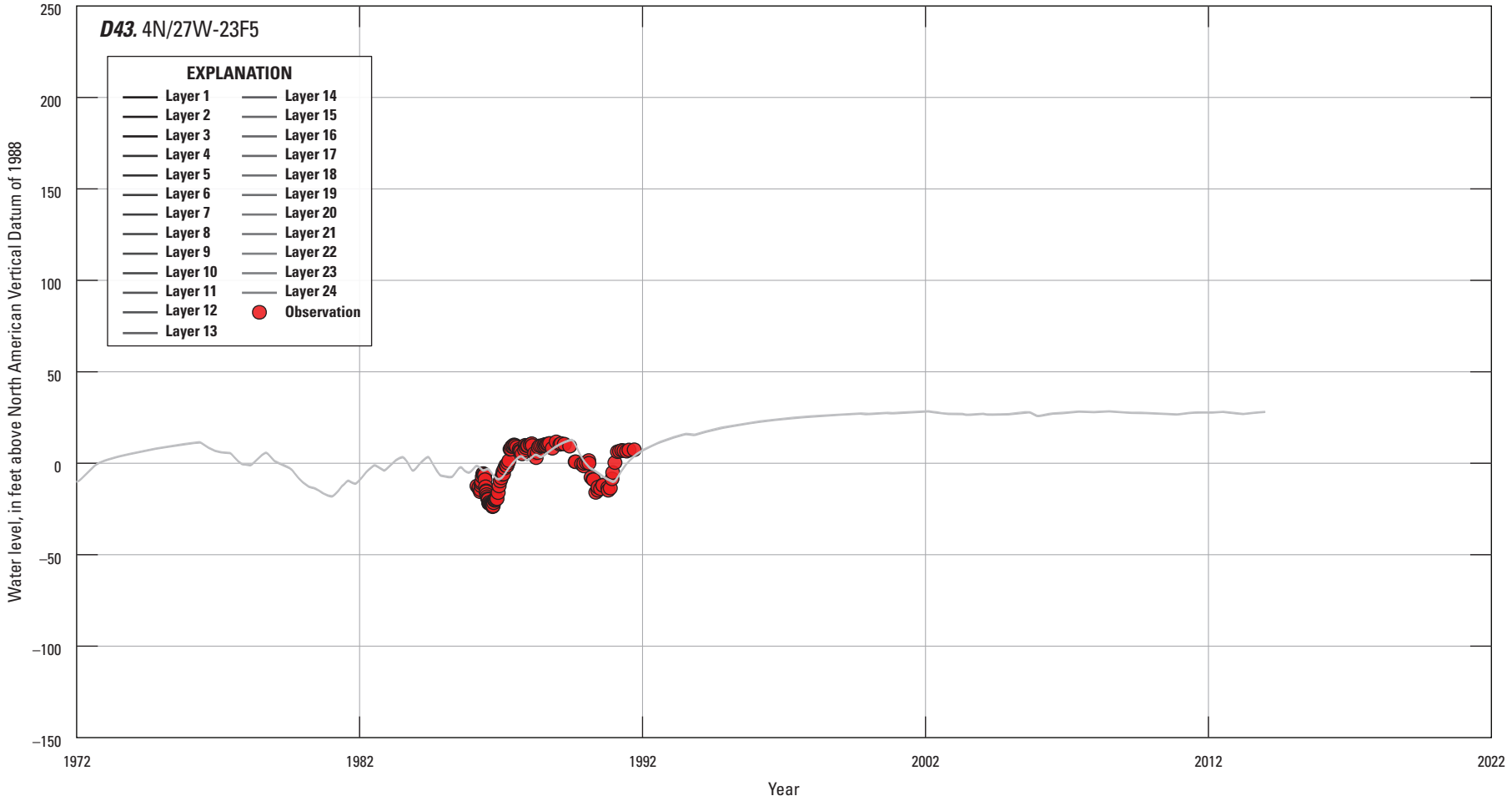

Figure 19. —Continued

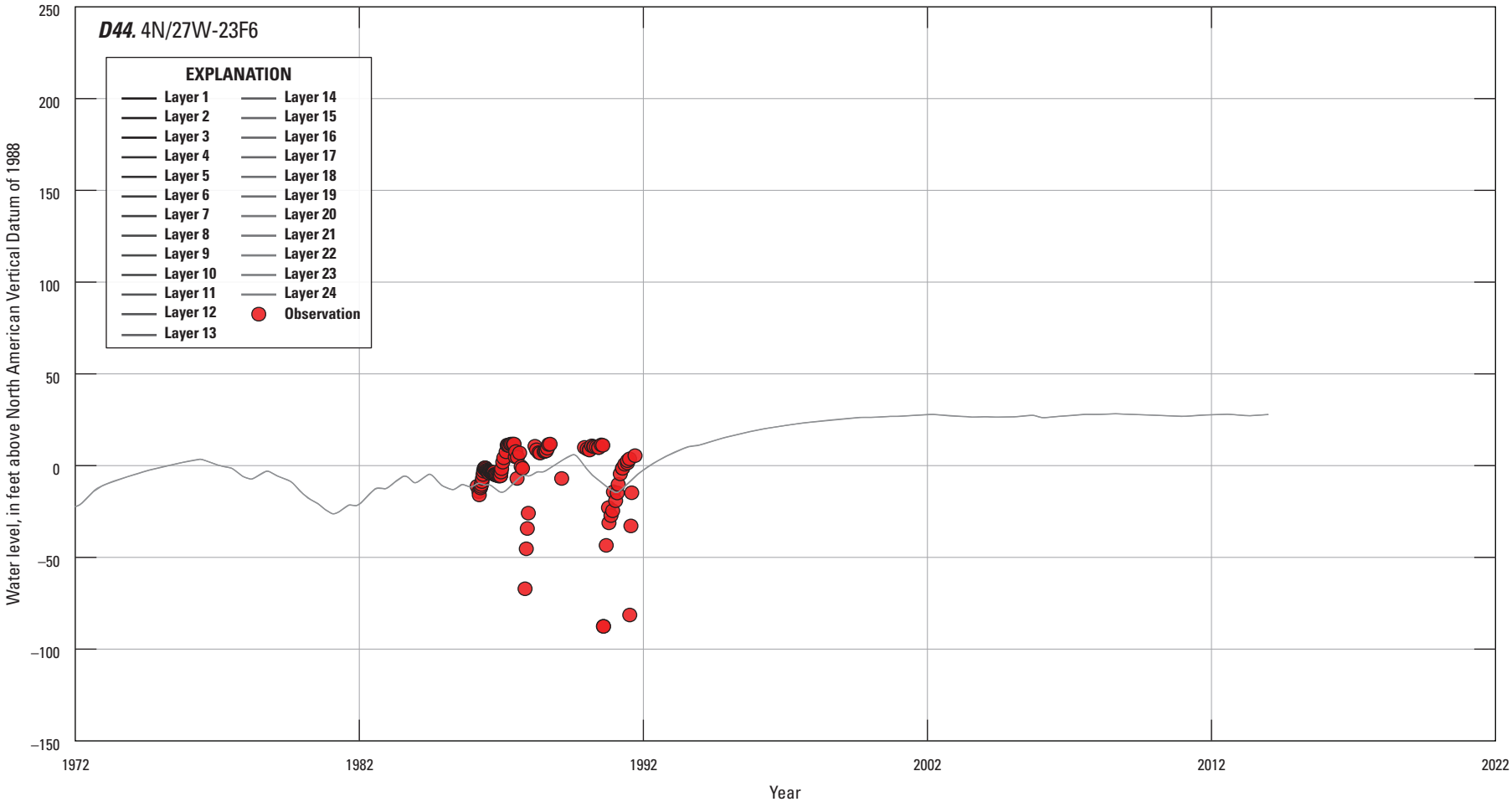

Figure 19. —Continued

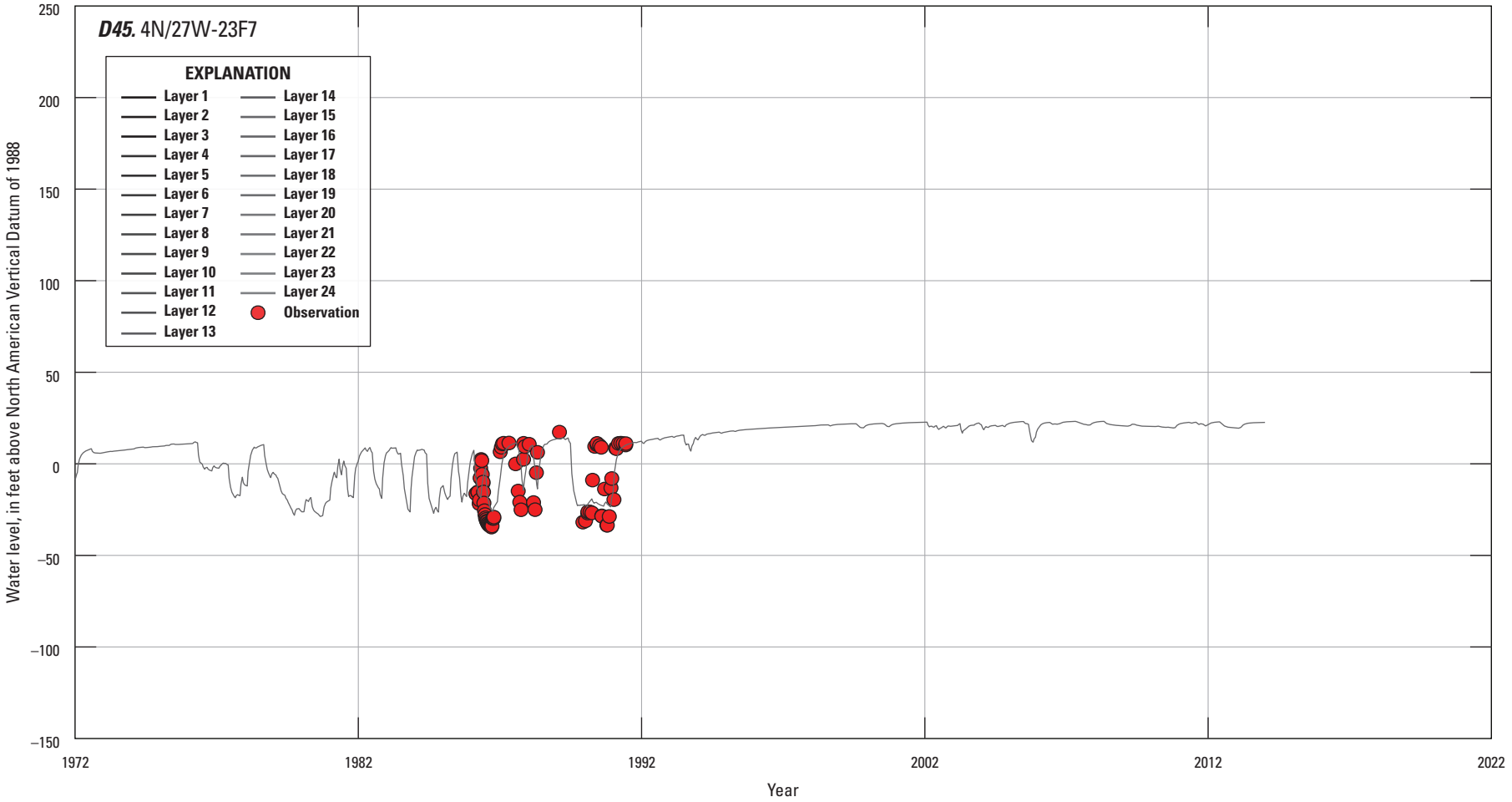

Figure 19. —Continued

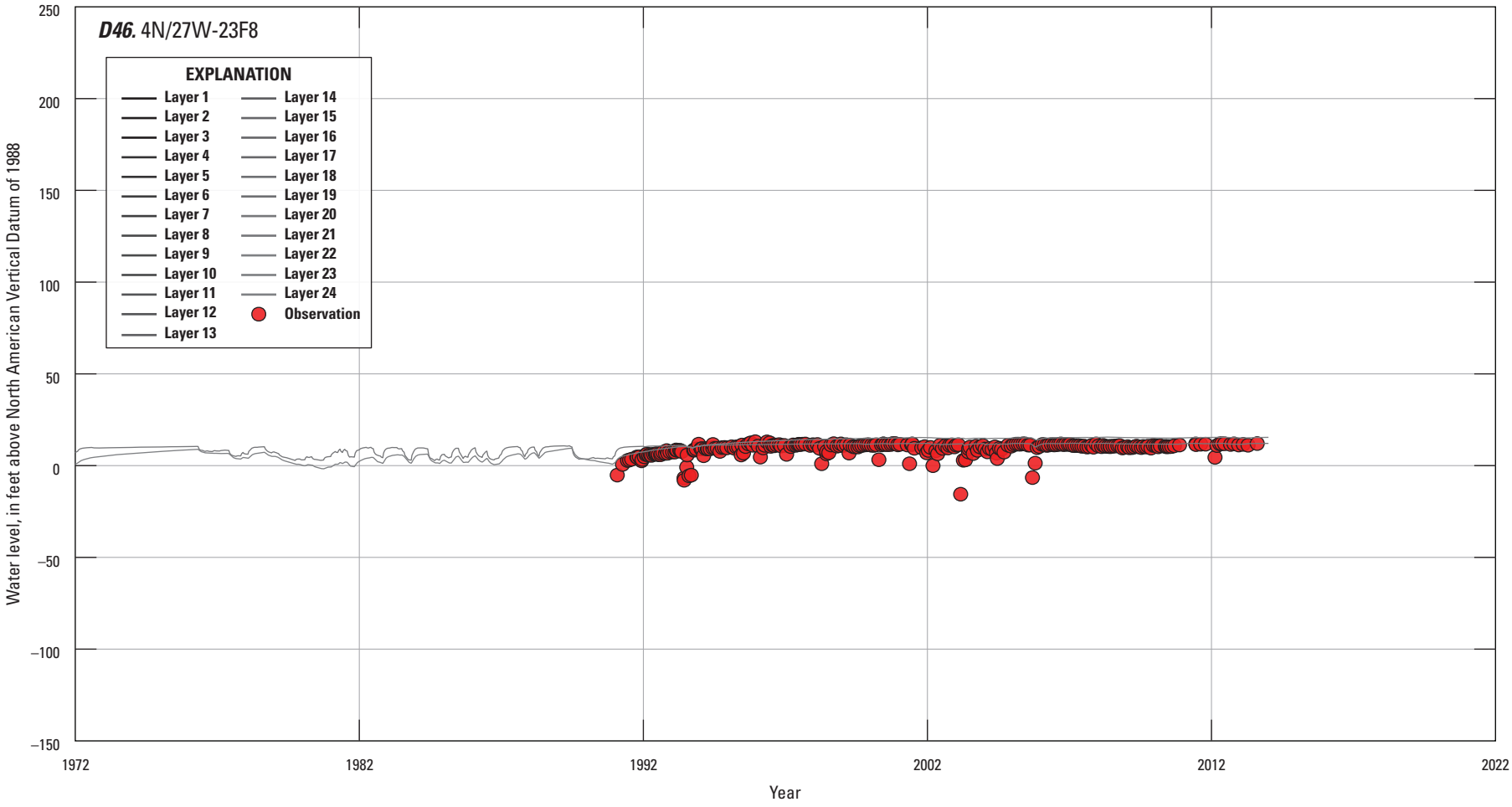

Figure 19. —Continued

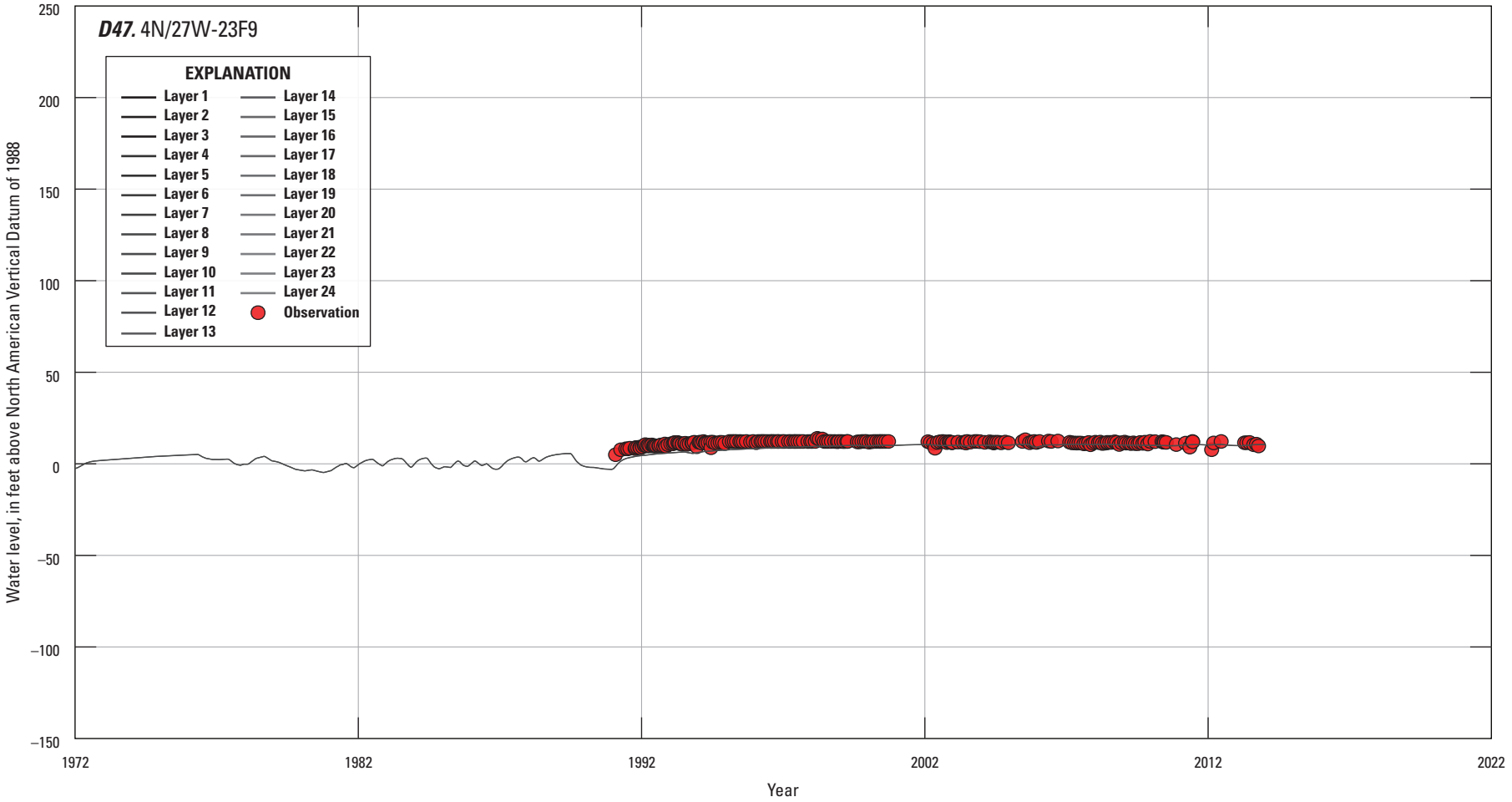

Figure 19. —Continued

West Foothill Subbasin

West Foothill subbasin simulated hydrographs showed a reasonable fit to measured data, with most hydrographs matching water levels as well as changes in water levels through time (fig. 19*A*). As would be expected, water-level changes were strongly influenced by the production wells in this region. Wells 4N/27W-07D1, 4N/27W-07M6, 4N/28W-12H4, and 4N/28W-12R3 are near the major production wells in West Foothill subbasin, including Los Robles and La Cumbre Mutual Water Company (LCM) wells #9 and #16 (figs. 9, 19*A*). Of the four wells, the fit of simulated to measured water levels was worst for well 4N/27W-07M6 (fig. 19*A*). From 1975 to 1977, the simulated hydraulic heads in well 4N/27W-07M6 declined because of pumping from the LCM #9 production well; however, measured water levels did not decline during this time. Wells 4N/27W-07M6 and LCM #9 are both perforated in the upper and lower producing zones. Additionally, wells LCM #9 and 4N/27W-07M6 are both in a narrow zone between the Northeast More Ranch fault and the unnamed fault, less than a third of a mile from each other (fig. 9). With no known barrier separating well 4N/27W-07M6 from LCM #9, this well proved difficult to calibrate. This indicated that groundwater flow is restricted between these two wells in some way that is not addressed by the conceptual model.

Wells 4N/28W-12B1, 4N/28W-12C2, and 4N/28W-01R1–2 are on the western side of the West Foothill subbasin (fig. 9). The nearest production well is Los Robles, which is slightly down gradient from these wells. In general, measured and simulated changes in head were very similar for these wells (fig. 19*A*). Simulated hydraulic heads and measured water levels were a reasonable match for wells 4N/28W-01R1–2; however, water levels for wells 4N/28W-12B1 and 4N/28W-12C2 were overestimated (fig. 19*A*). Matching water levels in wells 4N/28W-01R1–2 and 4N/28W-12C2 proved to be difficult because these wells are both perforated in the upper producing zone, are less than 0.5 mi apart, but had a water-level difference of approximately 20 ft, with lower water levels in well 4N/28W-12C2. No outflow exists on the west side of well 4N/28W-12C2 large enough to drive this water-level difference between the wells. In addition, even though it is closer to the nearest production well, water-levels fluctuated less in well 4N/28W-01R1 than in well 4N/28W-12C2. This indicates that wells 4N/28W-01R1–2 have a weak hydraulic connection to the south. This could be explained by a local decrease in sediment coarseness or layer thickness around wells 4N/28W-01R1–2 not captured in the HFM.

East Foothill Subbasin

In general, the hydrographs from wells (4N/27W-05P1 and 4N/27W-08M5–6), in the East Foothill subbasin, showed simulated trends in hydraulic head matching those measured (fig. 19*B*). One exception is well 4N/27W-05P1, in the northern part of the basin, because the seasonal variability in simulated hydraulic heads did not match the measured data; the simulated results were less variable than measured data. The lack of variability in the simulated results could be associated with unknown pumping near the well or be caused by the manner in which creeks were simulated. There could be unknown or unreported pumping that, if included, could affect the simulated results. Perhaps more importantly, San Roque Creek is less than 100 ft from well 4N/27W-05P1, and the creeks in the model area are simulated using constant-stage streams in the RIV package; therefore, seasonal variability of the stream stages, which likely affect water levels in these wells, were not addressed.

Monitoring wells 4N/27W-08M5–6 are in the middle of the East Foothill subbasin, approximately 1,400 ft southwest of the San Roque Park production wells and approximately 2,100 ft northwest of the McKenzie Park production wells (fig. 9). Wells 4N/27W-08M5–6 are perforated in the lower and upper producing zones, respectively. The simulated hydraulic heads and measured water levels for well 4N/27W-08M5 were very similar in terms of magnitude and trend (fig. 19*B*). Simulated hydraulic heads and measured water levels in well 4N/27W-08M6 followed a similar pattern, with simulated heads having slightly more drawdown and recovery than the measured data. The declines in simulated hydraulic heads and measured water levels in wells 4N/27W-08M5–6 corresponded to increased pumping in the East Foothill subbasin from 1984 to 1991 and from 2007 to 2013, and the period of increasing water levels during the 1990s and early 2000s corresponded to a time of relatively little pumping (fig. A–8). In addition to being consistent with the measured water levels at these wells, the simulated vertical gradient between these wells was consistent with the measured data.

Storage Unit III

In general, simulated hydraulic heads matched measured water levels well for the west side of Storage Unit III, but there were greater errors in simulated values on the east side (fig. 19*C*). Simulated hydraulic heads for wells in the west side of Storage Unit III, including wells 4N/27W-18C2–3 and 4N/27W-18Q1 and 18Q4, matched measured water levels during periods of high pumping, such as 1988–93 and 2010–13, fairly well. However, simulated heads were consistently higher than measured water levels during periods of low pumping, such as 1994–2008. Toward the east side of Storage Unit III, simulated hydraulic heads poorly matched measured water levels and seasonal changes in water levels (for example, well 4N/27W-21F2; fig. 19*C*). This is difficult to see given the hydrograph's scale, but the simulated seasonal fluctuations were under simulated. The eastern side of Storage Unit III consists of a thin layer of alluvium with underlying shale, which is bounded by the Mesa fault to the north and a mesa to the south with elevations up to 450 ft. The thin layer of alluvium could have low transmissivity values, allowing runoff from the mesa to the south to seasonally influence water levels in this area. Because runoff from the mesa is not simulated in the SBFTM, this could explain discrepancies between measured and simulated heads in this area.

Storage Unit I

Simulated hydrographs for selected wells in the western part of Storage Unit I (4N/27W-07Q5, 4N/27W-07R3, 4N/27W-16C1–2, 4N/27W-16E2, 4N/27W-17J1, 4N/27W-08R2, and 4N/27W-17L2–4; fig. 9) were generally in agreement with the measured data in terms of values and trends. Wells 4N/27W-07Q5 and 4N/27W-07R3 are in the westernmost corner of Storage Unit I (fig. 9), and the simulated hydraulic heads matched measured water levels fairly well in terms of value and trend (fig. 19*D*). To the east, simulated hydraulic heads and measured water levels near Mission Creek fit reasonably (for example, wells 4N/27W-16C1–2, 4N/27W-16E2, and 4N/27W-17J1). Well 4N/27W-08R2 is close to where Mission Creek runs along the East More Ranch fault (fig. 9). Measured water levels from this well showed influences from both Foothill subbasins and Storage Unit I. This indicated that well 4N/27W-08R2 could either pass through the East More Ranch fault at depth or is in the East More Ranch fault zone. Wells 4N/27W-17L2–4 are close to the Mesa fault (fig. 9). Simulated hydraulic heads and measured water levels fit reasonably for the shallow well 4N/27W-17L4, which was perforated above the upper producing zone, but did not fit as well for the deeper wells 4N/27W-17L2 and 4N/27W-17L3, which were perforated in the upper and lower producing zones, respectively (fig. 19*D*). Measured water levels in wells 4N/27W-17L2 and 4N/27W-17L3 indicated an influence from Storage Unit III, where water levels were relatively low during the post-1991 recovery. This indicated the well cluster could cross the Mesa fault at depth.

Simulated hydrographs for selected wells in the eastern part of Storage Unit I (4N/27W-14K2, 4N/27W-15J2, 4N/27W-15K1, 4N/27W-15E1–2, 4N/27W-16R1, 4N/27W-21B1, and 4N/27W-22E1–2), which are near the main Storage Unit I production wells (fig. 9), generally matched measured water levels. Wells 4N/27W-14K2 and 4N/27W-15J2 are east of the main production wells and are perforated in the upper producing zone and in the upper and middle producing zones, respectively. The simulated hydraulic heads and drawdown matched the measured data in both wells (fig. 19*D*). Well 4N/27W-15K1 is just north of the main production wells and is perforated in the lower producing zone (fig. 9). Simulated hydraulic heads and measured water levels were similar, but simulated drawdowns were slightly greater than measured drawdowns (fig. 19*D*). Wells 4N/27W-15E1–2, northwest of the main production wells (fig. 9), are perforated in the upper and lower producing zones and in the lower producing zone, respectively. In general, for both of these wells, simulated hydraulic heads were less than measured water levels, but amounts of drawdown were similar (fig. 19*D*). The measured water levels from 15E2 were much more variable in the early 1990s and 2010s than the simulated hydraulic heads (fig. 19*D*), however. West of the main production wells, well 4N/27W-16R1 is perforated in the lower producing zone, well 4N/27W-21B1 is perforated in the upper producing zone, and wells 4N/27W-22E1–2 are both perforated in the upper aquitard. Simulated hydraulic heads and measured water levels matched fairly well, although simulated drawdown was greater than measured during the pumping events between 1980 and 1990 for well 4N/27W-16R1, and it was less than measured in well 4N/27W-21B1 (fig. 19*D*). For wells 4N/27W-21B1 and 4N/27W-22E2, simulated heads were less than measured water levels during the recovery period following 1991 (fig. 19*D*).

In addition to the wells in the eastern part of Storage Unit I, there are a number of monitoring-well clusters between the production wells and the coastline (for example, 4N/27W-22B2–6, 4N/27W-22B8–11, 4N/27W-22A2–4, 4N/27W-22G2–4, 4N/27W-23E1–4, 4N/27W-23E5, 4N/27W-23F2–4, and 4N/27W-23F5–9; fig. 9). Monitoring wells 4N/27W-22B2–6 and 22B8–11 are within 300 ft of the Vera Cruz well, one of the main production wells in the Santa Barbara groundwater basin (fig. 9). Wells 22B2–6 are perforated in the upper producing zone, middle zone, lower producing zone, lower aquitard, and the three producing zones, respectively, and wells 22B8–11 are perforated in the lower aquitard, lower producing zone, middle producing zone, and upper producing zone, respectively. Water-level data were collected at wells 22B2–6 primarily during mid-1970s to the early 1990s, whereas data were collected at wells 22B8–11 primarily during the early 1990s to 2013 Overall, simulated hydraulic heads and measured water levels matched fairly well for these wells, except for wells 22B3 and 22B6 (fig. 19*D*). Monitoring well 4N/27W-22B3 was assumed to be perforated in the middle zone, which, with the exception of the middle producing zone, is generally composed of fine-grained material; therefore, the simulated response of the hydraulic heads to pumping was less variable than that shown by the measured data. Monitoring well 4N/27W-22B6 is perforated throughout all three producing zones in an area where there was a large vertical gradient between these zones. The lower simulated hydraulic heads for this well could, therefore, be partially due to the manner in which SBFTM averages the heads in each layer to produce a representative head value for the monitoring well. The direction of the vertical gradient was simulated accurately in wells 4N/27W-22B9 and 22B11, with highest heads in the lower producing zone (22B9) and lowest heads in the upper producing zone (22B11). The simulated vertical gradient between the lower and middle producing zones was slightly exaggerated; simulated hydraulic heads in the lower producing zone were slightly higher than measured during the recovery period from 1991 to 2013 (fig. 19*D*).

Monitoring wells 4N/27W-22A2–4 and 4N/27W-22G2–4 are about 0.25 mi southeast and south, respectively, from the Vera Cruz production well (fig. 9). Both sets of monitoring wells are between the main production wells and the coast and are about 0.5 mi from the coast. Monitoring wells 4N/27W-22A2–4 are perforated in the upper producing zone, middle producing zone, and lower producing zone, respectively.

Monitoring wells 4N/27W-22G2–4 are perforated in the upper aquitard, middle producing and lower producing zones, respectively. Simulated hydraulic heads, drawdowns, and vertical gradients were all in agreement with the measured data for both sets of monitoring wells (fig. 19*D*). In both wells, simulated and measured drawdowns were greater at depth, and the vertical difference in simulated hydraulic head and measured water levels from the lower to the upper zones was about 15 ft during the post-1991 recovery years.

Monitoring wells 4N/27W-23E1–4, 4N/27W-23E5–6, 4N/27W-23F2–4, and 4N/27W-23F5–9 are within 1.0 mi southeast of the Vera Cruz production well (fig. 9). Simulated hydraulic heads, drawdowns, and vertical differences in simulated hydraulic heads were similar to measured data for wells 4N/27W-23E1–5 and 4N/27W-23F2–9. Measured and simulated drawdowns for the upper, middle, and lower producing zones were all similar, with much smaller drawdowns in the upper aquitard layer (4N/27W-23E4).

Water-Level Data Fit

A simple method to assess overall model fit is to plot the simulated hydraulic heads against the measured water-level (fig. 20). For a perfect fit, all points should show a 1:1 relation (fall on the 1:1 diagonal line). The root mean square error (RMSE) between measured water-level elevations and simulated hydraulic heads was 14.7 ft. Given the scale of the SBFTM, simulated hydraulic heads reasonably matched measured water-level elevations. The average residual was –2.7 ft and the standard deviation was 14.5 ft. The average residual indicates a slight bias towards underpredicting measured water-level elevations. The residuals ranged from –156.4 to 159.5 ft; these extremes possibly represent errors in the databases, measurements that represent pumping conditions, or seasonal variations beyond the ability of the model to simulate. More than 54 percent of the simulated hydraulic heads were within 8 ft of measured water-level elevations, more than 80 percent were within 16 ft, and more than 95 percent were within 30 ft.

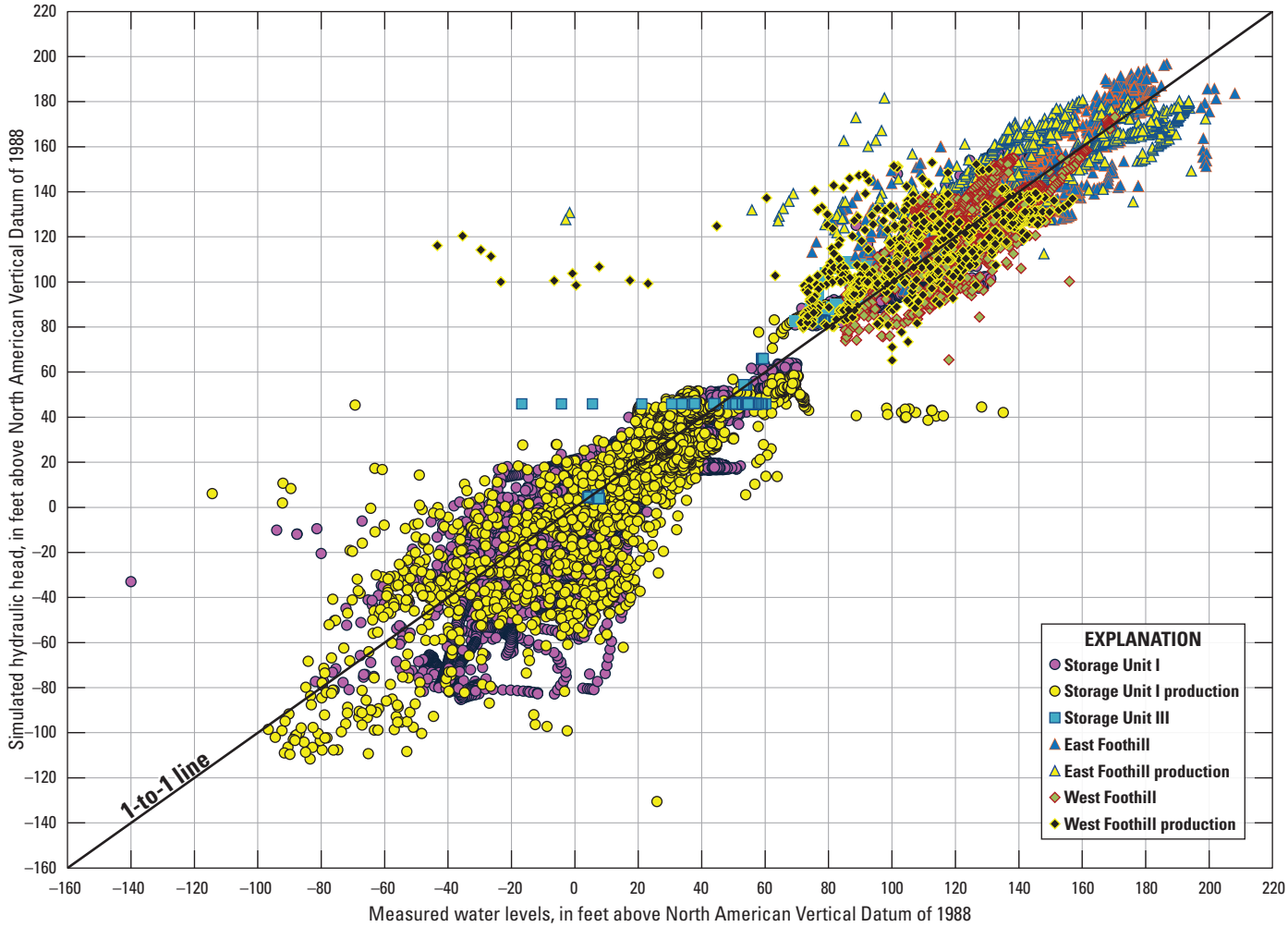

Figure 20. Simulated hydraulic heads compared with measured water levels by subbasin and well type for the Santa Barbara flow and transport model, Santa Barbara, California.

Figure 20 indicates that, overall, the SBFTM matched water levels above sea level (NAVD88) fairly well; however, it did not match water levels below sea level as well, as indicated by the greater spread in the plot of negative (below sea level) water levels. Simulated hydraulic heads in the Foothill subbasins, Storage Unit III, and the upper part of Storage Unit I, which were consistently above sea level, matched measured water levels fairly well. Simulated hydraulic heads and measured water levels in Storage Unit I that were below sea level did not match well during heavy pumping events. There were two primary factors contributing to the water-level discrepancy at these times. First, much of the measured data were from production wells or monitoring wells very close to production wells, which could result in discrepancies between the measured and simulated results (fig. 20). Water levels have a large spatial variation near pumping wells, and the SBFTM's cell dimensions are substantially greater than the well diameters; therefore, the accuracy of simulated water levels very near or in active production wells is limited. Second, recovery of water levels near the main production wells is rapid. Slight deviations between simulated and measured recovery rates lead to very large, short-term discrepancies in head. This overestimation of low water level elevations could result in underestimation of seawater intrusion should seawater reach the production wells.

Simulated Chloride Concentrations and Model Data Fit

Contours of simulated chloride concentrations for January 1972 and July 1990 are shown in figure 21. The chloride contours for January 1972 show conditions prior to seawater intruding during the 1980s and early 1990s, whereas the chloride contours for July 1990 show conditions near the peak of the historical groundwater pumpage and seawater intrusion. In general, the simulated chloride concentrations for January 1972 show limited seawater intrusion in the upper, middle, and lower producing zones; the greatest seawater intrusion occurred in the middle producing zone (figs. 21*A*, *C*, *E*). Simulated chloride concentrations in the upper producing zone were less than 2,000 mg/L in all onshore model cells (fig. 21*A*). Simulated chloride concentrations were greater than 2,000 mg/L in the middle producing zone as far as 1,600 ft inland and about 2,300 ft from the Vera Cruz production well (fig. 21*C*). Simulated chloride concentrations were greater than 2,000 mg/L in the lower producing zone as far as 1,000 ft inland and about 2,640 ft from the Vera Cruz production well (fig. 21*E*).

Between January 1972 and July 1990, the simulated chloride plume moved toward the production wells in response to increased pumpage from the main production wells in Storage Unit I in all three producing zones. In the upper producing zone, the simulated 1,500 mg/L contour advanced about 790 ft toward the Vera Cruz production well and about 550 ft toward the Corporation Yard production well (figs. 21*A, B*). Simulated chloride concentrations were higher in July 1990 in the middle producing zone; the 1,500 mg/L contour moved beyond U.S. Route 101 in some areas to about 0.5 mi inland (figs. 21*C, D*). The 1,500 mg/L contour advanced toward the Vera Cruz and Corporation Yard wells, about 200 and 880 ft, respectively. In the lower producing zone, the 1,500 mg/L contour advanced toward the Vera Cruz and Corporation Yard wells about 540 and 610 ft, respectively (figs. 21*E, F*).

Figure 22 shows simulated and measured chloride breakthrough curves for selected wells in Storage Unit I where the coastal monitoring wells are on the seaward side of U.S. Route 101 and the inland monitoring wells are on the inland side U.S. Route 101. Coastal wells 4N/27W-23E1, 4N/27W-23E5, and 4N/27W-23F4 are perforated in the lower producing zone. The trend of increasing measured chloride concentrations from the late 1970s to the early 1990s was reasonably well simulated in these wells (fig. 22*A*). The trend of decreasing measured chloride concentrations in these wells from the early 1990s through 2014 was steeper than that indicated by simulated chloride concentrations, although simulated chloride concentrations decreased during this period.

Well 4N/27W-23F8 is near the coast and is perforated in the middle producing zone. The simulated and measured chloride concentrations for this well generally were between 15,000 and 18,000 mg/L. There were some notably lower measurements that are thought to be outliers or erroneous data. Simulated concentrations were close to measured, although measured concentrations appeared to decline slowly or not at all from 1990 to 2014, whereas simulated concentrations continuously declined during this period (fig. 22*A*).

Measured chloride concentrations in wells perforated in the upper producing zone (4N/27W-23E3, 4N/27W-23F2, 4N/27W-23F7) increased only slightly during the 1980s; however, the simulated chloride concentrations increased more than measured, such that simulated concentrations in wells 24N/27W-23E3 and 4N/27W-23F2 increased to about 1,500 mg/L by 1990, compared to a maximum measured concentrations of 20 and 30 mg/L, respectively (fig. 22*A*).

The simulated chloride concentrations were in agreement with the measured data for wells perforated in the upper aquitard (4N/27W-23E4 and 4N/27W-23F9) and middle zone (4N/27W-23E6 and 4N/27W-23F6), where the chloride concentrations increased minimally during the 1980s (fig. 22*A*).

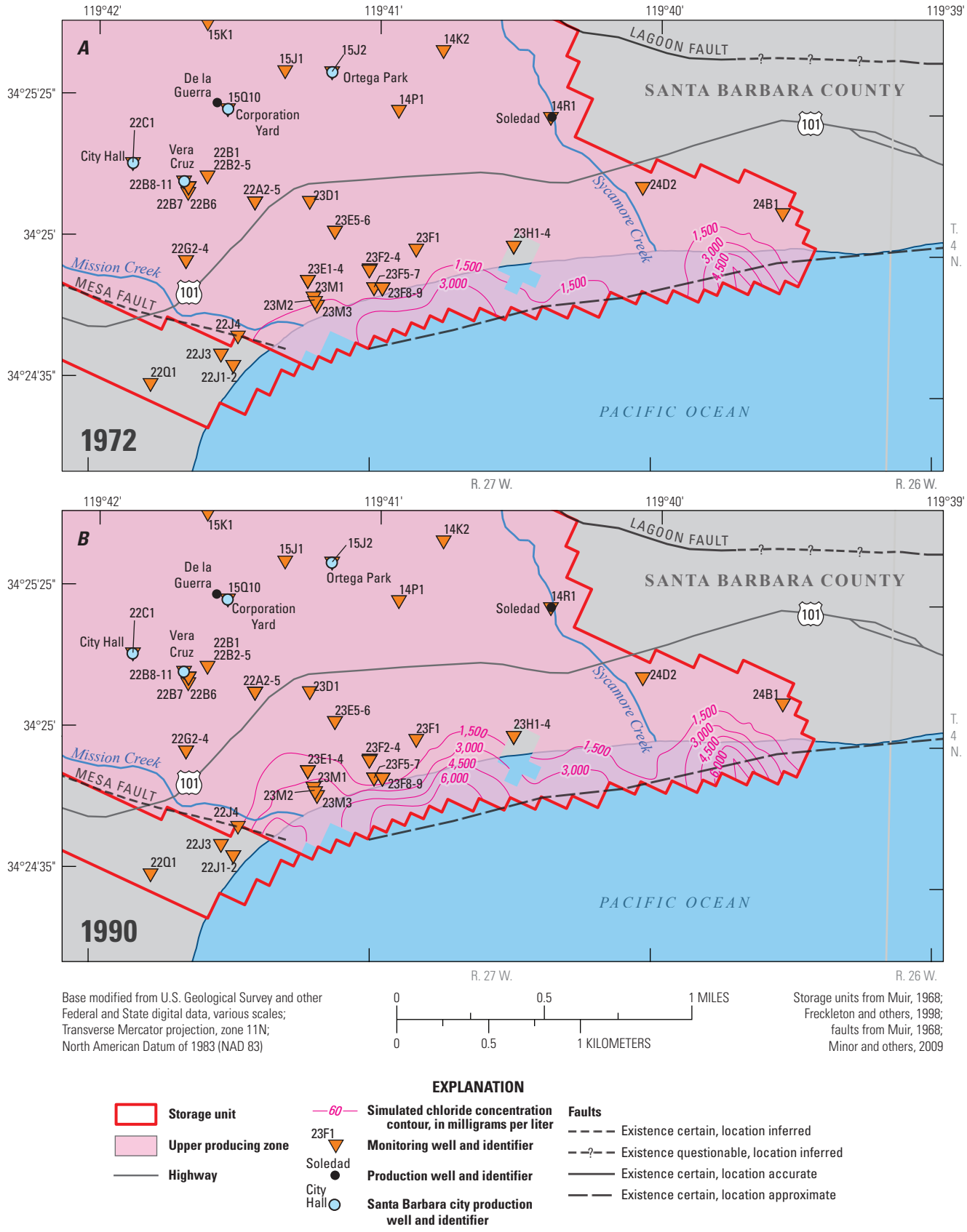

Figure 21. Simulated chloride concentration contours for different years and producing zones for the Santa Barbara groundwater basin, California: *A*, upper, January 1972; *B*, upper, July 1990; *C*, middle, January 1972; *D*, middle, July 1990; *E*, lower, January 1972; and *F*, lower, July 1990.

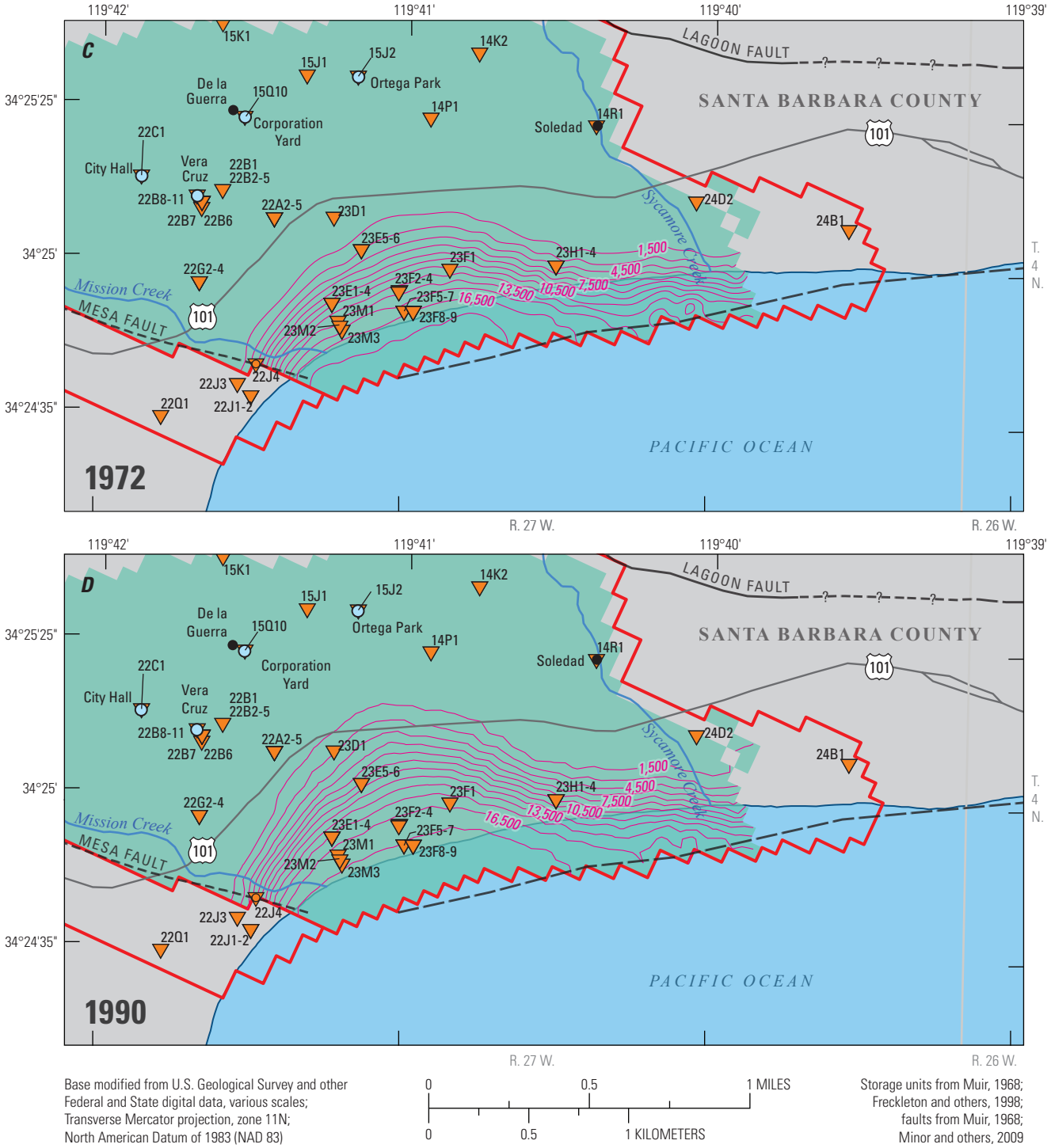

Figure 21. —Continued

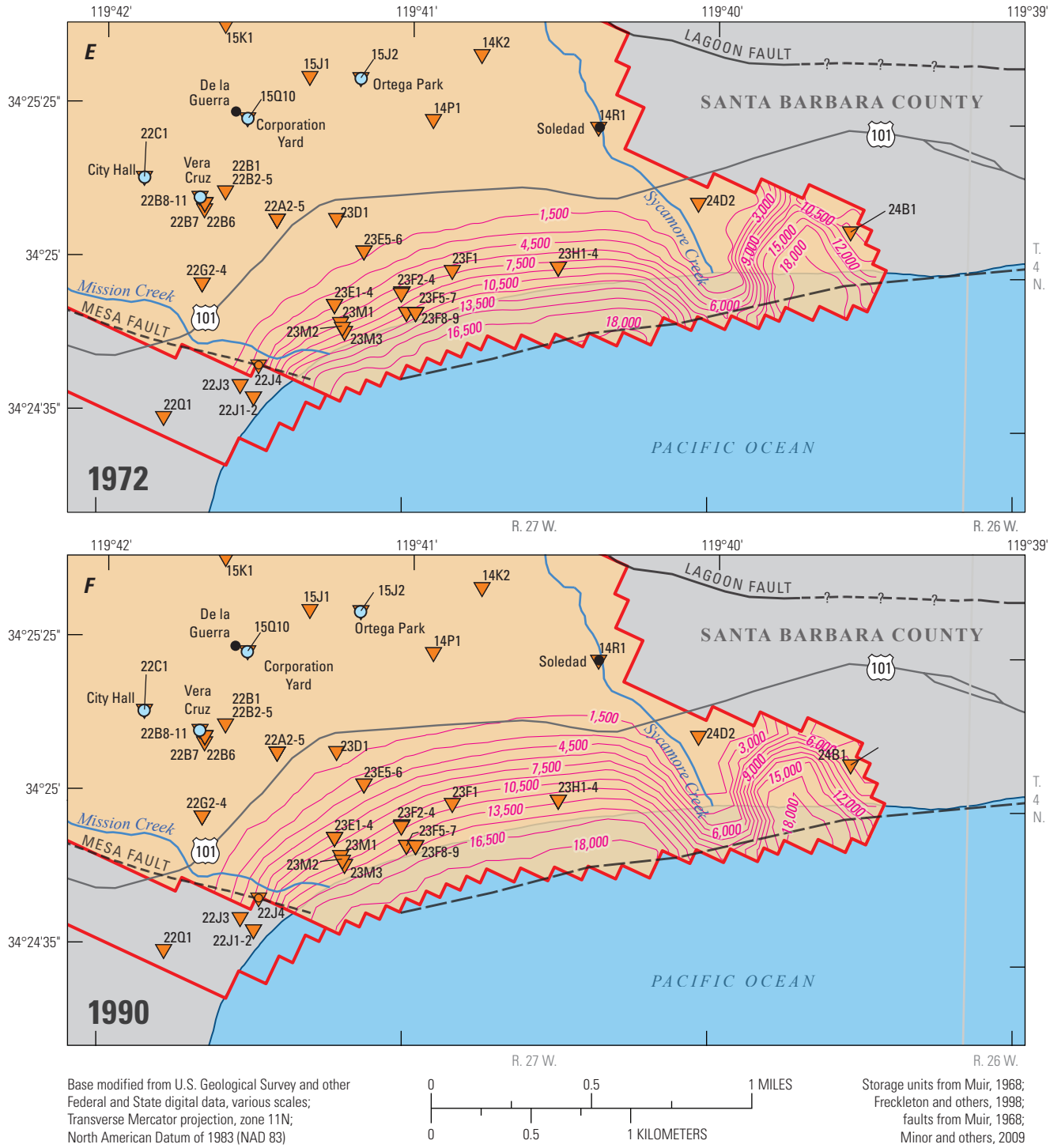

Figure 21. —Continued

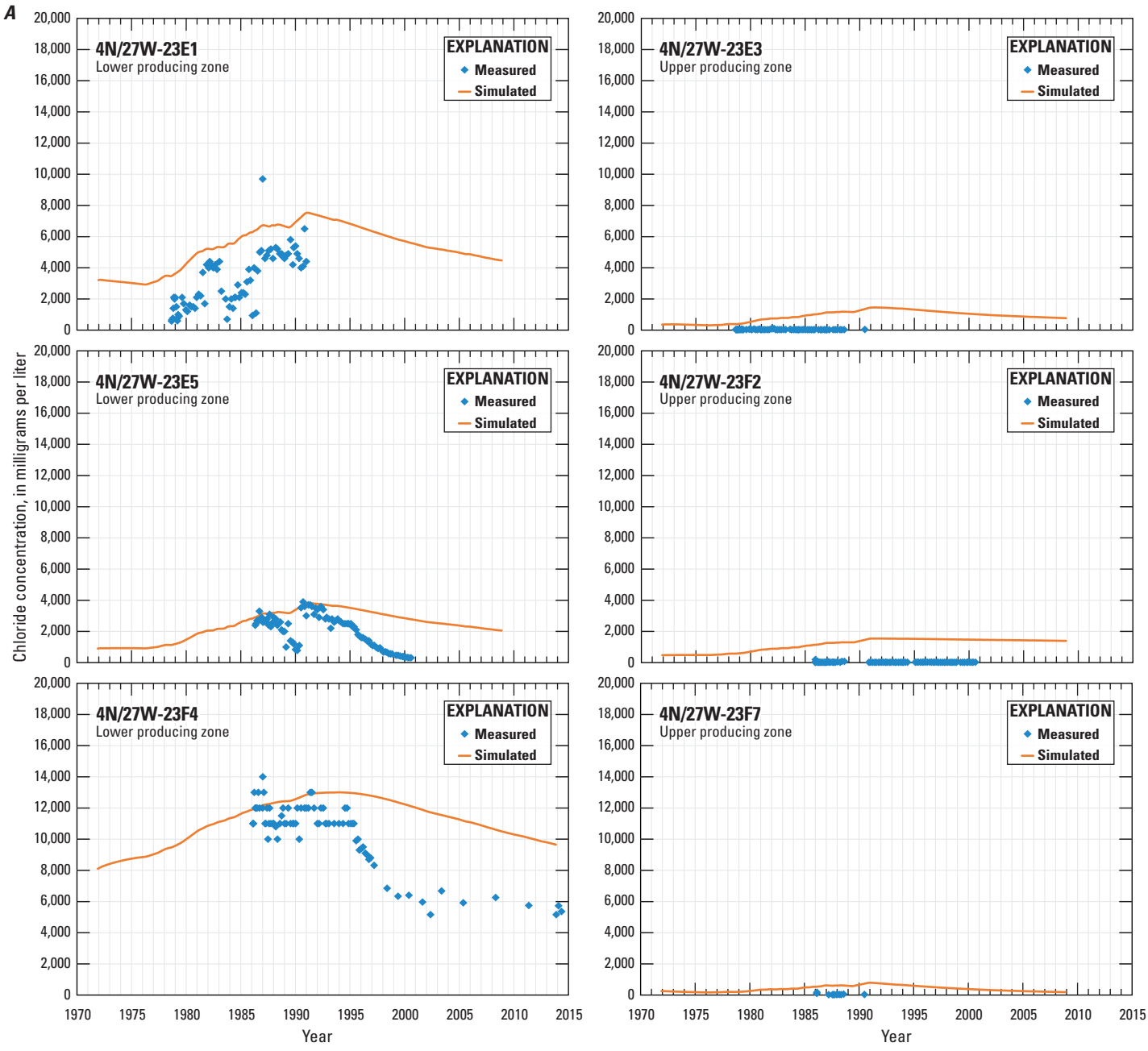

Figure 22. Simulated and measured chloride breakthrough curves for selected wells in Storage Unit I, Santa Barbara groundwater basin, California: *A*, coastal monitoring wells, and *B*, inland monitoring wells.

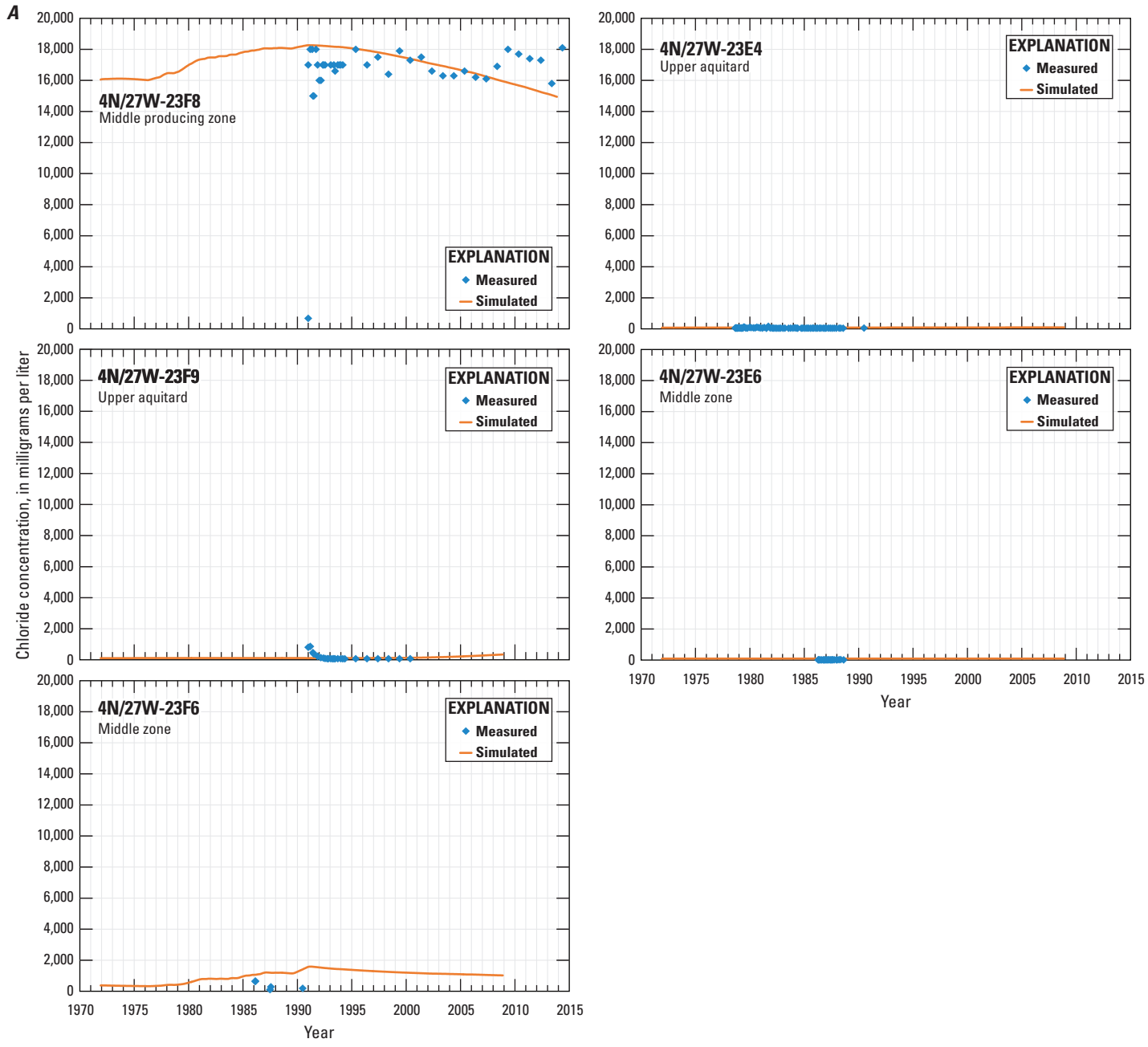

Figure 22. —Continued

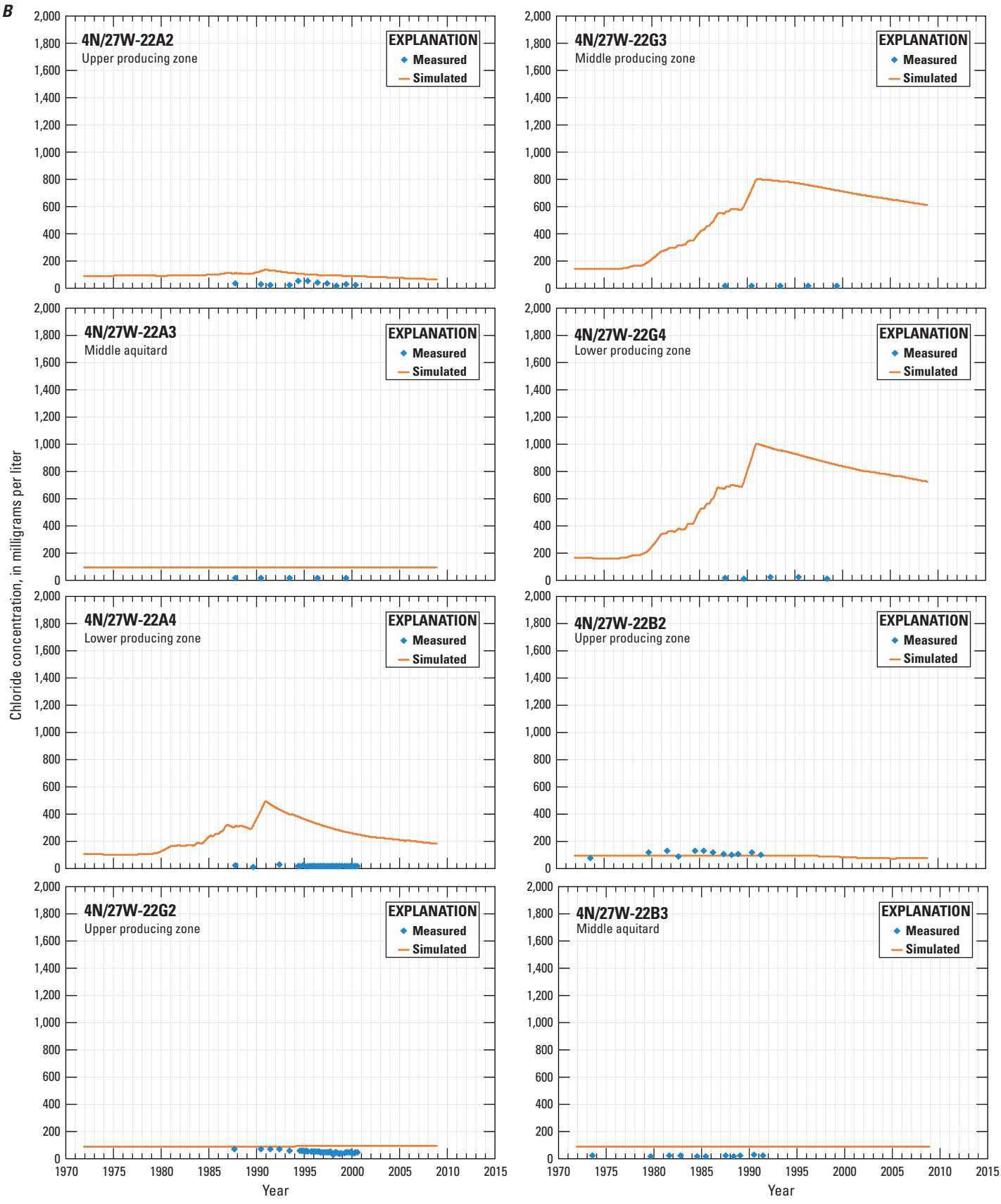

Figure 22. —Continued

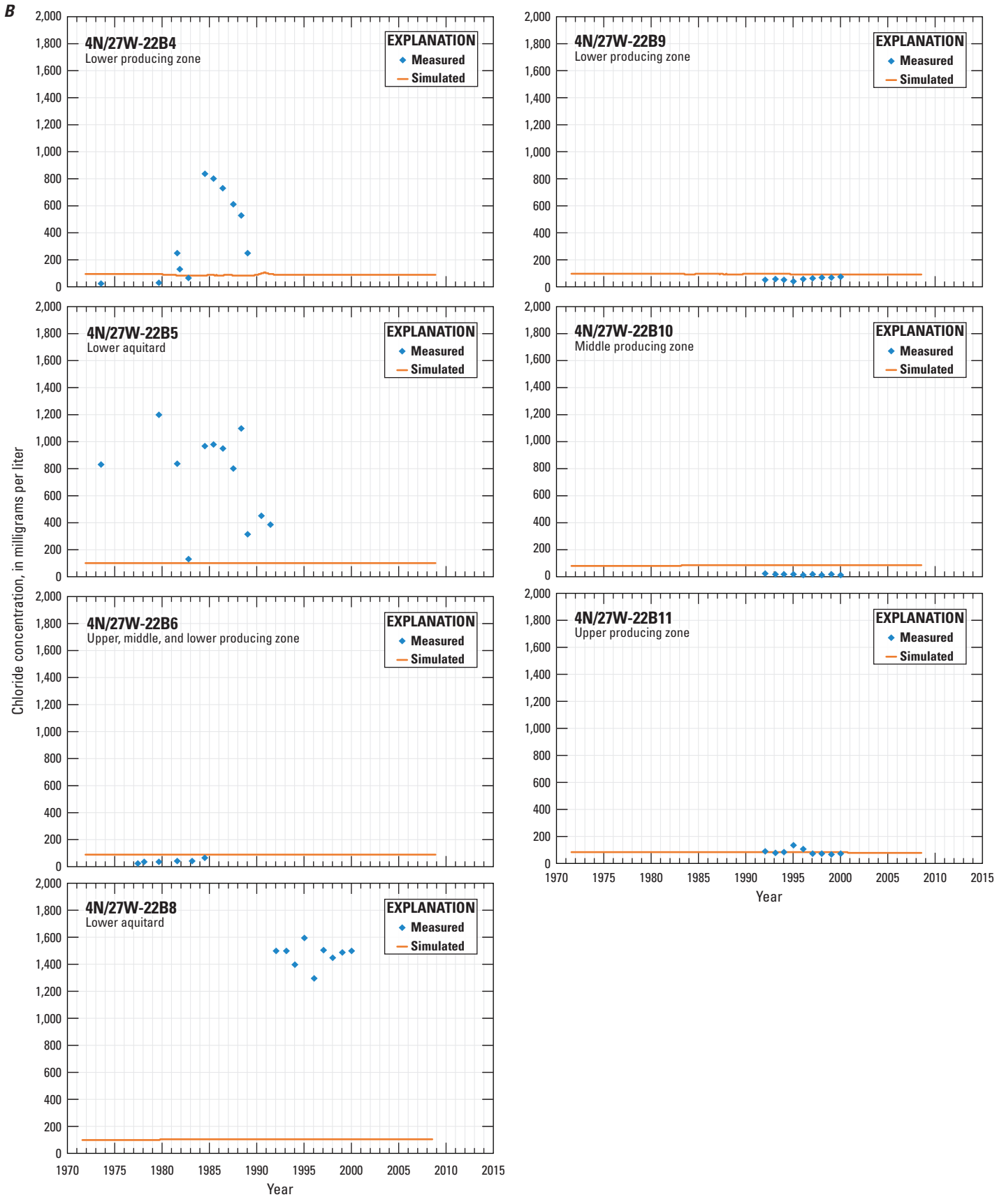

Figure 22. —Continued

For conditions farther inland, monitoring wells 4N/27W22A2–4 and 4N/27W22G2–4 are about 0.25 mi from the Vera Cruz production well and 0.5 mi from the coast (fig. 10). Measured chloride concentrations in these wells were consistently low, ranging from 10 to 60 mg/L. Simulated concentrations in wells 4N/27W22A2–3 (perforated in the upper producing zone and middle aquitard, respectively) were also consistently low; however, the simulated concentrations for well 22A4 (perforated in the lower producing zone) were greater that measured (fig. 22*B*). Simulated concentrations in wells 4N/27W22G2–4 increased in the middle and lower producing zones (22G3 and 4, respectively) during and after the 1980s, peaking at about 1,000 mg/L. Simulated chloride concentrations in the upper producing zone (well 4N/27W-22G2) were consistently low, at about 90 mg/L.

Monitoring wells 4N/27W-22B2–6 and 4N/27W-22B8–11 are the farthest inland sites used for monitoring chloride; they are near the Vera Cruz production well (fig. 10). In general, the measured and simulated chloride concentrations were generally low for these wells. Measured and simulated concentrations were less than 100 mg/L for the wells perforated above the lower producing zone. Wells 4N/27W22B4, 5, and 8, are perforated in the lower producing zone or the lower aquitard and have measured chloride concentrations as high as 1,600 mg/L; however, simulated chloride concentrations for these wells were substantially lower, at about 100 mg/L (fig. 22*B*). Recall that barium and boron concentrations in excess of the concentration of the two constituents in ocean water indicated that seawater intrusion was not the source of the elevated chloride concentrations in the deeper Vera Cruz wells (Martin, 1984). Because the SBFTM only simulates elevated chloride concentrations from seawater intrusion, it was not expected to match these chloride concentrations.

A simple method of assessing overall model fit is to plot the simulated chloride concentration against the measured chloride concentration (fig. 23). In a perfect fit, all points show a 1:1 relation (fall on the 1:1 diagonal line). The RMSE between measured and simulated chloride concentration was 1,586.5 mg/L. Given the scale of the SBFTM, simulated chloride concentration reasonably matched measured chloride concentration. The average residual was –426.0 mg/L, and the standard deviation was 1,529.0 mg/L. The average residual indicated a bias toward underpredicting the measured chloride concentrations. The residuals ranged from –6,449.0 to 4,889.4 mg/L; these extremes possibly represent errors in simulating the movement of the seawater intrusion front due to limitations of the model. More than 50 percent of the simulated chloride concentrations were within 600 mg/L of measured chloride concentration, more than 81 percent were within 1,900 mg/L, and more than 94 percent were within 3,600 mg/L.

As stated previously, the underestimation of low water levels at the production wells could lead to an underestimation of seawater intrusion. However, there are a number of other assumptions and discrepancies in the model that could lead to an overestimation of seawater intrusion. A comparison of simulated and measured chloride concentrations indicated that the SBFTM matched them fairly well both at high and low concentrations, but tended to slightly overestimate chloride concentrations, especially at lower concentrations (fig. 23). The slight overestimation of low chloride concentrations was related to the SBFTM slightly overestimating the advance of the chloride front during periods of heavy pumping and underestimating the retreat of the chloride front during periods of low pumping. Some of the chloride data from wells 4N/27W-23F4, and 23F8 were rounded to the nearest 1,000 mg/L at chloride concentrations above 10,000 mg/L. As a result, discrete jumps in measured chloride values can be seen in figure 23 for many of the measured chloride concentrations above 10,000 mg/L.

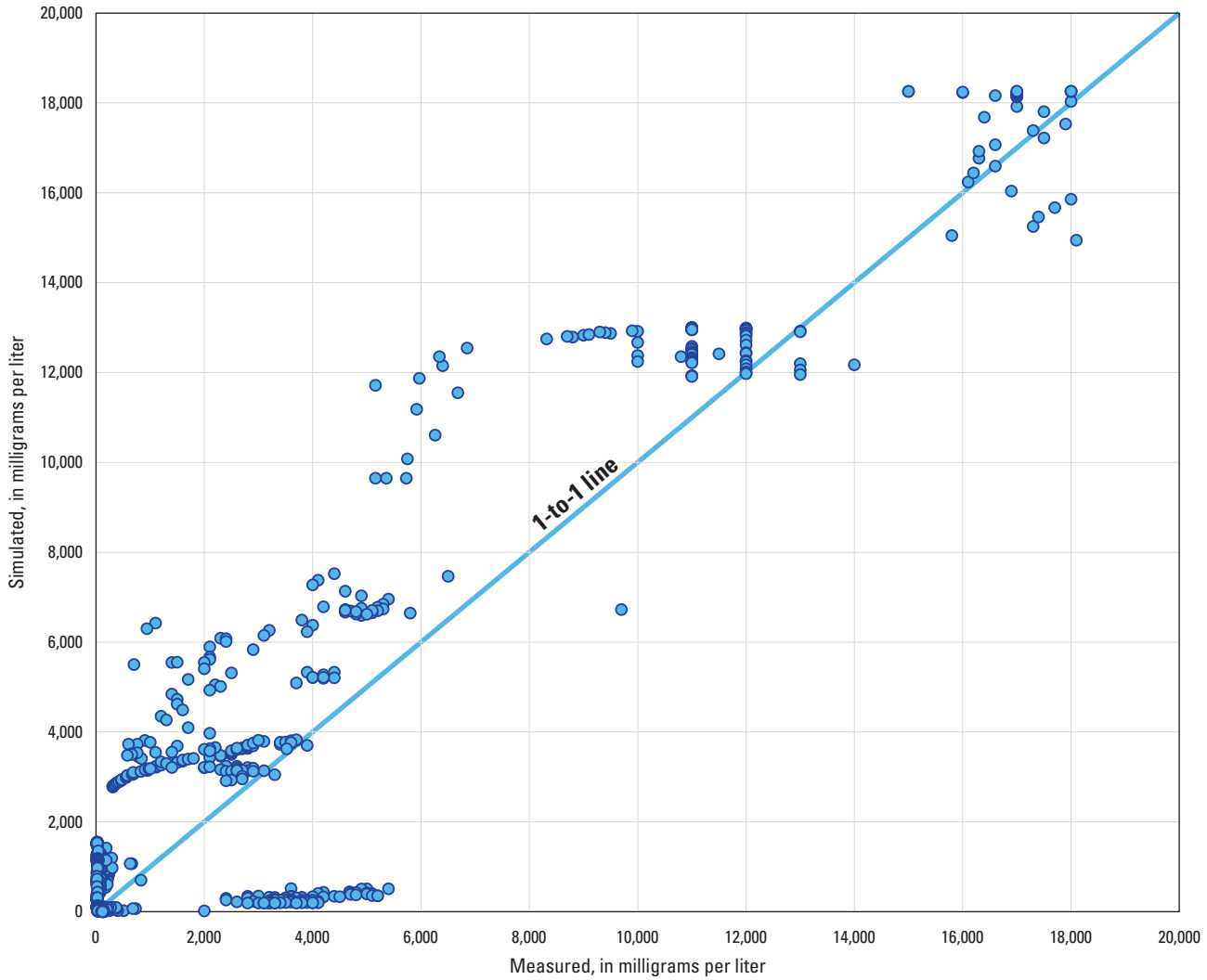

Figure 23. Simulated chloride concentrations compared with measured chloride concentrations for selected monitoring wells in Storage Unit I, Santa Barbara groundwater basin, California.

Model Limitations and Appropriate Use

A groundwater-flow and solute-transport model is a valuable tool for testing the conceptualization of the groundwater-flow system and for predicting the response of the system to changes in aquifer stresses. However, a model is only an approximation of the actual aquifer system and is not expected to exactly mimic the system being simulated. The model relies on estimates of aquifer properties and stresses, which have some degree of uncertainty.

Water levels and chloride concentrations simulated by the model are average values for the volume represented by each model cell. Simulated heads can vary considerably from measured water levels because of well location, depth, and construction. For example, wells may be perforated over a depth represented by more than one model layer, whereas corresponding measured water levels could represent an unknown composite of the hydraulic head across this perforated interval. The size of the model cells and the length of the stress periods of the model used in this work were appropriate when considering the resolution of available data and the regional scale of the simulation, however. Because model uncertainty increases substantially as the size of the area of interest decreases, the model generally is not appropriate for addressing detailed, local-scale problems. However, the regional model presented in this work can be used in the development of boundary conditions for other refined, local-scale groundwater models.

The SBFTM assumes constant stage for each creek in the model area. Streams in the model area are known to vary in stage. These seasonal fluctuations in stage, which could influence groundwater flow, are not simulated by the SBFTM. The SBFTM was constructed using a 56-layer model grid, with cell thickness for most of the model set to 20 ft. The model grid follows land surface, which sometimes differs from the path of groundwater flow in Storage Unit I, where the lower producing zone crosses multiple model layers as it increases in depth toward the coast. As the lower producing zone crosses model layers, the horizontal model connections between the lower producing zone and the surrounding confining layer can lead to additional flow between the producing zone and the aquitard. Layers in the SBFTM were all treated as confined; therefore, model layers could not go dry, and the SBFTM might overestimate groundwater flow near the water table during times when the water table is relatively low.

The bottom of the SBFTM was assumed to be a no-flow boundary, which does not allow flow or transport between the deep zone (bottom of the model) and the underlying bedrock. Previous studies have indicated that the underlying shale contains water with high chloride concentrations and that this water is a source of high chlorides in some wells perforated in the deep and lower producing zones. Therefore, it is a limitation in some parts of the model domain that the SBFTM does not simulate the transport of chlorides from the underlying shale to the deep zone and underestimates chloride concentrations in the deep zone and some areas of the lower producing zone.

The pumpage data available in the study area before 1971 were incomplete. Overall, pumpage from the major production wells in the study area was often known, but the amount of pumpage from each production well could not always be determined. When the distribution of pumpage could not be determined from data, the simulated pumpage distribution was approximated by parameter estimation, and might not reflect the actual distribution of pumpage; therefore, the early time responses to pumping might not be accurate. In addition, agricultural pumpage was not estimated for the model.

The amount of underflow from adjacent uplands (small-catchment recharge) was unknown and was determined by parameter estimation; therefore, the model might not accurately simulate the total underflow from adjacent uplands. Small-catchment recharge zones were aligned with the canyons to simulate separate recharge rates from different canyons. The model only simulates variations in small-catchment recharge on a zone-by-zone basis, and the model does not simulate variations on a smaller scale. That is, the model averages variations in small-catchment recharge that might exist in each zone and applies recharge homogenously across the zone, which could affect model accuracy.

The middle zone consists of fine-grained deposits interspersed with occasional coarse-grained water-bearing deposits. The coarse-grained water-bearing deposits in the middle zone vary in thickness and some could be substantially less than 20 ft thick, the approximate thickness of SBFTM model cells. The transport of chlorides could take a circuitous path through thin connecting lenses of coarse-grained deposits. The 20-ft-thick cells of the SBFTM can only approximate transport along such a small, circuitous path. Transport of chlorides through thin connecting lenses can lead to concentrating chlorides primarily in the connecting lenses and not in the rest of the model cell. Circuitous paths across connected coarse-grained lenses can lead to longer transport times because the chlorides must travel a greater distance. Therefore, the model discretization of 20 ft-thick cells might limit the model's ability to accurately predict transport time and concentrations of chlorides if interconnected coarse-grained lenses exist on a smaller scale.

Despite the uncertainty and these limitations, the SBFTM provides a conservative estimate of the amount of pumping permissible before seawater intrusion becomes an issue, because the SBFTM slightly overestimates the amount of seawater intrusion and slightly underestimates the dilution rate of seawater after the intrusion event. These simulation errors are conservative in terms of, for example, engineering solutions for seawater intrusion. That is, any engineering solution based on the simulated results would be designed for higher chloride concentrations than what might be found in reality, which would result in a conservative design.

In addition, the SBFTM can be used to estimate the effects of water-resource management strategies both on water levels and on seawater intrusion, assuming current and future climate scenarios. In addition, it can be coupled with an optimization algorithm to identify water-resource management strategies that optimize a given objective (or objectives) subject to a set of constraints. The SBFTM has been coupled with a multi-objective evolutionary algorithm, and the results are presented in chapter D.

Summary and Conclusions

In order to simulate seawater intrusion under various water-management scenarios, estimate the sustainability of the Santa Barbara and Foothill groundwater basins, and determine optimal strategies to manage the groundwater basins, a three-dimensional, density-dependent groundwater-flow and solute-transport model (SBFTM) of the groundwater basins was developed. The simulation time series used annual stress periods from 1929 to 1971 and monthly stress periods from 1972 to 2013. The SBFTM uses 250-by-250 ft cells and was divided into 56 layers to simulate flow in the upper, middle, and lower producing zones and the surrounding zones. The SBFTM was calibrated using 24,884 water-level observations, 1,064 chloride-concentration observations, and 254 parameters. The parameters represent hydraulic parameters (hydraulic conductivity, storage, and others), transport parameters (dispersivity, porosity, and others), conductance properties (fault, general-head boundary, and drains), creek properties (bed conductance and stage), and recharge or discharge parameters.

Parameter sensitivities varied over about two orders of magnitude for the 30 most sensitive parameters. The 30 most sensitive parameters are of varying types, including those controlling small-catchment recharge, pumping, horizontal and vertical hydraulic conductivity, porosity, and flow between the SBFTM and the ocean. The SBFTM was most sensitive to parameters controlling recharge, pumping, and hydraulic conductivity. The sensitivity of recharge and pumping parameters was most likely amplified by faults limiting flow out of Storage Unit I, making recharge and pumping the main mechanisms of inflow and outflow in Storage Unit I.

Analyses of the simulated hydrologic budget indicated that the sources of simulated recharge were primarily small catchments and creeks. Small catchments were the primary source of recharge during wetter periods, when pumping was limited. Creek leakage was the primary source of recharge during dry years. It was assumed that the creek stages are always greater than zero; therefore, the creeks are a constant source of water to the model.

The primary groundwater sink was pumping. Between 1929 and 2013, pumpage varied greatly; generally, pumping rates were higher during drier periods, and pumping rates were lower during wetter periods. Overall, groundwater pumping resulted in a net loss of about 11,400 acre-feet (acre-ft) of groundwater storage between 1929 and 2013.

Overall, the SBFTM replicated the natural groundwater-flow direction from the Sycamore, Mission, Lauro, and Aliso Canyons southwest through the Foothill groundwater basin and southeast through the Santa Barbara groundwater basin. In addition, the model replicated the change in direction of groundwater flow from northwest-to-southeast to a radial path toward the pumping center in the southeastern part of Storage Unit I caused by pumping during the late 1980s and early 1990s. The simulated radial-flow pattern extended to the offshore fault, which reversed the direction of flow across the fault, resulting in the simulation of seawater intrusion into the middle and lower producing zones.

Overall, the SBFTM simulated the areal distribution of seawater intrusion and the rising limb of chloride breakthrough curves well. The SBFTM simulated the areal distribution and response of chloride to pumpage. Seawater intrusion was overestimated during the 1990s, however. Regarding the chloride breakthrough curves, the SBFTM generally simulated the rising limbs of the measured breakthrough curves; however, the falling limbs were overestimated. This was caused by a combination of the SBFTM overestimating the advance of the chloride front during periods of heavy pumping and underestimating the retreat of the chloride front during periods of low pumping.

Overall, the SBFTM replicated the measured hydrographs. Measured values and trends were replicated as well as vertical gradients. The SBFTM simulates seawater intrusion but slightly overestimates the amount of seawater intrusion and slightly underestimates the dilution rate of seawater after the intrusion event.

References Cited

California Department of Water Resources, 1996, 1996 South central coast land use survey data: Sacramento, Calif., State of California, digital map accessed on July 12, 2011, at http://www.water.ca.gov/landwateruse/lusrvymain.cfm, currently available at https://www.water.ca.gov/Programs/Water-Use-And-Efficiency/Land-And-Water-Use/Land-Use-Surveys.

Daly, C., and Bryant, K., 2013, The PRISM climate and weather system—An introduction: Prism Climate Group, 5 p., accessed January 21, 2015, at http://www.prism.oregonstate.edu/documents/PRISM_history_jun2013.pdf.

Doherty, J.E., 2010, PEST—Model-independent parameter estimation, user manual (5th ed.), addendum to the PEST manual: Watermark Numerical Computing, 336 p.

Freckleton, J.R., Martin, P., and Nishikawa, T., 1998, Geohydrology of Storage Unit III and a combined flow model of the Santa Barbara and Foothill ground-water basins, Santa Barbara County, California: U.S. Geological Survey Water-Resources Investigations Report 97–4121, 80 p., http://pubs.er.usgs.gov/publication/wri974121.

Freeze, R.A., and Cherry J.A., 1979, Groundwater: Englewood Cliffs, N.J., Prentice-Hall, 604 p., http://hydrogeologistswithoutborders.org/wordpress/1979-toc/.

Goldman, C.R., and Horne, A.J., 1983, Limnology: New York, McGraw-Hill Book Co., 464 p.

Harbaugh, A.W., Banta, E.R., Hill, M.C., and McDonald, M.G., 2000, MODFLOW-2000, the U.S. Geological Survey modular ground-water model—User guide to modularization concepts and the ground-water flow process: U.S. Geological Survey Open-File Report 2000–92, 121 p., https://pubs.er.usgs.gov/publication/ofr200092.

Hill, M.C., 1990, Preconditioned conjugate-gradient 2 (PCG2), a computer program for solving ground-water flow equation: U.S. Geological Survey Water-Resources Investigations Report 90–4048, 43 p., https://pubs.er.usgs.gov/publication/wri904048.

Hsieh, P.A., and Freckleton, J.R., 1993, Documentation of a computer program to simulate horizontal-flow barriers using the U.S. Geological Survey's modular three-dimensional finite-difference ground-water flow model: U.S. Geological Survey Open-File Report 92–477, 32 p., https://pubs.er.usgs.gov/publication/ofr92477.

Langevin, C.D., Thorne, D.T., Jr., Dausman, A.M., Sukop, M.C., and Guo, W., 2008, SEAWAT version 4: A computer program for simulation of multi-species solute and heat transport: U.S. Geological Survey Techniques and Methods book 6, chap. A22, 39 p., https://pubs.er.usgs.gov/publication/tm6A22.

Martin, P., 1984, Ground-water monitoring at Santa Barbara, California; Phase 2—Effects of pumping on water levels and on water quality in the Santa Barbara ground-water basin: U.S. Geological Survey Water Supply Paper 2197, 31 p., https://pubs.er.usgs.gov/publication/wsp2197.

McDonald, M.G., and Harbaugh, A.W., 1988, A modular three-dimensional finite-difference ground-water flow model: U.S. Geological Survey Techniques of Water-Resouces Investigations book 6, chap. A1, 586 p., https://pubs.er.usgs.gov/publication/twri06A1.

McFadden, M.C., Polinoski, K.G., and Martin, P.M., 1991, Measurement of streamflow gains and losses on Mission Creek at Santa Barbara, California; July and September 1987: U.S. Geological Survey Water-Resources Investigations Report 91–4002, 15 p., https://pubs.er.usgs.gov/publication/wri914002.

Minor, S.A., Kellogg, K.S., Stanley, R.G., Gurrola, L.D., Keller, E.A., and Brandt, T.R., 2009, Geologic map of the Santa Barbara coastal plain area, Santa Barbara County, California: U.S. Geological Survey Scientific Investigations Map 3001, scale 1:25,000, 1 sheet, pamphlet, 38 p., https://pubs.er.usgs.gov/publication/sim3001.

Muir, K.S., 1968, Ground-water reconnaissance of the Santa Barbara-Montecito area, Santa Barbara County, California: U.S. Geological Survey Water Supply Paper 1859–A, 28 p., https://pubs.er.usgs.gov/publication/wsp1859A.

U.S. Census Bureau, 2017, QuickFacts from the U.S. Census Bureau, Santa Barbara city, California, accessed September 2017 at https://www.census.gov/quickfacts/fact/table/santabarbaracitycalifornia/HSD310215.

U.S. Department of Agriculture, 2008, Natural Resources Conservation Service, Soil Survey Geographic (SSURGO) database for Santa Barbara County, California, south coastal part: National Resources Conservation Service, accessed on July 12, 2011, at https://www.nrcs.usda.gov/wps/portal/nrcs/surveylist/soils/survey/state/?stateId=CA.

U.S. Geological Survey, 2013, USGS 11119745 Mission C A Rocky Nook Park A Santa Barbara CA: U.S. Geological Survey National Water Information System database, accessed November 2013, at https://waterdata.usgs.gov/nwis/uv?site_no=11119745.

Zheng, C., 2006, MT3DMS v5.2 supplemental user's guide: Tuscaloosa, Ala., University of Alabama, Department of Geological Sciences, 41 p., http://inside.mines.edu/~epoeter/583/14/discussion/mt3dms_v5_supplemental.pdf.

Zheng, C., 2010, MT3DMS v.5.3 supplemental user's guide: Tuscaloosa, Ala., University of Alabama, Department of Geological Sciences, 51 p., https://hydro.geo.ua.edu/mt3d/mt3dms_v5_supplemental.pdf.

Zheng, C., and Wang, P.P., 1999, MT3DMS—A modular three-dimensional multispecies transport model for simulation of advection, dispersion, and chemical reactions of contaminants in groundwater systems; Documentation and user's guide: Tuscaloosa, Ala., University of Alabama, Contract Report SERDP-99-1, 221 p., https://hydro.geo.ua.edu/mt3d/mt3dmanual.pdf.

Chapter D: Multi-Objective Simulation-Optimization Model

By Zachary P. Stanko and Tracy Nishikawa

Introduction

The city of Santa Barbara is interested in identifying management strategies that maximize the available groundwater resources while limiting drawdown and any associated seawater intrusion. In order to identify the best strategies, the U.S. Geological Survey (USGS) and the city cooperatively developed a simulation-optimization model, which uses the Santa Barbara flow and solute-transport model (SBFTM), described in chapter C, to derive optimal management strategies and estimate maximum pumping rates for a range of potential future climatic conditions. The SBFTM was used to develop a collection of predictive simulations that can be used to produce optimal pumping schedules and optimal pumping rates for each climatic condition. These simulations have different management horizons (time periods over which pumpage is optimized), initial groundwater levels, chloride concentrations, and climatic conditions. Overall, five management-optimization scenarios were developed in a multi-objective framework to obtain optimal pumping rates for all of the city's managed wells that maximize withdrawals, while minimizing drawdown and seawater intrusion.

This chapter describes the groundwater-management problem, reviews the multi-objective framework and optimization methods used to approximate optimal solutions for multiple competing objectives, defines the selected future-management scenarios, and presents the resulting solutions that optimizes pumping under the constraints and objectives of each of the scenarios. The simulated scenarios have management horizons ranging from 2 to 10 years; initial conditions from historically low to relatively high-water levels; and climatic conditions ranging from typical of the recent past to those of a 10-year drought.

Following the availability of imported water from the California State Water Project (SWP) in 1997 and the construction of a desalination plant, Nishikawa (1998) used a groundwater-flow model of the Santa Barbara groundwater basin to optimize pumping rates. Using a flow-only simulation, that is, the transport of chloride and computation of its concentrations were not simulated, the optimization was formulated as a linear-programming (LP) problem with a single minimize-cost objective function. Mild nonlinearities in the groundwater model, due to simulation of drains, were resolved with a simple iterative method. A 5-year management horizon was used, which corresponded to the city's design drought of calendar year 1947–51. The decision variables—or the choices involved in making management decisions, in this case associated with the water sources available for use—were the monthly pumpage from groundwater wells, imported water from the SWP, as well as water supply available from local surface water and desalination. Constraints included groundwater levels, pumping-well capacity, and water demand. Results of the 1998 study showed that a minimum-cost solution could be met by maximizing the lowest cost water source (surface water, when available) and continuously pumping the inland wells. The 1998 study also showed that desalinated water (the highest cost water source) was not used during the design drought of 1947–51. Note that the 1998 study was based on rules and regulations for surface water in effect at the time; since then, a Biological Opinion for the Cachuma Project (Cachuma Operation and Maintenance Board, 2017) has been issued and is under reconsultation by the Bureau of Reclamation and National Marine Fisheries Service.

Literature Review

Optimization methods have been widely used for water-resources management. A general overview of optimization methods will first be presented followed by a discussion of their applications to water-resources management.

Optimization Methods

A variety of techniques can be used to formulate and solve optimization problems. For the purposes of this study, there are two general techniques for solving large-scale (characterized by a large number of decision variables) optimization problems: mathematical programming and global search. Strict mathematical programming techniques can guarantee convergence to a local optimum but require that the underlying functions have certain inherent features (for example, continuity, differentiability, and convexity) to find a solution. Mathematical programming techniques require differentiability, because gradient information is required; this is computationally intensive. For additional information regarding mathematical programming techniques, see Nocedal and Wright (2006).

Global-search techniques can find or approximate a global optimum without gradient information; instead, a randomized search strategy is used. A global search is not associated with the features of the underlying mathematics. The functional relationships between inputs and outputs of an embedded or linked simulation model are not important for the global-search optimization techniques; therefore, problems that are highly nonlinear, discontinuous, or not differentiable are solvable. In addition, running simulations external to the optimization allows the use of parallel computing to conduct the global search in a computationally efficient manner (McKinney and Lin, 1994). For additional information regarding global-search techniques, see Coello and others (2007).

Frequently, an optimization problem has more than one objective. Different project goals can conflict with each other. These goals could make an optimization problem infeasible if incorporated as constraints, so alternatively, they can be posed as separate objectives. Given complex relationships among competing objectives, a multi-objective optimization problem can be formulated to find compromise solutions. Instead of a unique solution, a multi-objective optimization produces a set of solutions from which a decision maker can choose the solution that most aligns with the most important needs at the time. No single solution in the set can be better than other solutions in the set with respect to all objectives; this concept is called Pareto optimality (Coello and others, 2007). A Pareto-optimal solution is a feasible solution that cannot improve any of the objectives without worsening at least one other objective. To illustrate this concept of Pareto-optimality, figure 1 demonstrates a Pareto-optimal solution for a generic two-objective problem. For more detailed discussion of multi-objective optimization, see Coello and others (2007).

Evolutionary algorithms (EA) are a class of global-search techniques that can work with any problem formulation regardless of the nonlinearities and extent of complexity related to the embedded simulation model. These are a class of methods that treat the solutions of the optimization problem

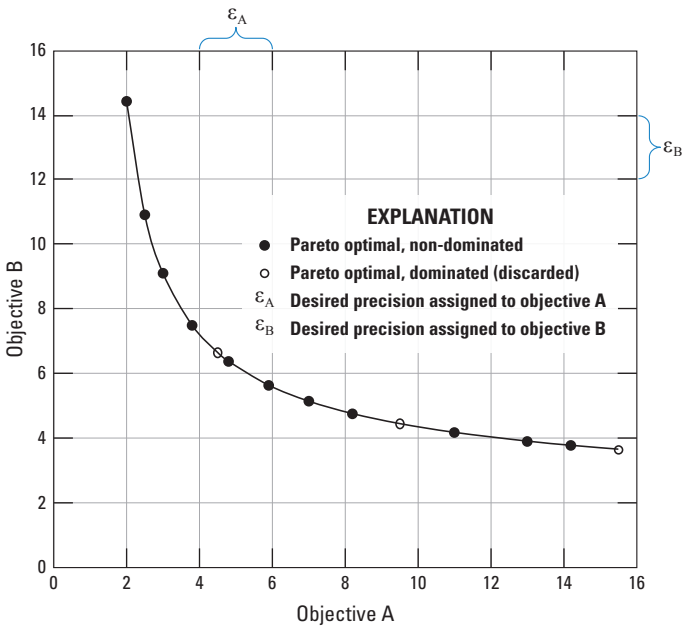

Figure 1. Concepts of Pareto-optimality are shown with two generic objectives, which are assumed to be minimization; no single point is optimal because a decrease in one objective causes an increase in the other, so any point on the curve is considered Pareto-optimal (Kollat and Reed, 2006).

as individuals in a population that are manipulated by a set of operators (mutation, combination, and selection) to evolve toward an optimal solution. The objective function of an EA is viewed as a measure of fitness for each individual solution in the population, and each iteration of selecting solutions from a population, and operating on them, is termed a generation (Coello and others, 2007). A genetic algorithm (GA) is a type of EA that primarily utilizes mutation and crossover combination to operate on variables of individual solutions that are encoded as genes on a chromosome. The concept of 'survival of the fittest' is used in GAs to rank solutions; the objective criteria are evaluated as a measure of fitness. For additional information regarding GAs and their genetic operators, the reader is referred to Coello and others (2007).

Use of EAs has been successful in a wide range of problem types, especially multi-objective optimization. A major advantage when using an EA is the ability to randomly search a large solution space in an intelligent and efficient manner without being overly susceptible to stopping prematurely in a sub-optimal region (local optima). The major disadvantage is that an EA can be slow to produce nearly optimal solutions if the problem dimensions are too high. For multi-objective problems, multi-objective evolutionary algorithms (MOEAs) have been shown to efficiently search large-scale problems with up to six objectives (Kasprzyk and others, 2009).

Groundwater-Management Models

Groundwater-flow and solute-transport models are often linked with optimization methods to solve groundwater-management problems. This linkage is the basis of a simulation-optimization model, which in the context of groundwater modeling, is also called a groundwater-management problem. When the simulation model is differentiable, or a gradient can be approximated, mathematical programming can be used. Examples of mathematical programming techniques that have been linked to groundwater models include linear programming (Molz and Bell, 1977; Lefkoff and Gorelick, 1986), nonlinear programming (Ahlfeld and others, 1988; Wang and Ahlfeld, 1994; McKinney and Lin, 1995; Das and Datta, 2000), successive linear programming (Nishikawa, 1998; Ahlfeld and Baro-Montes, 2008), and dynamic programming (Willis, 1979; Chang and others, 1992; Culver and Shoemaker, 1992, 1997). Many additional simulation-optimization review papers summarize the applications of these methods (for example, Gorelick, 1983; Yeh, 1992; Wagner, 1995; Ahlfeld and Mulligan, 2000; Mayer and others, 2002).

For groundwater-management problems specifically addressing seawater-intrusion issues, the simple approach, which constrains freshwater hydraulic heads along the coast to be above sea level, only works if the aquifer is relatively thin (Abarca and others, 2006). Singh (2014) reviews a range of simulation-optimization techniques for seawater-intrusion problems, including applications of GAs and multi-objective formulations. When the underlying flow and transport simulation model is complex, GAs are often applied (Qahman and others, 2005). Studies often use some type of EA to find solutions to single-objective seawater-intrusion problems (Qahman and others, 2005; Abd-Elhamid and Javadi, 2011). Various multi-objective optimization techniques also have been applied to seawater-intrusion problems (Cieniawski and others, 1995; Gordon and others, 2001). Dhar and Datta (2009) present an application of a GA to a multi-objective optimization of a seawater-intrusion model, where the two conflicting objectives were to (1) maximize total pumpage from all production wells and (2) to minimize pumpage from barrier wells.

Because EAs are particularly well-suited for multi-objective optimizations, they have been applied to water-resource problems (Sreekanth and Datta, 2015). Nicklow and others (2010) reviewed some applications of MOEAs to water-resource problems and specifically addressed numerous studies that use MOEAs to overcome some of the inherent difficulties of optimizations involving groundwater models. In a recent comparison among MOEAs, 10 algorithms were tested on several water-resource applications (Reed and others, 2013). The proprietary MOEA algorithm developed by Hadka and Reed (2013), referred to as Borg, consistently outperformed the others on the basis of various metrics used to evaluate algorithm effectiveness (the quality of solutions attained) and efficiency (the time it takes to attain these solutions). A study that assessed the performance of several MOEAs on a management plan for a contaminated lake, considering robust decision-making criteria and environmental-pollution constraints, also found Borg to surpass other algorithms in nearly all metrics (Ward and others, 2015).

After consulting with city personnel, it was determined that a multi-objective optimization technique was appropriate to address the city's water-resource management problem. Four objectives were identified as important goals of the study: maximize pumpage, minimize seawater intrusion, minimize total drawdown, and minimize the maximum drawdown. Given the complex nonlinear SEAWAT model and the number of decision variables, an MOEA was chosen instead of a mathematical-programming technique. The main advantages of using an MOEA for this study are that a gradient approximation is not required and that a high degree of parallelization is possible.

For this study, Borg was used to solve the multi-objective optimization using the SEAWAT groundwater-flow and solute-transport model. Borg was chosen as the optimization algorithm for this study for several reasons: (1) it is very efficient in automatically sorting, evolving, and retaining solutions; (2) it can be used in parallel to efficiently make use of multiple processors on multiple computers; (3) the algorithm is self-tuning, so there are no search or operation parameters to determine prior to using the algorithm; and (4) it is designed to effectively approximate Pareto-optimal solutions (Pareto curve) for multiple competing objectives. The first three reasons can be lumped together as features that allow the algorithm to proceed toward the optimal solution(s) at the fastest possible rate. The fourth reason (an approximate Pareto curve) can allow water managers to make the best possible decision in accordance with their preferences; for the purposes of this study the approximate Pareto-optimal solutions will be referred to as Pareto-optimal solutions. Once the Pareto curve is produced, a variety of decisions can be made with knowledge of the potential sacrifices or tradeoffs without any additional model runs. The alternative approach, to weigh each objective in advance, is very limiting and obscures possible solutions if those weights do not accurately represent future preferences. In Kasprzyk and others (2015), a comparison of the two approaches illustrates the benefits of a full multi-objective formulation.

Solution Space Discretization

In a continuous solution space, there are an infinite number of Pareto-optimal solutions. In order to choose from among the infinite number of solutions, a precision is assigned to each objective, defined by an epsilon value (ε value) that represents its favorability. Setting this ε value imposes a grid on the solution space to prevent searching for too many solutions that have similar objective values (fig. 1). Lesser values of ε with respect to the objective values themselves places more emphasis on solutions closer to the absolute minimum of a single objective. Greater values of ε with respect to the objective values themselves indicate that fewer trade-off solutions are desired with respect to an objective and an overall minimization of this objective is less important. Lesser values of ε allow for more trade-off analysis in the optimal solutions, but can also retain many solutions that differ only slightly. For example, a large ε_A (for objective A) represents less preference for maximizing A. Additionally, a lesser ε_B accepts more solutions in the full range of the objective B values. Each ε can be thought of as the weight of the objective (relative to its magnitude) on the overall decision making. The rectangular domain defined by ε_A, ε_B is termed the ε neighborhood, in which there is only one solution that is non-dominated, or optimal in the Pareto sense. For example, in figure 1 only one solution in each grid block is retained as Pareto-optimal (solid points). By defining the grid with ε_A and ε_B, the solid points dominate the hollow points as determined by the point's distance to the origin (Kollat and Reed, 2006). For additional information regarding ε dominance, the reader is referred to Hadka and Reed (2013).

For this report, additional ε values were chosen post-optimization to highlight optimization results; they were not chosen intentionally to reflect objective-function preference. If a water manager wishes to change the objective-function preference, a different set of ε values would be used and, potentially, the highlighted solutions would be different. This change in ε values would not require any additional model runs, however; all necessary information was generated in the original optimization runs.

Problem Formulation

As stated previously, the simulation-optimization problem was formulated as a multi-objective programming problem. In general, the objectives were to maximize pumpage and to minimize seawater intrusion and drawdown in production wells. The drawdown objective was formulated as two separate objective functions: minimize total drawdown to address an overall decline in water levels across all basins and minimize the maximum drawdown to address water-level declines around individual wells. In general, the constraints included pump-capacity limits, chloride drinking-water standards, and water-level limits. The decision variables were quarterly pumpage by well. The managed wells for all scenarios included the following city wells: Alameda Park, City Hall, Corporation Yard, Hope Avenue, Lincolnwood, Los Robles, Ortega Park, San Roque Park (2), Santa Barbara High School, Val Verde, and Vera Cruz (fig. 2). The Lincolnwood well, although not managed by the city at the time of this study, was included as a surrogate for a future city well that could be added in the Foothill groundwater basin. Note that background and unmanaged pumpage were not included because the focus of this study was the management of the city's wells. In addition, during times when the city's wells were pumped, most pumpage was from the city wells. The general formulation can be summarized as follows:

Objective A: Pumpage

$$minimize \sum_{i=1}^{nqtr} \sum_{j=1}^{npw} q_{ij} \tag{1}$$

Objective B: Seawater intrusion

$$minimize \sum_{i=1}^{nco} \sum_{k=1}^{ncw} c_{ik} \tag{2}$$

Objective C_t: Total drawdown

$$minimize \sum_{i=1}^{nyr} \sum_{j=1}^{npw} \left(h_{ij} - H_{j,0} \right) \tag{3}$$

Objective C_m: Maximum drawdown

$$minimize \max_{\substack{1 \le i \le nyr \\ 1 \le j \le npw}} \left(h_{ij} - H_{j,0} \right) \tag{4}$$

subject to:

Constraint 1

$$\left(250 \frac{mg}{L} - S_{ij} \right) \ge 0 \forall i = 1, \ldots, nper \; ; j = 1, \ldots, npw \tag{5}$$

Constraint 2

$$\left(q_{ij} - Q_{j,max} \right) \ge 0 \forall i = 1, \ldots, nqtr \; ; j = 1, \ldots, npw \tag{6}$$

Constraint 3

$$\sum_{j \in \Omega} q_{ij} \ge Q_{OTP} \forall i = 1, \ldots, nqtr \tag{7}$$

Constraint 4

$$h_{ij} - H_{j,min} \ge 0 \forall i = 1, \ldots, nyr \; ; j = 1, \ldots, npw \tag{8}$$

where

q_{ij} is the pumpage rate (negative out of aquifer) for pumping well j at time i,

c_{ik} is the concentration for chloride monitoring well k at time i,

h_{ij} is the weighted average hydraulic head for pumping well j at time i,

$H_{j,0}$ is the initial hydraulic head for pumping well j,

$H_{j,min}$ is the minimum acceptable hydraulic head for pumping well j,

S_{ij} is the weighted average solute concentration for pumping well j at time i,

$Q_{j,max}$ is the maximum pumpage rate for pumping well j,

$nqtr$ is the total number of quarters,

nco is the total number of concentration observations,

nyr is the total number of years,

npw is the total number of pumping wells,

ncw is the total number of chloride monitoring wells,

Q_{OTP} is the minimum flow to the Ortega treatment plant, and

Ω is the set of all wells that feed the Ortega plant (Alameda Park, City Hall, SBHS, Corporation Yard, Ortega Park, Vera Cruz).

Objective A maximizes the total pumpage for the management horizon (pumping out of the aquifer is negative in the model; therefore, the minimization used in the aforementioned formulation). Objective B minimizes the sum of chloride concentrations at 14 monitoring sites (wells 4N/27W-22A2, -22A4, -22B9, -22B10, -22B11, -22G3, -22G4, -23E3, -23E5, -23F2, -23F4, -23F5, -23F7 and -23F8; fig. 2) for all stress periods in the simulation. These monitoring sites represented existing monitoring locations near the leading edge of the observed seawater intrusion. For the purposes of this study, the sum of chloride concentrations is called "seawater intrusion"; therefore, objective B minimizes seawater intrusion. Objective C_t minimizes the sum of any drawdown below the initial hydraulic head in all city production wells during all stress periods (fig. 2). Although the intentions of objectives A and B are straightforward, the intent of objective C_t could be to control the loss of production and storage capacity and to control seawater intrusion. Objective C_m ensures that drawdowns are not too large in wells that might not directly affect seawater intrusion, such as those in the Foothill groundwater basin. For objectives C_t and C_m, weighted average heads were calculated using the percentage of total pumping coming from each layer as the weights.

Four constraints were defined initially in this problem formulation. Constraint 1 was a water-quality constraint. The chloride concentrations in water pumped from city production wells must remain below the water-quality standards for chloride concentrations. In this case, the secondary drinking-water standard for chloride of 250 milligrams per liter (mg/L), as defined by the U.S. Environmental Protection Agency, was used (U.S. Environmental Protection Agency, 2017). Concentrations were calculated as a weighted average of concentrations in each model layer penetrated by the well screen using the same weights that were used to calculate the average heads; the constraint must be honored in all layers at all times. Constraint 2 was a well-capacity constraint; a well could not pump at a rate greater than the capacity of its pump (table 1). Constraint 3 maintained a minimum flow from the Alameda, City Hall, Santa Barbara High School (SBHS), Corporation Yard, Ortega, and Vera Cruz wells to the city-operated Ortega treatment plant (fig. 2). Constraint 4 ensured that the water levels (weighted average heads) at each production well were maintained above a safe operating level (table 1).

Optimization Scenarios

To exploit the information that can be generated by the calibrated simulation model, five optimization scenarios were developed in consultation with city of Santa Barbara personnel. These scenarios allow water managers to evaluate a range of optimal solutions, given various states of the system (water levels and chloride concentrations) and potential climatic conditions. These scenarios are described in table 2. Three scenarios (1, 2, and 5) consisted of a multi-objective formulation to allow for variations in management preferences. The other two scenarios (3 and 4) were designed to examine the results of the optimizations with respect to sustainable groundwater yield and basin response to changes in pumping.

In general, initial conditions (water level or chloride concentration) can greatly affect the optimal solutions. The solutions are also affected by the amount of precipitation that recharges the basin, and this input is highly uncertain; therefore, a range of possible climatic conditions was evaluated. In this study, precipitation was used as a surrogate for climate; for example, the surrogate for a dry climatic condition was low precipitation. Additionally, because optimizing exact pumping rates for every well in every month for 10 years creates a problem so large it is nearly unsolvable in a realistic timeframe, aggregation techniques were used to reduce the number of management actions to be optimized (decision variables). For this study, monthly stress periods were grouped into 3-month quarters (January–March, April–June, and so on) to simplify the problem.

The five optimization scenarios were characterized by their problem formulation (objectives, constraints, and decision variables), initial conditions, management horizon, and climatic conditions. The details of the five scenarios are summarized in table 2.

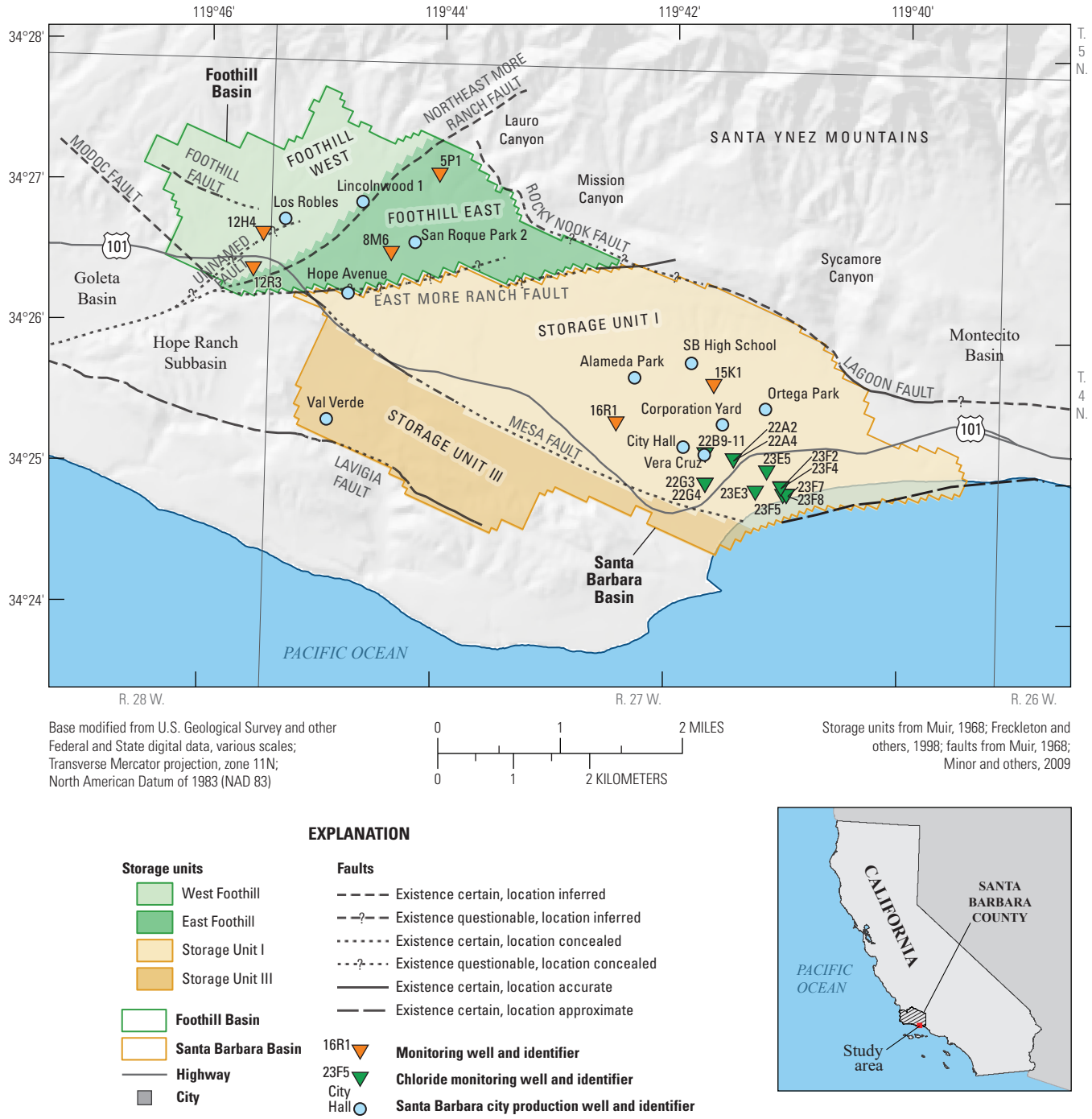

Figure 2. Locations of selected production wells, monitoring wells, and chloride monitoring wells, Santa Barbara and Foothill groundwater basins, Santa Barbara, California.

Table 1. Maximum pumping capacities for city of Santa Barbara production wells, Santa Barbara, California.

[cfd, cubic feet per day; ft, feet; gpm, gallons per minute; m, meters]

Well name	GPM	CFD	Minimum head (m)	Minimum head (ft)
Alameda Park	9,507	1,830,225	–33.5	–110
City Hall	10,695	2,058,930	–73.2	–240
Corporation Yard	8,558	1,647,529	–39.3	–129
Hope Avenue	5,767	1,110,225	–0.9	–3
Lincolnwood 1	10,902	2,098,781	25.0	82
Los Robles	5,887	1,133,326	–9.1	–30
Ortega Park	11,175	2,151,337	–63.4	–208
San Roque Park (2)	16,762	3,226,909	–17.4	–57
Santa Barbara High School	9,152	1,761,882	–42.7	–140
Val Verde	10,902	2,098,781	–27.4	–90
Vera Cruz	15,214	2,928,898	–74.7	–245

Table 2. A summary of the optimization scenarios, Santa Barbara multi-objective management model, Santa Barbara, California.

[The total number of decision variables is included as a gauge for problem size. **Abbreviation**: N/A, not applicable]

Optimization	Description	Management horizon	Climate pattern (precipitation simulated)	Initial water levels and concentrations	Decision variables (number of decision variables)
Scenario 1	Relatively high water levels followed by 10-years of typical past climate	10-year (40 quarters)	Typical past (1978–87)	High water levels (1998 groundwater levels and chloride concentrations)	Quarterly pumpage by well (440)
Scenario 2	Relatively high water levels followed by a 10-year drought	10-year (40 quarters)	10-year drought (1972, 1976, 1977, 1981, 1984, 1985, 1987, 1988, 1989, and 1990)	High water levels (1998 groundwater levels and chloride concentrations)	Quarterly pumpage by well (440)
Scenario 3	Time required for the lowest historical water levels (1990) to recover to highest historical water levels (1998)	N/A	Typical past and 10-year drought	Low water levels (1990 groundwater levels and chloride concentrations)	N/A
Scenario 4A	Pumpage decision rule as a function of measured chlorine concentration and allowable change in chlorine concentration	10-year (40 quarters)	Typical past and 10-year drought	2013 conditions (2013 groundwater levels and chloride concentrations)	Total pumpage by subbasin (30)
Scenario 4B	Pumpage decision rule as a function of measured water level and allowable drawdown	10-year (40 quarters)	Typical past and 10-year drought	2013 conditions (2013 groundwater levels and chloride concentrations)	Total pumpage by subbasin (30)
Scenario 5A	Short-term management assuming typical past to dry precipitation	2-year (8 quarters)	Typical past-to-dry (1998–99)	2013 conditions (2013 groundwater levels and chloride concentrations)	Quarterly pumpage by well (88)
Scenario 5B	Short-term management assuming dry to typical past precipitation	2-year (8 quarters)	Dry-to-typical past(1977–78)	2013 conditions (2013 groundwater levels and chloride concentrations)	Quarterly pumpage by well (88)
Scenario 5C	Short-term management assuming dry to dry precipitation	2-year (8 quarters)	Dry-to-dry (1989–90)	2013 conditions (2013 groundwater levels and chloride concentrations)	Quarterly pumpage by well (88)

Scenario 1

Scenario 1 identifies Pareto-optimal pumping schedules based on the assumptions of relatively high initial groundwater levels, followed by 10 years of typical climatic conditions. To represent high initial groundwater levels, those from 1998 (fig. 3), which corresponded to the end of a 6-year period of low pumpage (see fig. A–8), were chosen. Therefore, simulated hydraulic heads and chloride concentrations from 1998 in the calibrated model were used as initial conditions. The scenario used a 10-year management horizon characterized by typical precipitation (1978–87; fig. A–2). The optimization formulation was the same as the general formulation described previously.

Scenario 2

Scenario 2 identifies optimal pumping schedules based on the assumptions of relatively high initial groundwater levels, followed by a 10-year drought. As in scenario 1, relatively high water levels and associated chloride concentrations were used as initial conditions (1998 water levels and chloride concentrations). However, this 10-year management horizon was characterized by a very dry precipitation record. Figure A–2 shows the annual precipitation in Santa Barbara measured at the Santa Barbara County building and the cumulative departure from the mean. The dry precipitation record used for this scenario was an aggregate of 10 dry years from the calibration period (1972, 1976, 1977, 1981, 1984, 1985, 1987, 1988, 1989, and 1990; fig. A–2) replicated chronologically to simulate an extreme drought during the 10-year management horizon. For comparison, the average annual precipitation for the simulated drought was 11.4 in., and the average annual precipitation for the drought of 2012–16 was 10.2 in. Like scenario 1, the objectives and constraints for this scenario were the same as the general formulation.

Scenario 3

In contrast to the other scenarios, scenario 3 simulated the time required for the lowest historical water levels (1990) to recover to the highest historical water levels (1998; fig. 3). Hence, the initial conditions were based on 1990 simulated hydraulic heads and chloride concentrations. Most of the groundwater from wells in the Storage Unit I subbasin is treated at the Ortega groundwater treatment plant prior to distribution. For modeling purposes, the minimum operational flowrate to the treatment plant was assumed to be 300 gallons per minute (gal/min), or 484 acre-feet per year (acre-ft/yr; Kelley Dyer, Water Resources Supervisor, Public Works Department, Santa Barbara, Calif., written commun., 2014). Typical and dry climatic conditions were used over 10 years to assess the sensitivity of basin recovery to precipitation, assuming the minimal pumping from Storage Unit I.

Scenario 4

Scenario 4 was designed to produce tools that can help water managers make decisions regarding groundwater pumpage in response to newly collected water-level or chloride field data. For this study, these tools will be called “decision rules,” which are defined as formulas or principles used to choose a course of action in response to any given input of data.

The resulting decision-rule curves show the optimal pumping rates for a chosen well for a range of water levels and chloride concentrations. The 10-year typical period in scenario 1 and the 10-year drought period in scenario 2 were used for the 10-year management horizon. Two approaches were used to reflect how potential chloride concentration and drawdowns could affect the total optimal pumpage. Each approach can be used to identify a Pareto-optimal solution that reflects specific conditions (measured chloride concentrations or drawdown) and the resulting pumpage that satisfies management goals. Once a decision about total pumpage is made, the pumping schedule by well can be obtained from the optimization results from scenarios 1 or 2, depending on the climatic condition. Whenever new measurements are taken, optimal pumping schedules can be updated without re-running the simulation-optimization model.

Scenario 4A

In scenario 4A, the first step was to assume a measured chloride concentration at selected coastal monitoring wells. The next step was to search the Pareto-optimal solutions for simulated chloride concentrations equal to the assumed measured value at each selected well. An optimal total pumpage for Storage Unit I for the following year and associated change in chloride concentration were recorded and plotted for each simulated chloride concentration in the selected well. This rule-curve can be referenced to new chloride measurements to retrieve an optimal pumpage volume.

Scenario 4B

In scenario 4B, the first step was to store the maximum annual drawdown for each production well in the Foothill groundwater basin. The next step was to store the associated total pumpage for Storage Unit I and Foothill groundwater basin for those 10 years. The total optimal pumpage for Storage Unit I and Foothill groundwater basin was presented for each simulated maximum drawdown value.

Scenario 5

In scenario 5, a suite of potential, future pumping estimates was evaluated relative to a short-term climatic condition defined by a 2-year precipitation record. The management horizon was reduced to 2 years, and the initial conditions replicated those from the end of the calibration period (2013 water levels and chloride concentrations).

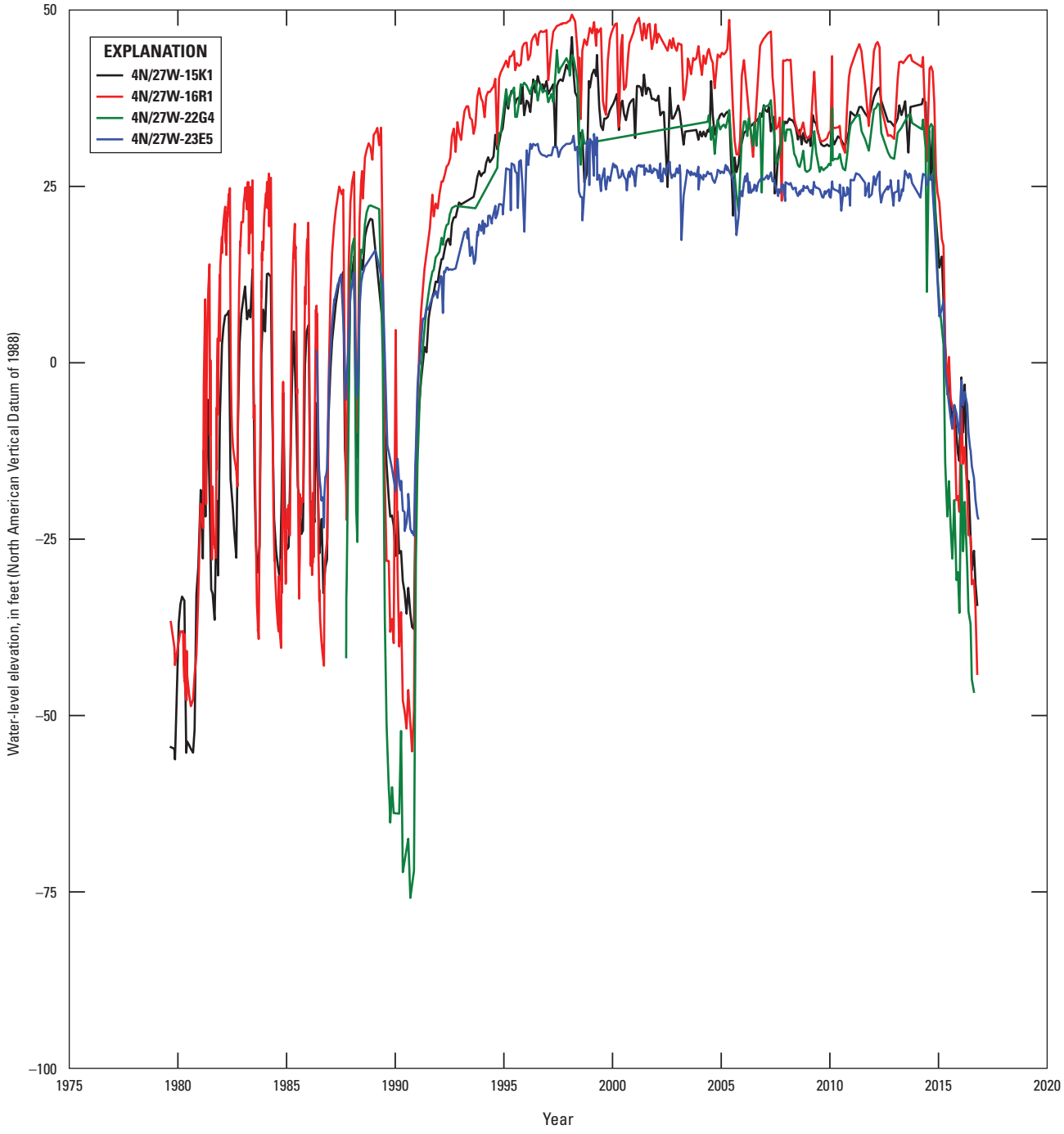

Figure 3. Hydrograph showing measured water levels for wells 4N/27W-15K1, 4N/27W-16R1, 4N/27W-22G4, and 4N/27W-23E5 in Storage Unit I, Santa Barbara groundwater basin, Santa Barbara, California.

Simulation-Optimization Results

In order to determine the best possible approximation of the true Pareto-optimal solution set, each scenario was formulated and run until minimum improvement was observed. For more information regarding MOEA convergence criteria, the reader is referred to Ward and others (2015). The ε values for all scenarios were ε_A = 1,000, ε_B = 10, ε_{Ct} = 10, and ε_{Cm} = 1 for objectives A, B, C_t, and C_m, respectively. Scenarios 1 and 2 were run for 90,000 function evaluations each (a function evaluation is defined as one forward run of the simulation model), after which, changes in the pumpage objective were less than 1 percent of total pumpage. Scenario 5 optimizations were run for 80,000 function evaluations, or to the point where improvements to all objectives were nearly stagnant.

Results for each scenario are presented and discussed separately. The values of each objective are converted to units that allow for practical interpretation. Objective A, pumpage, is presented as the sum of all quarterly pumping volumes (acre-ft) divided by the simulation time for an average pumping rate in acre-feet per year (acre-ft/yr). Objective B, seawater intrusion, is presented as formulated, that is, the sum of concentrations (mg/L) in all the model cells that make up the chloride-monitoring well and over all observation times. Objective C_t is shown as total drawdown in feet; objective C_m is the maximum drawdown in feet.

Because many Pareto-optimal solutions are generated, a few must be selected for further consideration and discussion purposes. Two strategies were employed to select optimal pumping solutions. First, the ε-dominance criterion was used to sort the solutions according to preference in each objective. This was done in the Borg MOEA with ε values, defined previously. Second, after filtering by ε dominance, Pareto-optimal pumpage rates by well (schedules) were selected from the remaining Pareto set according to the following convention:

Schedule $\{x\}_A$ maximize objective A-pumpage

Schedule $\{x\}_B$ minimize objective B-seawater intrusion

Schedule $\{x\}_{Ct}$ minimize objective C_t-total drawdown

Schedule $\{x\}_{Cm}$ minimize objective C_m-maximum drawdown

Schedule $\{x\}_D$ best overall compromise among the four objectives

Schedule $\{x\}_E$ best compromise among objectives B, C_t, and C_m

where

$\{x\}$ is the scenario number.

For example, schedule 1_A is the solution that minimized objective A (or maximized pumpage) for scenario 1. Schedule $\{x\}_E$ can be considered the best compromise among the environmental mitigation objectives (that is, seawater intrusion and both drawdown objectives).

Selection of the pumping schedules was intended to simplify the presentation of overall Pareto-optimal results. The complete Pareto-optimal solution set is given as hundreds of different pumping schedules for each scenario. Each of these schedules is optimal in the sense that no other solution can improve any of the objective values without worsening at least one other objective value. Selection of the pumping schedule from the solution set can be made according to the needs of the time. For example, given a projected water demand, the Pareto-optimal schedule that most closely matches the demand with pumpage might be chosen. It is important to point out that this schedule might not be one of the example schedules examined in this report. If minimizing seawater intrusion was paramount to all other objectives, however, then schedule $\{x\}_B$ pumpage would be a good guide for the available basin yield.

Although identifying schedules $\{x\}_A$, $\{x\}_B$, and $\{x\}_C$ is straightforward—the best performing solution in each of the objectives—all possible pumping schedules need to be ranked to identify schedules $\{x\}_D$ and $\{x\}_E$. Schedules $\{x\}_D$ and $\{x\}_E$ were identified by using scaled objective scores (SOS) for each Pareto-optimal solution. The use of SOS is a normalization that maps each objective value to the common interval [0, 1] to more easily compare the ranking of each schedule in each objective. It is calculated as follows:

$$SOS = \left(1 - \left|\frac{obj - min}{max - min}\right|\right) \quad (9)$$

where

obj is the objective-function value of a given pumping schedule,

min is the minimum value of the objective,

max is the maximum value of the objective, and

| | is the absolute value.

Because all objectives were formulated as minimizations, a score of 1 is the best possible value obtained in the Pareto-optimal set for that objective, and 0 is the worst possible value. Using the SOS, schedule $\{x\}_D$ is defined as the largest sum of scores for all four objectives, and schedule $\{x\}_E$ is the largest sum of scores for objectives B, C_t, and C_m.

Scenario 1

With relatively high-water levels as the initial conditions and typical precipitation used during a 10-year management horizon, this optimization produced the best possible yield for the basin under favorable conditions. The city can choose a pumping schedule according to the tradeoffs among the four objectives that meet the needs at that time. Figure 4 shows the 912 Pareto-optimal solutions for scenario 1, with pumping schedules 1_A through 1_E highlighted for clarity. Schedules with little seawater intrusion varied between about 26,000 and 24,200 acre-ft of pumpage (fig. 4). The schedules with the least seawater intrusion around schedule 1_B had more total drawdown and greater maximum drawdown than those that allowed a modest amount of seawater intrusion at a similar total pumpage. The scenario 1 results also indicated that about 31,300 acre-ft was the maximum yield for the basin during a 10-year period under typical conditions. All scenario 1 results assumed the simulated recharge pattern reasonably represented that of the precipitation record from 1978 to 1987.

The results indicated that the total chloride concentration (objective B) and total drawdown (objective C_t) were sensitive to total pumpage (objective A) in different ways (fig. 4). One might expect that chloride concentration and drawdown would simply increase with pumpage; however, because the spatial distribution of pumpage varies, this is not always the case. For example, the increased pumpage could be from the Foothill groundwater basin, where drawdown has little effect on seawater intrusion. Schedules 1_B and 1_{Ct} both had more pumpage than schedule 1_{Cm}, but less seawater intrusion (fig. 4); at the same time, schedule 1_B had moderate overall drawdown, yet schedules 1_{Ct}, 1_{Cm}, 1_D, and 1_E had an overall increase in water levels (negative drawdown). Tradeoffs were complex, and relationships among various objectives were not immediately apparent; however, overall, more pumpage resulted in more drawdown and more seawater intrusion. Schedules with similar total drawdown (for example, 300 ft, fig. 4) can result in a wide range of seawater intrusion. Conversely, schedules with similar pumpage have a relatively narrow range of seawater intrusion.

Table 3 presents the selected Pareto-optimal results for the total pumpage, total chloride concentration, total drawdown, and maximum drawdown for schedules 1_A–1_E. Schedules 1_A, 1_B, 1_{Ct}, and 1_{Cm} resulted in the greatest objective values for objectives A, B, C_t, and C_m (31,300 acre-ft, 2.74E7 mg/L, -790 ft, and 41 ft, respectively). Schedules 1_B through 1_E resulted in similar total pumpage values—a range of 900 acre-ft after 10 years. The best overall compromise solution, schedule 1_D, represented the largest SOS for the four objectives. In this case, schedule 1_D resulted in less total pumpage than schedules 1_A, 1_B, $1_{Ct, or}$ 1_{Cm}, but more pumpage than schedule 1_E. Schedule 1_E was the best compromise among the environmental mitigation objectives and resulted in the least amount of pumpage (table 3).

Figure 5 presents the SOS for each schedule in table 3, illustrating the relative tradeoffs on a common scale. The extreme solutions (schedules 1_A, 1_B, 1_{Ct}, and 1_{Cm}) all exhibited poor performance in at least one objective, relative to the highest attainable value (a score of 1). Schedule 1_B showed that a small decrease in overall seawater intrusion resulted in a large increase in total drawdown and maximum drawdown when compared to Schedules 1_C through 1_E. The compromise solutions (schedules 1_D and 1_E) showed a better balance among the environmental objectives (B and C) than the extreme solutions. Schedules 1_{Ct} and 1_D, appeared to be similar, but showed that for a small decrease in pumpage, better scores for objectives B and C_m were attained. Furthermore, schedule 1_E showed that high SOS (greater than 0.8) for all three environmental objectives was possible if pumpage could be reduced to about 25,000 acre-ft (table 3), but this would also result in lower water levels throughout the basin and a larger maximum drawdown compared to scenario 1_D (slightly worse objective C_t and C_m scores; fig. 5).

The selected Pareto-optimal pumping schedules for the Storage Unit I and Foothill groundwater basin are shown in figure 6, and the pumpage values by individual well for Schedule 1_D are presented in appendix D–1. These pumping schedules present a range of Pareto-optimal operations under typical rainfall. All schedules had relatively high pumpage during the first three quarters of year 10 because there is no year 11 as far as the optimization is concerned, implying that the state of the basin after year 10 is of no concern to the model beyond meeting the constraints. This is discussed in greater detail in the "Limitations" section of this chapter. Also, pumpage was usually large in the first quarter of each schedule, which indicates that the initial conditions were not violating any constraints and the system could be heavily pumped for one quarter, if less pumpage was imposed in the following quarters. It is also apparent from figure 6 that schedule 1_A did not necessarily result in more pumpage in each quarter. In fact, in some quarters (8, 12, and 15, for example), schedule 1_A (fig. 6*A*) had less pumpage from Storage Unit 1 than schedule 1_E (fig. 6*F*), and in some other quarters (21, 25, and 33, for example) schedule 1_A had less pumpage from the Foothill groundwater basin than schedule 1_D (fig. 6*E*). Among all the schedules, the general timing of the large pumpage and small pumpage quarters was highly variable.

In summary, the optimal annual pumping for schedule 1_D ranged from 1,829 to 3,418 acre-ft and averaged 2,558 acre-ft/yr for the 10-year period. Of this amount, the annual city pumpage in the Foothill basin ranged from 535 to 862 acre-ft and averaged 746 acre-ft/yr; and the annual city pumpage in Storage Unit I ranged from 925 to 2,457 acre-ft and averaged 1,620 acre-ft/yr. Although not presented in figure 6, the annual city pumpage in Storage Unit III ranged from 128 to 239 acre-ft and averaged 191 acre-ft/yr.

Figure 7 shows the contours of simulated hydraulic head in the upper, middle, and lower producing zones after 10 years of pumping, assuming schedule 1_D pumpage. A cone of depression formed around the wells in the three producing zones of Storage Unit I (fig. 7). In addition, there was a depression in the lower producing zone around the Hope Avenue well (fig. 7*C*), which could reflect the proximity of the well to the East More Ranch fault. An additional cone of depression was evident in the lower producing zone of the Foothill groundwater basin around the Los Robles well (fig. 7*C*).

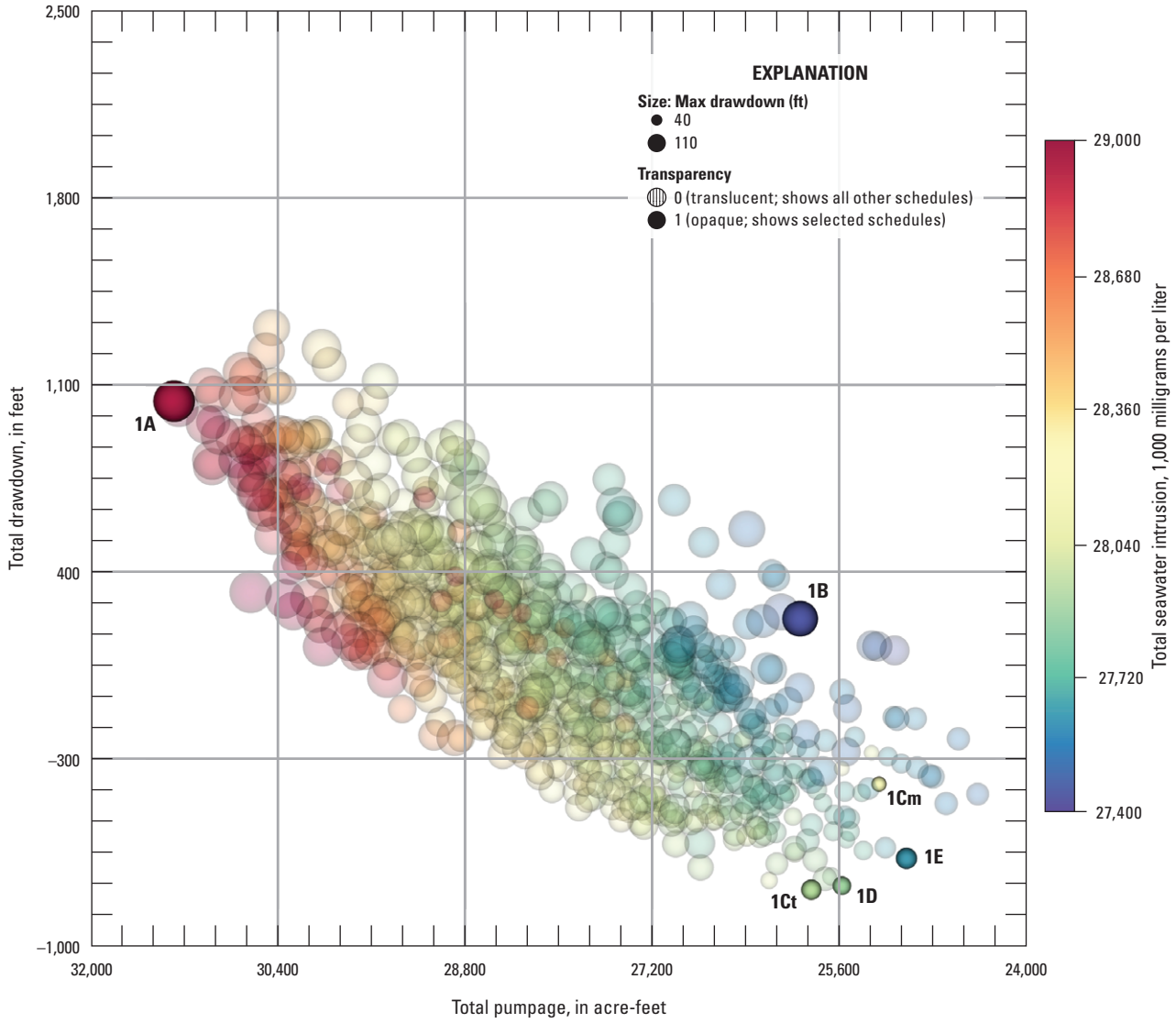

Figure 4. Selected Pareto-optimal solutions for scenario 1, Santa Barbara multi-objective management model, Santa Barbara, California.

Table 3. Values for the four objectives for selected Pareto-optimal pumping schedules, scenario 1, Santa Barbara multi-objective management model, Santa Barbara, California.

[Objective A is also shown divided by storage unit. **Abbreviations**: acre-ft, acre-feet; ft, feet; mg/L, milligrams per liter]

Schedule	Objective A total pumpage (acre-ft)	Objective B seawater intrusion (1,000 mg/L)	Objective Ct total drawdown (ft)	Objective Cm maximum drawdown (ft)	Storage Unit I pumpage (acre-ft)	Foothill pumpage (acre-ft)	Storage Unit III pumpage (acre-ft)
1_A	31,300	28,900	1,040	74	20,100	9,200	2,000
1_B	25,900	27,400	230	67	15,100	8,800	2,100
1_{Ct}	25,800	27,900	-790	48	16,400	7,600	1,900
1_{Cm}	25,300	28,200	-390	41	16,300	7,300	1,600
1_D	25,600	27,900	-770	46	16,200	7,500	1,900
1_E	25,000	27,600	-670	49	15,500	7,600	1,900

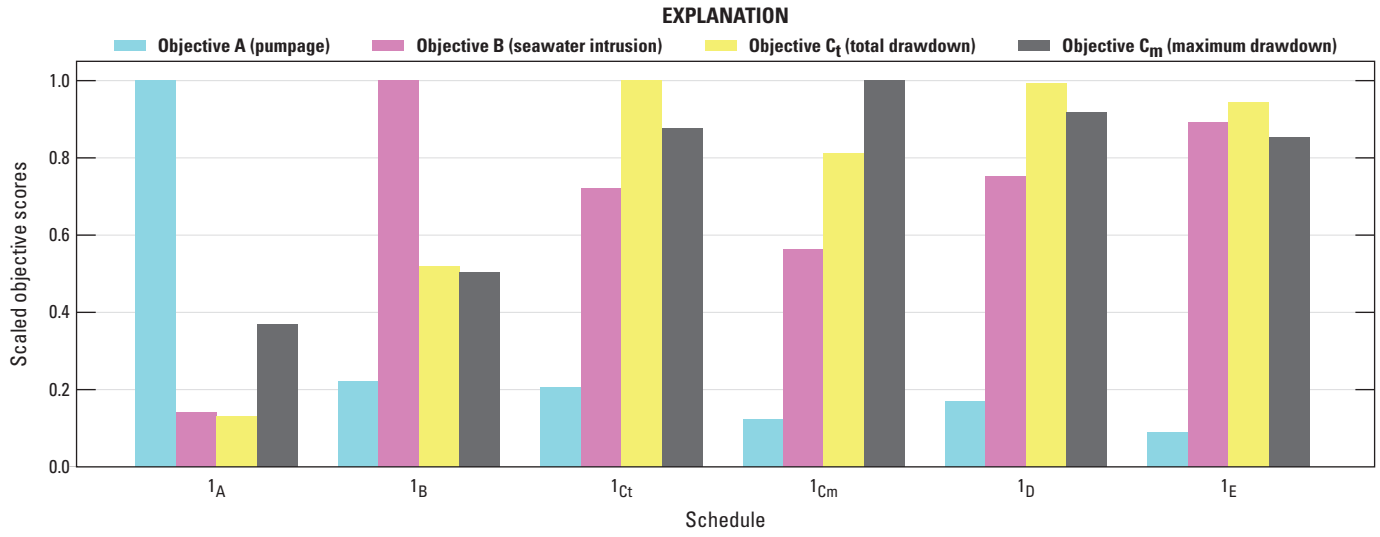

Figure 5. Scaled objective scores for schedules 1_A through 1_E, Santa Barbara multi-objective management model, Santa Barbara, California.

Figure 8 shows a vertical section of simulated chloride concentration and contours of simulated chloride concentrations for the middle and lower producing zones, assuming schedule 1_D pumpage. Some of the monitoring wells near the coast that were used to establish the seawater-intrusion objective are also shown in the vertical section. Wells 4N/27W-22A2 and 23F2 are perforated in the upper producing zone. Well 22A2 was near the leading edge of seawater intrusion in the upper producing zone, whereas well 23F2 is perforated near the top of the middle producing zone (fig. 8*A*). The mean simulated chloride concentrations at wells 22A2 and 23F2 at the end of the 10-year simulation were 130 and 1,900 mg/L, respectively. The simulated results for well 22A2 indicated that pumping from the City Hall or Vera Cruz wells could induce an upward migration of seawater from the top of the middle producing zone (fig. 8*A*). Wells 4N/27W-22A4 and 23F4 are perforated in the lower producing zone. Well 22A4 was near the leading edge of the seawater intrusion in the lower producing zone, whereas well 23F4 was near the centroid of the lower seawater plume (fig. 8) and its simulated chloride concentration was about 70-percent seawater. At the end of the 10-year simulation, the mean simulated chloride concentrations at wells 22A4 and 23F4 were 870 and 13,400 mg/L, respectively.

Simulated chloride breakthrough curves for the coastal monitoring wells, assuming schedule 1_D pumpage, are shown in figure 9. Higher chloride concentrations in the lower producing zone (wells 23F4 and 23F5) and the middle producing zone (well 23F8) are apparent. Overall, the rate of change in chloride concentration was greater in the lower producing zone than in the other two zones. For example, the rate of increase in chloride concentrations in well 22G4, which is perforated in the lower producing zone, was higher than that of its companion well in the middle producing zone (well 22G3). The largest increase in chloride concentration was in well 23E5, which is perforated in the lower producing zone; the simulated chloride concentration increased from about 2,700 mg/L to about 4,200 mg/L (fig. 9).

For Schedule 1_D, the largest simulated chloride concentration at any production well was about 158 mg/L in the middle producing zone of the Corporation Yard well. This estimate of concentration is only for a single model layer in the entire perforated interval; therefore, the actual chloride concentration of extracted water would be likely be less because it would be mixed with less-saline water from other depths.

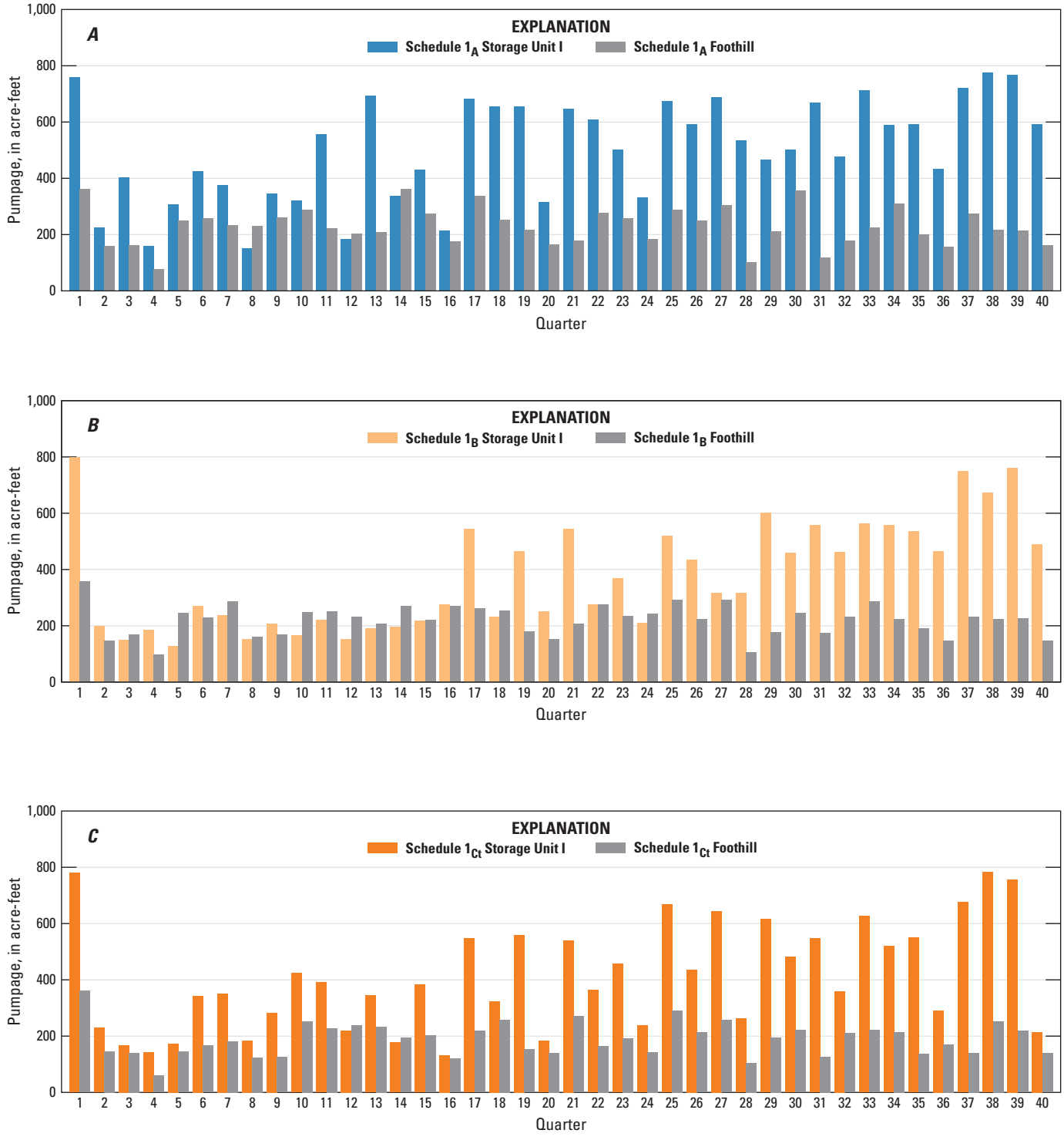

Figure 6. Quarterly pumpage for Storage Unit I and Foothill groundwater basin, Santa Barbara multi-objective management model, Santa Barbara, California, for *A*, schedule 1_A; *B*, schedule 1_B; *C*, schedule 1_{Ct}; *D*, schedule 1_{Cm}; *E*, schedule 1_D; and *F*, schedule 1_E.

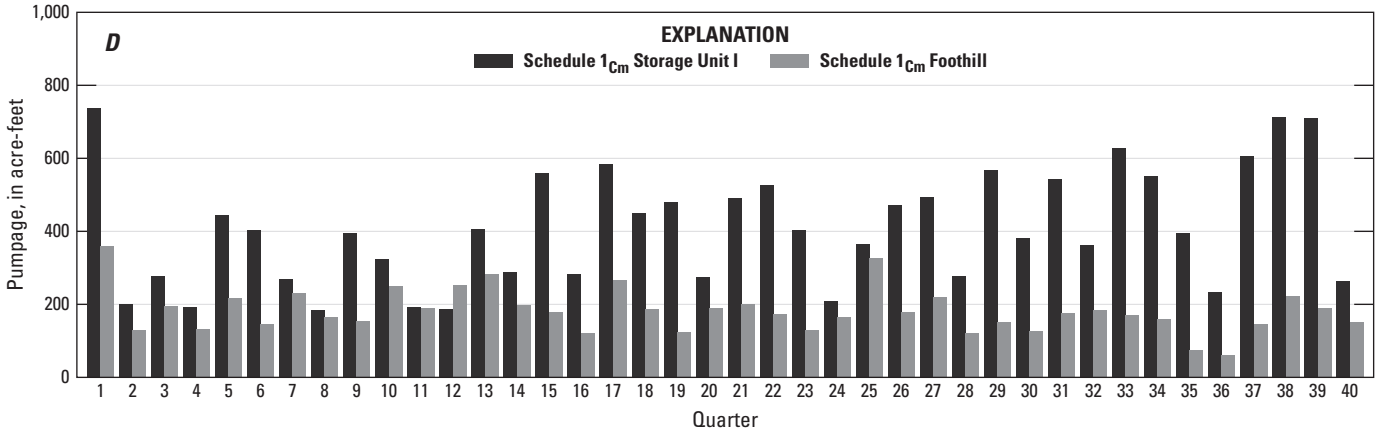

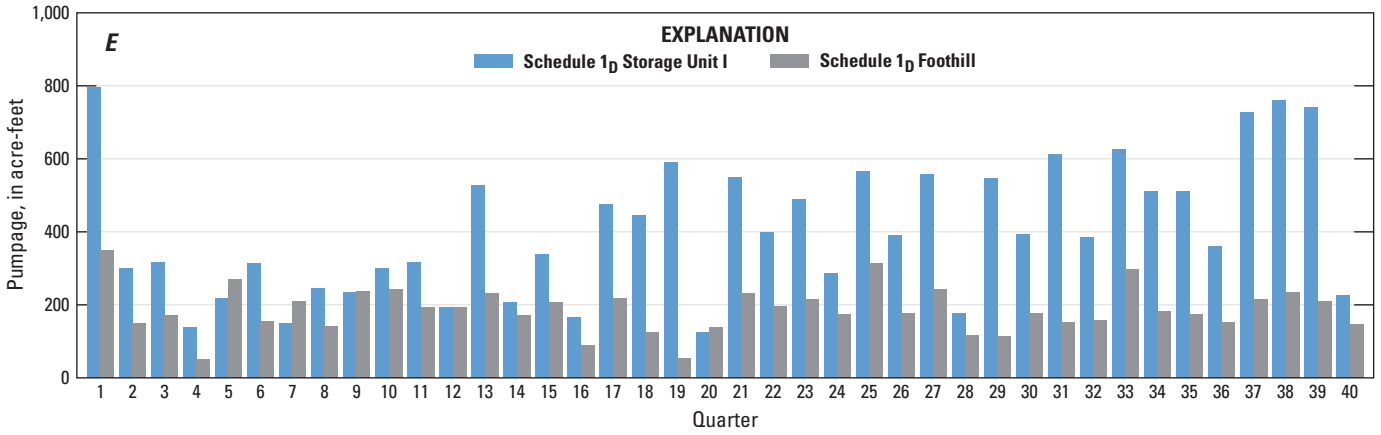

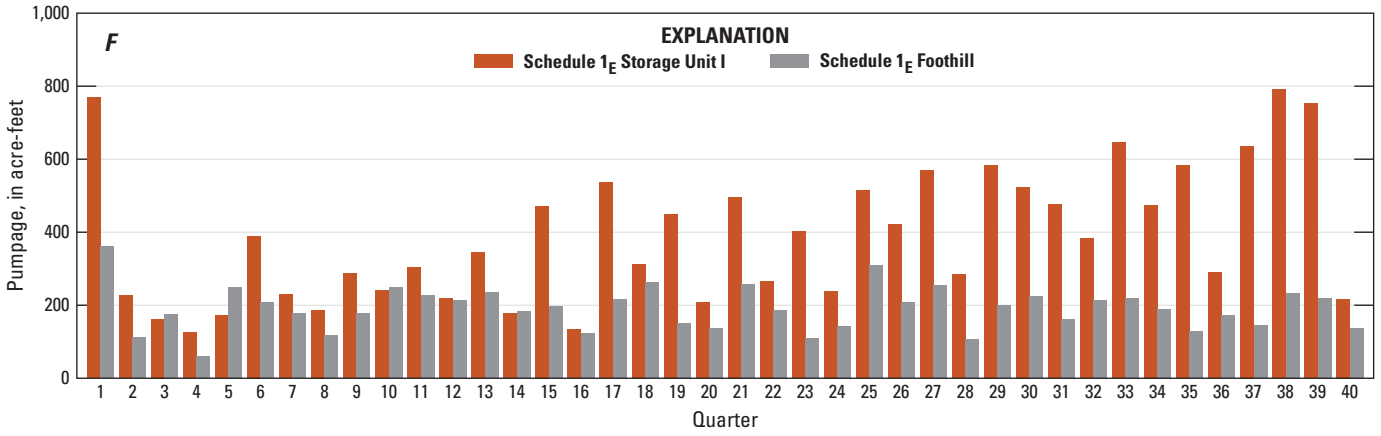

Figure 6. —Continued

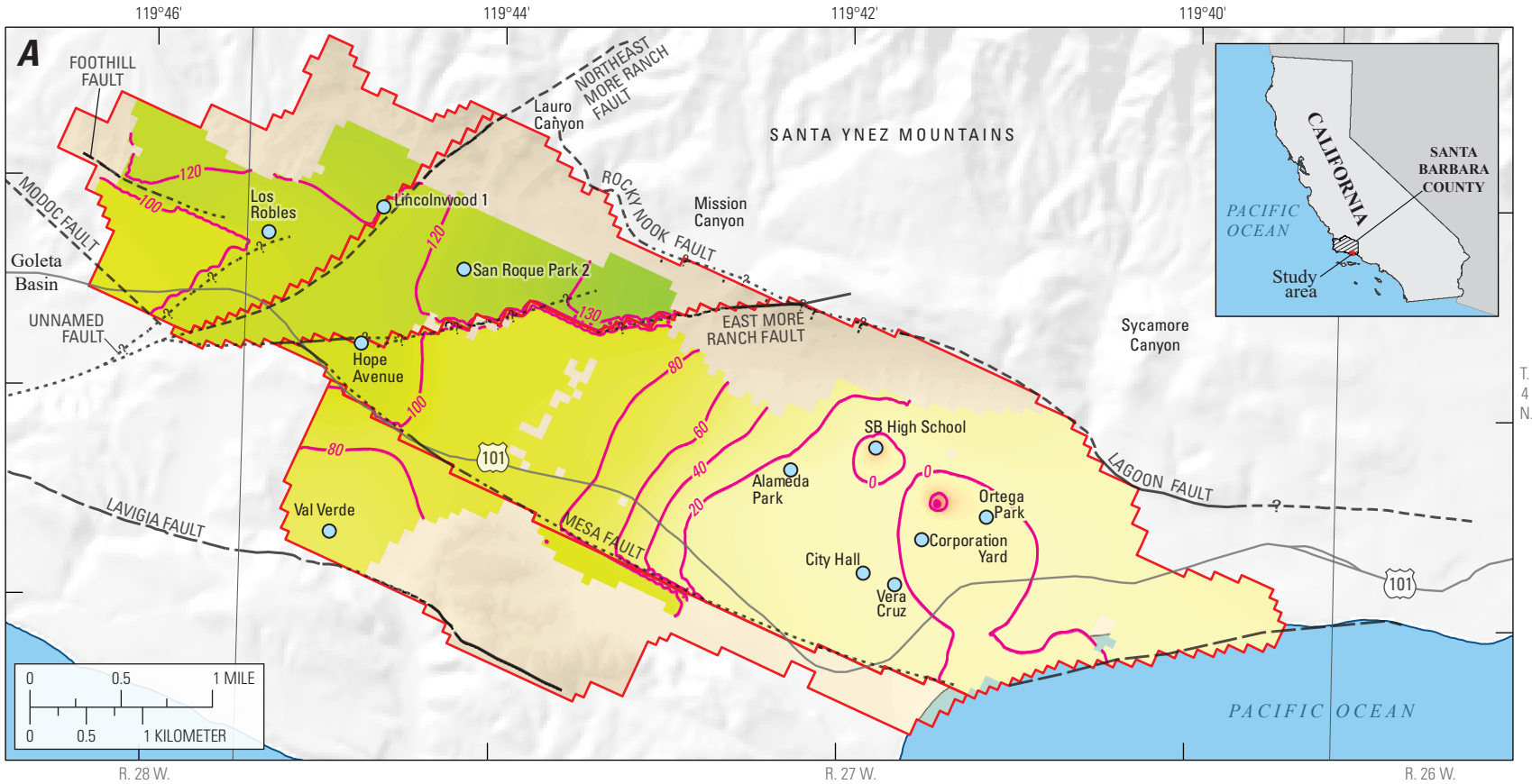

Base modified from U.S. Geological Survey and other Federal and State digital data, various scales; Transverse Mercator projection, zone 11N; North American Datum of 1983 (NAD 83)

Storage units from Muir, 1968; Freckleton and others, 1998; faults from Muir, 1968; Minor and others, 2009

EXPLANATION

Faults

- Existence certain, location inferred
- Existence questionable, location inferred
- Existence certain, location concealed
- Existence questionable, location concealed
- Existence certain, location accurate
- Existence certain, location approximate

Storage units

Simulated hydraulic head contours, in feet above North American Vertical Datum of 1988 (NAVD 88)

Highway

Vera Cruz — **Santa Barbara city production well and identifier**

Simulated hydraulic head, in feet above NAVD 88

High 250 200 150 100 50 0 –50 –100 Low –150

Figure 7. Contours of simulated hydraulic head after 10 years for schedule 1_D, Santa Barbara multi-objective management model, Santa Barbara, California: *A*, upper producing zone; *B*, middle producing zone; and *C*, lower producing zone.

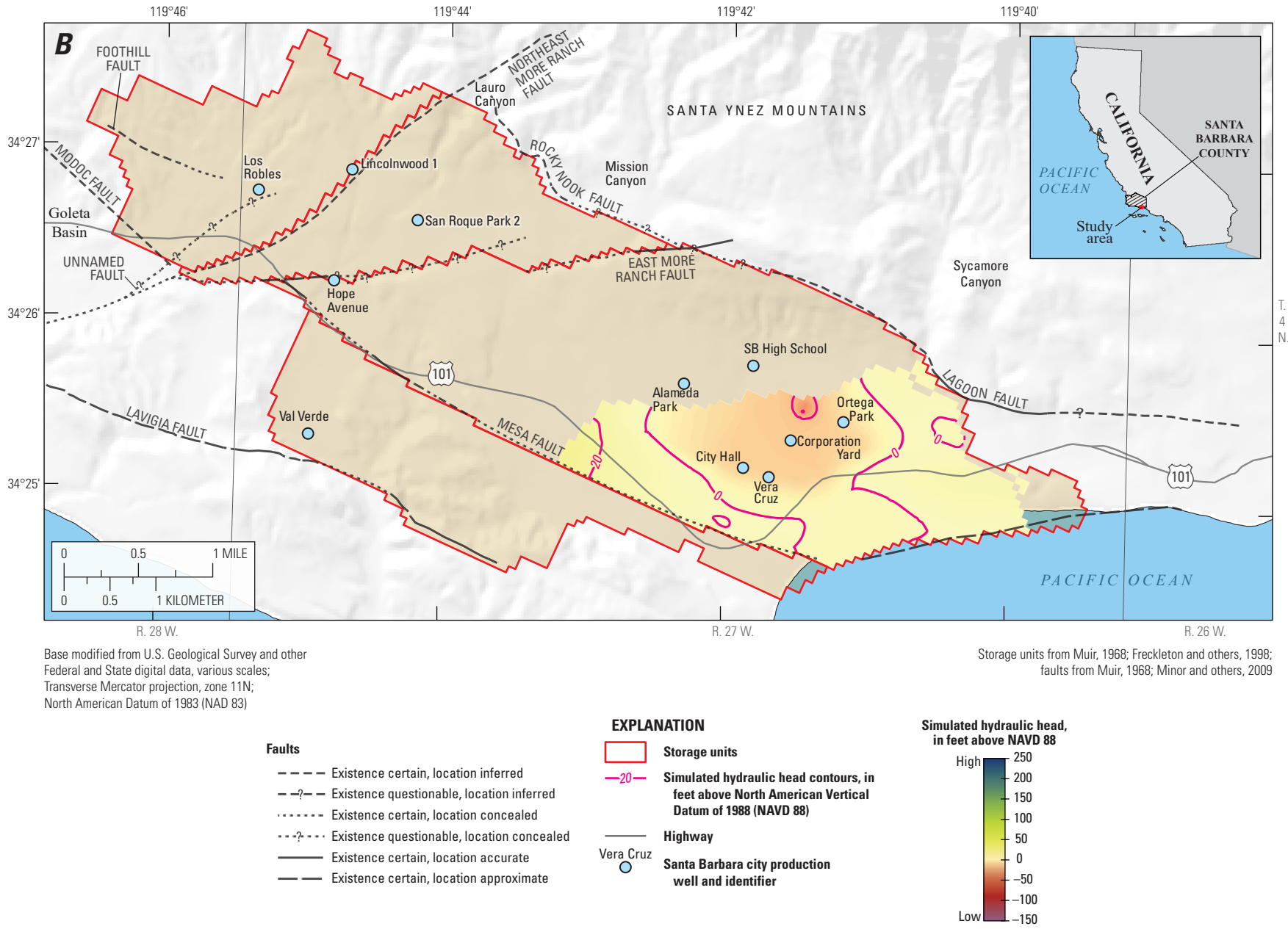

Base modified from U.S. Geological Survey and other Federal and State digital data, various scales; Transverse Mercator projection, zone 11N; North American Datum of 1983 (NAD 83)

Storage units from Muir, 1968; Freckleton and others, 1998; faults from Muir, 1968; Minor and others, 2009

Faults

- Existence certain, location inferred
- Existence questionable, location inferred
- Existence certain, location concealed
- Existence questionable, location concealed
- Existence certain, location accurate
- Existence certain, location approximate

EXPLANATION

- Storage units
- 20 — Simulated hydraulic head contours, in feet above North American Vertical Datum of 1988 (NAVD 88)
- Highway
- Vera Cruz — Santa Barbara city production well and identifier

Simulated hydraulic head, in feet above NAVD 88

High 250 200 150 100 50 0 –50 –100 Low –150

Figure 7. —Continued

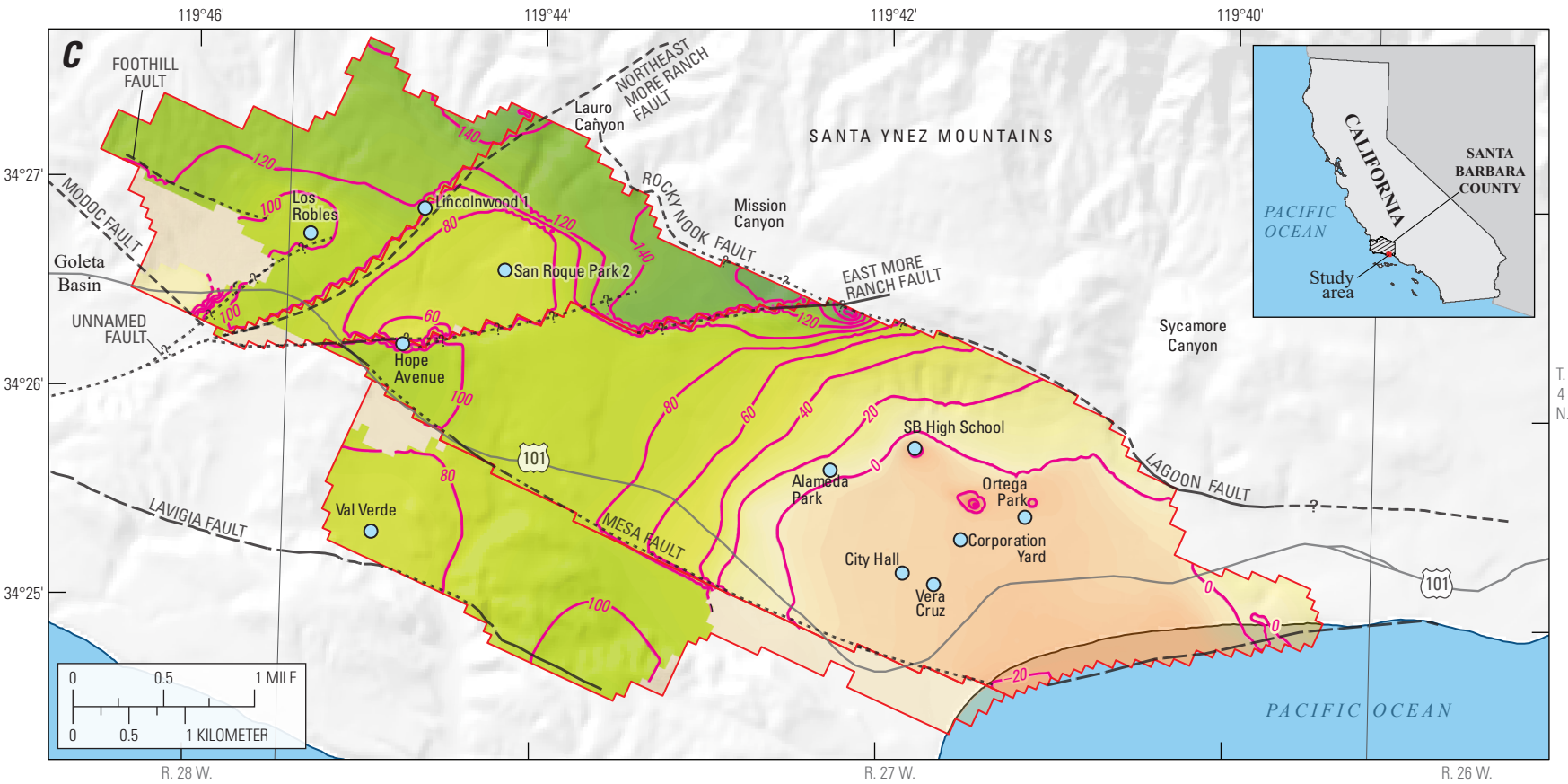

Base modified from U.S. Geological Survey and other Federal and State digital data, various scales; Transverse Mercator projection, zone 11N; North American Datum of 1983 (NAD 83)

Storage units from Muir, 1968; Freckleton and others, 1998; faults from Muir, 1968; Minor and others, 2009

EXPLANATION

Faults

- Existence certain, location inferred
- Existence questionable, location inferred
- Existence certain, location concealed
- Existence questionable, location concealed
- Existence certain, location accurate
- Existence certain, location approximate

Storage units

Simulated hydraulic head contours, in feet above North American Vertical Datum of 1988 (NAVD 88)

Highway

Vera Cruz — **Santa Barbara city production well and identifier**

Simulated hydraulic head, in feet above NAVD 88

High 250 200 150 100 50 0 –50 –100 Low –150

Figure 7. —Continued

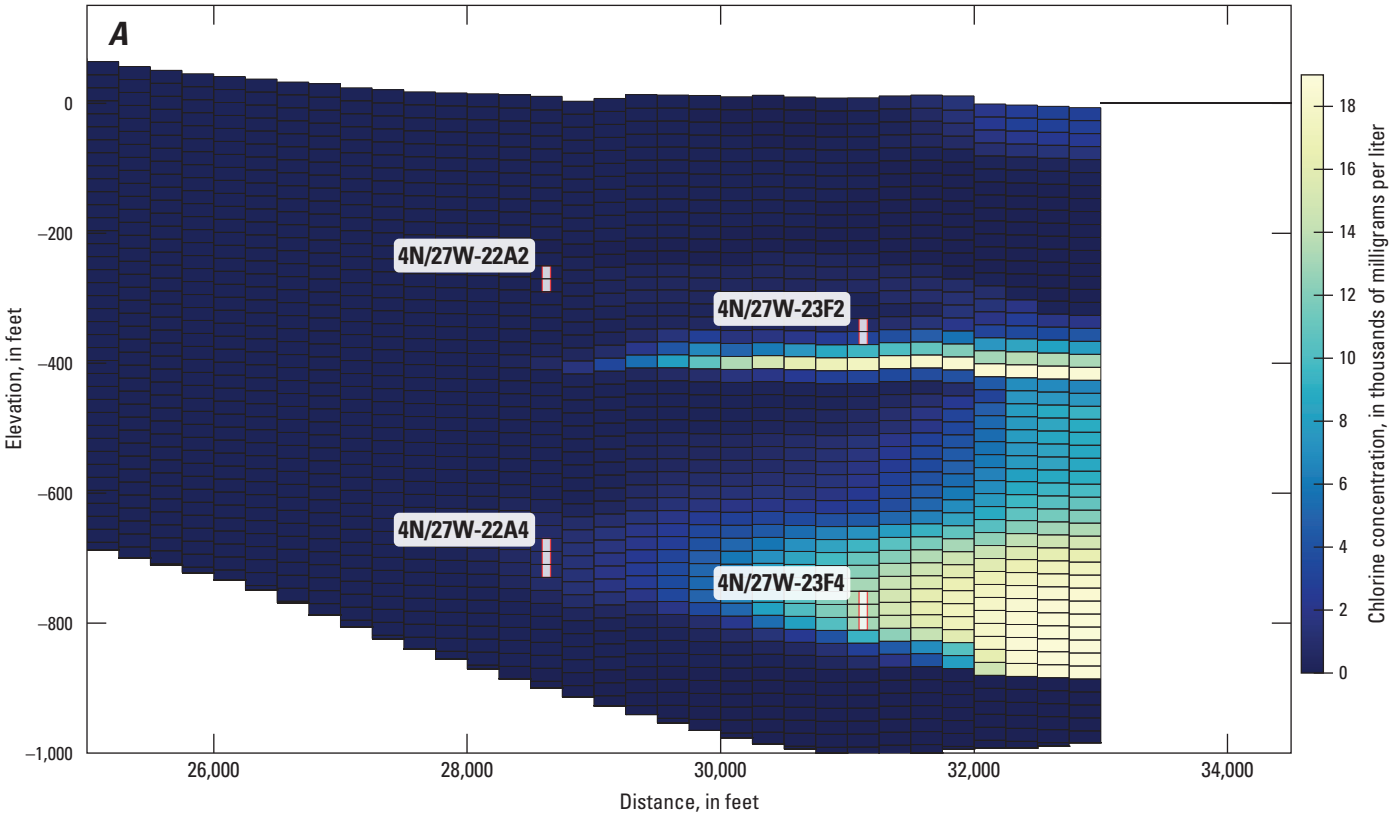

Figure 8. Simulated year-10 chloride concentration distribution for Storage Unit I, schedule 1_D, Santa Barbara multi-objective management model, Santa Barbara, California: *A*, section along model row 30; *B*, plan view of the middle producing zone; and *C*, plan view of the lower producing zone.

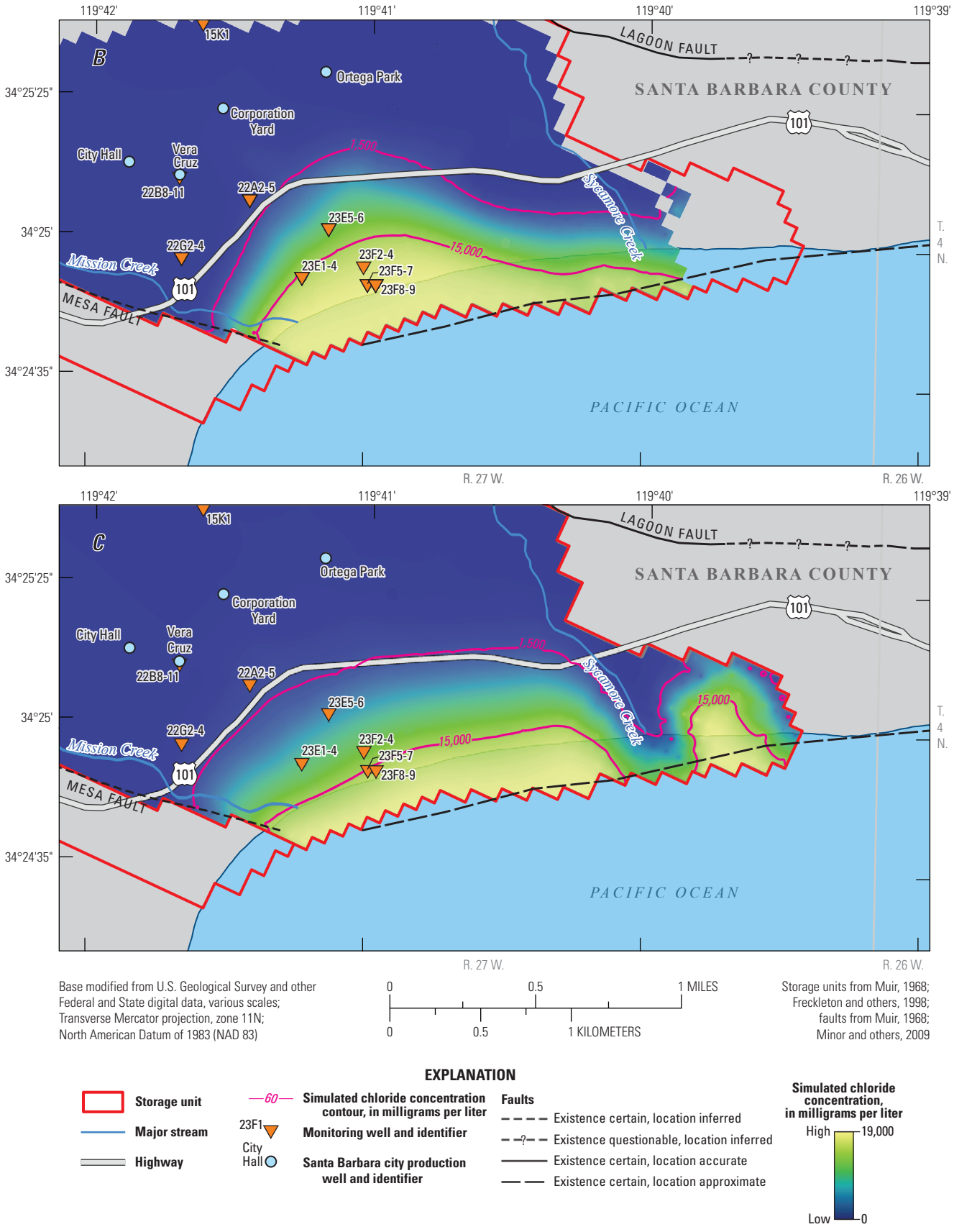

Figure 8. —Continued

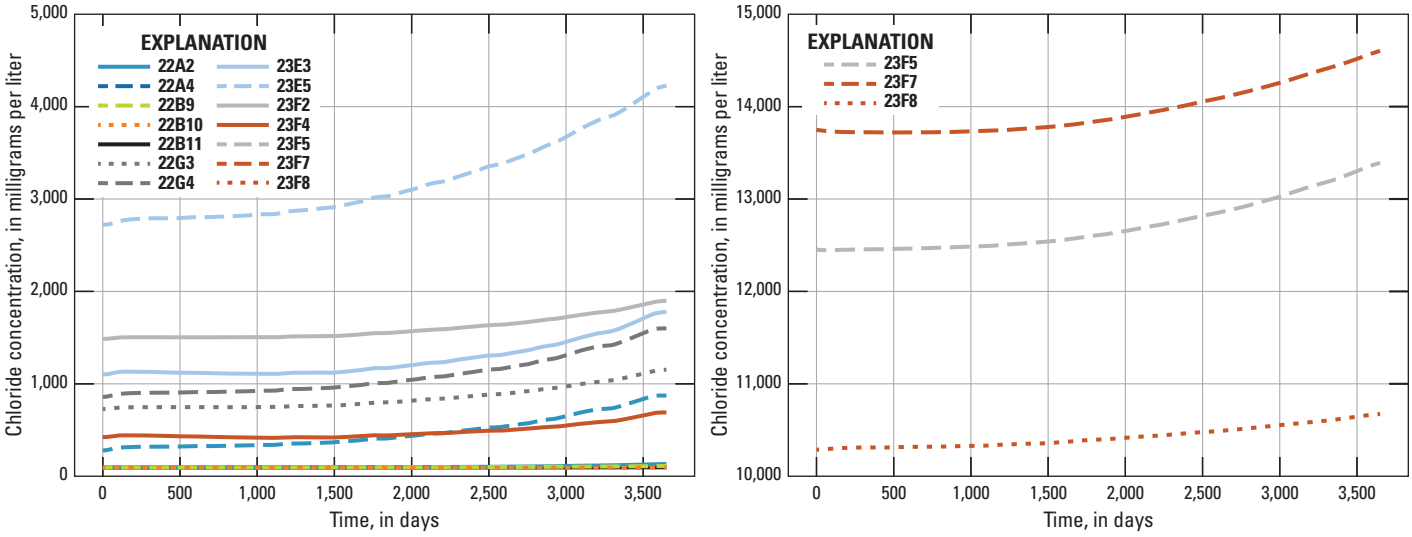

Figure 9. Simulated chloride breakthrough curves for selected monitoring wells for schedule 1_D, Santa Barbara multi-objective management model, Santa Barbara, California.

Scenario 2

Using relatively high-water levels for the initial conditions and dry climatic conditions during a 10-year management horizon, this optimization scenario produces the best possible yield of the basin under a simulated drought. The city can decide on a pumping schedule by choosing the tradeoff among the four objectives that meet their needs best at the time. Figure 10 shows the 629 Pareto-optimal solutions for scenario 2. A range of low seawater-intrusion values was only feasible for much larger drawdowns when compared to scenario 1 (fig. 4). Schedules 2_A, 2_B, 2_{Ct}, and 2_{Cm} represented the extreme solutions that achieved the lowest possible objective value (with respect to a minimization) for objectives A, B, C_t, and C_m, respectively (fig. 10). The scenario 2 tradeoffs differed from those of scenario 1 by having a smaller range of feasible values for objectives A and B, yet a larger range for objectives C_t and C_m. For scenario 2, schedules 2_{Ct}, 2_D, and 2_E were equivalent. Also notable is that there were no Pareto-optimal solutions for scenario 2 that resulted in negative total drawdown, as was found for scenario 1. In general, total pumpage and seawater intrusion were similar for scenarios 1 and 2; however, total drawdowns were larger in all schedules of scenario 2. All scenario 2 results assumed the simulated recharge pattern reasonably represents that of the dry precipitation record for a simulated 10-year drought.

Selected Pareto-optimal results are presented in table 4, and the associated SOS are shown in figure 11. The total pumpage, total chloride concentration, total drawdown, and maximum drawdown are shown for schedules 2_A–2_E in table 4. For scenario 2, the best overall compromise solution (schedule 2_D) and the best compromise between seawater intrusion and both drawdown objectives (schedule 2_E) were identical to those for schedule 2_{Ct} and are, therefore, not presented separately in table 4. Schedules 2_A, 2_B, 2_{Ct}, and 2_{Cm} resulted in the greatest values for objectives A, B, C_t, and C_m (30,000 acre-ft, 2.75E7 mg/L, 500 ft, and 54 ft, respectively, table 4). Achieving an SOS greater than 0.8 (fig. 11) for both drawdown objectives was possible for schedule 2_{Ct} at a total pumpage of about 26,200 acre-ft (table 4). Pumpage was greater for schedule 2_{Ct} than 2_{Cm}, but total drawdown was less and maximum drawdown was greater.

The tradeoffs for scenario 2 also showed that the lowest values of seawater intrusion were not attainable without a substantial drop in the SOS for the other three objectives (schedule 2_B compared to schedules 2_{Ct} and 2_{Cm} in fig. 11). Seawater intrusion increased for schedule 2_{Ct} and 2_{Cm} because minimizing either drawdown objective, much of which occurred in the Foothill groundwater basin, led to more pumpage in Storage Unit I. Similar to scenario 1, the SOS for objective B was very low for the schedule 2_A solution (fig. 11), making it an unlikely candidate for a management plan, but still valuable for its maximal dry-climate yield.

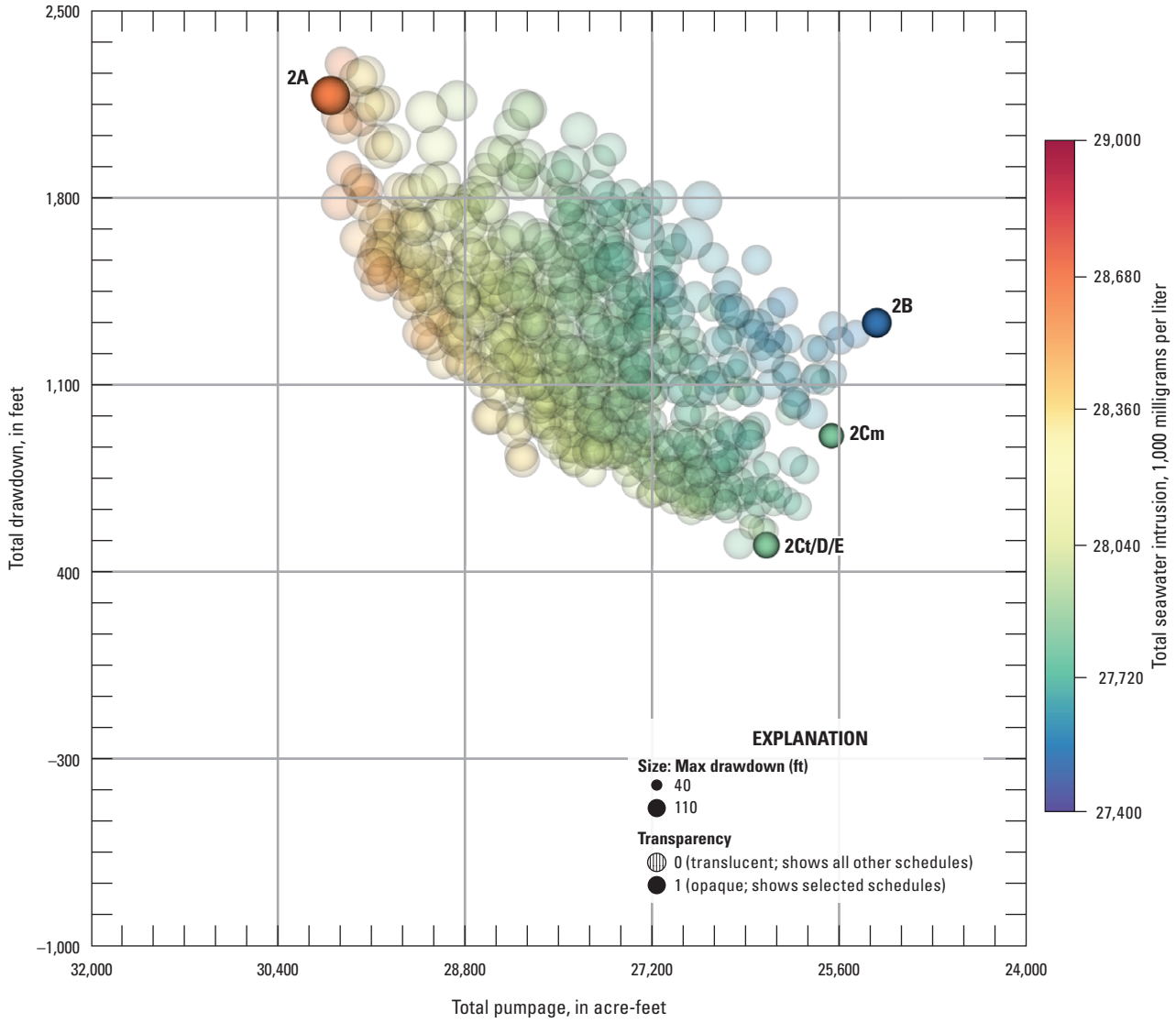

Figure 10. Selected Pareto-optimal solutions for scenario 2, Santa Barbara multi-objective management model, Santa Barbara, California.

Table 4. Values for the four objectives for selected Pareto-optimal pumping schedules, scenario 2, Santa Barbara multi-objective management model, Santa Barbara, California.

[Schedules 2_D and 2_E results are identical to Schedule 2_{Ct}. Objective A is also shown divided by storage unit. **Abbreviations**: acre-ft, acre-feet; ft, feet; mg/L, milligrams per liter]

Schedule	Objective A total pumpage (acre-ft)	Objective B seawater intrusion (1,000 mg/L)	Objective Ct total drawdown (ft)	Objective Cm maximum drawdown (ft)	Storage Unit I pumpage (acre-ft)	Foothill pumpage (acre-ft)	Storage Unit III pumpage (acre-ft)
2_A	30,000	28,600	2,180	71	18,900	9,100	2,000
2_B	25,300	27,500	1,330	60	14,900	8,500	1,900
$2_{Ct, D, E}$	26,200	27,800	500	56	16,100	8,100	2,000
2_{Cm}	25,700	27,800	910	54	15,600	8,100	2,000

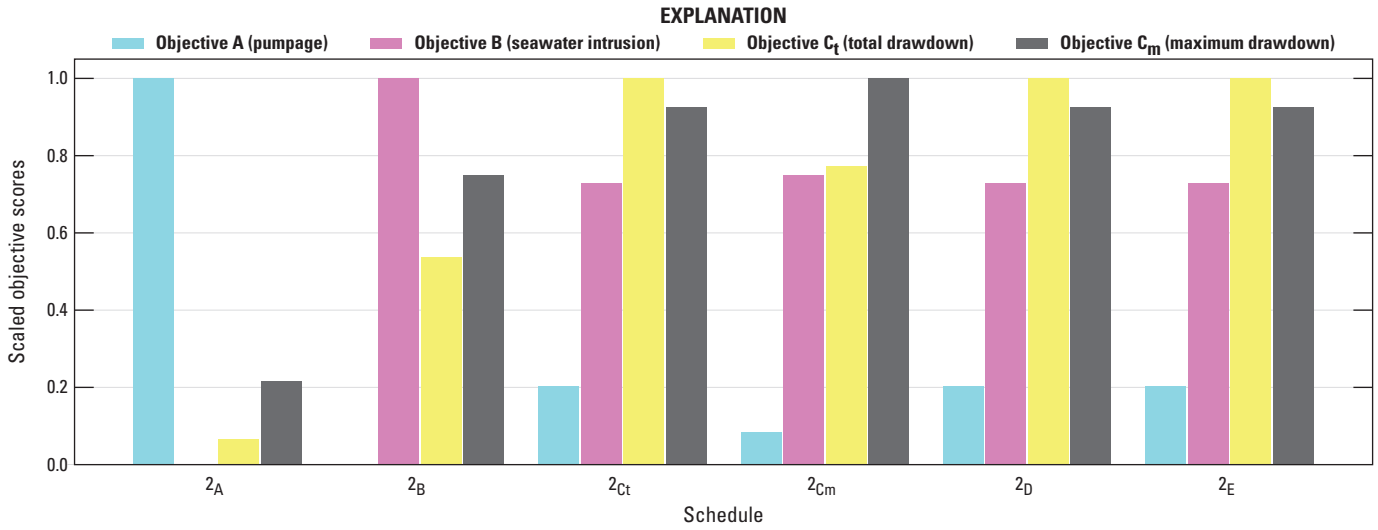

Figure 11. Scaled objective scores for schedules 2_A, 2_B, 2_{Ct}, 2_{Cm}, 2_D, and 2_E, Santa Barbara multi-objective management model, Santa Barbara, California.

The selected Pareto-optimal pumping schedules for the Storage Unit I subbasin and Foothill groundwater basin are shown in figure 12, and the pumpage by individual well for Schedule 2_D is presented in appendix D–2. The bars in figure 12 are divided into values of total pumping in Storage Unit I and Foothill groundwater basin. The nuances of these pumping schedules were similar to those of scenario 1 in terms of large initial pumpage in the first quarter, followed by a period of low pumpage, and then increased pumpage in the latter quarters of the 10-year management horizon. With few exceptions, the pumpage for schedule 2_A was generally larger in all quarters than for the other schedules. The temporal distribution of recharge was not considered, although it could also dictate which quarters receive more pumpage than others, depending on the assumed climatic conditions. An analysis of annual precipitation and the resulting pumpage, seawater intrusion, and drawdown was included as part of scenario 4.

In summary, the results for optimal annual pumping for schedule 2_D ranged from 1,617 to 3,463 acre-ft and averaged 2,623 acre-ft/yr for the 10-year period. Of this amount, the annual city pumpage from the Foothill groundwater basin ranged from 571 to 962 acre-ft and averaged 813 acre-ft/yr; the annual city pumpage from Storage Unit I ranged from 700 to 2,441 acre-ft and averaged 1,609 acre-ft/yr. Although not presented in figure 12, the annual city pumpage from Storage Unit III ranged from 169 to 251 acre-ft and averaged 201 acre-ft/yr. Figure 13 shows the contours of simulated hydraulic head for the upper, middle, and lower producing zones after 10 years of pumping for schedule 2_D (compromise schedule). A cone of depression formed around the Storage Unit I wells in the three producing zones (fig. 13). In addition, a cone of depression developed in the lower producing zone around the Hope Avenue well along the East More Ranch fault (fig. 13*C*). Additional depressions formed around the Val Verde well in Storage Unit III for the upper (fig. 13*A*) and lower (fig. 13*C*) producing zones.

Figure 14 shows a vertical section of chloride concentration and simulated chloride concentrations for the middle and lower producing zones, assuming schedule 2_D pumpage. The mean simulated chloride concentrations at wells 22A2 and 23F2 were 137 and 1,938 mg/L, respectively, at the end of the 10-year simulation. For the lower producing zones, the mean simulated chloride concentrations at wells 22A4 and 23F4 were 917 and 13,405 mg/L, respectively, at the end of the 10-year simulation. In the middle producing zone, the maximum simulated chloride concentration directly below well 22A2 was about 600 mg/L.

Simulated chloride breakthrough curves for the coastal monitoring wells, assuming schedule 2_D pumpage, showed trends similar to those for scenario 1 (fig. 15). The chloride concentration increase was still greatest in well 23E5, but the reduced pumpage in this schedule, compared to schedule 1_D, resulted in a higher final concentration (4,304 mg/L compared to 4,227 mg/L). Similarly, all other wells that showed seawater intrusion increased to a slightly higher concentration compared to schedule 1_D.

The results of scenario 2 showed that optimization of well pumpage identifies management schedules that mitigate seawater intrusion in a drier climatic condition. With less rainfall, there is less available groundwater, and the yield, considering the chloride and drawdown tradeoffs, is lower. Less pumping generally results in less seawater intrusion. Because the complex dynamics among the four objectives depend strongly on climate, choosing an optimal schedule from the Pareto curve that produces the desired pumpage results in a clear tradeoff between drawdown and seawater intrusion. In other words, if demand can be reduced when anticipating a drier climatic condition, an effective pumping schedule is available to meet any feasible drawdown and chloride specification without needing to re-run the model.

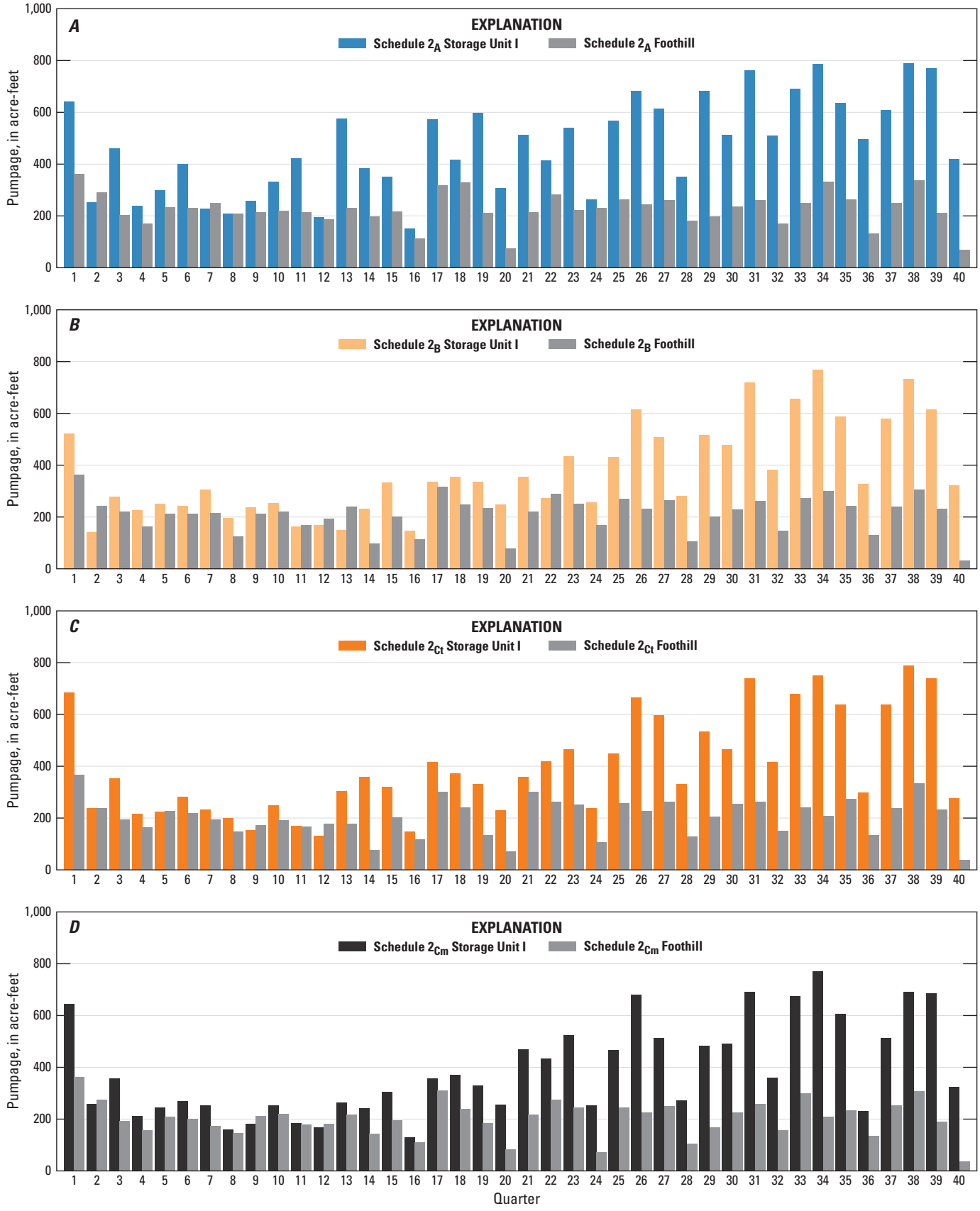

Figure 12. Scenario 2 quarterly pumpage for Storage Unit I and Foothill groundwater basin, Santa Barbara multi-objective management model, Santa Barbara, California, for *A*, schedule 2_A; *B*, schedule 2_B; *C*, schedules 2_{Ct}, 2_D, and 2_E; and *D*, schedule 2_{Cm}.

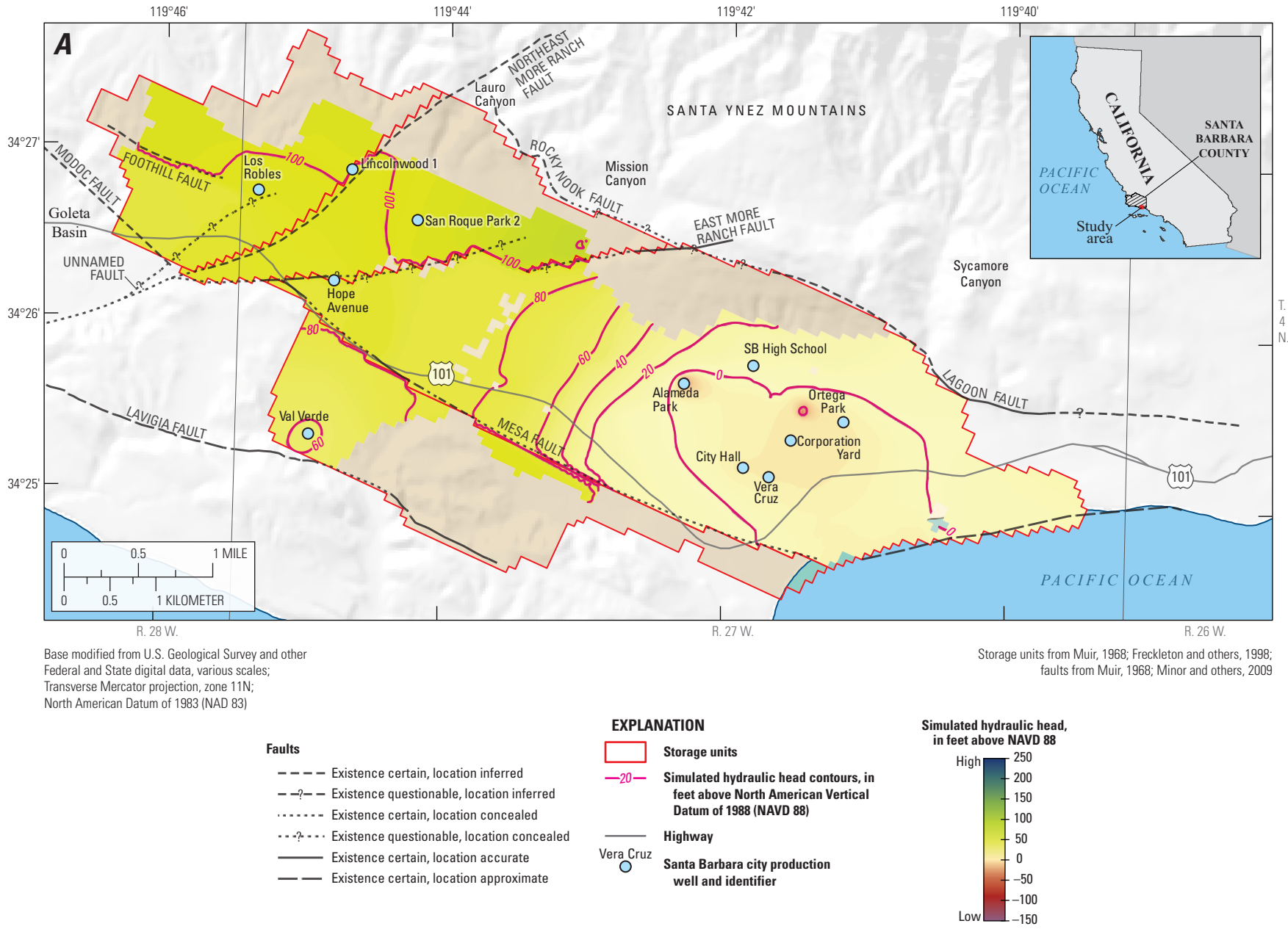

Figure 13. Contours of simulated hydraulic head after 10 years for scenario 2, schedule 2_D, Santa Barbara multi-objective management model, Santa Barbara, California: *A*, upper producing zone; *B*, middle producing zone; and *C*, lower producing zone.

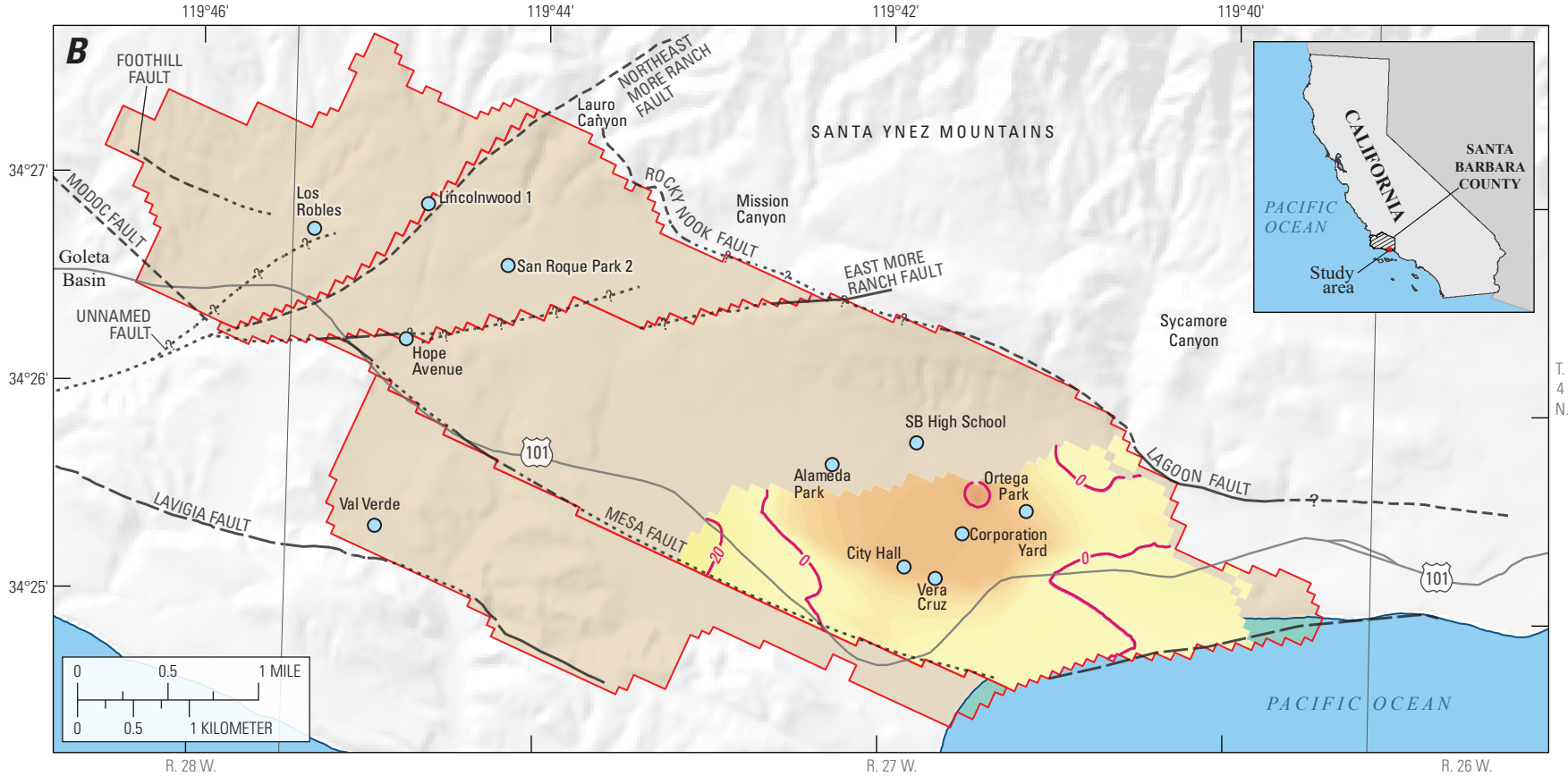

Base modified from U.S. Geological Survey and other Federal and State digital data, various scales; Transverse Mercator projection, zone 11N; North American Datum of 1983 (NAD 83)

Storage units from Muir, 1968; Freckleton and others, 1998; faults from Muir, 1968; Minor and others, 2009

EXPLANATION

Faults

- Existence certain, location inferred
- Existence questionable, location inferred
- Existence certain, location concealed
- Existence questionable, location concealed
- Existence certain, location accurate
- Existence certain, location approximate

- **Storage units**
- **Simulated hydraulic head contours, in feet above North American Vertical Datum of 1988 (NAVD 88)**
- **Highway**
- Vera Cruz — **Santa Barbara city production well and identifier**

Simulated hydraulic head, in feet above NAVD 88

High 250 200 150 100 50 0 –50 –100 Low –150

Figure 13. —Continued

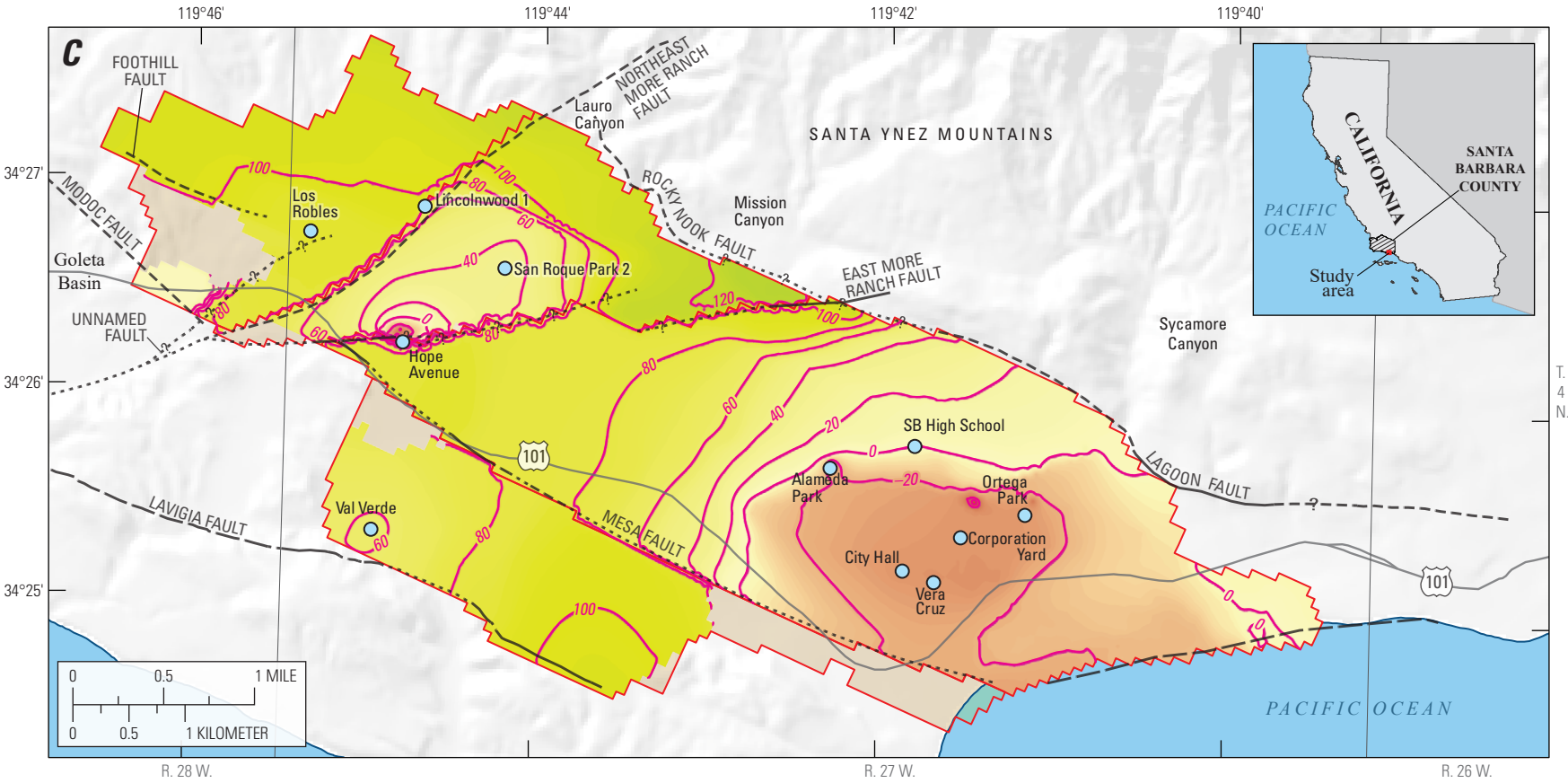

Base modified from U.S. Geological Survey and other Federal and State digital data, various scales; Transverse Mercator projection, zone 11N; North American Datum of 1983 (NAD 83)

Storage units from Muir, 1968; Freckleton and others, 1998; faults from Muir, 1968; Minor and others, 2009

Faults

- Existence certain, location inferred
- Existence questionable, location inferred
- Existence certain, location concealed
- Existence questionable, location concealed
- Existence certain, location accurate
- Existence certain, location approximate

EXPLANATION

- Storage units
- Simulated hydraulic head contours, in feet above North American Vertical Datum of 1988 (NAVD 88)
- Highway
- Vera Cruz — Santa Barbara city production well and identifier

Simulated hydraulic head, in feet above NAVD 88

High 250, 200, 150, 100, 50, 0, –50, –100, –150 Low

Figure 13. —Continued

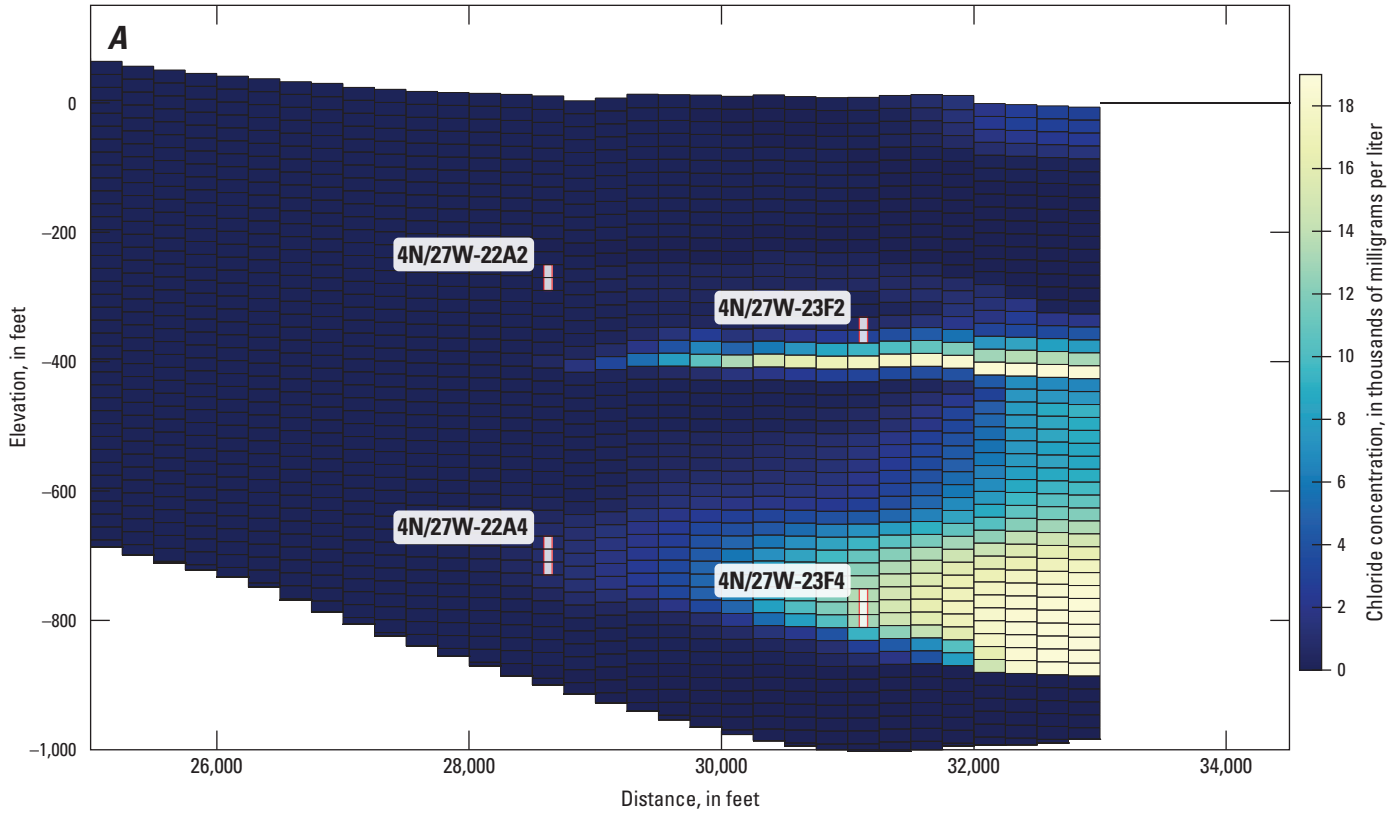

Figure 14. Simulated year-10 Storage Unit I chloride concentration distribution for schedule 2_D, Santa Barbara multi-objective management model, Santa Barbara, California: *A*, section along model row 30; *B*, plan view of middle producing zone; and *C*, plan view of the lower producing zone.

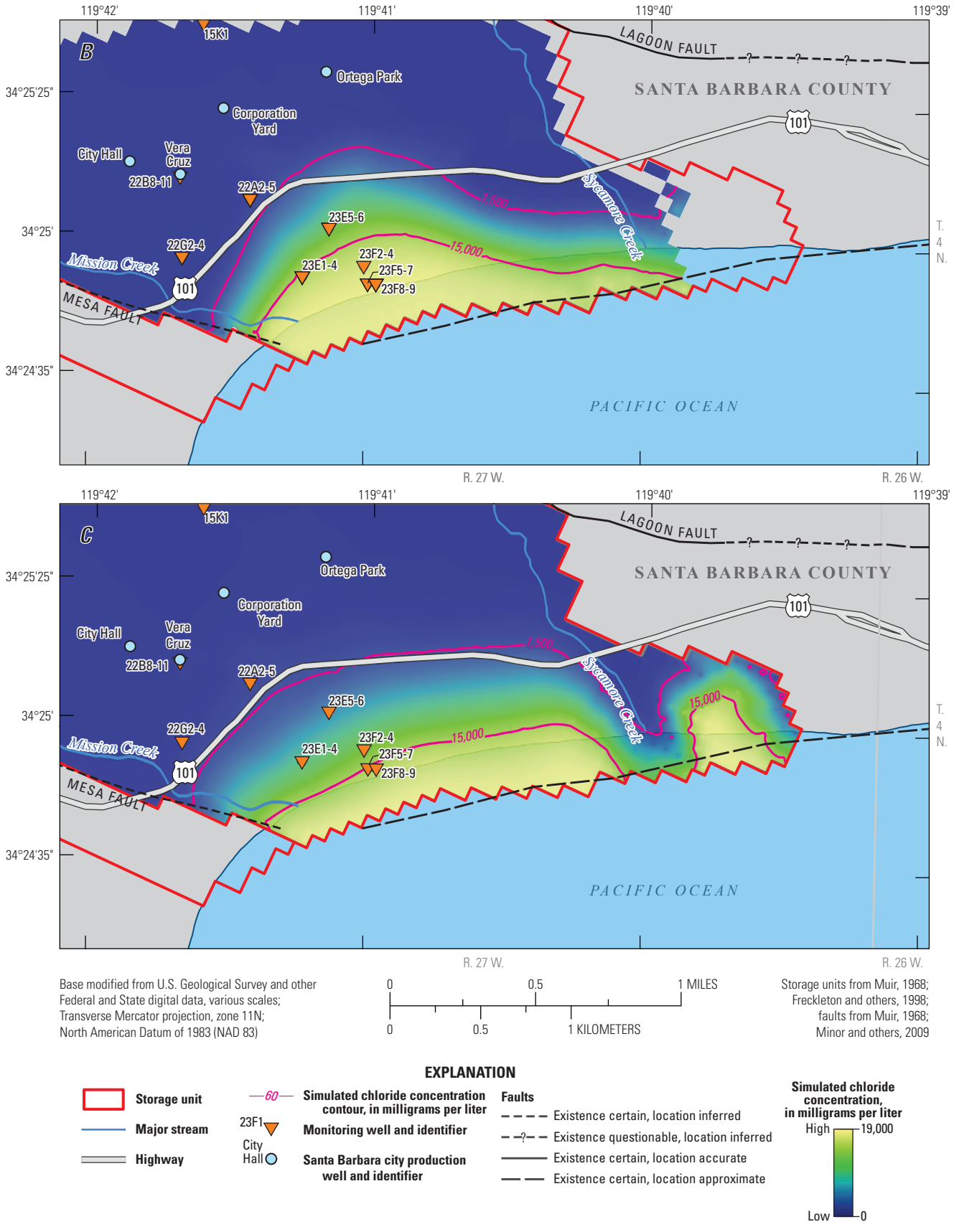

Figure 14. —Continued

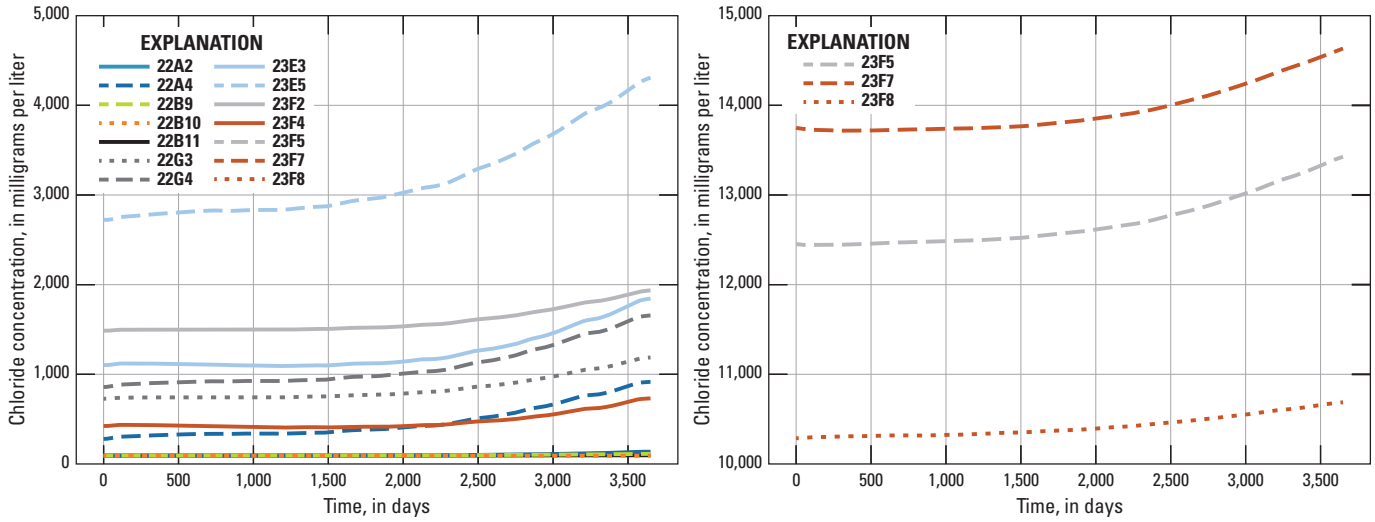

Figure 15. Simulated chloride breakthrough curves for selected monitoring wells for schedule 2_D, Santa Barbara multi-objective management model, Santa Barbara, California.

Scenario 3

Scenario 3 assumed 484 acre-ft/yr was pumped from the six production wells in Storage Unit I (based on assumed minimum flowrates for Ortega groundwater treatment-plant operations); there was no pumpage from Foothill groundwater basin or Storage Unit III. The pumpage was assigned to each well in Storage Unit I by scaling the quarterly pumpage for schedule 1_D (typical) and schedule 2_D (dry), such that the total annual pumpage was 484 acre-ft. See appendix D–3 for the quarterly pumpage by well. This scenario simulated minimal initial water levels (1990), the 10-year typical precipitation used in scenario 1, and the 10-year drought used in scenario 2.

Figure 16*A–B* shows drawdown hydrographs with respect to 1998 water levels for four monitoring wells in Storage Unit I (4N/27W-15K1, -16R1, -22G4, and -23E5), assuming typical and dry climatic conditions, respectively. Instead of using initial conditions to calculate drawdown, the 1998 high water level for each well was used as the reference point; therefore, as drawdown approached zero, the simulated hydraulic heads approached 1998 water levels. For both climatic conditions, the simulated hydraulic heads recovered quickly in the first year, after which the hydraulic heads recovered more slowly. For the typical climatic condition, only well 16R1 recovered to 1998 levels after 10 years; for the dry climatic condition, none of the wells recovered to 1998 conditions (as indicated by 0 ft of drawdown in fig. 16). These results indicated that Storage Unit I would not be able to completely recover to 1998 water levels within 10 years under a typical or dry climatic condition while constantly extracting 484 acre-ft/yr from Storage Unit I; however, water levels appeared to stabilize as they approached about 0–5 ft below 1998 levels for a typical climatic condition and about 3–8 ft below 1998 levels for a dry climatic condition.

Figure 16*C–D* shows drawdown hydrographs for four monitoring wells in the Foothill groundwater basin (4N/27W-12R3, -12H4, -5P1, and -8M6), assuming typical and dry climatic conditions, respectively. As with the Storage Unit I drawdown hydrographs, zero drawdown equaled the simulated water levels from 1998. For the Foothill groundwater basin, initial water levels from 1990 were not as far below 1998 levels as those for Storage Unit I. With no pumping simulated in the Foothill groundwater basin, there was a smooth recovery to water levels between about 30 and 70 ft above 1998 levels for a typical climatic condition (fig 16*C*) and to between about 20 and 60 ft above 1998 levels for a dry climatic condition (fig 16*D*).

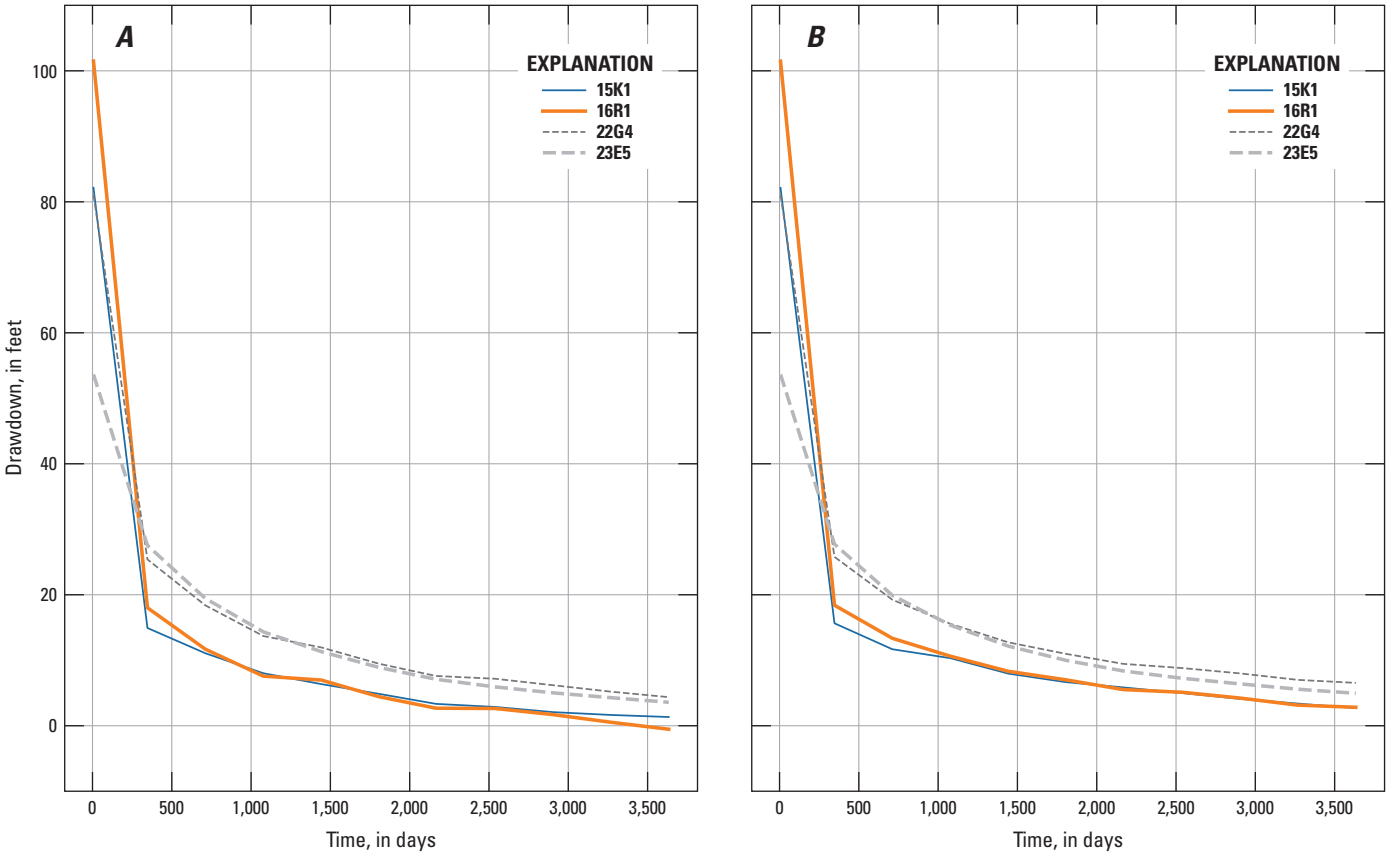

Figure 16. Simulated drawdowns with respect to 1998 water levels for selected wells and total pumpage equaling 484 acre-feet per year (acre-ft/yr), scenario 3, Santa Barbara multi-objective management model, Santa Barbara, California, for *A*, Storage Unit I (SU1) with a 10-year typical climatic condition; *B*, Storage Unit I with a 10-year dry climatic condition; *C*, the Foothill groundwater basin with a 10-year typical climatic condition; and *D*, the Foothill groundwater basin with a 10-year dry climatic condition.

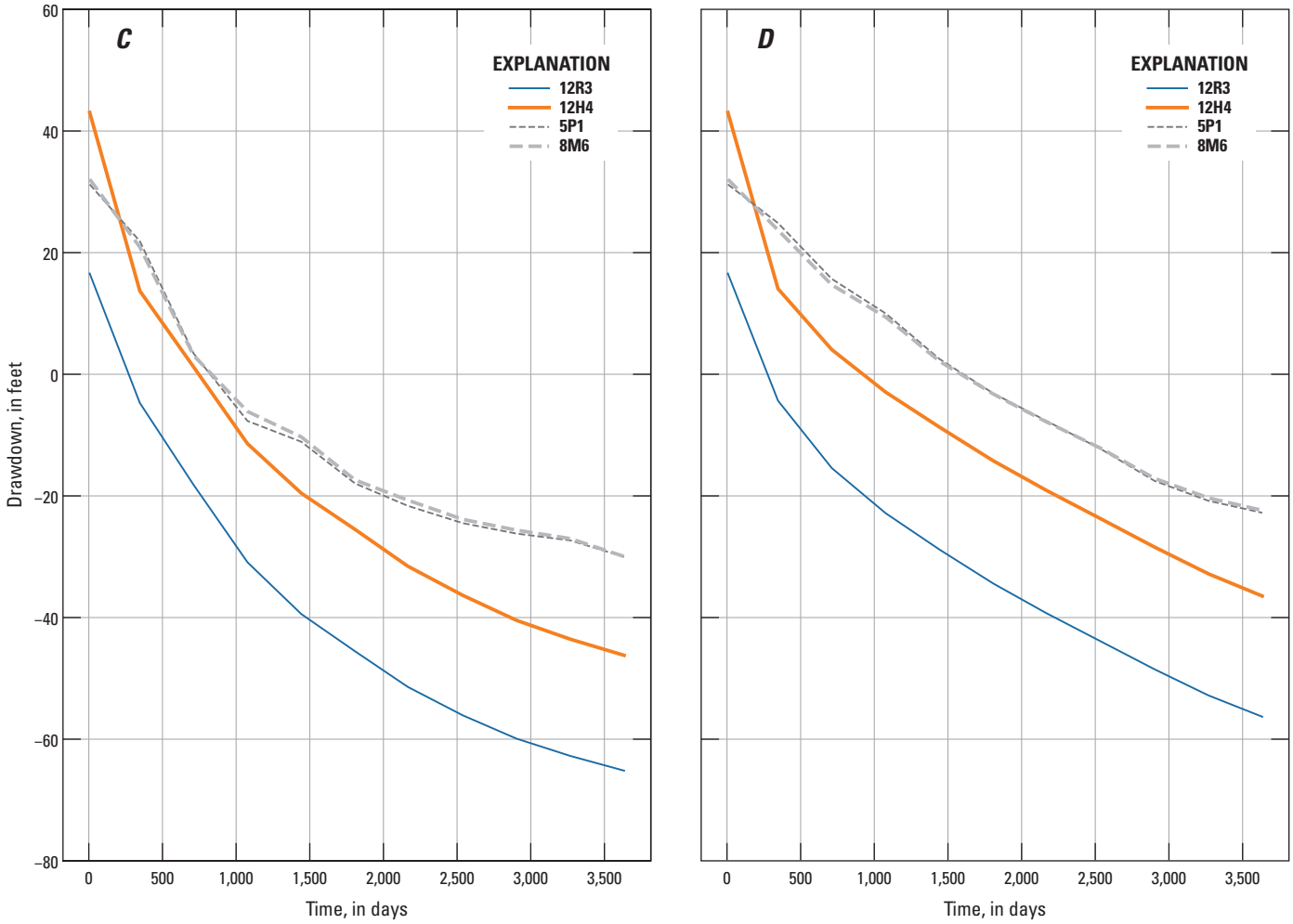

Figure 16. —Continued

Figure 17 shows contours of simulated year-10 drawdowns with respect to 1998 water levels for the upper, middle, and lower producing zones for scenario 3, assuming typical conditions. Note that the hydrographs in figure 16 are for a single model cell in the well's perforated interval, and the contours in figure 17 are based on a depth-averaged, simulated hydraulic head in each producing zone. The hydrographs and contours, therefore, are not directly comparable. In the upper producing zone, drawdowns ranged from 0 to 10 ft throughout most of Storage Unit I and ranged from –20 to –60 ft in the Foothill groundwater basin (fig. 17*A*). In the middle producing zone, drawdowns ranged from 0 to 10 ft in Storage Unit I (fig. 17*B*). In the lower producing zone, the drawdown was more than 0 ft and less than 20 ft throughout most of Storage Unit I and ranged from –20 to –80 ft in the Foothill groundwater basin (fig. 17*C*). The recovery would likely have been greater in all the producing zones if not for the pumping to supply the Ortega treatment plant.

Figure 18 shows contours of the initial (1990) chloride distribution for the middle and lower producing zones (fig. 18*A*) and the simulated year-10 chloride concentrations for the middle and lower producing zones for scenario 3, assuming typical conditions (fig. 18*B*). The simulated results indicated the extent of seawater intrusion after 10 years of pumping 484 acre-ft/yr from Storage Unit I. The changes in the 15,000-mg/L contours show seawater intrusion was retreating near the coast both for the middle and lower producing zones (fig. 18*B*).

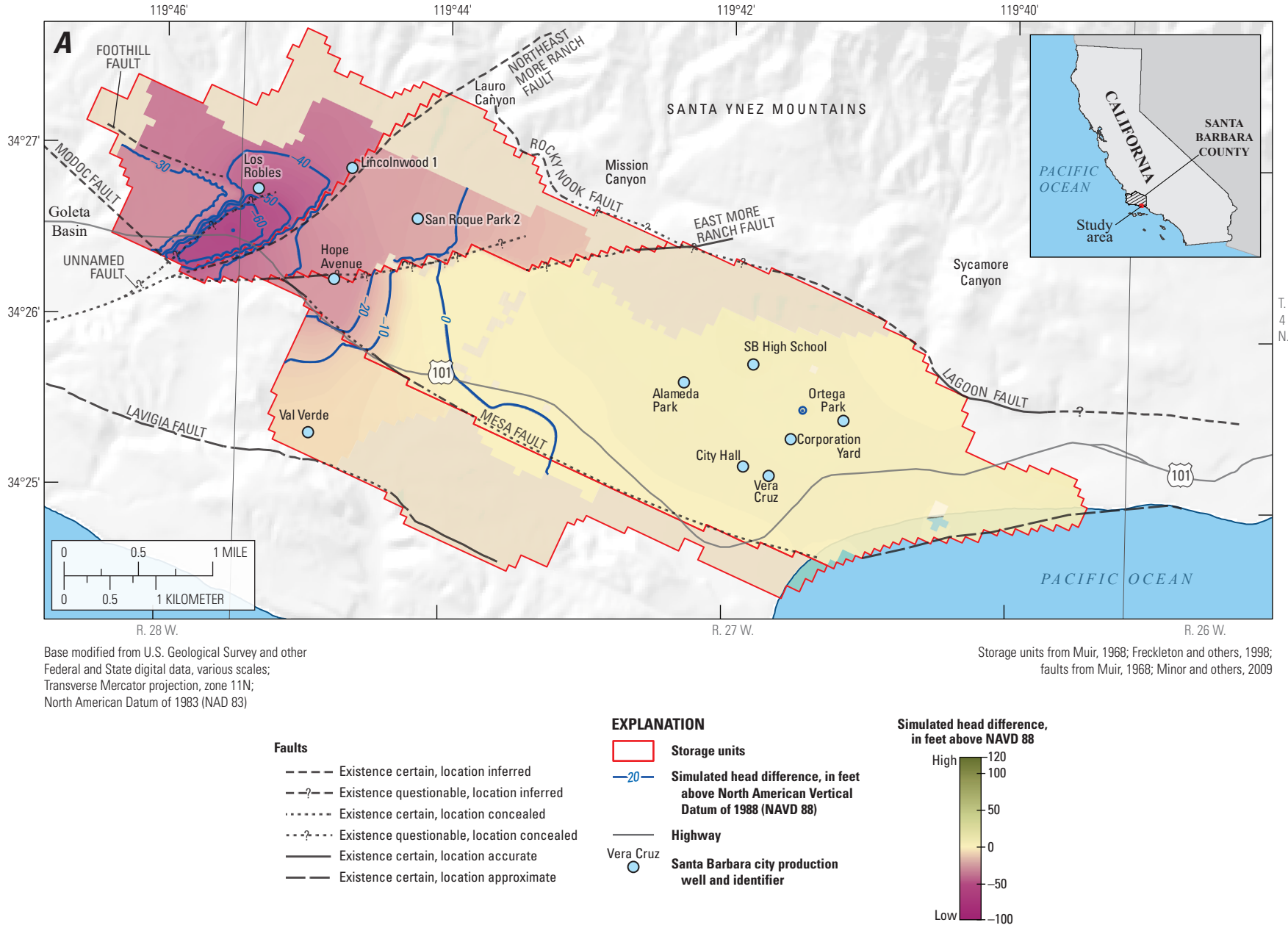

Figure 17. Contours of simulated year-10 drawdowns with respect to 1998 water levels, assuming typical conditions, scenario 3, Santa Barbara multi-objective management model, Santa Barbara, California, for the *A*, upper producing zone; *B*, middle producing zone; and *C*, lower producing zone.

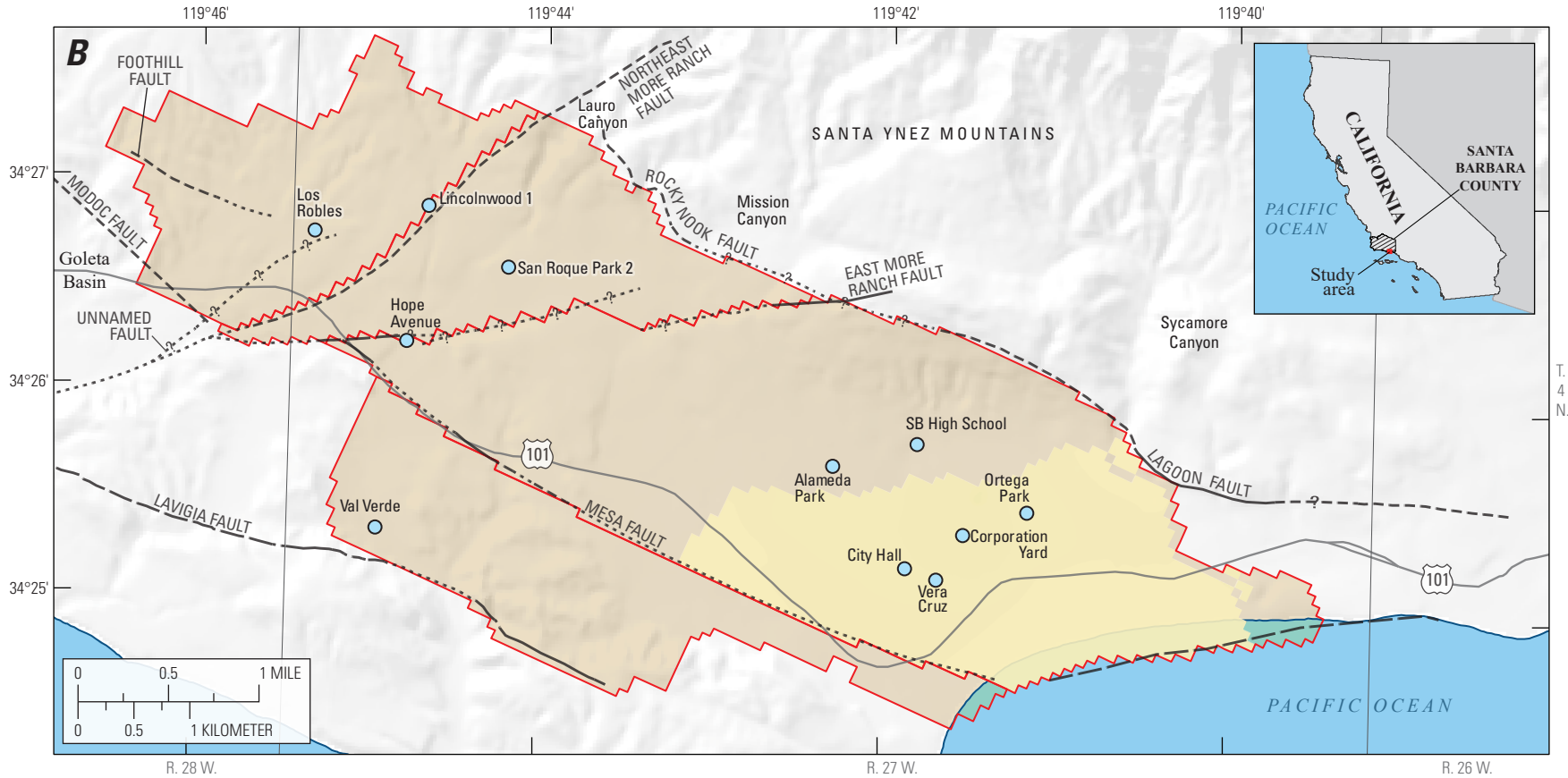

Base modified from U.S. Geological Survey and other Federal and State digital data, various scales; Transverse Mercator projection, zone 11N; North American Datum of 1983 (NAD 83)

Storage units from Muir, 1968; Freckleton and others, 1998; faults from Muir, 1968; Minor and others, 2009

Faults

- Existence certain, location inferred
- Existence questionable, location inferred
- Existence certain, location concealed
- Existence questionable, location concealed
- Existence certain, location accurate
- Existence certain, location approximate

EXPLANATION

- **Storage units**
- **Highway**
- Vera Cruz — **Santa Barbara city production well and identifier**

Simulated head difference, in feet above NAVD 88

High 120, 100, 50, 0, −50, −100 Low

Figure 17. —Continued

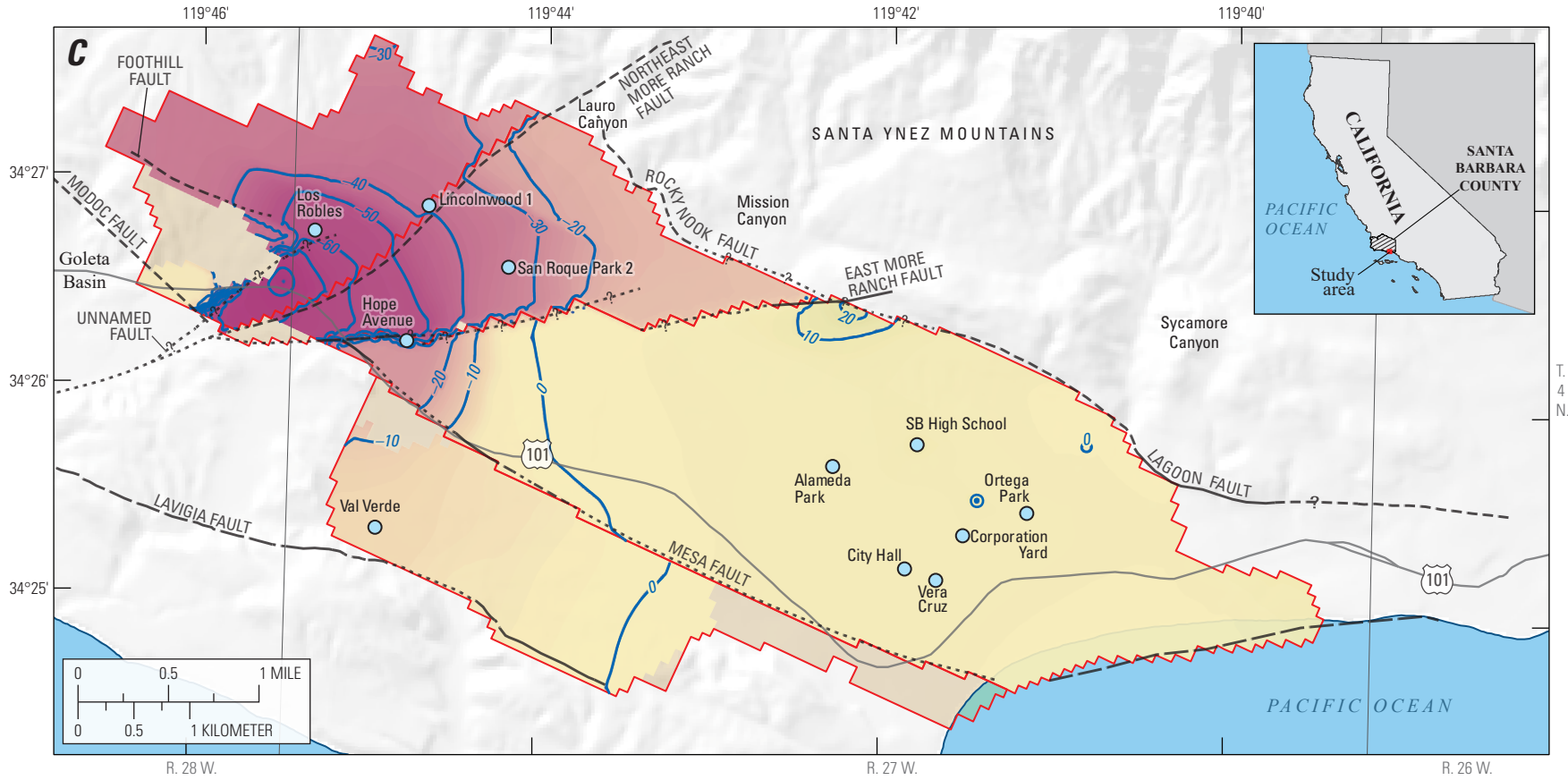

Base modified from U.S. Geological Survey and other Federal and State digital data, various scales; Transverse Mercator projection, zone 11N; North American Datum of 1983 (NAD 83)

Storage units from Muir, 1968; Freckleton and others, 1998; faults from Muir, 1968; Minor and others, 2009

Faults

- Existence certain, location inferred
- Existence questionable, location inferred
- Existence certain, location concealed
- Existence questionable, location concealed
- Existence certain, location accurate
- Existence certain, location approximate

EXPLANATION

- Storage units
- Simulated head difference, in feet above North American Vertical Datum of 1988 (NAVD 88)
- Highway
- Vera Cruz — Santa Barbara city production well and identifier

Simulated head difference, in feet above NAVD 88

High 120, 100, 50, 0, −50, Low −100

Figure 17. —Continued

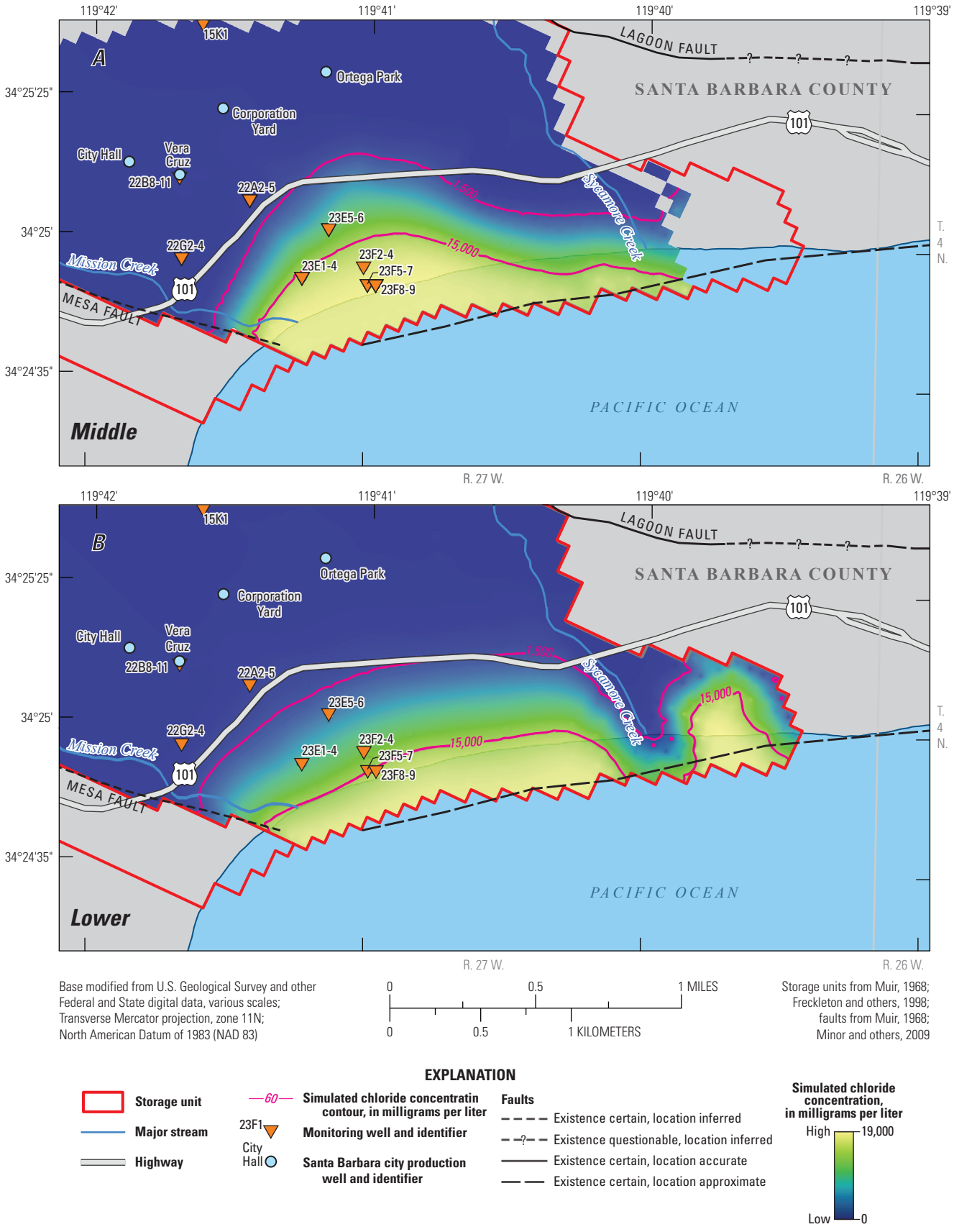

Figure 18. Contours, assuming a typical climatic condition, scenario 3, Santa Barbara multi-objective management model, Santa Barbara, California, of *A*, initial (1990) chloride concentrations in the middle producing zone; *B*, initial (1990) chloride concentrations in the lower producing zone; *C*, simulated year-10 chloride concentrations in the middle producing zone; and *D*, simulated year-10 chloride concentrations in the lower producing zone.

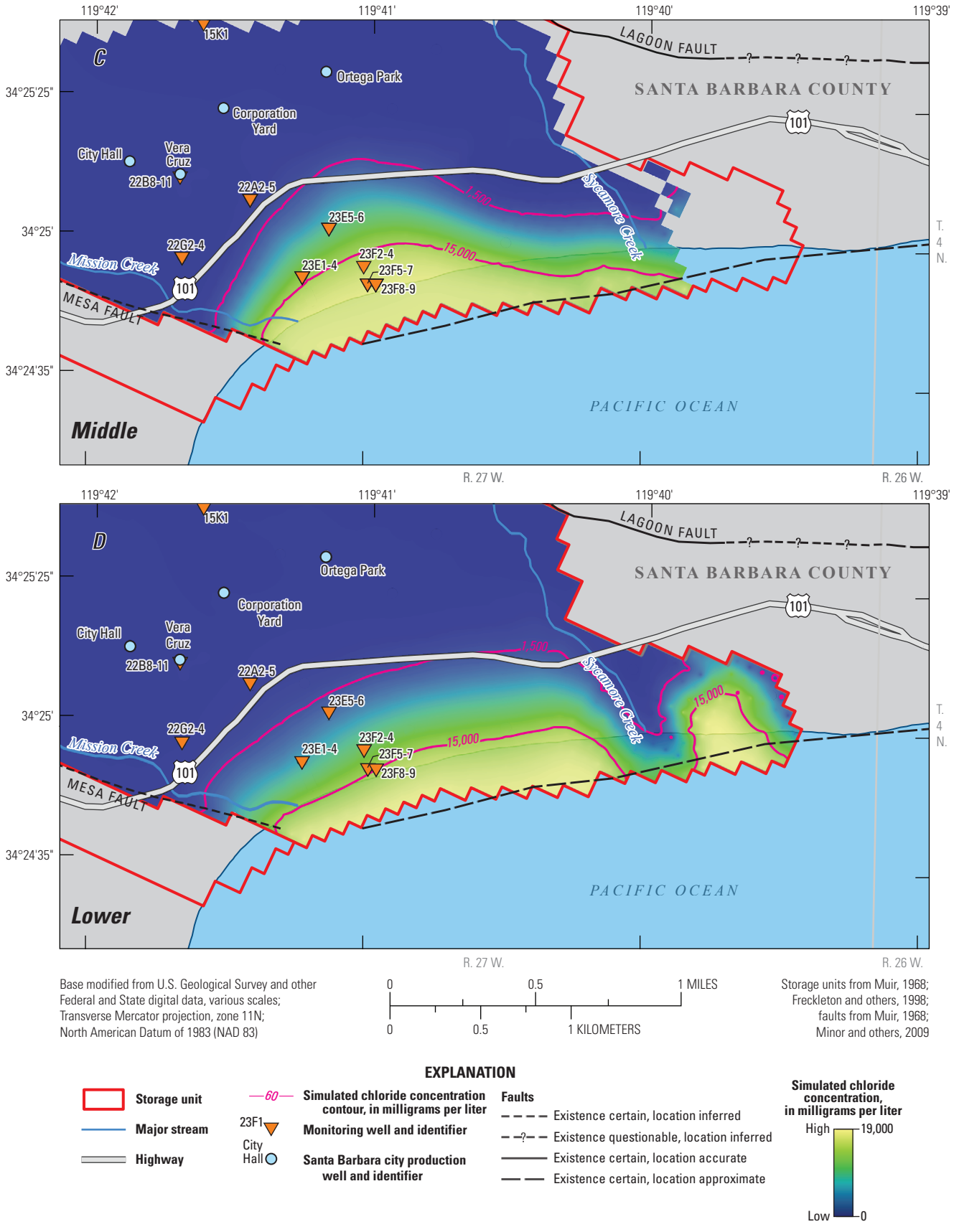

Figure 18. —Continued

Figure 19 shows contours of simulated year-10 drawdown with respect to 1998 water levels for the upper, middle, and lower producing zones for scenario 3, assuming dry conditions. In the upper producing zone, drawdowns ranged from 0 to 10 ft throughout most of Storage Unit I and ranged from –20 to –60 ft in the Foothill groundwater basin (fig. 19*A*), yet were slightly greater than the simulated drawdowns for a typical climatic condition (fig. 17*A*). In the middle producing zone, drawdowns ranged from 0 to 10 ft in Storage Unit I (fig. 19*B*) and were similar to those of a typical climatic condition (fig. 17*B*). In the lower producing zone, drawdowns ranged from more than 0 ft to less than 70 ft throughout most of Storage Unit I and ranged from 0 to –70 ft in the Foothill groundwater basin (fig. 19*C*). The simulated drawdown in the northern part of Storage Unit I (fig. 19*C*) could be the result of less natural recharge associated with the dry climatic condition. In general, the water-level recovery for the upper zone, assuming dry conditions, was similar to that for the typical climatic condition, yet water-level contours were slightly farther inland, indicative of less recharge; for the lower zone under dry conditions, water-level recovery was less than that for the typical climate throughout both subbasins.

Figure 20 shows contours of simulated year-10 chloride concentrations for the middle and lower producing zones for scenario 3, assuming dry conditions. The changes in the 15,000- mg/L contours show seawater intrusion was retreating near the coast, particularly in the middle producing zone (fig. 20). In general, there was little difference in the chloride contours between dry and typical climatic conditions, indicating that climate did not substantially affect seawater intrusion under the same pumpage schedule.

Scenario 4

The two cases in scenario 4 were designed to produce decision rules to support management decisions based on the optimal results. The initial conditions for scenario 4 were designed to emulate recent conditions; therefore, simulated 2013 hydraulic heads and chloride concentrations are used as initial conditions. The goal of scenario 4A was to provide a decision rule for groundwater pumpage as a function of allowable change in measured chloride concentration in selected coastal monitoring wells. For example, a water manager would choose an allowable maximum increase in chloride concentration for the year according to the measured concentration in a given well; the result of the decision rule would be the optimal total pumpage for Storage Unit I for the allowable maximum chloride increase in the following year. The goal of scenario 4B was to provide a decision rule for groundwater pumpage as a function of desired maximum drawdown in selected wells in the Foothill groundwater basin. For example, a water manager would choose an allowable maximum drawdown in a given well for 10 years of pumping. The result of the decision rule would be the optimal total 10-year pumpage for Storage Unit I and Foothill groundwater basin.

In this scenario, 10-year simulations were made using the Pareto-optimal pumping schedules for the typical (scenario 1) and dry (scenario 2) climatic conditions. Recall that scenario 1 had 912 Pareto-optimal solutions (fig. 4), and scenario 2 had 629 Pareto-optimal solutions (fig. 10). The epsilon values were adjusted such that a reasonably large number of Pareto-optimal pumping schedules were identified—in this case, about 100 such pumping schedules were identified for each scenario—and such that the schedules represented the full range of objective values. Scenario 1 had 127 Pareto-optimal pumping schedules using ε_A, ε_B, ε_{Ct}, and ε_{Cm} values of 500, 20, 200, and 5, respectively (fig. 21*A*). Scenario 2 had 97 Pareto-optimal pumping schedules using ε_A, ε_B, ε_{Ct}, and ε_{Cm} values of 500, 20, 50, and 5, respectively (fig. 21*B*). Figures 21*A* and *B* represent subsets of the entire Pareto-optimal solutions as defined by these ε values. The decision-rule curves for scenarios 4A and 4B were produced from the subsets of Pareto-optimal results for scenarios 1 and 2 by running a 10-year simulation for each solution in the subsets and searching for specific levels of chloride concentration or maximum drawdown in selected monitoring or production wells.

Scenario 4A

For this scenario, the decision-rule curves were generated from the 10-year simulation results using the following steps:

1. Assume measured chloride concentrations at selected monitoring sites.
2. Search the scenario 1 and 2 Pareto-optimal pumping schedules for simulated chloride concentrations that equal the assumed measured chloride concentration at each monitoring site.
3. If the simulated value equals the assumed measured concentration, then the total pumpage in Storage Unit I for the following year and the associated change in chloride concentration are saved.

Figure 22 shows example decision-rule curves for two monitoring wells (4N/27W-23E3 and 23E5) assuming typical and dry climatic conditions. Assume that 800 mg/L and 2,000 mg/L chloride concentrations were measured in wells 23E3 and 23E5, respectively. For well 23E3, assuming typical climatic conditions and an allowable increase in measured chloride concentration of 76 mg/L, the Pareto-optimal results indicated that during the year following the time when 800 mg/L was measured, about 1,937 acre-ft of water was pumped from Storage Unit I. This results in one point on the rule curve. Each red circle in figure 22 represents a similar analysis for every point on the Pareto front, assuming a concentration of 800 mg/L was reached at well 23E3. A threshold of 2,000 mg/L was applied to well 23E5, and similar analyses were performed (fig. 22).

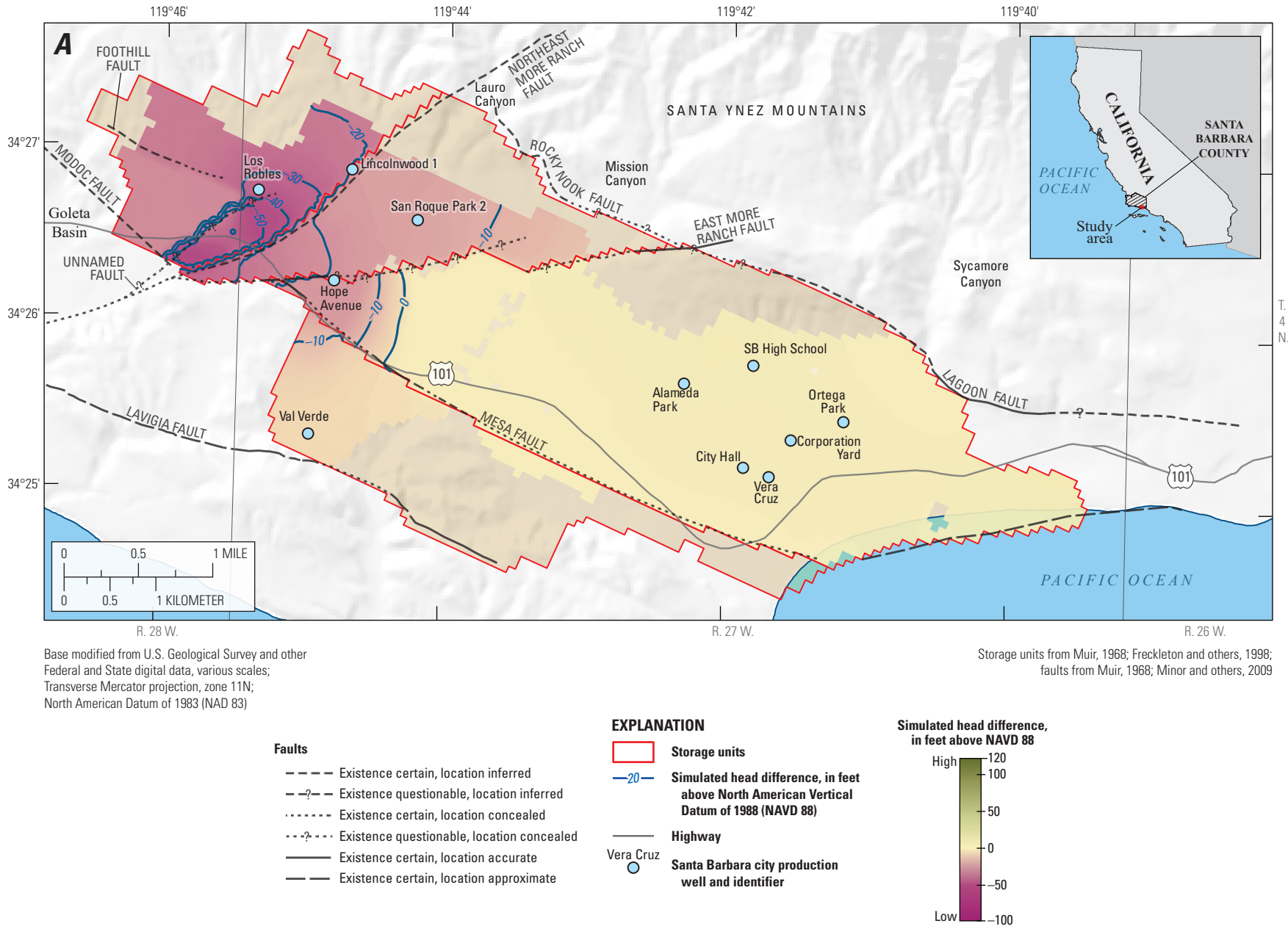

Figure 19. Contours of simulated year-10 drawdown with respect to 1998 water levels, assuming dry climatic condition, scenario 3, Santa Barbara multi-objective management model, Santa Barbara, California, for the *A*, upper producing zone, *B*, middle producing zone, and *C*, lower producing zone.

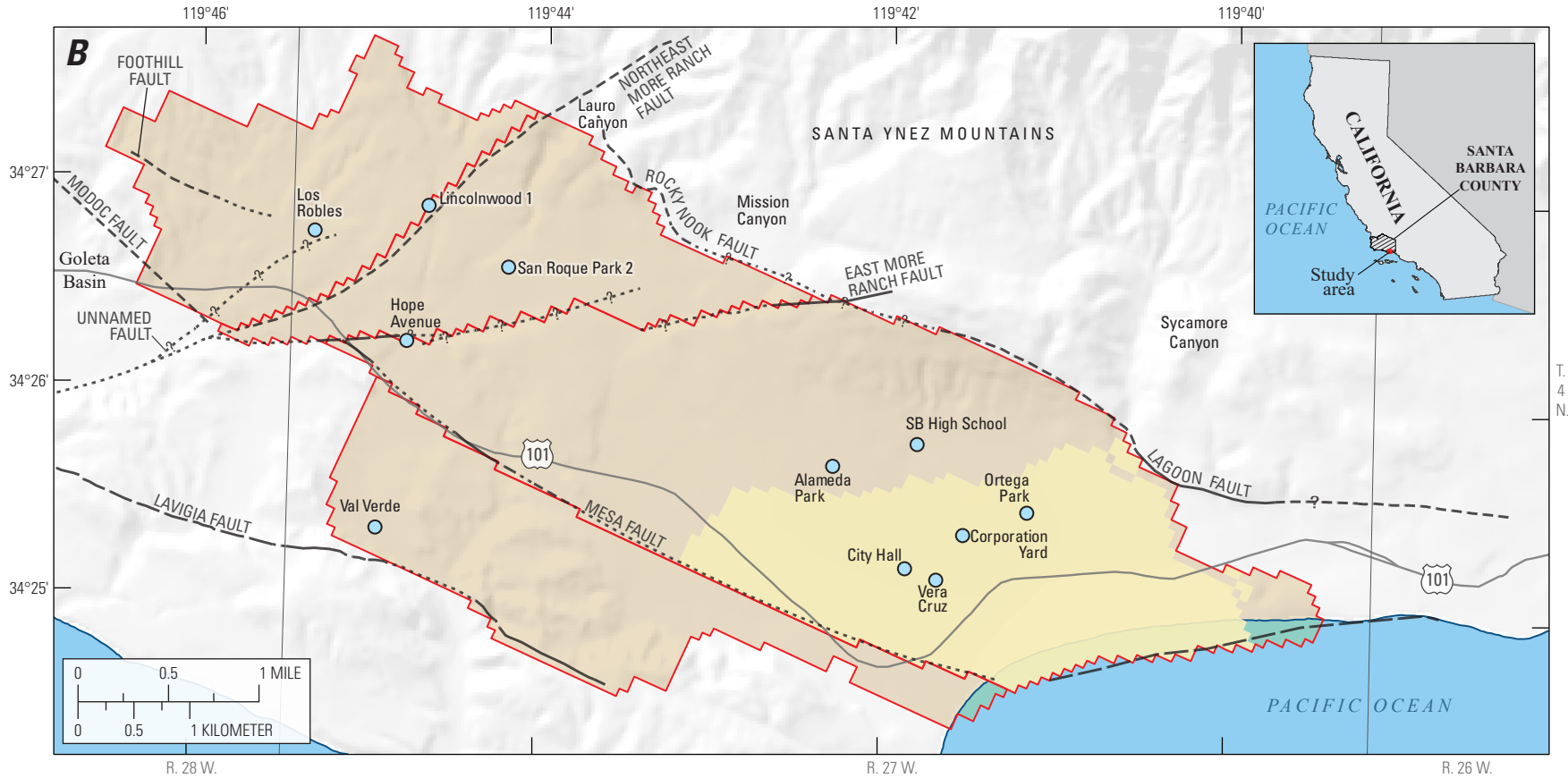

Base modified from U.S. Geological Survey and other Federal and State digital data, various scales; Transverse Mercator projection, zone 11N; North American Datum of 1983 (NAD 83)

Storage units from Muir, 1968; Freckleton and others, 1998; faults from Muir, 1968; Minor and others, 2009

Faults

- Existence certain, location inferred
- Existence questionable, location inferred
- Existence certain, location concealed
- Existence questionable, location concealed
- Existence certain, location accurate
- Existence certain, location approximate

EXPLANATION

- Storage units
- Highway
- Vera Cruz — Santa Barbara city production well and identifier

Simulated head difference, in feet above North American Vertical Datum of 1988

High 120, 100, 50, 0, −50, Low −100

Figure 19. —Continued

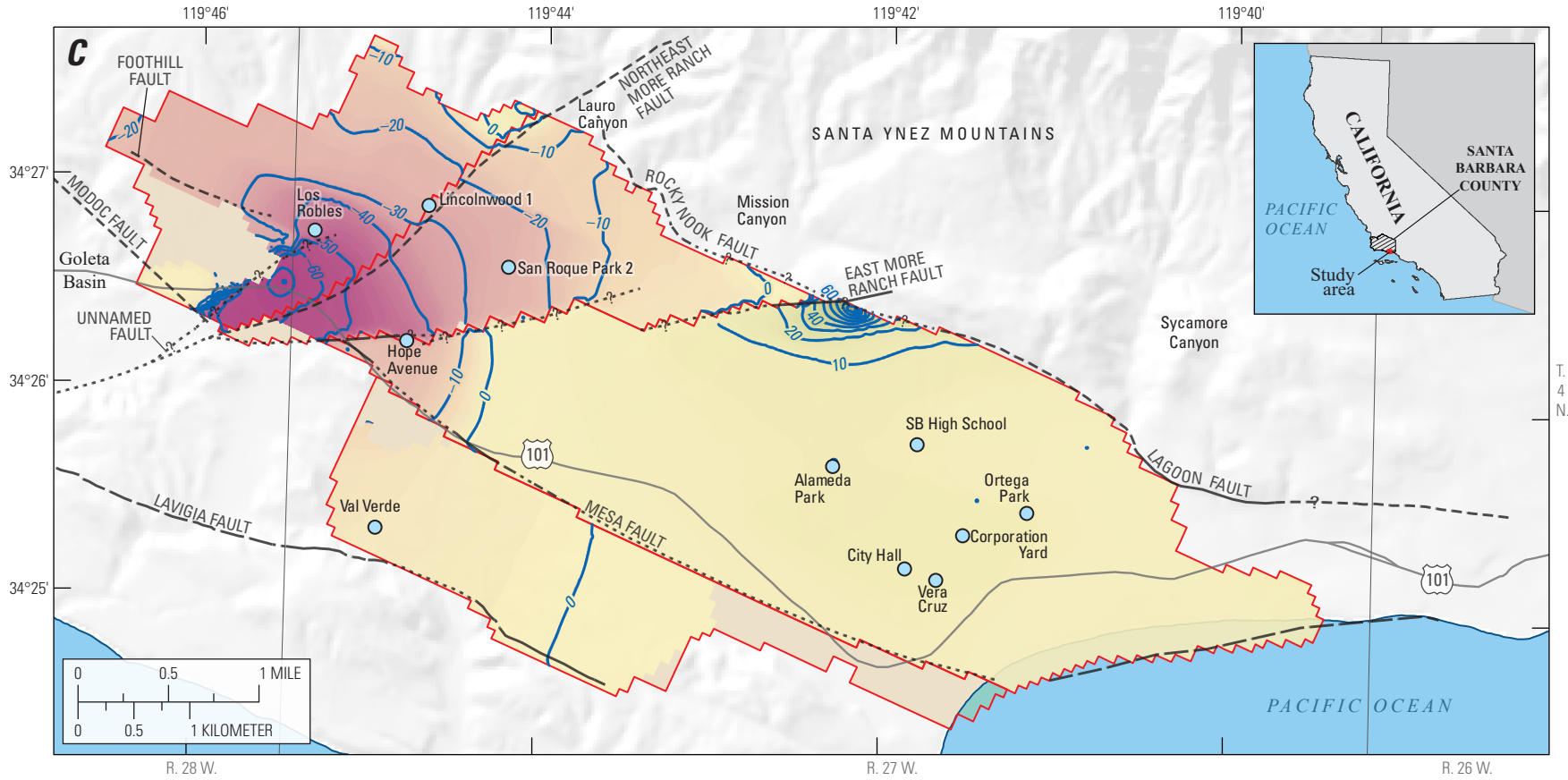

Base modified from U.S. Geological Survey and other Federal and State digital data, various scales; Transverse Mercator projection, zone 11N; North American Datum of 1983 (NAD 83)

Storage units from Muir, 1968; Freckleton and others, 1998; faults from Muir, 1968; Minor and others, 2009

Faults

- Existence certain, location inferred
- Existence questionable, location inferred
- Existence certain, location concealed
- Existence questionable, location concealed
- Existence certain, location accurate
- Existence certain, location approximate

EXPLANATION

- Storage units
- −20 — Simulated head difference, in feet above North American Vertical Datum of 1988 (NAVD 88)
- Highway
- Vera Cruz — Santa Barbara city production well and identifier

Simulated head difference, in feet above NAVD 88

High 120, 100, 50, 0, −50, Low −100

Figure 19. —Continued

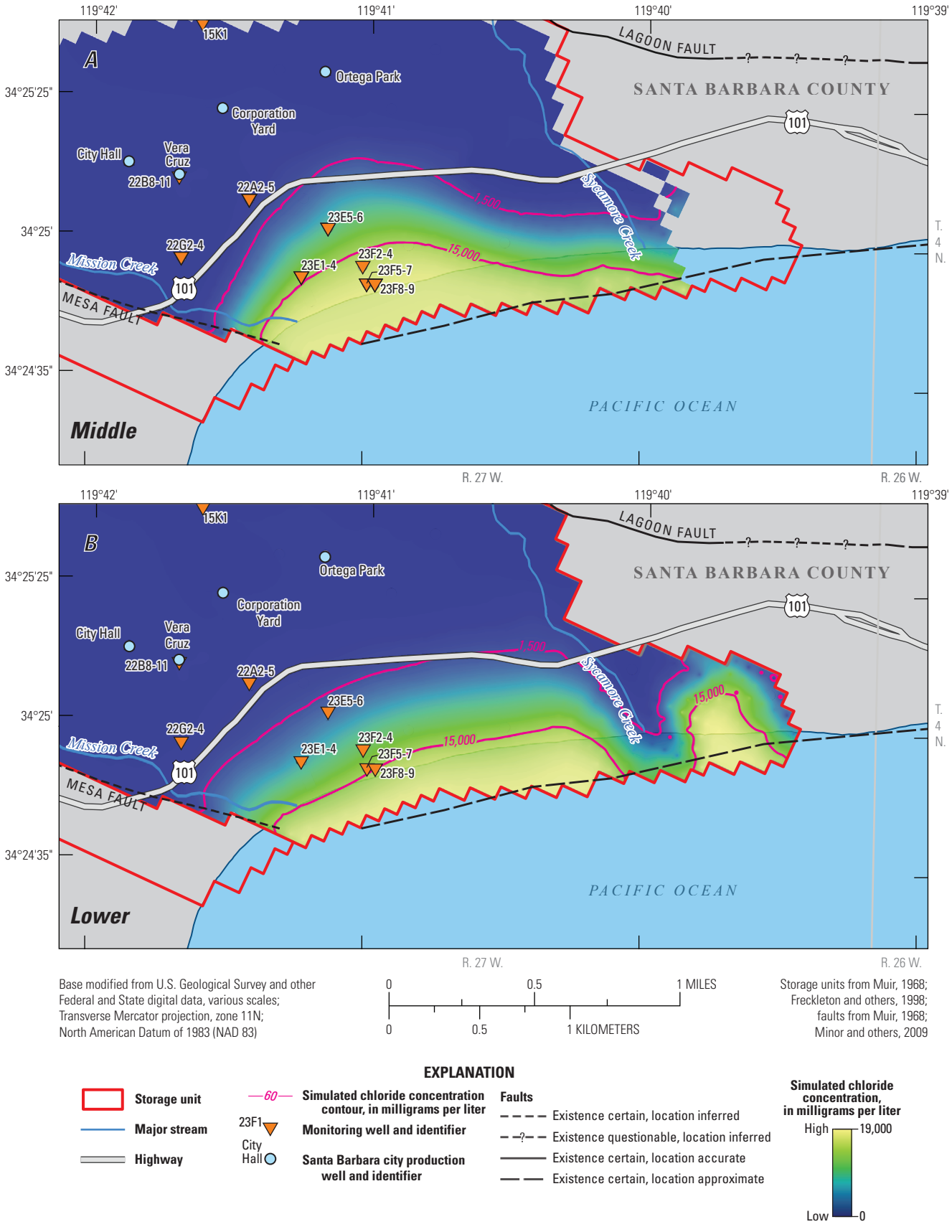

Figure 20. Contours; assuming a dry climatic condition, scenario 3, Santa Barbara multi-objective management model, Santa Barbara, California, of simulated year-10 chloride concentrations for *A*, the middle producing zone, and *B*, the lower producing zone.

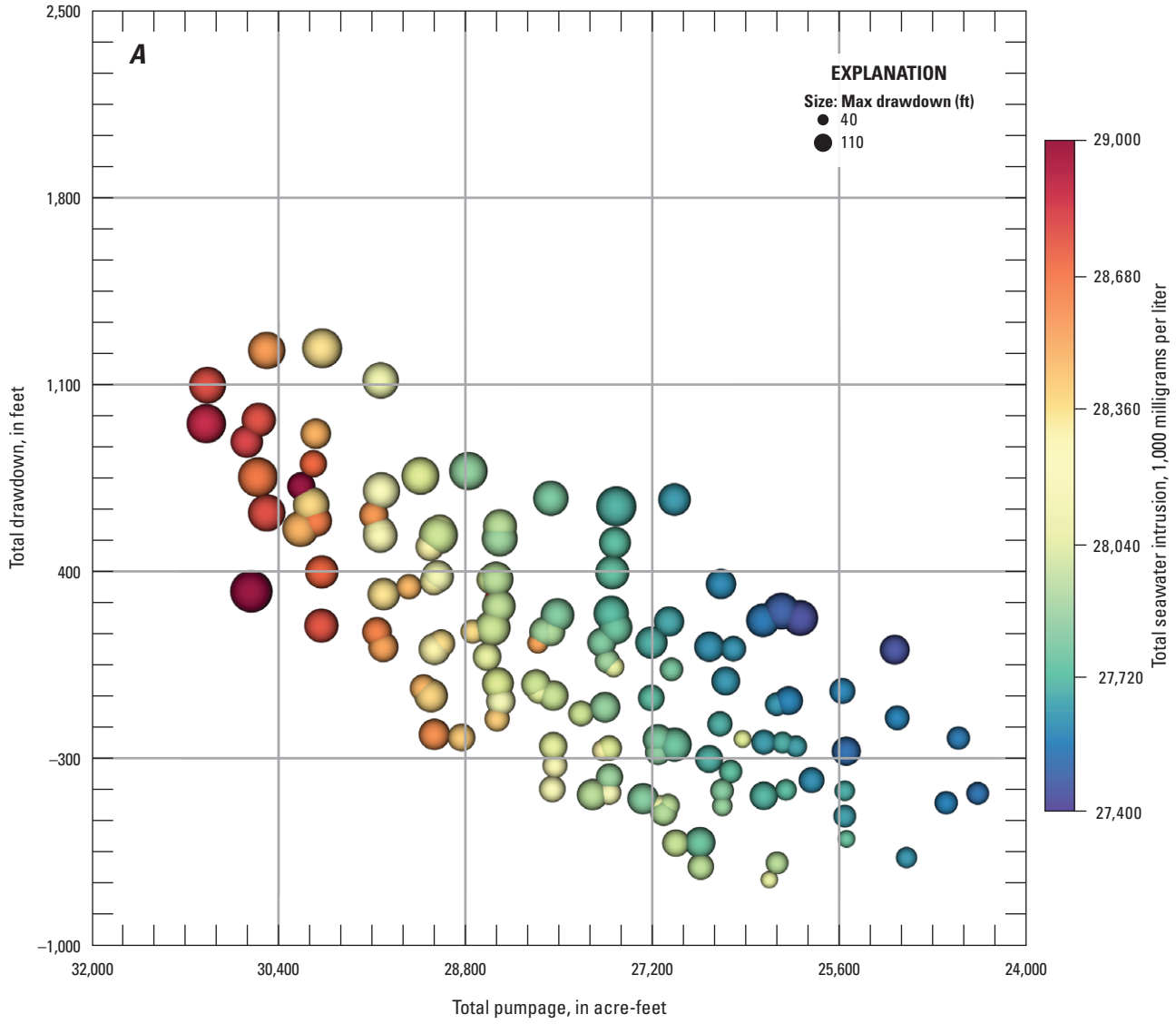

Figure 21. Subsets of Pareto-optimal solutions, Santa Barbara multi-objective management model, Santa Barbara, California, for *A*, scenario 4A, and *B*, scenario 4B.

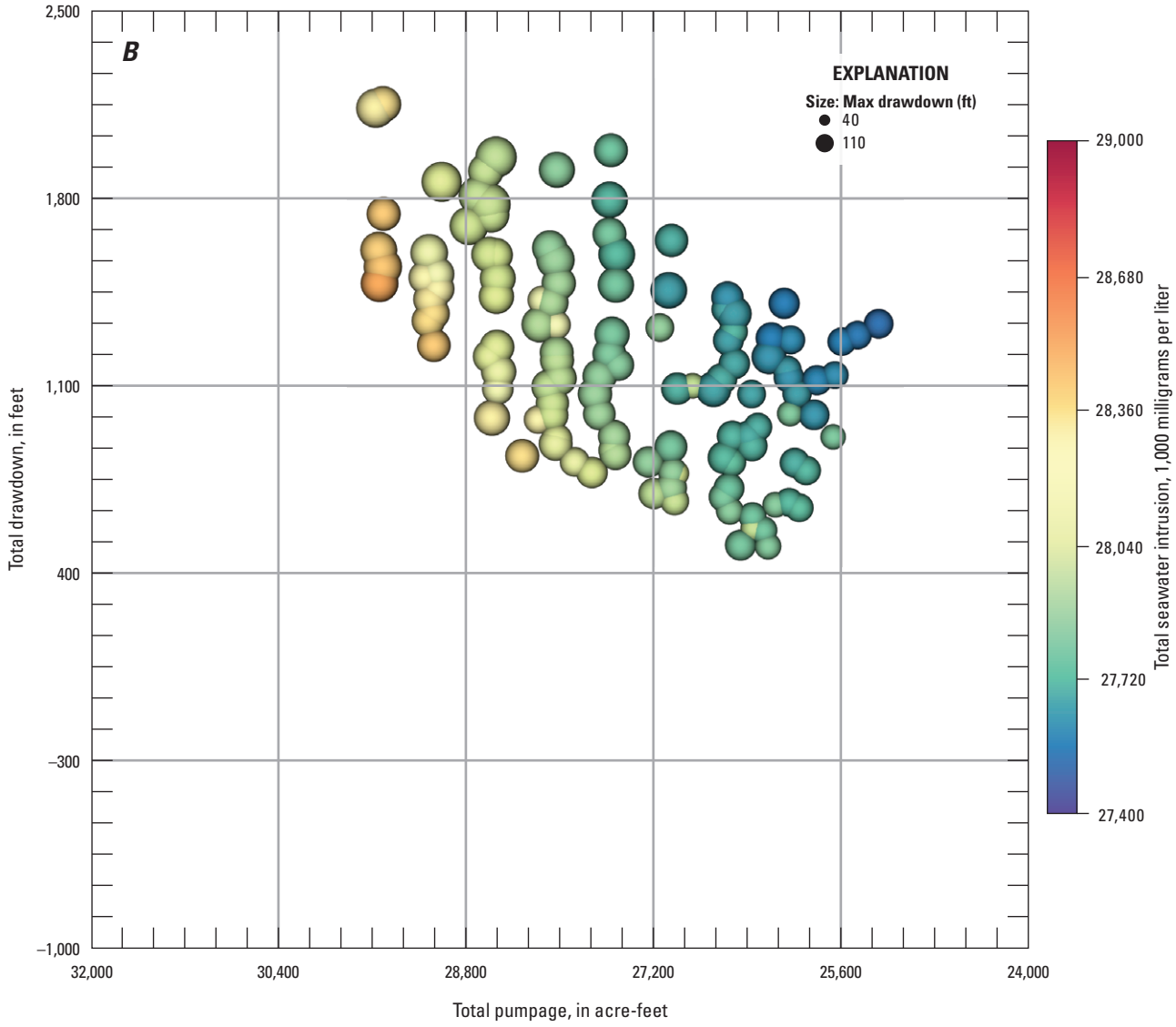

Figure 21. —Continued

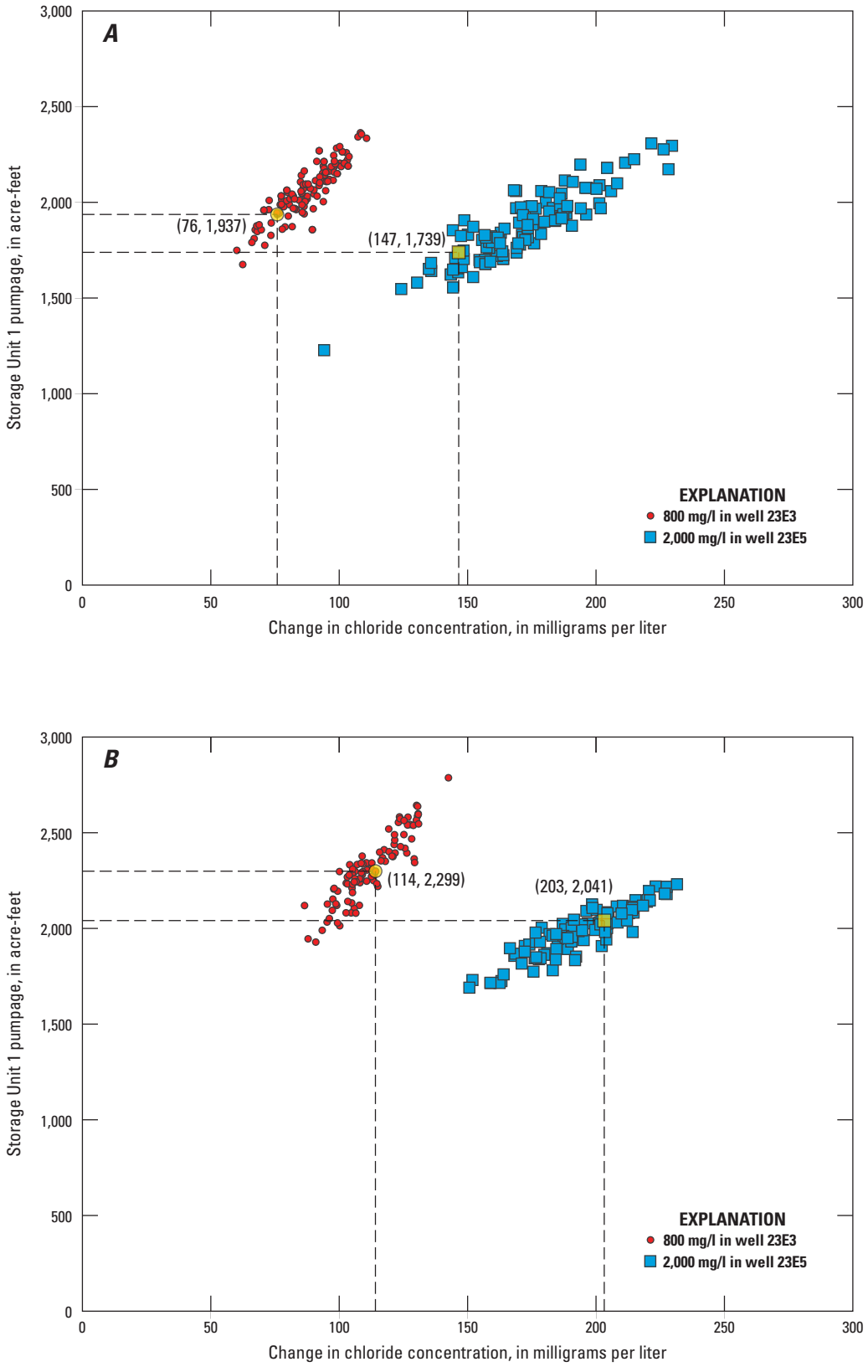

Figure 22. Example decision-rule curves for wells 4N/27W-23E3 and 4N/27W-23E5 used to assess total pumpage from Storage Unit I on the basis of observed chloride concentrations in selected monitoring wells, Santa Barbara multi-objective management model, Santa Barbara, California. The pumpage and change in chloride concentration are for the year following the measured level. *A*, scenario 1 (typical climatic condition), and *B*, scenario 2 (dry climatic condition). The highlighted dot and square represent schedules 1_D and 2_D pumpage for scenarios 1 and 2, respectively.

As an example of interpreting the decision rules, consider the decision rule for well 23E3, assuming a dry climatic condition (fig. 22*B*) and that a chloride concentration of 800 mg/L was measured in the well. Further assume that an increase of about 114 mg/L was deemed allowable for this well during the year following when the measurement was taken, then the total Pareto-optimal pumpage from Storage Unit I would be about 2,299 acre-ft. Note that the decision rule was only valid for points shown in figure 22; it would not be appropriate to interpolate between points for a given well.

An alternative approach to interpreting the decision rules is to identify a desired total pumpage and then determine the resulting change in chloride concentration. For example, again consider well 23E3, assuming a dry climatic condition (fig. 22*B*) and that a chloride concentration of 800 mg/L was measured in the well. Further assume that the city desired to pump a total of about 2,300 acre-ft in a year. Pumping 2,300 acre-ft increased chloride concentrations by about 100 mg/L to 114 mg/L (fig. 22*B*). The differences in chloride concentrations resulted from differing pumping patterns. The city could choose the pumping pattern with the least change in chloride concentration or by other criteria. For points clustered near each other, the specific pumping schedules associated with each point near the desired pumpage value would have to be inspected and compared in order to make a decision about which schedule to choose.

Scenario 4B

For this scenario, decision-rule curves were created to assess the effect of allowable drawdown in Foothill groundwater basin wells on potential management decisions. Note that decision-rule curves are not presented for Storage Unit I wells, because it was determined that seawater intrusion was a higher priority in this basin than drawdown. The decision-rule curves were generated from the 10-year simulation results using the following steps:

1. The maximum annual drawdown for each production well in Foothill groundwater basin for 10 years of pumping was stored.

2. The associated total pumpage for Storage Unit I and Foothill groundwater basin for those 10 years was stored separately.

The Los Robles well decision rules for Foothill groundwater basin pumpage under typical and dry climatic conditions are shown in figures 23*A* and 23*B*, respectively. The Los Robles well decision rules for pumpage in Storage Unit I, under typical and dry climatic conditions, are shown in figures 23*C* and 23*D*, respectively. The decision rules for all production wells in Storage Unit I and the Foothill groundwater basin are presented in appendix D–4.

As an example of interpreting the decision rules, consider the decision rule for the Los Robles well, assuming a typical climatic condition (fig. 23*A*). Further assume that a maximum drawdown of 22 ft was desired for a 10-year management horizon. The decision rule indicated that the total pumpage from the city wells in Foothill groundwater basin was about 7,461 acre-ft for the 10-year period.

Consider the total pumpage for Storage Unit I, assuming a typical climatic condition, as indicated by the decision rule for the Los Robles well (fig. 23*C*). Further assume that a maximum drawdown of 22 ft was desired during a 10-year management horizon. The decision rule indicates that the total pumpage from the city wells in Storage Unit I was about 16,203 acre-ft for the 10-year period.

Many of the decision rules for pumpage in Storage Unit I as a function of maximum, annual drawdown at wells in the Foothill groundwater basin either were very disperse (for example, the Hope Avenue, Lincolnwood 1, and San Roque Park (2) wells in appendix D–4) or were slightly nonlinear (for example, the Los Robles well). This could indicate that drawdown in the Foothill groundwater basin is not a strong function of the total pumpage for Storage Unit I, probably because Storage Unit I and Foothill groundwater basin are hydraulically disconnected by the East More Ranch fault.

Scenario 5

Scenario 5 investigated the short-term (2-year) effects of extreme climatic conditions on the optimal pumping schedules. Specifically, three cases were investigated: typical-to-dry (scenario 5A, 1998–99), dry-to-typical (scenario 5B, 1977–78), and dry-to-dry (scenario 5C, 1989–90) periods. The Pareto-optimal solutions and pumping schedules for the three scenario-5 cases are shown in figure 24 and presented in tables 5–7. Overall, the Pareto curves were similar for scenarios 5A and 5B, but shifted toward less drawdown and toward less pumpage for scenario 5C. In general, all the pumping schedules resulted in water-level recovery for all the scenarios, except for schedules $5A_A$, $5B_A$, and $5B_B$, which resulted in water-level declines. In addition, schedule $5A_B$ resulted in a water-level recovery, whereas for the other two climatic conditions, schedule B resulted in a water-level decline (scenario $5B_B$) or no change in water level (scenario $5C_B$).

The results for all three scenario-5 cases indicated that schedule A pumpage resulted in similar seawater intrusion, but large differences in drawdown; schedules B and C pumpage varied in their yield more than the other schedules for all the scenarios; and the schedule D pumpage for all the scenarios results in similarly large increases in water levels. With no regard for future availability beyond the 2-year horizon, the total pumpage for schedules A and D were similar for scenarios 5A and 5B (tables 5 and 6); however, the total schedule $5A_{Cm}$ pumpage (about 6,800 acre-ft, table 5) was nearly 1,000 acre-ft greater than the pumpage of Schedule $5B_{Cm}$ (about 5,800 acre-ft, table 6), indicating that pumpage was sensitive to the climate in year two when minimizing the maximum drawdown. Conversely, pumpage with respect to total drawdowns appeared more sensitive to the climate in year one, because the yield for schedules $5B_{Ct}$ and $5C_{Ct}$ (year one was dry) were similar and that of schedule $5A_{Ct}$ was larger. When minimizing seawater intrusion, pumpage was largest in scenario $5C_B$ (5,900 acre-ft; table 7) and smallest in scenario $5A_B$ (5,000 acre-ft; table 5).

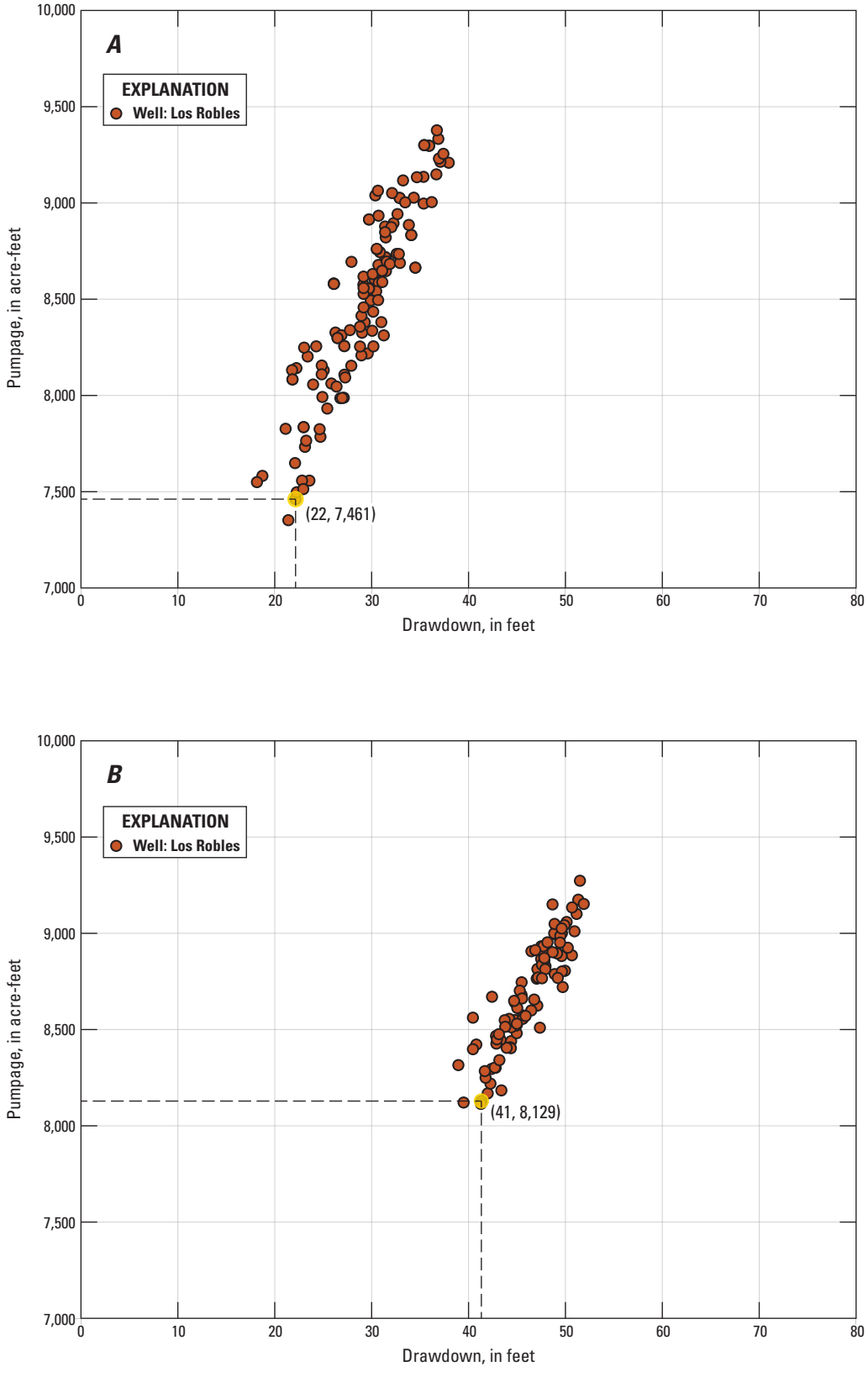

Figure 23. Example decision-rule curves for the Los Robles well, Santa Barbara multi-objective management model, Santa Barbara, California, for *A*, total 10-year pumpage Foothill groundwater basin scenario 1; *B*, total 10-year pumpage Foothill groundwater basin scenario 2; *C*, for total 10-year pumpage Storage Unit I scenario 1; and *D*, for total 10-year pumpage, Storage Unit I scenario 2.

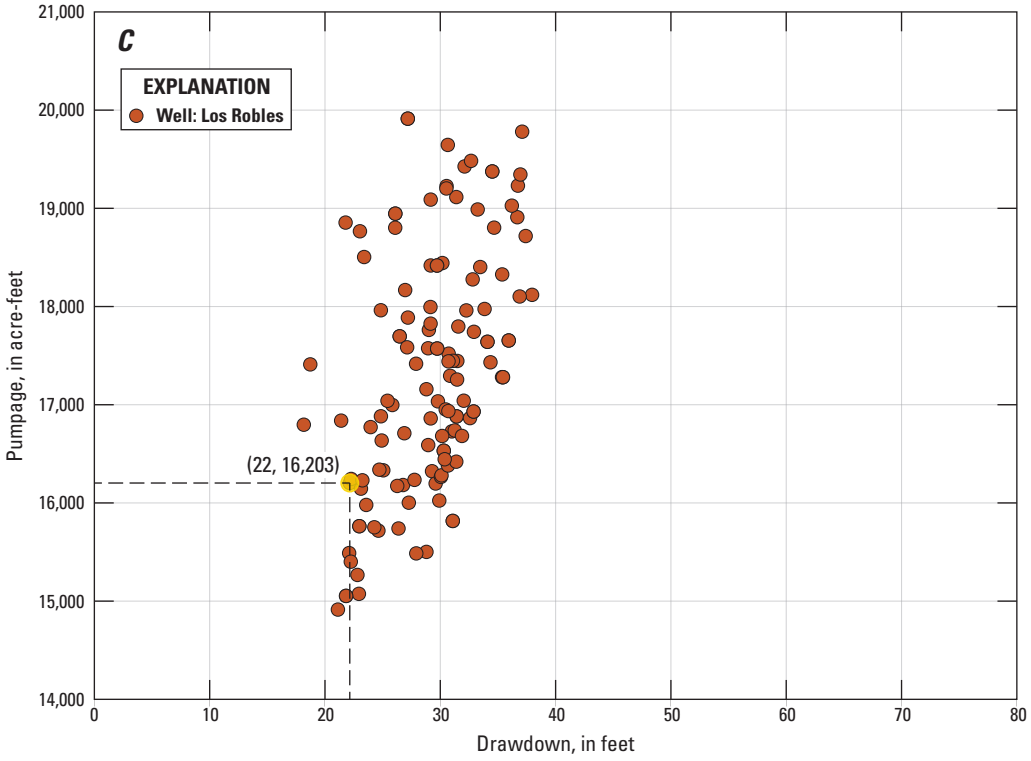

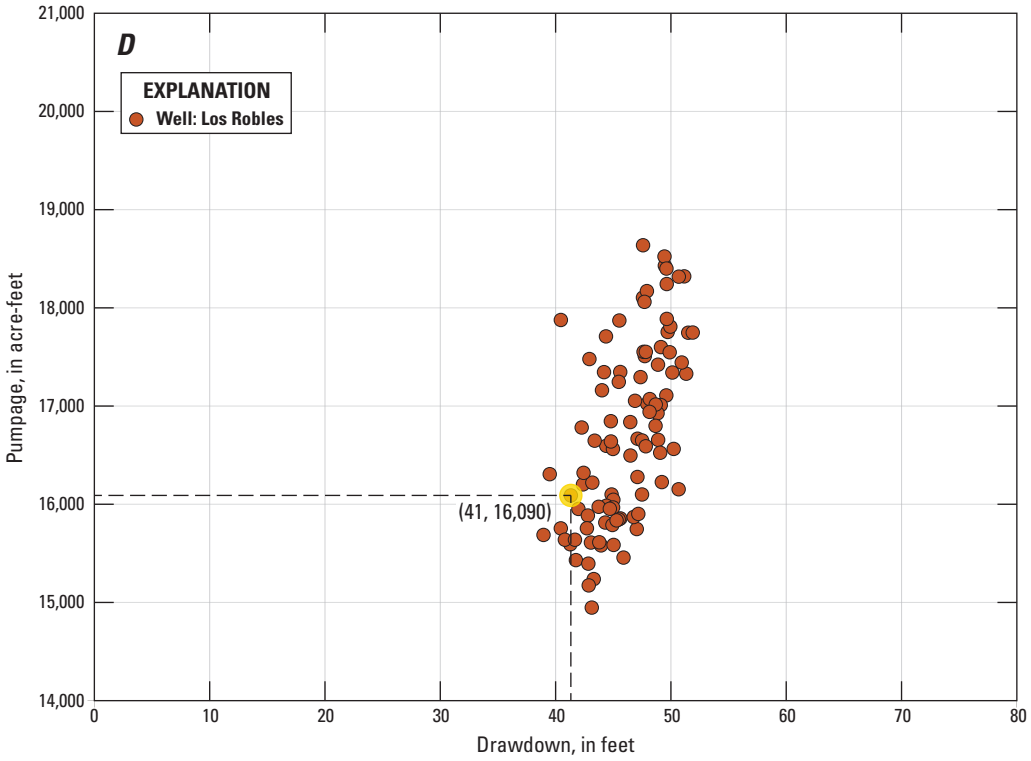

Figure 23. —Continued

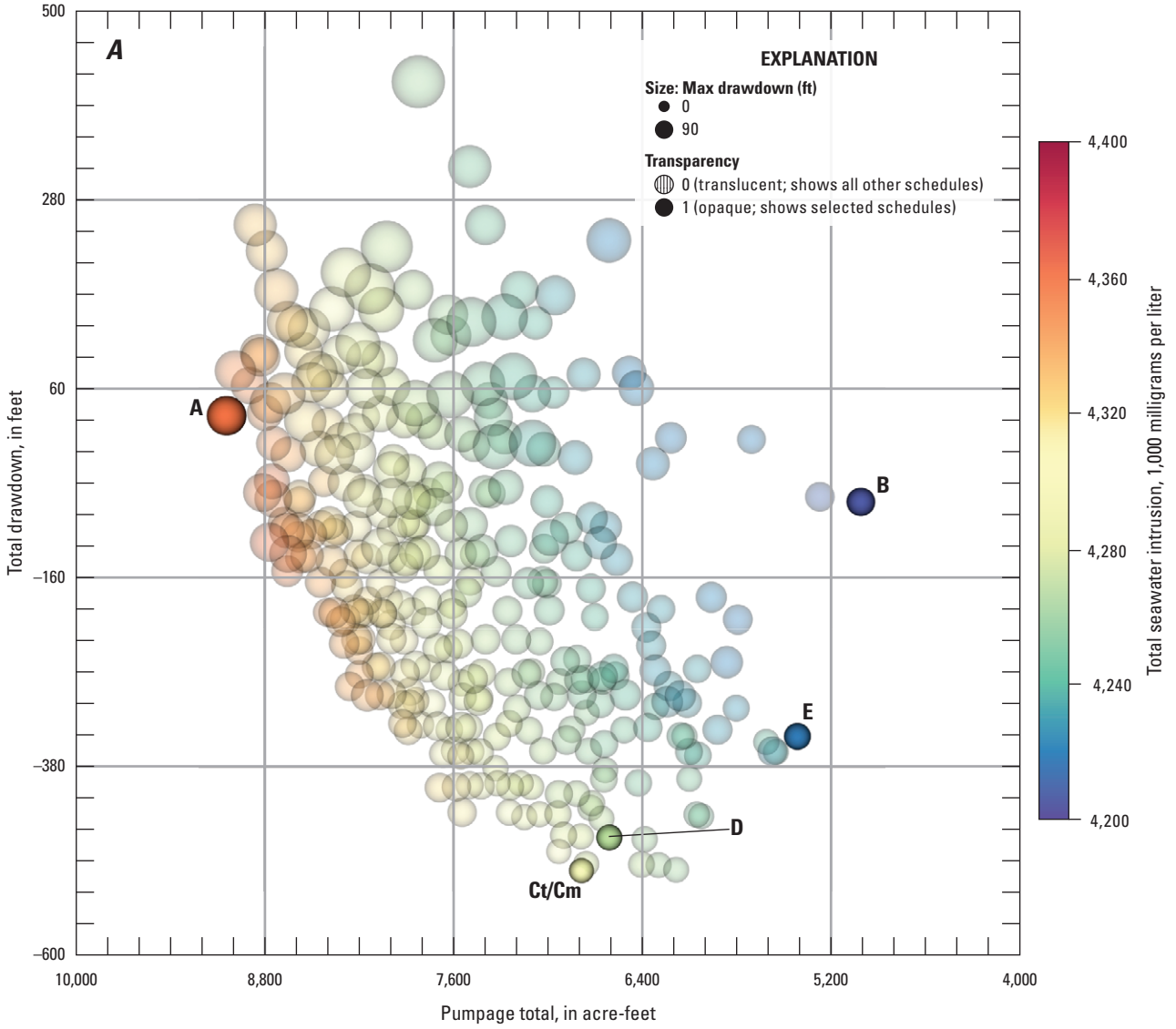

Figure 24. Selected Pareto-optimal solutions relative to seawater intrusion, maximum drawdown, total pumpage, and total drawdown, Santa Barbara multi-objective management model, Santa Barbara, California, for *A*, scenario 5A (typical-dry); *B*, scenario 5B (dry-typical); and *C*, scenario 5C (dry-dry).

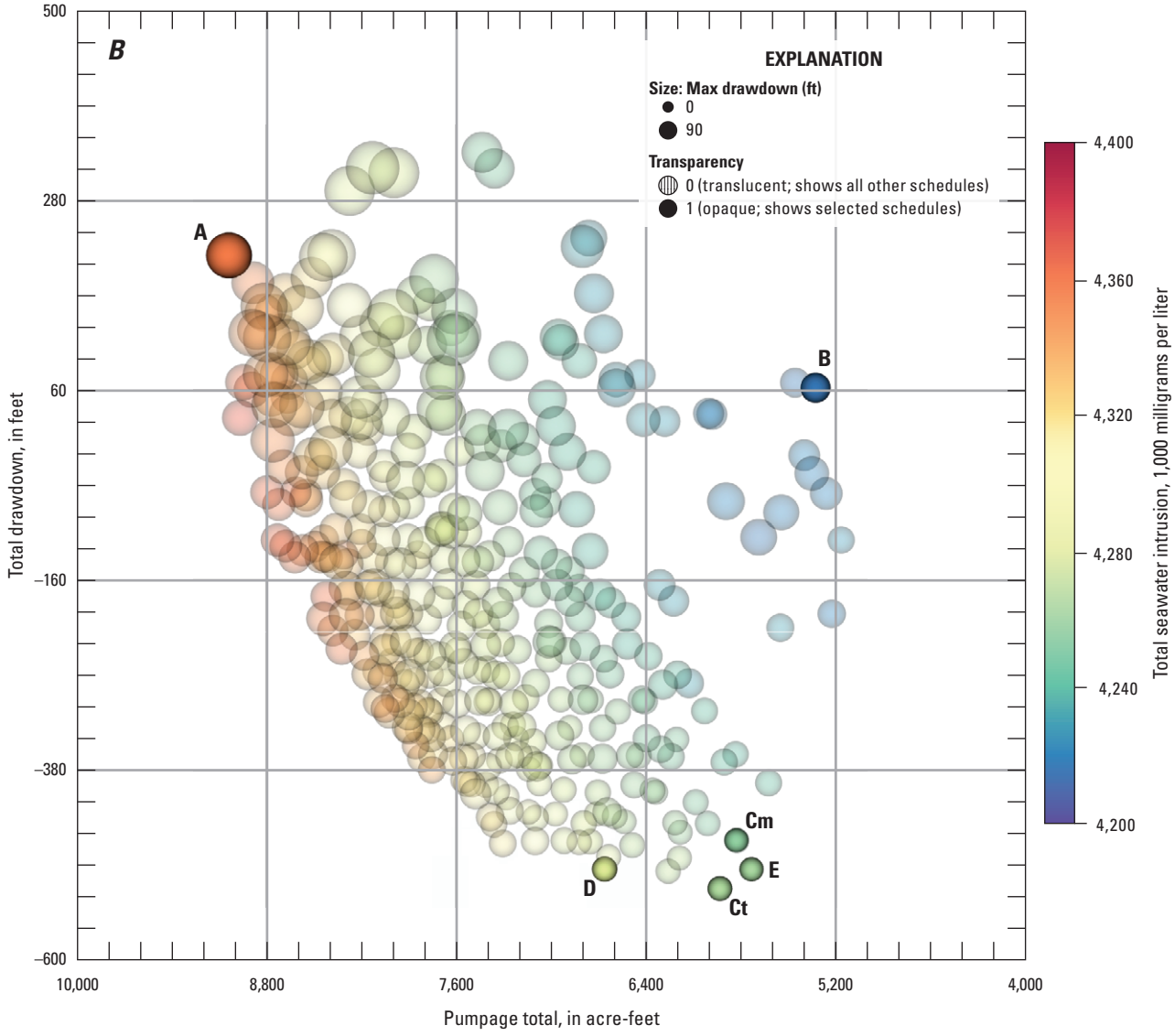

Figure 24. —Continued

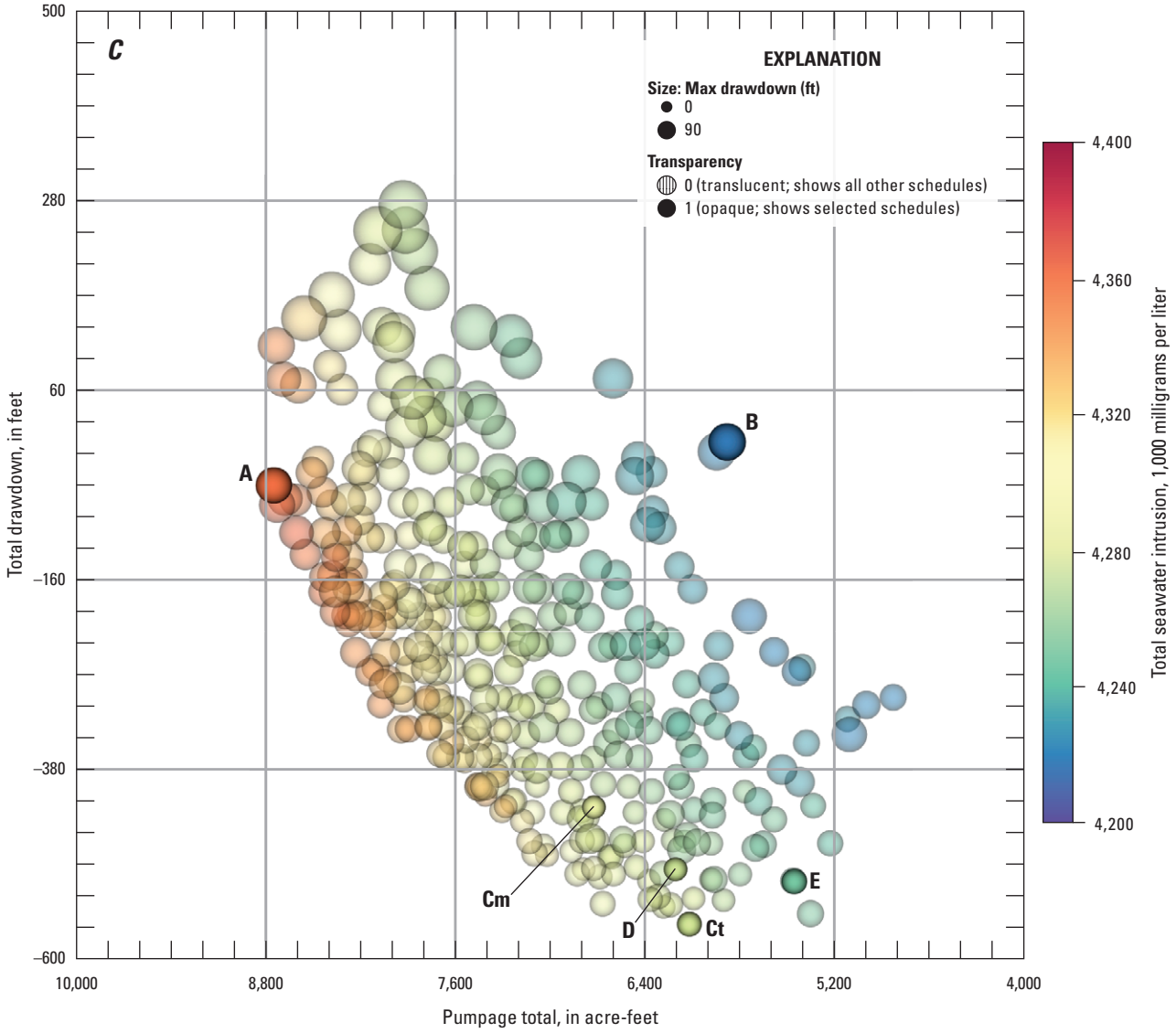

Figure 24. —Continued

Table 5. Objective values for scenario 5A, Santa Barbara multi-objective management model, Santa Barbara, California.

[acre-ft, acre-feet; ft, feet; mg/L, milligrams per liter]

Schedule	Objective A total pumpage (acre-ft)	Objective B seawater intrusion (1,000 mg/L)	Objective Ct total drawdown (ft)	Objective Cm maximum drawdown (ft)
$5A_A$	9,000	4,357	30	47
$5A_B$	5,000	4,205	–70	19
$5A_{Ct}$	6,800	4,299	–500	10
$5A_{Cm}$	6,800	4,299	–500	10
$5A_D$	6,600	4,266	–460	12
$5A_E$	5,400	4,216	–340	14

Table 6. Objective values for scenario 5B, Santa Barbara multi-objective management model, Santa Barbara, California.

[acre-ft, acre-feet; ft, feet; mg/L, milligrams per liter]

Schedule	Objective A total pumpage (acre-ft)	Objective B seawater intrusion (1,000 mg/L)	Objective Ct total drawdown (ft)	Objective Cm maximum drawdown (ft)
$5B_A$	9,000	4,355	220	62
$5B_B$	5,300	4,214	60	22
$5B_{Ct}$	5,900	4,263	–520	9
$5B_{Cm}$	5,800	4,254	–460	7
$5B_D$	6,700	4,279	–490	10
$5B_E$	5,700	4,260	–490	7

Table 7. Objective values for scenario 5C, Santa Barbara multi-objective management model, Santa Barbara, California.

[acre-ft, acre-feet; ft, feet; mg/L, milligrams per liter]

Schedule	Objective A total pumpage (acre-ft)	Objective B seawater intrusion (1,000 mg/L)	Objective Ct total drawdown (ft)	Objective Cm maximum drawdown (ft)
$5C_A$	8,700	4,358	–50	38
$5C_B$	5,900	4,215	0	41
$5C_{Ct}$	6,100	4,275	–560	9
$5C_{Cm}$	6,700	4,289	–420	6
$5C_D$	6,200	4,273	–490	6
$5C_E$	5,500	4,246	–510	11

For comparison among the three scenario-5 cases, schedule D, the best compromise among all four objectives, was selected from each case. The contours of simulated hydraulic heads for year two for the three cases are shown in figures 25–27 for the upper, middle, and lower producing zones, respectively (figure parts *A*–*C*). In general, the simulated contours for each producing zone were similar in form for scenarios 5A–C, with the lowest water levels for all producing zones in Storage Unit I (figs. 25–27). The simulated hydraulic heads in Storage Unit I, however, were slightly lower for scenario 5B than for scenarios 5A and 5C. The differences were most obvious in the upper producing zone (figs. 25*A*, 26*A*, and 27*A*) of Storage Unit I and the lower producing zone of the Foothill groundwater basin.

The contours of simulated chloride concentrations at the end of year two for the three cases are shown in figure 28 for the middle and lower aquifers. The distribution of chloride was similar among the scenarios; however, the seawater intruded slightly farther inland for scenario 5B than for scenarios 5A and 5C.

The total quarterly pumpage by storage unit for schedules A (maximize pumping) and B (minimize seawater intrusion) of scenario 5 is presented in figure 29. In general, when maximizing the pumpage, a greater percentage of the total pumpage was extracted from Storage Unit I. However, when minimizing seawater intrusion, a greater percentage of the total pumpage was sometimes from the Foothill groundwater basin in quarters 2, 3, and 4 (see, for example, quarter 3 and 4 in fig. 29*A*).

For scenario 5, the SOS illustrated different tradeoff dynamics depending on the climatic condition. Figure 30 shows the SOS for the six pumping schedules of scenarios 5A–C. The tradeoff dynamics for schedule D were similar for all three climatic conditions ($5A_D$, $5B_D$, and $5C_D$). Schedule E shows the relative tradeoff in pumpage for each climatic condition when prioritizing the three environmental objectives compared to an equal preference for minimizing all objectives in schedule D.

For scenario 5A (typical-to-dry), the extreme solutions for maximizing pumpage and minimizing seawater intrusion showed substantial tradeoffs: the best score for objective A ($5A_A$) resulted in the worst score for objective B, and the best score for objective B ($5A_B$) resulted in the worst score for objective A, indicating that maximizing pumpage resulted in maximum seawater intrusion, and minimal seawater intrusion resulted in minimal pumpage (fig. 30*A*). The solution for minimizing total drawdown, schedule $5A_{Ct}$ was the same as $5A_{Cm}$ for this climatic condition, indicating that the solution that resulted in the minimal total drawdown also resulted in the minimal maximum drawdown (fig. 30*A*). Comparing the compromise solutions ($5A_D$ and $5A_E$) showed that the objective B score for schedule $5A_E$ increased as its objective A, C_t, and C_m scores decreased, indicating that to improve the seawater-intrusion results from schedule D, one must accept slightly worse drawdown results.

In scenario 5B (dry-to-typical), the maximum pumpage solution (schedule $5B_A$) had scores below 0.3 for all other objectives; however, none were zero, indicating that there were worse solutions for each objective that also resulted in less pumpage (fig. 30*B*). Similarly, the minimal seawater-intrusion solution (schedule $5B_B$) did not result in the least pumpage, although the score was less than 0.1. Both solutions for the drawdown objectives ($5B_{Ct}$ and $5B_{Cm}$, fig. 30*B*) showed a larger tradeoff for objective A (scores below 0.2) than objective B (scores between 0.6 and 0.8). To achieve the minimal total drawdown (schedule $5B_{Ct}$), there was a slightly larger tradeoff in objective B and a slightly smaller tradeoff in objective A compared to the minimum maximum drawdown (schedule $5B_{Cm}$), indicating that the solution that minimized the maximum drawdown resulted in less seawater intrusion and less pumpage than schedule $5B_{Ct}$. The compromise solutions (schedules $5B_D$ and $5B_E$) resulted in scores greater than 0.9 for the drawdown objectives with scores less than 0.7 for objective B and less than 0.4 for objective A. Between schedules $5B_D$ and $5B_E$, a small tradeoff in maximum drawdown resulted in more pumpage, but more seawater intrusion as well.

For the extreme solutions in the dry-to-dry climate of scenario 5C, schedule $5C_A$ had a score near zero for objective B, yet the minimum seawater-intrusion solution (schedule $5C_B$) had a score greater than 0.2 for objective A (fig. 30*C*). These scores indicated that there were few solutions that maximized pumpage that resulted in more seawater intrusion (schedule $5C_A$), whereas there were relatively more solutions that increased seawater intrusion, but had less pumpage (schedule $5C_B$). For the drawdown objectives, the results indicated that Schedule $5C_{Cm}$ allowed more pumpage than schedule $5C_{Ct}$, but with more seawater intrusion and total drawdown. For the compromise solutions (schedules $5C_D$ and $5C_E$), the results indicated that schedule $5C_E$ allowed less seawater intrusion than schedule $5C_D$ with less pumpage, slightly less total drawdown, and a slightly greater maximum drawdown.

The simulated breakthrough curves for scenarios 5A–C, assuming schedule-D pumpage, are shown in figure 31. Much like the results presented in tables 5–7, the flat breakthrough curves indicated that the chloride concentrations were fairly insensitive to pumping schedule, except for well 23E5, which had the largest increase in concentration (fig. 31). The increase in simulated chloride concentrations in well 23E5 for schedule $5B_D$ (fig. 31*B*) reflected the greater total pumpage for that scenario than for schedules $5A_D$ and $5C_D$ (tables 5–7). The chloride breakthroughs for scenario 5B (fig. 31*B*) were noticeably different than the other two climatic conditions in the second year, where typical precipitation was simulated.

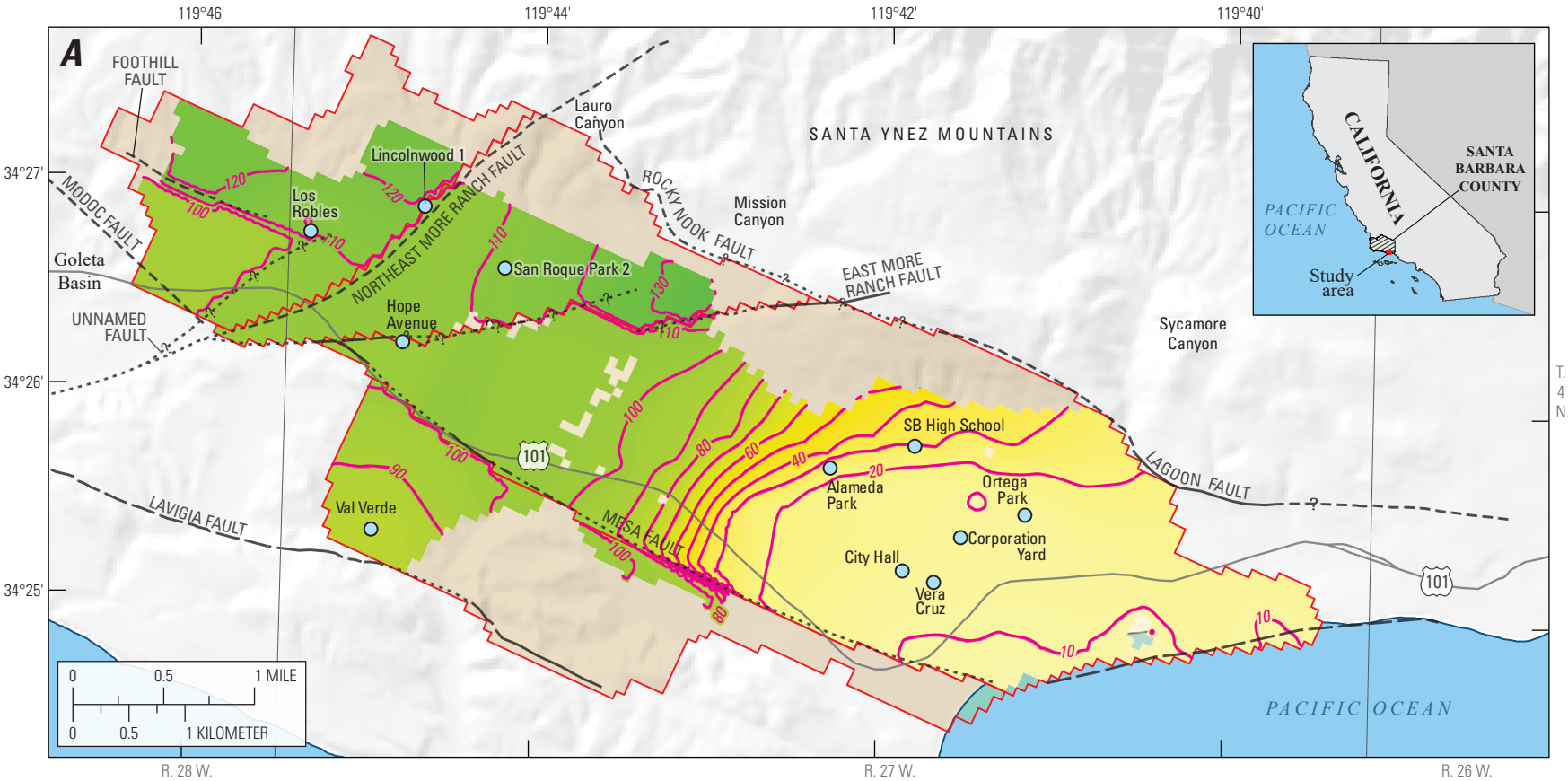

Base modified from U.S. Geological Survey and other Federal and State digital data, various scales; Transverse Mercator projection, zone 11N; North American Datum of 1983 (NAD 83)

Storage units from Muir, 1968; Freckleton and others, 1998; faults from Muir, 1968; Minor and others, 2009

EXPLANATION

Faults

- Existence certain, location inferred
- Existence questionable, location inferred
- Existence certain, location concealed
- Existence questionable, location concealed
- Existence certain, location accurate
- Existence certain, location approximate

Storage units

Simulated hydraulic head contours, in feet above North American Vertical Datum of 1988 (NAVD 88)

Highway

Vera Cruz — **Santa Barbara city production well and identifier**

Simulated hydraulic head, in feet above NAVD 88

High 248 200 150 100 50 0 Low

Figure 25. Contours of simulated hydraulic heads for year two, Santa Barbara multi-objective management model, Santa Barbara, California, for pumping schedule $5A_D$: *A*, upper producing zone; *B*, middle producing zone; and *C*, lower producing zone.

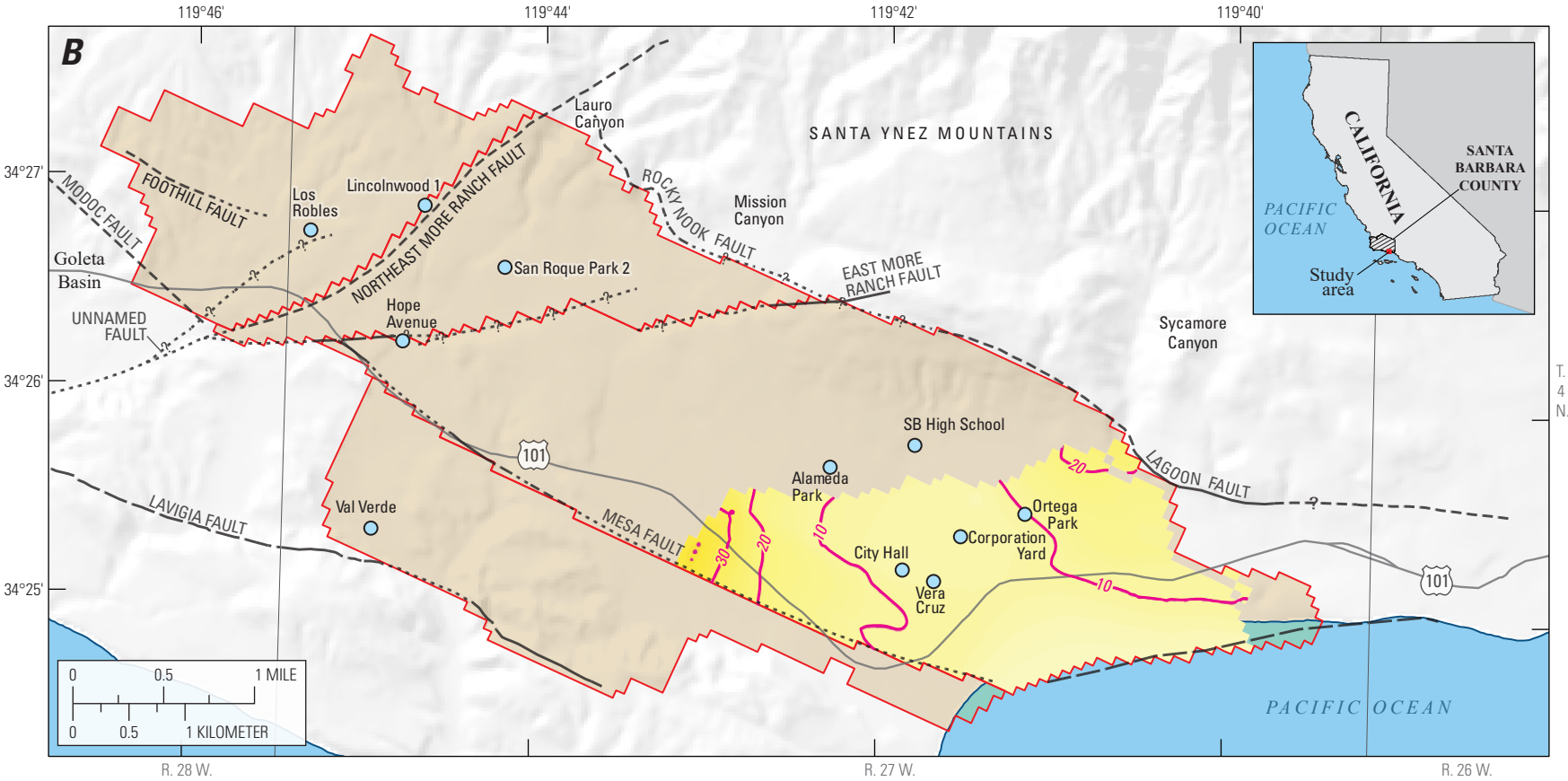

Base modified from U.S. Geological Survey and other Federal and State digital data, various scales; Transverse Mercator projection, zone 11N; North American Datum of 1983 (NAD 83)

Storage units from Muir, 1968; Freckleton and others, 1998; faults from Muir, 1968; Minor and others, 2009

Faults

- Existence certain, location inferred
- Existence questionable, location inferred
- Existence certain, location concealed
- Existence questionable, location concealed
- Existence certain, location accurate
- Existence certain, location approximate

EXPLANATION

- Storage units
- 20 — Simulated hydraulic head contours, in feet above North American Vertical Datum of 1988 (NAVD 88)
- Highway
- Vera Cruz — Santa Barbara city production well and identifier

Simulated hydraulic head, in feet above NAVD 88

High 248, 200, 150, 100, 50, 0 Low

Figure 25. —Continued

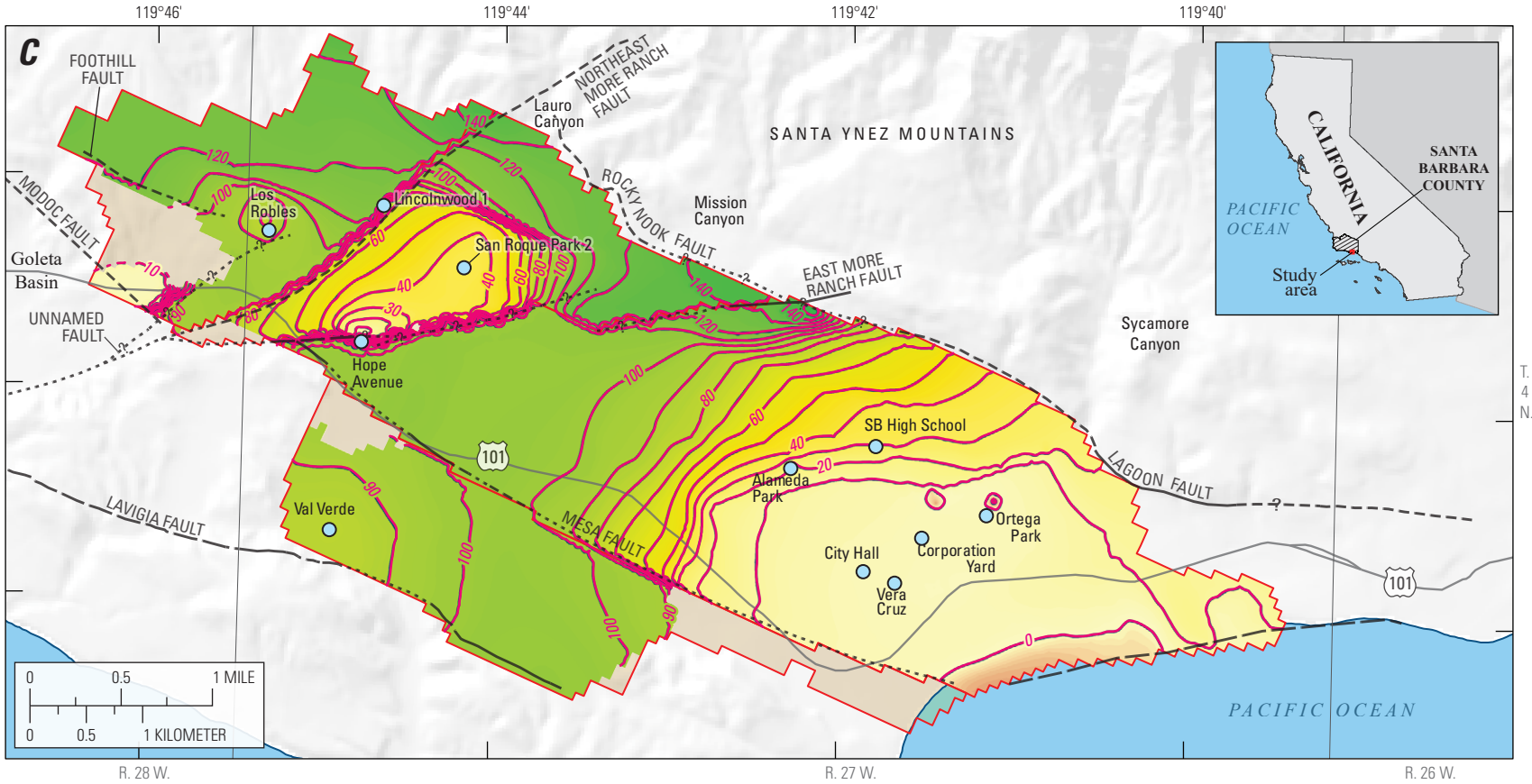

Base modified from U.S. Geological Survey and other Federal and State digital data, various scales; Transverse Mercator projection, zone 11N; North American Datum of 1983 (NAD 83)

Storage units from Muir, 1968; Freckleton and others, 1998; faults from Muir, 1968; Minor and others, 2009

Faults

- Existence certain, location inferred
- Existence questionable, location inferred
- Existence certain, location concealed
- Existence questionable, location concealed
- Existence certain, location accurate
- Existence certain, location approximate

EXPLANATION

- **Storage units**
- **Simulated hydraulic head contours, in feet above North American Vertical Datum of 1988 (NAVD 88)**
- **Highway**
- Vera Cruz — **Santa Barbara city production well and identifier**

Simulated hydraulic head, in feet above NAVD 88

High 248, 200, 150, 100, 50, 0 Low

Figure 25. —Continued

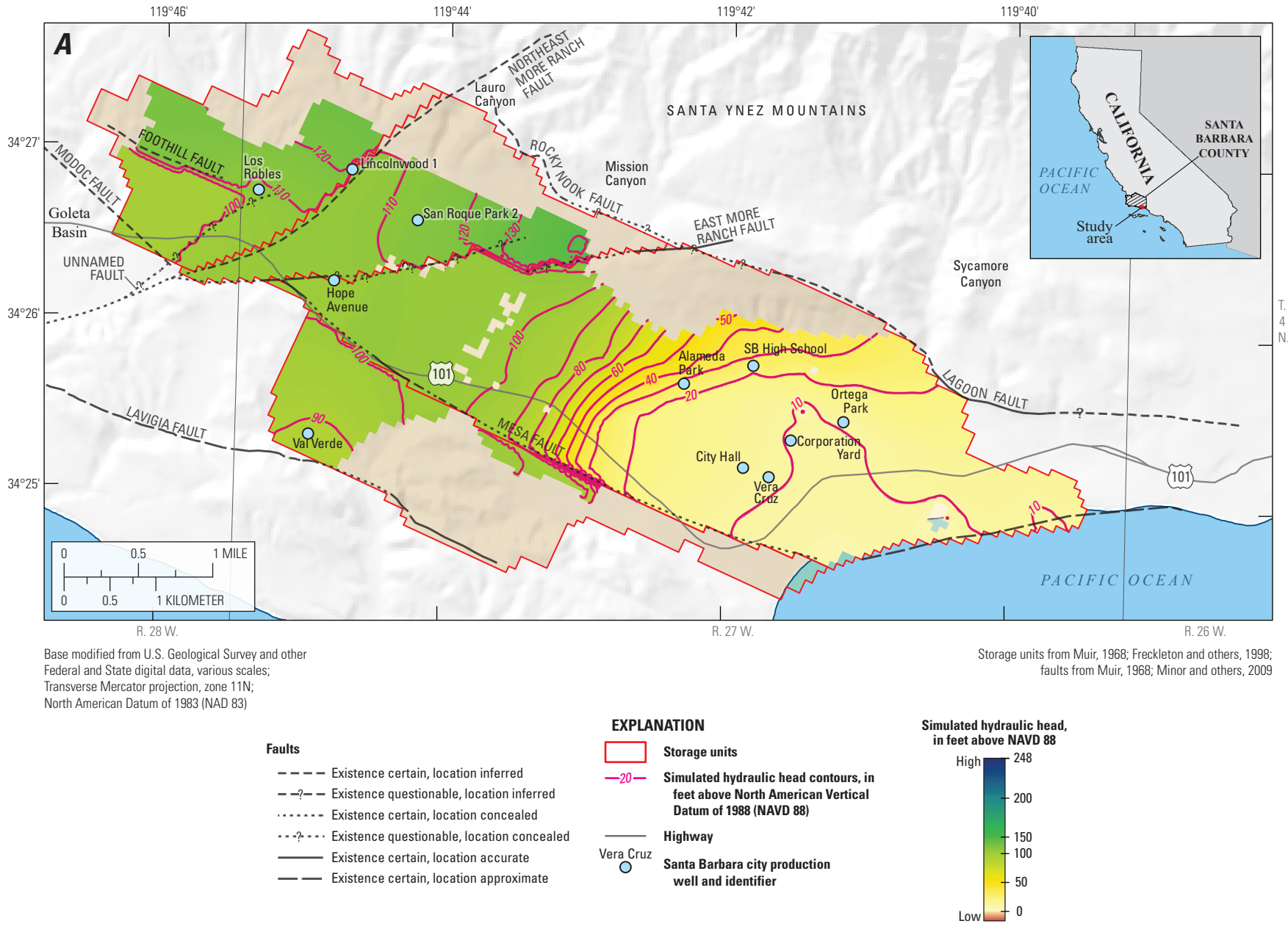

Figure 26. Contours of simulated hydraulic heads for year two, Santa Barbara multi-objective management model, Santa Barbara, California, for pumping schedule $5B_D$: *A*, upper producing zone; *B*, middle producing zone; and *C*, lower producing zone.

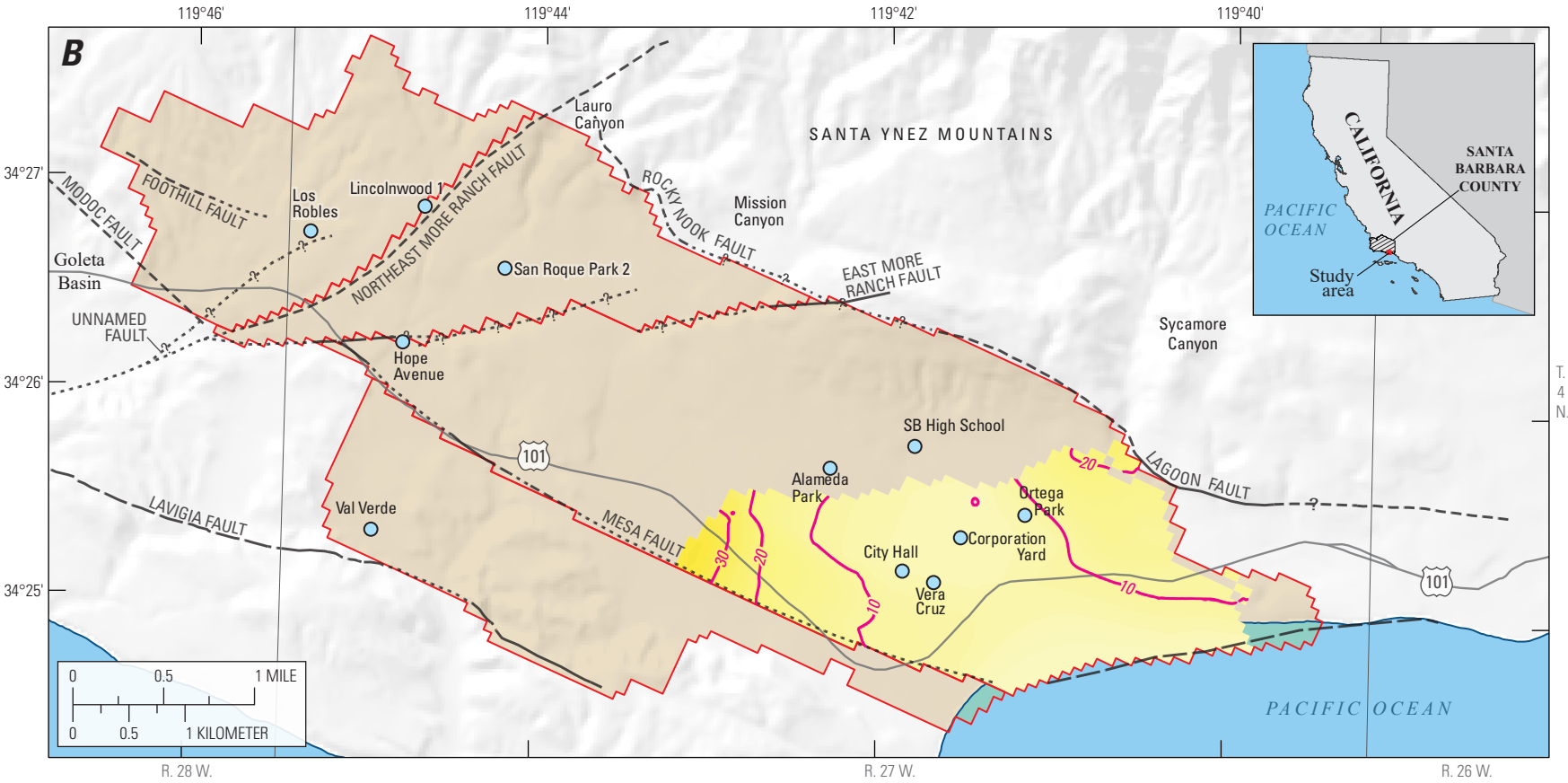

Base modified from U.S. Geological Survey and other Federal and State digital data, various scales; Transverse Mercator projection, zone 11N; North American Datum of 1983 (NAD 83)

Storage units from Muir, 1968; Freckleton and others, 1998; faults from Muir, 1968; Minor and others, 2009

Faults

- Existence certain, location inferred
- Existence questionable, location inferred
- Existence certain, location concealed
- Existence questionable, location concealed
- Existence certain, location accurate
- Existence certain, location approximate

EXPLANATION

- Storage units
- 20 — Simulated hydraulic head contours, in feet above North American Vertical Datum of 1988 (NAVD 88)
- Highway
- Vera Cruz — Santa Barbara city production well and identifier

Simulated hydraulic head, in feet above NAVD 88

High 248, 200, 150, 100, 50, 0 Low

Figure 26. —Continued

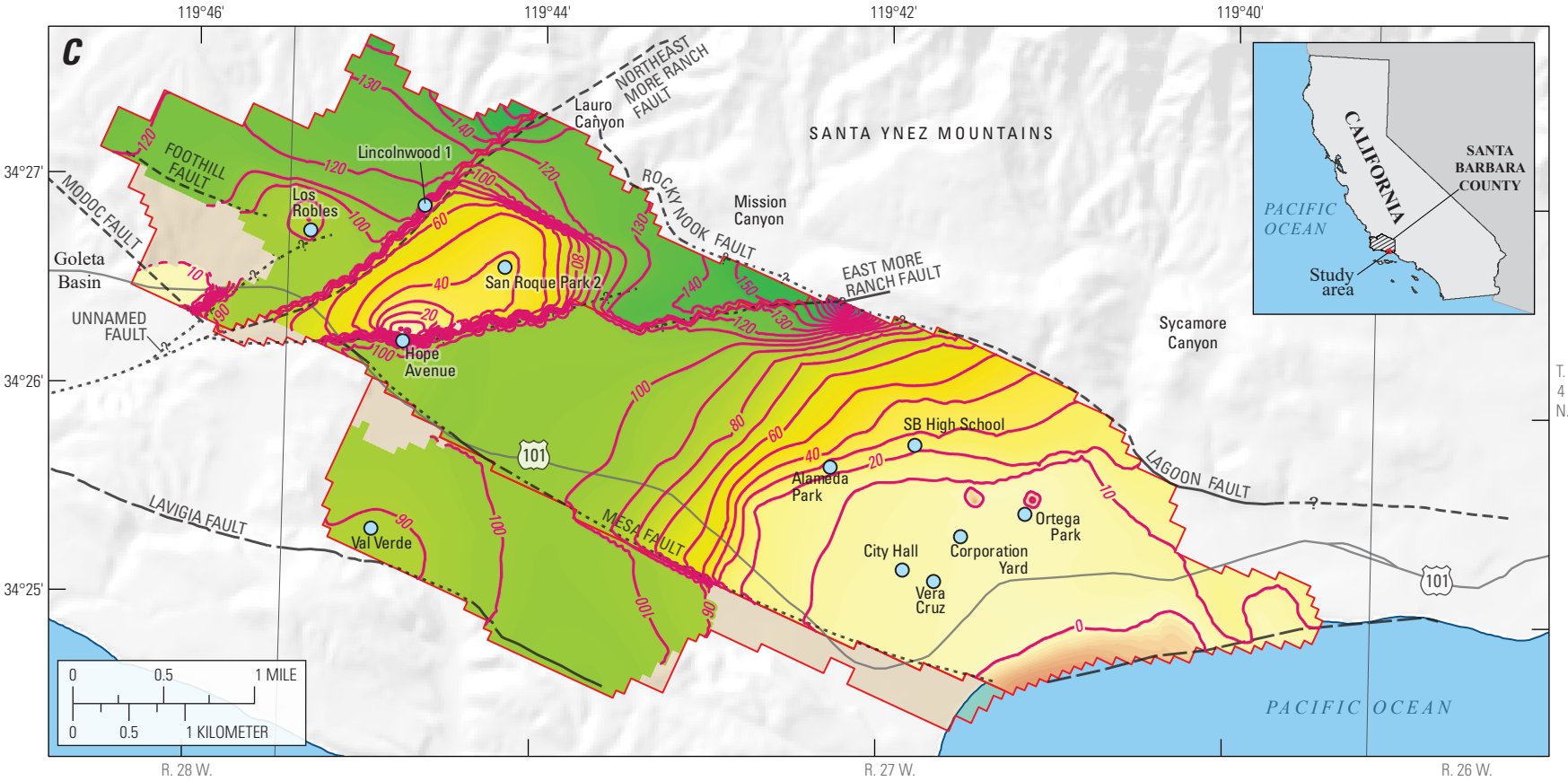

Base modified from U.S. Geological Survey and other Federal and State digital data, various scales; Transverse Mercator projection, zone 11N; North American Datum of 1983 (NAD 83)

Storage units from Muir, 1968; Freckleton and others, 1998; faults from Muir, 1968; Minor and others, 2009

Faults

- Existence certain, location inferred
- Existence questionable, location inferred
- Existence certain, location concealed
- Existence questionable, location concealed
- Existence certain, location accurate
- Existence certain, location approximate

EXPLANATION

- Storage units
- 20 — Simulated hydraulic head contours, in feet above North American Vertical Datum of 1988 (NAVD 88)
- Highway
- Vera Cruz — Santa Barbara city production well and identifier

Simulated hydraulic head, in feet above NAVD 88

High 248, 200, 150, 100, 50, 0 Low

Figure 26. —Continued

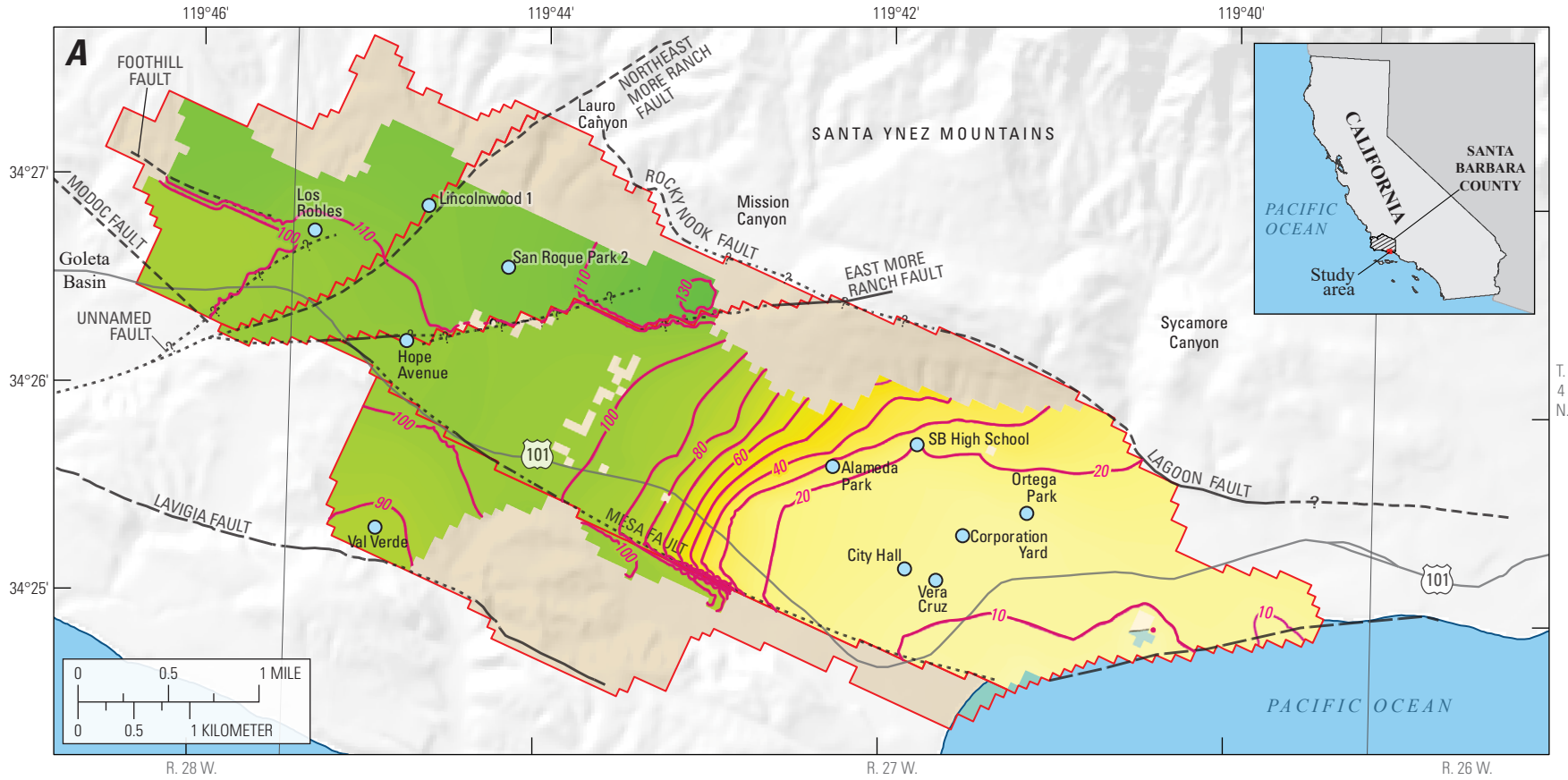

Base modified from U.S. Geological Survey and other Federal and State digital data, various scales; Transverse Mercator projection, zone 11N; North American Datum of 1983 (NAD 83)

Storage units from Muir, 1968; Freckleton and others, 1998; faults from Muir, 1968; Minor and others, 2009

EXPLANATION

Faults

- Existence certain, location inferred
- Existence questionable, location inferred
- Existence certain, location concealed
- Existence questionable, location concealed
- Existence certain, location accurate
- Existence certain, location approximate

Storage units

Simulated hydraulic head contours, in feet above North American Vertical Datum of 1988 (NAVD 88)

Highway

Vera Cruz — **Santa Barbara city production well and identifier**

Simulated hydraulic head, in feet above NAVD 88

High 248 200 150 100 50 0 Low

Figure 27. Contours of simulated hydraulic heads for year two, Santa Barbara multi-objective management model, Santa Barbara, California, for pumping schedule $5C_D$: *A*, upper producing zone; *B*, middle producing zone; and *C*, lower producing zone.

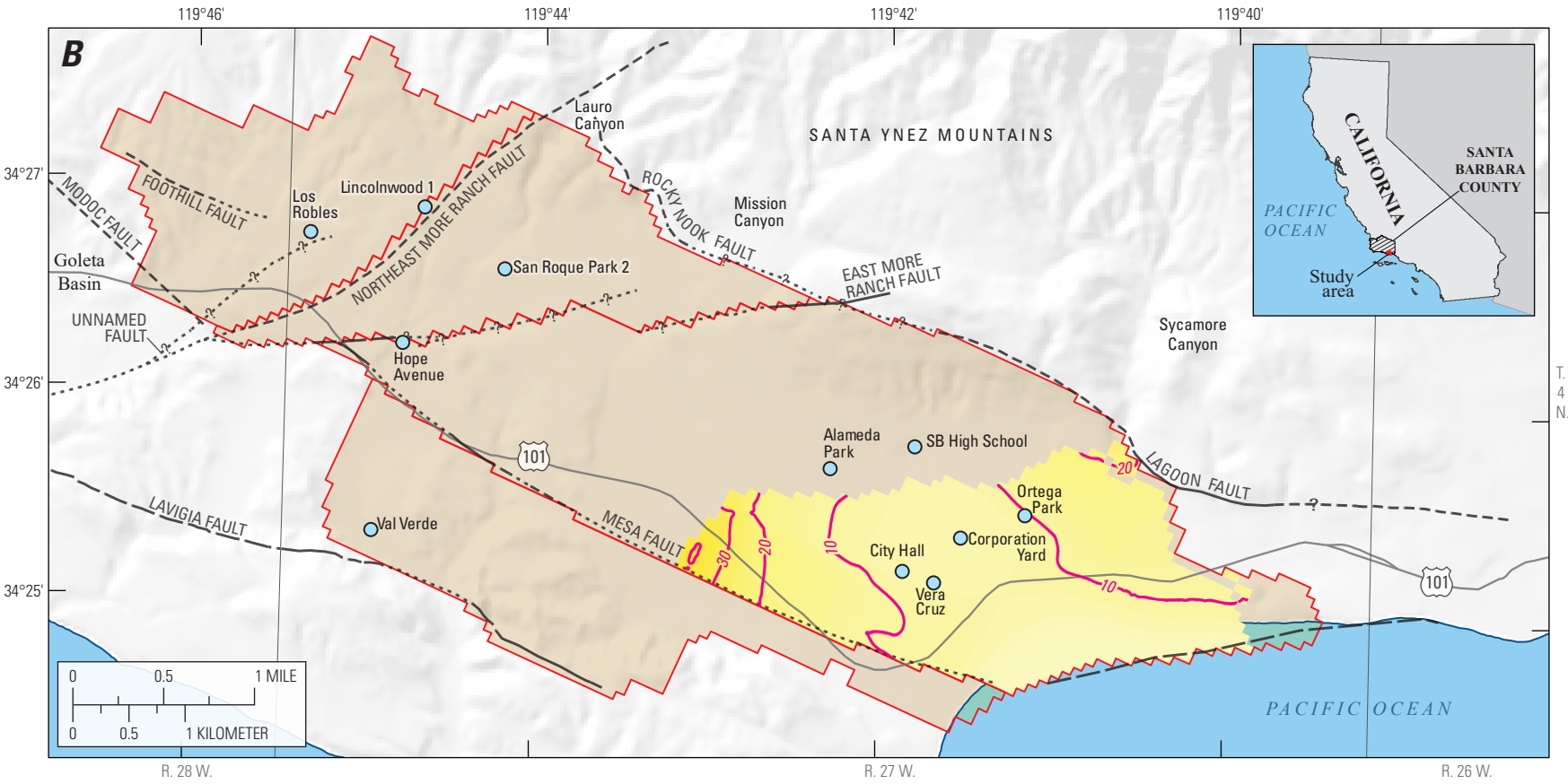

Base modified from U.S. Geological Survey and other Federal and State digital data, various scales; Transverse Mercator projection, zone 11N; North American Datum of 1983 (NAD 83)

Storage units from Muir, 1968; Freckleton and others, 1998; faults from Muir, 1968; Minor and others, 2009

Faults

- Existence certain, location inferred
- Existence questionable, location inferred
- Existence certain, location concealed
- Existence questionable, location concealed
- Existence certain, location accurate
- Existence certain, location approximate

EXPLANATION

- Storage units
- 20 — Simulated hydraulic head contours, in feet above North American Vertical Datum of 1988 (NAVD 88)
- Highway
- Vera Cruz — Santa Barbara city production well and identifier

Simulated hydraulic head, in feet above NAVD 88

High 248, 200, 150, 100, 50, 0 Low

Figure 27. —Continued

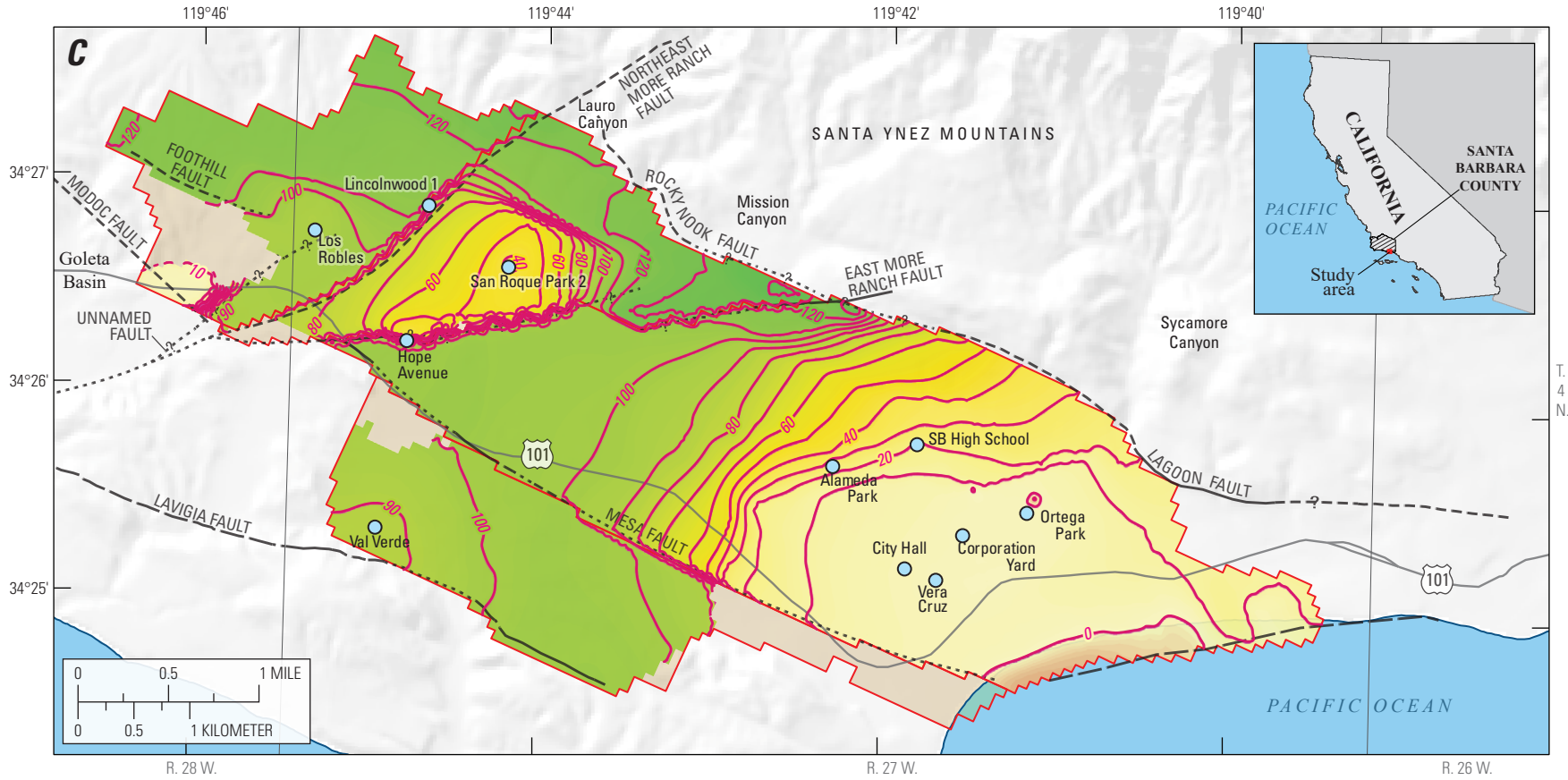

Base modified from U.S. Geological Survey and other Federal and State digital data, various scales; Transverse Mercator projection, zone 11N; North American Datum of 1983 (NAD 83)

Storage units from Muir, 1968; Freckleton and others, 1998; faults from Muir, 1968; Minor and others, 2009

Faults

- Existence certain, location inferred
- Existence questionable, location inferred
- Existence certain, location concealed
- Existence questionable, location concealed
- Existence certain, location accurate
- Existence certain, location approximate

EXPLANATION

- **Storage units**
- **Simulated hydraulic head contours, in feet above North American Vertical Datum of 1988 (NAVD 88)**
- **Highway**
- Vera Cruz — **Santa Barbara city production well and identifier**

Simulated hydraulic head, in feet above NAVD 88

High 248 200 150 100 50 0 Low

Figure 27. —Continued

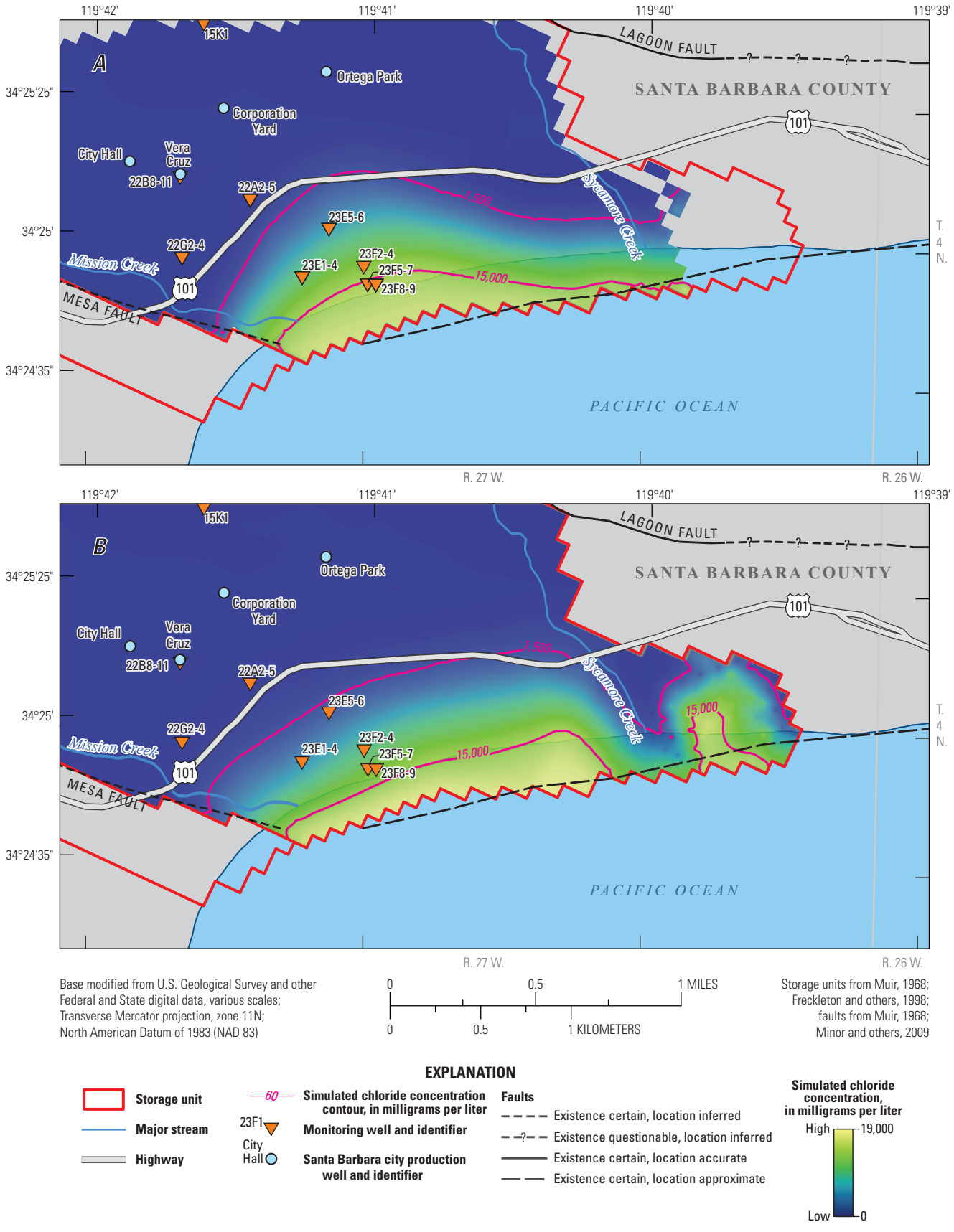

Figure 28. Contours of simulated chloride concentrations for year two, Santa Barbara multi-objective management model, Santa Barbara, California for pumping schedule: *A*, $5A_D$ in the middle producing zone; *B*, $5A_D$ in the lower producing zone; *C*, $5B_D$ in the middle producing zone; *D*, $5B_D$ in the lower producing zone; *E*, $5C_D$ in the middle producing zone; and *F*, $5C_D$ in the lower producing zone.

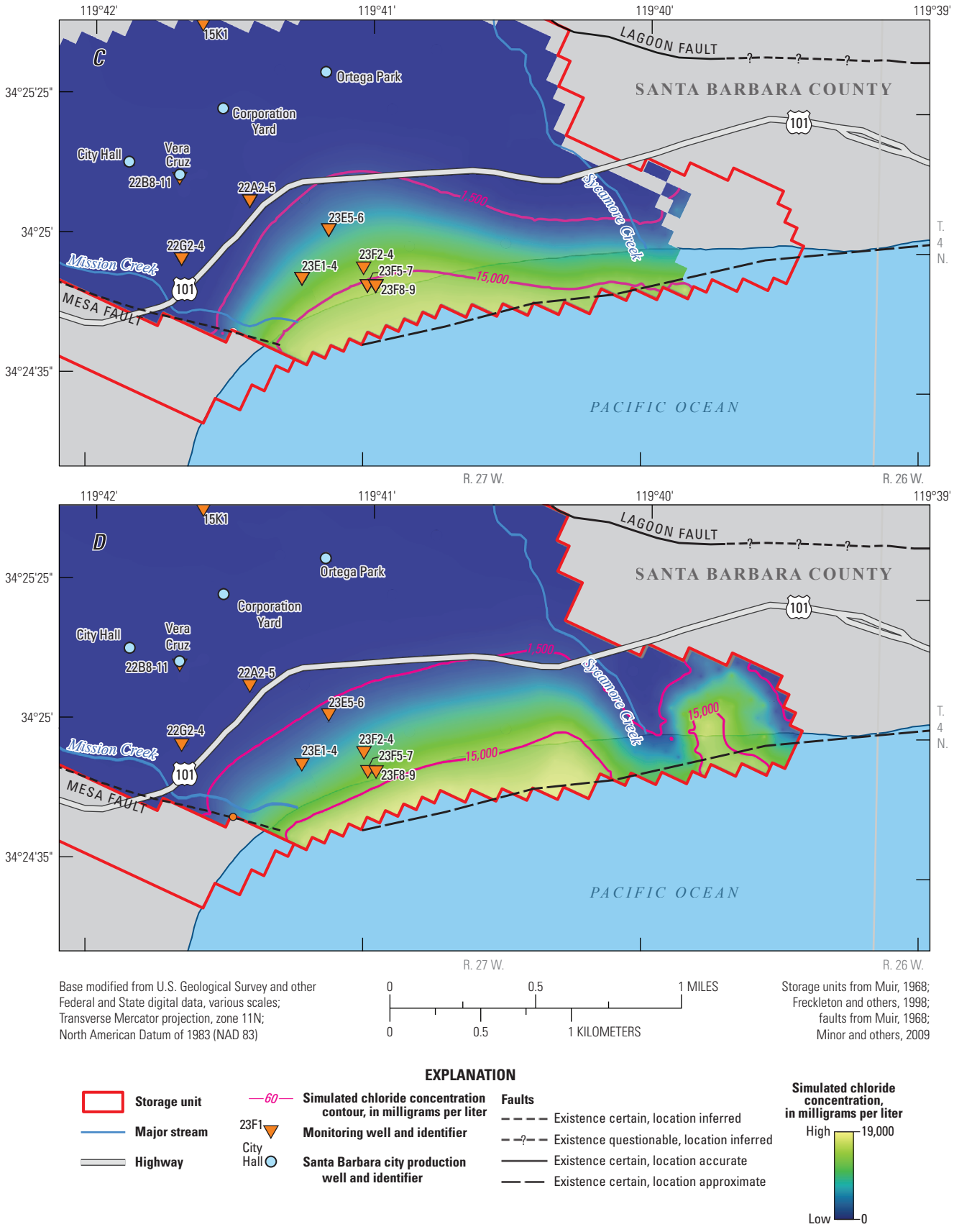

Figure 28. —Continued

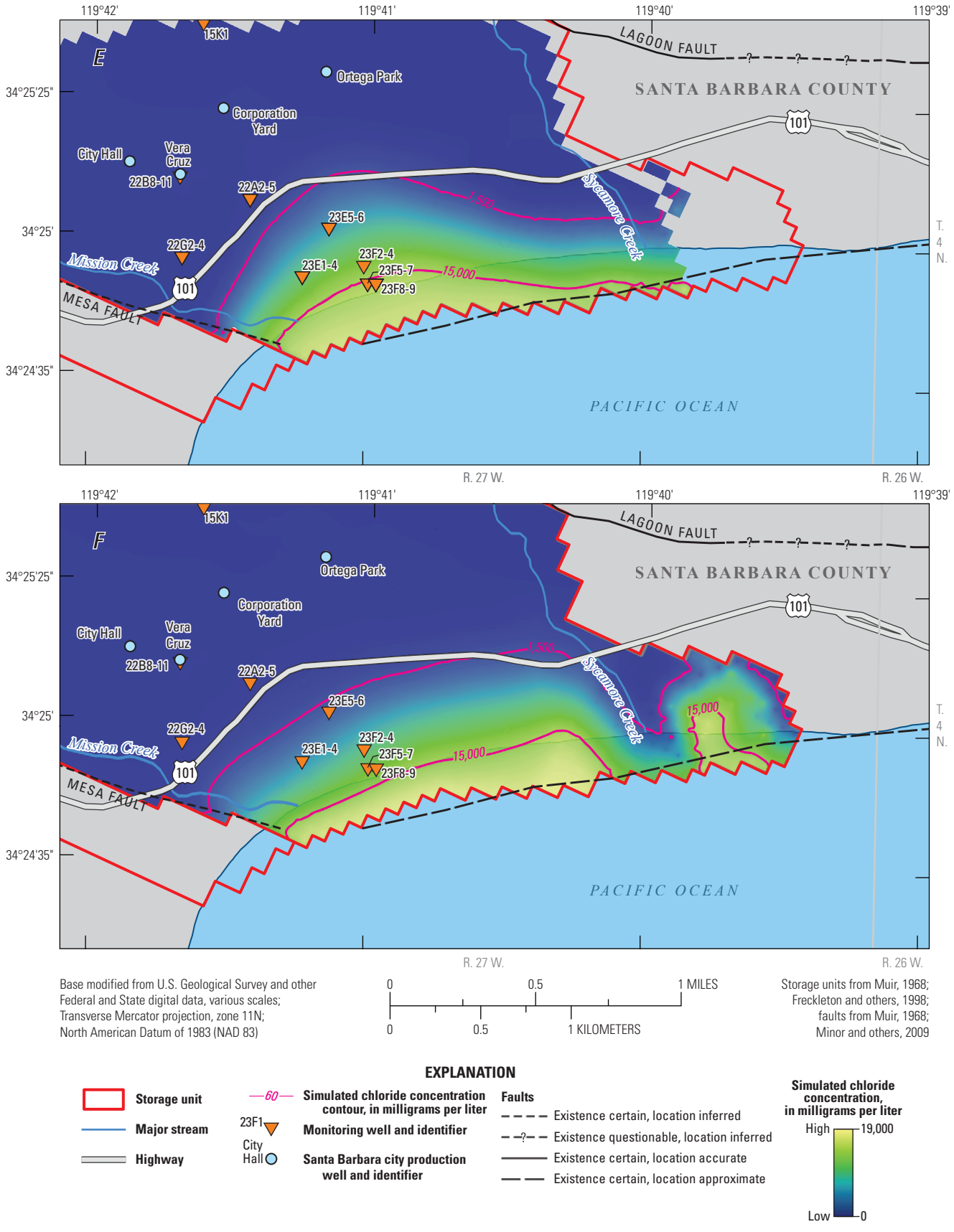

Figure 28. —Continued

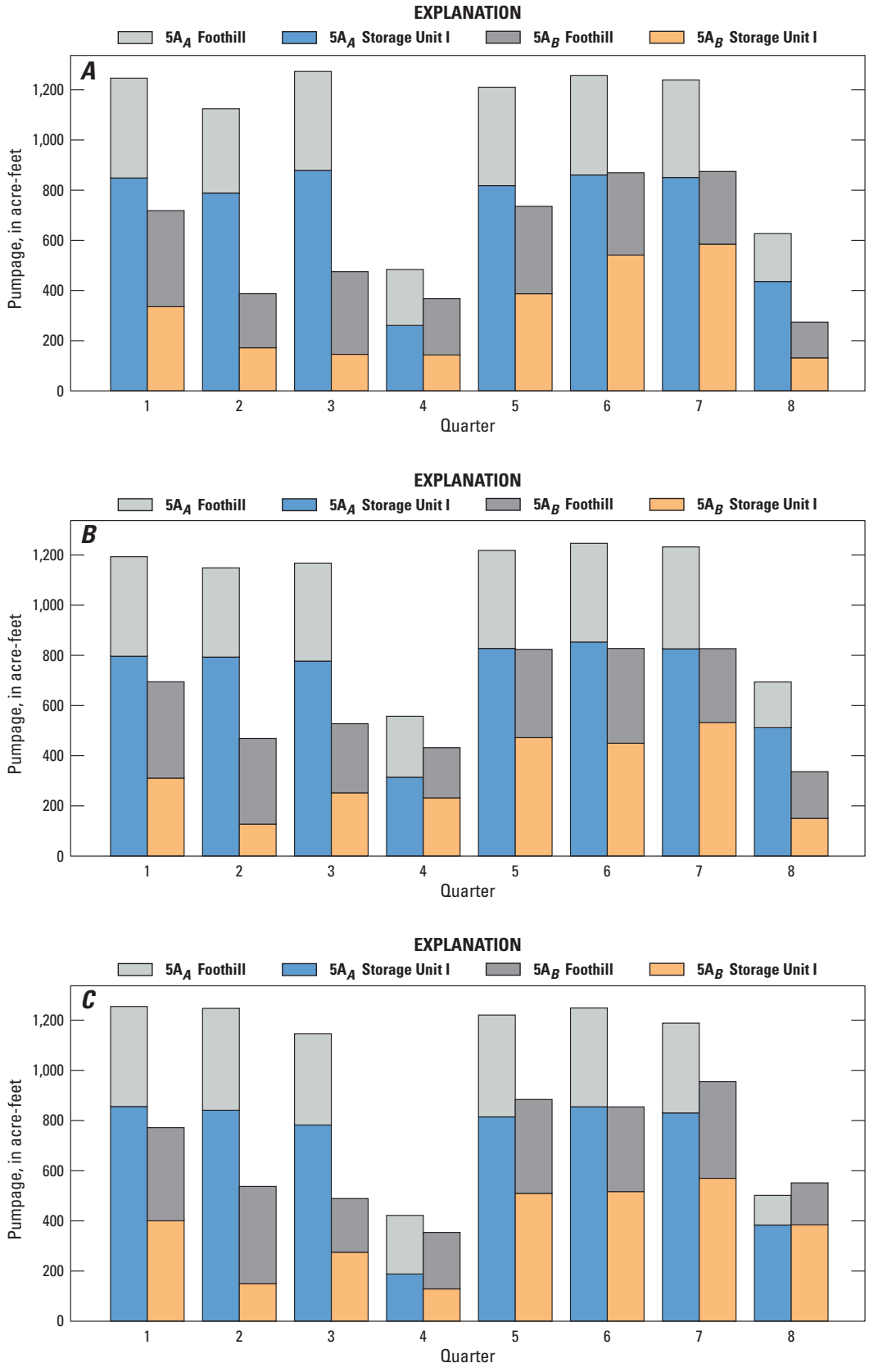

Figure 29. Pumping schedules A and B (maximum pumpage and minimum seawater intrusion, respectively), Storage Unit I and Foothill groundwater basin, Santa Barbara multi-objective management model, Santa Barbara, California, for scenarios *A*, 5A; *B*, 5B; and *C*, 5C.

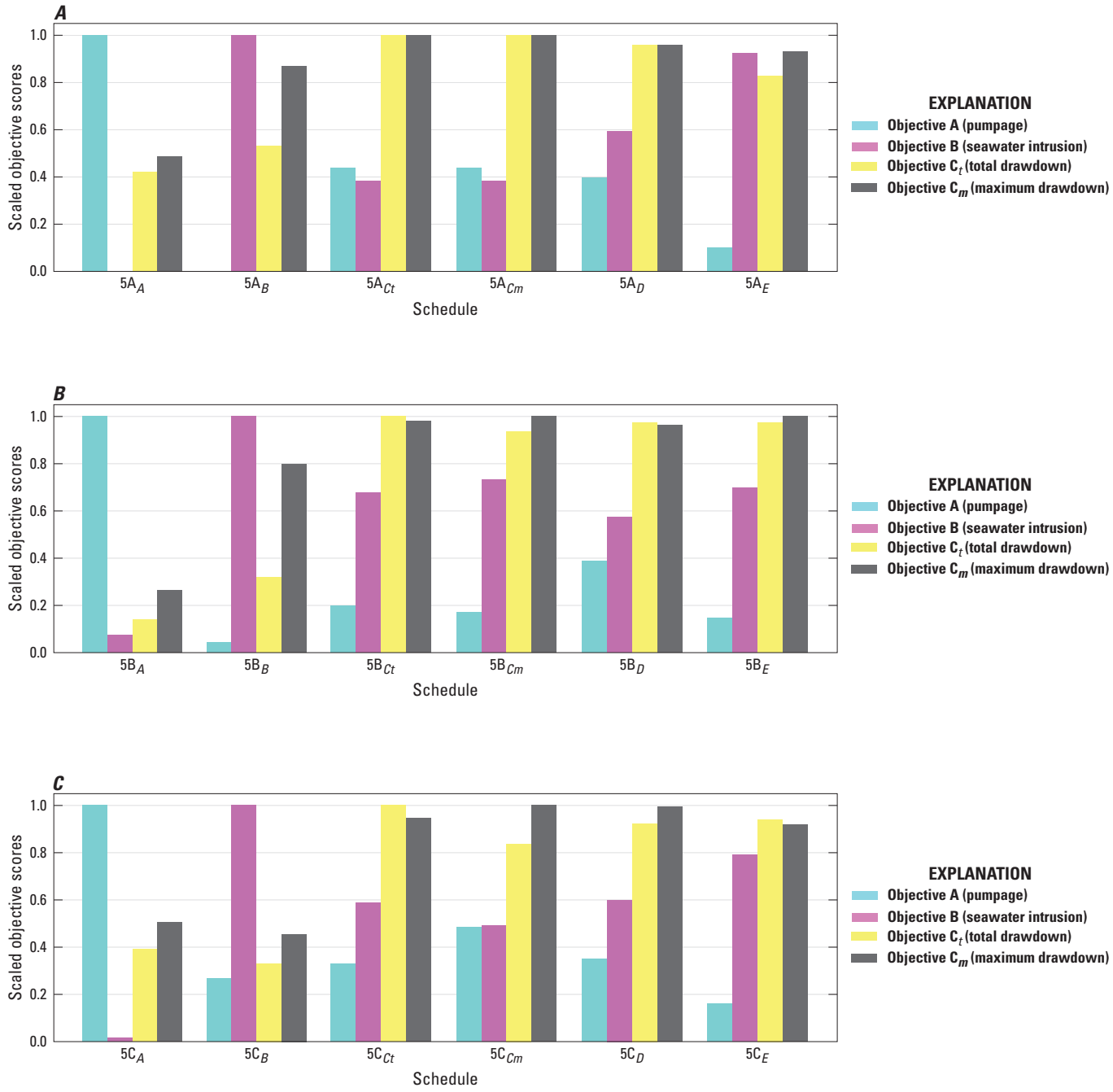

Figure 30. Scaled objective scores by scenario 5 pumping schedule used in the Santa Barbara multi-objective management model, Santa Barbara, California: *A*, 5A; *B*, 5B; and *C*, 5C.

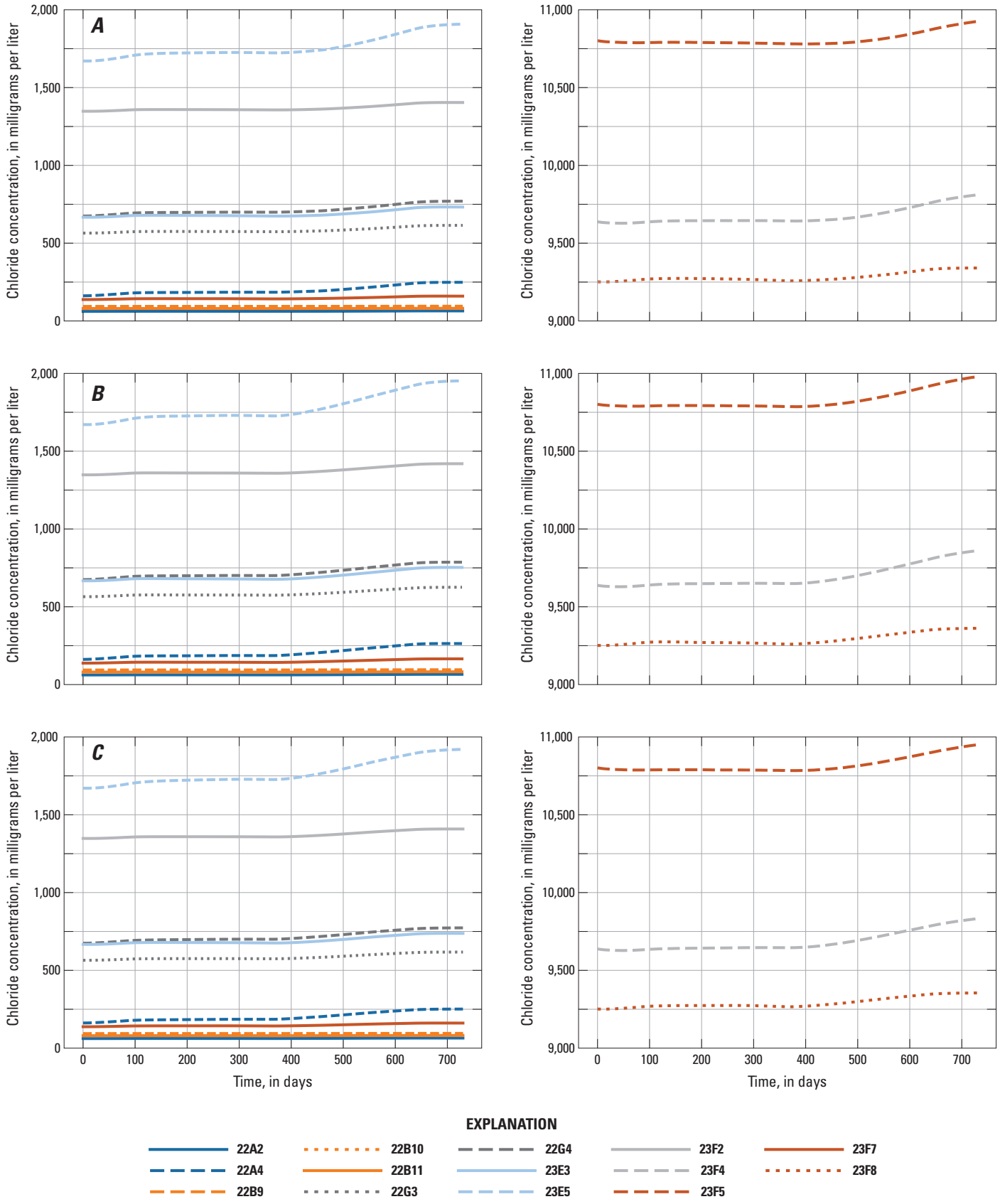

Figure 31. Breakthrough curves of simulated chloride concentrations for selected monitoring wells, Santa Barbara multi-objective management model, Santa Barbara, California, for *A*, schedule $5A_D$; *B*, schedule $5B_D$; and *C*, schedule $5C_D$.

Limitations

The simulation-optimization model described in this chapter has limitations because the underlying SEAWAT model is an approximation of reality, future precipitation is uncertain, and the optimization technique cannot guarantee a global optimum. The limitations of the simulation model are discussed in chapter C and include uncertainties in the stresses, hydraulic parameters, and measured data and various simplifying assumptions made during the modeling process. The implications of these simulation-model limitations for the optimization results were not examined and were beyond the scope of the study. The assumed climatic conditions were intended to span a large range of precipitation, which accounts for some uncertainty in rainfall data, but the optimization necessarily assumes the simulation is an adequate representation of the natural system. Given the inherent limitations of the simulation and the necessary simplifications in the problem formulation—for example, aggregation of monthly pumping into quarterly pumping—the optimization problem is one for which a global solution can only be approximated.

Undoubtedly, future precipitation could vary and not match the values used in any of the scenarios; therefore, the Pareto-optimal results only represent an empirical range of pumpage given specific climatic patterns. Although the Pareto-optimal pumping schedules can be adjusted (by scaling all values by a constant fraction) to meet demand, the corresponding system states cannot be scaled accordingly. It is safe to assume, however, that if a chosen Pareto-optimal pumping schedule produced acceptable seawater intrusion and drawdowns, scaling down the pumpage would not increase these effects to unacceptable levels. It must also be assumed that no additional stress to the system is incurred during the simulation period. Pareto-optimal results might no longer be optimal if an additional well (unaccounted for in the model) began pumping.

Although Borg was selected as the optimization algorithm partly because of its superior performance avoiding common EA perils (such as search stagnation in local optima), a global optimum can never be assured, even given a large number of simulation runs. If the optimization were allowed to run infinitely, slightly different Pareto-optimal solutions could be produced. The overall approximate Pareto fronts produced by Borg were monitored, and once no differences were observed for several generations of the algorithm, the optimization was determined to be complete. Exact values (as opposed to general magnitudes and trends) for schedules on the Pareto front are not ultimate answers to any problem. Instead, they represent what is feasible and optimal with respect to the problem formulation and the simulation model.

An additional limitation involves utilizing the optimal results for the entire management horizon. The last few stress periods of any scenario can show increased pumpage strictly because there was no further restriction on system state (water levels and chloride concentrations) beyond the end of the simulation (final condition). In other words, in a 10-year simulation, there is no year 11; therefore, pumpage can increase in year 10 until all of the constraints become binding. This can leave the system in a poor state moving forward, and seawater intrusion, for example, could continue increasing. The rates of seawater intrusion or water-level declines were not considered. Additionally, the first year of the optimal schedule can be considerably influenced by the initial condition. To account for changes to and uncertainty in the initial condition, the first year of the pumping schedules could also be discarded. Consequently, the middle 8 years of any 10-year optimization result is more reliable for planning and management guidance. Similar limitations are present in the 2-year simulations of scenario 5; however, it is difficult to determine the effects of the initial and final conditions because of the short management horizon.

Summary and Conclusions

The city of Santa Barbara is interested in identifying management strategies that maximize the available groundwater resources, while limiting seawater intrusion and groundwater drawdown. In order to identify the best management strategies, the U.S. Geological Survey in cooperation with the city of Santa Barbara undertook a simulation-optimization study that used the Santa Barbara flow and solute-transport model, described in chapter C of this report, to obtain optimal management strategies and estimate maximum pumping rates for a range of potential future climatic conditions.

The simulation-optimization problem was formulated as a multi-objective optimization problem and was solved using the Borg multi-objective evolutionary algorithm (MOEA). Borg was chosen as the optimization algorithm for this study for several reasons: (1) it is very computationally efficient; (2) it can run in parallel; (3) it requires little user input; and (4) it can solve for multiple competing objectives. The first three points allow the algorithm to proceed toward the optimal solutions at the fastest possible rate. The fourth point is advantageous for large, complex optimization problems because it is difficult to formulate the optimization problem in a way that produces only one optimal solution.

Results for each optimization are presented in Pareto-optimal surfaces in four objective dimensions: objective A sought to maximize total pumpage; objective B sought to minimize seawater intrusion; objective C_t sought to minimize total drawdown; and objective C_m sought to minimize the maximum drawdown. The decision variables were quarterly pumpage for 11 production wells. Strict optimization constraints were pumping capacities for each well implemented as variable bounds. Additional constraints were drinking-water-quality standards for chloride concentration at production wells, minimum-head specifications, and minimum flow to the Ortega groundwater-treatment plant.

Five scenarios were designed to assess the optimization results with respect to an uncertain future climatic condition. Scenario 1 was an optimization of a 10-year simulation assuming a typical climatic condition. Scenario 2 was an optimization of the same 10-year simulation model as scenario 1 but assumed a dry climatic condition to replicate a 10-year drought. Scenario 3 was designed to determine the potential for aquifer recovery if pumpage was limited to the minimum flow required to supply the Ortega groundwater-treatment plant. Scenario 4 was presented to create decision-rule curves from the database of scenario-1 and scenario-2 optimization results. These decision-rule curves allow water managers to adapt pumping schedules on the basis of chloride concentrations or drawdown measurements at select monitoring wells. Scenario 5 was an optimization of a 2-year simulation under three different climatic conditions: typical-to-dry (scenario 5A), dry-to-typical (scenario 5B), and dry-to-dry (scenario 5C). Scenario 5 demonstrated the sensitivity of Pareto-optimal results to short-term climatic conditions.

For each Pareto optimal solution in scenarios 1, 2, and 5, a pumping schedule, a set of chloride breakthrough curves, and water-level contours were produced. Six pumping schedules (A, B, C_t, C_m, D, and E) were identified in each Pareto-optimal set to illustrate the tradeoffs among the four objectives. The goals of pumping schedules A–E were to maximize pumpage; minimize seawater intrusion; minimize total drawdown; minimize maximum drawdown; achieve the best overall compromise among the four objectives; and achieve the best compromise among objectives B, C_t, and C_m.

The results of scenarios 1 and 2 presented the tradeoffs among the four conflicting objectives for a 10-year horizon. The maximum yield of scenario 1 (schedule 1_A) was 31,300 acre-feet (acre-ft); that of scenario 2 (schedule 2_A) was 30,000 acre-ft. These schedules are not necessarily preferable, but identify the extent to which the basins can be pumped. The best compromises among all objectives for the two climatic conditions were schedules 1_D and 2_D. Schedule 1_D represents optimal pumping schedules, assuming typical climatic conditions, and resulted in an average yield of 2,558 acre-feet per year (acre-ft/yr), ranging from 1,829 to 3,418 acre-ft/yr. Schedule 2_D represents optimal pumping schedules, assuming dry climatic conditions, and resulted in an average yield of 2,623 acre-ft/yr, ranging from 1,617 to 3,463 acre-ft/yr. Schedule 2_D resulted in more pumpage and less seawater intrusion than schedule 1_D; however, schedule 2_D resulted in much larger drawdowns as well.

Scenario 3 showed the potential for aquifer recovery from 1990 water levels to 1998 water levels under minimal pumpage and either typical or dry climatic conditions during a 10-year simulation. Aquifer recovery was illustrated by hydrographs that showed drawdown relative to 1998 water levels. There were minor differences in the recovery between the typical and dry climatic conditions. The drawdown at selected Storage Unit I wells stabilized between about 0 and 5 feet (ft) with a typical climatic condition and about 3 to 8 ft for the dry climatic condition. Therefore, despite minimal pumpage, the water levels did not recover to 1998 levels after 10 years of typical or dry climatic condition. Also, there was little difference between the extents of simulated seawater intrusion after 10 years for these climatic conditions. This scenario demonstrated that simulated seawater intrusion was not sensitive to recharge, even with pumpage substantially decreased.

The scenario-4 results produced decision-rule curves that can be used to help make management decisions without needing to run a simulation. The optimizations of scenarios 1 and 2 produced a set of feasible pumping schedules from which a subset was selected for further analysis. The rule curves were produced as a reference for when additional field measurements are taken of water levels and chloride concentrations. In the case of a measured concentration, a curve was produced that showed simulated results that matched that concentration and the associated Pareto-optimal pumpage in Storage Unit I and the ensuing seawater intrusion. For the case of measured water levels, each decision-rule curve showed a subset of Pareto-optimal pumpage, separated by storage unit, for each production well. Combined, these curves provide an approach to adapt production management as measurements are taken in the future. In other words, total pumpage by storage unit can be adjusted to future conditions, and the associated Pareto-optimal pumping schedule can be derived from these results.

For scenario 5, the Pareto optimal results illustrated the effect of short-term precipitation patterns on preferred pumping schedules. In general, the Pareto optimal results for Scenario 5A (typical-to-dry) and 5B (dry-to-typical) showed a greater range of pumpage and drawdown than scenario 5C (dry-to-dry). The solution for the objective of minimal seawater intrusion (schedule B) for the typical-to-dry simulation (schedule $5A_B$) had substantially less total drawdown (in fact, simulated hydraulic heads increased for schedule $5A_B$) than schedules $5B_B$ and $5C_B$. For the minimal maximum-drawdown solution (schedule C_m), there was much less pumpage in the dry-to-typical climatic condition (schedule $5B_{Cm}$) than in the other two climatic conditions (schedules $5A_{Cm}$ and $5C_{Cm}$). The best compromise solution (schedule D) in the typical-to-dry climatic condition (schedule $5A_D$) also had less simulated seawater intrusion than schedules $5B_D$ and $5C_D$. The simulated hydraulic heads were similar for each producing zone in each climatic condition; any differences were most notable in the lower producing zone of the Foothill groundwater basin and the upper producing zone of Storage Unit I. The quarterly pumping schedules by well showed the increase in Foothill groundwater basin pumpage for minimal seawater-intrusion solutions. The tradeoffs among all three objectives were more pronounced in the scenario-5B results. Very little difference was noticeable in the chloride breakthrough curves for all three climatic conditions, however.

The Borg MOEA offers the most efficient way of collecting simulation results by using Pareto-optimality and searching the decision-variable space in a logical manner. Typically, unanticipated climatic conditions or changing management preferences would require additional simulations and, possibly, an additional study altogether. In this study, the Pareto-optimal results for two climatic conditions (typical and dry) provide the city with a collection of simulation results to help make decisions without additional model simulations.

The Pareto-optimal results for each scenario can be used for assessing the differences between scenarios or for assessing the tradeoffs among the four competing objectives. The differences between scenario-1 and scenario-2 results showed the effect on basin yield, when simulating typical precipitation, and indicated that it was beneficial to simulate a drought. In scenario 2, the complex dynamics among the four objectives depended strongly on climate and choosing an optimal schedule from the Pareto curve that produced the desired pumpage results in a clear tradeoff between drawdown and seawater intrusion.

Further conclusions can be drawn from scenarios 1 and 2 by investigating scenarios 3 and 4. Considering scenario-3 results, the best-case scenario (10-year typical precipitation), assuming minimal pumpage, was a return to water levels about 0–10 ft lower than those in 1998. The basin responded quickly when pumping was reduced, but the rate of the response was greatly diminished after a few years. At that point, drawdown stabilized at about 0–10 ft less than 1998 levels with continued pumping of 484 acre-ft/yr from Storage Unit I. The scenario-4 results provide a way to mitigate further seawater intrusion or excessive drawdown. As data are collected, regardless of the pumping schedule that is implemented, management actions can be adapted to prevent unnecessary losses in yield, increases in chlorides, or decreases in water levels.

Lastly, the scenario-5 results were also useful for assessing the consequences of assuming typical or dry precipitation for 2-year climatic conditions. Objective B values did not vary over a wide range among the pumping schedules of all scenarios, meaning seawater intrusion was relatively insensitive to a 2-year precipitation pattern. Results showed that optimal pumpage was more sensitive to climate in year one when minimizing total drawdown, and conversely, optimal pumpage was more sensitive to climate in year two when minimizing the maximum drawdown. The maximum pumpage in each scenario (schedule A) was distributed more to Storage Unit I than the Foothill groundwater basin in all quarters. For the minimal seawater-intrusion pumpage (schedule B), there were some quarters in which a larger portion of pumpage came from the Foothill groundwater basin than from Storage Unit I. The dry-to-dry precipitation pattern of scenario 5C generally represented conservative estimates of optimal pumpage, seawater intrusion, and drawdown. These conservative pumping schedules from drier climate simulations ensured the short-term annual yield of the basin would not jeopardize future yield if precipitation remained low.

References Cited

Abarca, E., Vázquez-Suñé, E., Carrera, J., Capino, B., Gámez, D., and Batlle, F., 2006, Optimal design of measures to correct seawater intrusion: Water Resources Research, v. 42, no. 9, p. 1–14.

Abd-Elhamid, H.F., and Javadi, A.A., 2011, A cost-effective method to control seawater intrusion in coastal aquifers: Water Resources Management, v. 25, no. 11, p. 2755–2780.

Ahlfeld, D.P., and Baro-Montes, G., 2008, Solving unconfined groundwater flow management problems with successive linear programming: Journal of Water Resources Planning and Management, v. 134, no. 5, p. 404–412.

Ahlfeld, D.P., and Mulligan, A.E., 2000, Optimal management of flow in groundwater systems: San Diego, California, Academic, 185 p.

Ahlfeld, D.P., Mulvey, J.M., Pinder, G.F., and Wood, E.F., 1988, Contaminated groundwater remediation design using simulation, optimization, and sensitivity theory; 1. Model development: Water Resources Research, v. 24, no. 3, p. 431–441.

Cachuma Operation and Maintenance Board, 2017, National Marine Fisheries Service biological opinion: accessed October 2017, at http://fmp.cachuma-board.org/nmfs.htm.

Chang, L.C., Shoemaker, C.A., and Liu, P.L.F., 1992, Optimal time-varying pumping rates for groundwater remediation; Application of a constrained optimal control algorithm: Water Resources Research, v. 28, no. 12, p. 3157–3171.

Cieniawski, S.E., Eheart, J.W., and Ranjithan, S., 1995, Using genetic algorithms to solve a multiobjective groundwater monitoring problem: Water Resources Research, v. 31, no. 2, p. 399–409.

Coello, C.A.C., Lamont, G.B., and Van Veldhuizen, D.A., 2007, Evolutionary algorithms for solving multi-objective problems (2d ed.), Genetic and Evolutionary Computation Series: Boston, Mass., Springer, 800 p.

Culver, T.B., and Shoemaker, C.A., 1992, Dynamic optimal control for groundwater remediation with flexible management periods: Water Resources Research, v. 28, no. 3, p. 629–641.

Culver, T.B., and Shoemaker, C.A., 1997, Dynamic optimal ground-water reclamation with treatment capital costs: Journal of Water Resources Planning and Management, v. 123, no. 1, p. 23–29.

Das, A., and Datta, B., 2000, Optimization based solution of density dependent seawater intrusion in coastal aquifers: Journal of Hydrologic Engineering, v. 5, no. 1, p. 82–89.

Dhar, A., and Datta, B., 2009, Saltwater intrusion management of coastal aquifers; I : linked simulation-optimization: Journal of Hydrologic Engineering, v. 14, no. 12, p. 1263–1272.

Freckleton, J.R., Martin, P., and Nishikawa, T., 1998, Geohydrology of Storage Unit III and a combined flow model of the Santa Barbara and Foothill ground-water basins, Santa Barbara County, California: U.S. Geological Survey Water-Resources Investigations Report 97–4121, 80 p., http://pubs.er.usgs.gov/publication/wri974121.

Gordon, E., Shamir, U., and Bensabat, J., 2001, Optimal extraction of water from regional aquifer under salinization: Journal of Water Resources Planning and Management, v. 127, no. 2, p. 71–77.

Gorelick, S.M., 1983, Review of distributed parameter groundwater management modeling methods: Water Resources Research, v. 19, no. 2, p. 305–319.

Hadka, D.M., and Reed, P.M., 2013, Borg; An auto-adaptive many-objective evolutionary computing framework: Evolutionary Computation, v. 1, no. 2, p. 231–259, http://doi.org/10.1162/EVCO_a_00075.

Kasprzyk, J.R., Reed, P.M., Kirsch, B.R., and Characklis, G.W., 2009, Managing population and drought risks using many-objective water portfolio planning under uncertainty: Water Resources Research, v. 45, no. 12, 18 p., doi:10.1029/2009WR008121.

Kasprzyk, J.R., Reed, P.M., and Hadka, D.M., 2015, Battling Arrow's Paradox to discover robust water management alternatives: Journal of Water Resources Planning and Management, v. 142, no. 2, 04015053, http://doi.org/10.1061/(ASCE)WR.1943-5452.0000572.

Kollat, J.B., and Reed, P.M., 2006, Comparing state-of-the-art evolutionary multi-objective algorithms for long-term groundwater monitoring design: Advances in Water Resources, v. 29, no. 6, p. 792–807, doi:10.1016/j.advwatres.2005.07.010.

Lefkoff, L.J., and Gorelick, S.M., 1986, Design and cost analysis of rapid aquifer restoration systems using flow simulation and quadratic programming: Ground Water, v. 24, no. 6, p. 777–790.

Mayer, A.S., Kelley, C.T., and Miller, C.T., 2002, Optimal design for problems involving flow and transport phenomena in saturated subsurface systems: Advances in Water Resource, v. 25, no. 8–12, p. 1233–1256.

McKinney, D.C., and Lin, M.D., 1994, Genetic algorithm solution of groundwater management models: Water Resources Research, v. 30, no. 6, p. 1897–1906.

McKinney, D.C., and Lin, M.D., 1995, Approximate mixed-integer nonlinear programming methods for optimal aquifer remediation design: Water Resources Research, v. 31, no. 3, p. 731–740.

Minor, S.A., Kellogg, K.S., Stanley, R.G., Gurrola, L.D., Keller, E.A., and Brandt, T.R., 2009, Geologic map of the Santa Barbara coastal plain area, Santa Barbara County, California: U.S. Geological Survey Scientific Investigations Map 3001, scale 1:25,000, 1 sheet, pamphlet, 38 p., https://pubs.er.usgs.gov/publication/sim3001.

Muir, K.S., 1968, Ground-water reconnaissance of the Santa Barbara-Montecito area, Santa Barbara County, California: U.S. Geological Survey Water Supply Paper 1859–A, 28 p., https://pubs.er.usgs.gov/publication/wsp1859A.

Molz, F.J., and Bell, L.C., 1977, Head gradient control in aquifers used for fluid storage: Water Resources Research, v. 13, no. 4, p. 795–798.

Nicklow, J., Reed, P.M., Savic, D., Dessalegne, T., Harrell, L., Chan-Hilton, A., Karamouz, M., Minsker, B., Ostfeld, A., Singh, A., Zechman, E., and ASCE Task Committee on Evolutionary Computation in Environmental and Water Resources Engineering, 2010, State of the art for genetic algorithms and beyond in water resources planning and management: Journal of Water Resources Planning and Management, v. 136, no. 4, p. 412–432.

Nishikawa, T., 1998, A water-resources optimization model for Santa Barbara, California: ASCE Journal of Water Resources Planning and Management, v. 124, no. 5, p. 252–263.

Nocedal, J., and Wright, S.J., 2006, Numerical optimization: New York, Springer Science and Business Media, 664 p.

Qahman, K., Larabi, A., Ouazar, D., Naji, A., and Cheng, A.H.-D., 2005, Optimal and sustainable extraction of groundwater in coastal aquifers: Stochastic Environmental Research and Risk Assessment, v. 19, no. 2, p. 99–110.

Reed, P.M., Hadka, D.M., Herman, J.D., Kasprzyk, J.R., and Kollat, J.B., 2013, Evolutionary multiobjective optimization in water resources; The past, present, and future: Advances in Water Resources, 51, p. 438–456, http://doi.org/10.1016/j.advwatres.2012.01.005.

Singh, A., 2014, Optimization modelling for seawater intrusion management: Journal of Hydrology, v. 508, p. 43–52.

Sreekanth, J., and Datta, B., 2015, Review; Simulation-optimization models for the management and monitoring of coastal aquifers: Hydrogeology Journal, v. 23, no. 6, p. 1155–1166.

U.S. Environmental Protection Agency, 2017, Secondary drinking water standards; Guidance for nuisance chemicals: accessed on January 11, 2017, at https://www.epa.gov/dwstandardsregulations/secondary-drinking-water-standards-guidance-nuisance-chemicals.

Wagner, B.J., 1995, Recent advances in simulation-optimization groundwater management modeling: Review in Geophysics, v. 33, p. 1021–1028.

Wang, W., and Ahlfeld, D.P., 1994, Optimal groundwater remediation with well locations as a decision variable; Model development: Water Resources Research, v. 30, no. 5, p. 1605–1618.

Ward, V.L., Singh, R., Reed, P.M., and Keller, K., 2015, Confronting tipping points; Can multi-objective evolutionary algorithms discover pollution control tradeoffs given environmental thresholds?: Environmental Modelling and Software, v. 73, p. 27–43, http://doi.org/10.1016/j.envsoft.2015.07.020.

Willis, R.L., 1979, A planning model for the management of groundwater quality: Water Resources Research, v. 15, no. 6, p. 1305–1312.

Yeh, W.W.-G., 1992, Systems analysis in groundwater planning and management: Journal of Water Resources Planning and Management, v. 118, no. 1, p. 224–237.

Appendix D–1: Schedule 1D Pumpage, by Well, Santa Barbara Multi-Objective Management Model, Santa Barbara, California

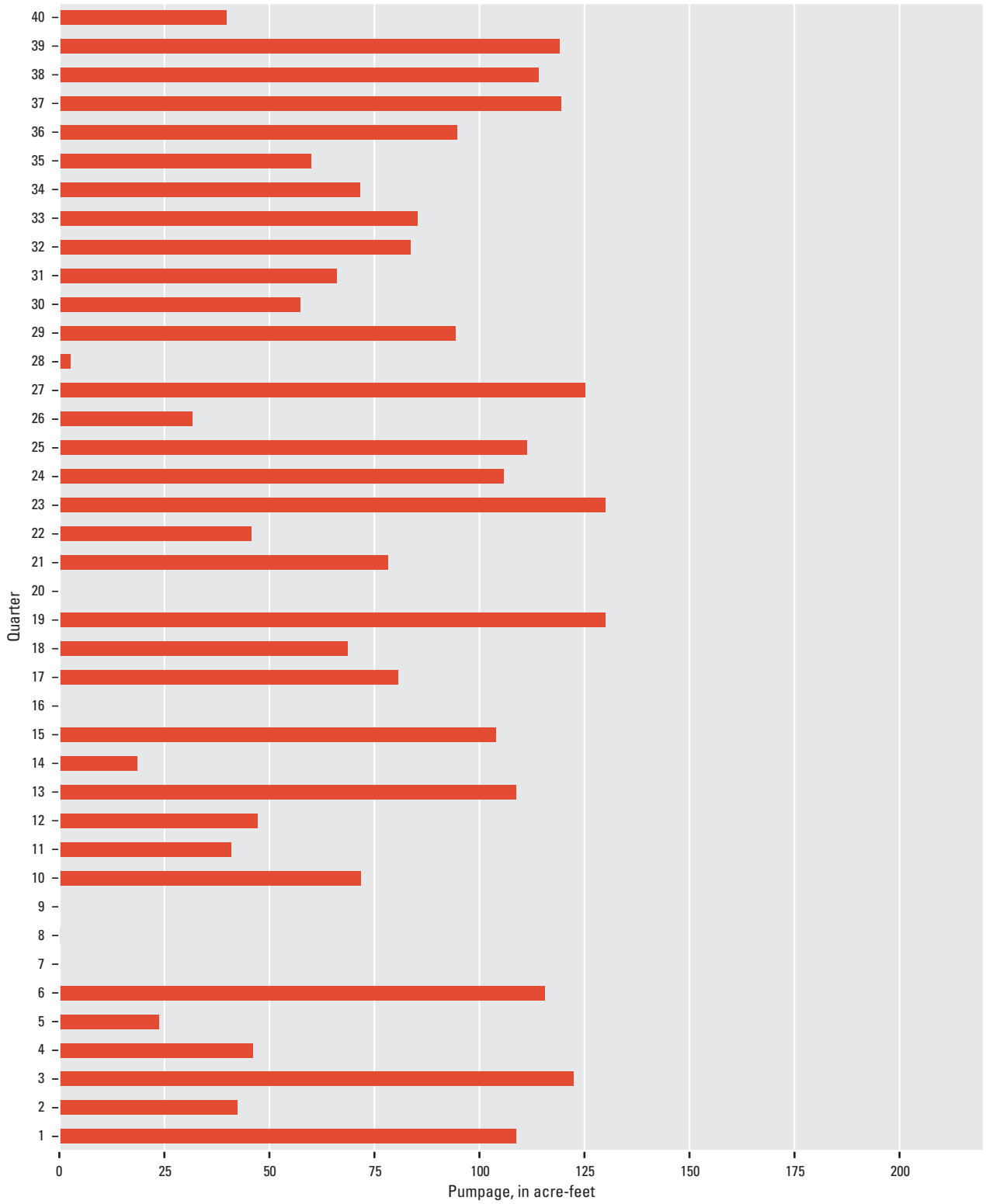

Figure D1–1. Optimal quarterly pumpage for the Alameda Park well, schedule 1_D, Santa Barbara, California.

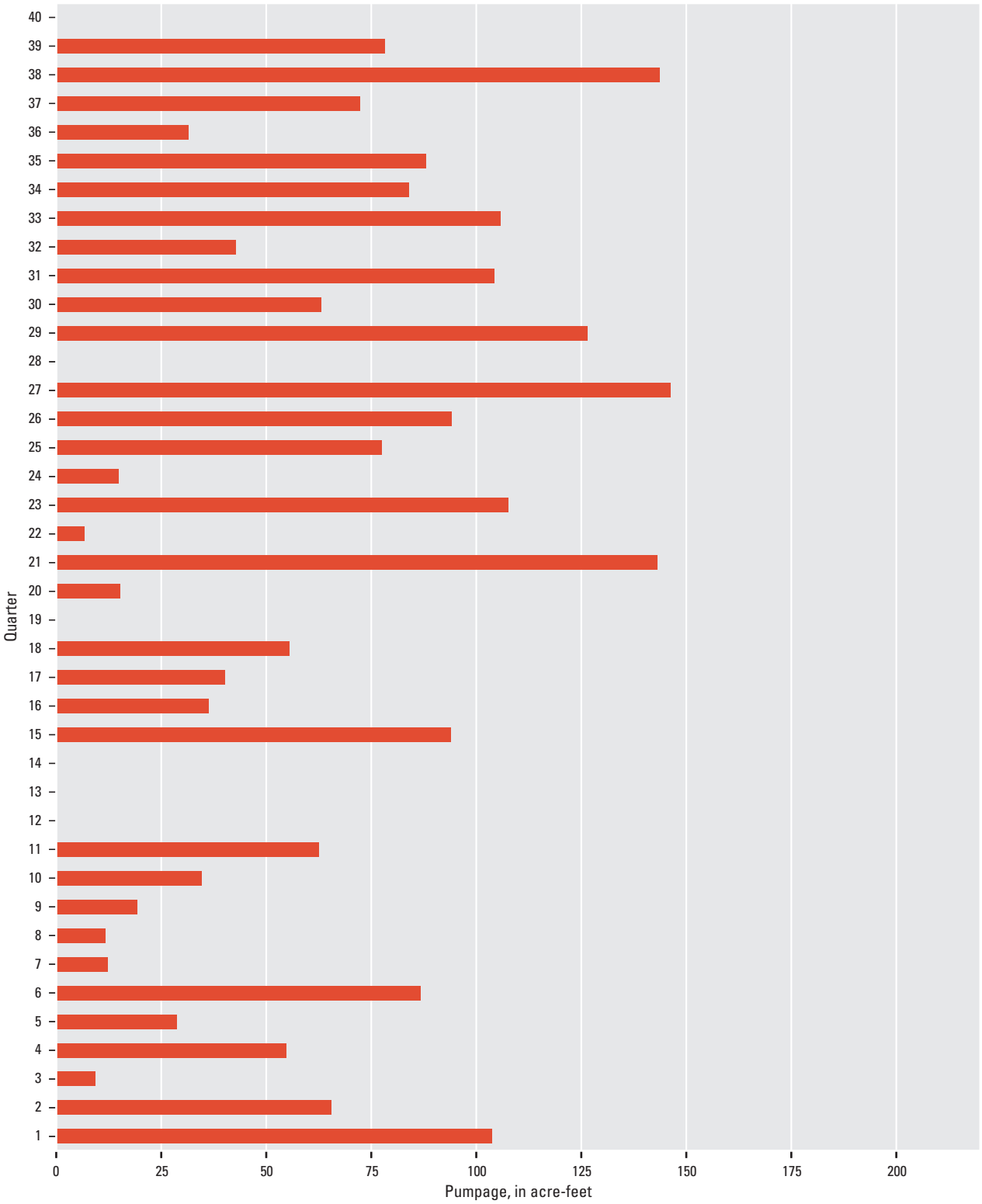

Figure D1–2. Optimal quarterly pumpage for the City Hall well, schedule 1_D, Santa Barbara, California.

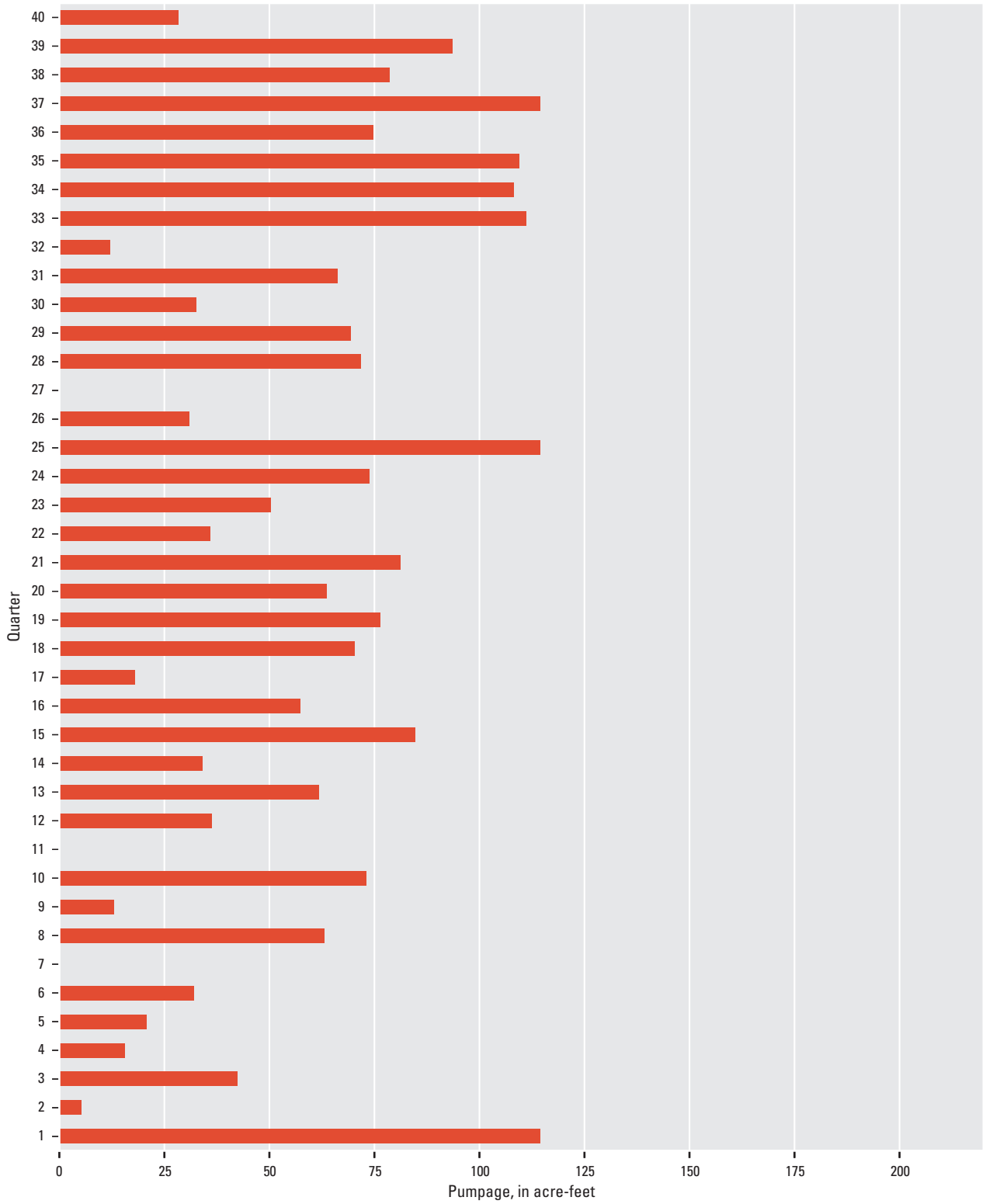

Figure D1–3. Optimal quarterly pumpage for the Corporation Yard well, schedule 1_D, Santa Barbara, California.

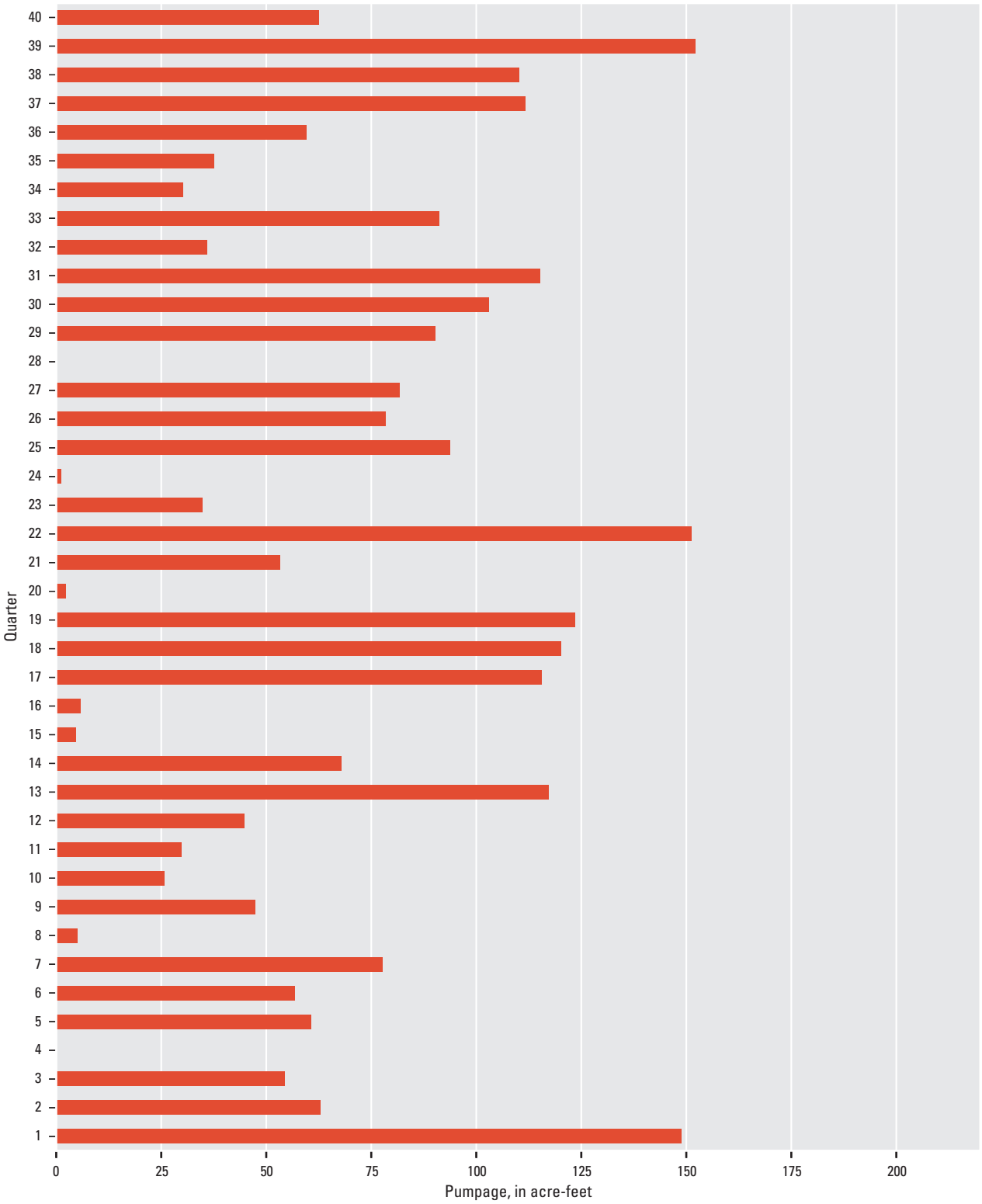

Figure D1–4. Optimal quarterly pumpage for the Ortega Park well, schedule 1_D, Santa Barbara, California.

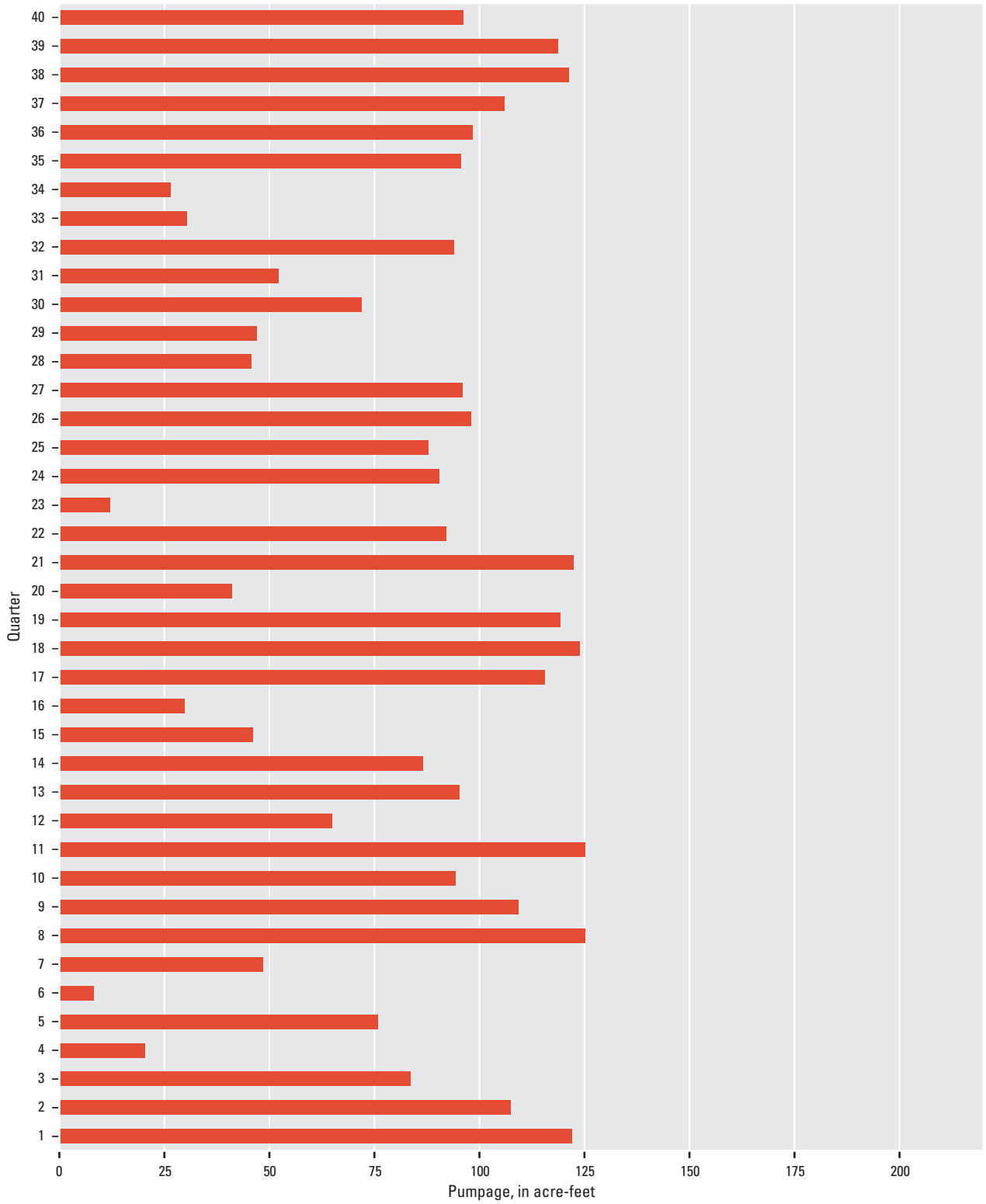

Figure D1–5. Optimal quarterly pumpage for the Santa Barbara High School well, schedule 1_D, Santa Barbara, California.

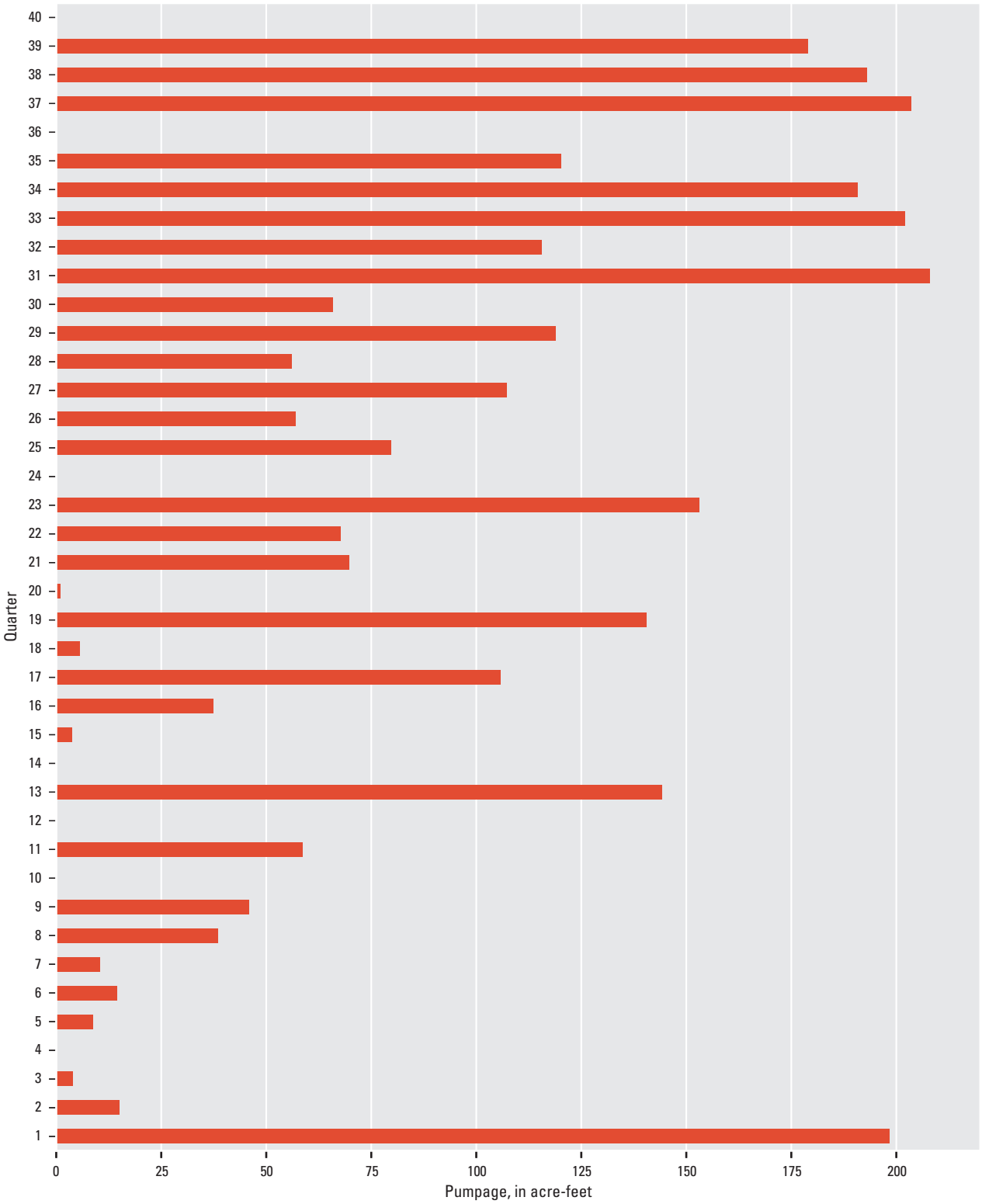

Figure D1–6. Optimal quarterly pumpage for the Vera Cruz well, schedule 1_D, Santa Barbara, California.

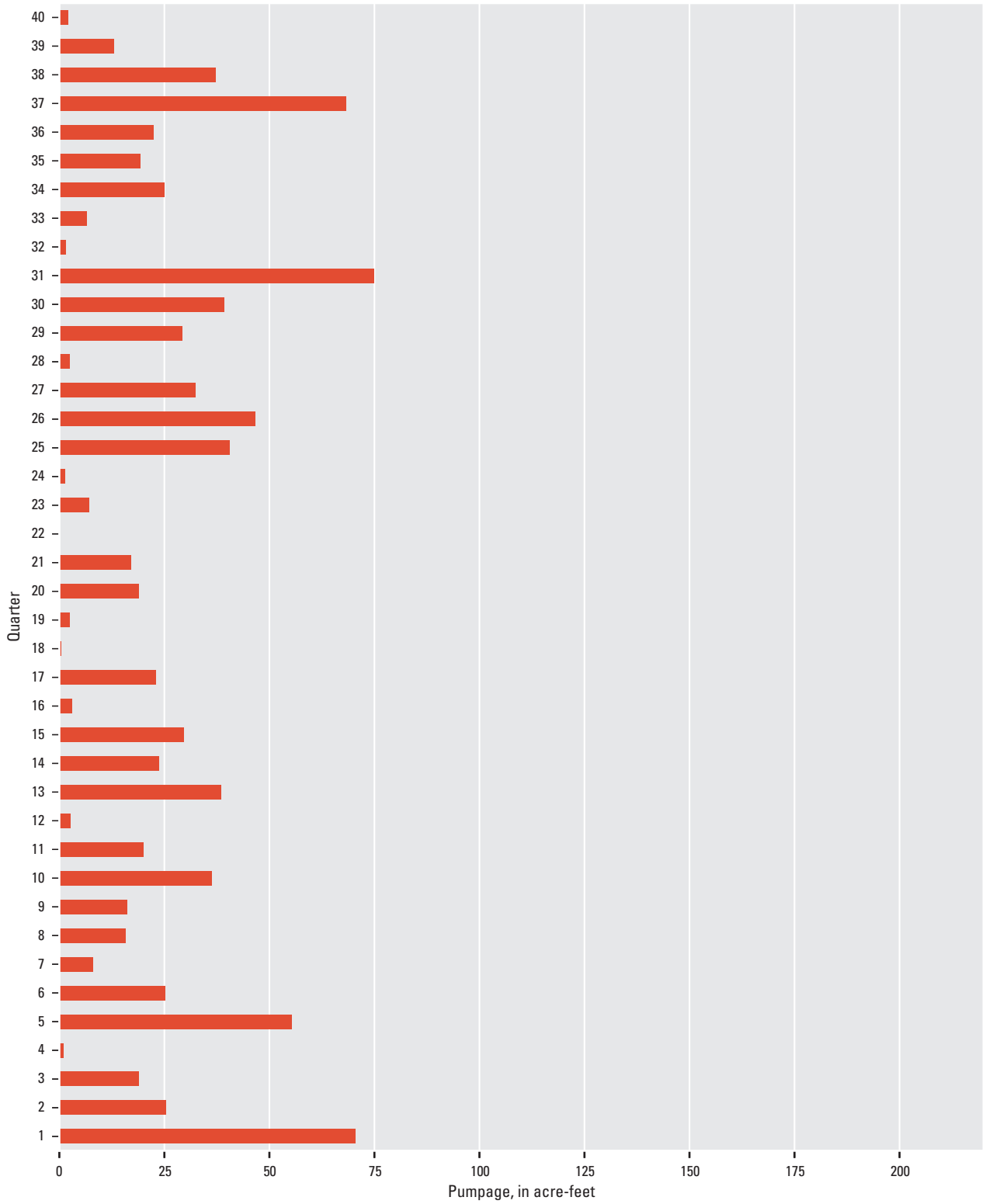

Figure D1–7. Optimal quarterly pumpage for the Hope Avenue well, schedule 1_D, Santa Barbara, California.

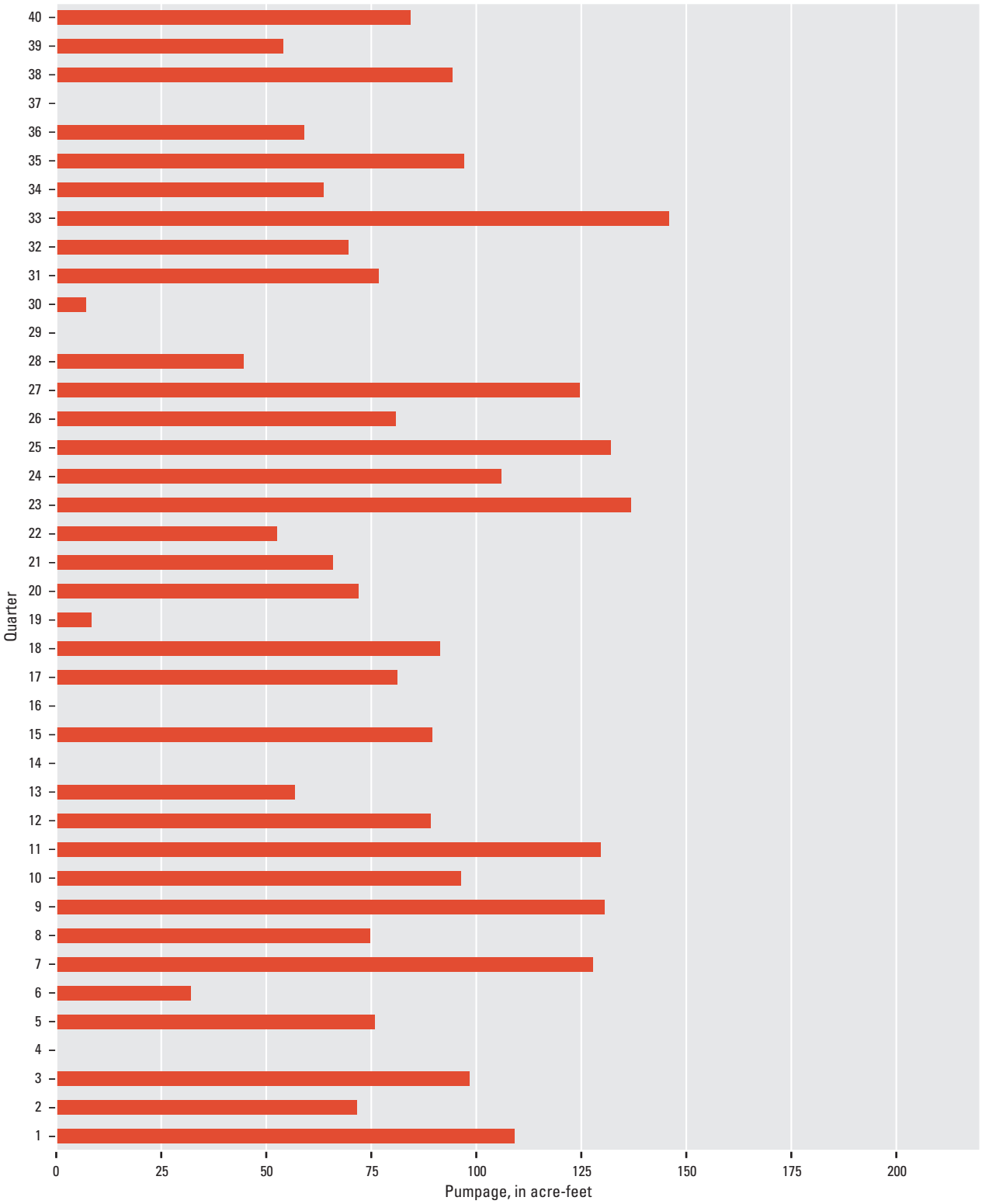

Figure D1–8. Optimal quarterly pumpage for the Lincolnwood 1 well, schedule 1_D, Santa Barbara, California.

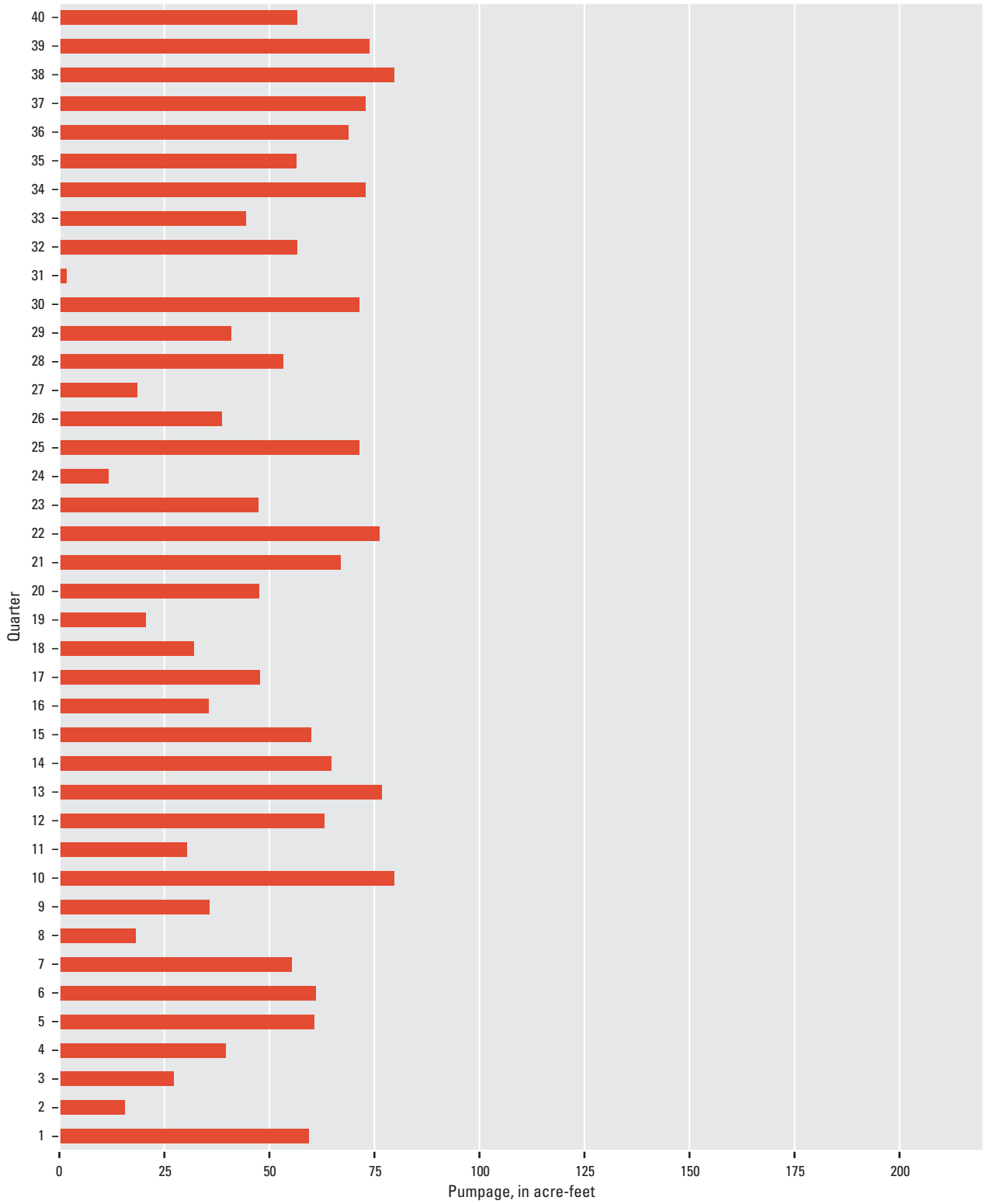

Figure D1–9. Optimal quarterly pumpage for the Los Robles well, schedule 1_D, Santa Barbara, California.

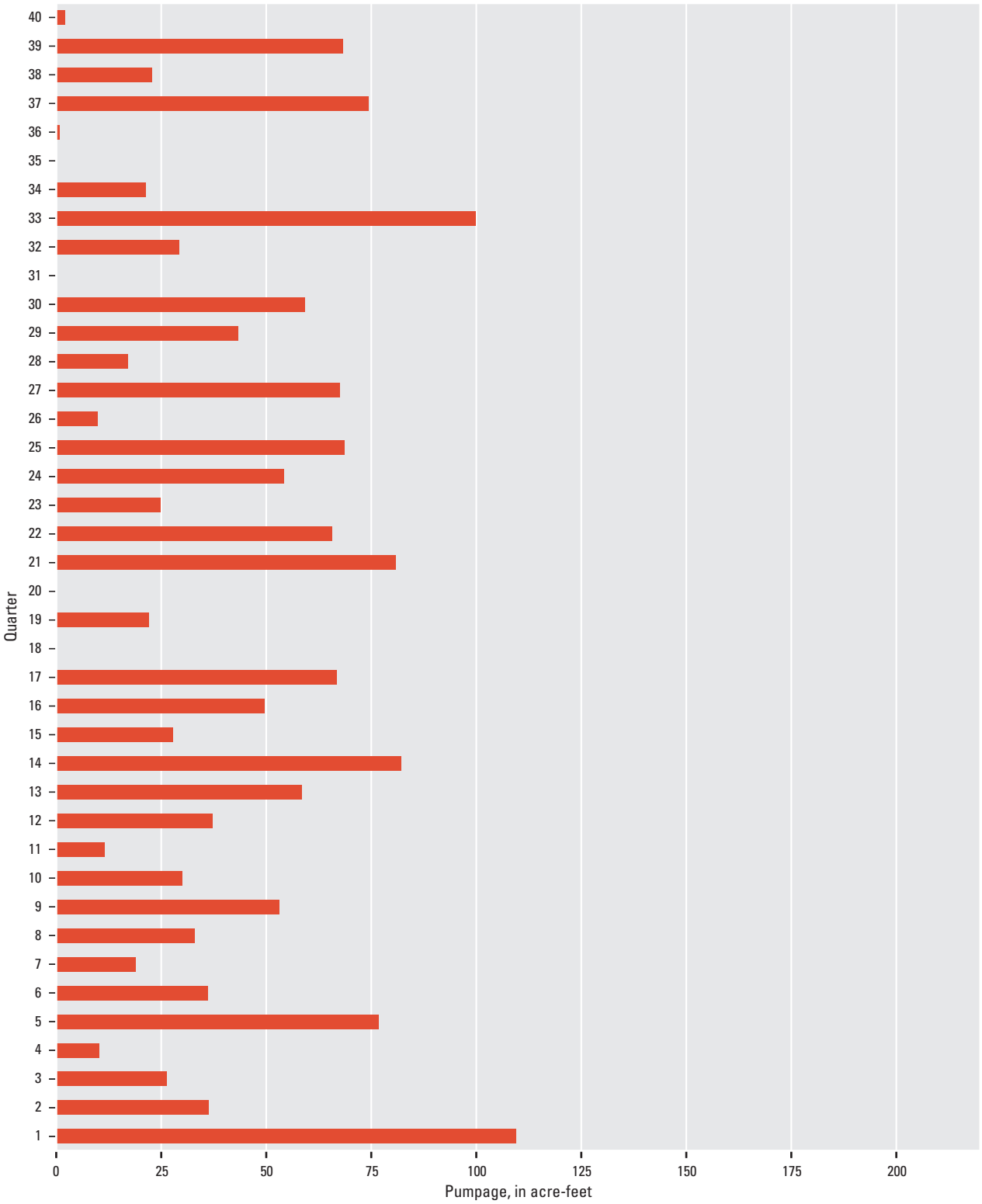

Figure D1–10. Optimal quarterly pumpage for the San Roque Park 2 well, schedule 1_D, Santa Barbara, California.

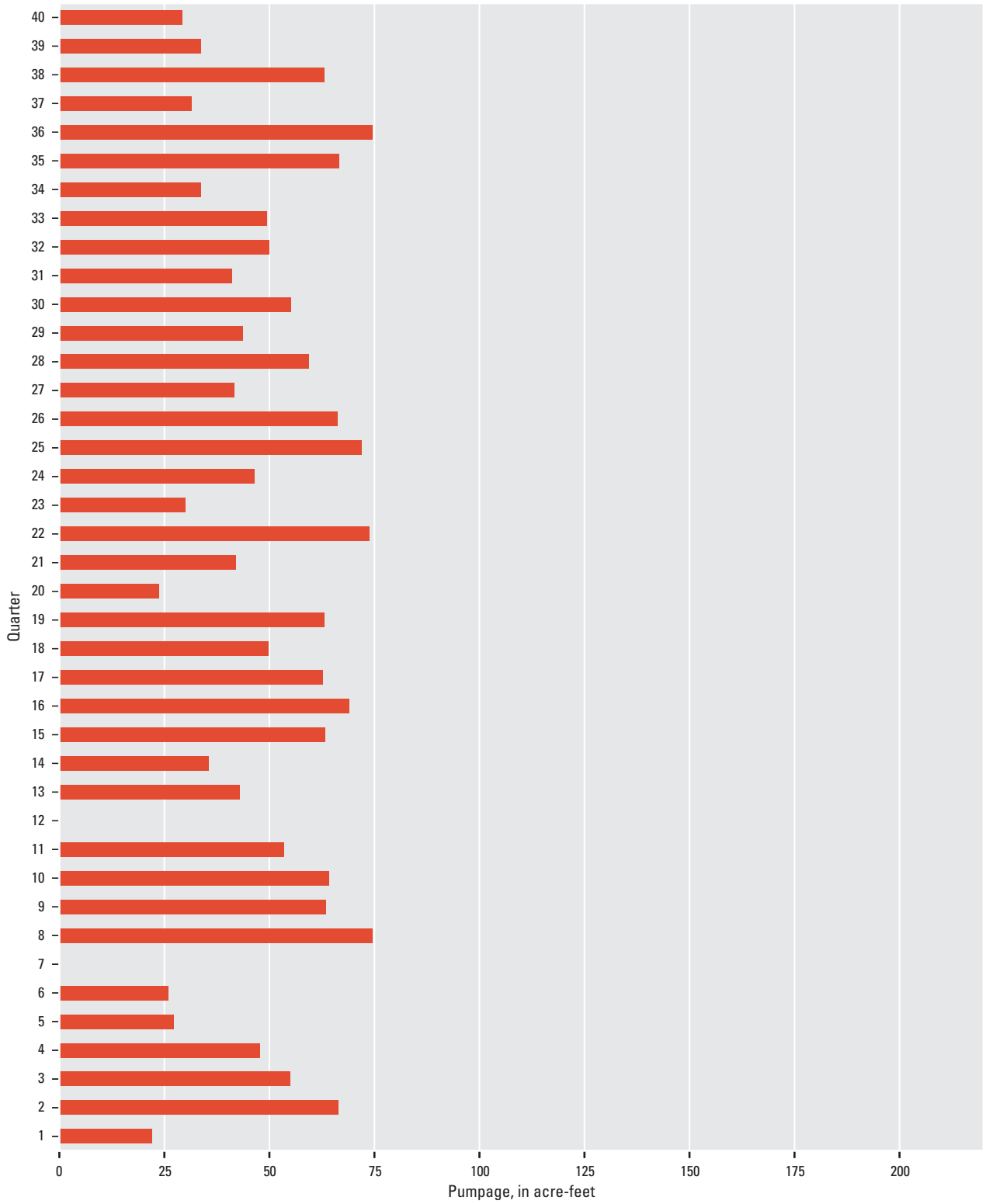

Figure D1–11. Optimal quarterly pumpage for the Val Verde well, schedule 1_D, Santa Barbara, California.

Appendix D–2: Schedule 2D Pumpage, by Well, Santa Barbara Multi-Objective Management Model, Santa Barbara, California

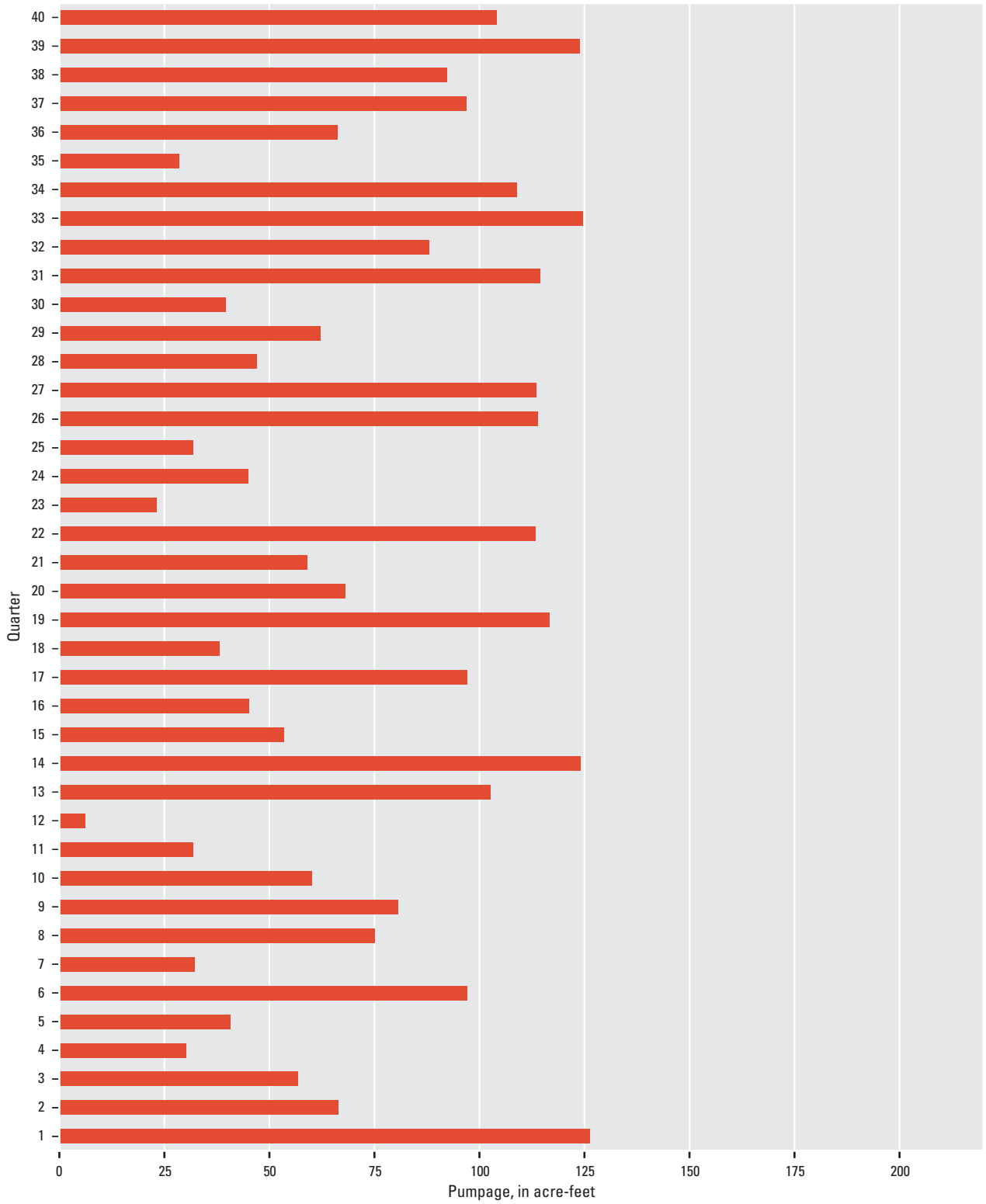

Figure D2–1. Optimal quarterly pumpage for the Alameda Park well, schedule 2_D, Santa Barbara, California.

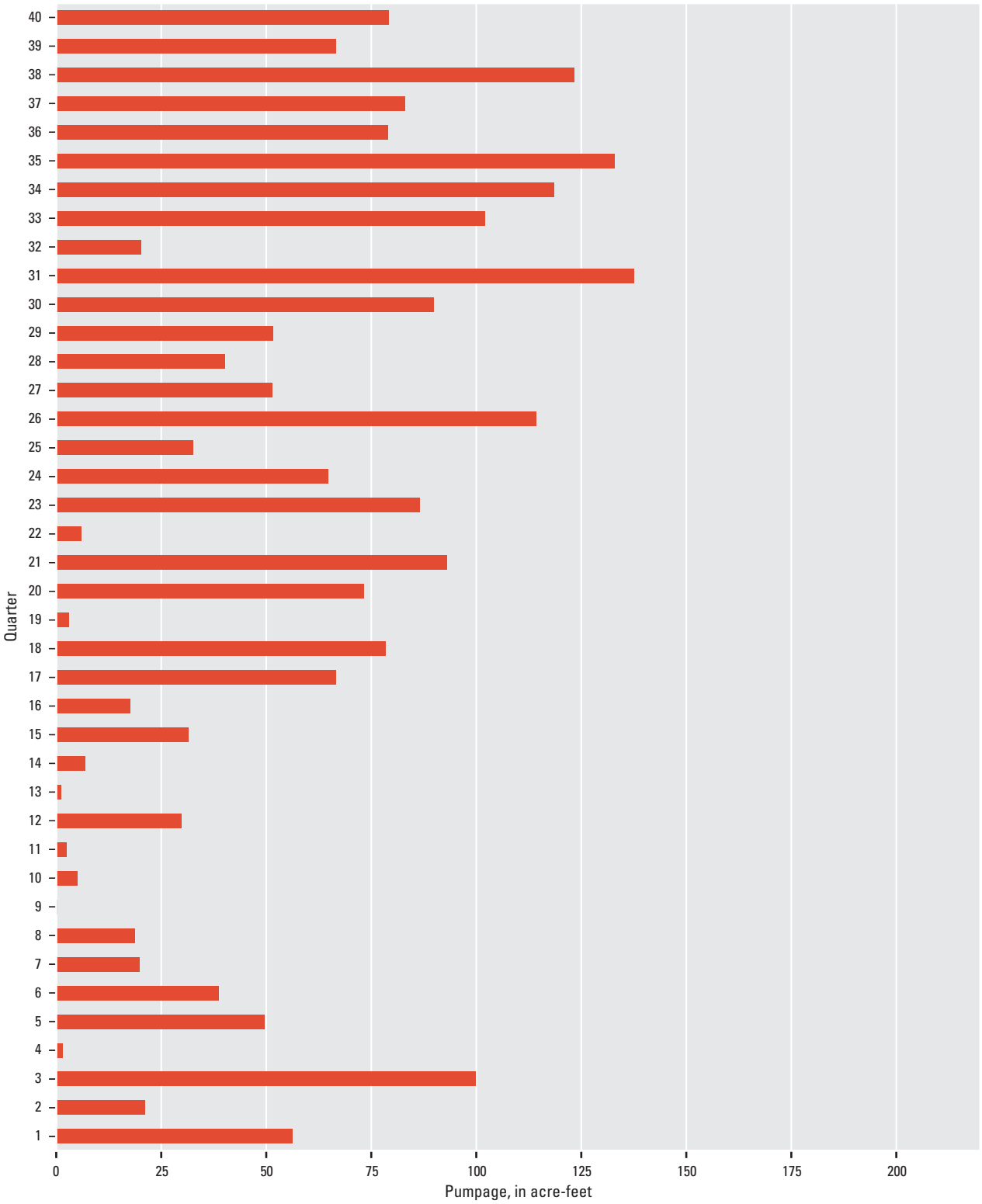

Figure D2–2. Optimal quarterly pumpage for the City Hall well, schedule 2_D, Santa Barbara, California.

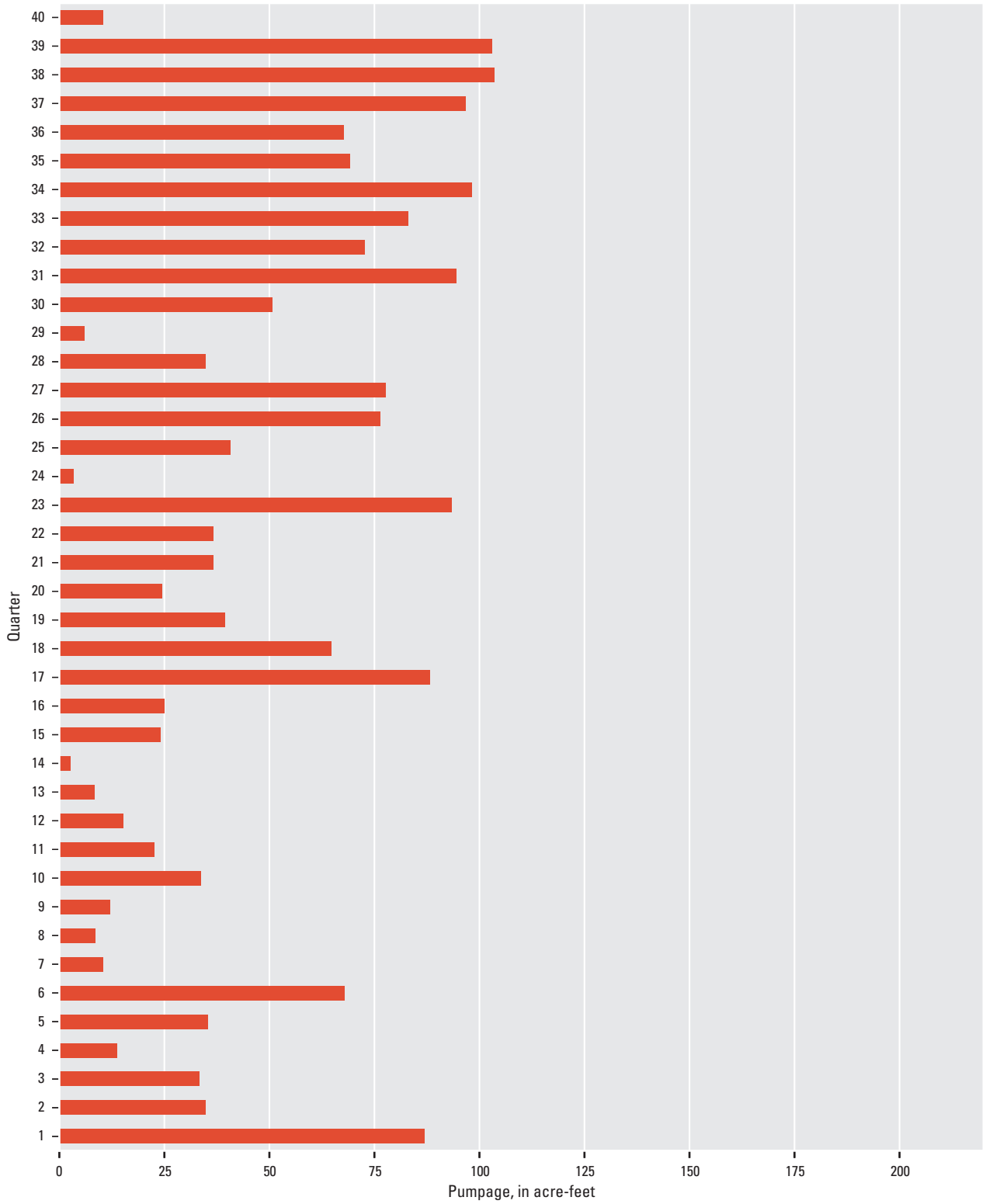

Figure D2–3. Optimal quarterly pumpage for the Corporation Yard well, schedule 2_D, Santa Barbara, California.

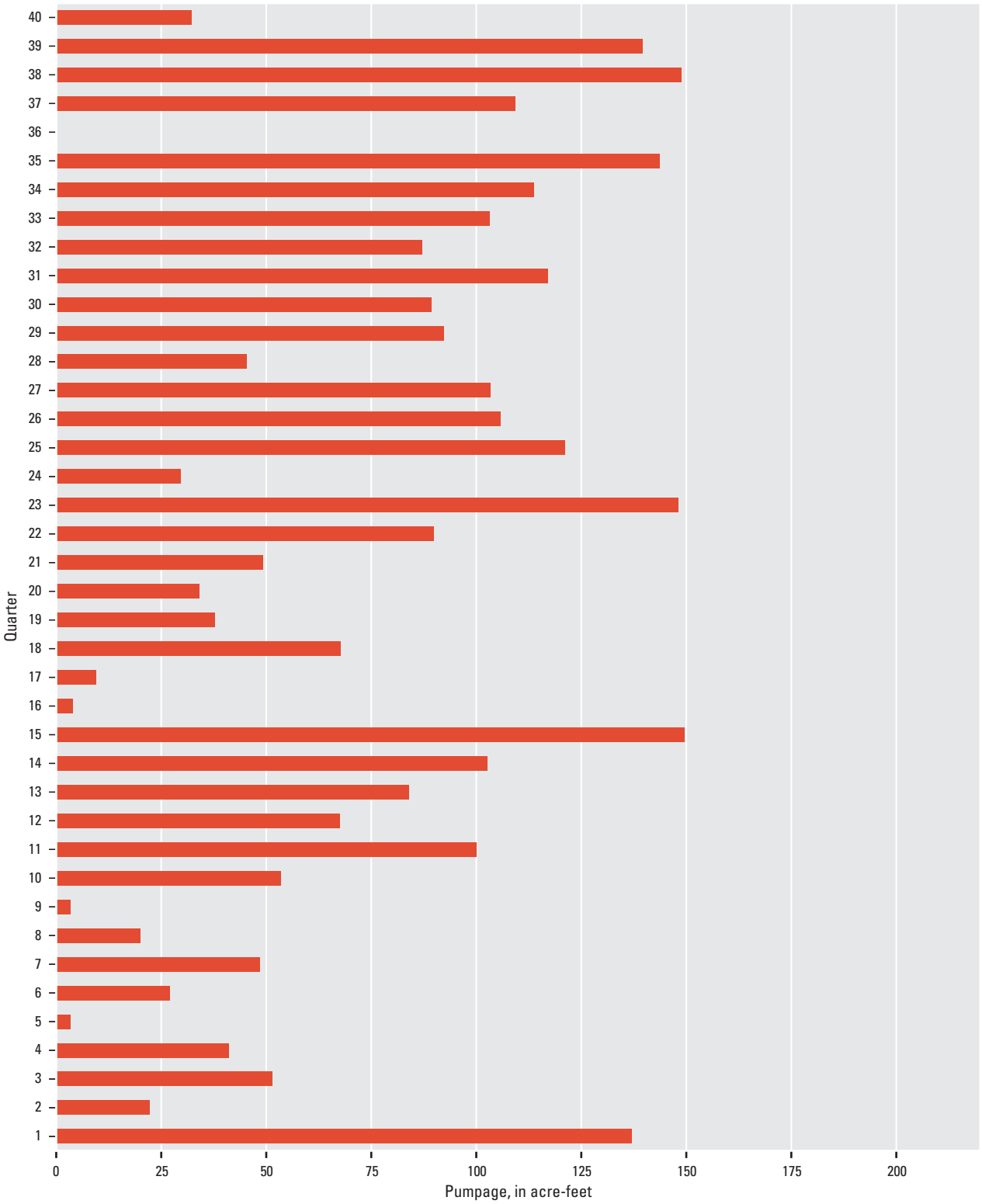

Figure D2–4. Optimal quarterly pumpage for the Ortega Park well, schedule 2_D, Santa Barbara, California.

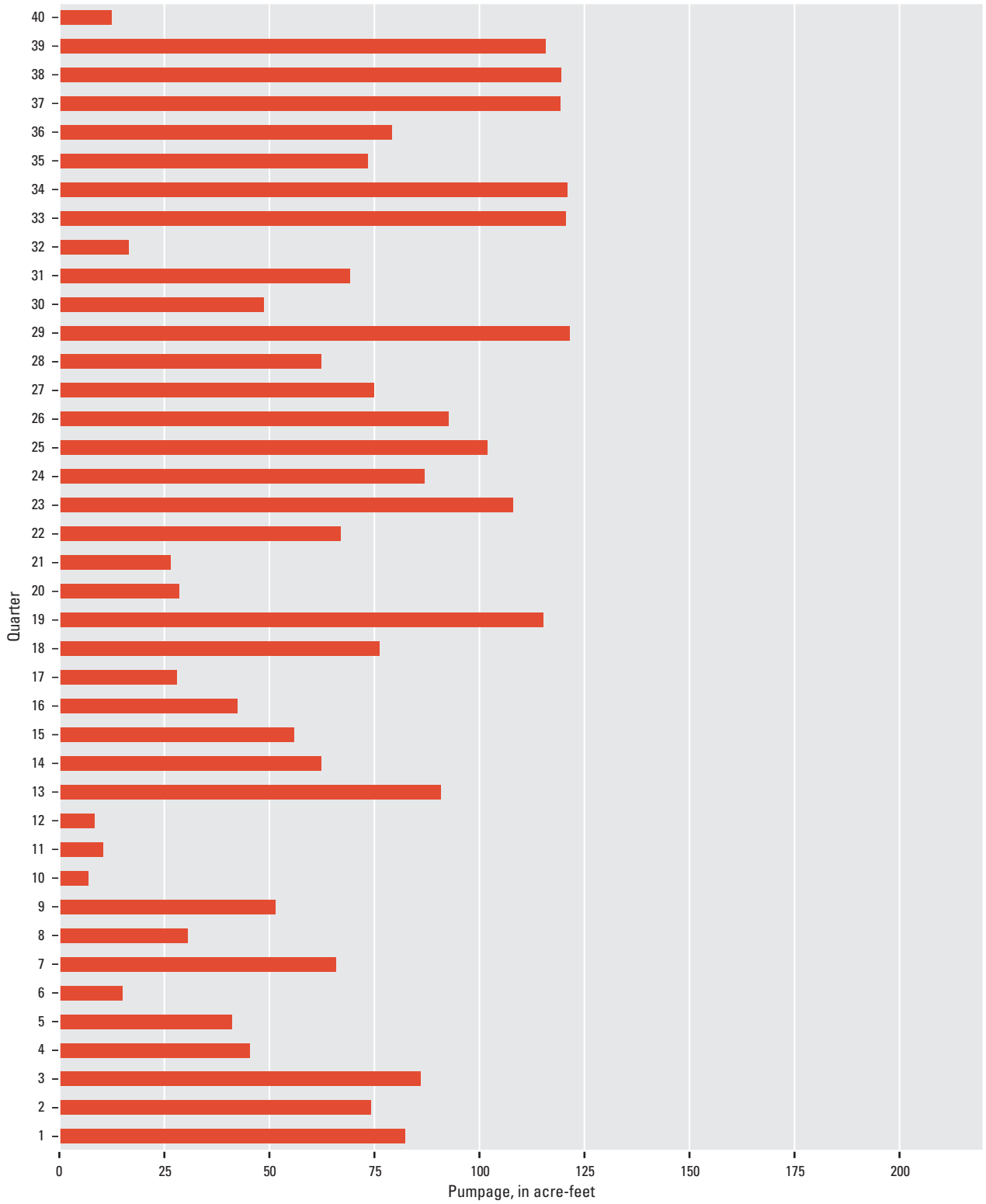

Figure D2–5. Optimal quarterly pumpage for the Santa Barbara High School well, schedule 2_D, Santa Barbara, California.

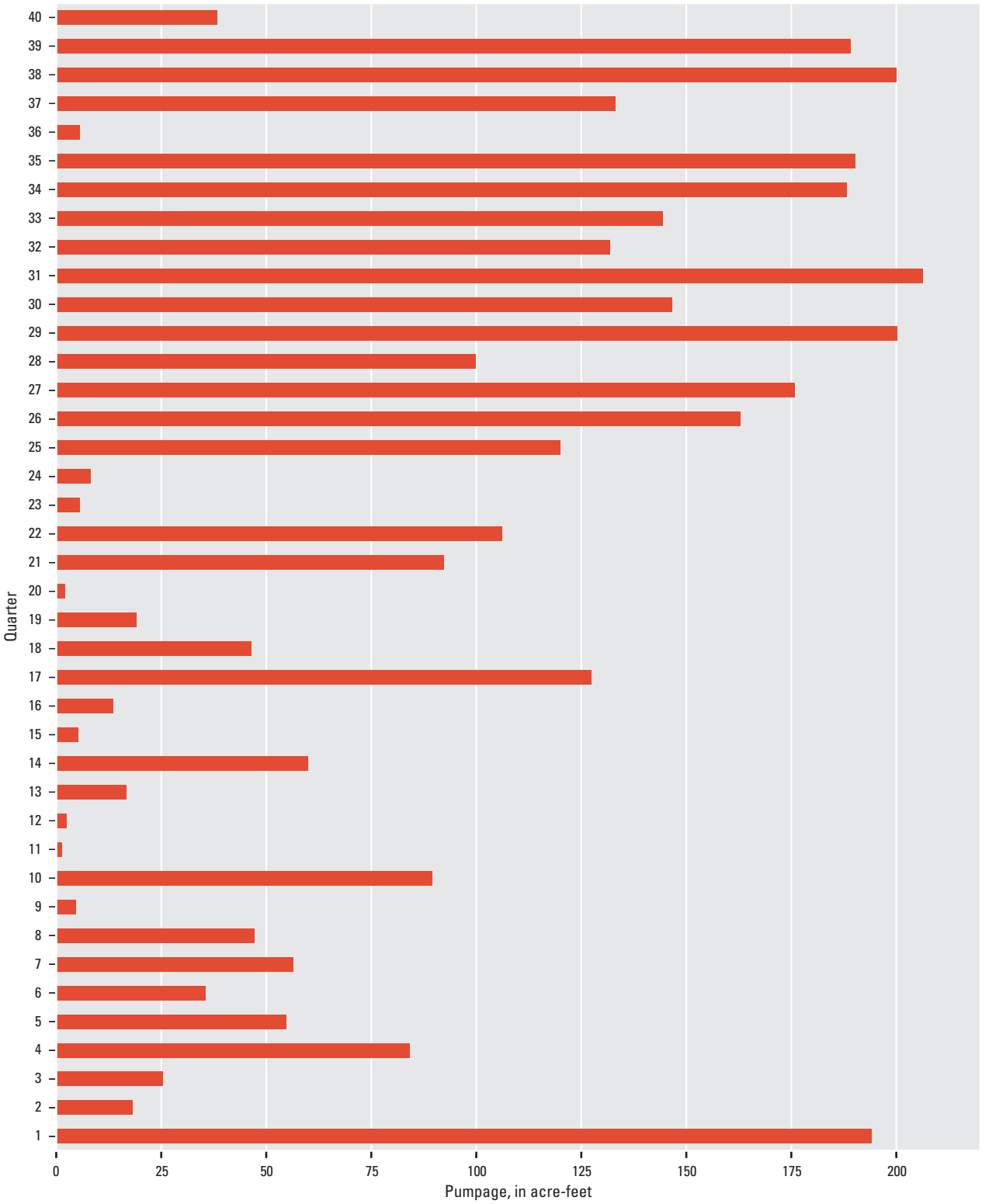

Figure D2–6. Optimal quarterly pumpage for the Vera Cruz well, schedule 2_D, Santa Barbara, California.

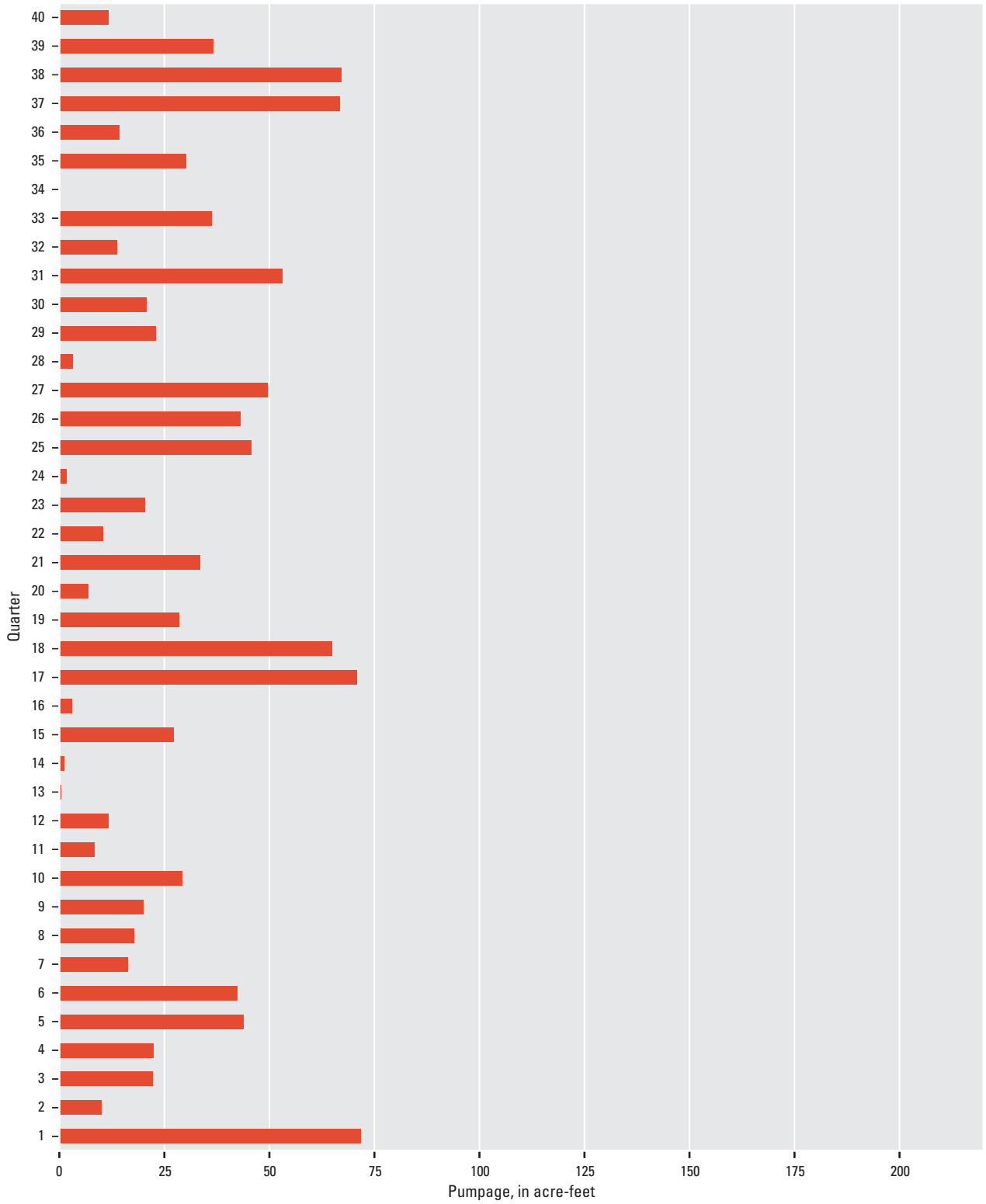

Figure D2–7. Optimal quarterly pumpage for the Hope Avenue well, schedule 2_D, Santa Barbara, California.

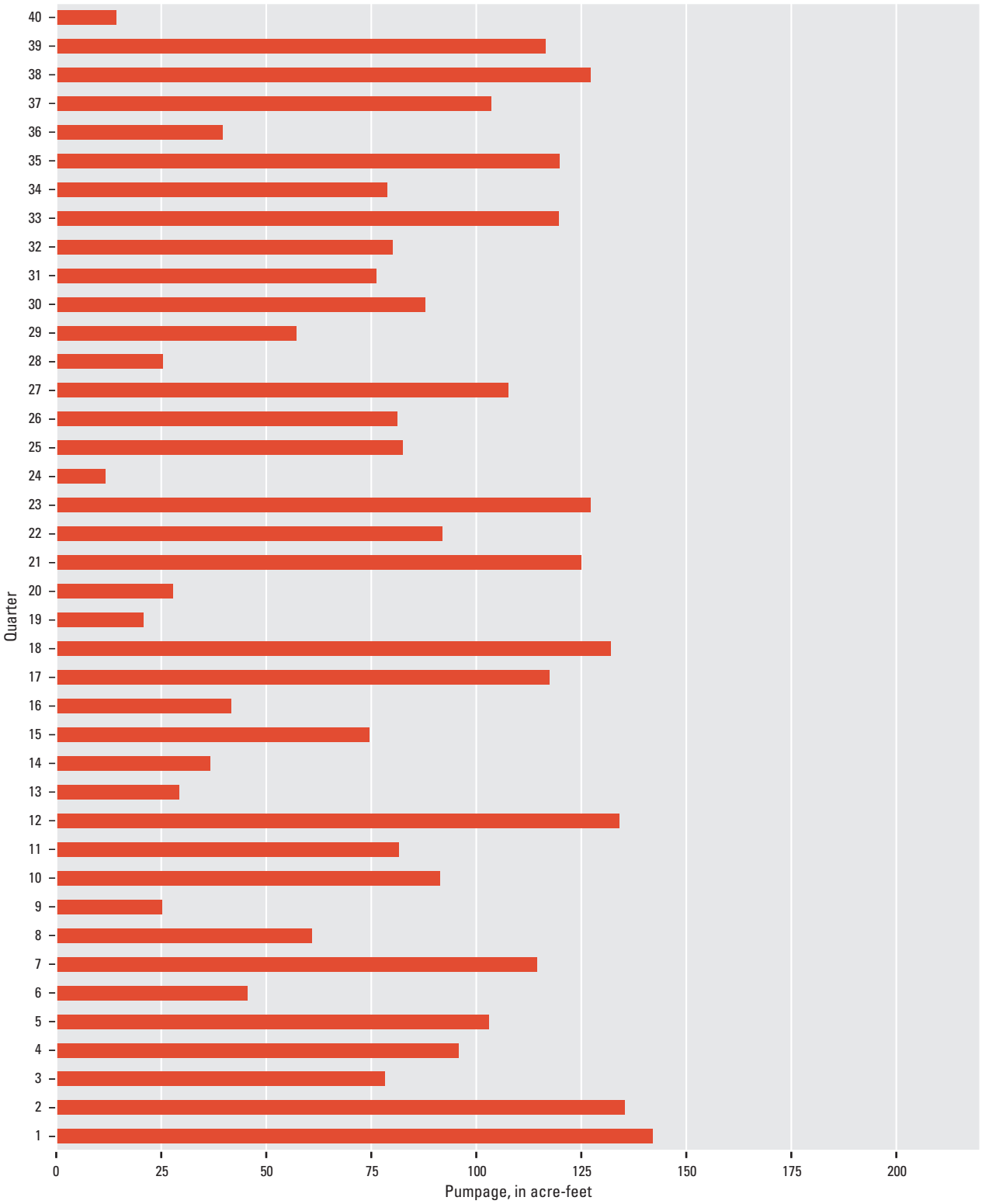

Figure D2–8. Optimal quarterly pumpage for the Lincolnwood 1 well, schedule 2_D, Santa Barbara, California.

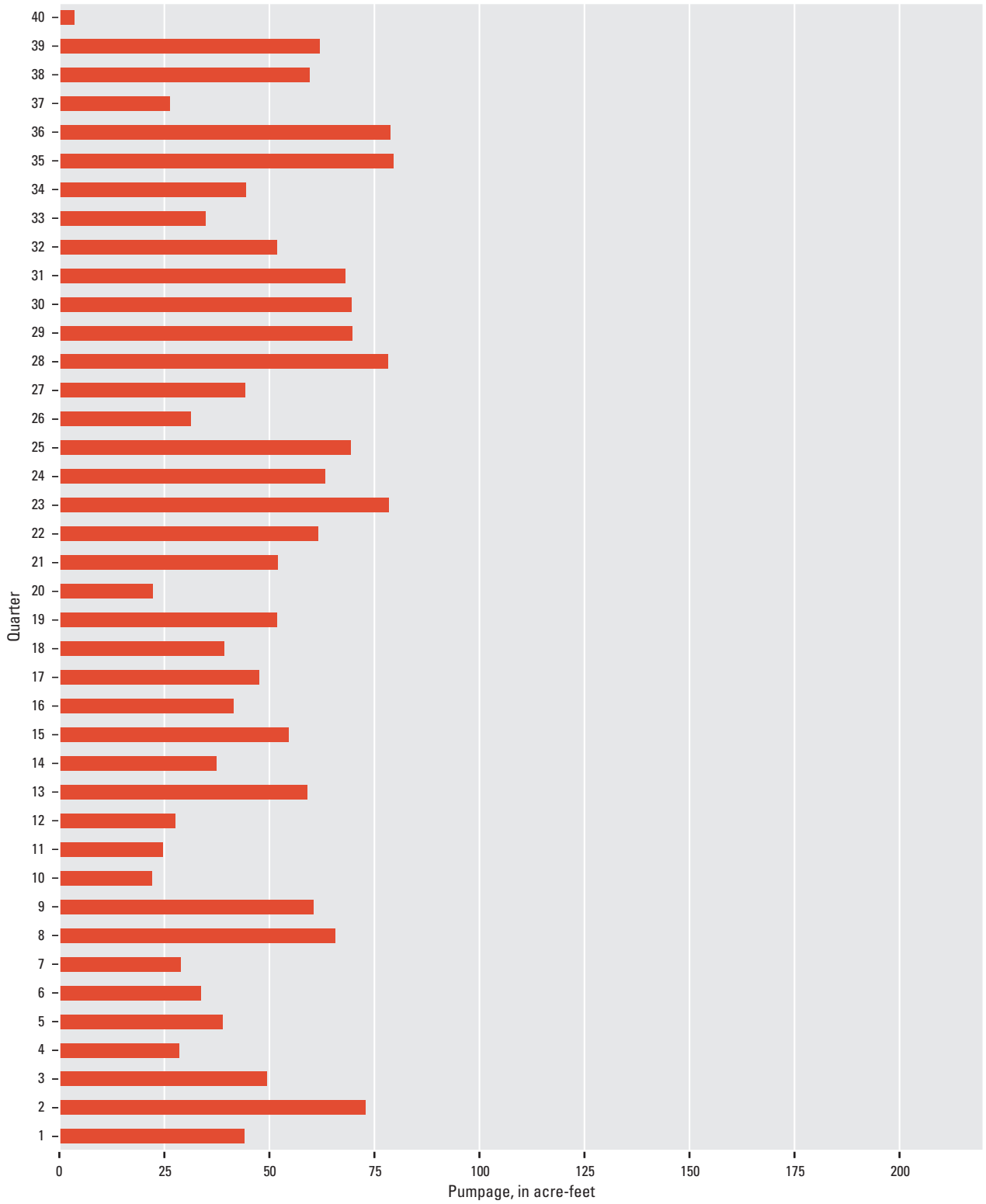

Figure D2–9. Optimal quarterly pumpage for the Los Robles well, schedule 2_D, Santa Barbara, California.

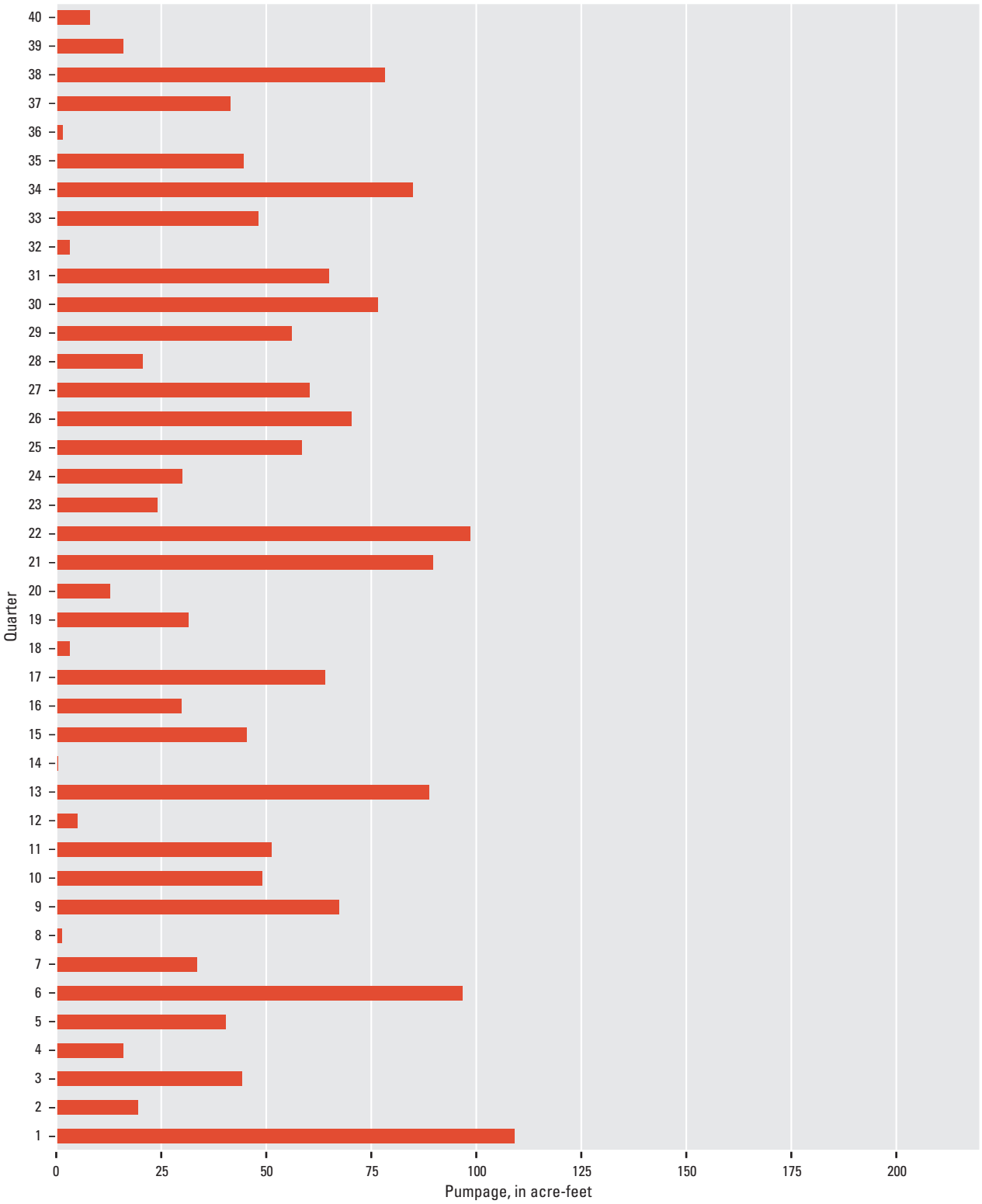

Figure D2–10. Optimal quarterly pumpage for the San Roque Park 2 well, schedule 2_D, Santa Barbara, California.

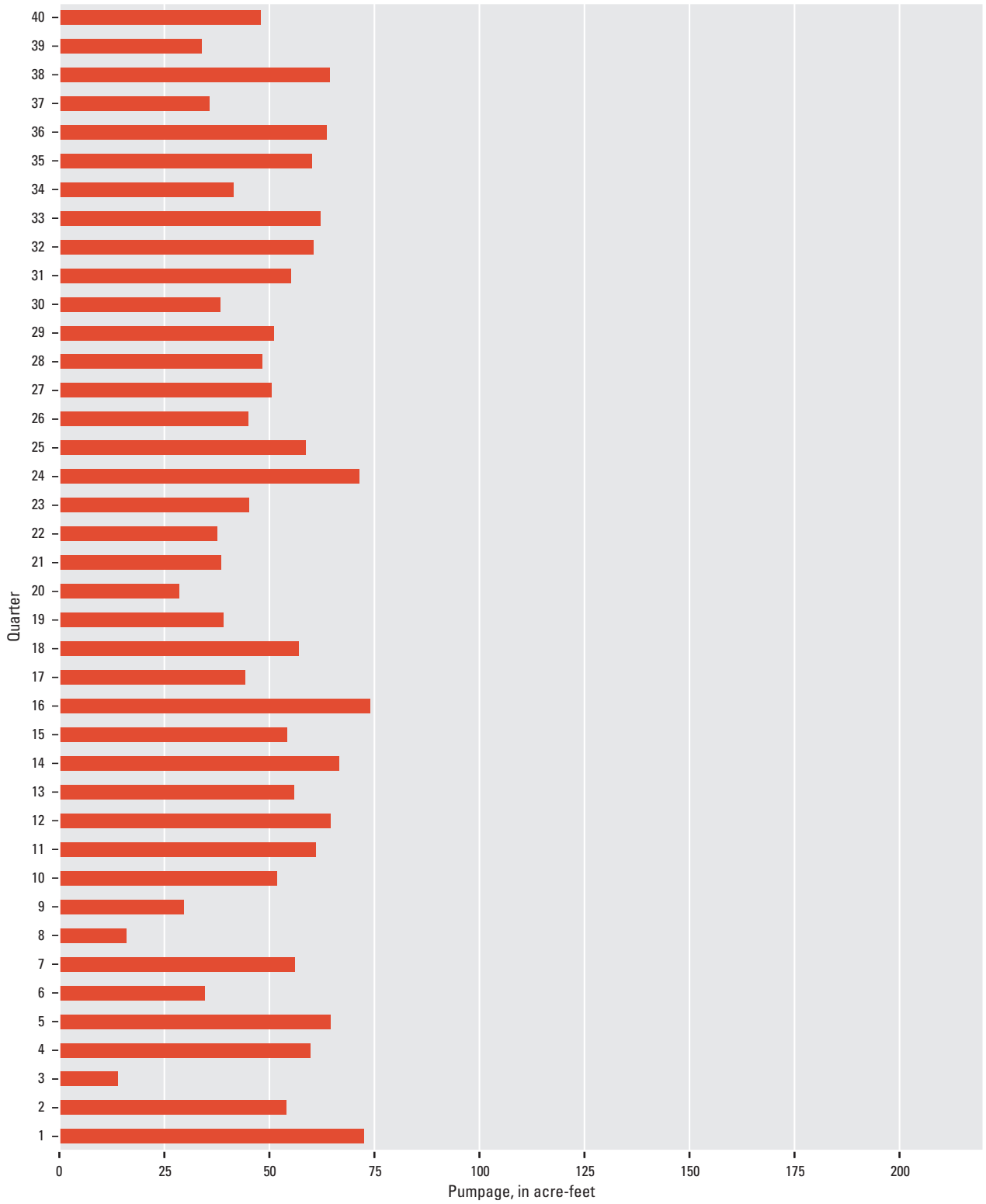

Figure D2–11. Optimal quarterly pumpage for the Val Verde well, schedule 2_D, Santa Barbara, California.

Appendix D–3: Scenario 3 Pumpage, by Well, Santa Barbara Multi-Objective Management Model, Santa Barbara, California

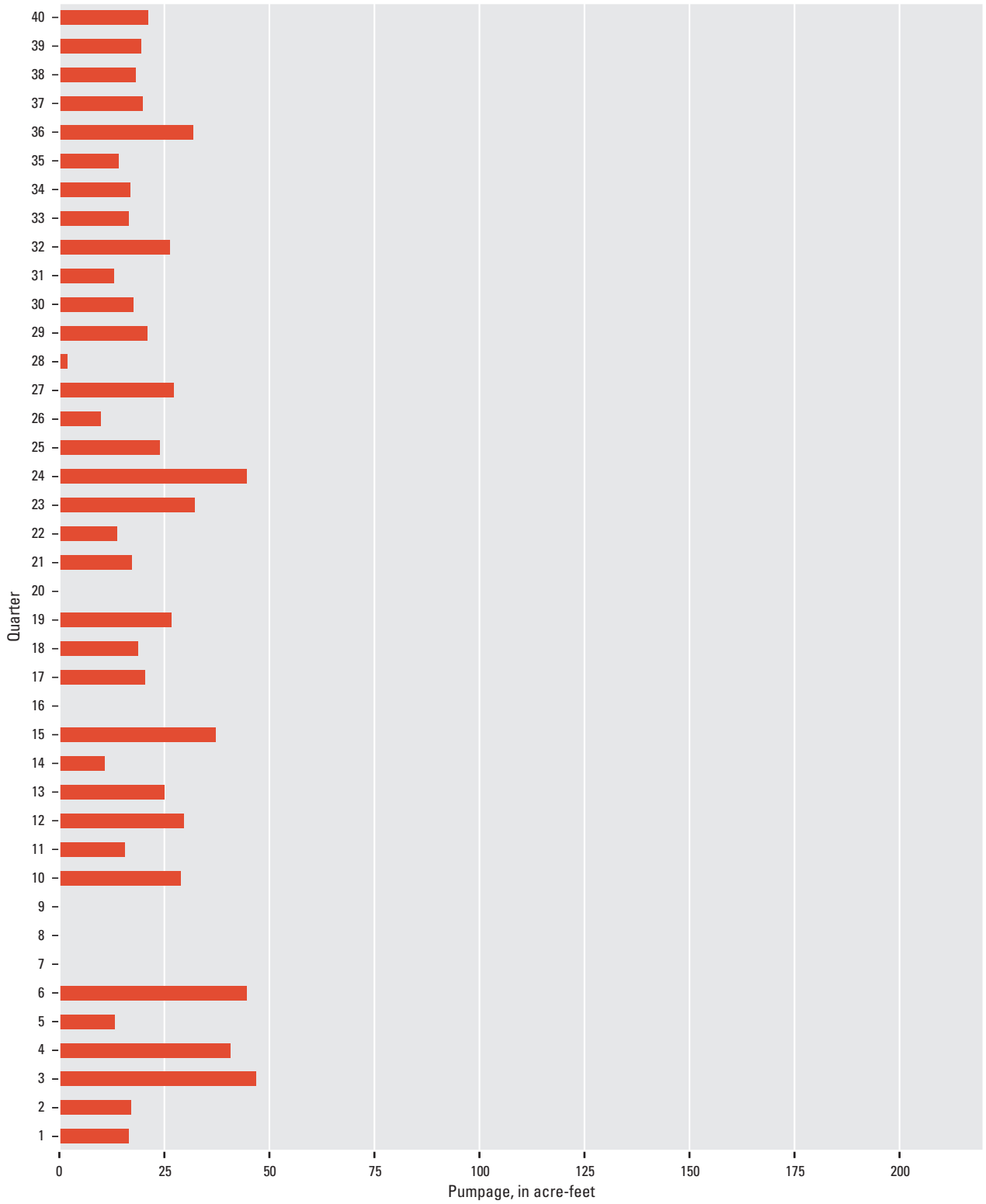

Figure D3–1. Quarterly pumpage (scaled from schedule 1_D to meet the demand of the Ortega water treatment plant) for the Alameda Park well, scenario 3, typical conditions, Santa Barbara, California.

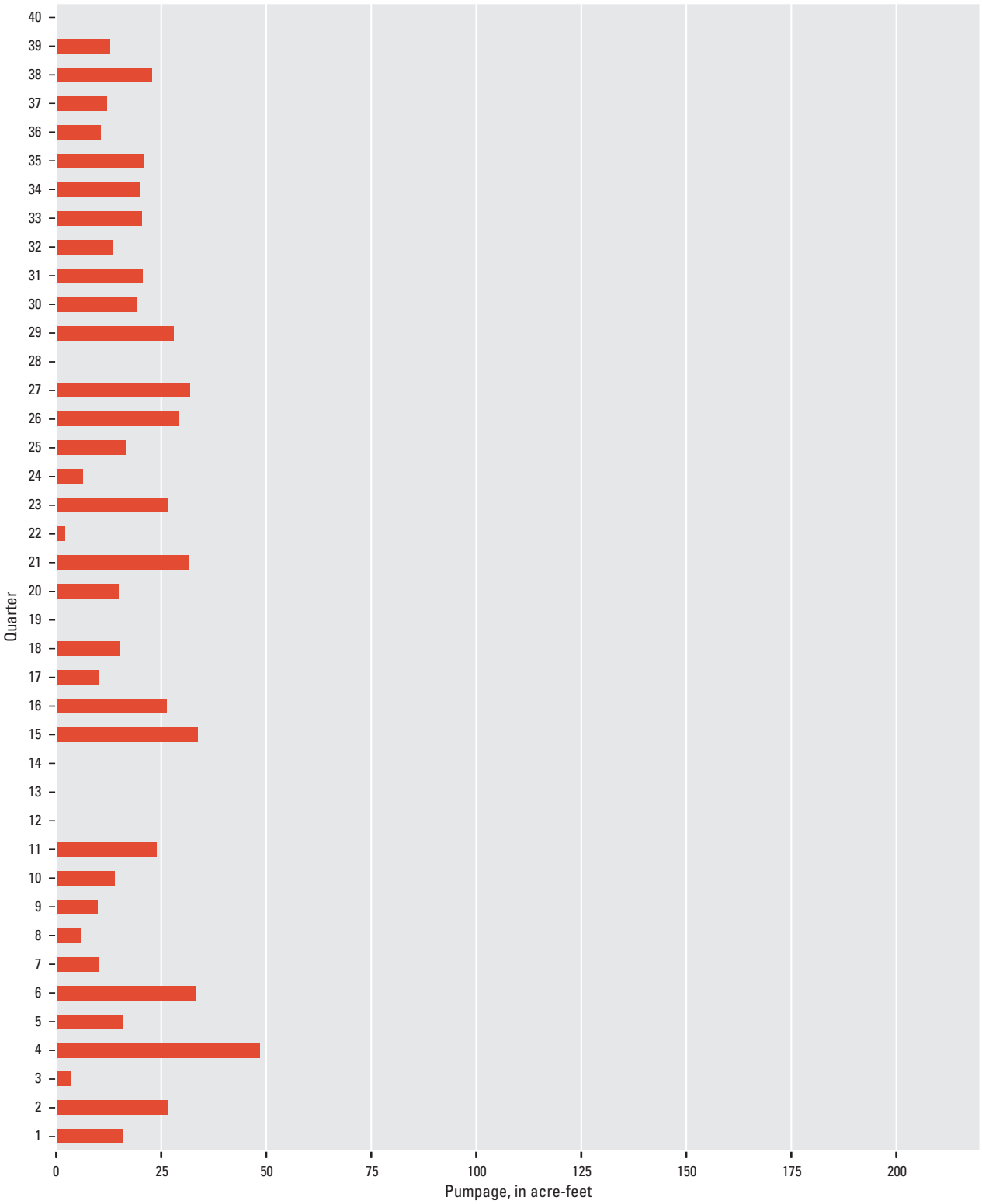

Figure D3–2. Quarterly pumpage (scaled from schedule 1_D to meet the demand of the Ortega water treatment plant) for the City Hall well, scenario 3, typical conditions, Santa Barbara, California.

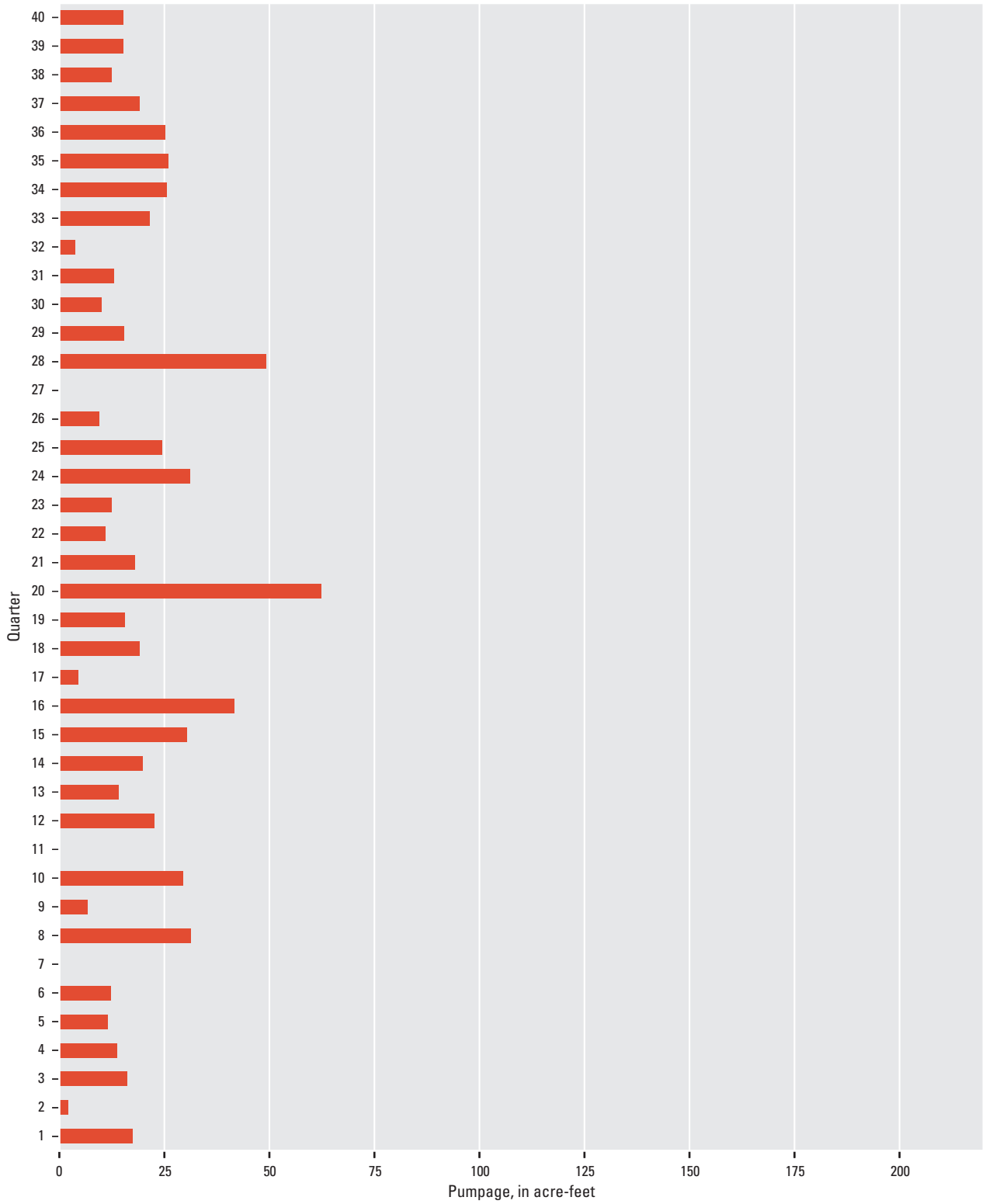

Figure D3–3. Quarterly pumpage (scaled from schedule 1_D to meet the demand of the Ortega water treatment plant) for the Corporation Yard well, scenario 3, typical conditions, Santa Barbara, California.

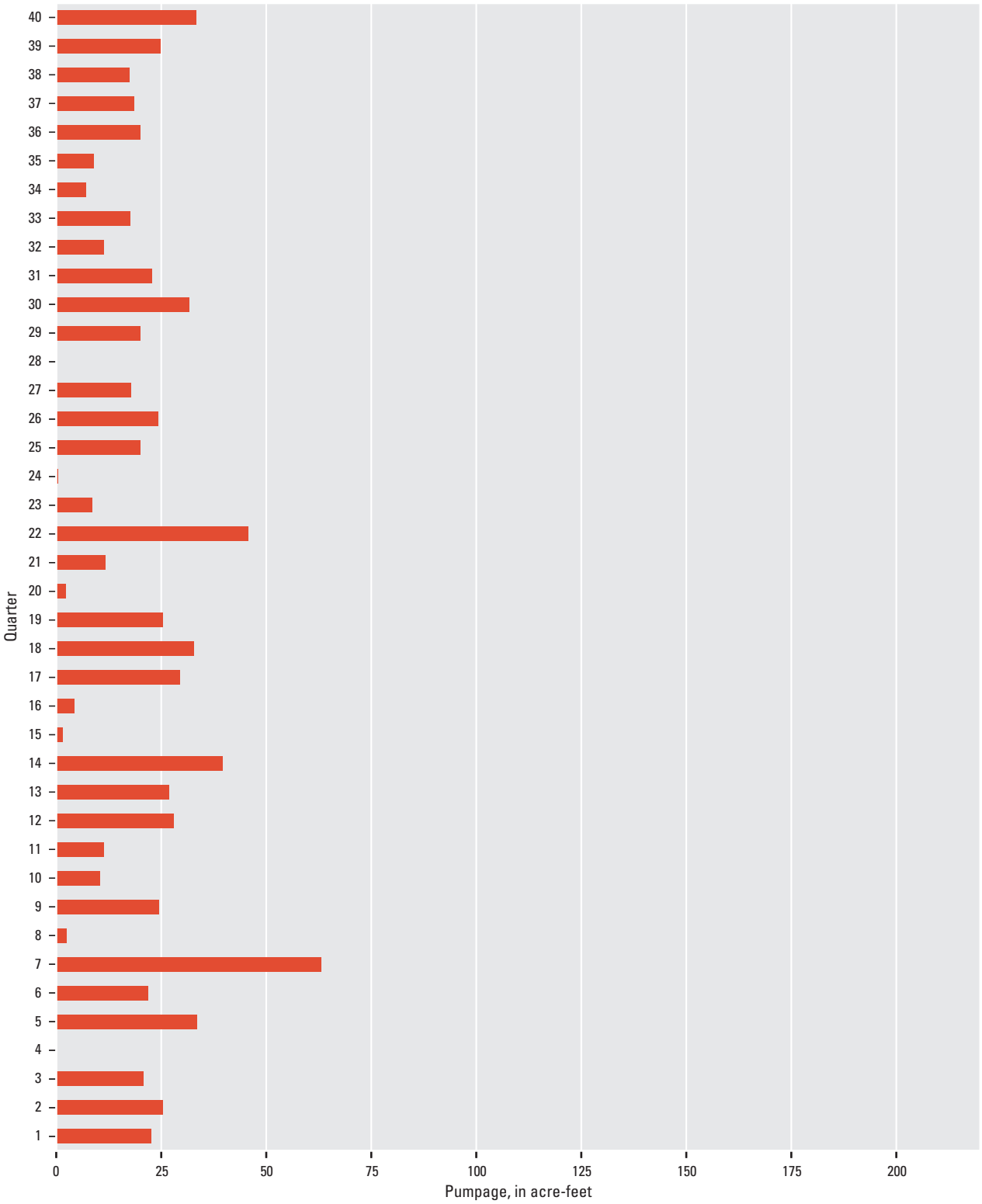

Figure D3–4. Quarterly pumpage (scaled from schedule 1_D to meet the demand of the Ortega water treatment plant) for the Ortega Park well, scenario 3, typical conditions, Santa Barbara, California.

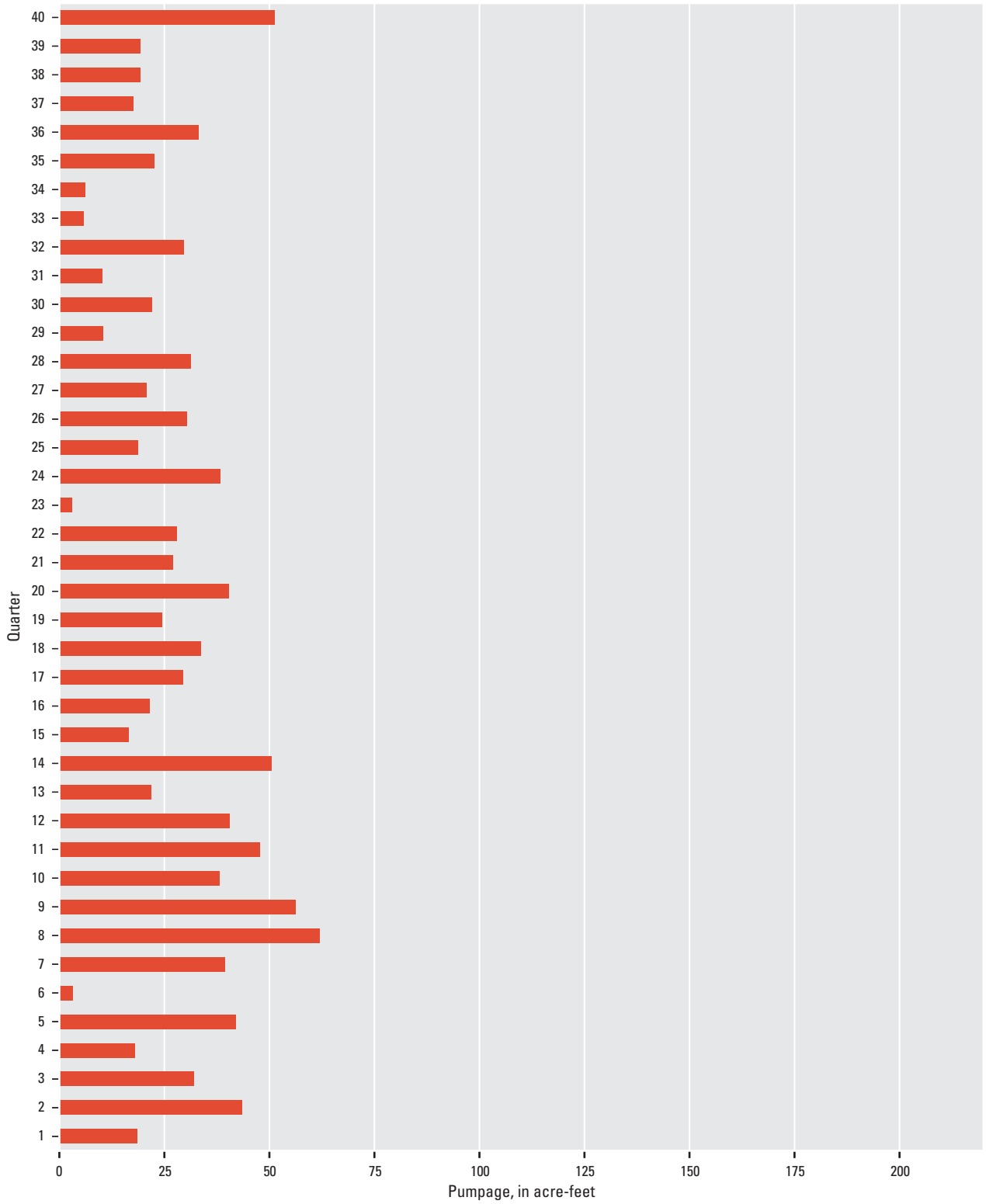

Figure D3–5. Quarterly pumpage (scaled from schedule 1_D to meet the demand of the Ortega water treatment plant) for the Santa Barbara High School well, scenario 3, typical conditions, Santa Barbara, California.

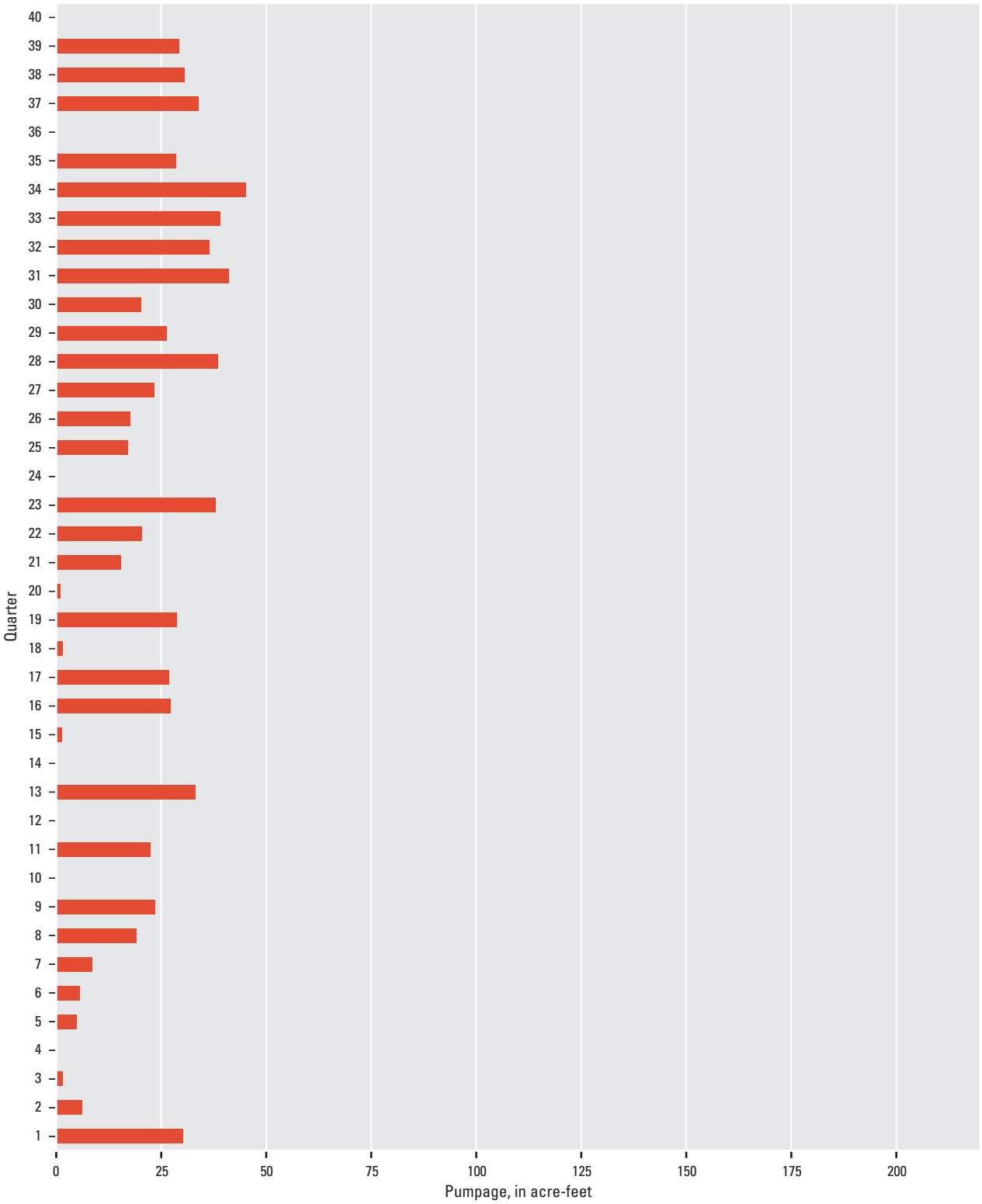

Figure D3–6. Quarterly pumpage (scaled from schedule 1_D to meet the demand of the Ortega water treatment plant) for the Vera Cruz well, scenario 3, typical conditions, Santa Barbara, California.

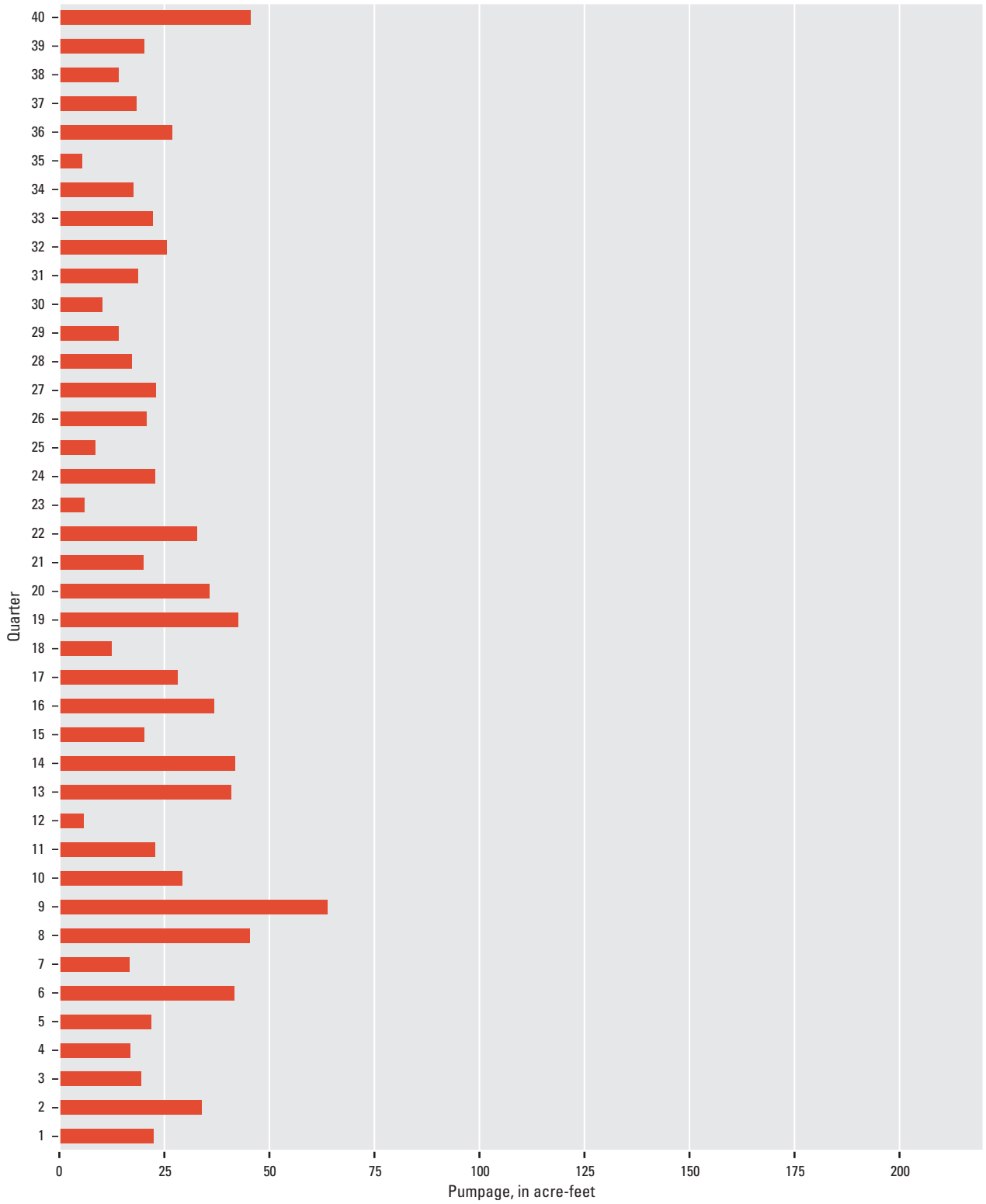

Figure D3–7. Quarterly pumpage (scaled from schedule 2_D to meet the demand of the Ortega water treatment plant) for the Alameda Park well, scenario 3, drought conditions, Santa Barbara, California.

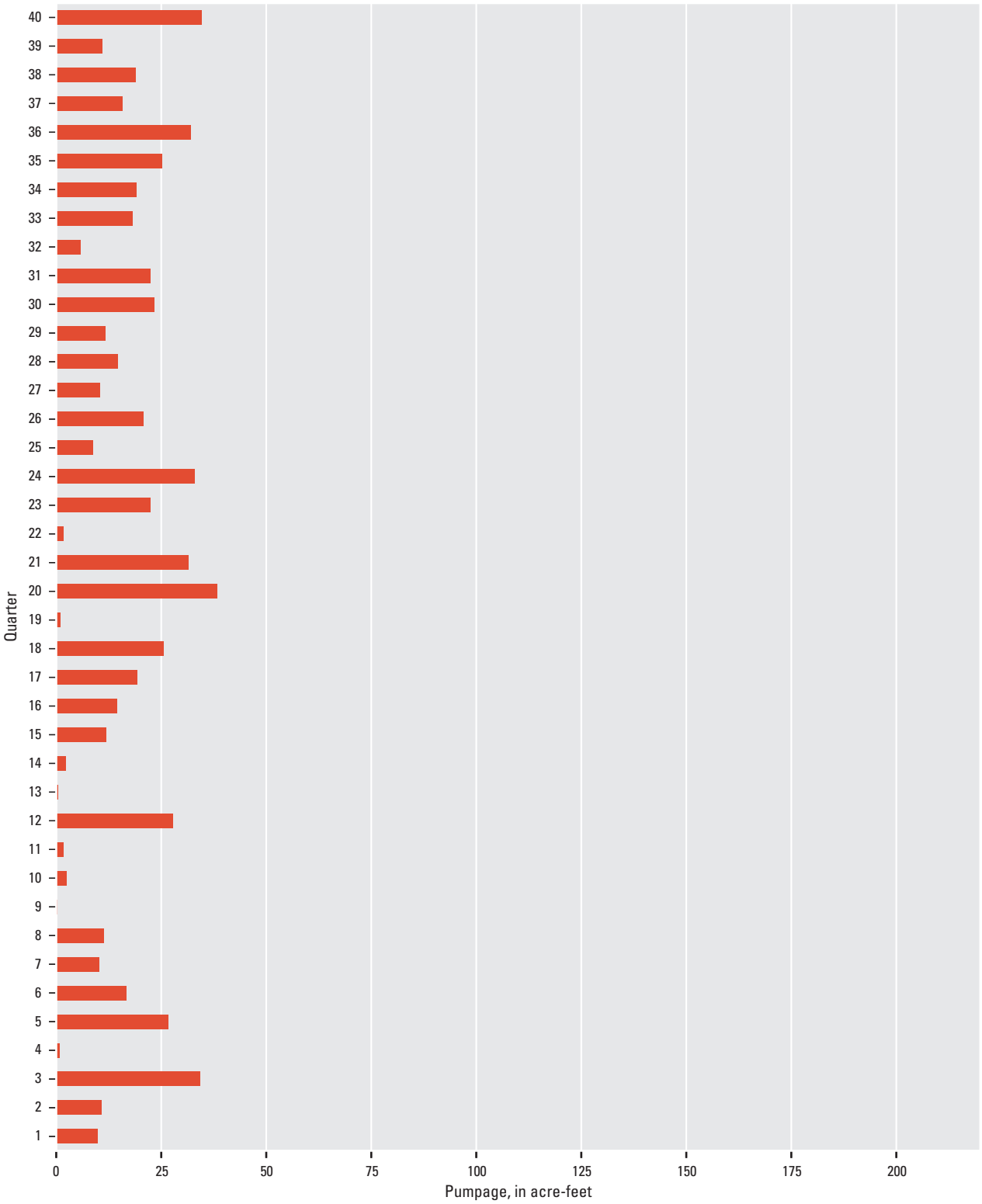

Figure D3–8. Quarterly pumpage (scaled from schedule 2_D to meet the demand of the Ortega water treatment plant) for the City Hall well, scenario 3, drought conditions, Santa Barbara, California.

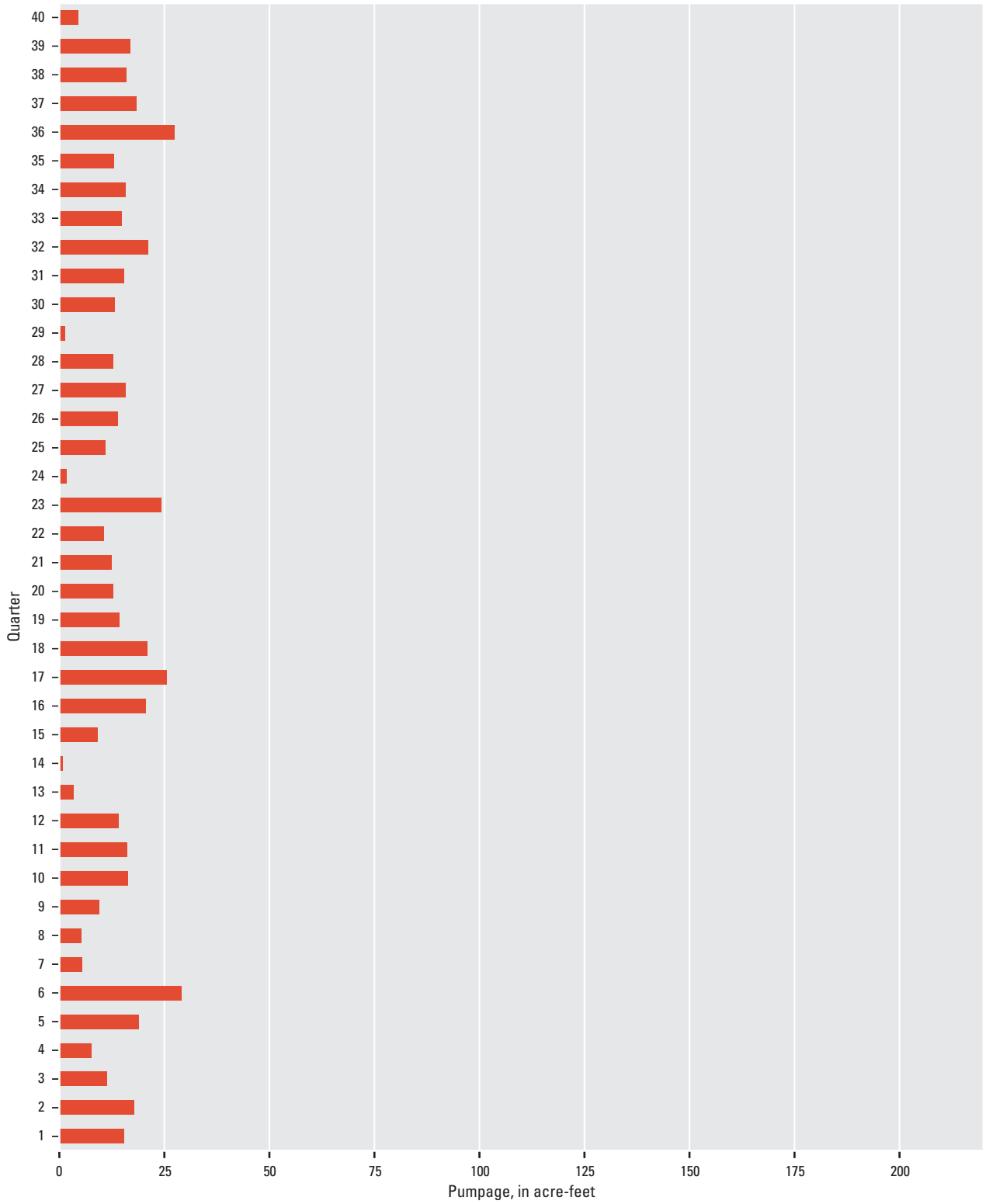

Figure D3–9. Quarterly pumpage (scaled from schedule 2_D to meet the demand of the Ortega water treatment plant) for the Corporation Yard well, scenario 3, drought conditions, Santa Barbara, California.

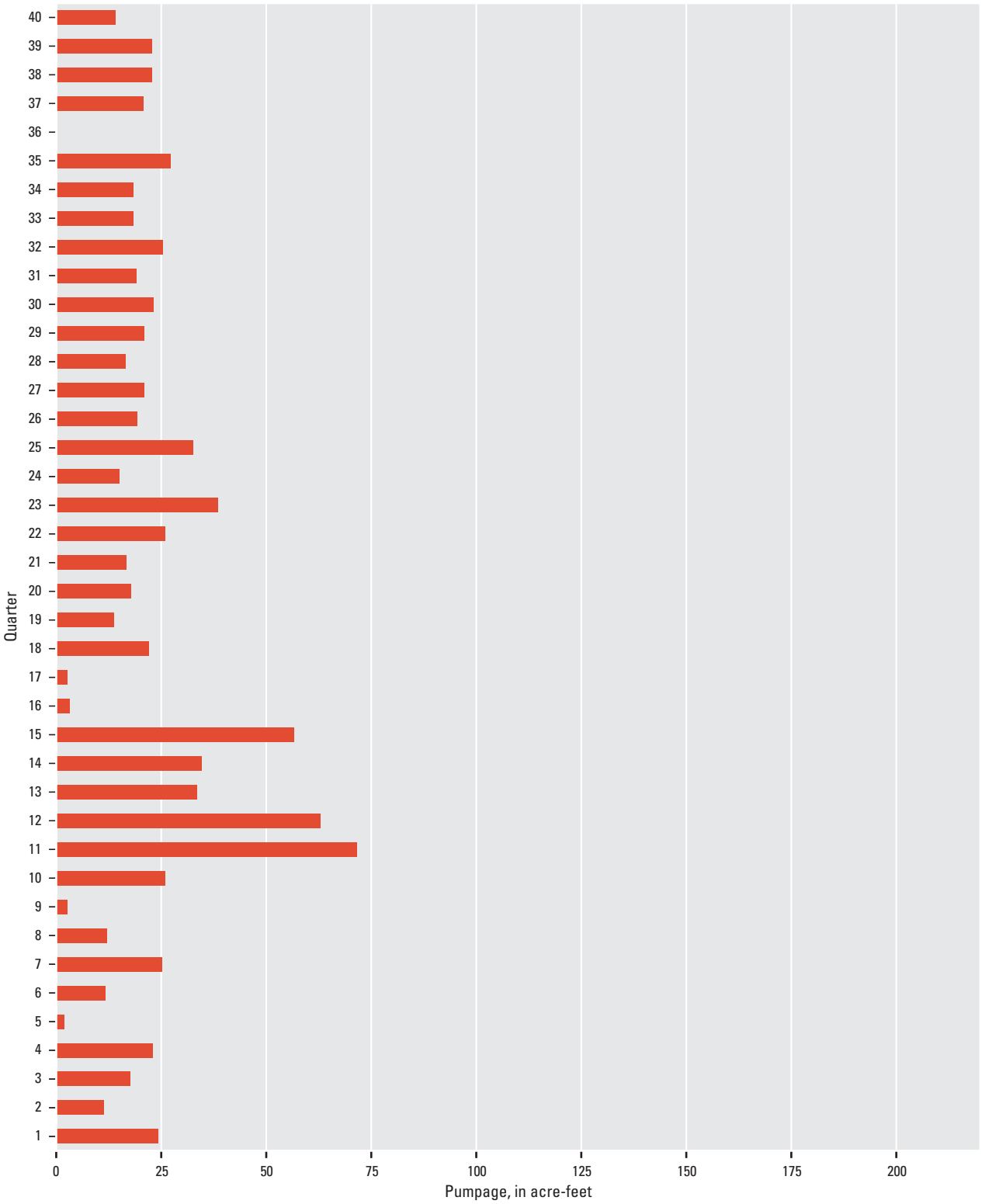

Figure D3–10. Quarterly pumpage (scaled from schedule 2_D to meet the demand of the Ortega water treatment plant) for the Ortega Park well, scenario 3, drought conditions, Santa Barbara, California.

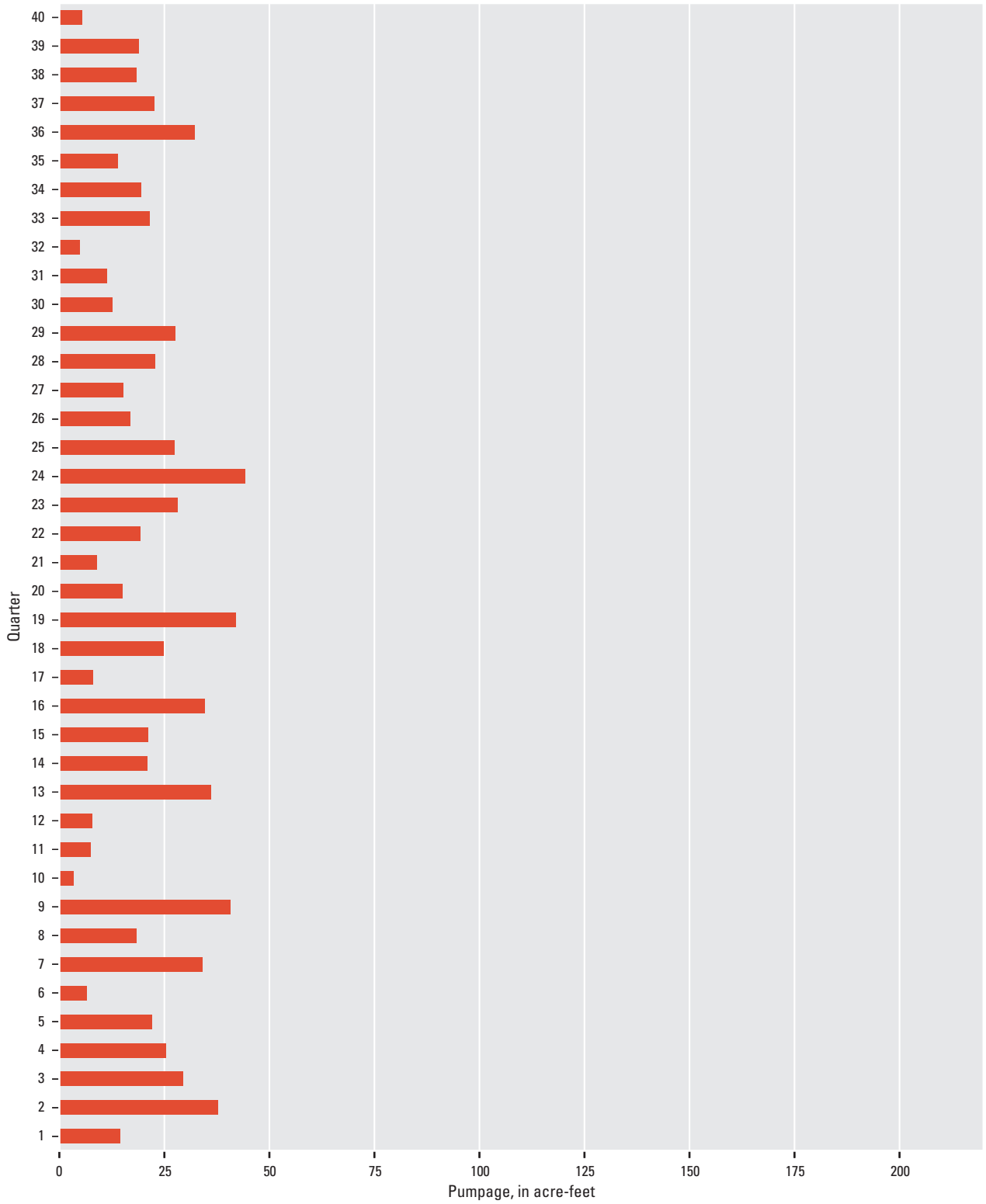

Figure D3–11. Quarterly pumpage (scaled from schedule 2_D to meet the demand of the Ortega water treatment plant) for the Santa Barbara High School well, scenario 3, drought conditions, Santa Barbara, California.

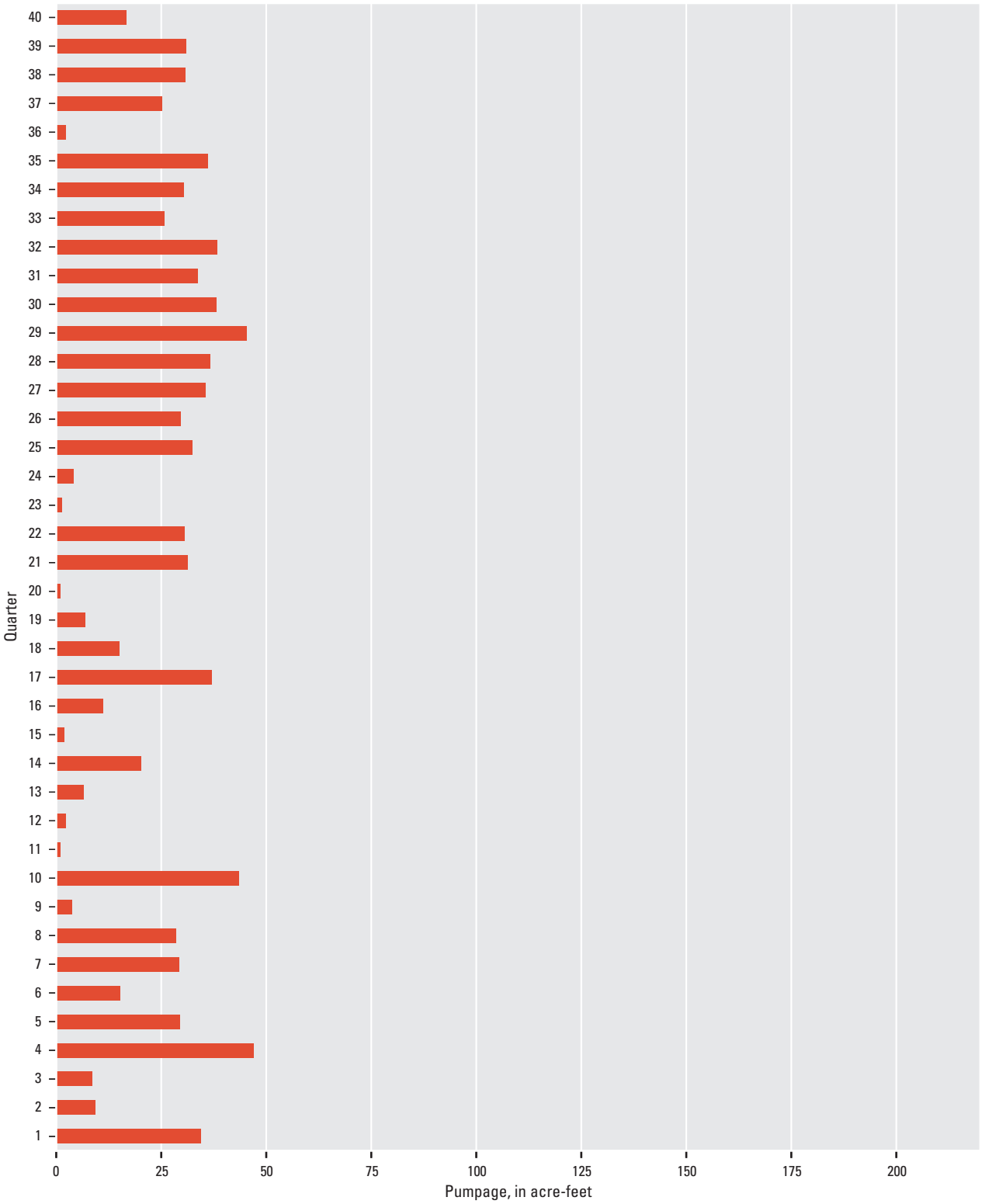

Figure D3–12. Quarterly pumpage (scaled from schedule 2_D to meet the demand of the Ortega water treatment plant) for the Vera Cruz well, scenario 3, drought conditions, Santa Barbara, California.

Appendix D–4: Scenario 4B Decision Rules, Santa Barbara Multi-Objective Management Model, Santa Barbara, California

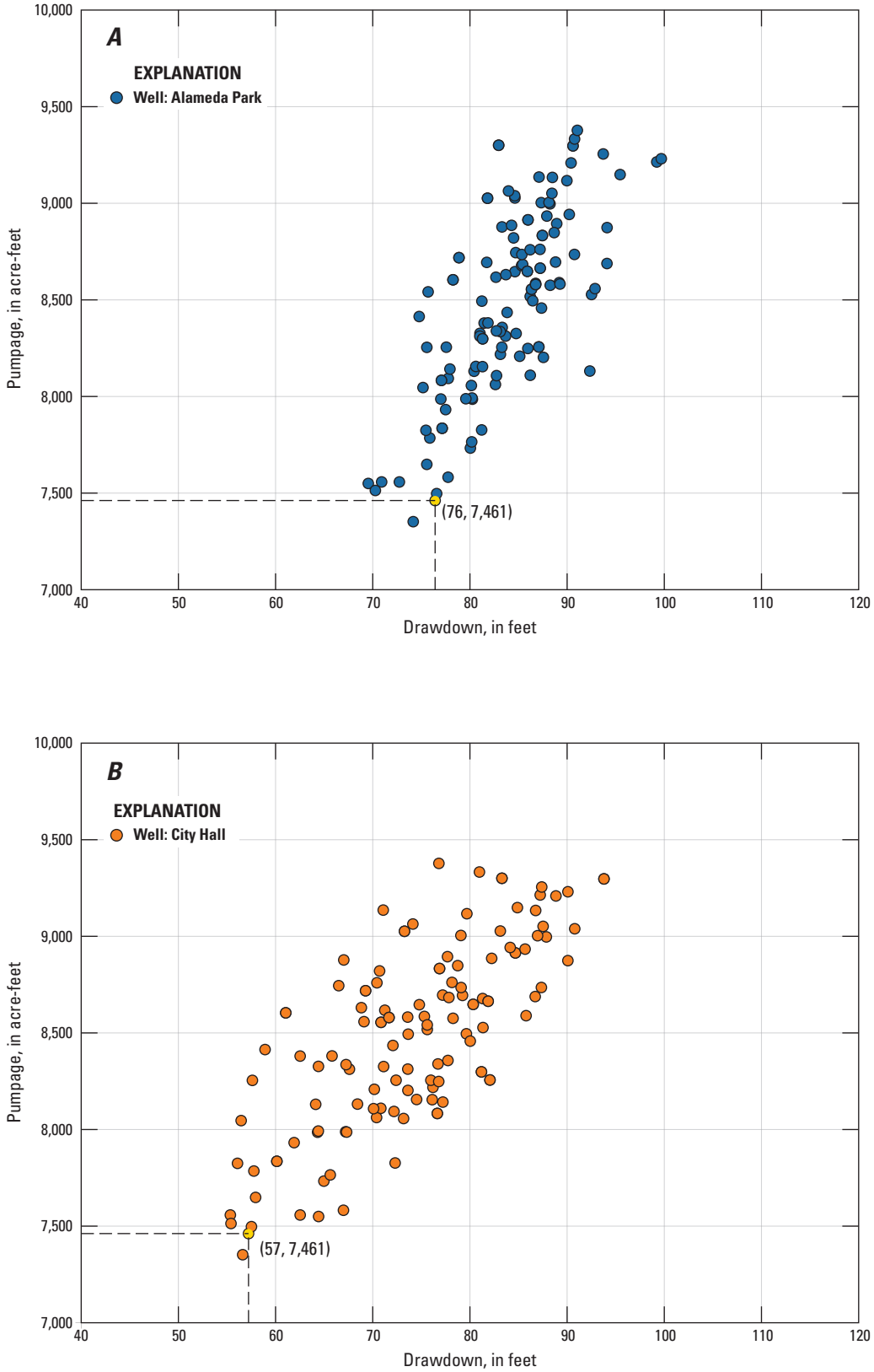

Figure D4–1. Decision rules for total Foothill groundwater basin pumpage as a function of maximum drawdown at the city of Santa Barbara production wells assuming scenario 1 (typical) precipitation, Santa Barbara groundwater basin, Santa Barbara, California (the yellow dot represents the total schedule 1_D pumpage for Foothill groundwater basin), *A*, Alameda Park; *B*, City Hall; *C*, Corporation Yard; *D*, Hope Avenue; *E*, Lincolnwood 1; *F*, Los Robles; *G*, Ortega Park; *H*, San Roque Park 2; *I*, Santa Barbara High School; *J*, Val Verde; and *K*, Vera Cruz.

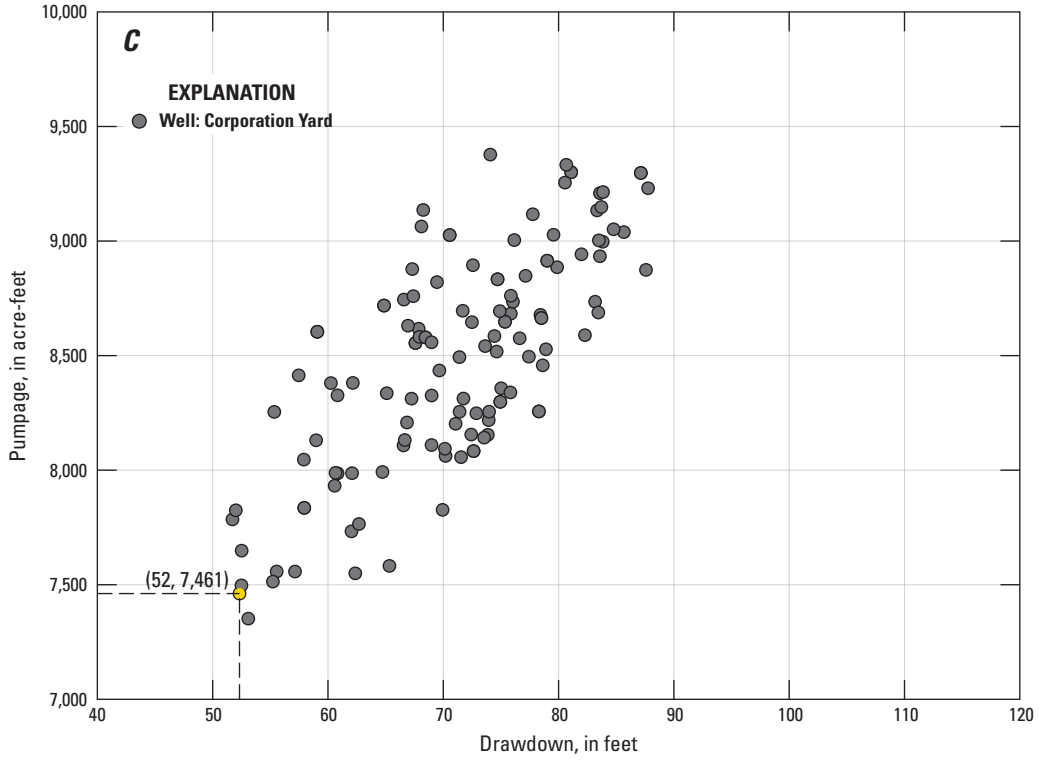

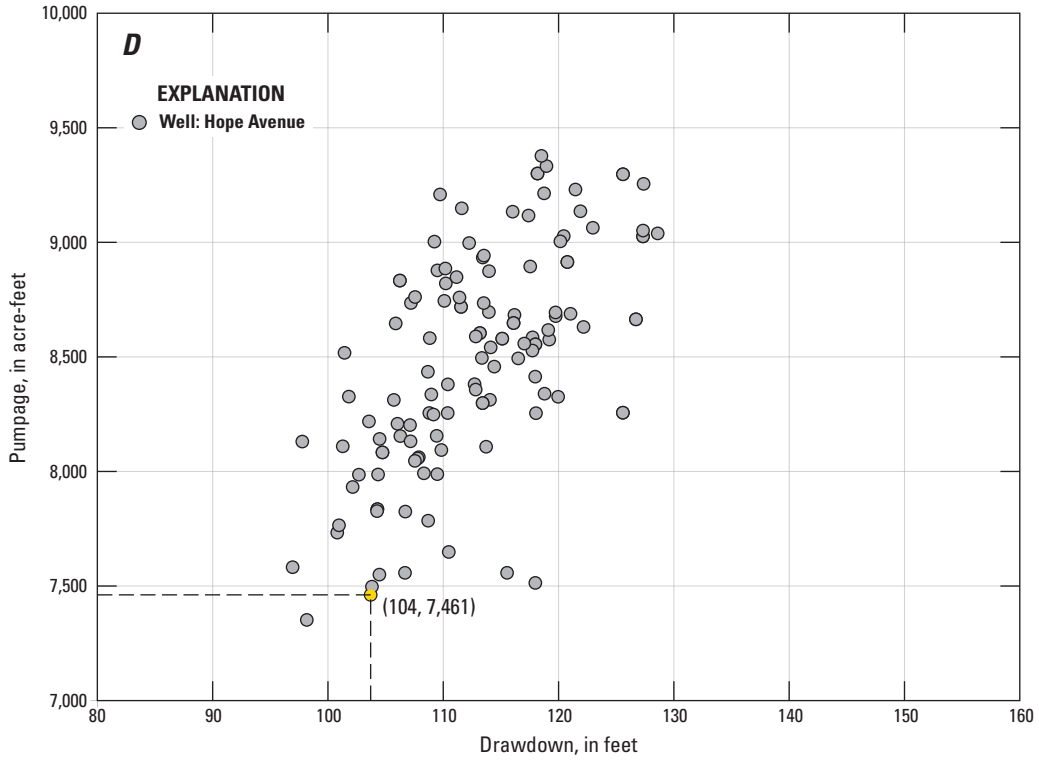

Figure D4–1. —Continued

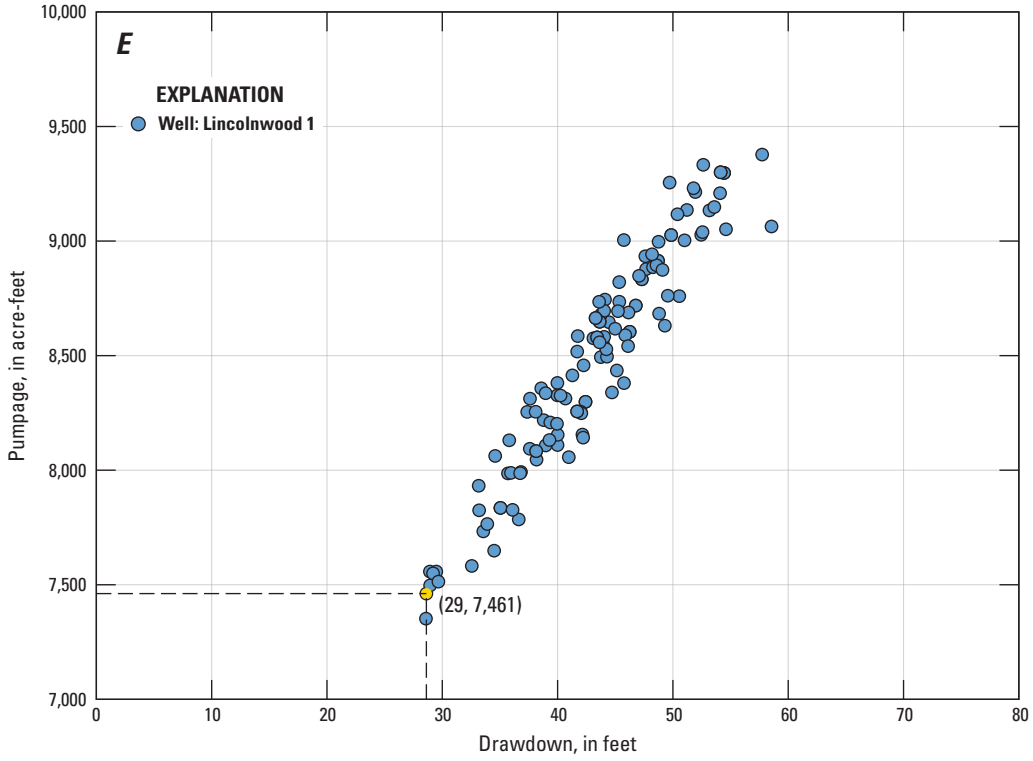

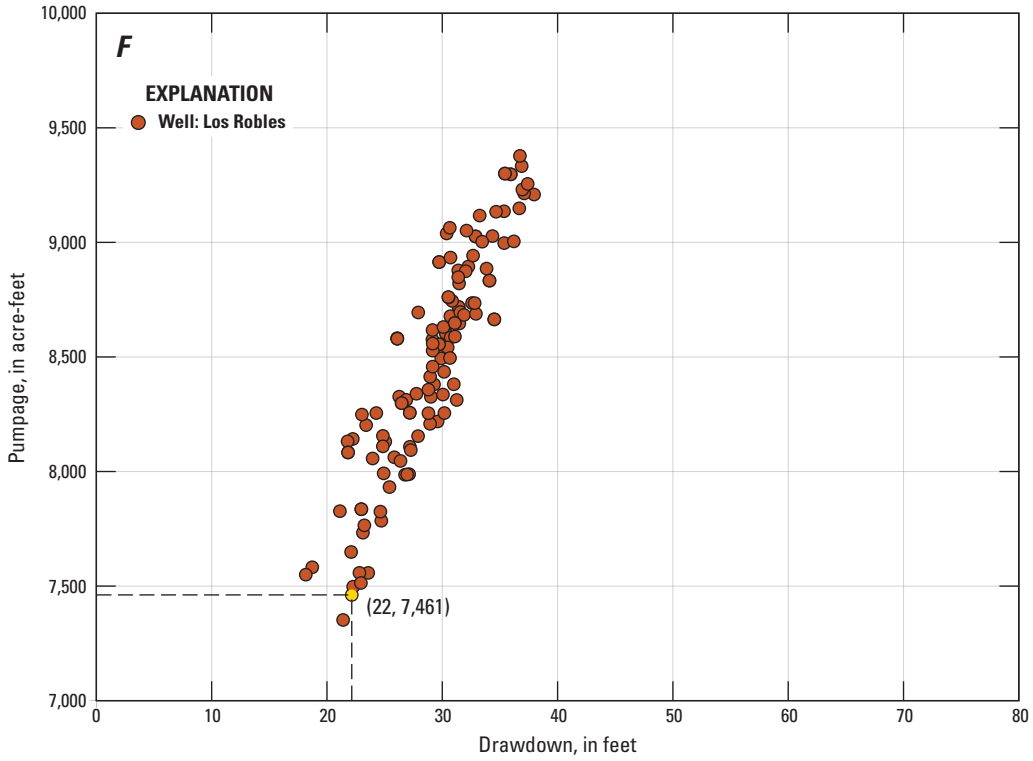

Figure D4–1. —Continued

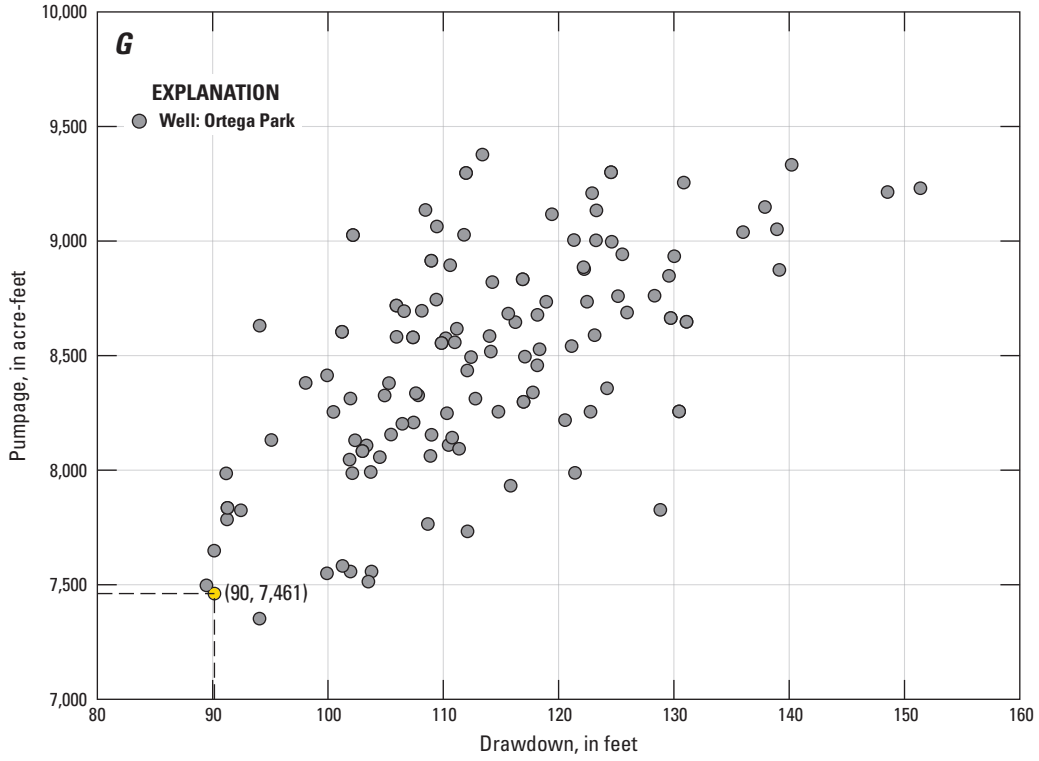

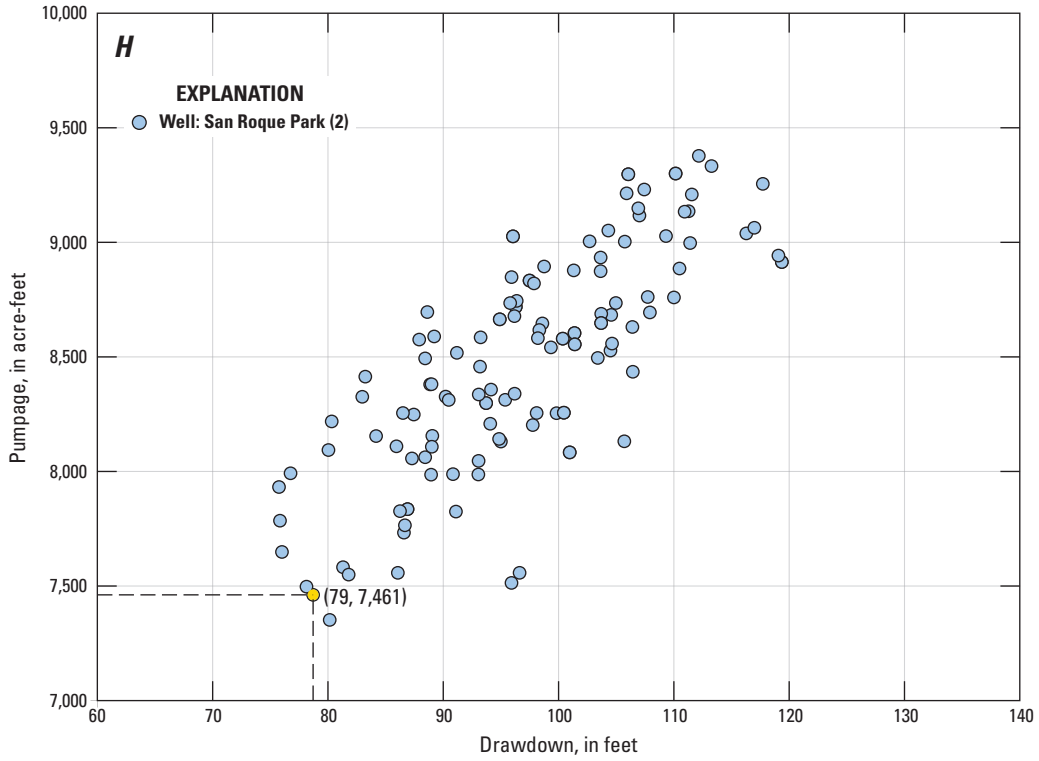

Figure D4–1. —Continued

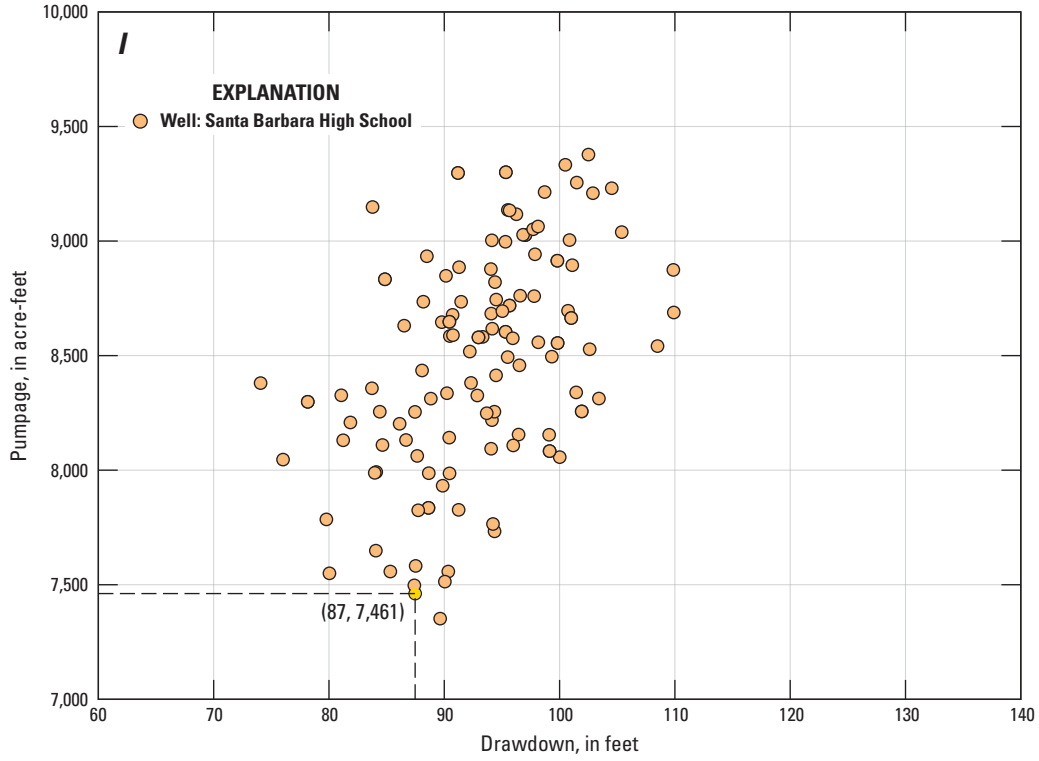

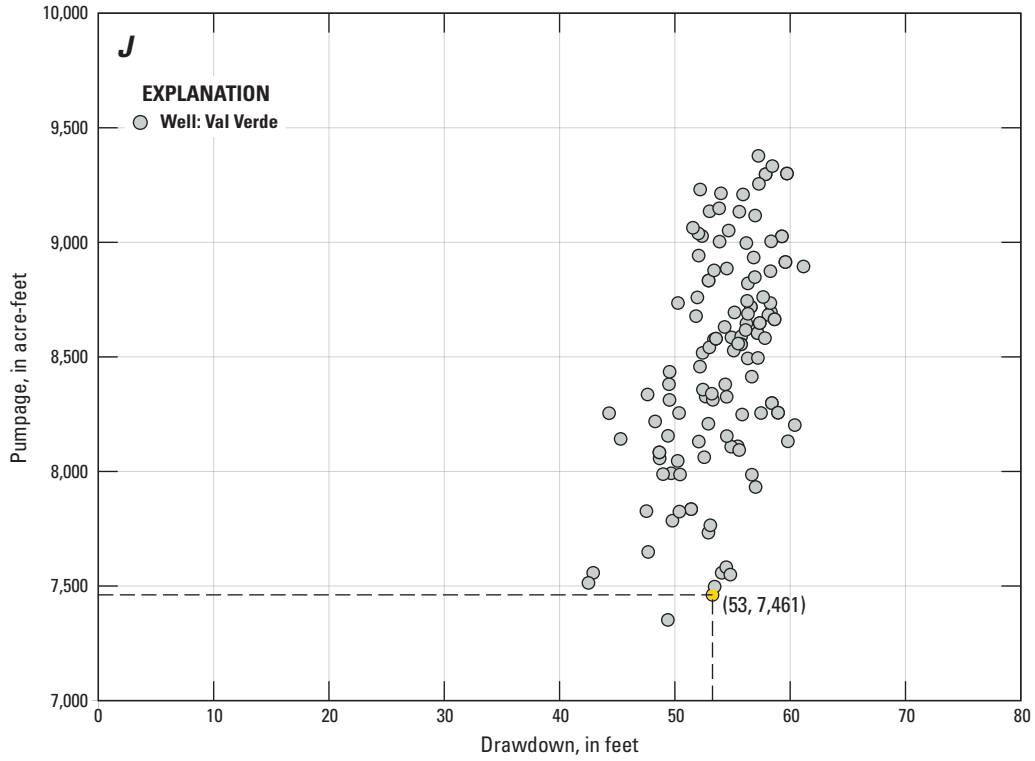

Figure D4–1. —Continued

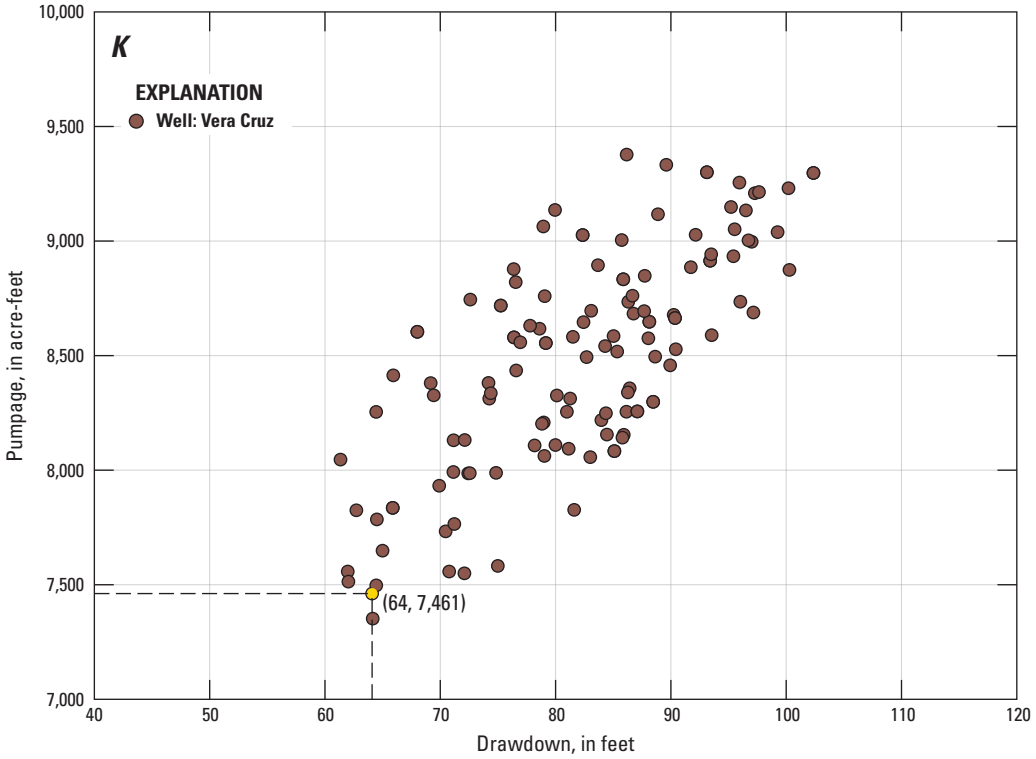

Figure D4–1. —Continued

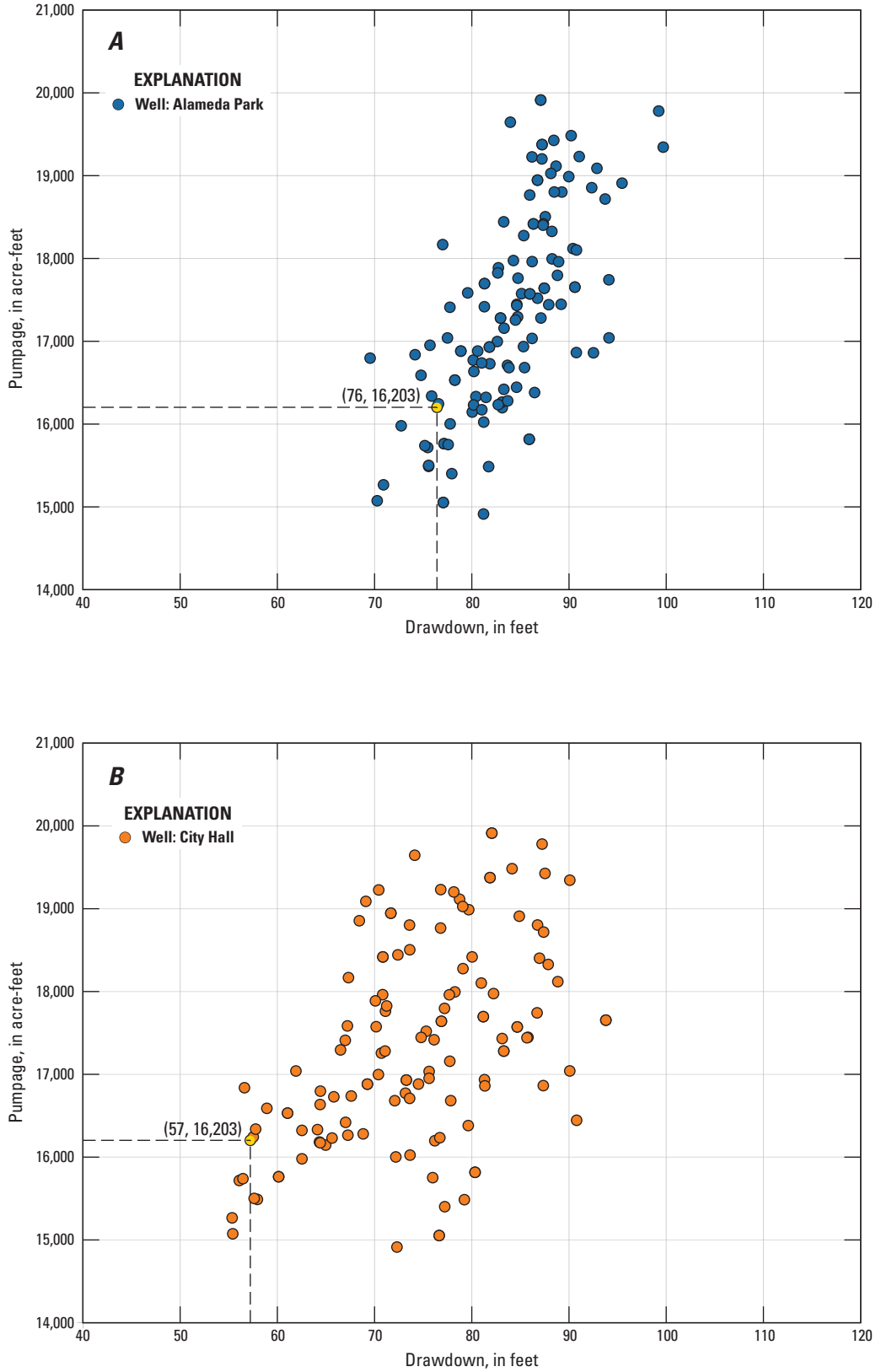

Figure D4–2. Decision rules for total Storage Unit I pumpage as a function of maximum drawdown at the city of Santa Barbara production wells assuming scenario 1 (typical) precipitation, Santa Barbara groundwater basin, Santa Barbara, California (the yellow dot represents the total schedule 1_D pumpage for Storage Unit I), *A*, Alameda Park; *B*, City Hall; *C*, Corporation Yard; *D*, Hope Avenue; *E*, Lincolnwood 1; *F*, Los Robles; *G*, Ortega Park; *H*, San Roque Park 2; *I*, Santa Barbara High School; *J*, Val Verde; and *K*, Vera Cruz.

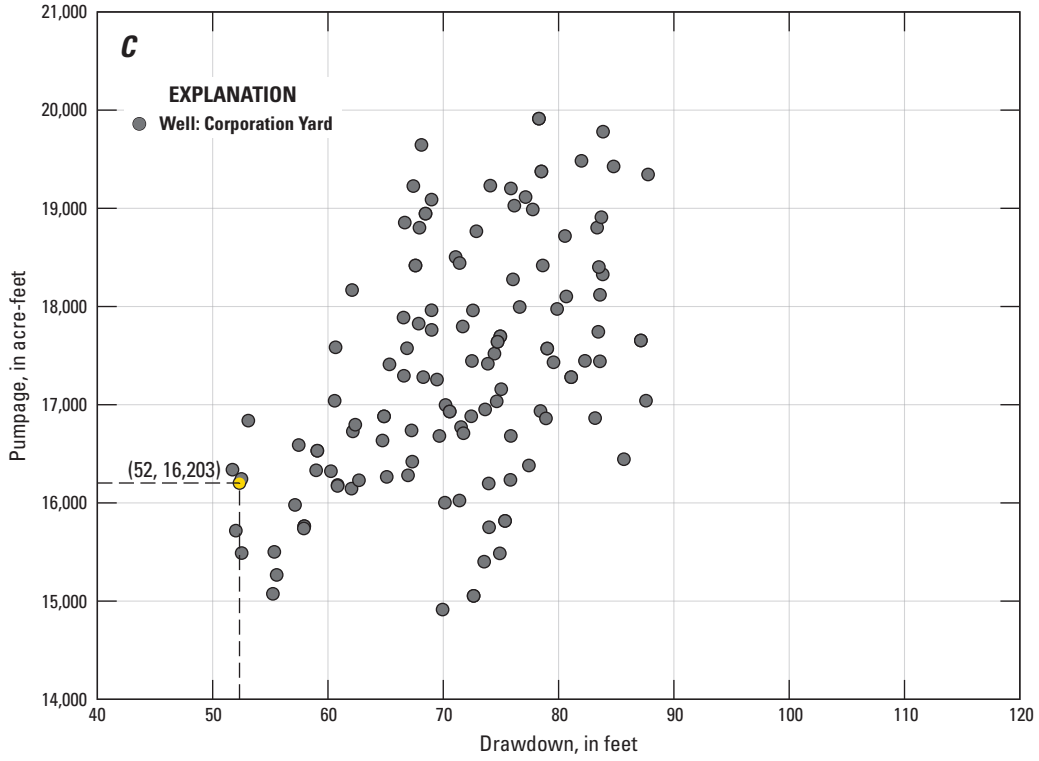

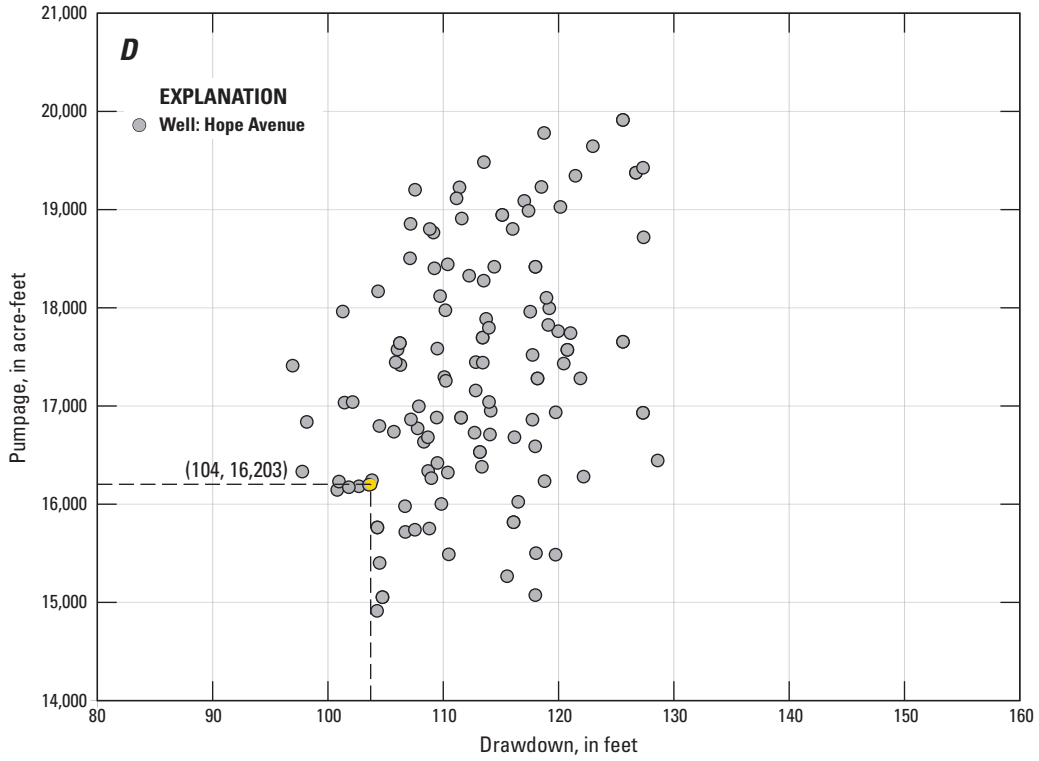

Figure D4–2. —Continued

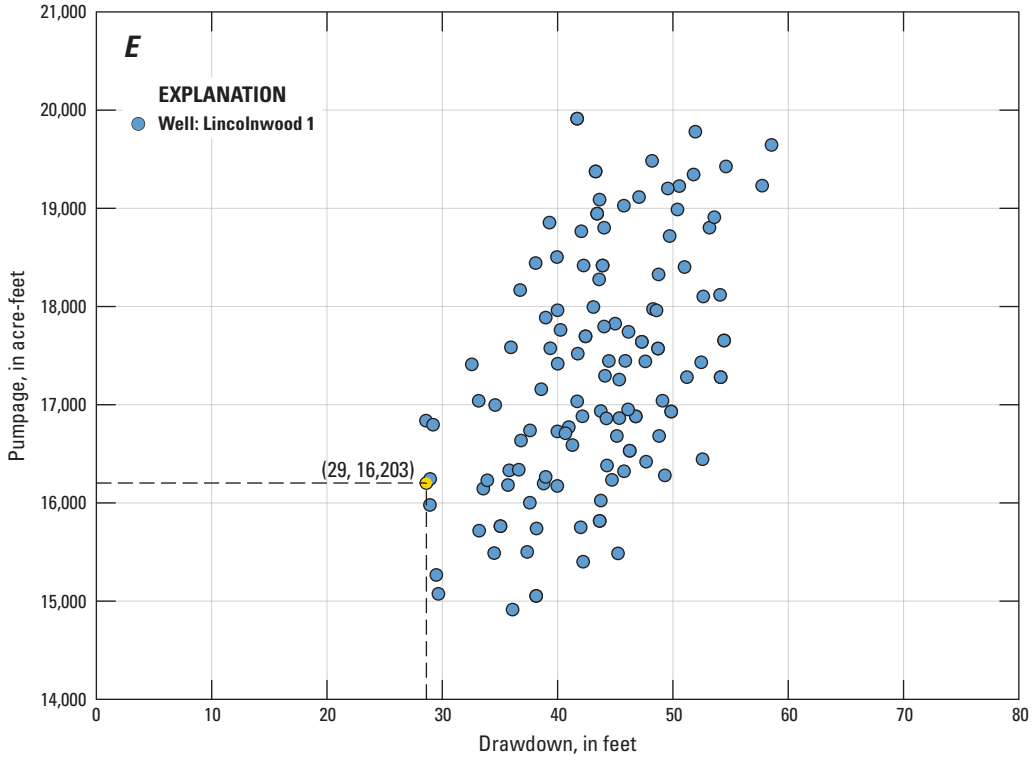

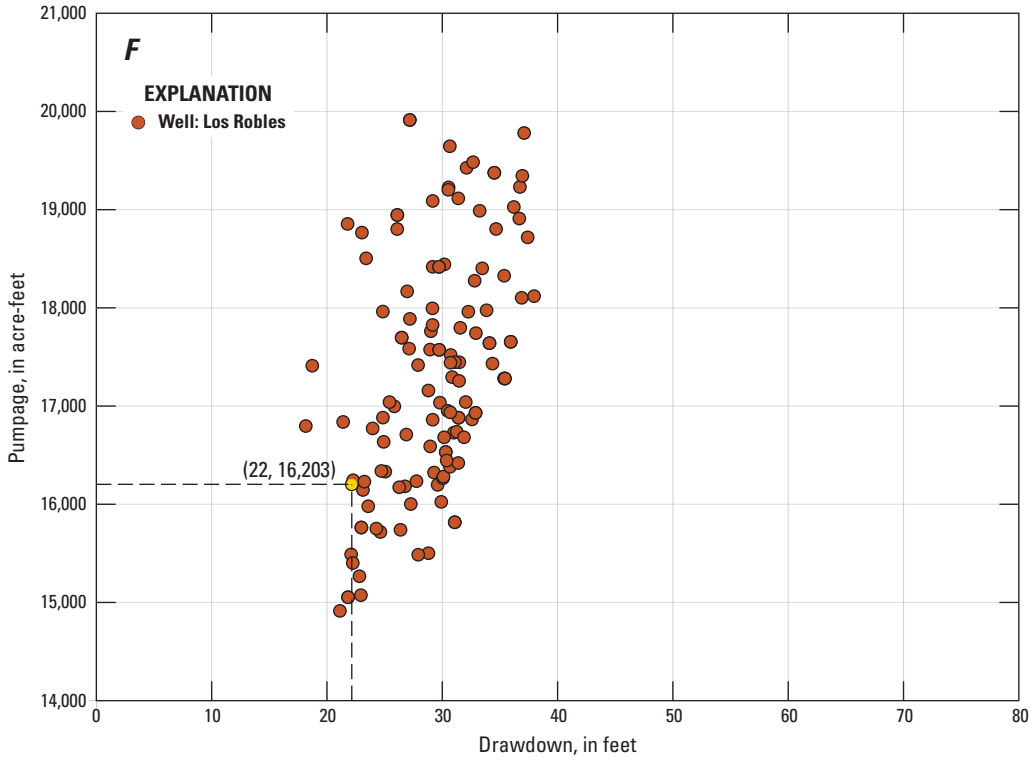

Figure D4–2. —Continued

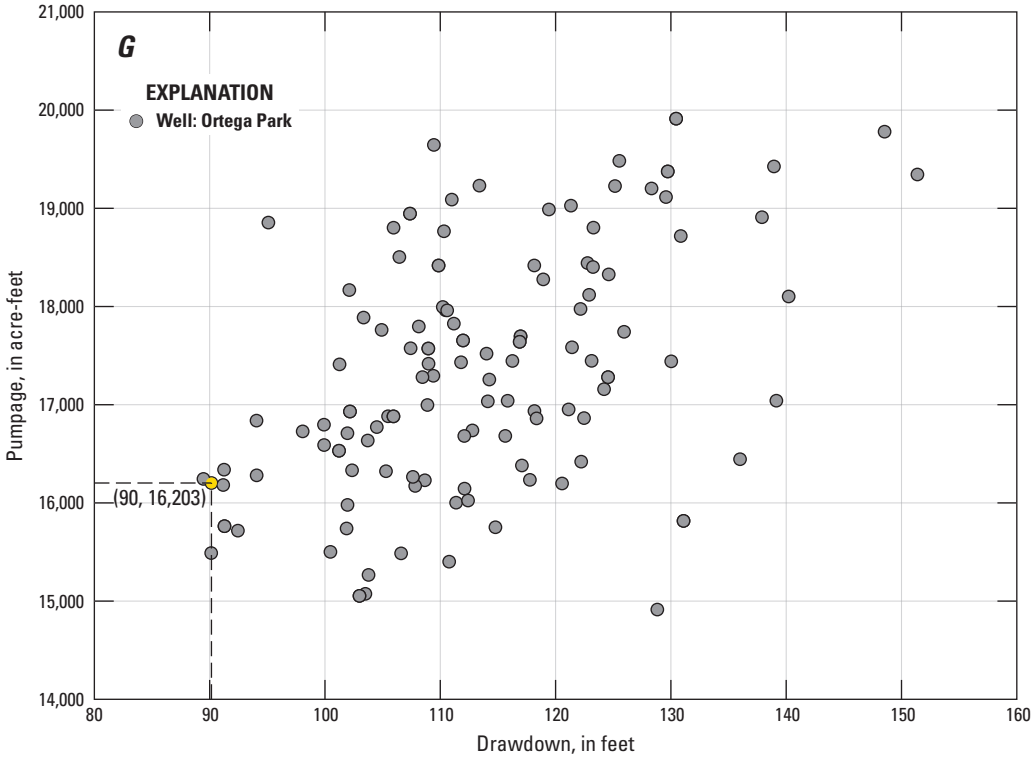

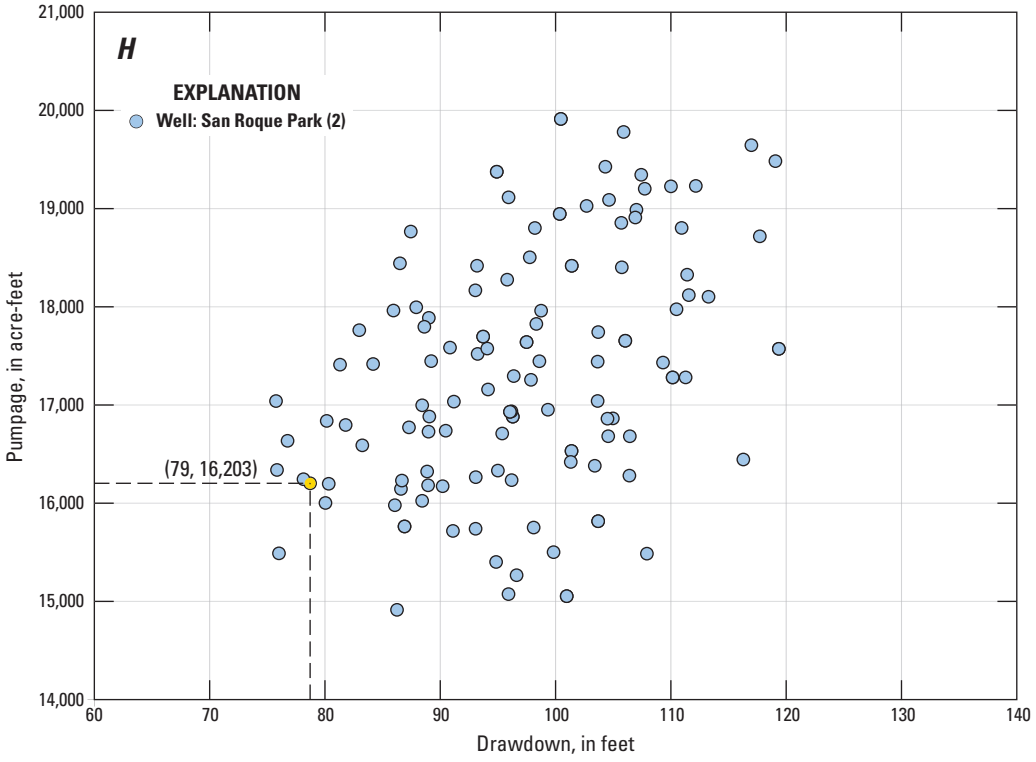

Figure D4–2. —Continued

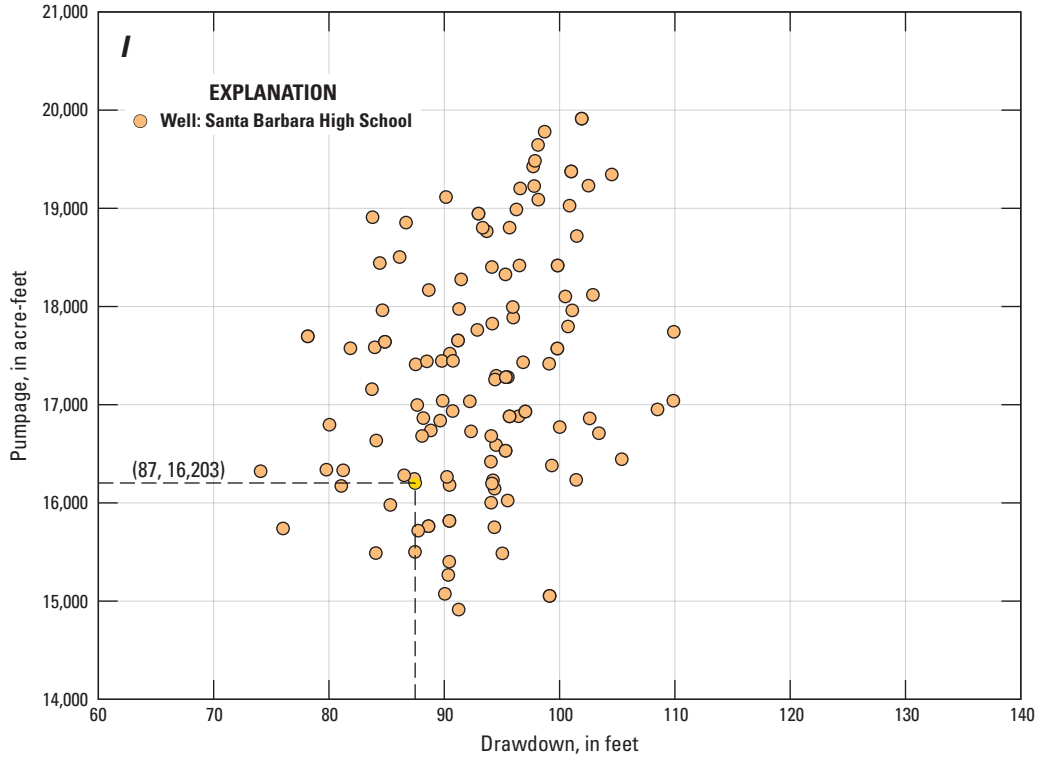

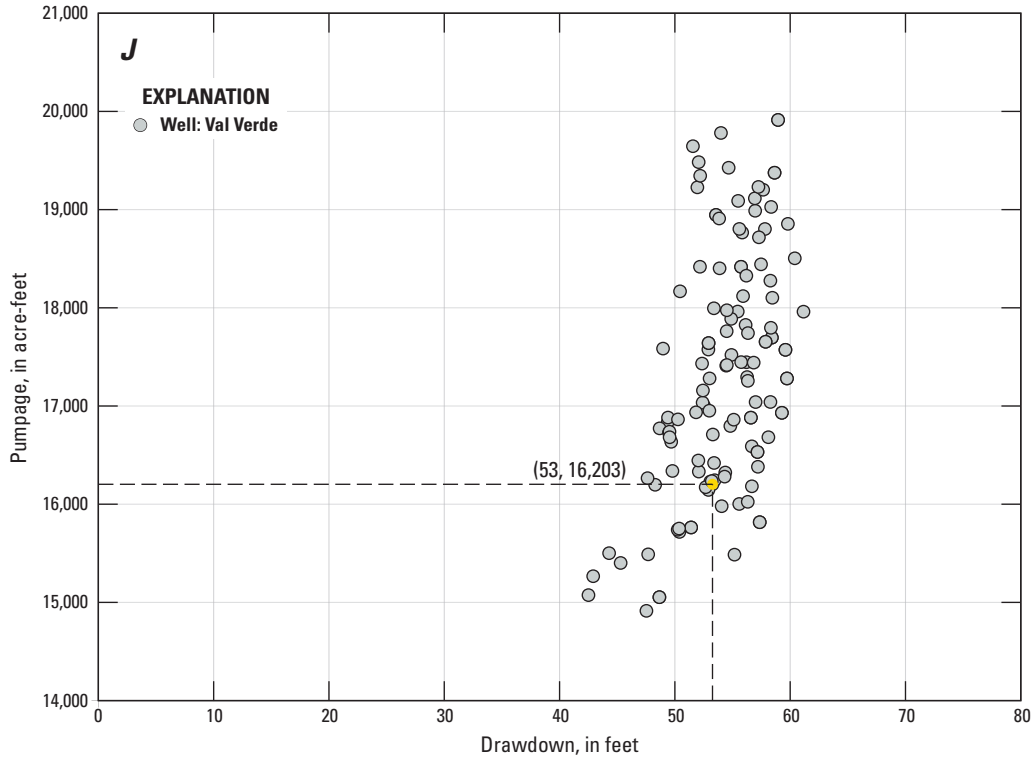

Figure D4–2. —Continued

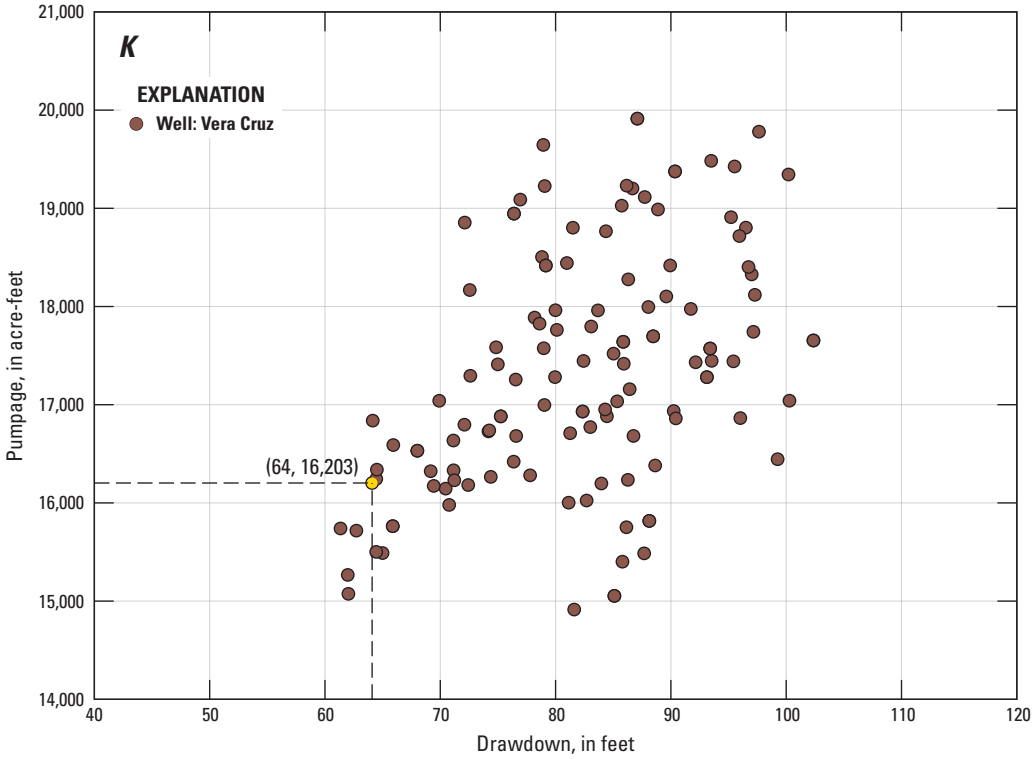

Figure D4–2. —Continued

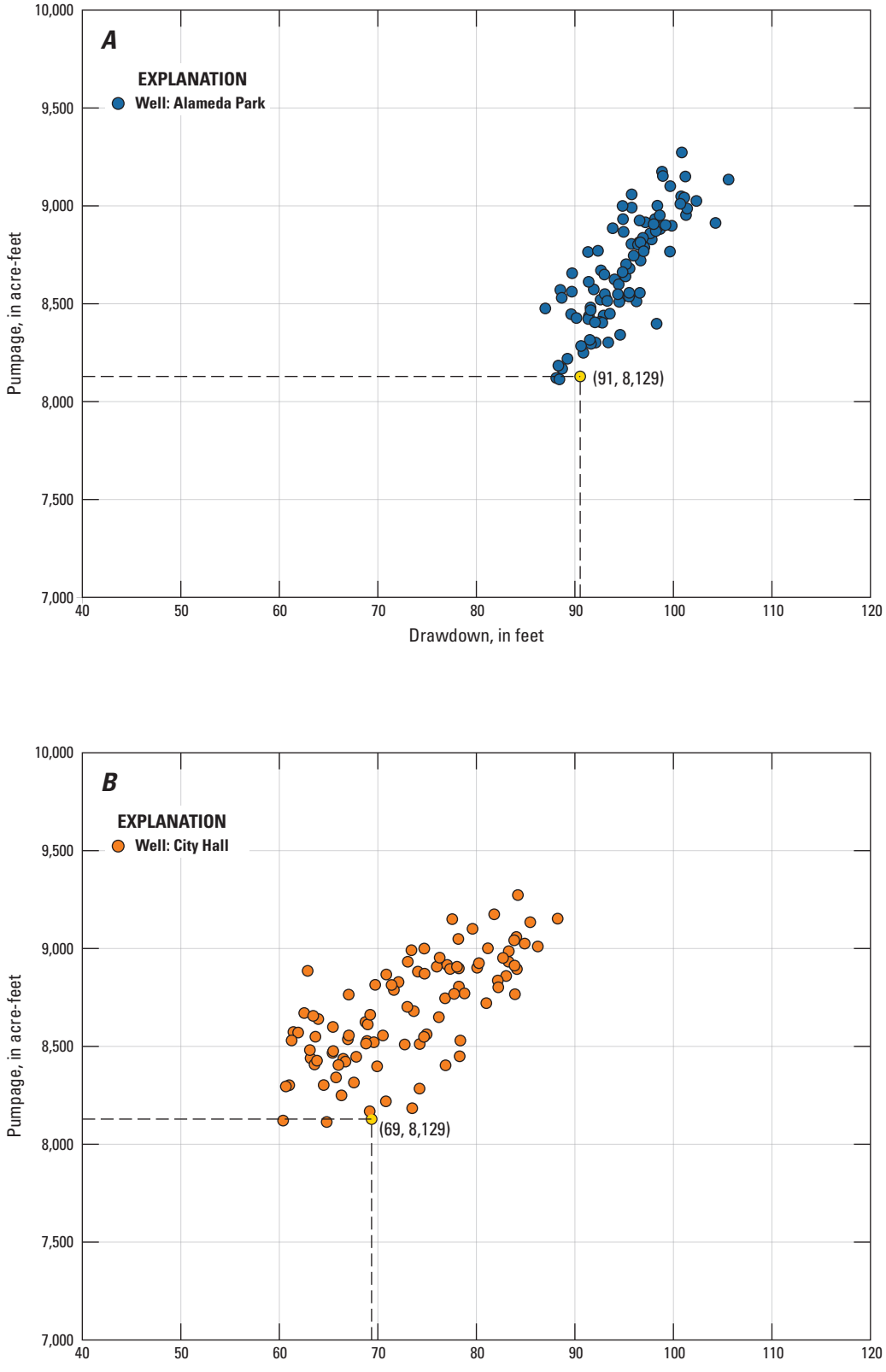

Figure D4–3. Decision rules for total Foothill groundwater basin pumpage as a function of maximum drawdown at the city of Santa Barbara production wells assuming scenario 2 (dry) precipitation, Santa Barbara groundwater basin, Santa Barbara, California (the yellow dot represents the total schedule 2_D pumpage for Foothill groundwater basin), *A*, Alameda Park; *B*, City Hall; *C*, Corporation Yard; *D*, Hope Avenue; *E*, Lincolnwood 1; *F*, Los Robles; *G*, Ortega Park; *H*, San Roque Park 2; *I*, Santa Barbara High School; *J*, Val Verde; and *K*, Vera Cruz.

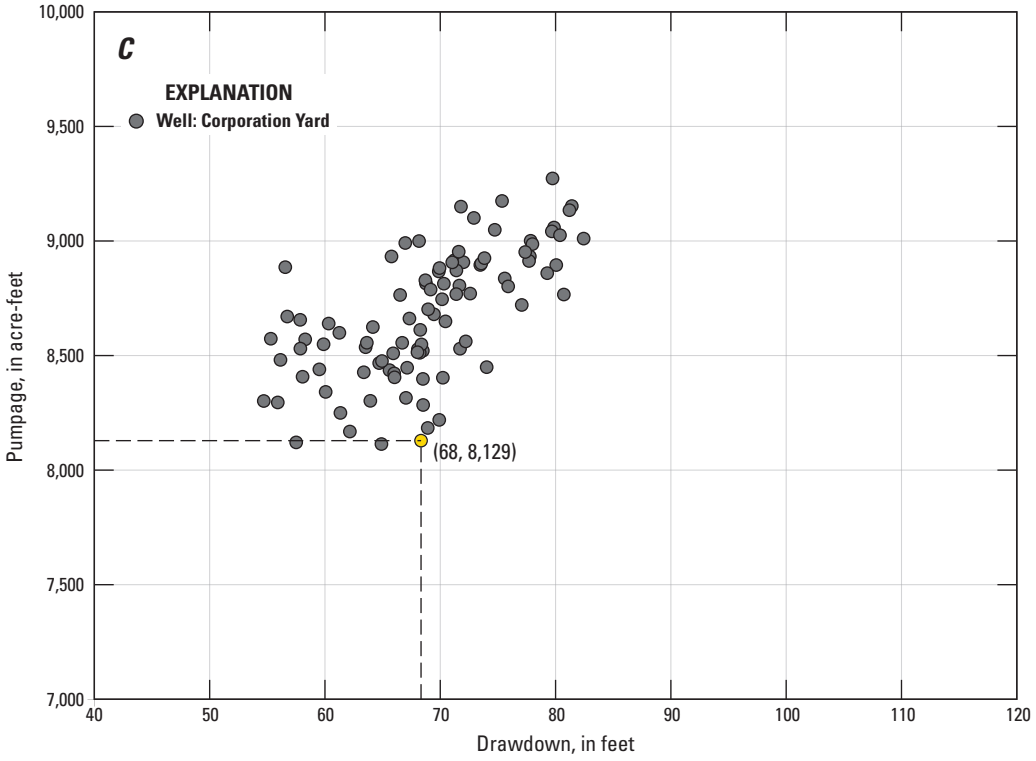

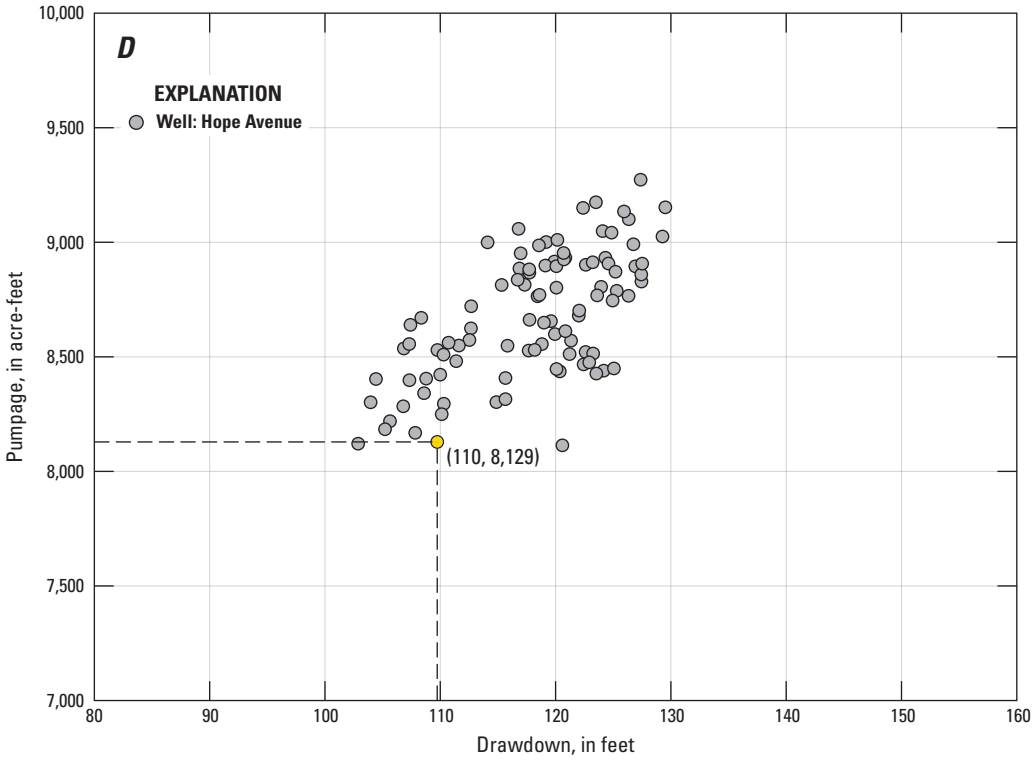

Figure D4–3. —Continued

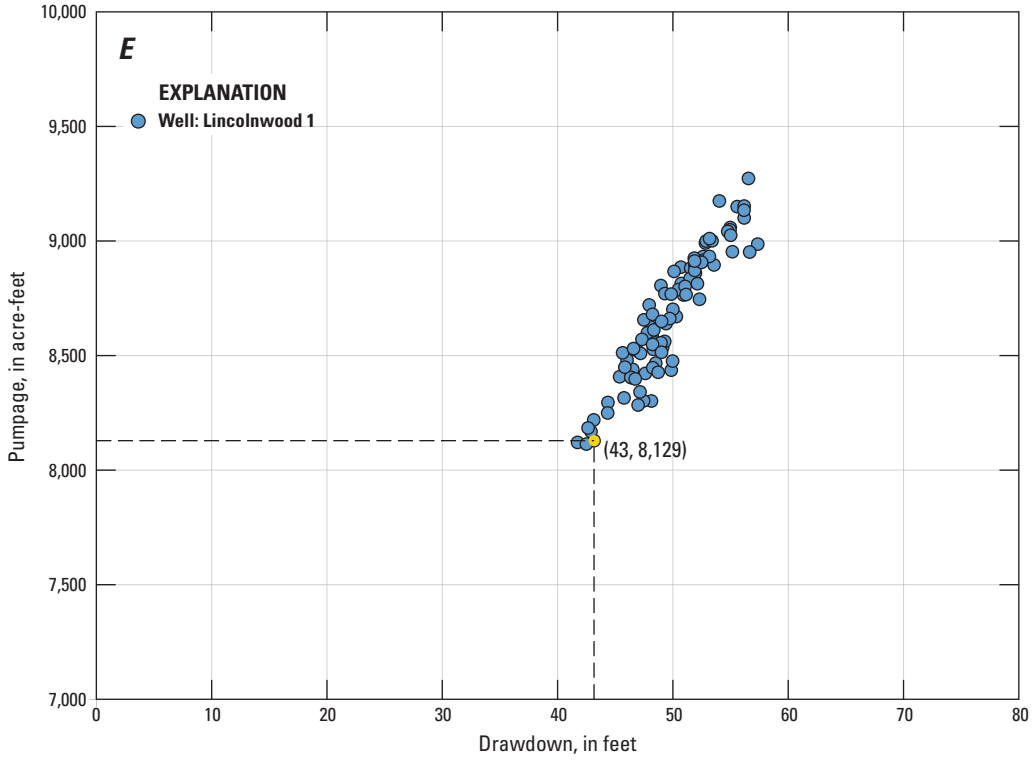

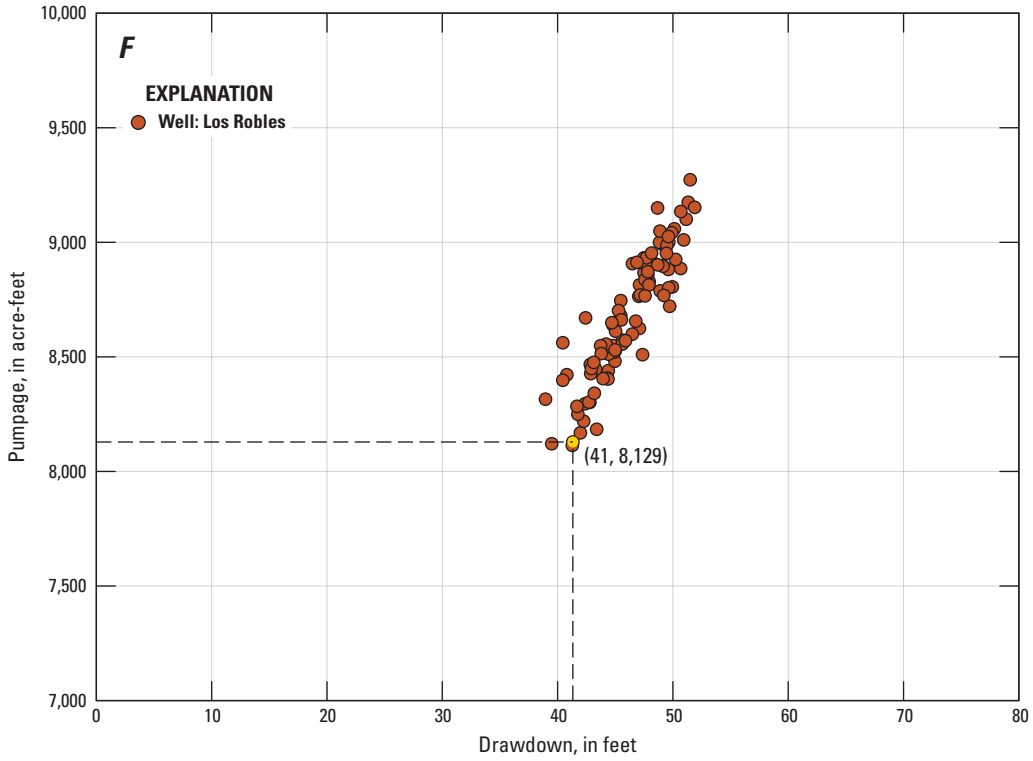

Figure D4–3. —Continued

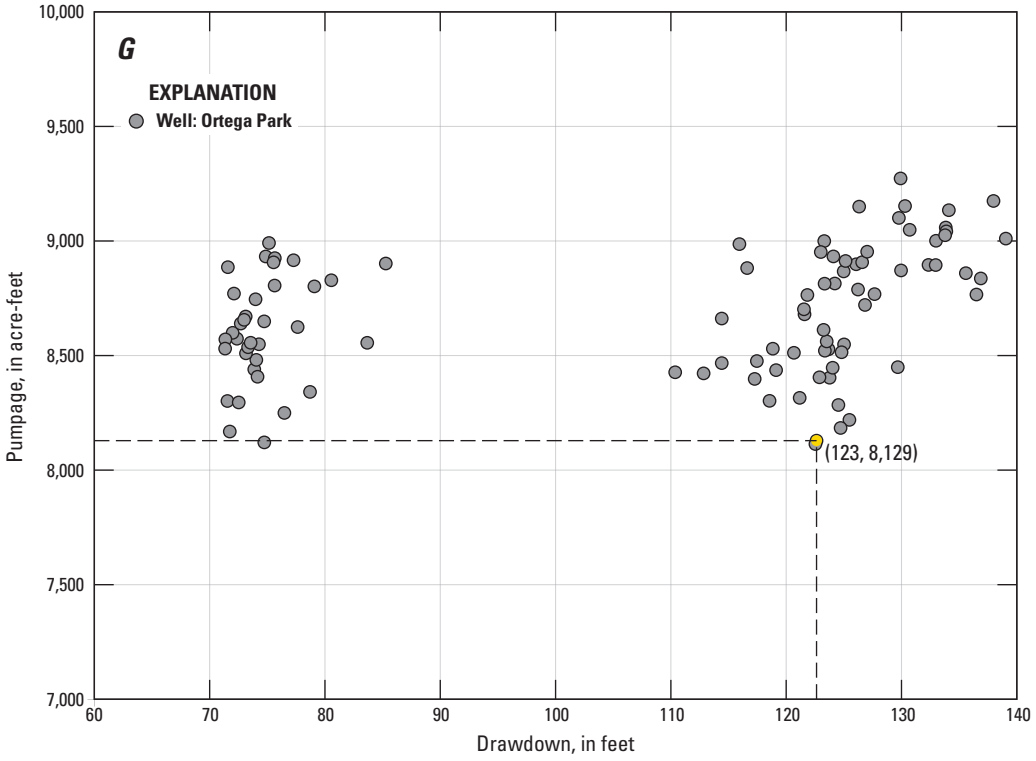

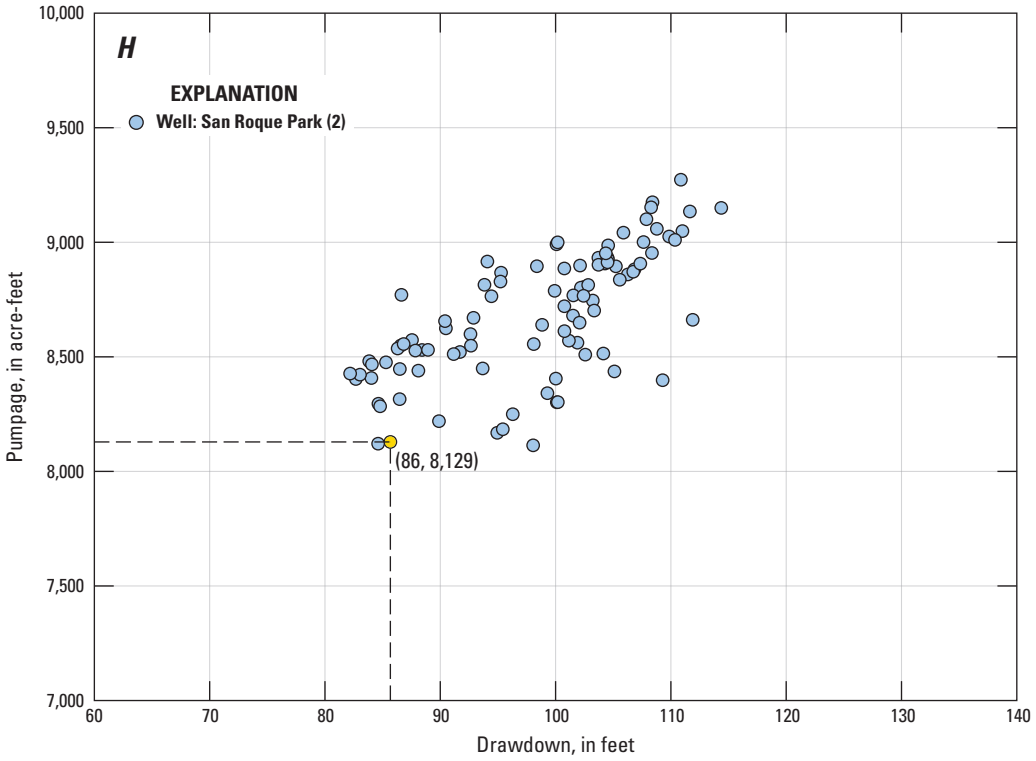

Figure D4–3. —Continued

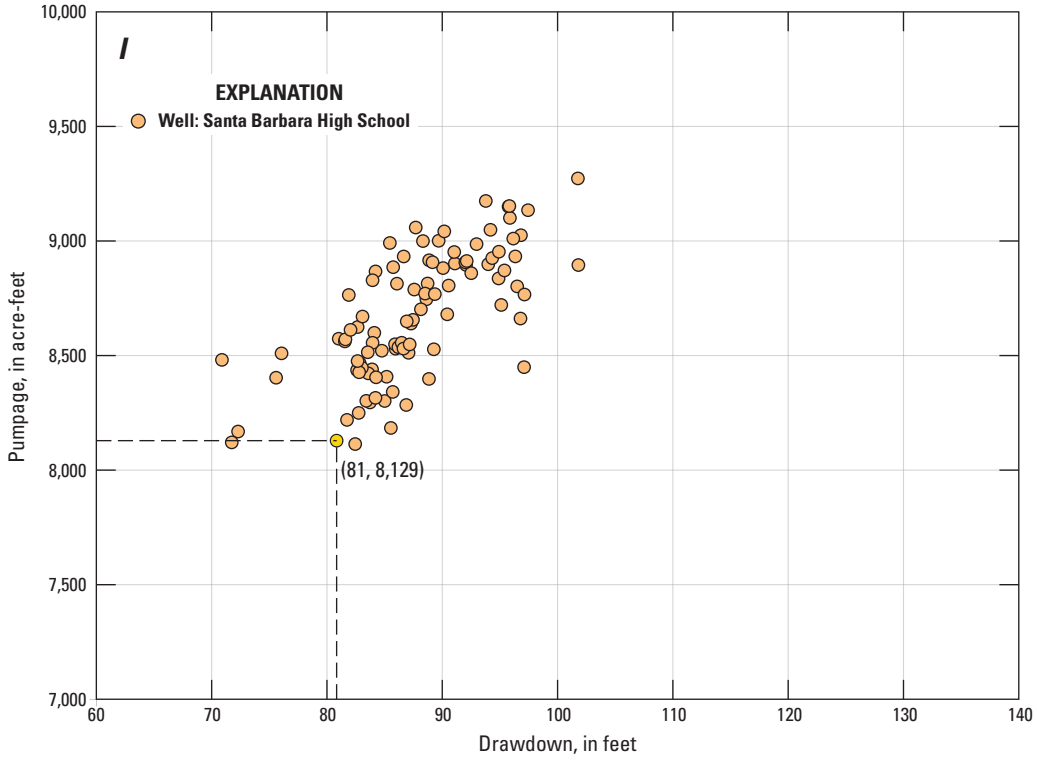

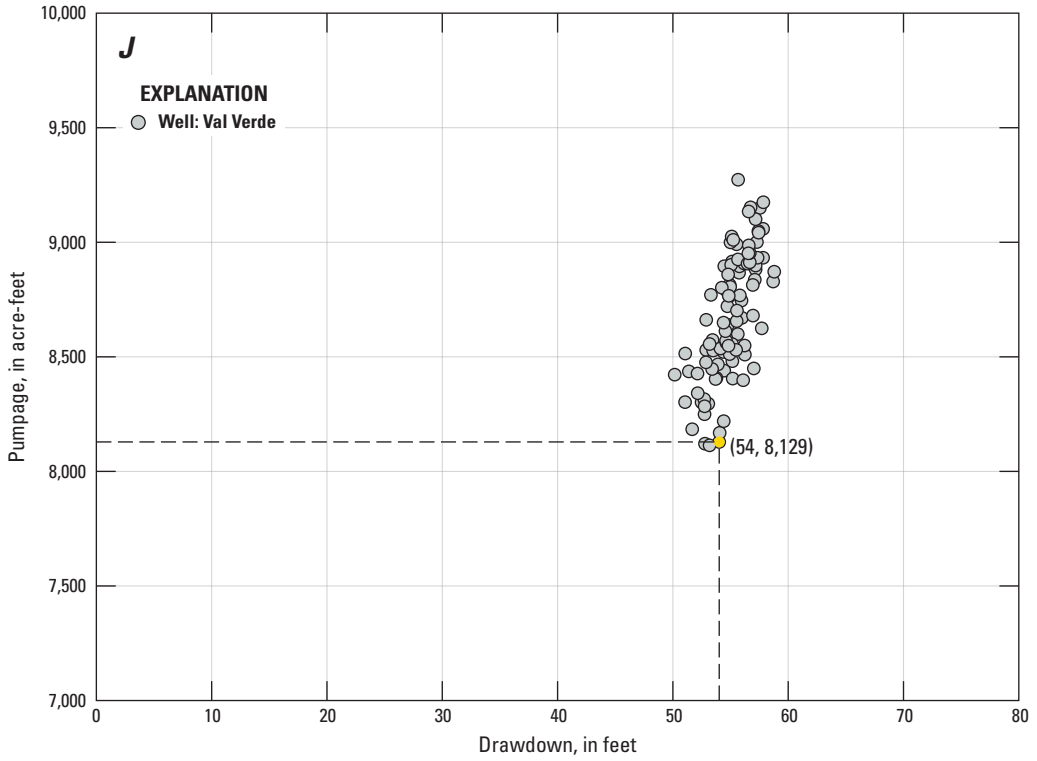

Figure D4–3. —Continued

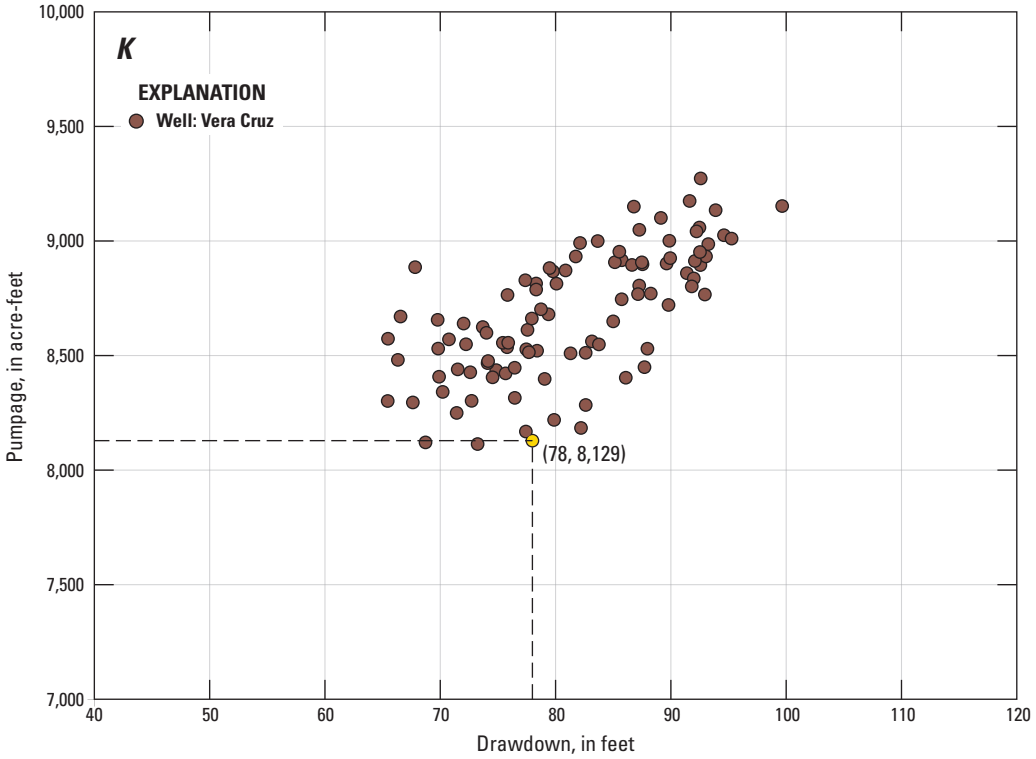

Figure D4–3. —Continued

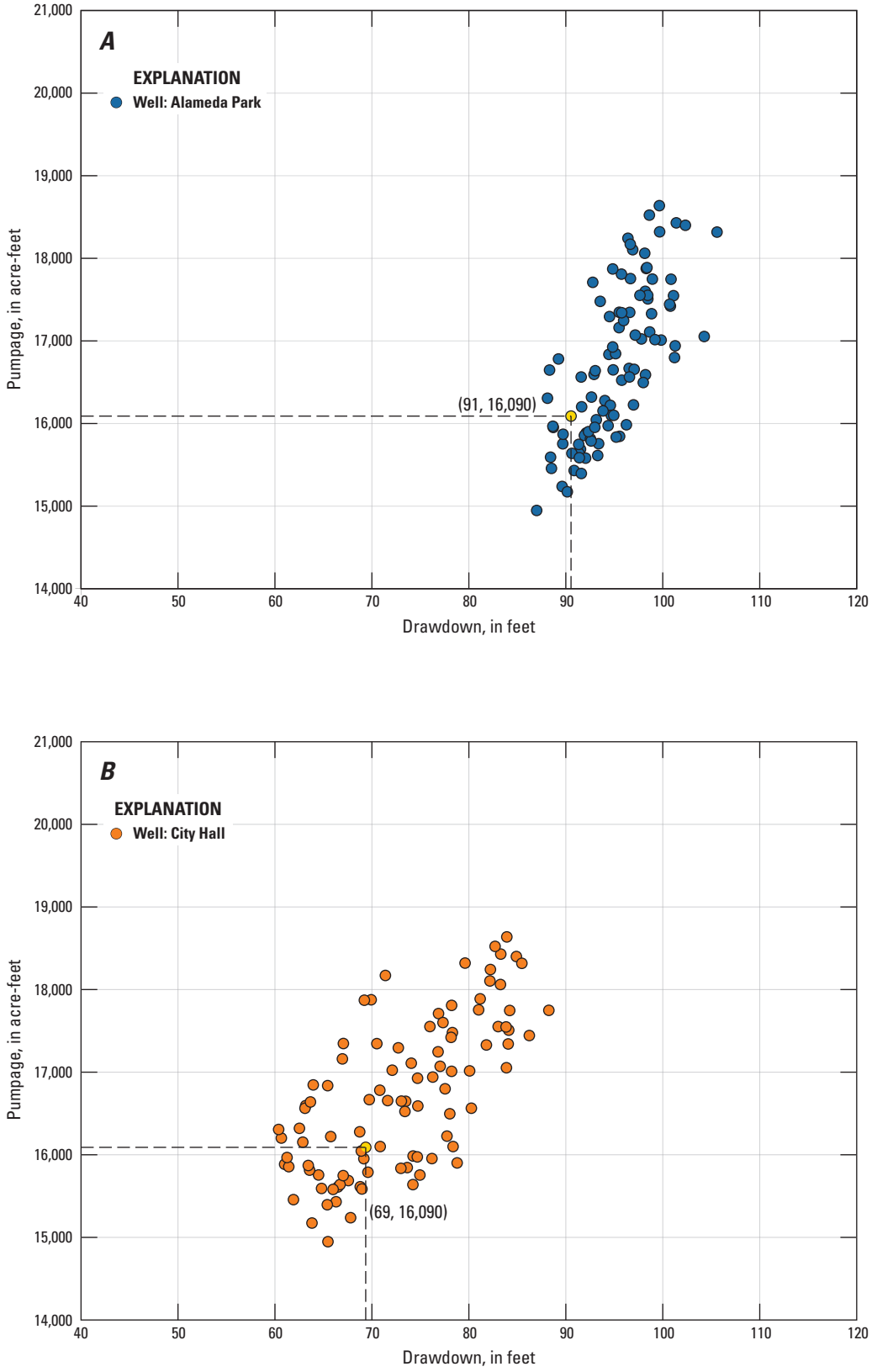

Figure D4–4. Decision rules for total Storage Unit I pumpage as a function of maximum drawdown at the city of Santa Barbara production wells assuming scenario 2 (dry) precipitation, Santa Barbara groundwater basin, Santa Barbara, California (the yellow dot represents the total schedule 2_D pumpage for Storage Unit I), *A*, Alameda Park; *B*, City Hall; *C*, Corporation Yard; *D*, Hope Avenue; *E*, Lincolnwood 1; *F*, Los Robles; *G*, Ortega Park; *H*, San Roque Park 2; *I*, Santa Barbara High School; *J*, Val Verde; and *K*, Vera Cruz.

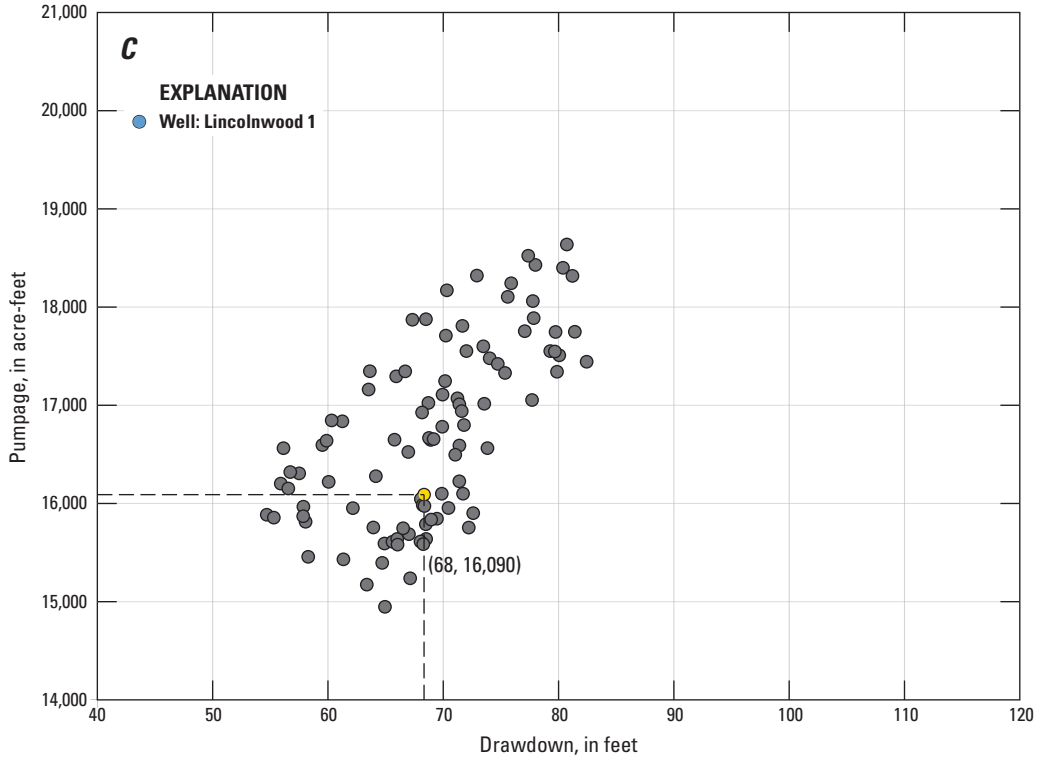

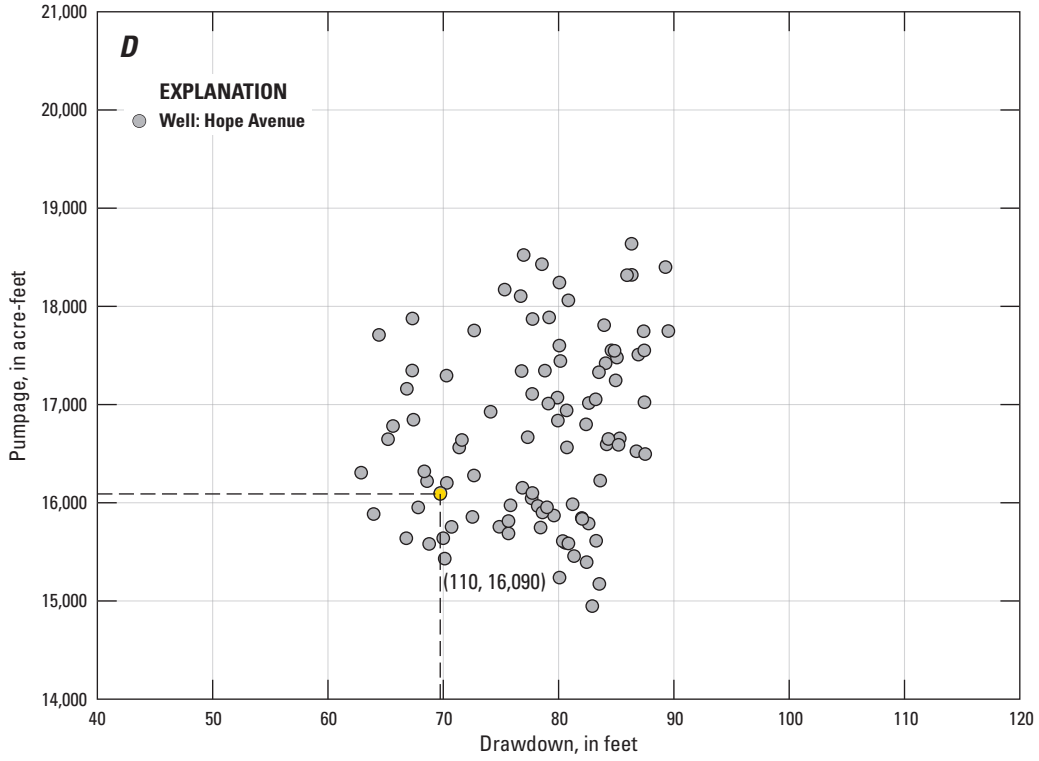

Figure D4–4. —Continued

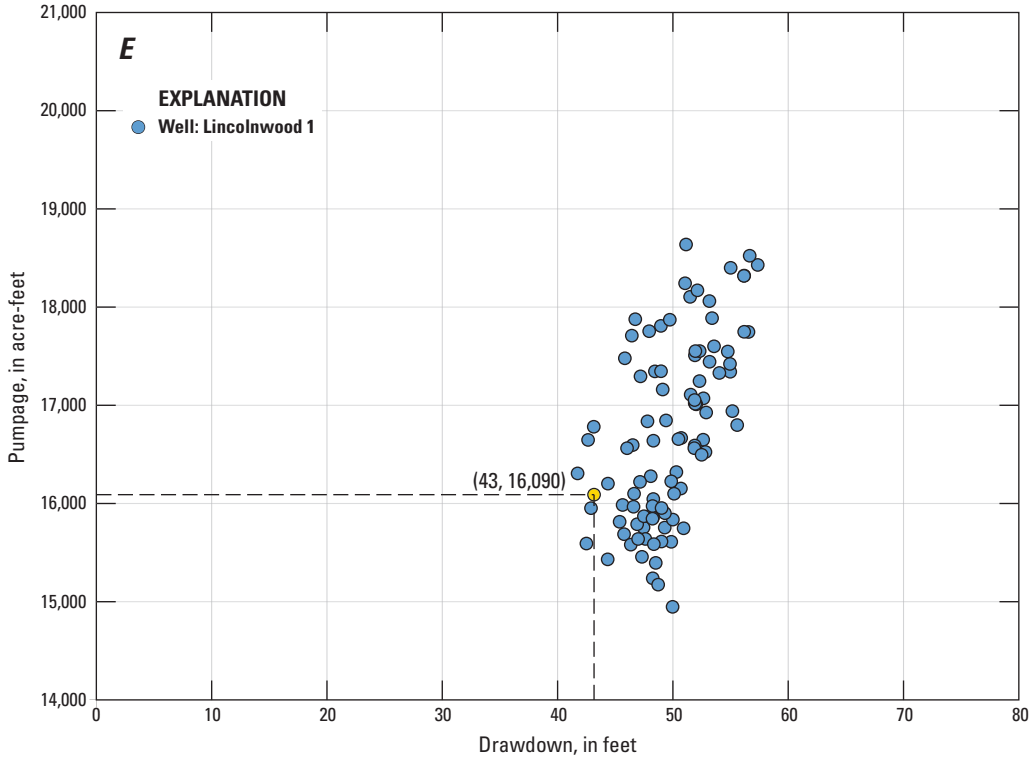

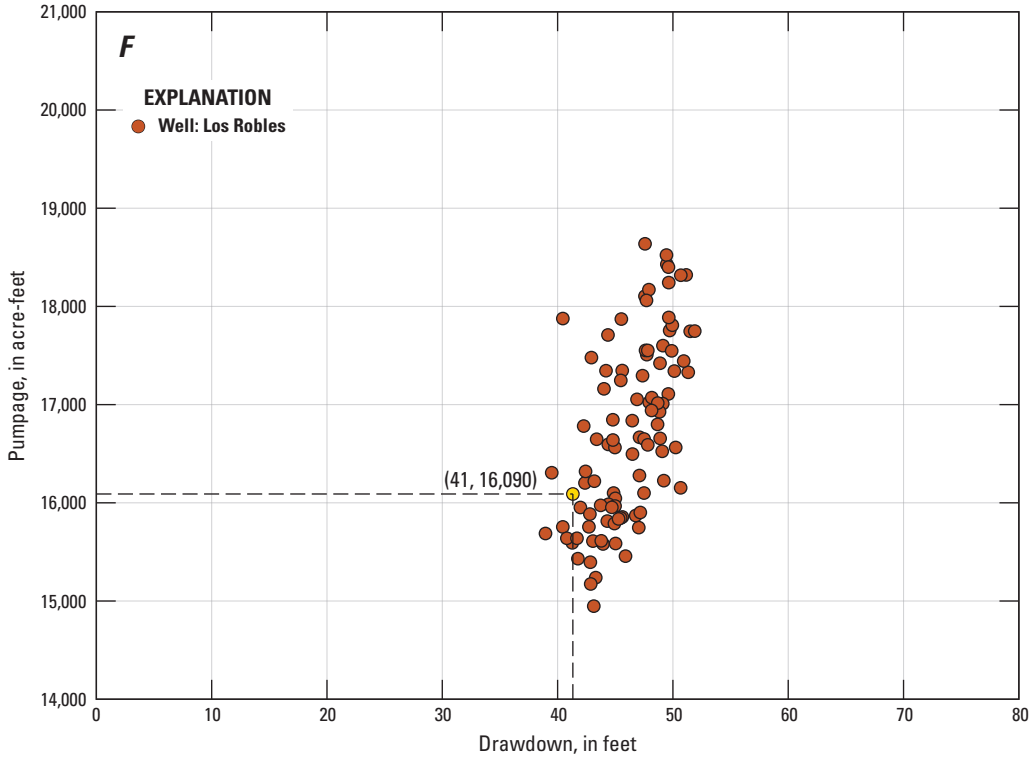

Figure D4–4. —Continued

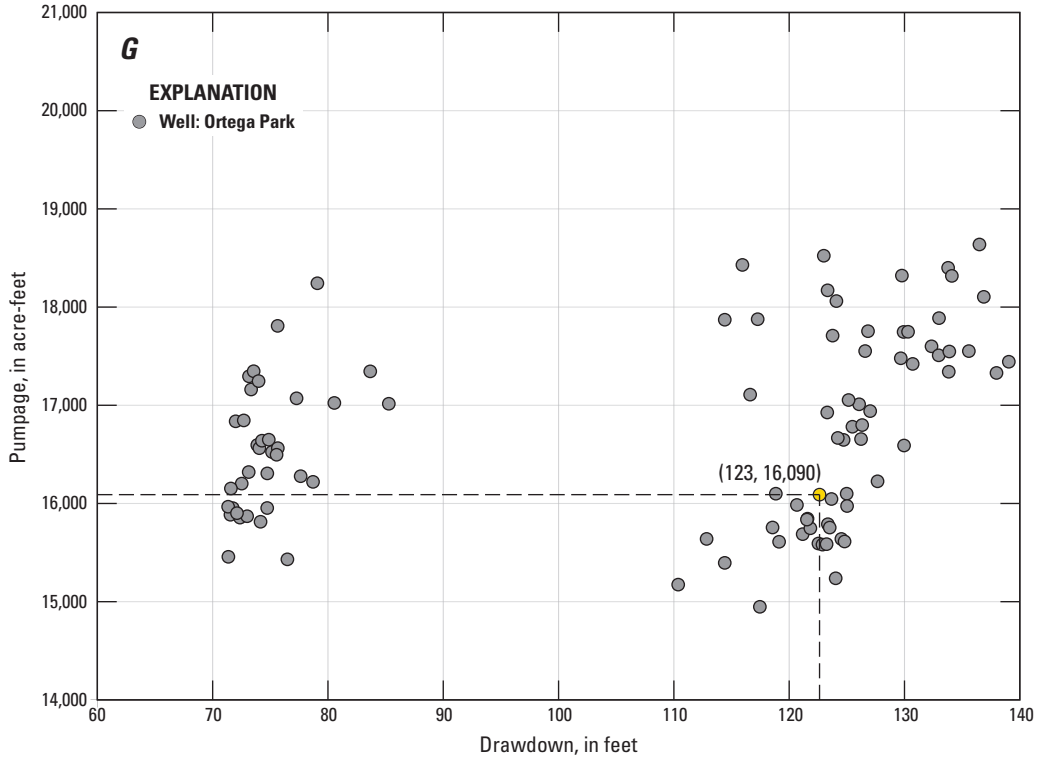

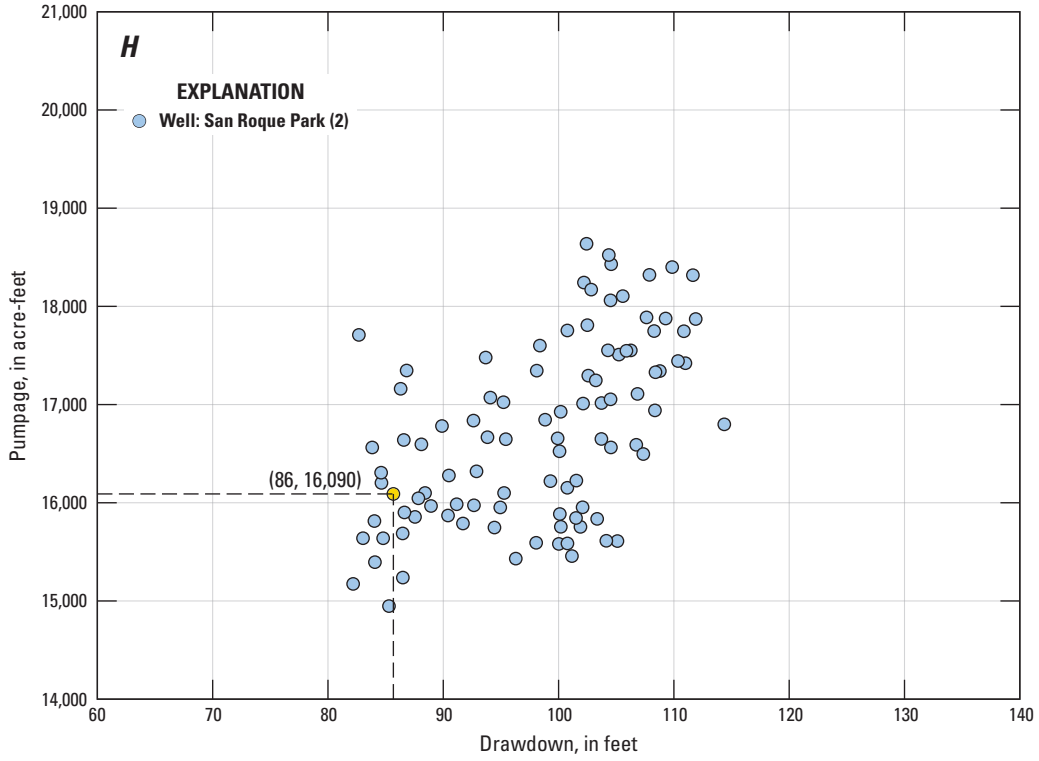

Figure D4–4. —Continued

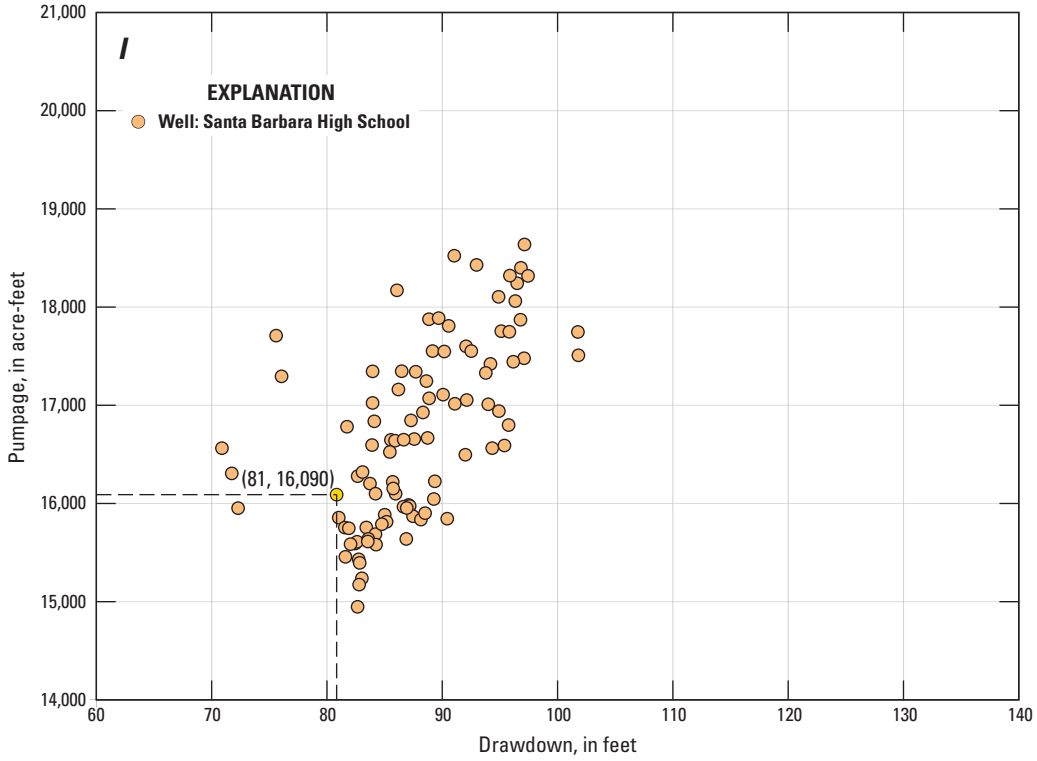

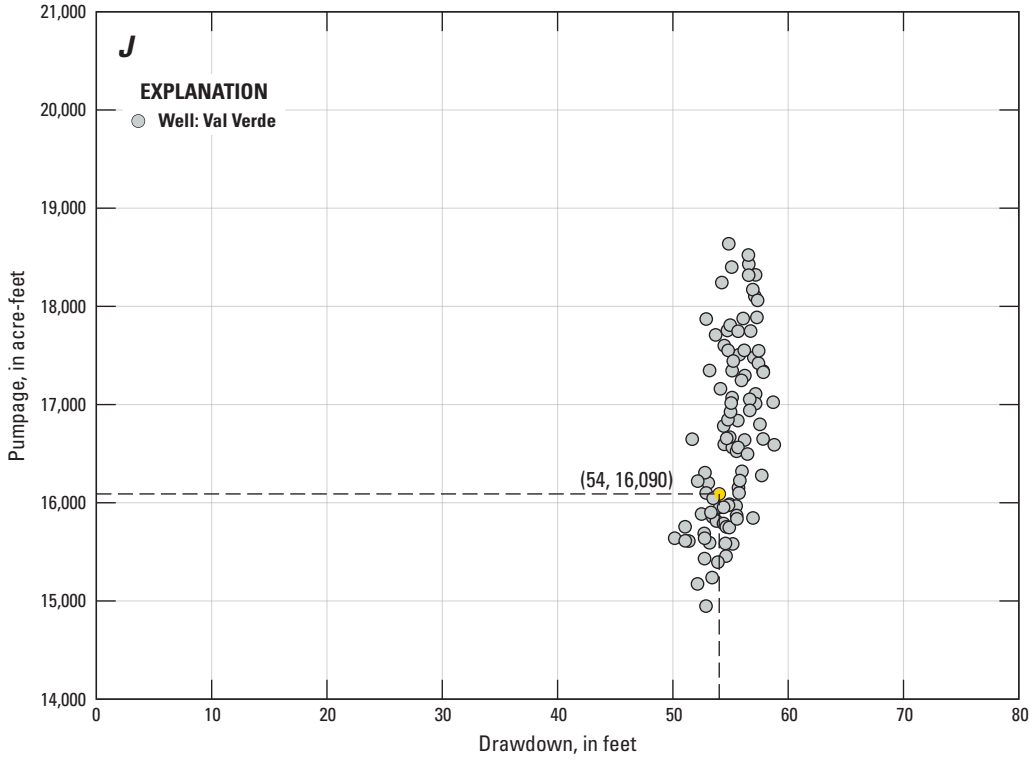

Figure D4–4. —Continued

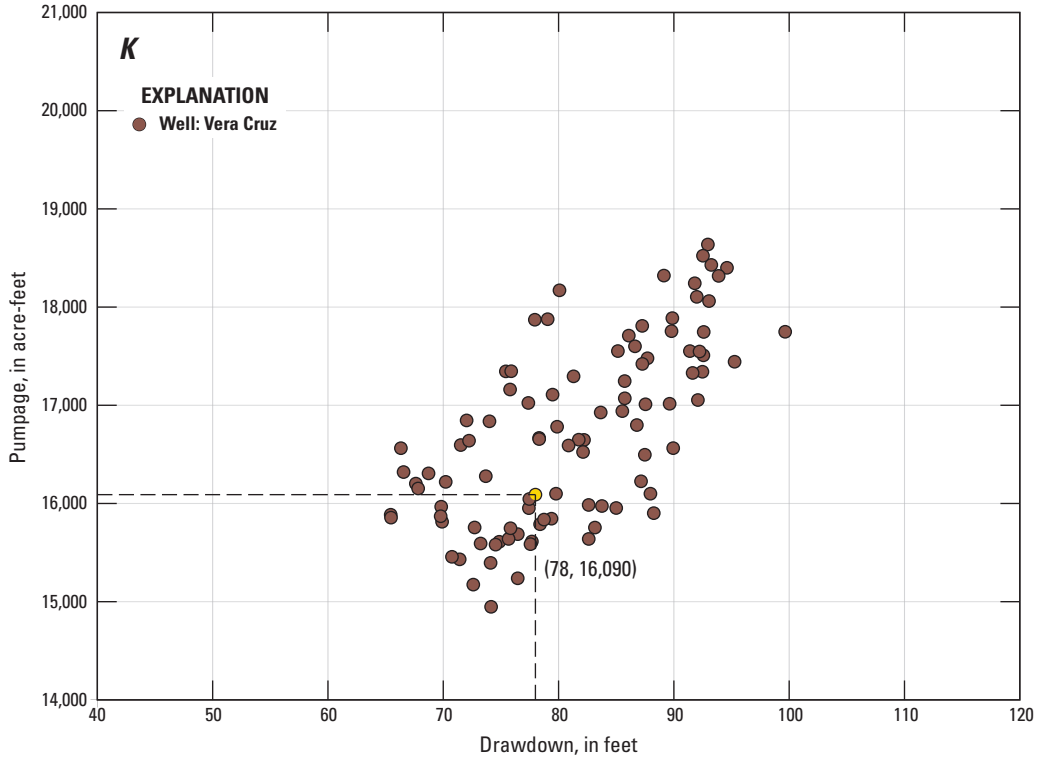

Figure D4–4. —Continued

Publishing support provided by the U.S. Geological Survey
Science Publishing Network, Sacramento Publishing Service Center

For more information concerning the research of this report, contact the
Director, California Water Science Center
U.S. Geological Survey
6000 J Street, Placer Hall
Sacramento, California 95819
http://ca.water.usgs.gov

ISSN 2328-0328 (online)
https://doi.org/10.3133/sir20185059